

PROCEEDINGS BOOK

 **IFEC2023**
DECEMBER 25-26, 2023
SIRNAK, TÜRKIYE

INTERNATIONAL FUTURE ENGINEERING CONFERENCE

EDITORS

ASSOC. PROF. DR. MAHMUT DİRİK

ASSOC. PROF. DR. ASAF TOLGA ULGEN

IKSAD PUBLISHING HOUSE

ISBN: 978-625-367-594-3



CONFERENCE ID

CONFERENCE TITLE

1st International Future Engineering Conference
-IFEC2023-

DATE and PLACE

December 25-26, 2023 / Şirnak, Türkiye

PARTICIPATION

Keynote & Invited

ORGANIZATION

Governory of Şirnak
Şirnak University
Şirnak University, Technology Transfer Office
Şirnak Chamber of Industry and Commerce
IKSAD-Institute of Economic Development and Social Research

PARTICIPANTS COUNTRY

Algeria, Bulgaria, Egypt, Georgia, Hungary, India, Iraq, Kazakhstan, Kosovo, Kuwait, Malasia, Morocco, Nigeria, Pakistan, Romania, Russia, Saudi Arabia, Serbia, Slovenia, Spain, Tunisia, Türkiye, Ukraine, Vietnam

Number Of Accepted Papers-**103**

Number Of Rejected Papers-**41**

The number of abstracts from foreign countries-**65**

The number of abstracts from Türkiye-**38**

Honorary Board

Cevdet Atay

Governor of Şirnak, Türkiye

Prof. Dr. Abdurrahim ALKIŞ

Rector of Sirnak University, Türkiye

Prof. Dr. Oscar CASTILLO

Tijuana Institute of Technology, MX

Conference Heads

Assoc. Prof. Dr. Mahmut DİRİK

Assoc. Prof. Dr. Asaf Tolga ULGEN

Organizing Board Members

Assoc. Prof. Dr. Mehmet HASKUL

Assist. Prof. Dr. Edip TASKESEN

Assoc. Prof. Dr. Ahmet TURŞUCU

Assoc. Prof. Dr. Abdullah BAŞÇI

Assist. Prof. Dr. Sedat ÖZCANAN

Assoc. Prof. Dr. Sedat ÇELİK

Coordinator

Atabek MOVLYANOV

Erciyes University, Faculty of Engineering, Energy Systems Eng. department

SCIENTIFIC BOARD MEMBERS

Prof. Dr. Antonio Rodríguez DIAZ
Prof. Dr. Zulfiqar HABİB
Prof. Dr. Valentina E. BALAS
Prof. Dr. Luis MARTINEZ
Prof. Dr. José Luis VERDEGAY
Prof. Dr. Maya LAMBOVSKA
Prof. Dr. Fevrier VALDEZ
Prof. Dr. Pedro Ponce CRUZ
Prof. Dr. Dmitry NAZAROV
Prof. Dr. Said BROUMI
Prof. Dr. Alfian MA'ARIF
Prof. Dr. Mahmut Tahir NALBANTÇILAR
Prof. Dr. Musa AYDIN
Prof. Dr. M. Ali AKÇAYOL
Prof. Dr. Osman BİLGİN
Prof. Dr. İhsan ALP
Prof. Dr. Abdulkadir ŞENGÜR
Prof. Dr. Ali KARCI
Prof. Dr. Davut HANBAY
Prof. Dr. Murat KARABATAK
Prof. Dr. Mehmet ÖZKAYNAK
Prof. Dr. Memet ŞAHİN
Prof. Dr. İlhan TARIMER
Prof. Dr. Fevzi HANSU
Prof. Dr. E. Mustafa EYYUBOĞLU
Prof. Dr. Mehmet ŞİMŞEK
Prof. Dr. Erkan TANYILDIZI
Prof. Dr. Melih INAL
Prof. Dr. Gürcan YILDIRIM
Assoc. Prof. Dr. Mehmet Hilal ÖZCANHAN
Assoc. Prof. Dr. S. A. EDALATPANAH
Assoc. Prof. Dr. Ömerülfaruk ÖZGÜVEN
Assoc. Prof. Dr. Baha SEN
Assoc. Prof. Dr. Tuncay ERCAN
Assoc. Prof. Dr. Derya AVCI
Assoc. Prof. Dr. Sait Ali UYMAZ
Assoc. Prof. Dr. Aytuğ ONAN
Assoc. Prof. Dr. Adnan Fatih KOCAMAZ
Assoc. Prof. Dr. Sait Barış GÜNER
Assoc. Prof. Dr. Vakkas ULUÇAY
Assoc. Prof. Dr. Emrah AYDEMİR
Assoc. Prof. Dr. Zafer CÖMERT
Assoc. Prof. Dr. Faruk SERİN
Assoc. Prof. Dr. Nuh ALPASLAN
Assoc. Prof. Dr. Şehmus BADAY
Assoc. Prof. Dr. Melih KUNCAN
Assoc. Prof. Dr. Murat CANAYAZ
Assoc. Prof. Dr. Murat KARAKOYUN
Assoc. Prof. Dr. Buket DOĞAN
Assoc. Prof. Dr. Kazım HANBAY
Assoc. Prof. Dr. Fatih ERTAM
Assoc. Prof. Dr. Yasemin GÜLTEPE
Assoc. Prof. Dr. Recep ÖZDAĞ
Assist. Prof. Dr. Ahmet Arif AYDIN

Assist. Prof. Dr. Bekir ÇIRAK
Assist. Prof. Dr. Emrah DÖNMEZ
Assist. Prof. Ali ARI
Assist. Prof. Dr. Abdulkadir AYANOĞLU
Assist. Prof. Dr. Sedat GOLGİYZ
Assist. Prof. Dr. Esra N. YOLAÇAN
Assist. Prof. Dr. Mahmut KAYA
Assist. Prof. Dr. Emir ÖZTÜRK
Assist. Prof. Dr. Nuh AZGINOĞLU
Assist. Prof. Dr. Abdullatif BABA
Assist. Prof. Dr. Mustafa KAYA
Assist. Prof. Dr. M. Gökhan BAKAL
Assist. Prof. Dr. Cüneyt ÖZDEMİR
Assist. Prof. Dr. Alper Turan ALAN
Assist. Prof. Dr. FATİH OKUMUŞ
Assist. Prof. Dr. Mutlu TEKİR
Assist. Prof. Dr. Fatih ILKBAHAR
Assist. Prof. Dr. Ali ŞENOL
Assist. Prof. Dr. Oğuzhan KENDİRLİ
Assist. Prof. Dr. Kenan ZENGİN
Assist. Prof. Dr. Murat KOCA
Assist. Prof. Dr. İSA AVCI
Assist. Prof. Dr. BUKET TOPTAŞ
Assist. Prof. Dr. Çiğdem Sazak TURGUT
Assist. Prof. Dr. Abdullah ELEWI
Assist. Prof. Dr. Ahmet ÇELİK
Assist. Prof. Dr. Burcu Yurekli YILMAZEL
Assist. Prof. Dr. Venera ADANOVA
Assist. Prof. Dr. Ali Osman SELVİ
Assist. Prof. Dr. Güliz TOZ
Assist. Prof. Dr. Kenan İNCE
Assist. Prof. Dr. Mehmet KARA
Assist. Prof. Dr. Yahya DOĞAN
Assist. Prof. Dr. İlker ÖZÇELİK
Assist. Prof. Dr. Hakan GÜNDÜZ
Assist. Prof. Dr. Yıldırım YILMAZ
Assist. Prof. Dr. Emre OLCA
Assist. Prof. Dr. Ece Gelal SOYAK
Assist. Prof. Dr. Hüseyin GÜRBÜZ
Assist. Prof. Dr. Fatih ARLI
Assist. Prof. Dr. Hakan DUMRUL
Assist. Prof. Dr. Serdal DAMARSEÇKİN
Dr. Arfat Ahmad Khan
Dr. Mohammad Javad EBADI
Dr. Mutlucan BAYAT
Dr. Berna ARI
Dr. Khandan ROŞHANAEL
Dr. Sultan N. TURHAN
Dr. Mubbashar SADDIQUE
Dr. Ahmet DEVELİ
Dr. Esra SÖĞÜT
Dr. Emrah ASLAN

PHOTO GALLERY











observer hall 3



Selman İLBE...



Hamza Alah... >

Kaydediliyor...

Kalan: 09:19:17



1st International Future Engineering Conference -IFEC2023-

December 25-26, 2023 / Sırnak, Türkiye

EXPLORING BUILDING-INTEGRATED PHOTOVOLTAIC/THERMAL SYSTEMS

Lecturer Mazlum CENGİZ, Sırnak
University, Machinery and Metal Technologies,
Sırnak-Türkiye
mazlumcengiz@sirnak.edu.tr (Responsible
Author)
ORCID: 0002-3724- 6894

Lecturer Dr. Yahya CELEBİ, Sırnak
University, Motor Vehicles and Transportations,
Sırnak-Türkiye
yahya.celebi@outlook.com,
ORCID: 0002-4686-9794

Prof. Dr. Huseyin AYDIN, Batman
University, Faculty of Engineering, Department
of Mechanical Engineering, Batman-Türkiye
huseyin.aydin@batman.edu.tr,
ORCID: 0002-5415-0405

The screenshot displays a Zoom meeting interface with a grid of participants. The participants visible are:

- H2_KUMAR NEERAJ
- Observer hall 2
- Hall2-Onur SİLAHTAR
- TRSC
- Hall-2, Abdurrahim ERAT
- Ahmet
- Woyengitonye Butler Abadani
- Observer hall 2
- Mehmet Haskul
- H2 Sabri UZUNER
- Muhammed Tayyip Koçak
- BRAKNI Oumai...
- Hall2 Alpay TOK
- Murat CANAYAZ
- Observer-3
- Zohaib Hassan Sain - S(2)
- Hall-3, Hutu Dana
- Hall-3, Hamid Zoug...
- Khalid Reggab

The shared PowerPoint presentation is titled "International Congress on ES (Presentation 2) - PowerPoint" and is displayed in the bottom half of the screen. The slide content includes:

EXPLORING THE TRANSFORMATIVE IMPACT: AI'S INFLUENCE ON ADVANCEMENTS IN INDUSTRIAL RESEARCH

Presenter: Zohaib Hassan Sain

The participant list on the right side of the screen shows 7 participants:

- O... (Ortak oturum sahibi, ben)
- Zohaib Hassan Sain - S(2), H...
- AD AMIN Danladi Bello
- BT Bashir Tanimu
- HH Hall-3, Hamid Zougari
- HH Hall-3, Hutu Dana
- KR Khalid Reggab

Observer H-1

Mouna Bedoui

Murat CANAYAZ

H-1 -yashvanth M

Mahmut Dirik

Rasim ÇEKİK

Rasim ÇEKİK

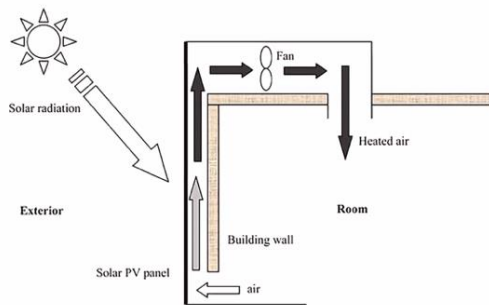
observer hall 3



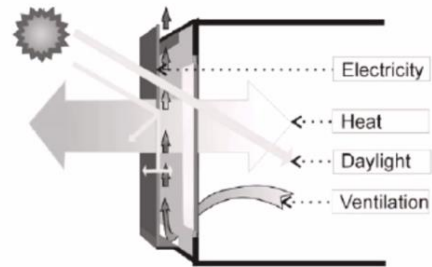
Kaydediliyor...

Kalan: 09:12:53

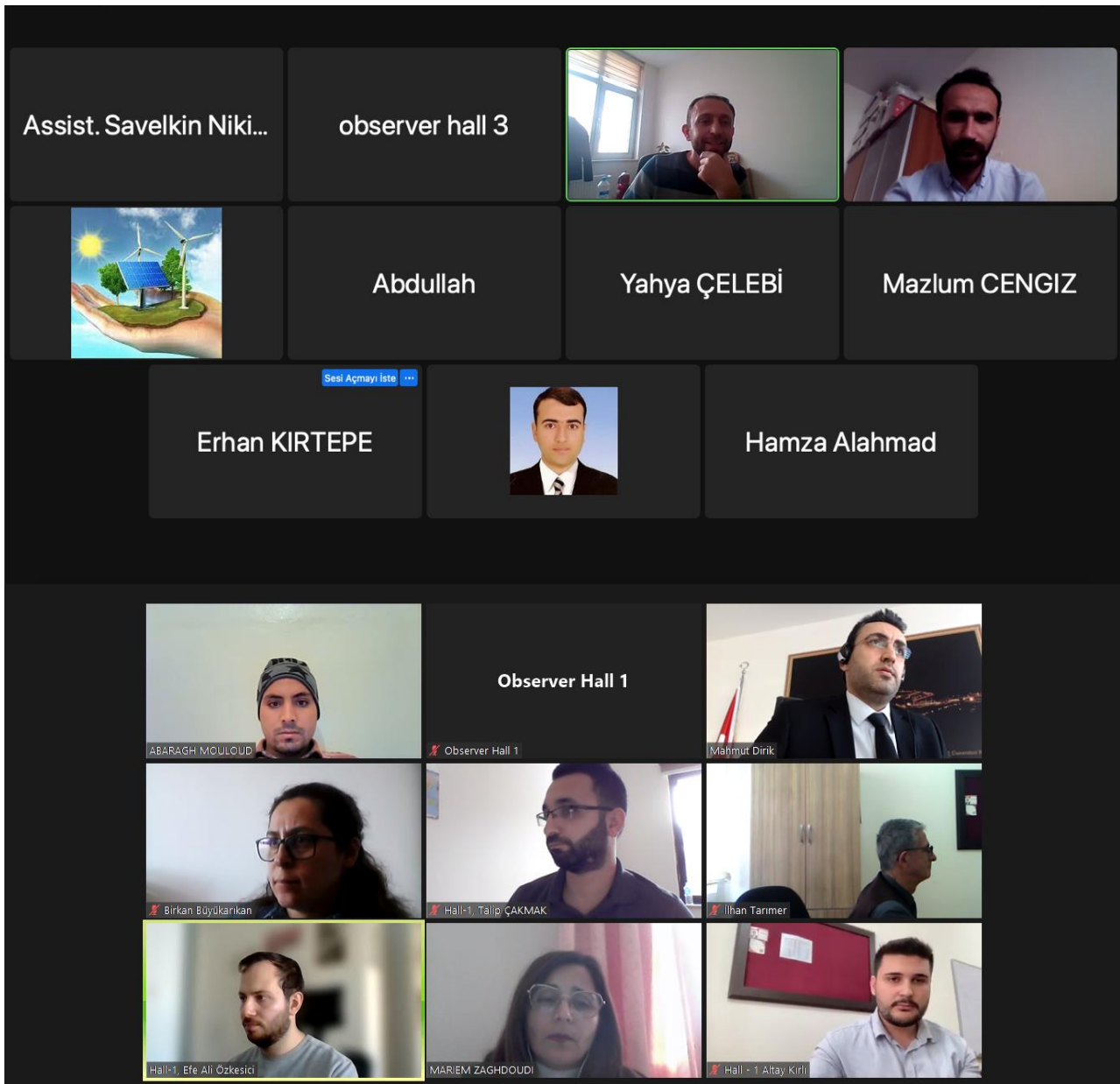
Working principle of BIPV/T Systems



A façade BIPV/T system with air circulation



The ventilation mode of a façade BIPV/T system with air circulation





1st International Future Engineering Conference -IFEC2023-

December 25-26, 2023 / Sirnak, Türkiye

Conference Program

Important, Please Read Carefully (Online Presentations)

- To be able to attend a meeting online, login via <https://zoom.us/join> site, enter ID "Meeting ID or Personal Link Name" and solidify the session.
- The Zoom application is free and no need to create an account.
- The Zoom application can be used without registration.
- The application works on tablets, phones and PCs.
- The participant must be connected to the session 5 minutes before the presentation time.
- All congress participants can connect live and listen to all sessions.
- Moderator is responsible for the presentation and scientific discussion (question-answer) section of the session.

Points to Take into Consideration - TECHNICAL INFORMATION (Online Presentations)

- Make sure your computer has a microphone and is working.
- You should be able to use screen sharing feature in Zoom.
- Attendance certificates will be sent to you as pdf at the end of the congress.
- Requests such as change of place and time will not be taken into consideration in the congress program.

Before you login to Zoom please indicate your hall number, name and surname

exp. Hall-1, Ethem KILIÇ

Participant Countries: Algeria, Bulgaria, Egypt, Georgia, Hungary, India, Iraq, Kazakhstan, Kosovo, Kuwait, Malasia, Morocco, Nigeria, Pakistan, Romania, Russia, Saudi Arabia, Serbia, Slovenia, Spain, Tunisia, Türkiye, Ukraine, Vietnam

-Opening Ceremony-

Date: **25.12.2023**

Ankara Local Time: **10:00-10:40**

Place: **Sirnak University**

Zoom Meeting ID: 851 7785 3338

Zoom Passcode: 252623

Head IFEC **Assoc. Prof. Dr. Mahmut DİRİK**

President of IKSAD Institute **Dr. Mustafa Latif EMEK**

President of Şirnak Chamber of Industry and Commerce **Osman GELİŞ**

Rector of Şirnak University **Prof. Dr. Abdurrahim ALKIŞ**

Mayor of Şirnak **Mehmet YARKA**

Governor of Şirnak **Cevdet ATAY**

-Invited Speeches-

Date: **25.12.2023**

Ankara Local Time: **10:40-11:40**

Place: **Sirnak University**

Prof. Dr. Mehmet Emin ERKAN

Dicle Üniversitesi

Prof. Dr. Oscar CASTILLO

Tijuana Institute of Technology

Prof. Dr. İlhan TARIMER

Muğla Sıtkı Koçman Üniversitesi

ONLINE PRESENTATIONS

25.12.2023 / Hall-1, Session-1



ANKARA LOCAL TIME



13⁰⁰ : 15⁰⁰



MEETING ID: 851 7785 3338



PASSCODE: 252623

HEAD OF SESSION: Assoc. Prof. Dr. Mahmut DİRİK

AUTHORS	AFFILIATION	TOPIC TITLE
Assist. Prof. Dr. Birkan BÜYÜKARIKAN	Isparta University of Applied Sciences, Türkiye	Examination of image color transfer applications with deep learning models
İlhan TARIMER Oruç Altay KIRLI Ayşe ELDEM	Muğla University, Türkiye Karamanoğlu Mehmetbey University, Türkiye	Artificial Intelligence Support in Ensuring Driving Balance of a Two-Wheeler
İlhan TARIMER Abdul JALEEL Gizem AKTAŞ	Muğla Sıtkı Koçman University, Türkiye Riyadh Bank, Saudi Arabia Residorm Kötekli, Türkiye	A Review in Identifying Blockchain Problem Statement
Assist. Prof. Dr. Yıldırım YILMAZ Res. Assist. Talip ÇAKMAK	Recep Tayyip Erdogan University, Türkiye	Time Series Analysis and Data Mining for Robust Short-term Compressive Strength Forecasting in Geopolymer Mortar: An ARIMA Model Data-Driven Approach
Efe Ali ÖZKESİCİ Assist. Prof. Dr. Osman GÖKALP	İzmir Kâtip Çelebi University, Türkiye	Brain Tumor Classification with Vision Transformers
Assist. Prof. Dr. Murat ASLAN	Şırnak University, Türkiye	A performance comparison of some recent metaheuristics in accordance with different criteria
Assoc. Prof. Dr. Mahmut DİRİK	Şırnak University, Türkiye	AI-Based Analysis of Socioeconomic and Ethnic Influences on Student Performance
Alaa Iskandar Dr. Bela Kovacs	University of Miskolc Miskolc, Hungary	Comparative Analysis of Swarm Robotics Design Through Reinforcement Learning and Particle Swarm Optimization
Alaa Iskandar Dr. Bela Kovacs	University of Miskolc Miskolc, Hungary	Reward Design Strategies in Reinforcement Learning for Collective Behavior Generation

ONLINE PRESENTATIONS

25.12.2023 / Hall-2, Session-1



ANKARA LOCAL TIME



13 00 : 15 00



MEETING ID: 851 7785 3338



PASSCODE: 252623

HEAD OF SESSION: Assoc. Prof. Dr. Ahmet TURŞUCU

AUTHORS	AFFILIATION	TOPIC TITLE
Assoc. Prof. Dr. Ahmet TURŞUCU	Sirnak University, Türkiye	Examination Of The Albedo Parameter On Some Elements With Atomic Number Varying Between 4 And 30
Lect. Abdurrahim ERAT Prof. Dr. Ahmet Mete VURAL	Şirnak University, Türkiye Gaziantep University, Türkiye	An Assessment Of Pulse Width Modulation Methods For Dc-Dc Modular Multilevel Converters
Dr. Res. Assist. Onur SİLAHTAR Assoc. Prof. Dr. Özkan ATAN	Van Yüzüncü Yıl University, Türkiye	CubeSat Tracking Control Using Sliding Mode Controller and Fuzzy Sliding Mode Controller
Dr. Res. Assist. Onur SİLAHTAR Assoc. Prof. Dr. Özkan ATAN	Van Yüzüncü Yıl University, Türkiye	Target Detection and Tracking Using Image Processing and Intuitionistic Fuzzy Controller
Assist. Prof. Dr. Özgül KARATAŞ	Konya Technical University, Türkiye	Electron Spin Resonance Study on Spin Susceptibility of Graphite Nanoparticles
S. Satheeskumaran K. Sasikala N. Sharath Babu Kumar Neeraj	Anurag Univerity, India Vels Univerity, India	Edge Computing Assisted Intelligent Healthcare Monitoring System for Elderly People
Kelven Kenn Simon Mohd Hairul Izhan Jubberin	Keningau Vocational College, Malaysia	Humidity and Temperature Sensing Laundry Rack
HELLALI Lallouani MOUSSA Oussama Saad Belhamdi AKKA Ali	University of Msila, Algeria Higher Normal School of Boussada, Algeria	Scalar Control Based on Interval Type-2 Fuzzy Logic of Dual Star Induction Machine

ONLINE PRESENTATIONS

25.12.2023 / Hall-3, Session-1



ANKARA LOCAL TIME

13⁰⁰ : 15⁰⁰



MEETING ID: 851 7785 3338

PASSCODE: 252623

HEAD OF SESSION: Prof. Dr. Jose A. R. CEMBRANOS

AUTHORS	AFFILIATION	TOPIC TITLE
Assist. Prof. Dr. Dicle ÖZCAN ELÇİ	Şırnak University, Türkiye	An Assessment of The Status of Women in Stem Fields In Turkey
Prof. Dr. Jose A. R. CEMBRANOS	Universidad Complutense de Madrid, Spain	Audiovisual Engineering for Educational Innovation
Assoc Prof. Dr. C.Vijai Assist. Prof. M. Elayaraja	Dr. Sagunthala R&D Institute of Science and Technology, India St.Peter's Institute of Higher Education and Research, India	A Move towards Cashless Economy: A Case of Continuous Usage of Mobile Wallets in India
Assoc. Prof. Dr. Ihor PONOMARENKO Dmytro PONOMARENKO	State University of Trade and Economics, Ukraine International University of Business and Law, Ukraine	The Impact of Using AI Chatgpt on Digital Marketing
Suzana KNEŽEVIĆ Milena MILOJEVIĆ Maja DOŠENOVIĆ MARINKOVIĆ Goran STANIŠIĆ	Academy of Applied Studies Šabac, Serbia	Application of Robotic Milking of Cows in the Function of Sustainable Farm Development in The Republic of Serbia
Milena Nikodijević Nemanja Vučković	University of Niš, Republic of Serbia International University of Novi Pazar, Republic of Serbia	The Investigation of Direct Dye Sorption on Linen Fabric
Yulia KOBERNIK Dr. Varvara GETMANTSEVA	Russian State University named after A.N. Kosygin, Russia	Development of An Interactive Module for Designing Addressable Clothing
Khalid Reggab	Ziane Achour University, Algeria	Energy spectrum of non relativistiv shrodinger equation for nonlinear potential

ONLINE PRESENTATIONS

25.12.2023 / Hall-4, Session-1



ANKARA LOCAL TIME



13 00 : 15 00



MEETING ID: 851 7785 3338



PASSCODE: 252623

HEAD OF SESSION: Prof. Dr. Lazim ABDULLAH

AUTHORS	AFFILIATION	TOPIC TITLE
Prof. Dr. M. Tahir NALBANTÇILAR Yakup ANIT	Ankara Hacı Bayram Veli University, Türkiye Sirnak University, Türkiye	Comparative Evaluation of Methods Used in Determining the Liquefaction Potential of Soils
AOUARI Issam BENAHMED Baizid MEHMET Palanci ROUABEH Aïcha	University of Djelfa, Algeria Arel Istanbul University, Türkiye University of Bouira, Algeria	Estimation of ground motion duration during the Boumerdes earthquake of May 21, 2003 in the north of Algeria
Amira Chekrit Abdelmadjid Hacene Chaouche	Badji Mokhtar University, Algeria	Effects of uncertainties in soil and structural properties on lateral load distribution along a pile in proximity to an undrained slope
Assist. Prof. Dr. Subhojit Chattaraj Assist. Prof. Dr. Sandeepan Saha Assist. Prof. Dr. Sandip Sarkar Dipak Paul	Greater Kolkata College of Engineering and Management, India	Importance of Resource Allocation to Maintain Health and Safety at Construction Site
Assist. Prof. Dr. Sandeepan Saha Assist. Prof. Dr. Subhojit Chattaraj Sahali Halder Trishita Giri	Greater Kolkata College of Engineering and Management, India	Importance of Strategies to Avoid Construction Site Fatalities: A Review Approach
Mohammed KHATTAB Oday JARADAT Samya HACHEMI Hicham BENZETTA	University Mohamed Khider Biskra, Algeria Université Ziane Achour – Djelfa, Algeria	Sustainable concrete: Using marble wastes as an environmentally friendly aggregate
Prof. Dr. Lazim ABDULLAH	Universiti Malaysia Terengganu Kuala Nerus, Malaysia	Application Of Single-Valued Neutrosophic-Dematel To Investigate Causal Effects Of Criteria Of Sustainable Urban Transport
Amina OUAHBI Youness BOUHAIJ Abdeslam EL BOUARI Omar TANANE	HASSAN II University, Morocco	Development of a solid catalyst derived from sardine scales and eggshells for biodiesel synthesis

ONLINE PRESENTATIONS

25.12.2023 / Hall-1, Session-2



ANKARA LOCAL TIME



15³⁰ : 17³⁰



MEETING ID: 851 7785 3338



PASSCODE: 252623

HEAD OF SESSION: Dr. Edip TAŞKESEN

AUTHORS	AFFILIATION	TOPIC TITLE
Dr. Fatih ARLI	Sirnak University, Türkiye	Z-Scheme Photocatalytic Systems For Photoelectrochemical Water Splitting
Dr. Hakan DUMRUL Dr. Edip TAŞKESEN Ali BULUT	Sirnak University, Türkiye	Use of Solar Drying Systems In Different Industrial Sectors
Ojlan OĞUZ Dr. Edip TAŞKESEN Hamza ALAHMAD	Sirnak University, Türkiye	Thermal Insulation and Materials in Buildings
Yusuf DEĞİŞMAN Regaib DİRİK Serdal DAMARSEÇKİN	Sirnak University, Türkiye	Hydroelectric Power Plants and Their Impaction Energy
Assist. Prof. Dr. K.R.Padma K.R.Don	SriPadmavati Mahila Visva Vidyalayam (Women's) University, India Bharath University, India	An Updated Review on Blends of Fuel Based on Biomass as a Potential Replacement For the Forthcoming Renewable Energy System
Mariem Zaghdoudi Issam Attar Majdi Hazam Hatem Oueslati	Research and Technology Center of Energy (CRTE), Tunisia	Investigating the Performance of a Water-Based PV/T System
Islam Zuzaku Skender Demaku Donika Sylejmani	University of Pristina, "HASAN PRISHTINA", Kosovo	The Ecological Risk Of Contamination With Toxic Metals In The Soils, Waste And Ash, Around The "Trepça" Complex, The "Kosovo" Thermal Power Plants And The New Ferronickel Complex
Hicham Sayhi Amor Bourek Abdelkarim Ammar Ilyes Dahnoun	University of Biskra, Algeria University of M'hamed BOUGARA of Boumerdes, Algeria	Modeling and Control with MPPT Speed for Wind Energy Conversion System (WECS) Based on Permanent Magnet Synchronous Generator (PMSG)
ABARAGH Mouloud Elmostafa HROUR Jamal GUERROUM	Sultan Moulay Slimane University, Morocco	Relativistic elastic scattering of a hydrogen atom ($2s-2s$) by electron impact in the presence of a circularly polarized laser field

ONLINE PRESENTATIONS

25.12.2023 / Hall-2, Session-2



ANKARA LOCAL TIME



15³⁰ : 17³⁰



MEETING ID: 851 7785 3338



PASSCODE: 252623

HEAD OF SESSION: Assoc. Prof. Dr. Mehmet HASKUL

AUTHORS	AFFILIATION	TOPIC TITLE
Assoc. Prof. Dr. Mehmet HASKUL Prof. Dr. Murat KISA	Şırnak University, Türkiye Harran University, Türkiye	Free Vibration Analysis of Stepped Beam With Varying Cross-Section With A Crack
Mehmet Said Bayraklılar Muhammed Tayyip Koçak	Siirt University, Türkiye Istanbul University of Health and Technology, Türkiye	Optimization of FDM Parameters to Increase the Compressive Strength of ABS Parts
Dr. BRAKNI Oumaima Dr. Amrouche Fethia Dr. Abdallah Mohammedi Prof. KERBOUA ZIARI Yasmina	University of Science and Technology Houari Boumediene (USTHB), Algeria Centre de Développement des Énergies Renouvelables, Algeria University of Batna 2, Algeria	Analyzing the Impact of Flow Field Channel Design Variations on PEMFC Performance: A Computational Fluid Dynamics (CFD) Study with Constriction and Enlargement Configurations
Radhiyah M. Aljarrah Ali M. Aljawdah	University of Kufa, Iraq University of Babilon, Iraq	Study the Effect of Doping with Silver Nanoparticles on the Properties of Zirconium Dioxide Membranes and their Effect on it as a Gas Sensor
Woyengitonye Butler Abadani	Federal Polytechnic, Nigeria	Investigation of Soil Aggressivity to Underground Storage Pipes and Tanks: Implications of Corrosion Control
Hicham Sayhi Amor Bourek Abdelkarim Ammar Ilyes Dahnoun	University of Biskra, Algeria University of M'hamed BOUGARA of Boumerdes, Algeria	Sensorless Maximum Power Extraction Control Using Perturb and Observe (P&O) Method from Permanent Magnet Synchronous Generator (PMSG) based Wind Energy Conversion System (WECS)
Imoh Ime Ekanem Aniekan Essienubong Ikpe	Akwa Ibom State Polytechnic, Nigeria	A Technical Survey on Energy Potentials of Point Focus Solar Collector System: A Sustainable Resource for Energy Mix Augmentation
Husain M. Ahmad Ahmad B. Alazmi Muammer Catak	American University of the Middle East, Kuwait	Designing a Prototype for Both Transmitter and Receiver Sections of Morse Code Communication Using Arduino Uno
Dr. Sabri UZUNER Alpay TOK	University of Duzce, Türkiye Dr. Engin PAK Cumayeri Vocational School, Türkiye	Semi-Autonomous Military Equipment Transport Vehicle with Target Tracking

ONLINE PRESENTATIONS

25.12.2023 / Hall-3, Session-2



ANKARA LOCAL TIME



15³⁰ : 17³⁰



MEETING ID: 851 7785 3338



PASSCODE: 252623

HEAD OF SESSION: Dr. Zohaib Hassan Sain

AUTHORS	AFFILIATION	TOPIC TITLE
Prof. Dr. Mehmet Emin ERKAN Prof. Dr. Aydın VURAL	Dicle University, Türkiye	Microbiological quality parameters of pickled Soryaz samples collected from sales points in Şırnak
Bashir Tanimu Al-Amin Danladi Bello Sule Argungu Abdullahi Morufu Ajibola Ajibke	Ahmadu Bello University Zaria, Nigeria	Assessment of precipitation and temperature gridded dataset for Nigeria
Huțu Dana Amariei Sonia	Stefan cel Mare University of Suceava, Romania	Pastry Products with a Low Sugar Content Through the use of Substitutes
Assoc. Prof. M. As. Michailov	SWU "Neofit Rilski", Bulgaria	Environmental Protection as a Recognized Necessity for Human Society
Dr. Zohaib Hassan Sain	Superior University, Pakistan	Exploring Chat-GPT'S Pivotal Role in Shaping the Landscape of Industry 4.0
Dr. Zohaib Hassan Sain	Superior University, Pakistan	Exploring the Transformative Impact: AI'S Influence on Advancements in Industrial Research
Hamid Zouggari Mahir Fatima-Zahra Albourine Abdallah	Ibn Zohr University, Morocco	Polypyrrole- Embedded Phosphate Nanoparticles: An Efficient Approach for Heavy Metal Removal in Wastewater Treatment
Assoc. Prof. Irina Nikolayevna Ivashchenko Sivoplyasova Alina Olegovna	Kuban State University, Russia	The Effect of Synthetic Materials on a Biological System

ONLINE PRESENTATIONS

25.12.2023 / Hall-4, Session-2



ANKARA LOCAL TIME



15³⁰ : 17³⁰



MEETING ID: 851 7785 3338



PASSCODE: 252623

HEAD OF SESSION: Assist. Prof. Avinash Kumar

AUTHORS	AFFILIATION	TOPIC TITLE
Dhruv Kohli Devang Khurana Barinder Singh Amanpreet Kaur Paras Sachdeva	Chitkara University, India	Exploring the Capabilities of Unity 3D Gaming Software
Assoc. Prof. Ihor PONOMARENKO Dmytro PONOMARENKO	State University of Trade and Economics, Ukraine International University of Business and Law, Ukraine	The Impact Of Using AI CHATGPT On Digital Marketing
Assist. Prof. Avinash Kumar	Mangalayatan University, India	Forward Hunting for Malware and Ransomware Detection to Decrease Risk
Assist. Prof. Saptadeepa Kalita	Sharda University, India	A Novel Periodontal Disease Grade Classification Methodology using Convolutional Neural Network
Oyewale Mustapha Akinola Adaramola Ojo Jayeola	Federal Polytechnic Ilaro, Nigeria	Enhancing Network Security: An Intrusion Detection and Prevention Approach
MUKTHA D. S. Sagaya Aurelia	CHRIST University, India	A Case Study on Cisco Packet Tracer and GNS3 Simulators: A Practical Viewpoint
Usman Mahmud Mohammed Hassan Abubakar Ado Abubakar Abdulkadir Bichi Armaya'u Zango Umar	Al-Qalam University, Nigeria Bayero University, Nigeria Yusuf Maitama Sule University, Nigeria	A Free Data Redundancy Method for Sentiment Classification in Movie Review Using Ensemble Machine Learning Approach
Nguyen THÍ HANG Nguyen MANH HUNG Pham Thi THU THUY Nguyen HONG NHUNG Nguyen KHANH LINH	Thai Nguyen high School for the Gifted, Vietnam Women's Union Thai Nguyen Province, Vietnam Khanh Hoa High School, Vietnam Iris School, Vietnam	Solution to Supporting Women's Integration and Digital Transformation in Industry 4.0
Yassir Soulaïmani Nehéz Károly	University of Miskolc, Hungary	Enhancing Efficiency: The Integration of Blockchain Technology with Internet of Things

ONLINE PRESENTATIONS

26.12.2023 / Hall-1, Session-3



ANKARA LOCAL TIME



10⁰⁰ : 12⁰⁰



MEETING ID: 851 7785 3338



PASSCODE: 252623

HEAD OF SESSION: Assoc. Prof. Dr. Mahmut DİRİK

AUTHORS	AFFILIATION	TOPIC TITLE
Assoc. Prof. Dr. Murat CANAYAZ	Van Yüzüncü Yıl University, Türkiye	Deep Learning In The Diagnosis Of Ear Diseases: Effective And Rapid Solutions
Assist. Prof. Dr. Ahmet ÇELİK	Kütahya Dumlupınar University, Türkiye	Realization Of Milk Quality Classification With C4.5 Decision Tree Algorithm: Performance Measurement According To F1 Score and MCC Metrics
Assist. Prof. Dr. Rasım ÇEKİK	Sirnak University, Türkiye	DDoS Attacks Detection with A Rule-Based Approach Using Rough Set
Assoc. Prof. Dr. Mahmut DİRİK	Sirnak University, Türkiye	Al-Jazari: Ancient Wisdom's Influence on Modern Technology
Dastan Begaliyev Masoud Riazi	Nazarbayev University, Kazakhstan	Drilling Stick Slip Prediction Using Machine Learning
Yashvanth M Shivani Singh Assoc. Prof. Dr. Shalini R	Jain Deemed to be University, India	Role of Big Data in Indian Banking Operations
Oyewale Mustapha Akinola Adaramola Ojo Jayeola	The Federal Polytechnic Ilaro, Nigeria	Enhancing Network Security: An Intrusion Detection and Prevention Approach
Belgacem Bouallegue Mouna Bedoui Hosam El-Sofany Mohsen Macchout	King Khalid University, Saudi Arabia University of Monastir, Tunisia Cairo Higher Institute for Engineering, Egypt University of Monastir, Tunisia	A Proposed AES-CBC Algorithm to improve IoT Systems Security
Idris Lawal Bagiwa	Hassan Usman Katsina Polytechnic, Nigeria	A Systematic Review on Vehicular Ad Hoc Network (VANET) Security challenges and Solutions

ONLINE PRESENTATIONS

26.12.2023 / Hall-2, Session-3



ANKARA LOCAL TIME



10⁰⁰ : 12⁰⁰



MEETING ID: 851 7785 3338



PASSCODE: 252623

HEAD OF SESSION: Prof. Mamoun Lyes Hennache

AUTHORS	AFFILIATION	TOPIC TITLE
A. Raza I. A. Khan	Government College University, Pakistan	Synthesis of Binder-Free and Highly Conducting MoS ₂ Nanoflowers Like Electrode Material for Supercapacitor Applications
Ibrahim Chouidira Djala Eddine Khodja	University of M'Sila, Algeria	Evaluation of the Effectiveness of Fault-Tolerant Operation of Broken Bars Using Direct Torque Control in an Induction Machine
Ibrahim Chouidira Djala Eddine Khodja	University of M'Sila, Algeria	Hysteresis Control for Compensation of Current Harmonics by Using Active Parallel Filter
Prof. Mamoun Lyes Hennache Ali Hennache	Yildirim Beyazit University, Türkiye Imam Mohammad Ibn Saud Islamic University, Kingdom of Saudi Arabia	Electronic Disasters: The Hidden Dangers And Toxicity Of Emf's Pollution Produced In The 21st Century And Their Negative Effects On The Environment And Human Health
Prof. Mamoun Lyes Hennache Ali Hennache	Yildirim Beyazit University, Türkiye Imam Mohammad Ibn Saud Islamic University, Kingdom of Saudi Arabia	Superconducting Materials And Their Impact On The Development Of Electronic Devices
Assoc. Prof. Kassayeva Assyl Zhvlamanovna Assoc. Prof. Sagindvkova Elvira Umirovna	Caspian University of Technology and Engineering, Kazakhstan	Converting the energy of sea waves into electrical energy
Reshmi Soyinka V Vaduhammal V Sneka C Dr. V Thiyagarajan	Sri Sivasubramaniya Nadar College of Engineering, India	Design and Analysis of Reduced Switch Multilevel Inverters for Electric Vehicle Applications
Abdelkader BOUAZZA	University of Tiaret, Algeria	Strategic Energy Optimization in a Hybrid Power System With Photovoltaic, Wind, and Battery Integration Using a Three-Level Converter
KOULALI Mostefa	University of Tiaret, Algeria	Dynamic Fuzzy Control Strategy for Integrating Photovoltaic, Fuel Cell, and Battery System via Three-Level T Type Inverter

ONLINE PRESENTATIONS

26.12.2023 / Hall-3, Session-3



ANKARA LOCAL TIME



10 00 : 12 00



MEETING ID: 851 7785 3338



PASSCODE: 252623

HEAD OF SESSION: Assist. Prof. Dr. Hüseyin GÜRBÜZ

AUTHORS	AFFILIATION	TOPIC TITLE
Selman İLBEYOĞLU Assist. Prof. Dr. Hüseyin GÜRBÜZ	Şırnak University, Türkiye	The Current Status and Future Projection of Pem Fuel Cells
Assist. Prof. Dr. Abdullah TURAN Hebat GUNEL	Şırnak University, Türkiye	Blade Pitch Angle Control of a Wind Turbine With Pi-Pd Designed With The Weighted Geometric Center Method
Dr. Edip TAŞKESEN Ruzgar ÜREN Selman İLBEYOĞLU Ceylan ÜREN	Şırnak University, Türkiye	The Role and Importance of Coal in Energy Production
Dr. Edip TAŞKESEN Dr. Fatih ARLI Hamza ALAHMAD Elif Nur BİLEN	Şırnak University, Türkiye	Electrochemical Energy Conversion and Storage Systems
Dr. Edip TAŞKESEN Dr. Hakan DUMRUL Hamza ALAHMAD	Şırnak University, Türkiye	Electrocatalytic Technique Investigation in Biodiesel Production
Lect. Mazlum CENGİZ Lect. Yahya CELEBİ Prof. Dr. Huseyin AYDIN	Şırnak University, Türkiye	Exploring Building-Integrated Photovoltaic/Thermal Systems
Assist. Prof. Dr. Erhan KIRTEPE Dr. Mert Sinan TURGUT	Şırnak University, Türkiye Ege University, Türkiye	Theoretical Analysis of an Organic Rankine Cycle With Parabolic Trough Collector in Şırnak Climate Conditions
Assoc. Prof. Kassayeva Assylkanym Zhulamanovna Res. Assist. Savelkin Nikita Kirillovich	Yessenov University, Kazakhstan	Hydrogen - fuel of the future
Maïssa Bouselsal Fateh Mebarek - Oudina	Faculty of Sciences University, Algeria	Evaluation the Performance of Shell/Tube Heat Exchangers Using Hybrid Nano Fluid

ONLINE PRESENTATIONS

26.12.2023 / Hall-4, Session-3



ANKARA LOCAL TIME



10⁰⁰ : 12⁰⁰



MEETING ID: 851 7785 3338



PASSCODE: 252623

HEAD OF SESSION: Assoc. Prof. Dr. Ümit ERDEM

AUTHORS	AFFILIATION	TOPIC TITLE
Huda Assi ALBAYATI Prof. Dr. Waleed M. SH. ALABDRABA Assist. Prof. Dr. Cem GÖL	Bolu Abant İzzet Baysal University, Türkiye Tikrit University, Iraq	Production, Improvement and Characterization of Activated Carbon Fibers From Date Palms
Assist. Prof. Dr. Huseyin AGGUMUS Assist. Prof. Dr. Abdullah TURAN	Şırnak University, Türkiye	Determination Of The Optimum Placement Of The Semi-Active Control Element Used In Structural Vibration Control
Assoc. Prof. Dr. Asaf Tolga ULGEN Assoc. Prof. Dr. Ümit ERDEM Prof. Dr. Gürçan YILDIRIM	Şırnak University, Türkiye Kirikkale University, Türkiye Abant İzzet Baysal University, Türkiye	Change of key mechanical performance parameters of Bi-2223 ceramic phase with CdO addition in main matrix
Assoc. Prof. Dr. Asaf Tolga ULGEN Assoc. Prof. Dr. Ümit ERDEM Prof. Dr. Gürçan YILDIRIM	Şırnak University, Türkiye Kirikkale University, Türkiye Abant İzzet Baysal University, Türkiye	Influence of applied loads and CdO impurity on mechanical stabilization and granularity
Ayesha Rafiq Prof. Dr. Matloob Ahmad	Government College University Faisalabad, Pakistan	Recent Methodologies in Synthesizing Thienothiophenes: A Promising Framework for the Development of Biologically Active Compounds
TAFRAOUT Fatima	University Abdelmalek Essaâdi, Morocco	Development of Composites Based on Biodegradable Polymers and Local Mineral Materials and their Applications in Wastewater Treatment
U. Elaiyarsan J. Paulmar Pushparaj C. Asokan S. Prathiban	Easwari Engineering College, India SNS College of Technology, India	Investigation on Mechanical and wear behaviour of flyash reinforced AA6068 aluminium alloy fabricated through powder metallurgy technique
Z. Kovziridze N. Nijaradze G. Tabatadze T. Cheishvili Ts. Danelia N. Darakhvelidze	Georgia Technical University, Georgia	Smart nanocomposite in the TiC-BN-SiC-B ₄ C-SiAlON-Al ₂ O ₃ system
Dr. Matej Babič	Complex Systems and Data Science Laboratory, Slovenia	Modelling topographical properties of 3D printing metal material

CONTENT

CONFERENCE ID	I
SCIENTIFIC & REVIEW COMMITTEE	II
PHOTO GALLERY	III
PROGRAM	IV
CONTENT	V
FOREWORDS	I-III
PROCEEDINGS	1-457

Author	Title	No
Birkan BÜYÜKARIKAN	Examination of image color transfer applications with deep learning models	1
İlhan TARIMER Oruç Altay KIRLI Ayşe ELDEM	Artificial Intelligence Support in Ensuring Driving Balance of a Two-Wheeler	2
İlhan TARIMER Abdul JALEEL Gizem AKTAŞ	A Review in Identifying Blockchain Problem Statement	15
Yıldıran YILMAZ Talip ÇAKMAK	Time Series Analysis and Data Mining for Robust Short-term Compressive Strength Forecasting in Geopolymer Mortar: An ARIMA Model Data-Driven Approach	24
Efe Ali ÖZKESİCİ Osman GÖKALP	Brain Tumor Classification with Vision Transformers	31
Murat ASLAN	A performance comparison of some recent metaheuristics in accordance with different criteria	37
Mahmut DIRİK	AI-Based Analysis of Socioeconomic and Ethnic Influences on Student Performance	46
Alaa Iskandar Bela Kovacs	Comparative Analysis of Swarm Robotics Design Through Reinforcement Learning and Particle Swarm Optimization	56
Alaa Iskandar Bela Kovacs	Reward Design Strategies in Reinforcement Learning for Collective Behavior Generation	57
Ahmet TURŞUCU	Examination Of The Albedo Parameter On Some Elements With Atomic Number Varying Between 4 And 30	58
Abdurrahim ERAT Ahmet Mete VURAL	An Assessment Of Pulse Width Modulation Methods For Dc-Dc Modular Multilevel Converters	63
Onur SİLAHTAR Özkan ATAN	CubeSat Tracking Control Using Sliding Mode Controller and Fuzzy Sliding Mode Controller	71
Onur SİLAHTAR Özkan ATAN	Target Detection and Tracking Using Image Processing and Intuitionistic Fuzzy Controller	72
Özgül KARATAŞ	Electron Spin Resonance Study on Spin Susceptibility of Graphite Nanoparticles	73
S. Satheeskumaran K. Sasikala N. Sharath Babu Kumar Neeraj	Edge Computing Assisted Intelligent Healthcare Monitoring System for Elderly People	74
Kelven Kenn Simon Mohd Hairul Izhaz Jubberin	Humidity and Temperature Sensing Laundry Rack	75
HELLALI Lallouani MOUSSA Oussama Saad Belhamdi AKKA Ali	Scalar Control Based on Interval Type-2 Fuzzy Logic of Dual Star Induction Machine	76
Dicle ÖZCAN ELÇİ	An Assessment of The Status of Women in Stem Fields In Turkey	77
Jose A. R. CEMBRANOS	Audiovisual Engineering for Educational Innovation	78
C.Vijai M. Elayaraja	A Move towards Cashless Economy: A Case of Continuous Usage of Mobile Wallets in India	79
Ihor PONOMARENKO Dmytro PONOMARENKO	The Impact of Using AI Chatgpt on Digital Marketing	87

Suzana KNEŽEVIĆ Milena MILOJEVIĆ Maja DOŠENOVIĆ MARINKOVIĆ Goran STANIŠIĆ	Application of Robotic Milking of Cows in the Function of Sustainable Farm Development in The Republic of Serbia	92
Milena Nikodijević Nemanja Vučković	The Investigation of Direct Dye Sorption on Linen Fabric	93
Yulia KOBERNIK Varvara GETMANTSEVA	Development of An Interactive Module for Designing Addressable Clothing	94
Khalid Reggab	Energy spectrum of non relativistic shrodinger equation for nonlinear potential	99
M. Tahir NALBANTÇILAR Yakup ANIT	Comparative Evaluation of Methods Used in Determining the Liquefaction Potential of Soils	100
AOUARI Issam BENAHMED Baizid MEHMET Palanci ROUABEH Aïcha	Estimation of ground motion duration during the Boumerdes earthquake of May 21, 2003 in the north of Algeria	111
Amira Chekrit Abdelmadjid Hacene Chaouche	Effects of uncertainties in soil and structural properties on lateral load distribution along a pile in proximity to an undrained slope	119
Subhojit Chattaraj Sandeepan Saha Sandip Sarkar Dipak Paul	Importance of Resource Allocation to Maintain Health and Safety at Construction Site	120
Sandeepan Saha Subhojit Chattaraj Sahali Halder Trishita Giri	Importance of Strategies to Avoid Construction Site Fatalities: A Review Approach	121
Mohammed KHATTAB Oday JARADAT Samya HACHEMI Hicham BENZETTA	Sustainable concrete: Using marble wastes as an environmentally friendly aggregate	122
Lazim ABDULLAH	Application Of Single-Valued Neutrosophic-Dematel To Investigate Causal Effects Of Criteria Of Sustainable Urban Transport	127
Amina OUAHBI Youness BOUHAIJ Abdeslam EL BOUARI Omar TANANE	Development of a solid catalyst derived from sardine scales and eggshells for biodiesel synthesis	141
Fatih ARLI	Z-Scheme Photocatalytic Systems For Photoelectrochemical Water Splitting	142
Hakan DUMRUL Edip TAŞKESEN Ali BULUT	Use of Solar Drying Systems In Different Industrial Sectors	151
Ojlan OĞUZ Edip TAŞKESEN Hamza ALAHMAD	Thermal Insulation and Materials in Buildings	161
Yusuf DEĞİŞMAN Regaib DİRİK Serdal DAMARSEÇKİN	Hydroelectric Power Plants and Their Impaction Energy	166
K.R.Padma K.R.Don	An Updated Review on Blends of Fuel Based on Biomass as a Potential Replacement For the Forthcoming Renewable Energy System	175
Mariem Zaghoudi Issam Attar Majdi Hazam Hatem Oueslati	Investigating the Performance of a Water-Based PV/T System	176
Islam Zuzaku Skender Demaku Donika Sylejmani	The Ecological Risk Of Contamination With Toxic Metals In The Soils, Waste And Ash, Around The "Trepça" Complex, The "Kosovo" Thermal Power Plants And The New Ferronickel Complex	179
Hicham Sayhi Amor Bourek Abdelkarim Ammar Ilyes Dahnoun	Modeling and Control with MPPT Speed for Wind Energy Conversion System (WECS) Based on Permanent Magnet Synchronous Generator (PMSG)	180
ABARAGH Mouloud Elmostafa HROUR Jamal GUERROUM	Relativistic elastic scattering of a hydrogen atom ($2s-2s$) by electron impact in the presence of a circularly polarized laser field	181
Mehmet HASKUL Murat KISA	Free Vibration Analysis of Stepped Beam With Varying Cross-Section With A Crack	182

Mehmet Said Bayraklılar Muhammed Tayyip Koçak	Optimization of FDM Parameters to Increase the Compressive Strength of ABS Parts	195
BRAKNI Oumaima Amrouche Fethia Abdallah Mohammedi KERBOUA ZIARI Yasmina	Analyzing the Impact of Flow Field Channel Design Variations on PEMFC Performance: A Computational Fluid Dynamics (CFD) Study with Constriction and Enlargement Configurations	196
Radhiyah M. Aljarrah Ali M. Aljawdah	Study the Effect of Doping with Silver Nanoparticles on the Properties of Zirconium Dioxide Membranes and their Effect on it as a Gas Sensor	197
Woyengitonye Butler Abadani	Investigation of Soil Aggressivity to Underground Storage Pipes and Tanks: Implications of Corrosion Control	198
Hicham Sayhi Amor Bourek Abdelkarim Ammar Ilyes Dahnoun	Sensorless Maximum Power Extraction Control Using Perturb and Observe (P&O) Method from Permanent Magnet Synchronous Generator (PMSG) based Wind Energy Conversion System (WECS)	213
Imoh Ime Ekanem Aniekan Essienubong Ikpe	A Technical Survey on Energy Potentials of Point Focus Solar Collector System: A Sustainable Resource for Energy Mix Augmentation	214
Husain M. Ahmad Ahmad B. Alazmi Muammer Catak	Designing a Prototype for Both Transmitter and Receiver Sections of Morse Code Communication Using Arduino Uno	215
Sabri UZUNER Alpay TOK	Semi-Autonomous Military Equipment Transport Vehicle with Target Tracking	222
Mehmet Emin ERKAN Aydin VURAL	Microbiological quality parameters of pickled Soryaz samples collected from sales points in Şırnak	224
Bashir Tanimu Al-Amin Danladi Bello Sule Argungu Abdullahi Morufu Ajibola Ajibke	Assessment of precipitation and temperature gridded dataset for Nigeria	228
Hutu Dana Amariei Sonia	Pastry Products with a Low Sugar Content Through the use of Substitutes	244
M. As. Michailov	Environmental Protection as a Recognized Necessity for Human Society	245
Zohaib Hassan Sain	Exploring Chat-GPT'S Pivotal Role in Shaping the Landscape of Industry 4.0	246
Zohaib Hassan Sain	Exploring the Transformative Impact: AI'S Influence on Advancements in Industrial Research	247
Hamid Zougari Mahir Fatima-Zahra Albourine Abdallah	Polypyrrole- Embedded Phosphate Nanoparticles: An Efficient Approach for Heavy Metal Removal in Wastewater Treatment	248
Irina Nikolayevna Ivashchenko Sivoplyasova Alina Olegovna	The Effect of Synthetic Materials on a Biological System	249
Dhruv Kohli Devang Khurana Barinder Singh Amanpreet Kaur Paras Sachdeva	Exploring the Capabilities of Unity 3D Gaming Software	251
Ihor PONOMARENKO Dmytro PONOMARENKO	The Impact Of Using AI CHATGPT On Digital Marketing	261
Avinash Kumar	Forward Hunting for Malware and Ransomware Detection to Decrease Risk	266
Saptadeepa Kalita	A Novel Periodontal Disease Grade Classification Methodology using Convolutional Neural Network	267
Oyewale Mustapha Akinola Adaramola Ojo Jayeola	Enhancing Network Security: An Intrusion Detection and Prevention Approach	268
MUKTHA D. S. Sagaya Aurelia	A Case Study on Cisco Packet Tracer and GNS3 Simulators: A Practical Viewpoint	269
Usman Mahmud Mohammed Hassan Abubakar Ado Abubakar Abdulkadir Bichi Armaya'u Zango Umar	A Free Data Redundancy Method for Sentiment Classification in Movie Review Using Ensemble Machine Learning Approach	270
Nguyen THÍ HANG Nguyen MANH HUNG Pham Thi THU THUY Nguyen HONG NHUNG Nguyen KHANH LINH	Solution to Supporting Women's Integration and Digital Transformation in Industry 4.0	271
Yassir Soulaïmani Nehéz Károly	Enhancing Efficiency: The Integration of Blockchain Technology with Internet of Things	272

Murat CANAYAZ	Deep Learning In The Diagnosis Of Ear Diseases: Effective And Rapid Solutions	273
Ahmet ÇELİK	Realization Of Milk Quality Classification With C4.5 Decision Tree Algorithm: Performance Measurement According To F1 Score and MCC Metrics	274
Rasim ÇEKİK	DDoS Attacks Detection with A Rule-Based Approach Using Rough Set	281
Mahmut DIRİK	Al-Jazari: Ancient Wisdom's Influence on Modern Technology	291
Dastan Begaliyev Masoud Riazi	Drilling Stick Slip Prediction Using Machine Learning	301
Yashvanth M Shivani Singh Shalini R	Role of Big Data in Indian Banking Operations	302
Oyewale Mustapha Akinola Adaramola Ojo Jayeola	Enhancing Network Security: An Intrusion Detection and Prevention Approach	309
Belgacem Bouallegue Mouna Bedoui Hosam El-Sofany Mohsen Macchout	A Proposed AES-CBC Algorithm to improve IoT Systems Security	310
Idris Lawal Bagiwa	A Systematic Review on Vehicular Ad Hoc Network (VANET) Security challenges and Solutions	311
A. Raza I. A. Khan	Synthesis of Binder-Free and Highly Conducting MoS ₂ Nanoflowers Like Electrode Material for Supercapacitor Applications	312
Ibrahim Chouidira Djala Eddine Khodja	Evaluation of the Effectiveness of Fault-Tolerant Operation of Broken Bars Using Direct Torque Control in an Induction Machine	313
Ibrahim Chouidira Djala Eddine Khodja	Hysteresis Control for Compensation of Current Harmonics by Using Active Parallel Filter	314
Mamoun Lyes Hennache Ali Hennache	Electronic Disasters: The Hidden Dangers And Toxicity Of Emf's Pollution Produced In The 21st Century And Their Negative Effects On The Environment And Human Health	315
Mamoun Lyes Hennache Ali Hennache	Superconducting Materials And Their Impact On The Development Of Electronic Devices	326
Kassayeva Assyl Zhvlamanovna Sagindvkova Elvira Umirovna	Converting the energy of sea waves into electrical energy	340
Reshmi Soyinka V Vaduhammal V Sneka C V Thiagarajan	Design and Analysis of Reduced Switch Multilevel Inverters for Electric Vehicle Applications	341
Abdelkader BOUAZZA	Strategic Energy Optimization in a Hybrid Power System With Photovoltaic, Wind, and Battery Integration Using a Three-Level Converter	342
KOULALI Mostefa	Dynamic Fuzzy Control Strategy for Integrating Photovoltaic, Fuel Cell, and Battery System via Three-Level T Type Inverter	343
Selman İLBEYOĞLU Hüseyin GÜRBÜZ	The Current Status and Future Projection of Pem Fuel Cells	344
Abdullah TURAN Hebat GUNEL	Blade Pitch Angle Control of a Wind Turbine With Pi-Pd Designed With The Weighted Geometric Center Method	352
Edip TAŞKESEN Ruzgar ÜREN Selman İLBEYOĞLU Ceylan ÜREN	The Role and Importance of Coal in Energy Production	364
Edip TAŞKESEN Fatih ARLI Hamza ALAHMAD Elif Nur BİLEN	Electrochemical Energy Conversion and Storage Systems	374
Edip TAŞKESEN Hakan DUMRUL Hamza ALAHMAD	Electrocatalytic Technique Investigation in Biodiesel Production	383
Mazlum CENGİZ Yahya CELEBI Dr. Huseyin AYDIN	Exploring Building-Integrated Photovoltaic/Thermal Systems	389
Erhan KIRTEPE Mert Sinan TURGUT	Theoretical Analysis of an Organic Rankine Cycle With Parabolic Trough Collector in Şirnak Climate Conditions	400

Kassayeva Assylkanym Zhulamanovna Savelkin Nikita Kirillovich	Hydrogen - fuel of the future	410
Maissa Bouselsal Fateh Mebarek - Oudina	Evaluation the Performance of Shell/Tube Heat Exchangers Using Hybrid Nano Fluid	411
Huda Assi ALBAYATI Waleed M. SH. ALABDRABA Assist. Prof. Dr. Cem GÖL	Production, Improvement and Characterization of Activated Carbon Fibers From Date Palms	412
Huseyin AGGUMUS Abdullah TURAN	Determination Of The Optimum Placement Of The Semi-Active Control Element Used In Structural Vibration Control	424
Asaf Tolga ULGEN Ümit ERDEM Gürçan YILDIRIM	Change of key mechanical performance parameters of Bi-2223 ceramic phase with CdO addition in main matrix	430
Asaf Tolga ULGEN Ümit ERDEM Gürçan YILDIRIM	Influence of applied loads and CdO impurity on mechanical stabilization and granularity	439
Ayesha Rafiq Matloob Ahmad	Recent Methodologies in Synthesizing Thienothiophenes: A Promising Framework for the Development of Biologically Active Compounds	449
TAFRAOUT Fatiha	Development of Composites Based on Biodegradable Polymers and Local Mineral Materials and their Applications in Wastewater Treatment	450
U. Elaiyarsan J. Paulmar Pushparaj C. Asokan S. Prathiban	Investigation on Mechanical and wear behaviour of flyash reinforced AA6068 aluminium alloy fabricated through powder metallurgy technique	451
Z. Kovziridze N. Nijaradze G. Tabatadze T. Cheishvili Ts. Danelia N. Darakhvelidze	Smart nanocomposite in the TiC-BN-SiC-B ₄ C-SiAlON-Al ₂ O ₃ system	452
Matej Babič	Modelling topographical properties of 3D printing metal material	453

Foreword-1

It is with great pleasure that I present the proceedings of the 1st International Future Engineering Conference (IFEC 2023), organized collaboratively by Şırnak University, the Governorship of Şırnak, Şırnak Chamber of Commerce and Industry, IKSAD, and Şırnak University Technology Transfer Office Inc. Held on December 25-26, 2023, the conference uniquely combined both in-person and online formats.

In the centennial year of our Republic, IFEC 2023 has ignited Turkey's inherent potential, offering outcome-driven outputs for sustainable development and growth. The conference stands as a comprehensive roadmap in the engineering world, embodying innovation, fostering collaboration, and promoting forward-thinking. This inaugural event at Şırnak University has created an academic hub where scientists from various engineering disciplines converge to exchange knowledge, solve common problems, and discuss groundbreaking innovations.

Our world is witnessing rapid technological advancements, especially in areas such as artificial intelligence, sustainable infrastructure, robotics, the Internet of Things, biotechnology, augmented reality, energy storage, superconducting materials, and quantum computing. These developments, known as "Industry 4.0" in Germany, "Industry 5.0" by the European Council, and "Society 5.0" in Japan, are driving transformative changes. Thus, we are advancing towards a new era, marked by concepts like the "digital transformation age, industry 5.0, society 5.0, and a super-intelligent society." Engineering and basic science education play a critical role at the forefront of this technological progression.

The primary goal of IFEC is to highlight and encourage the symbiotic relationship between industry and academia. The conference not only bridges theoretical knowledge with practical application but also fosters international collaboration. It is crucial in continuing advancements in engineering and resonating our collective efforts on a global scale. IFEC has incorporated primary scientific and R&D areas into its engineering disciplines spectrum. This diversity reflects our solution-oriented objectives against the multifaceted challenges of the modern world. The conference offers thematic sessions, panel discussions, and technical presentations, providing researchers with a platform for presentation and a unique environment for discussion and discovery. Additionally, IFEC promotes activities in innovation, economic growth, social change, and regional development.

Aligning with our country's development policies, IFEC transcends mere knowledge exchange, offering a rich environment for cultural interaction and collaboration. The conference's diversity, attracting over 120 distinguished scientists, industry leaders, and innovative thinkers from 25 different countries ranging from Algeria to Vietnam and India to Spain, presents a significant opportunity for knowledge sharing. In presenting this proceedings book, we hope to encapsulate the essence of IFEC - a hub of innovation, a crossroads of global expertise, and a guidepost for future engineering advancements. We trust the research outcomes shared here will inspire our readers and encourage them to contribute to the ever-evolving field of engineering.

Prof. Dr. Mehmet Emin Erkan

Dicle University

Foreword-2

Esteemed Colleagues,

The International Future Engineering Conference (IFEC 2023), innovatively organized under the auspices of Şırnak University, transcends the conventional scope of a scientific meeting. I must first extend my profound gratitude to Assoc. Prof. Dr. Mahmut Dirik and Assoc. Prof. Dr. Asaf Tolga Ülgen for their extraordinary energy and dedication in orchestrating this successful conference. Their leadership spearheaded a team that achieved significant synergy in both the academic and industrial sectors.

The triumph of the conference is intimately tied to the contributions of everyone involved. Thus, I wish to express my sincere appreciation for the efforts of every individual and institution that supported the organization. Each has played an indispensable role in pushing the frontiers of science and engineering.

IFEC 2023 harbored substantial potentials for the scientific community, extending well beyond a mere event. The continuation of this conference is crucial, not just for Şırnak University, but for the entire scientific world. Tracking and advancing current technologies and engineering research is feasible through such platforms, which serve not only as conduits for knowledge exchange but also as catalysts for global collaborations and the genesis of innovative ideas.

I am proud to be part of the inception of such a pioneering endeavor. Şırnak University, with this conference, has demonstrated its commitment to contributing to the future of science and technology. Future activities of IFEC will undoubtedly shed more light on research in this field and provide valuable contributions to the international scientific community.

I eagerly anticipate being a part of this exhilarating conference at the next IFEC event.

Sincerely,

Prof. Dr. Oscar CASTILLO

Tijuana Institute of Technology

Foreword-3

The International Future Engineering Conference (IFEC 2023), hosted by Şırnak University, emerged as a prestigious event bringing together numerous engineering experts and researchers from the global stage. The conference presented an effective platform for the exchange of knowledge, focusing on advanced technologies and future trends in engineering. A wide range of participants from various engineering disciplines shared their research through keynote presentations, panel discussions, and technical sessions. Three main speakers and numerous presenters from both local and international arenas added value to the conference and emphasized the importance of academic collaboration.

IFEC 2023 contributed to the promotion of new research, the strengthening of international cooperation, and the advancement of innovations in the field of engineering. The conference agenda varied from the application of deep learning models in image color transfer applications to the examination of Blockchain Issue Reporting, and the Scalar Control of Double Star Induction Machines using Fuzzy Logic. Additionally, it included studies on the Performance Analysis of Water-Based PV/T Systems, the Role of AI and ChatGPT in Digital Marketing, Resource Management for Health and Safety in the Construction Sector, Load Distribution Along Slopeless Slopes, the Energy Potentials of Point Focus Solar Collector Systems, and the Role of ChatGPT in Shaping the Industry 4.0 Landscape. Important research was presented, including the Exploration of the Capabilities of Unity 3D Game Software. All these studies have made significant contributions to both the academic community and the industry.

IFEC 2023 witnessed a series of accomplishments celebrating the future of science and technology and set larger goals for the 2024 conference. We look forward to the continued intensive efforts in science and technology to support this progress. We hope to see you at the next IFEC conference.

Sincerely,

Prof. Dr. İlhan TARIMER

Muğla Sıtkı Koçman University

EXAMINATION OF IMAGE COLOR TRANSFER APPLICATIONS WITH DEEP LEARNING MODELS

Birkan BÜYÜKARIKAN

Asst. Prof. Dr. Isparta University of Applied Sciences, Uluborlu Selahattin Karasoy Vocational School, Department of Computer Technologies, Isparta-Türkiye, (Responsible Author) ORCID: 0000-0002-9703-9678

Abstract

One of the subjects that has been studied for a long time in computer vision applications is color transfer. Color transfer aims to create new images by transferring the related color from a reference to the target image. Color transfer is also evaluated in image enhancement applications. Researchers have used traditional and deep learning approaches to execute these applications. The traditional color transfer approach consists of sequential image processing steps and is expressed mathematically. All these steps involve long, laborious processes. Therefore, it becomes difficult to obtain natural effects in images created with this approach, and only linear problems can be solved. For this reason, deep learning, which has a strong place in computer vision, has been intensively used in color transfer applications in recent years. The deep learning approach creates models that can solve complex lighting and nonlinear problems. In addition, these models can be easily developed for different applications. This study reviewed color transfer applications with a deep learning approach. This study was carried out as a summary of the latest approaches based on deep learning. As a result of the examinations, extremely useful and valuable images can be created by transferring the colors to the images. The number of images can be increased with this approach, which is especially applied to data sets containing a limited number of images. In addition, it is believed that the performance of deep learning models used for classification and recognition applications with the help of images developed with this approach will increase, and color transfer will be widely used in many subjects.

Keywords: Color transfer, deep learning, computer vision

Introduction

The appearance characteristics of the image reflect the viewer's visual perception (Liu, 2022). Color is an important feature used by people to perceive the appearance characteristics of an image. Various image correction tools are used in applications to change the image's color. These tools involve several trivial operations. Color transfer, an image processing method, can be applied to change the color distribution in the image without using these tools (Song & Liu, 2016). Color transfer involves the task of converting the color in the target image into the desired color information in the reference image (Lee et al., 2020). By changing the color, the appearance of the target image also changes, and the target image has similar colors to the source image (Dumoulin et al., 2016; Gatys et al., 2016; Song & Liu, 2016; Lee et al., 2020). Therefore, different interpretations of the same scene can be achieved with different styles of images (Zhao et al., 2020).

Traditional and state-of-the-art approaches are used extensively for color transfer applications in research. Traditional approaches consist of interconnected steps based on image processing, and these steps are processed sequentially. A problem with one of these steps will cause the final results to fail (Liu et al., 2018). Also, color and color tone adjustments depend on image content and need fine-tuning. Recently, deep learning has shown unique capabilities to solve these complex problems encountered in traditional methods (Yan et al., 2016). In deep learning, color properties and relationships are learned through the layers. Therefore, higher-level semantic relations are transferred to the target image (Gatys et al., 2016; Chen et al., 2017; 2018). Gatys et al. (2016) pioneered transferring styles from one image to another with CNN. Since the transfer application can be carried out without ground truth training data, researchers have turned to studies on transferring not only style but also color, texture, and appearance (Jing et al., 2019).

This study aims to present color transfer applications based on a deep learning approach. In this study, the importance of color transfer applications was mentioned, and these applications were summarized. Other

sections of this study are organized as follows. In Section 2, color transfer applications with the deep learning approach are examined, and in the last section, the results and limitations are mentioned.

Color Transfer Application with Deep Learning

Color references are created using color effects such as color, tone, illumination, weather conditions, props, and artistic (He et al., 2019; Liu, 2022). All these effects used for color transfer are performed on RGB and grayscale images (Levin et al., 2004). Research on the image or video color transfer using deep learning is introduced in this section.

Deep learning-based color transfer across images has typically been employed in research applications for image enhancement and correction (Liu, 2022). For these applications, it's critical to develop new algorithms or enhance existing ones (Xu & Ding, 2022). Additionally, two crucial difficulties related to this issue in these applications are producing the proper color match between the reference image and the source image and maintaining the source image content after color transfer (Wu & Deng, 2020). New vision tasks and methods have emerged for color transfer with deep learning, which is used to realize these applications and can learn high-level features from images (Tumanyan et al., 2022). One of the first deep learning applications for color transfer by Yan et al. (2016) suggested a deep neural network to demonstrate how to express the color correction problem in images. They stated, however, that inaccurately labeling the reference image could have a negative impact on the images since it would spread to the target images features. He et al. (2017) proposed a model based on pre-trained VGG19 for color transfer semantically related images. Their proposed model achieves local color transfer and can avoid unwanted distortions (at the edges or detailed patterns). Lee et al. (2020) proposed a deep neural network that exploits the color histogram analogy to transfer the color of a reference image to a specific target image. Their proposed model was a modified version of U-Net and ResNet. Xu & Ding (2022) used VGG19 for color transfer and evaluated the images they produced in terms of color quality. He et al. (2017), Lee et al. (2020), Xu & Ding (2022), and Zhang et al. (2022) applied their work to well-known CNN models.

On the other hand, colorizing 3D images is generally a complex task that requires expertise and effort. Zhang et al. (2022) used the VGG19 model to colorize 3D images automatically. On the other hand, different emotions in images or videos are conveyed to people with different colors (Zhang et al., 2022). Therefore, when transferring colors in these applications, the focus is on the color of the reference image (Liu et al., 2018). Considering the emotional factors of the reference image, Liu et al. (2018) proposed a new color transfer method that takes advantage of the basic structure of VGG19, which can process emotional images end-to-end. Their proposed method considers both emotion classification and local semantic information. They stated that color correction can be done with this method in areas such as film/television post-production, visual effects production (VFX), and artwork design. However, they stated that the limited number of training and test sets used for image coloring would cause network instability.

Another area of color transfer application is the improvement of images caused by illumination. Liu et al. (2019) proposed a transfer application for images with complex illumination. In their study, they first converted the RGB images to the HSV color space and gave the images produced with the V value to the input of the CNN model. Using the hierarchical feature maps they extracted from CNN, the images' histograms were reshaped, the images obtained from here were converted to RGB color space, and the illumination was transferred to the images.

Models developed with the deep learning strategy provide more stable color transfers by considering local and global color distribution characteristics (Yang et al., 2022). Color transfer can be used in various complex scenes and in the digital restoration of old image archives, medical image colorization, art restoration, image enhancement in remote sensing, and infrared image enhancement (Xu & Ding, 2022). Transferring color to a grayscale image is a significant image processing problem known as colorization (Levin et al., 2004). Iizuka et al. (2016) automatically colored grayscale images with a CNN model. Their model has a fusion layer combining local information in image patches with global knowledge. Here, the model was trained end-to-end. Limmer & Lensch (2016) proposed a CNN model based on transferring the color spectrum of the RGB image to near-infrared reflectance images. They noted that correctly coloring objects fails when object appearance and color are unrelated.

Conclusion

This study presents an overview of image color transfer based on a deep learning approach, and studies in the literature are summarized. Studies in literature include image and video color transfer applications. Studies generally appear to be based on the VGG19 model. The color features obtained with various layer combinations of VGG19 express the image better. In addition, these applications will also contribute to the development of new proposed models. However, the inadequacy of hardware in deep learning, the need for more images, and the image processing process taking a long time are some of the problems that still need to be solved in this field.

References

- Chen, D., Yuan, L., Liao, J., Yu, N. & Hua, G. (2017). Stylebank: An explicit representation for neural image style transfer. *Proceedings of the IEEE conference on computer vision and pattern recognition*, 1897-1906. <https://doi.org/10.1109/CVPR.2017.296>.
- Chen, D., Yuan, L., Liao, J., Yu, N. & Hua, G. (2018). Stereoscopic neural style transfer. *Proceedings of the IEEE Conference on Computer Vision and Pattern Recognition*, 6654-6663. <https://doi.org/10.1109/CVPR.2018.00696>.
- Dumoulin, V., Shlens, J. & Kudlur, M. (2016). A learned representation for artistic style. *arXiv preprint arXiv:1610.07629*.
- Gatys, L. A., Ecker, A. S. & Bethge, M. (2016). Image style transfer using convolutional neural networks. *Proceedings of the IEEE conference on computer vision and pattern recognition*, 2414-2423. <https://doi.org/10.1109/CVPR.2016.265>.
- He, M., Liao, J., Yuan, L. & Sander, P. V. (2017). Neural color transfer between images. *arXiv preprint arXiv:1710.00756*, 2.
- He, M., Liao, J., Chen, D., Yuan, L. & Sander, P. V. (2019). Progressive color transfer with dense semantic correspondences. *ACM Transactions on Graphics (TOG)*, 38 (2), 1-18. <https://doi.org/10.1145/3292482>.
- Iizuka, S., Simo-Serra, E. & Ishikawa, H. (2016). Let there be color! joint end-to-end learning of global and local image priors for automatic image colorization with simultaneous classification. *ACM Transactions on Graphics (TOG)*, 35 (4), 1-11. <https://doi.org/10.1145/2897824.2925974>.
- Jing, Y., Yang, Y., Feng, Z., Ye, J., Yu, Y. & Song, M. (2019). Neural style transfer: A review. *IEEE transactions on visualization and computer graphics*, 26 (11), 3365-3385. <https://doi.org/10.1109/TVCG.2019.2921336>.
- Lee, J., Son, H., Lee, G., Lee, J., Cho, S. & Lee, S. (2020). Deep color transfer using histogram analogy. *The Visual Computer*, 36, 2129-2143. <https://doi.org/10.1007/s00371-020-01921-6>.
- Levin, A., Lischinski, D. & Weiss, Y. (2004). *Colorization using optimization*. In: ACM SIGGRAPH 2004 Papers. Eds, p. 689-694. <https://doi.org/10.1145/1186562.1015780>.
- Limmer, M. & Lensch, H. P. (2016). Infrared colorization using deep convolutional neural networks. *2016 15th IEEE International Conference on Machine Learning and Applications (ICMLA)*, 61-68. <https://doi.org/10.1109/ICMLA.2016.0019>.
- Liu, D., Jiang, Y., Pei, M. & Liu, S. (2018). Emotional image color transfer via deep learning. *Pattern Recognition Letters*, 110, 16-22. <https://doi.org/10.1016/j.patrec.2018.03.015>.
- Liu, S., Song, Z., Zhang, X. & Zhu, T. (2019). Progressive complex illumination image appearance transfer based on CNN. *Journal of Visual Communication and Image Representation*, 64, 102636. <https://doi.org/10.1016/j.jvcir.2019.102636>.
- Liu, S. (2022). An Overview of Color Transfer and Style Transfer for Images and Videos. *arXiv preprint arXiv:2204.13339*, 1-12.

- Song, Z.-C. & Liu, S.-G. (2016). Sufficient image appearance transfer combining color and texture. *IEEE Transactions on Multimedia*, 19 (4), 702-711. <https://doi.org/10.1109/TMM.2016.2631123>.
- Tumanyan, N., Bar-Tal, O., Bagon, S. & Dekel, T. (2022). Splicing vit features for semantic appearance transfer. *Proceedings of the IEEE/CVF Conference on Computer Vision and Pattern Recognition*, 10748-10757. <https://doi.org/10.1109/CVPR52688.2022.01048>.
- Wu, L. & Deng, T. (2020). Computer network security analysis modeling based on spatio-temporal characteristics and deep learning algorithm. *Journal of Physics: Conference Series*, 042111. <https://doi.org/10.1088/1742-6596/1648/4/042111>.
- Xu, M. & Ding, Y. (2022). Color Transfer Algorithm between Images Based on a Two-Stage Convolutional Neural Network. *Sensors*, 22 (20), 7779. <https://doi.org/10.3390/s22207779>.
- Yan, Z., Zhang, H., Wang, B., Paris, S. & Yu, Y. (2016). Automatic photo adjustment using deep neural networks. *ACM Transactions on Graphics (TOG)*, 35 (2), 1-15. <https://doi.org/10.1145/2790296>.
- Yang, H., Tian, F., Qi, Q., Wu, Q. J. & Li, K. (2022). Underwater image enhancement with latent consistency learning-based color transfer. *IET Image Processing*, 16 (6), 1594-1612. <https://doi.org/10.1049/ipr2.12433>.
- Zhang, M., Liao, J. & Yu, J. (2022). Deep exemplar-based color transfer for 3D model. *IEEE transactions on visualization and computer graphics*, 28 (8), 2926-2937. <https://doi.org/10.1109/TVCG.2020.3041487>.
- Zhao, H.-H., Rosin, P. L., Lai, Y.-K. & Wang, Y.-N. (2020). Automatic semantic style transfer using deep convolutional neural networks and soft masks. *The Visual Computer*, 36, 1307-1324. <https://doi.org/10.1007/s00371-019-01726-2>.

ARTIFICIAL INTELLIGENCE SUPPORT IN ENSURING DRIVING BALANCE OF A TWO-WHEELER

İlhan TARIMER

Information Systems Engineering, Institute of Natural Sciences. Muğla University, 48100, Muğla, Turkey

Oruç Altay KIRLI

Information Systems Engineering, Technology Faculty. Muğla University, 48100, Muğla, Turkey

Ayşe ELDEM

Computer Engineering, Engineering Faculty. Karamanoğlu Mehmetbey University, 70200, Karaman, Turkey

Abstract

Due to the rapid increase in the number of vehicles compared to the capacity of roadways today, traffic congestion has become a significant problem. As a solution to this issue, we can observe that two-wheeled vehicles, which occupy less space in traffic and can facilitate the transportation of more vehicles and individuals per square meter, are gaining prominence. The rapid growth of traffic congestion sometimes brings along vital risks. In the event of an emergency, emergency response teams turn to two-wheeled motorcycles to quickly reach the scene and escape from congested traffic. This enables fast intervention. However, in the high-speed drives of emergency teams, accidents can occur depending on the condition of the road.

The Autonomous Support Legs we have developed aim to enhance the safety of two-wheeled vehicles. The main objective of our project remains to maintain the idea of practicality for two-wheeled vehicles while providing a safe driving experience similar to four-wheeled vehicles. The autonomous system produced as a result of this project provides protection from both directions by being placed on the rear wheel chassis of two-wheeled vehicles, similar to support wheels attached to bicycles. This system only operates when two-wheeled vehicles are moving at slow speeds, and it can pose a serious danger at high speeds and in turns.

In this project, the autonomous system we have created uses advanced artificial intelligence and machine learning to analyze when and which support leg needs to be deployed, aiming to prevent potential accidents. Therefore, the safety of two-wheeled vehicles is increased, and the goal is to prevent possible accidents through the developed system.

Keywords: Artificial intelligence, Autonomous Systems, Two Wheeler Safety

Introduction

According to road monitoring data in our country, it has entered the top 10 countries with the most congested traffic. The presence of heavy traffic in crowded cities is a significant issue for automobile drivers. In large cities, it is essential to consider the state of traffic when moving from one place to another. Being stuck in traffic for hours means not being able to reach your destination on time. For this reason, people are turning to more practical two-wheeled vehicles. However, one of the most significant concerns in the preference for two-wheeled vehicles is the fear of having an accident while using these vehicles. In a study conducted in 2007, it was observed that out of 749,456 accidents, 32,239 of them were motorcycle accidents [1]. This number is significant, considering the use of motorcycles in traffic. In our country, the rate of motorcycle usage is 14.8% among other modes of transportation [2].

When examining accidents that occur in our country, it is observed that accidents are concentrated in Istanbul, Ankara, and Izmir, where traffic is most congested [3].

A study conducted in European Union countries revealed that the mortality rate for two-wheeled vehicles is 20 times higher than that of other vehicles [4].

When considering the analyzed data, it becomes evident that making two-wheeled vehicles a safer mode of transportation is of significant importance, both for emergency response teams and individuals who rely on two-wheeled vehicles.

1. Literature Review / Theoretical Background

In contemporary times, one of the most significant challenges for motorcycles and other two-wheeled vehicles is issues related to balance. According to the laws of physics, two-wheeled vehicles that are not subject to equal forces tend to lean to the side [5]. The proposed project aims to prevent accidents that may occur in the event of possible wheel skidding by autonomously ensuring the balance of two-wheeled vehicles.

Some studies in the literature have focused on the goal of enabling two-wheeled vehicles to maintain balance on their own [6]. However, these existing studies primarily address the static balance of two-wheeled vehicles or their ability to move forward without additional intervention. There is no research available regarding the development of an autonomous system that attempts to maintain the balance of a moving motorcycle and aims to prevent accidents.

Therefore, the objective of this proposed study is to address these safety issues in two-wheeled vehicles during motion and prevent potential accidents.

2. Methodology

The primary goal of this study is to explore and utilize the Arduino microcontroller platform, which enables students in various fields, particularly engineering and applied sciences, to carry out their projects more easily and effectively.

In the initial step, it is necessary to select the most suitable microcontroller model that aligns with the project's objectives. In this study, the Arduino Nano model was preferred, as it offers sufficient ports despite its compact size. It is also emphasized that the microcontroller should possess the required features to operate reliably in confined spaces.

The MPU-6050 sensor, to be used in the system, is employed to track the inertial motion of a two-wheeled vehicle by collecting six-axis data (three axes for the gyroscope and three axes for the accelerometer) on the microcontroller. This sensor's data processing capabilities will be crucial for achieving the project's objectives.

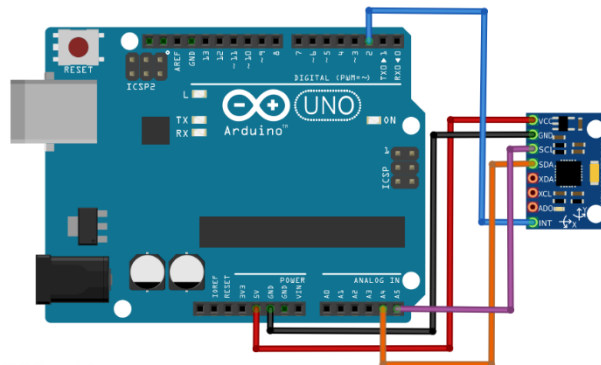


Figure 1: MPU-6050 Arduino Connection Diagram

Below is the code block required to connect the MPU-6050 sensor to the Arduino platform:

```

MPU6050 mpu;

int16_t ax, ay, az, gx, gy, gz;

double Setpoint, Input, Output;
PID pid(&Input, &Output, &Setpoint, 2, 0.1, 1);

void setup() {
  Wire.begin();
  mpu.initialize();
  pid.SetMode(AUTOMATIC);
  Setpoint = 0;
  Serial.begin(9600);
}

void loop() {
  mpu.getMotion6(&ax, &ay, &az, &gx, &gy, &gz);
  float angle = atan2(-ay, az) * 180 / M_PI;
  Input = angle;
  pid.Compute();
  delay(10);
}

```

DC motors that convert electrical energy into mechanical energy are explained and the concept of magnetic flux is discussed in detail. Additionally, the functionality and advantages of Arduino Motor Shield, which is used as a motor control card, are emphasized.

To determine the weight to be installed on DC motors, you need to take into account the torque capacity of the motor and the speed of the motor. The formula you can use to make this calculation is given below.

$$M_{\max} = N \cdot m_{(\max)} / (\text{Torque length}) \times G$$

In this formula:

Maximum Weight (kg) = Maximum Torque (N.m) / (Motor's Torque Arm (m) x Gravity Acceleration (m/s²))

Where:

F, W - Maximum Weight represents the maximum weight the motor can carry (in kilograms).

Maximum Torque stands for the DC motor's maximum torque capacity (in Newton meters).

TM - Motor's Torque Arm represents the distance over which the motor is effective in producing torque (in meters).

g - represents the acceleration due to gravity, representing Earth's gravitational pull.

For example, let's assume a DC motor has a maximum torque capacity of 0.2 N.m and a motor's torque arm of 0.1 meters:

$$\text{Maximum Weight (kg)} = 0.2 \text{ N.m} / (0.1 \text{ m} \times 9.81 \text{ m/s}^2) \approx 0.204 \text{ kg.}$$

According to this calculation, this DC motor can carry approximately 0.204 kg (204 grams) of weight.

During the programming process, the Arduino microcontroller is programmed using the C# programming language, while an artificial intelligence system is developed using Python. This allows for the creation of a plan to ensure that the sensors work correctly under specific conditions.

The selection of high carbon steel material for the side supports to be used on the microcontroller platform is explained, highlighting the material's advantages in terms of durability and lightness.

The sensor placement forms the basis of tests conducted in a laboratory environment, and based on the results of these tests, the artificial intelligence system is trained.

The following diagram illustrates the workflow of this autonomous system.

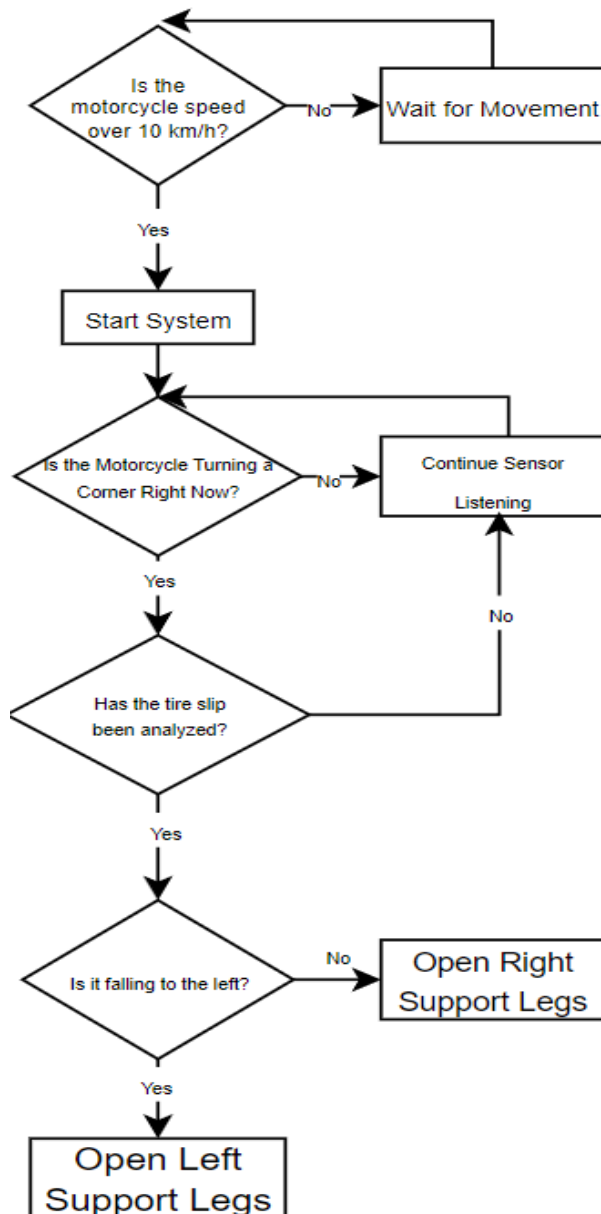


Figure 2: Flow Chart of Autonomous System

In the final stage, it is planned to conduct statistical analyses of the collected data and examine significant differences between different groups. This study demonstrates how various statistical domains contribute to the project's focal points and data collection processes. Data analysis has enabled the evaluation of the data collected by the sensors used in the project through fundamental statistical work. This examination involves organizing, cleaning, summarizing, and visualizing the data, providing a detailed analysis of essential

statistical parameters such as the distribution of motor speed, accelerometer data, and other sensor data. Additionally, the project's performance evaluation has been quantitatively assessed using statistical metrics, including accuracy, precision, speed, and energy efficiency.

Comparative analysis includes the statistical comparison of different motor models and artificial intelligence algorithms. These comparisons have been conducted using statistical tests and analysis methods, such as ANOVA and t-tests, to evaluate the performance of various motor types. Furthermore, error analysis has statistically examined errors in autonomous systems, determining the type, frequency, and magnitude of errors. Design optimization has been achieved by optimizing motor parameters and design variables using statistical experimental design.

Lastly, trend analysis has included time-series analyses to monitor the project's long-term performance and forecast future improvements. These statistical studies have significantly contributed to better understanding the data, improving the design, and objectively evaluating the project's success. These analyses provide essential guidance for the development and optimization processes of autonomous systems.

3. Findings

In this study, the support legs shown below (Figure: 3) and added to the vehicle were designed and these designs were drawn in 3D. The drawings were made to scale and prepared for production (Figure: 3 and Figure: 4).

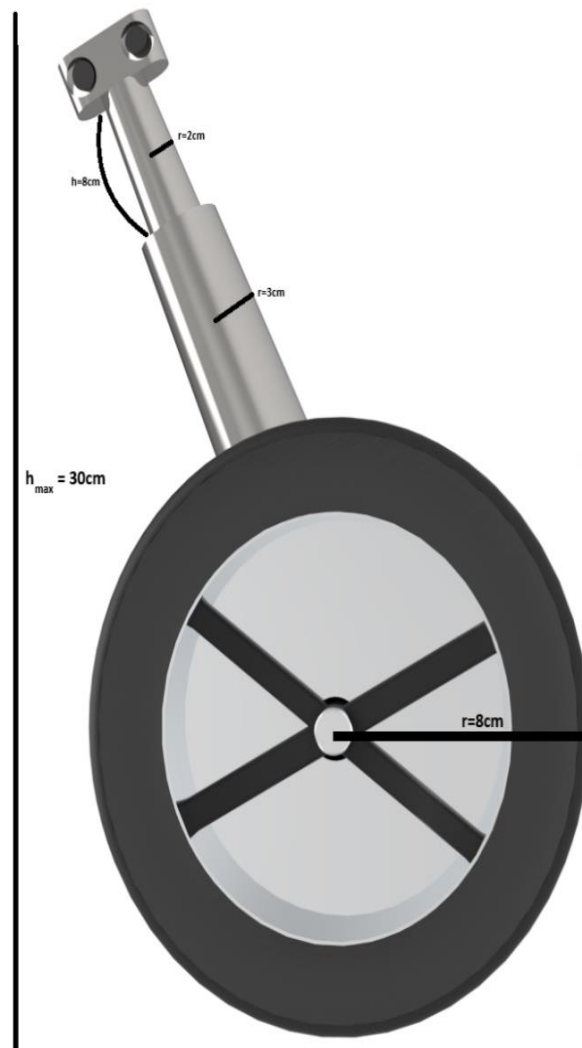


Figure 3: Support Leg Dimensions

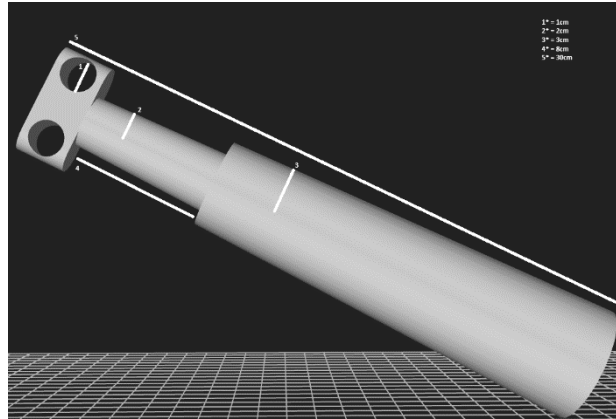


Figure 4: Support Leg Mounting Bar Dimensions

An interlocking structure has been created to ensure that the support leg works quickly in times of danger and does not compromise driving safety when it is not necessary. In this way, the system will operate at the desired angle and can intervene quickly. The support leg can be mounted on the right and left chassis of the engine (Figure: 5).

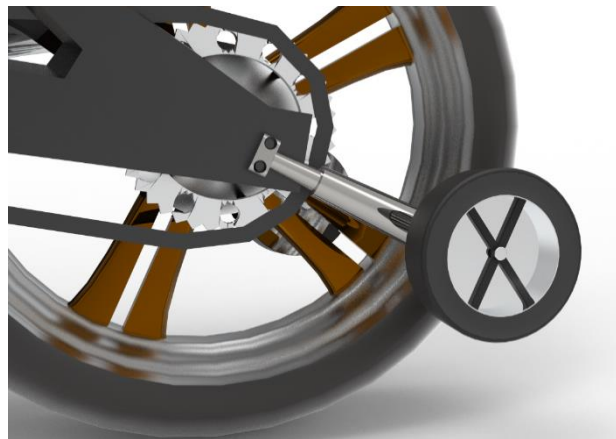


Figure 5: Support Leg Installation Situation.

The support leg is fixed on the chassis at 2 different points to ensure stability. Additionally, support legs can be placed at different angles depending on the chassis geometry of the motorcycle to be applied (Figure 6).



Figure 6: Structure of the Support Leg

One of the most important problems encountered in the developed autonomous system is the contact angle of the support wheels with the road. A variable angle attachment point was developed so that the support wheel can contact the road at the maximum angle (Figure 7).



Figure 7: Variable Angle Wheel Mount

Thanks to the variable-tilt wheel connection, the motorcycle ensures maximum efficiency by maintaining full contact with the road surface at all times, regardless of the angle at which it approaches the road.

Upon examining the research data obtained from our studies, it is evident that electric motors with different torque values and mounting brackets are used based on the weight and chassis design of each motorcycle. Let's calculate the required torque for a motorcycle weighing 180 kg, for instance.

First, we consider the weight of the motorcycle and the height of the support leg. Then, we include the wheel's radius and the acceleration due to gravity (typically 9.81 m/s^2) in our calculations.

$$\text{Moment (N.m)} = \text{Force (N)} \times \text{Lever Arm (m)}$$

To calculate the force (F), we can use the gravitational force generated when applying the motorcycle's weight to the center of the support leg:

$$\text{Force (F)} = \text{Weight (W)} = \text{Mass (m)} \times \text{Gravity Acceleration (g)}$$

The mass of the motorcycle (m) is given in kilograms, so we can use the mass:

$$\text{Mass (m)} = 180 \text{ kg}$$

Gravity acceleration (g) is generally assumed to be approximately 9.81 m/s^2 . Now we can calculate the force:

$$F = m * g$$

$$F = 180 \text{ kg} * 9.81 \text{ m/s}^2$$

$$F \approx 1765.8 \text{ N}$$

Now, using the force applied to the wheel and the radius of the support leg, we can calculate the torque:

$$\text{Moment (N.m)} = \text{Force (N)} \times \text{Lever Arm (m)}$$

The lever arm is the radius of the support leg (r), and we need to convert 8 cm to meters (0.08 m):

$$\text{Moment} = 1765.8 \text{ N} * 0.08 \text{ m}$$

$$\text{Moment} \approx 141.26 \text{ N.m}$$

Therefore, for a motorcycle weighing 180 kg to support a wheel with a height of 30 cm and a radius of 8 cm, the required torque is approximately 141.26 N.m. This torque represents the maximum torque the motor needs to provide to the support leg. Based on these results, the system we developed can be applied to all vehicles, depending on the specifications of the motorcycle in use.

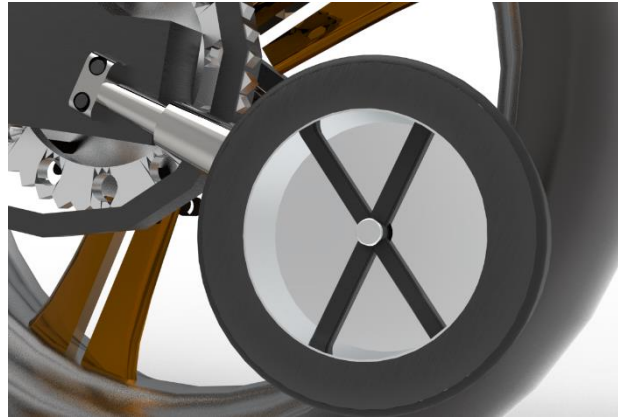


Figure 8: Structure of the Support Leg

In our developed project, a design optimization has been created to enable the support leg to provide balance. (Figure 8) The working principle of the design we developed is as follows: if the motorcycle's rear wheel skids according to the data from the sensors when entering a turn, the support leg system is activated after analyzing which direction and angle it skids. For example, if it is determined that a motorcycle is skidding to the left in a left turn, and the motorcycle begins to tilt to the left at a 30-degree angle, the system intervenes. Since the data entered for the support leg varies depending on the motorcycle to be applied, the angle and length at which the support leg needs to be opened in advance have been determined. Accordingly, to save a 180kg motorcycle from falling when it is tilting at a 30-degree angle to the left, the support leg aims to prevent it by opening at a 15cm angle. The active range of the support leg varies according to the angles at which this dangerous situation occurs. For example, if it had been detected that the same motorcycle was skidding at a 40-degree angle, the support leg would intervene by opening at a 10cm angle.

This study focuses on the severity of traffic problems and motorcycle accidents in our country. According to road monitoring data, our country is among the top ten countries with the most congested traffic, especially in major cities, traffic congestion has become an inevitable reality of daily life. While this presents a significant problem for drivers, it has also increased the need for fast and convenient transportation. However, the use of two-wheeled vehicles (motorcycles) to meet this need is limited due to safety concerns. In this context, a study focusing on this issue conducted in 2007 revealed that a significant portion of accidents in the country involved motorcycle accidents. This study, which focuses on addressing this problem, aims to reduce motorcycle accidents and make two-wheeled vehicles safer by using the Arduino microcontroller platform.

Additionally, research conducted in EU countries indicates that the mortality rates for two-wheeled vehicles are 20 times higher than for other modes of transportation. This highlights the seriousness of two-wheeled vehicle safety. In this context, the study focuses on the balance issues of two-wheeled vehicles and addresses the shortcomings in existing studies, which generally focus on static balance but lack solutions for maintaining balance and preventing accidents while in motion. Therefore, an Arduino-based autonomous system is developed, offering a new approach to the safety of two-wheeled vehicles. This study aims to provide engineering and applied science students and researchers in various fields with the opportunity to carry out their projects more effectively. In line with this goal, a system integrating the Arduino Nano microcontroller, MPU-6050 sensor, and DC motors has been developed. In addition, the Arduino microcontroller has been programmed using the C# programming language, and an artificial intelligence system has been integrated using Python. This study aims to make a significant contribution to the design and development of Arduino-based autonomous systems and offers an innovative approach to improving the safety of two-wheeled vehicles.

4. Discussion

When reviewing the literature, one can find approaches similar to our work. The study referenced as [7] is the closest to this work. In [7], the focus is primarily on motorcycle balance systems, while this study provides

a more general overview and explains how Arduino can be integrated into a wide range of control applications. While both articles provide valuable resources for readers interested in Arduino and microcontroller-based projects, the key difference that sets this study apart from the others is the emphasis on preventing accidents that may occur as a result of a wheel skid, not just keeping two-wheeled vehicles in balance. This study specifically aims at keeping two-wheeled vehicles balanced.

Another study referred to as [8] is a study on two-wheeled balance robots. In this study, instead of solving the balance problem with new approaches, the approaches used in the literature have been applied to the balance robot. However, when comparing this study to our work, this study solely focuses on achieving balance. In our study, while achieving balance, the safety of a motorcycle is the main goal, and the development of any accident-preventing system is also intended.

Another study, [9], focuses on warning the driver about potential dangers by placing sensors and various detectors on two-wheeled vehicles and communicating through a mobile device. In this study, a phone or tablet device is mounted on the motorcycle handlebar, detecting hazardous situations from the camera and notifying the driver. It also monitors the ride and provides reports to the driver. Additionally, it creates a network to communicate with other systems using this system, developing a system that can predict road stability in advance and provide warnings to the driver. The most significant difference between this project and our project is that it develops a hazard detection system and provides warnings only. In our project, we aim to detect hazards and prevent them in case of a potential accident.

Another project that worked on the balance of two-wheeled devices is the study numbered as [10]. In this study, a gyroscope is used to maintain the balance of a two-wheeled electric motorized device, but the focus is only on the ability of two-wheeled vehicles to maintain their own balance and prevent tipping over. There is no accident prevention system, which is our main goal. The contribution provided by this study is aimed to be utilized in our own study by using it in the balance analysis unit.

5. Results

This study has focused on the development of an Arduino microcontroller-based system that successfully controls the balance of two-wheeled autonomous vehicles. This system has made a significant contribution to important issues in our country, such as traffic problems and motorcycle accidents. In particular, the results of the project demonstrate its success in maintaining the balance of two-wheeled vehicles.

The artificial intelligence software plays a crucial role in controlling the movement of the two-wheeled autonomous vehicle and maintaining its balance. This software calculates the torques generated by the motors of each wheel, computes the friction forces based on the surfaces of the wheels and the vehicle's speed, and calculates the forces required to maintain balance. As a result, the vehicle optimizes its ability to maintain balance. Artificial intelligence algorithms monitor sensor data in real time, detect the vehicle's inclination, and adjust motor torques to maintain balance. This ensures the safe and desired movement of the vehicle and underscores the importance of artificial intelligence in balance control.

In the future, more comprehensive research and applications can be built upon this study. In particular, further development of artificial intelligence algorithms and advancements in sensor technology can offer more effective solutions for the safety of two-wheeled vehicles. Commercial and industrial applications of this technology can also be explored. In conclusion, this study serves as a starting point with the potential to address a significant issue related to the safety of two-wheeled vehicles and can inspire future research.

Acknowledgements

We would like to extend our gratitude to Muğla Sıtkı Koçman University and Karamanoğlu Mehmetbey University for their support in the realization of this study.

References

- [1] Özkan, S, İkizceli, İ, Akdur, O, Durukan, P, Güzel, M, Avrdar, A. (2009). Motosiklet kazalarına bağlı yaralanmalar. *Akademik Acil Tıp Dergisi*, 8(2), 25 - 29. <https://www.acarindex.com/akademik-acil-tip-dergisi/motosiklet-kazalarinabagli-yaralanmalar-500502>
- [2] Türkiye İstatistik Kurumu. (2022, 26 Ocak). Motorlu Kara Taşıtları Aralık 2021 Erişim Adresi: <https://data.tuik.gov.tr/Bulten/Index?p=Motorlu-Kara-Tasitlari-Aralik-2021-45703>
- [3] Yılmaz, V. & Erişoğlu, M. (2003). Türkiye'de trafik kazalarında riskli illerin istatistiksel olarak belirlenmesi. *Afyon Kocatepe Üniversitesi Fen Ve Mühendislik Bilimleri Dergisi*, 3 (1) , 129-146. <https://dergipark.org.tr/tr/pub/akufemubid/issue/1595/19835>
- [4] Sataloğlu, N. D., Aydın, B., ve Turla, A. (2010). Bisiklet ve motorsiklet kazası sonucu yaralanma ve ölümler. *Adli Tıp Bülteni*, 15(1), 13-20. <https://www.adlitipbulteni.com/archives/archive-detail/article-preview/bisiklet-ve-motorsikletkazas-sonucu-yaralanma-ve-/44393>
- [5] Gillespie, T. D. (1992). *Fundamentals of vehicle Dynamics*. Fondren Library
- [6] Sreehari M.D., Manikandan K., Pranjith K., Adithya V., Munga Balagi Jayanth Ram; Indu V., Meher Madhu Dharmana (2020). Design and analysis of e-bike with electrical regeneration and self-balancing assist. *The Institute of Electrical and Electronics Engineers, (ICOEI)(48184)*. <https://doi.org/10.1109/icoei48184.2020.9142889>
- [7] Çelik, U. (2014). Kendini dengeleyebilen iki tekerlekli aracın tasarımı ve kontrolü.
- [8] Taşlıalan, G., & Orhan, A. K. (2022). İki tekerlekli denge robotunun PID ile kontrolü. *Niğde Ömer Halisdemir Üniversitesi Mühendislik Bilimleri Dergisi*, 11(2), 1-1.
- [9] Smirnov, A., Kashevnik, A., Lashkov, I., Hashimoto, N., & Boyali, A. (2015, April). Smartphone-based two-wheeled self-balancing vehicles rider assistant. In *2015 17th Conference of Open Innovations Association (FRUCT)* (pp. 201-209). IEEE.
- [10] Govardhan, P., Thakre, A., Shende, N., Phadnis, N., Muley, S., & Scholar, U. G. (2017). Survey on self balancing two wheel electric prototype. *Int. J. Eng. Res. Gen. Sci*, 5(5), 32-36.
- [11] Işığışık, P. D. E. (2008). PERFORMANS ÖLÇÜMÜ, YÖNETİMİ VE İSTATİSTİKSEL ANALİZİ . *Istanbul University Econometrics and Statistics e-Journal* , 0 (7) , 1-23 . Retrieved from <https://dergipark.org.tr/en/pub/iuekois/issue/8988/112064>

A REVIEW IN IDENTIFYING BLOCKCHAIN PROBLEM STATEMENT

İlhan TARIMER

Department of Information Systems Engineering, Muğla Sıtkı Koçman University, 48100, Muğla, Turkey

Abdul Jaleel

Independent Consultant With Riyadh Bank, Riyadh, Saudi Arabia

Gizem AKTAŞ

Computer Engineer (Free Lancer), Residorm Kötekli, Menteşe–Muğla, Turkey

Abstract

All you need to know for understanding blockchain is that it is a “globally distributed ledger” that's it. We're actually going to ignore the “globally distributed” for a second and we're just going to discuss about ledger's in first section. From a layman perspective, a ledger is a record of transactions and account balances it's what's used in double entry accounting but more colloquially it's what your bank statement might look like at the end of every month. Ledgers have some properties among them are that they're immutable which means once you put a transaction in a ledger, you can never get rid of it. If you wanted to add a transaction, the ledger that's not allowed you have to add it at the end ledger's are data structures and the format has to be consistent like in a bank write like my checks have to look like. Blockchain is a secure-data-structure mechanism that holds the data in blocks form where each block is assigned a unique hash id and each block knows it's parent's blockhash. Blockchain is a secure-data-structure mechanism that holds the data in blocks form where each block is assigned a unique hash id and each block knows it's parent's blockhash. Using this technique one can create a historically accurate dataset but rather more blocks can be added that data can be timely accurate. Blocks can store data used by other users or transactions related. At using bitcoins your identity is a public key assigned to you, while you are registered into the system. Each person is assigned a unique pair of keys "public" & "private". While the public key is known to all the other nodes in the network but the private key is only known to you and you use it to decode and approve transactions by using your public key. This mechanism hides identity over the network; however, still one can find who you are using social engineering techniques. This problem is seen in the blockchain system where an identity is public. In this paper, the phenomena of the ‘blockchain’ is reviewed and discussed.

Key Words: Blockchain, Network, Global Ledger, Transaction

1. Introduction

Blockchain is a secure-data-structure mechanism that holds the data in blocks form where each block is assigned a unique hash id and each block knows it's Parent's blockhash. It basically stores all the transactions in a ledger. A transaction is an agreement between a buyer and a seller to exchange an asset for payment in the context of a blockchain. This is a message that represents the intent of the sender. When Altan declares that she wants to send one Bitcoin to Berke, he has to sign a message and broadcast it to the ledger. This message is a transaction wrapping up ledger's moving on to the idea of what it means for something to be globally distributed. Fig. 1 shows these ideas.

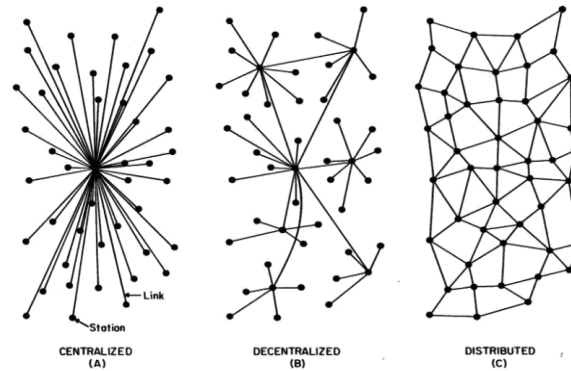


Figure 1. Transaction wrapping in a ledger.

This message is a transaction wrapping up ledger's moving on to the idea of what it means for something to be globally distributed. Fig. 1 shows these ideas. Figure 1 where there are many copies of the ledger maintained simultaneously ideally of equal importance in reality blockchains like Ethereum and bitcoin are a little more like the central picture. The ledger is still maintained in different places but certain ledger maintainers do more work than others [1 – 4]. For instance, recent studies have explored the applications of blockchain and distributed ledger technologies in biomedical and healthcare sectors, emphasizing their potential impact on data management and healthcare delivery [1]. Additionally, researchers have examined the broader implications of distributed ledger technology, especially in the financial sector, shedding light on its challenges and opportunities [4]. Furthermore, the World Bank has also contributed to the discourse on distributed ledger technology, offering insights into its applications and implications [2]. Reports prepared for institutions like the British Standards Institution have outlined the challenges and prospects for standards in the context of blockchain technologies, providing valuable insights into the evolving landscape [3]. These studies collectively contribute to our understanding of the diverse roles played by ledger maintainers across different sectors.

Once it is entered into a distributed context, there will be a problem called the double spend problem, just to point out a little more depth. Jaleel is now sending a transaction in a distributed context. He got his message that he wants to send a Bitcoin to Nevin. He signs it and broadcasts into the public sphere. As we now have many ledgers maintained simultaneously all over the world, Jaleel can't send his transaction to everyone at the same time and this is for a number of reasons one of them being network latency. One of them being that she may not actually know who all these ledger maintainers are in reality. Each ledger maintainer know that they forward messages that they receive to the other maintainers. Consequently, one may receive the same message twice. Finally, it should be considered that the case where Nevin is malicious and she's deliberately trying to send out the same message over and over and how do the ledger maintainers know. Not to execute and not to send more than one Bitcoin to Berke are the ledger itself assuming they can trust it.

The way the Bitcoin blockchain solves it is it gives each Bitcoin a unique identifier or something that looks and acts like a unique identifier. We have that context Jaleel trying to send multiple transactions clearly there needs to be a way to secure these transactions and it is known what's actually going on in the real world. But you know it in a distributed context that gets a little bit more complicated, because there's no bank that's where it is got to reach to the magic of cryptography.

Let's say, I send ten dollars to someone. It is not known that this is legitimate well. It's a signature in the analogue context it's pretty straightforward. In the digital world that gets trickier because there's no way to have his/her hand in anything to speak; because the signature looks a little bit more digital like this that begs the question how our digital signature is created everyone using public key cryptography. If you own any kind of crypto, then you know that you have two types of keys at your disposal. You've got a public key which is a public identifier of your existence cryptographically. Then you've got a private key which you need to keep it safe. It can't be recreated the signature you need to have the same message and the same private key. It's not enough to know like what the person is sending or to even get a hold of their private key you need both to recreate the same message and then the beauty of public key cryptography is that the signers'

public key can be used to verify. The individual you intend to sign the message actually summarizes it without ever needing to know their private key. It's the first rule of Bitcoin that there is no Bitcoin and what that means is that there's no file on your computer or hard drive that actually is a Bitcoin. There are only transactions on the ledger and if you have a record of everything, everyone has ever received you know who has what. In case of Nevin sends a transaction, he takes a transaction that he previously received from Jaleel and a hash of it. He includes that in the new transaction he's sending, the transaction has inputs and outputs and he crafts an output that is very similar to the input he received earlier.

If he sends one Bitcoin to İlhan, miners who see this transaction can look up not only that Berke actually has one Bitcoin to spend; but he specifically has the Bitcoin that matches this hash and this is the most simple type of transaction you'll see. A second key thing to note here is that all transactions have inputs and outputs and the sum of the inputs always has to equal the sum of the outputs but of course Nevin may want to send more or less than one Bitcoin to İlhan.

In that case he breaks up the outputs and sends whatever he doesn't want to send as half a Bitcoin back to himself and half a Bitcoin to İlhan. It can be thought that this is like giving cash, then receiving change and again the sum of the inputs in the sum of the outputs. These still have to be equal and then all outputs can be used going forward to craft new transactions. Apart blockchain, a block is just a collection of transactions that have been finalized. It can be minded that it is imagined like a shopkeeper taking the receipts and cash to the bank at the end of the day. It happens in every few minutes or seconds. The order of the blockchain is maintained by including the hash of the previous block. If even one letter in a previous transaction has been changed, this would be kind of like a macro version of the transaction inputs and outputs hashing that being seen because of the properties of hash functions.

2. Place Where Blocks Come From

This brings us to the concept of mining basically. A block is a set of transactions and it

considers how does a set of transactions get appended to the ledger. You can't connect a block to the ledger in which any miner wants to connect the new block to the to the ledger. When they want to do it, that would result in all sorts of chaos. That means that we need some kind of game that game is called proof of work for miners to earn the right to attach the next block to the chain. Basically, what happens is the miners or these computers which will soon be you will be forced to brute-force hashes of the state of the block. Unless two miners find a nonce at the same time because of network latency, we never know where certain miners are with a relation to one another.

This review paper aims to find out that a research area in blockchain which could be as below "scalability of Blockchain and how serious is the scalability issue; selecting the use cases for blockchain and identifying research problems".

2.1. Blockchain scalability and Seriousness of scalability issue

Bitcoin is currently being traded at the volume of around 300000 transactions per day. But the network can handle a maximum of only seven simple transactions per second and not more than three complex transactions per second [5–8]. For instance, Atzei et al. (2018) formalized Bitcoin transactions, providing insights into the underlying structure of the network [5]. Delgado-Segura et al. (2020) proposed a fair protocol for data trading based on Bitcoin transactions, offering potential solutions to transaction complexity issues [6]. Additionally, Zhao and Guan (2015) conducted a graph-based investigation of Bitcoin transactions, shedding light on the network's transaction patterns [7]. Furthermore, Vranken (2017) discussed the sustainability aspects of Bitcoin and blockchain technologies, highlighting their limitations in terms of scalability [8]. These studies collectively inform our understanding of the network's transaction capabilities.

This means that the network is currently operating at close to its maximum capacity etherium. Even though the hypothetical capacity for transactions of a single etherium note is over 1,000 transactions, the existing gas limit lowers on the other hand a blockchain focused on speed and scalability managed to grow up to four terabytes in under eight months. The reason is that just looking at regular cryptocurrencies and they're highly volatile market

prices a delay in transaction processing can lead to losses especially Volume traders and of course when it comes to dapps and other blockchain based applications processing speed limit could serve as a major obstacle to adoption, especially for mobile app's long waiting times would generally cause interrupted sessions (imagine trying to access YouTube via a 90s dial dial-up modem).

It could be analyzed that why users have not accepted blockchain technology far and wide but looking at it from the point of view of scalability. It's a good thing that blockchain apps might simply not be ready for prime time. Another scalability issue is of course energy it is no secret that the proof-of-work consensus mechanism used by bitcoin and Ethereum uses up a lot of energy and for blockchain. It's important to note that these issues pertaining to public blockchains in a private blockchain even one based on a Bitcoin protocol high speeds are achievable. The fundamental challenge when it comes to scaling of blockchain projects is rooted in something called the scalability trilemma (Fig. 2). This concept is connected to what we call a project management triangle.

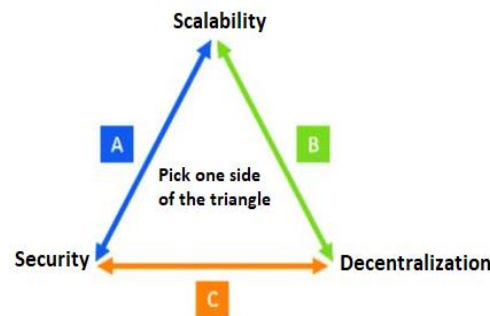


Figure 2. Scalability trilemma.

A block chain needs to be decentralized in terms of security and fast. It only can be two of those at the same time; the term was originally coined by Vitalik booted by himself. So, it's obvious that the etherium team is conscious of the problem and is already working on it to illustrate it.

Let's take a Bitcoin blockchain the network is relatively secure and fully decentralized which means that it can't be fast euros and ripple. On the other hand are faster and are said to be relatively secure but that means that they can't be fully decentralized.

De-centralized means that the ledger is distributed across multiple nodes of the network. It's a technology that is not house on a single server but distributed to all the network participants more importantly. Decentralization also refers to a level of control. There should be no center point of control rather than relying on a central authority to validate transactions the consensus protocol should validate data in an incorruptible and immutable way. Such decentralization should remove the need for trust and the network as no one should be able to manipulate [9–11]. Researchers have addressed the issue of trust in decentralized systems, particularly in the context of Bitcoin transactions. Möser, Böhme and Breuker (2014) introduced risk scoring methods for Bitcoin transactions, contributing to the understanding of transaction security [9]. Irwin and Turner (2018) examined challenges related to illicit Bitcoin transactions, emphasizing the importance of identifying the parties involved [10]. Wu et al. (2021) proposed a method for detecting mixing services in the Bitcoin transaction network, enhancing transaction transparency and security [11]. These studies collectively highlight the significance of trust and security in decentralized networks like Bitcoin.

Of course, it is meant that it is safe from hacks and exploits. It doesn't pertain to bugs or errors in code but rather the ability of the networks to withstand 51% attacks and Sibyl attacks. One actor assumes many identities when it comes to speed it means that blockchain can quickly process any transaction regardless of the volume and the number of n network participants. Such an independence between speed and number of participants is what most commonly referred to when scalability is thought. Of course, mostly the reality that a blockchain solution will never be faster than a traditional database running on a single server has already accepted. So, the benefits of de-centralization and security really need to outweigh. The true limits of speed is really well demonstrated by using the example of Bitcoin. It's consensus protocol proof of work in this protocol nodes have to spend a significant amount of computing power electricity before they can add the block to the chain. This is probably the best way to ensure that the network is secure but also by definition it

will never be able to compete in speed. The design of Bitcoin prioritizes security and decentralization over speed. So the lack of scalability when it comes to Bitcoin is really a feature, not a bug; but one that still hinders the network's development when Bitcoin cash forked from the main Bitcoin blockchain in 2017. The fundamental reason was dealing with its scalability issue. The approach that Bitcoin cash took was increasing the size of a single block first from bitcoins one megabyte to eight megabytes and then further to 32 megabytes.

A higher block size means more transactions. That can be processed per second but also has made full nodes more expensive to operate leading to centralized entities having more leverage on the network as of early 2019. It promises to limit the energy consumption and speed challenges of the current blockchain. There are already companies designing their products around Kasper and other layers to Ethereum scaling solutions. One such example is lucidity a blockchain based system that tracks advertising impressions on the blockchain to weed out suspect sites and bot fraud allows advertisers to more carefully direct their ad spending to publishers validated on the blockchain their implementation of a plasma cash scaling solution means that they can process the massive amount of transactions required to track advertising impressions throughout the entire ad delivery chain. One such example is lucidity a blockchain based system that tracks advertising impressions on the blockchain to weed out suspect sites. So outside of a higher block size and a proof of stake approach what are the current known solutions to blockchain scalability issues.

Let's start by looking into EOS a controversial project that clearly chooses security and speed over decentralization. Its consensus mechanism is called the delegated proof of stake or D POS. It was created by Don Letty and met the founder of steam it with D POS. Any EOS holder is encouraged to vote for 21 block producers. The producers are then incentivized to enforce the rules for preventing double spending and driving the network forward. But the transaction is being validated by only 21 nodes. The speed and energy efficiency of the network can be increased significantly. In addition network resources such as bandwidth RAM and CPU can also be purchased or rented with aol's tokens which ensures that only purposeful computation is happening on the blockchain. The EOS team claims that they can process up to 1 million transactions per second the technology is not there yet. The claimed performance is around 1200 TPS transactions per second. But according to some reports the actual limit is currently at 250 transactions. The trade-off here is the network significant centralization. It is caused by the validators being pre-selected by the ripple foundation since all the participants have to trust these nodes in order to perform operations on the blockchain. Some people refer to ripple as a by note blockchain in name. It is a distributed network of nodes with every node holding all transactions. This allegedly allows for 1,000 transactions to be processed each second. The solutions of the centralization issue here is that stellar lets almost anyone run a node. You do not need to be selected by some unaccountable central entity. One problem with stellar; however, is the lack of incentives as node operators do not get monetary rewards this keeps the transaction feeds very low.

But can also limit the motivation to participate other potential solutions include side chains or off chain resources to take the burden away from the main blockchain. Side chain is exactly what it sounds like a secondary blockchain layer designed to facilitate lower cost and higher speed transactions between two or more parties off chain solutions mean moving the entire computation process into the non-blockchain environment without increasing the risk. When it comes to offering solutions, it is identified two options off chain state channels and off chain computations state channels are mechanisms where blockchain interactions get conducted outside of the network. in order to ensure security and compliance with the rules a part of the blockchain is locked by a smart contract that requires participants to reach 100% consensus. To update this part of the blockchain, the state is then transferred back to the block chain in the state channel is closed in this sense the blockchain is used purely as a settlement layer to process the final transaction.

Transaction capacity can be increased with lower fees and processed information more quickly. An example of such an implementation is the Lightning Network of chain computations work in a very similar way. A trusted verifiable system executes computations outside of a blockchain this pertains primarily to operations that would be extremely expensive on the blockchain plasma. It ensures reliability and validity of those plasma chains, while the plasma blockchain does not disclose block contents on the route chain instead. The block header hashes are given to the route which is enough to determine block validity, if there is proof of fraud present on the main chain the block is rolled back and the block creator is penalized. Multiple other parties also develop different solutions to tackle the scalability issue and break the scalability tree limit. All the other data is stored off chain to sum up scalability is a huge issue that remains probably the biggest

obstacle to widespread adoption. The solution that becomes the most successful needs to resolve the scalability tree limit as we know blockchain operations will probably always be slower than traditional centralized computing and that's why these three benefits of DLT speed security and decentralization all need to be present in order to convince consumers. In addition, our current environmental challenges and general drive towards energy efficiency requires blockchain technologies to become much leaner in terms of consumption energy efficiency and increase in speed should therefore go hand-in-hand without compromising security.

2.2. Selecting use cases and identifying research problems for blockchain

Using a standard blockchain systems currently most of the applications are from financial sectors. These applications focus on decentralizing the financial systems currently got. For example, when to be looked at bitcoins, it is seen that it is a decentralized system which is developed by using blockchain technologies. It has attracted lots of investors over the past 10 years. The blockchain technology gives that trust investors need in terms of security and data integrity; however, there are some downsides to it too.

This is the reason why many new approaches to blockchain technology has emerged in the market. These systems brings new promises for the developers to bring new type of applications for blockchain. One of these technologies is Ethereum which is mainly created with a focus on expanding the blockchain application areas. Ethereum can do this by using a few things differently, as they've introduced new tools such as smart contracts, Ethereum virtual machine, Solidity, Ether and proof of work [12–14]. For instance, Schilling and Uhlig (2019) discuss the economic aspects of Bitcoin, shedding light on the foundational concepts that influence cryptocurrencies [12]. Tikhomirov (2018) provides an in-depth analysis of Ethereum's state of knowledge and research perspectives, offering valuable insights into its development [13]. Dannen (2017) introduces Ethereum and Solidity, providing beginners with the foundations of cryptocurrency and blockchain programming, emphasizing the practical applications of Ethereum technology [14].

Ethereum is a blockchain system developed to give developers the flexibility to use blockchain for other kinds of applications then financial like bitcoin. This system has few innovative ideas which can help developers use the power of blockchain for other apps like chat or voting system etc. Ethereum does this by using a technique called smart contracts. Smart contract is a system that helps to make a virtual contract between the 2 parties without the involvement of a third party. Ethereum virtual machine is responsible for executing the code used in smart contract. This helps in the decentralization of the application without involving a third party. As the Ethereum VM can execute the smart contract to complete a blockchain transaction, the average amount of transaction inside a single block can be easily calculated using the formula below:

$$\# \text{ of Transactions per Block} = \frac{\text{Block Size in Bytes}}{\text{Average Transaction Size in Bytes}} = \frac{1,048,576}{380.04} \cong 2,759.12$$

As for blockchain system it holds the data in blocks form where each block is assigned a unique hash ID and each block knows it's Parent's blockhash. This link “intellipaat.com” has prepared a visual flow of blockchain which is presented in Fig. 3 below.

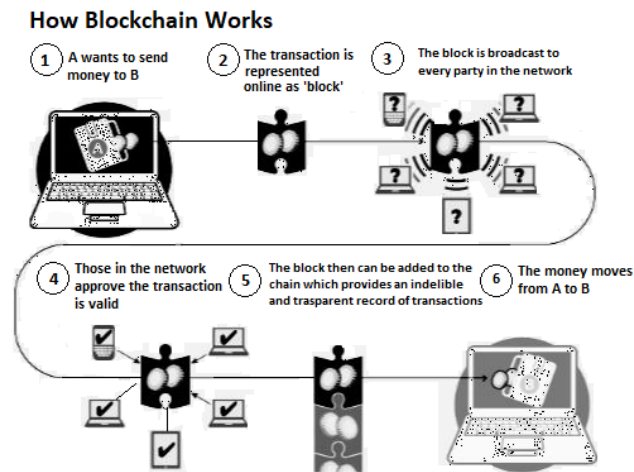


Fig. 3. Blockchain working

A single transaction has to go through these steps in order for the block to be properly validated and added to the previous blocks in chain. For ‘A’ to transfer the money to ‘B’ it has to go through all these validations steps.

With the consensus of all the parties in the network ‘A’ can send money to ‘B’ where everyone in the chain will recognise the fact that the transaction was real and can be legally made within the system. Because of ‘A’ doesn’t have any credit to send to ‘B’ and it still wants to send the money. In this case the transaction block will be created successfully but the money will not be transferred to ‘B’. But rather a failed money sending transaction will be added to the database of blocks in the network (Fig. 4).

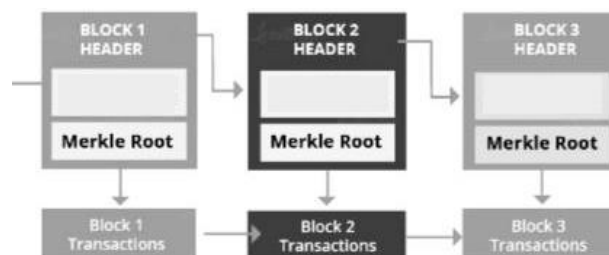


Figure 4. Adding money sending transaction

So, if compare the transactions speed of all digital transactions systems we can see in the Fig. 2 that visa is leading the transactions per second by a huge factor as compared to bitcoin or Ethereum.

3. Blockchain’s Key Characteristics

Consensus, provenance, immutability and finality are the blockchain’s a few key characteristics. Consensus is an algorithm that enables the blocks valids. A block is only considered valid if all the parties in the network agrees on it’s validity. This can be considered as the backbone of a blockchain network. The second characteristics provenance enables blockchain network parties to get the ownership of an asset and how it’s changing over time. This gives proof of the ownership of any asset within the blockchain network.

Immutability means that in a blockchain network no one has the authorization to modify a block once it’s been added to the transaction ledger. If the block was added by an error or human mistake then it can only be replaced by adding a new block to the ledger. Finality means that the ledger for all the transactions is created and all the parties must share the same ledger.

A blockchain is a technique that can help create a historically accurate dataset that can't be changed or modified but rather we can add more blocks so that data can be timely accurate. One can easily read the current value for any transaction by simply looking at the last block added for that transaction.

Blocks can also store other user related or transaction related data too but while using bitcoins like system your identity is the public key assigned to you while you register into the system. Each person is assigned a unique pair of keys "public" & "private" now the public key is known to all the other nodes in the network but the private key is only known to you and you use it to decode and approve any transaction made using your public key.

3.1. Main Issues and Security

Blockchain has an environmental cost: A blockchain system mostly relies on hashing and encryption algorithms to provide the security it needs for the distributed system. These algorithms needs huge amount of computational power to help users in gaining permissions within the network. So that no one can forge or falsify a transaction. The blockchain nature is that it grows exponentially, which is why the industry's biggest players are facing this issue of requiring huge amount of computation power in order to keep their network alive.

Lack of regulation creates a risky environment: As the growing use of blockchain in financial industry, their is a big risk of regulations from the governments. Because if you are an investor and you invest your money in the blockchain systems like bitcoins or ether etc. Even the big players can one day be shut down by the government for shady practices or secretly leave you open for hackers or maybe they can leave you out in the open without any protection for your coins. This is just because of the lack of regulations.

Blockchains can be slow and cumbersome: A blockchain network needs huge amount of storage for it's ledgers to be stored and not everybody can provide that much of capacity. This is a problem which is solved by using the cloud systems but that brings a new issue which makes the network very slow to work with. For example, a traditional payment system like 1 link etc can do thousands of transactions per second while in the blockchain system only 7 to 10 transactions can be made per second which is a huge difference. The end user simply expect things to work fast with the new technologies in the market.

Inside the blockchain world the network is considered as secured because that's one of the key features that a blockchain provides. But based on the previous knowledge of how once considered one of the most secure systems were hacked. The main reason being the difference between theory and practice. Because in theory a blockchain can be considered as full proof secure technology but in practice the programmers tend to make mistakes that leads to huge security flaws. For example, let's take a look at our current networks algorithms that are considered to be fully secured like WPA wifi protocols; however, researchers have been able to find bugs inside the code for WPA wifi. Even Though in theory it is still one of the most secure protocols, it is seen that it is hacked by identifying flaws in practice. Similarly, inside a blockchain system the practice can be different than what the theory says. Security is one of the most important concerns when it comes to blockchain because it is mainly used by big players like bitcoins & ether for financial systems.

4. Conclusions and Problems to be Worked on

There are some of the questions to be worked on future. In order to solve most of IoT' critical problems with blockchain technology up, initially it has been thought that Bitcoin and cryptocurrencies are for financial applications. But there are some early on examples of applications that are non-financial as domain name registries of land title and global identity registry systems.

The most popular blockchain based system is Bitcoin. Most people believe that Bitcoin transactions are slow and it takes ten minutes to inscribe on the chain. So, one should take care when to use this technology for the Internet of Things.

There are common issues that IoT devices are facing. Blockchain can help to solving the problems, as blockchain provides better solutions for IoT. The key points for exploring more are proof of work on how blockchain implementing the decentralized systems in practice and the problems that can occur while

implementing IoT blockchain system.

5. References

1. Tsung-Ting Kuo, Hyeon-Eui Kim, Lucila Ohno-Machado, 08.Sept.2017. "Blockchain Distributed Ledger Technologies for Biomedical and Health care Applications", *Journal of the American Medical Informatics Association*, Vol. 24, Iss. 6, P. 1211–1220, <https://doi.org/10.1093/jamia/ocx068>.
2. Natarajan Harish, Krause Solvej, Gradstein Helen, 2017. "Distributed Ledger Technology and Blockchain", *FinTech Note: No. 1.* © World Bank, Washington, USA. <https://openknowledge.worldbank.org/handle/10986/29053>.
3. Advait Deshpande, Katherine Stewart, Louise Lepetit, Salil Gunashekar, May 2017. Overview Report: Distributed Ledger Technologies/Blockchain: Challenges, Opportunities and the Prospects for Standards, Prepared for the British Standards Institution (BSI), P. 40.
4. Alexis Collomb, Klara Sok, 2019. "Blockchain / Distributed Ledger Technology (DLT): What Impact on the Financial Sector?", *Digiworld Economic Journal*, No. 103, 3rd Q. 2016, p. 93
5. Nicola Atzei, Massimo Bartoletti, Stefano Lande, Roberto Zunino, 07.Dec.2018. "A Formal Model of Bitcoin Transactions", Springer Conference paper, Int. Conf. on Financial Cryptography and Data Security (FC 2018), pp 541–56.
6. Sergi Delgado-Segura, Cristina Pérez-Solà, Guillermo Navarro-Arribas, Jordi Herrera-Joancomartí, June 2020. "A fair protocol for data trading based on Bitcoin transactions", *Future Generation Computer Systems*, Vol. 107, Pages 832-840.
7. Chen Zhao, Yong Guan, 20.Nov.2015. A Graph-Based Investigation Of Bitcoin Transactions, 11th International Conference on Digital Forensics, Orlando, USA, January 26-28, 2015, Springer Book Series.
8. Harald Vranken, 28.Oct.2017. "Sustainability of Bitcoin and Blockchains", *Journal of Current Opinion in Environmental Sustainability*, Volume 28, Pages 1-9.
9. Malte Möser, Rainer Böhme, Dominic Breuker, 08.Oct.2014. Towards Risk Scoring of Bitcoin Transactions, International Conference on Financial Cryptography and Data Security (FC 2014), Financial Cryptography and Data Security pp 16–32.
10. Angela S.M. Irwin, Adam B. Turner, 2.July.2018. "Illicit Bitcoin transactions: challenges in getting to the who, what, when and where", *Journal of Money Laundering Control*, ISSN: 1368-5201, Volume 21 Issue 3, pp.
11. Jiajing Wu, Jieli Liu, Weili Chen, Huawei Huang, Zibin Zheng, Yan Zhang, Detecting Mixing Services via Mining Bitcoin Transaction Network With Hybrid Motifs, Publisher: IEEE Transactions on Systems, Volume: 52 Issue: 4Page(s): 2237 – 2249, OI: 10.1109/TSMC.2021.3049278.
12. Linda Schilling, Herald Uhlig, Oct.2019. "Some Simple Bitcoin Economic", *Journal of Monetary Economics*, Volume 106, Pages 16-26.
13. Sergei Tikhomirov, 17.Feb.2018. Ethereum: State of Knowledge and Research Perspectives, Conference paper of International Symposium on Foundations and Practice of Security (FPS 2017), pp 206–221.
14. Chris Dannen, 2017. *Introducing Ethereum and Solidity: Foundations of Cryptocurrency and Blockchain Programming for Beginners*, New York, USA, ISBN-13: 978-1-4842-2534-9, DOI 10.1007/978-1-4842-2535-6, Library of Congress Control Number: 2017936045, Pages 17.

TIME SERIES ANALYSIS AND DATA MINING FOR ROBUST SHORT-TERM COMPRESSIVE STRENGTH FORECASTING IN GEOPOLYMER MORTAR: AN ARIMA MODEL DATA-DRIVEN APPROACH

Yıldıran YILMAZ

*Assist. Prof. Dr., Department of Computer Engineering, Recep Tayyip Erdogan University, Fener, Rize TR53100, Turkey
(Corresponding Author) ORCID: 0000-0002-5337-6090*

Talip ÇAKMAK

*Research Assistant, Department of Civil Engineering, Recep Tayyip Erdogan University, Fener, Rize TR53100, Turkey
ORCID: 0000-0003-0266-6132*

ABSTRACT

With a primary focus on leveraging time-series analysis and data mining methodologies, this paper delves into the realm of geopolymers, an eco-friendly and energy-efficient construction material. The target of the study is to specify the variables that affect the compressive strength of geopolymers and then utilize those variables to estimate the mechanical property (compressive strength (CS)) of mortars in the future. The study analysed the effects of factors such as compressive strength, obsidian, glass waste, fly ash, and heat on the CS of mortar. ARIMA model is adeptly employed to forecast the short-term compressive strength of geopolymers endowed with five distinct properties and subjected to varying temperatures. As a result of the analysis, the highest RMSE, MAE, MAPE, and R2 values were obtained as 1.207, 0.983, 0.025, and 0.941, respectively. Those results emphasize how well-sophisticated statistical modeling approaches could be employed to understand and estimate the dynamics of compressive strength in geopolymer mortars.

Keywords: Forecasting, Time series Analysis, ARIMA Model, Geopolymer, Obsidian, Data mining

Introduction

Geopolymer mortars are building materials that are of increasing interest and use in the contemporary construction industry. They are an environmentally friendly and energy-efficient building material developed as an alternative to traditional cement-based mortars [1]. A study by Ahmed et al. [2] concentrated on the application of geopolymer, notably fly ash (FA), which has been created as an ordinary Portland cement substitute due to the substantial carbon dioxide releases that the cement production labour has been producing lately. They developed various scale models to anticipate the mechanical property (CS) of fly ash based geopolymer mortar using test sets obtained from the literature. In their study, various data sets with different mixing ratios, different maturation times (from 1 to 28 days) and distinct maturation temperatures were used. Three different models including LR, MLR and NLR models were developed and these models were evaluated by statistical evaluations such as R², RMSE, SI, OBJ and MAE. The results of the investigation showed that the NLR model outperformed the LR and MLR models. For the NLR model, the values of R², RMSE, SI, and OBJ are 0.933, 4.294 MPa, 0.138, and 4.209, in that order. In another study [3], Wu et al. analysed the alkali equivalent (AE) and water glass modulus (WGM) effects of immersion experiments using artificial seawater. During 270 days, 300 samples underwent recurrent performance tests and an artificial immersion in saltwater. Mass loss and uniaxial compressive strength (UCS) were used as metrics for operation assessment, whereas AE (3–15%) and WGM (1.0–1.8) were utilized as motivating components. Furthermore, utilizing the experimental data, a support vector regression (SVR) model was created, and it demonstrated accurate prediction within a month or two. The authors in [4] conducted a contrast study on normal and self-compacting geopolymer mortar based on mixtures of fly ash - ground granulated blast furnace slag (GGBFS). The experiments included fresh properties, hardening properties and compressive strength tests. An artificial neural network (ANN) model advanced using the Tensorflow approach was used to forecast the compressive strength. Their model was trained on 150 data sets obtained from the literature and validated on data sets obtained in the laboratory. Manikandan et al. [5] considered the

mechanical and compressive strength properties of geopolymer concrete. The authors in [5] examined how different ratios of polypropylene (PP) fibres and rice husk ash (RHA) impacted the compressive and mechanical strength of geopolymer mortar. Using input factors including the RHA ratio, the density of sodium hydroxide (NaOH) liquid, and the quantity of polypropylene fibre, they also developed an artificial neural network (ANN) model to predict these features. As a consequence of the findings, it is possible to investigate the potential of geopolymer mortar for structural restoration and to determine whether it can be used to repair structural elements.

Prior research mentioned so far has primarily focused on small-scale laboratory tests, which may not fully reflect performance in real-world settings. In fact, the compressive strength of geopolymer mortars is unique owing to the special chemical reactions of the materials they contain [6]. The dataset used in our study includes compressive strength (CS), obsidian (OB), glass waste (GW), fly ash (FA), and HEAT as important properties for determining the compressive strength of geopolymer mortars. Understanding and predicting the effects of these properties on mortar compressive strength is crucial for building more sustainable and reliable structures in the construction industry. Our research aims to identify the elements that contribute to the compressive strength of geopolymer mortars and utilize these factors to predict the mortar's compressive strength in the future. To accomplish this, we have outlined the following contributions.

- This study explores the impact of variables which is such as fly ash (FA), glass waste (GW), obsidian (OB), and compressive strength (CS) on the compressive strength of mortars.
- By analysing the data set, we have successfully developed a 30-day forecast model for compressive strength using the ARIMA (1,0,0) method. We will discuss the performance of our model in the following sections.
- The results obtained can contribute to the development of strategies for more effective use of geopolymer mortars in the construction industry. Furthermore, the ability to predict compressive strength allows for more reliable planning of construction projects. This research aims to provide a basic reference for future building material developments and sustainable construction practices.

Related Works

Geopolymer mortars are a special type of material that stands out as sustainable and durable building materials. Previous studies in this field have focused on the strength properties of mortars, compressive strength and various production parameters [7]. Experimental studies on the strength properties of geopolymer mortars have proposed optimized blends to improve the compressive strength of mortars by studying the interaction of different components of the material [8]. In previous research, the effects of mortar components on the strength have been studied. The models used for the strength prediction of geopolymer mortars generally include regression analysis and time-series models [9], [10]. Some studies have emphasized the use of artificial intelligence-based models to understand the complex interactions that determine mortar properties and predict the future strength [11]. Chen et al. [12] determined the average profile depth using GEP to check the conformity of road surfacing used in the accreditation of car tires to the ISO 10844 standard. The highest R² value of 0.74 was obtained in the analysis of the data obtained from 54 samples depending on different parameters. Shagadan et al. [13] used ANN algorithm to estimate the compressive strength values depending on material factors. In the study, the compressive strengths obtained from silica fume with different milling times were predicted. The highest R² value in the study was obtained as 0.61 from the RBF neural network algorithm. Thiyagarajan et al. [14] performed time series analysis for the detection of microbial corrosion due to sewage temperature. They used different algorithms such as ARIMA, Prophet, ETS and Baget. In the 12-hour analysis, the ARIMA model showed the best prediction performance with an MAE of 0.1848 and the ETS model showed the lowest performance with an MAE of 0.1457. Ariza et al. [15] used different algorithms such as ANN, Markov Process, HMMs and Semi-Markov process to predict the deterioration process of infrastructure. As a result of the time series analysis, Semi-Markov process showed the best performance with 0.6086 MAE value and ANN algorithm showed the lowest performance with 0.3154 MAE value. Although models in strength prediction often provide an overview, there is a need for more detailed predictions for specific application conditions. Some earlier models may be sensitive to changes in certain parameters, which may affect the overall prediction accuracy.

To address the shortcomings in the previous literature, this study utilized the ARIMA (1,0,0) model to forecast the mechanical property of a specific geopolymer mortar for a period of 30 days. This study aimed to provide a basis for understanding the effects of specific properties (OB, GW, FA, and HEAT) on strength and to develop more specific prediction models for use in field conditions. The results provide practical guidance to researchers and industry experts who wish to evaluate the long-term performance of geopolymer mortars and optimize the use of the material.

Materials and Methods

Figure 1 demonstrates the comprehensive experimental workflow and analysis of the findings of the study. Distinct types of binders such as obsidian, waste glass and fly ash were mixed with 12 M NaOH and CEN standard sand to obtain geopolymer composite mortar samples. The mortars were kept in the molds for 24 hours under room conditions in order not to deform while the mortars were removed from the mold by taking the required setting. The demoulded specimens were subjected to 4 different temperature cures 75, 90, 105 and 120 °C for 72 hours. Mechanical tests were carried out on certain days to obtain compressive strength values. After obtaining the required results, a dataset was created for forecasting analysis.

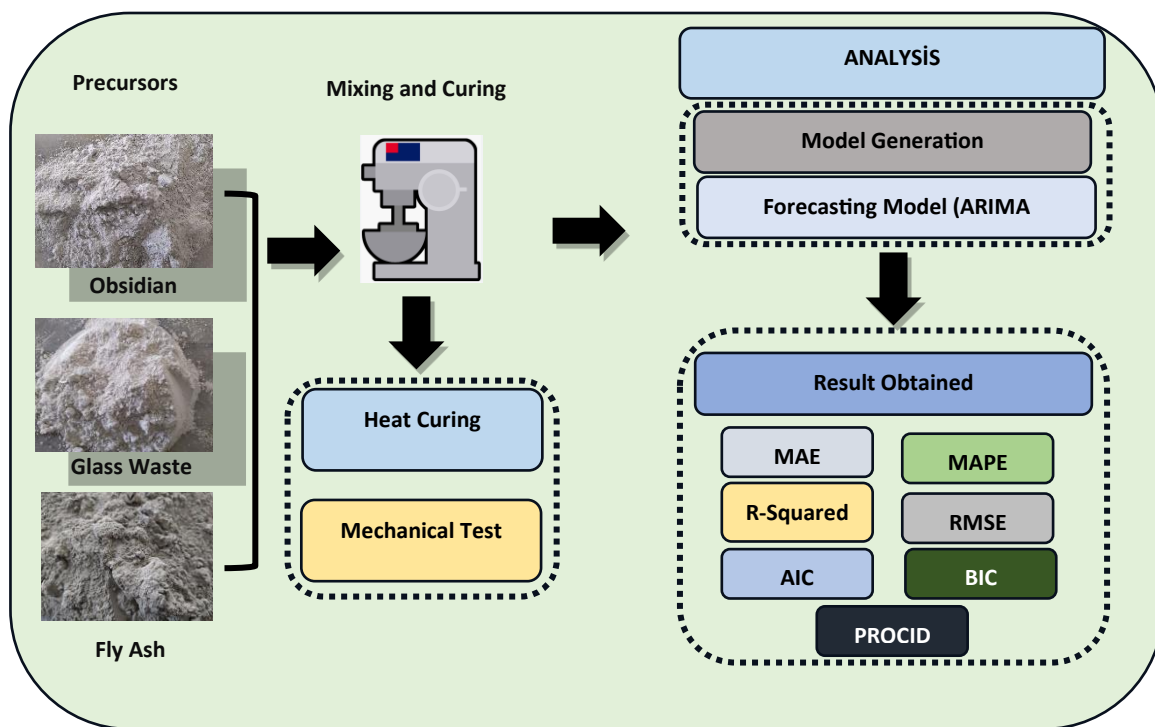


Figure 1. Flow chart of general process

Description of dataset and evaluation metrics

The dataset forms the basis of research focused on forecasting the compressive strength of geopolymer mortar. This dataset contained 88 different samples, and each sample had five different properties. These attributes numerically represent the specific properties and components of the geopolymer mortar. CS (compressive strength) is a numerical variable that signals the compressive strength of a geopolymer mortar. OB is a numerical variable indicating the percentage of obsidian in the geopolymer mortar. GW represents the amount of glass waste in the mortar. FA indicates the fly ash content. Fly ash is a vital factor that affects the chemical composition of mortars. Heat indicates the temperature at which the material is exposed. Temperature is another critical factor that affects the properties of mortar. The days were numerical variables representing the day on which the experiment was performed. In addition, the prediction results were

obtained using the ARIMA (1,0,0) model. The metrics used to evaluate the performance of this model are as follows:

The RMSE (Root Mean Square Error): Determines how much the model's predictions deviate from the actual values. A lower RMSE indicates better forecasting performance. The average of the absolute variations between the actual and anticipated values is known as the mean absolute error, or MAE for short. The average absolute error rate given as a percentage is displayed by the MAPE (Mean Absolute Percentage Error) calculation. PROCID represents the processing time of the prediction model. R² (R-squared) measures how well the model fits. The closer it is to 1, the more successful the model is. AIC (Akaike Information Criterion): It is a criterion that evaluates statistical model quality. Lower AIC values show better models. Bayesian Information Criterion (BIC): Like the AIC, it is a criterion that evaluates model quality. Lower BIC values indicate better models.

This dataset and the forecasting model results provide a valuable resource for understanding the factors affecting the compressive strength of geopolymers and for improving future compressive strength predictions.

Forecasting Method

In this study, the ARIMA (1,0,0) model was used to obtain the 30-day forecasts. Time-series data analysis and value prediction using ARIMA models are robust statistical techniques [16]. In the selection of the ARIMA model, the parameters (p, d, q), autocorrelation, and autocorrelation squared plots were analyzed to determine the trend and stationarity levels in the dataset. Our analyses led to the conclusion that the ARIMA (1,0,0) model was the best fit and can accurately represent the dataset's stationarity levels and has a first-order autoregressive term (AR(1)).

In order to train the ARIMA model, first, the dataset was converted to a format suitable for time-series analysis and the days in the dataset were used as the time-series index. The dataset was then split into training and test datasets at 80% and 20% accuracy, respectively. The ARIMA (1,0,0) model was applied to the training data and the parameters of the model were estimated. Our forecasting model was able to predict future values using the patterns learned from the training data. The performance of the model is evaluated using a test dataset.

Results

This study evaluated the performance of a time-series model for predicting Geopolymer Mortar Compressive Strength (CS). The model was trained using the ARIMA (1,0,0) algorithm. The 30-day forecasting results and performance evaluation metrics of the model are presented below:

Table 1. Performance evaluation results of the time-series analysis

Curing Temperature	RMSE	MAE	MAPE	POCID	R2	AIC	BIC
75 °C	1,207	0,983	0,025	100	0,941	-8,842	-12,8
90 °C	1,237	1,003	0,03	100	0,94	-8,545	-12,5
105 °C	0,739	0,603	0,017	100	0,941	-10,1	-14,1
120 °C	0,254	0,193	0,006	100	0,93	-13,4	-17,3

After the model was successfully trained on the training data, a 30-day forecast was performed. The forecast results are listed in Figure 2.

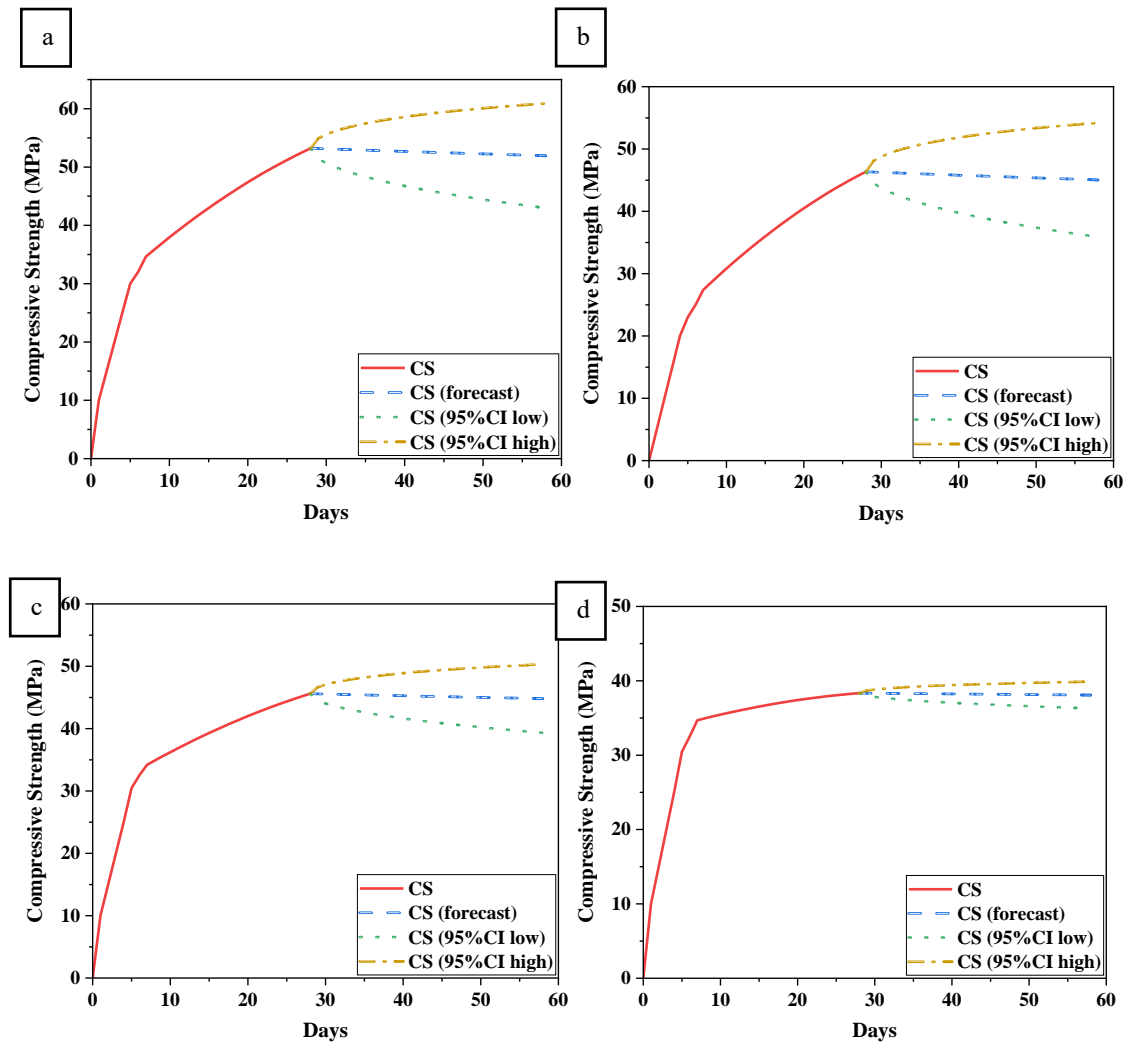


Figure 2. Actual and predicted data plot of geopolymer mortars exposed to various temperatures a) 75 °C, b) 90 °C, c) 105 °C, d) 120 °C.

The evaluation of the model according to the success metrics reveals a very positive result. The high R-squared value shows how well the model explains the data. The RMSE and MAE values indicate how close the model's predictions are to the true values, while the MAPE value measures the percentage error rate. In the structure of the time-series dataset, there are three features ("CS," "OB," "GW," "FA," "HEAT," and "Days") and a target variable ("CS (forecast)"). The data is organized into four sets. CS (forecast) represents the dependent variable that was forecasted.

These results suggest that the ARIMA (1,0,0) model is an effective tool for forecasting Geopolymer Mortar Strength (CS). However, future studies can further examine the reliability of the results obtained by comparing a larger data set and different models.

Discussion

The main purpose of this paper is to examine the 30-day strength prediction using the geopolymer mortar dataset. The ARIMA (1,0,0) model provided an excellent fit with a high R^2 value of 0.941. This shows how well the model fits the actual data set and its predictions are reliable. RMSE and MAE values are quite low (1,207 and 0,254, respectively). This shows how close the model's predictions are to the true values. The AIC and BIC values are -8,8426 and -12,8. Low AIC and BIC values show that the model is appropriate for

explaining the dataset and that adding more complexity is not necessary. MAPE Value was measured at 0,025, which can be considered a low error rate. The PROCID value was measured at 100. The higher value of this metric may indicate that the model may be inadequate in predictions in some cases. This study shows that the model used may be inadequate for certain situations. Future research could consider the use of more complex models or different methods. In order to improve the model's performance and generalizability, a bigger data set might be employed. With an emphasis on the strength predictions generated on the geopolymers mortar dataset, our study looked at the time series model's achievements and shortcomings. Future researchers can use the obtained results as a useful foundation to enhance and expand prediction models in this area.

Conclusion and Future Work

The investigation we conducted attempted to develop a forecasting model used to anticipate geopolymers mortar compressive strength. By applying the ARIMA (1,0,0) model to a dataset of 83 samples, the results obtained included an RMSE of 1.207, MAE of 0.983, MAPE of 0.025, PROCID of 100, and R2 of 0.941. Our findings demonstrated that the ARIMA model developed in this study exhibits high accuracy and efficiency in predicting the compressive strength of geopolymers mortars over a 30-day period. The low RMSE and MAE values indicate that the model's predictions are close to the actual values, while the high R2 value highlights the model's strong explanatory power.

Although this study provides a preliminary step towards predicting the one-month term of the compressive strength of geopolymers mortars, some recommendations for future research are as follows. Using a larger data set can increase the generalization ability of the model and include a wider variety of conditions. In addition to the existing features, adding variables such as environmental factors and weather conditions can improve the model's forecasting ability. These recommendations can guide future researchers to expand knowledge in this area and develop more robust prediction models.

References

- [1] Asadi, Iman, et al. "Phase change materials incorporated into geopolymers concrete for enhancing energy efficiency and sustainability of buildings: a review." *Case Studies in Construction Materials* 17 (2022): e01162.
- [2] Ahmed, Hemn Unis, et al. "Statistical methods for modelling the compressive strength of geopolymers mortar." *Materials* 15.5 (2022): 1868.
- [3] Wu, Yingjie, et al. "Time-Varying Pattern and Prediction Model for Geopolymers Mortar Performance under Seawater Immersion." *Materials* 16.3 (2023): 1244.
- [4] Ardhirra, P. J., and Dhanya Sathyan. "A comparative study of normal and self-compacting geopolymers mortar and its strength prediction using tensor flow approach." *Materials Today: Proceedings* 65 (2022): 1046-1055.
- [5] Manikandan, P., et al. "An Artificial Neural Network Based Prediction of Mechanical and Durability Characteristics of Sustainable Geopolymers Composite." *Advances in Civil Engineering 2022* (2022).
- [6] Dash, P. K., Parhi, S. K., Patro, S. K., & Panigrahi, R. (2023). Influence of chemical constituents of binder and activator in predicting compressive strength of fly ash-based geopolymers concrete using firefly-optimized hybrid ensemble machine learning model. *Materials Today Communications*, 37, 107485.
- [7] Ahmad, A., Ahmad, W., Chaiyasarn, K., Ostrowski, K. A., Aslam, F., Zajdel, P., & Joyklad, P. (2021). Prediction of geopolymers concrete compressive strength using novel machine learning algorithms. *Polymers*, 13(19), 3389.
- [8] Tanyildizi, H. (2021). Predicting the geopolymers process of fly ash-based geopolymers using deep long short-term memory and machine learning. *Cement and Concrete Composites*, 123, 104177.

- [9] Lokuge, W., Wilson, A., Gunasekara, C., Law, D. W., & Setunge, S. (2018). Design of fly ash geopolymer concrete mix proportions using Multivariate Adaptive Regression Spline model. *Construction and Building Materials*, 166, 472-481.
- [10] Kurt, Z., Yilmaz, Y., Cakmak, T., & Ustabas, I. (2023). A novel framework for strength prediction of geopolymer mortar: Renovative precursor effect. *Journal of Building Engineering*, 76, 107041.
- [11] Dao, D. V., Ly, H. B., Trinh, S. H., Le, T. T., & Pham, B. T. (2019). Artificial intelligence approaches for prediction of compressive strength of geopolymer concrete. *Materials*, 12(6), 983.
- [12] Shih-Huang Chen, Cheng-Kai Huang, Dita Adelfani, Yi-Yang Cheng, The preliminary study of the forecasting model between surface texture and various material parameters for the ISO 10844 test track, *Case Studies in Construction Materials*, Volume 19, 2023, e02523, ISSN 2214-5095, <https://doi.org/10.1016/j.cscm.2023.e02523>.
- [13] A. Shaqadan, I. Alshalout, M. Abojaradeh, R. Al-kasasbeh and A. Al-Khatib, "Developing Artificial Neural Networks Model for Concrete Mix Design," 2022 International Engineering Conference on Electrical, Energy, and Artificial Intelligence (EICEEAI), Zarqa, Jordan, 2022, pp. 1-5, doi: 10.1109/EICEEAI56378.2022.10050473
- [14] K. Thiyagarajan, S. Kodagoda ve N. Ulapane, "Beton Kanalizasyon Borusu Yüzey Sıcaklığının Kısa Süreli Zaman Serisi Tahmini", 2020 16. Uluslararası Kontrol, Otomasyon, Robotik ve Görme Konferansı (ICARCV), Shenzhen, Çin, 2020, s. 1194-1199, doi: 10.1109/ICARCV50220.2020.9305439
- [15] Santamaria Ariza M, Zambon I, S. Sousa H, Campos e Matos JA, Strauss A. Comparison of forecasting models topredict concrete bridge decks performance.*Structural Concrete*. 2020;21:1240–1253. <https://doi.org/10.1002/suco.201900434>SANTAMARIA ARIZAET AL.1253
- [16] Shumway, R. H., Stoffer, D. S., Shumway, R. H., & Stoffer, D. S. (2017). ARIMA models. *Time series analysis and its applications: with R examples*, 75-163.

BRAIN TUMOR CLASSIFICATION WITH VISION TRANSFORMERS

Efe Ali ÖZKESİCİ

*İzmir Kâtip Çelebi University, Faculty of Natural and Applied Science, Department of Software Engineering, İzmir – Türkiye,
(Responsible Author) ORCID: 0000-0002-8716-1063*

Assist. Prof. Dr. Osman GÖKALP

*Assist. Prof. Dr., İzmir Kâtip Çelebi University, Faculty of Natural and Applied Science, Department of Software Engineering,
İzmir – Türkiye, ORCID: 0000-0002-7604-8647*

ABSTRACT

Brain tumors stand as complex pathological conditions posing serious threats to human health. The hazardous nature of this disease underscores the importance of early diagnosis and effective treatment. In this context, technological methods offered by modern medicine, particularly advancements in artificial intelligence (AI) and image processing (IP), have made significant strides in the detection of brain tumors. The focal point of this study is to assess the potential of the Vision Transformer (ViT) deep learning model in the context of brain tumor detection. The detection of brain tumors requires precise analysis of complex MRI data, and artificial intelligence has emerged as an effective tool to overcome this challenge. Vision Transformer, distinguished by its ability to process large-scale visual datasets and its learning capacity, is a prominent AI model. This study is designed to evaluate the potential of Vision Transformer in the context of brain tumor detection. Experimental results on a common benchmark dataset show that ViT yields promising results against traditional CNN-based algorithms.

Keywords: Brain Tumor, MRI, Deep Learning, Image Processing, Artificial Intelligence, Vision Transformer

Introduction

Brain tumors are defined as growths of cells in or near the brain. Primary brain tumors originate in the brain, while secondary brain tumors consist of cancer cells spreading from other parts of the body to the brain. Noncancerous or benign brain tumors generally exhibit slow growth, whereas cancerous or malignant tumors tend to grow rapidly. Treatment options depend on the type, size, and location of the tumor; surgery and radiation therapy are commonly employed. Brain tumors can take various forms, with some being cancerous (malignant) and others noncancerous (benign). Symptoms vary depending on the tumor's size and location, encompassing headaches, vision problems, imbalance, and memory issues. Although the cause of brain tumors is often uncertain, factors such as age, race, radiation exposure, and genetic elements are considered risk factors. While there is no preventative measure for brain tumors, individuals at high risk are advised to consider regular screening tests. For several types of brain scans, including magnetic resonance imaging (MRI), well-known machine learning classification techniques have been used (Aldape et al., 2019). Due to the complexity of medical imaging, this topic is still challenging. With the aid of ongoing and upcoming research in this area, we can better understand the course of the disease and create new treatments. Deep learning, a subclass of machine learning, has been used for intelligent systems in many fields, particularly in the processing of medical pictures, and it can handle difficult decision-making tasks (Gassenmaier et al., 2021). Convolutional neural networks have shown promising results for illness diagnosis and organ segmentation (Litjens et al., 2017). CNNs combine the three key phases of a classification job, namely feature extraction, feature selection, and classification, in contrast to conventional machine learning approaches. In automated medical image analysis, convolutional neural networks have achieved major advancements. The Vision Transformer method is based on dividing an image into 16x16 sized pieces and removing their embeddings. Although CNNs have demonstrated success across diverse computer vision tasks and exhibit efficient performance on large-scale datasets, Vision Transformers present distinct advantages in situations where prioritizing global dependencies and fostering contextual understanding are paramount. Vision

Transformers outperform convolutional neural networks (CNN) while using fewer computational resources for training. In this study, we developed a classification model using a vision transformer. The experimental study showed ViT based approaches could be used as a model for automatic detection of brain tumors.

The remainder of this study is organized as follows. In the relevant study section, existing methods and research in the literature on brain tumor detection and classification are reviewed. The next section provides an overview of the entire methodology of this study, including the dataset used and how it was obtained, and how they were used together with ViT. Application details, results and evaluation are discussed in the next section. Results and final thoughts are mentioned in the last section of this article.

Related Works

Kang et al. (2023) presented RCS-YOLO, a rapid and high-accuracy object detector tailored for brain tumor detection. Leveraging the RCS-OSA module, their model exhibited notable performance improvements. The evaluation utilized the 2020 brain tumor dataset (Br35H), demonstrating precision, recall, AP50, AP50:95, FLOPs, and Frames Per Second (FPS) as comparative metrics. The results showcased RCS-YOLO's superiority over state-of-the-art detectors, outperforming YOLOv7 and YOLOv8l in terms of precision, AP50, and FPS, while reducing FLOPs. Additionally, an ablation study emphasized the efficacy of the RCS-OSA module, underscoring its contribution to enhanced accuracy and efficiency.

In another study, Ming Kang (2023) introduced CGFW-YOLOv8 for brain tumor detection, evaluated on the public Br35H dataset. Their model, BGF-YOLO, demonstrated significant improvements over baseline YOLOv8 and competing detectors in terms of precision, recall, and mean average precision (mAP). Ablation studies highlighted the contributions of components like the BRA, GFPN, and the fourth head, showcasing their impact on overall accuracy. Further experiments explored different multiscale feature fusion structures and attention mechanisms, with BGF-YOLO consistently outperforming alternatives. The proposed model's robustness was evident in its choice of regression loss, with CIoU yielding superior results compared to GIoU, DIoU, EIoU, SIoU, and WIoU.

These studies collectively emphasize advancements in object detection techniques tailored specifically for brain tumor detection, with a focus on precision, recall, and overall model efficiency.

Materials and Methods

In this section, the dataset containing brain MRI images is prepared and described for brain tumors. In addition, Vision Transformer explained. After that, how brain tumors can automatically be classified in this study with artificial intelligence is explained with the dataset containing brain MRI images.

Dataset

The dataset used in this study is an open database on Kaggle website (<https://www.kaggle.com/datasets/masoudnickparvar/brain-tumor-mri-dataset>). The dataset contains a total of 3255 images. In this dataset, there are four classes of images. "gomia_tumor", "meningioma_tumor", "no_tumor", "pituitary_tumor". The main purpose of this dataset is to help researchers develop a model with high accuracy to detect and classify the stage brain tumors.

Data Preparation

In the data preparation phase, libraries such as Tensorflow, Matplotlib, NumPy, and Pandas were installed and used. Afterward, paths to the images were identified and constants and seeds were determined for reproducibility. Then, the dataset was split into %80 train and %20 test batches consisting of 4 classes and determined the number of images for each class was. Images were copied and resampled from the train folder and split randomly with equal proportions in each class for the validation folder.

Data Preprocessing

Data was used in grayscale. Data were rescaled to 20x20 with the help of matplotlib. It is shown in Figure 1.

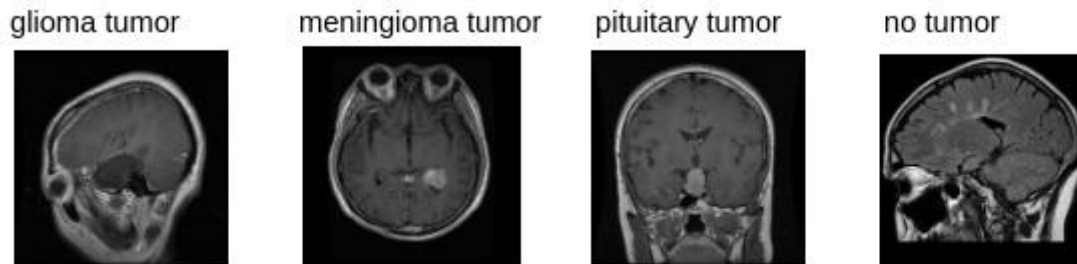


Figure 1. Brain MRI Images

Deep Learning

Deep learning is a subset of machine learning that involves the use of neural networks with multiple layers (deep neural networks) to model and analyze complex patterns in data. It leverages hierarchical representations of features, automatically learning relevant features from raw data without explicit programming. Deep learning algorithms learn to extract hierarchical features through the iterative optimization of model parameters, allowing them to automatically discover intricate patterns and representations in data. The depth of these networks enables them to capture intricate relationships, making deep learning a powerful tool for tasks such as image classification and autonomous decision making. Convolutional Neural Networks (CNNs) are crucial in deep learning for their effectiveness in image-related tasks. By automatically learning hierarchical features from pixel data, CNNs enable the extraction of intricate patterns, revolutionizing image recognition, classification, and other visual data analysis applications.

Vision Transformers

The Vision Transformer (ViT) is a recent breakthrough in computer vision that introduces a paradigm shift from convolutional neural networks (CNNs) to transformer architectures for image classification tasks. While both ViT and traditional CNNs eliminate the need for manually crafted features, ViT distinguishes itself by leveraging a self-attention mechanism to capture global contextual information from the entire image (Dosovitskiy et al., 2020). ViT divides an input image into fixed-size patches, linearly embeds each patch into high-dimensional vectors, and then processes them through a transformer encoder. This enables ViT to efficiently capture long-range dependencies and relationships among image regions. The attention mechanism allows each patch to attend to all other patches, enabling holistic understanding of the image. Pre-trained on large-scale datasets, ViT exhibits remarkable performance on various vision benchmarks, demonstrating its capability to generalize knowledge across diverse visual domains. As a transformer-based architecture, ViT showcases the potential of attention mechanisms beyond natural language processing, marking a significant stride in the fusion of vision and transformer-based models.

Overview of the Developed ViT Model

Patch Encoder using Keras Layer was added to ensure correct encoding of patches used in training. A normalization layer was created from the encoded paths. Multi-head attention layer was created from this created layer. A connection was created between these new layers and patches. Thus, a second layer was created. Normalization was applied to the second layer created and a third layer was created. MLP process was applied to the third layer created. The second and third layers created were added to each other. Normalization and MLP process was applied again to the newly formed layer. Thus, the model is ready for use. You can see the diagram of the model in Figure 2.

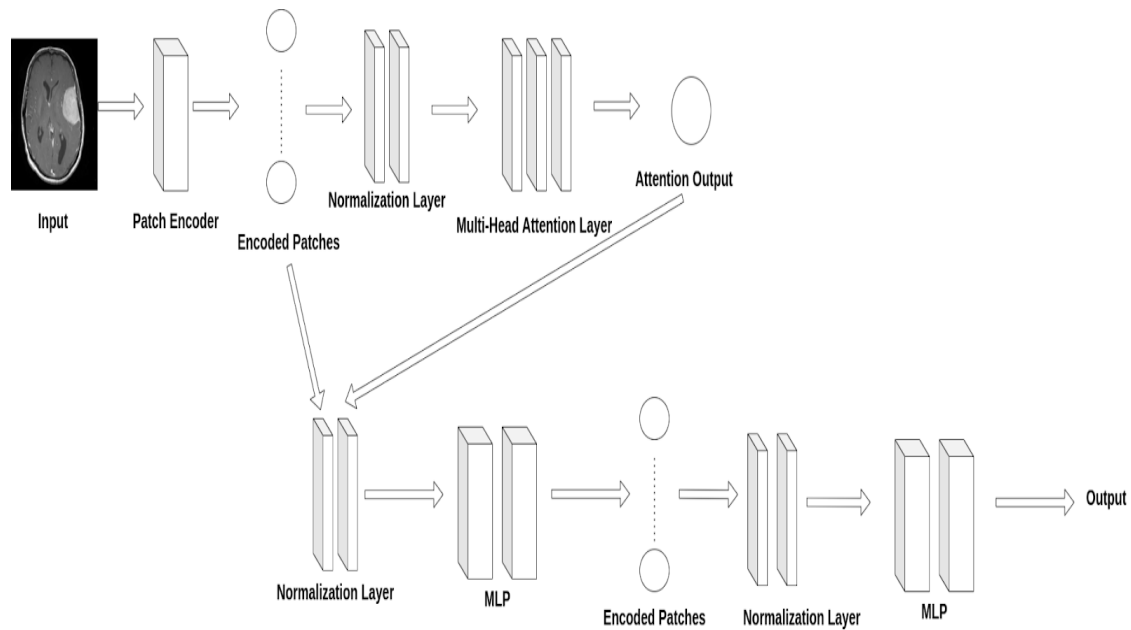


Figure 2. Diagram of ViT Model

Experimental Work

In this section, we evaluate the performance of ViT model with different metrics on dataset containing brain MRI images. During the experiments, the epoch value was set to 10. Data was rescaled to 20x20.

Metrics

The following metrics were used to evaluate the performance of the model described earlier.

- 1) *Accuracy*: It refers to the percentage of test samples that were successfully categorized.
- 2) *F1-score*: Calculating precision and recall is possible using the confusion matrix. After that, the F1-score is calculated as the harmonic mean of recall and precision.
- 3) *Precision*: Precision, on the other hand, shows how many of the values we estimated as positive are positive.

Performance Evaluation

In this section, the results obtained after experimental work is given and compared against other works that used the same dataset. Table 1 outlines the performance results of three models namely, the "ViT Model," "RCS-YOLO," and "BGF-YOLO." Notably, the "ViT Model" emerges as the standout performer, achieving an accuracy of 0.94, an F1-score of 0.947, and a precision of 0.954. These metrics collectively underscore the exceptional capability of the ViT Model in accurate classification, precision, and maintaining a harmonious balance between precision and recall. The ViT Model's robust performance positions it as a compelling choice for tasks requiring comprehensive understanding and precise predictions. In comparison, while "RCS-YOLO" also demonstrates commendable results in accuracy, F1-score, and precision, and "BGF-YOLO" exhibits promising accuracy and precision figures, the absence of F1-score information for the latter calls for careful consideration. The strong showing of the ViT Model across multiple metrics reinforces its effectiveness, making it a noteworthy candidate for applications demanding nuanced and accurate data analysis.

On the other hand, in the scope of this study, an examination was conducted on the outcomes obtained from a Convolutional Neural Network (CNN) model trained on a comparable dataset. The aforementioned model achieved results of 0.91 accuracy, an F-1 score of 0.85, and precision of 0.90 during the training on the same dataset. However, the results obtained from these experiments appear to be lower compared to the training results achieved with the Vision Transformer (ViT). The superior performance of the ViT model, particularly on intricate medical imaging data, underscores its efficacy. These findings suggest that the ViT model could provide a more sensitive and accurate solution for analogous medical imaging tasks. In this model, changes have been made to the fundamental CNN model. In the 9 layer CNN model, there are 14 stages as well as hidden layers that give us the best result in detecting the tumor. The input image first entered the convolution layer with 32 filters, and then entered the batch normalization and max pooling layers, respectively. After these processes, it entered the convolution layer with 64 filters and was processed again in the batch normalization and max pooling layers. After these operations, the flatten process was applied and finally the dense operations containing 512 and 2 layers were performed and the output was created. The diagram presented in Figure 3 is the projected methodology with a short narration.

The results are shown in Table 1.

Base Model Scores for Brain Tumor Detection	Accuracy	F1-Score	Precision
Trained ViT Model	0.94	0.947	0.954
RCS-YOLO	0.930	0.946	0.936
BGF-YOLO	0.974	-	0.919
Trained CNN Model	0.91	0.85	0.90

Table 1. Performance Evaluation Table With Base Model's and CNN Model

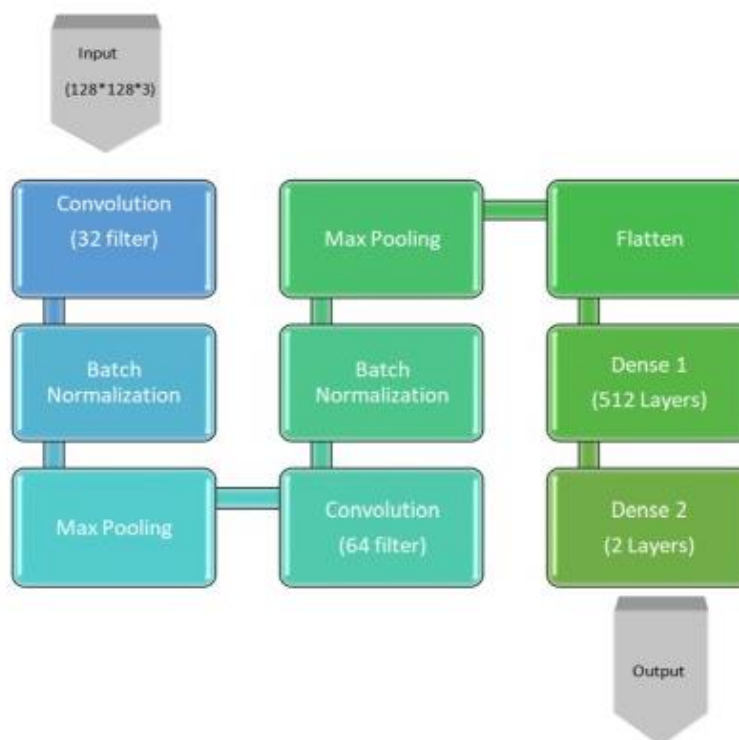


Figure 3. Diagram of Tested CNN Model

Conclusion

In conclusion, this research endeavors to assess the potential of the Vision Transformer (ViT) deep learning model in the domain of brain tumor detection. The ViT model, characterized by its adeptness in processing extensive visual datasets and its capacity for learning, emerges as a noteworthy artificial intelligence paradigm. Notably, ViT excels in highlighting global dependencies and enhancing contextual understanding, outperforming traditional Convolutional Neural Networks (CNNs) by using fewer computational resources.

The experimental findings underscore that ViT-based approaches hold promise for the automatic detection of brain tumors. The ViT Model, showcasing high accuracy, F1 score, and precision, accentuates its proficiency in achieving a harmonious balance between classification, precision, and recall. In comparison with other studies, ViT's robust performance is evident across various metrics.

The success of ViT can be attributed to its unique ability to process an image by dividing it into fixed-size patches and subsequently embedding these patches into high-dimensional vectors. This approach enhances the model's capacity to comprehend long-range dependencies and relationships among different regions of the image. The ViT Model's resilience in dealing with medical imaging complexities positions it as a compelling tool for nuanced and accurate data analysis tasks.

In summary, the ViT Model presents itself as a powerful and effective solution for tasks involving the detection of brain tumors and other complex medical imaging challenges. Future research endeavors may explore additional applications of ViT in diverse medical imaging contexts.

References

- Kenneth Aldape, Kevin M. Brindle, Louis Chesler, Rajesh Chopra, Amar Gajjar, Mark R. Gilbert, Nicholas Gottardo, David H. Gutmann, Darren Hargrave, Eric C. Holland, David T. W. Jones, Johanna A. Joyce, Pamela Kearns, Mark W. Kieran, Ingo K. Mellinghoff, Melinda Merchant, Stefan M. Pfister, Steven M. Pollard, Vijay Ramaswamy, Jeremy N. Rich, Giles W. Robinson, David H. Rowitch, John H. Sampson, Michael D. Taylor, Paul Workman and Richard J. Gilbertson 2019. Challenges To Curing Primary Brain Tumors, pp, 3-6
- Ingo K. Mellinghoff, M.D., Martin J. van den Bent, M.D., Deborah T. Blumenthal, M.D., Mehdi Touat, M.D., Katherine B. Peters, M.D., Jennifer Clarke, M.D., M.P.H., Joe Mendez, M.D., Shlomit Yust-Katz, M.D., Liam Welsh, M.D., Ph.D., Warren P. Mason, M.D., François Ducray, M.D., Yoshie Umemura 2023. Vorasidenib in IDH1- or IDH2-Mutant Low-Grade Glioma
- Alexey Dosovitskiy, Lucas Beyer, Alexander Kolesnikov, Dirk Weissenborn, Xiaohua Zhai, Thomas Unterthiner, Mostafa Dehghani, Matthias Minderer, Georg Heigold, Sylvain Gelly, Jakob Uszkoreit, Neil Houlsby 2020. An Image is Worth 16x16 Words: Transformers for Image Recognition at Scale
- Geert Litjens, Thijs Kooi, Babak Ehteshami Bejnordi, Arnaud Arindra Adiyoso Setio, Francesco Ciompi, Mohsen Ghafoorian, Jeroen A W M van der Laak, Bram van Ginneken, Clara I Sánchez 2017. A Survey On Deep Learning In Medical Image Analysis
- Mohammad Havaei, Axel Davy, David Warde-Farley, Antoine Biardc, Aaron Courvillec, Yoshua Bengio, Chris Palc, Pierre-Marc Jodoina, Hugo Larochellea, 2015. Brain Tumor Segmentation with Deep Neural Networks (BTSWDNN), p, 2-3
- Omid Nejati Manzari, Hamid Ahmadabadi, Hossein Kashiani, Shahriar B. Shokouhi, Ahmad Ayatollahi 2023. MedViT: A Robust Vision Transformer For Generalized Medical Image Classification
- Tahira Shehzadi, Khurram Azeem Hashmi, Didier Stricker, Muhammad Zeshan Afzal 2023. Object Detection With Transformers: A Review(ODWTR), p, 11-13
- Sebastian Gassenmaier, Saif Afat, Dominik Nickel, Mahmoud Mostapha, Judith Herrmann, Ahmed E. Othman 2021. Deep Learning–Accelerated T2-Weighted Imaging of The Prostate: Reduction Of Acquisition Time and Improvement of Image Quality
- Arkapravo Chattopadhyay, Mausumi Maitra 2022. MRI-Based Brain Tumour Image Detection Using CNN Based Deep Learning Method

A PERFORMANCE COMPARISON OF SOME RECENT METAHEURISTICS IN ACCORDANCE WITH DIFFERENT CRITERIA

Murat ASLAN

*Department of Computer Engineering, Faculty of Engineering, Şırnak University, Şırnak, Türkiye (Responsible Author)
ORCID: 0000-0002-7459-3035*

ABSTRACT

Optimization is primarily concerned with finding an optimal solution within a given search space. Optimization problems divided into two major categories: continuous optimization problems and discrete optimization problems. Usually, the first version of the metaheuristic methods is proposed to solve continuous optimization problems. In this study, a performance comparison of the three different recent metaheuristics is presented according to different criteria. These recent metaheuristics are slime mould algorithm (SMA), arithmetic optimization algorithm (AROA), and Archimedes optimization algorithm (AOA). SMA, AOA, and AROA algorithms are implemented on five different unimodal or multimodal benchmark problems such as sphere, rosenbrock, restring, ackley, and griewank problems to demonstrate and validate the effectiveness of the compared methods. The SMA, AOA, and AROA algorithms are compared with respect to various criteria such as population size, problem dimensionality, and stopping criterion. In the experiments, the first step is to examine the size of the population for four different values such as 10, 30, 50, and 100. Then, problem dimensionality is considered for four different values like 10, 30, 50 and 100 for all compared algorithms. Finally, the stopping criterion is chosen as the number of maximum iterations (MaxIter), and it is adjusted to 100, 500, 1000 and 10000 iterations. The SMA, AOA, and AROA algorithms are executed 30 independent runs for each problem, and the algorithms are compared in terms of the Best, Worst, Mean and Standard Division (Std.) criteria. The experimental results and comparisons show that the SMA method provides a better performance than the AOA and AROA methods for the problem considered in this study.

Keywords: Archimedes optimization algorithm, arithmetic optimization algorithm, benchmarks, continuous optimization, slime mould algorithm

1. Introduction

Metaheuristics are very effective methods for solving optimization problems. In addition, metaheuristic methods can be easily adapted to a wide variety of problems, depending on the structure of the problem at hand (Aslan, 2017; Karaboğa, 2011). Therefore, metaheuristic algorithms have been applied to the solution of many problems, such as graph coloring problem (Mahmoudi & Lotfi, 2015; Djelloul, Sabba, & Chikhi, 2014), wind turbine placement problem (Aslan, Gunduz, & Kiran, 2020; Beşkirli et al., 2018; Beşkirli, Koc, & Kodaz, 2019), energy demand forecasting problem (Aslan & Beşkirli, 2022; Özdemir, Dörterler, & Aydın, 2022; Sağlam, Spataru, & Karaman, 2022), urban land readjustment problem (Koc, Atay, & Babaoglu, 2022; Koc & Babaoglu, 2021; Kucukmehmetoglu & Geymen, 2016), 0-1 knapsack problem (Kong et al., 2015; Rizk-Allah & Hassanien, 2018; Xiang et al., 2014; Zhang et al., 2013), feature selection problem (Desuky et al., 2021; Emary, Zawbaa, & Hassanien, 2016; Hancer et al., 2015; Qiao, Peng, & Peng, 2006), community detection problem (Atay, Aslan, & Kodaz, 2018; Koc, 2022), traveling salesman problem (Ahmed; Ouaarab, Ahiod, & Yang, 2014; Gunduz & Aslan, 2021), and so on.

Optimization problems can be divided into two major categories: continuous optimization problems and discrete optimization problems according to the values of the decision variables (Aslan, Gunduz, & Kiran, 2019). Besides, the first version of metaheuristic methods is proposed for solving continuous optimization problems. Metaheuristic algorithms are inspired by the movements that occur in nature in order to achieve the desired goal. Metaheuristics do not guarantee the arrival at the exact solution in the search space. However, they do guarantee reaching a solution that is close to the exact solution, since they guide all

solutions in the solution space (Karaboğa, 2011). Metaheuristic methods are derived from biological, chemical, physical, swarm intelligence, social behavioral, and musical domains. In addition, there are also hybrid algorithms that are created by using some of these algorithms in combination (Aslan, 2017; Akyol & Alataş, 2012; Alataş, 2007).

In this study, three different newly proposed swarm intelligence, evolutionary or phenomena based metaheuristics are analyzed according to the different criteria on benchmark problems. These metaheuristic methods are slime mould algorithm (SMA) (Li et al., 2020), arithmetic optimization algorithm (AROA) (Abualigah et al., 2021), and Archimedes optimization algorithm (AOA) (Hashim et al., 2021). Benchmark problems are frequently used to compare the performance of optimization algorithms. Therefore, to demonstrate the effectiveness of the SMA, AROA, and AOA methods, experiments are conducted on five different unimodal or multimodal benchmark problems, such as the sphere, rosenbrock, restring, ackley, and griewank problems (Surjanovic & Bingham, 2013). The outline of the study is as follows: The basic SMA, AOA, and AROA methods are described in Section 2. The benchmark problems used in this study are explained in Section 3. Experimental results and comparisons of the SMA, AOA, and AROA methods are presented Section 4. And, the conclusions are given in Section 5.

2. Materials and Methods

2.1. Slime Mould Algorithm (SMA)

SMA, which has been proposed by Li et al. (2020), is a new population-based optimization algorithm inspired by the releasing behavior of slime mould (Li et al., 2020). The SMA algorithm has been implemented through the integration of the optimal food path with the help of a positive-negative feedback system. SMA's mathematical model consists of three phases: approach food, wrap food, and grabbing food. In order to find a food position with a better concentration, the slime mould mainly depends on this generated wave (Koc, 2022). The pseudo code of SMA is presented in Algorithm 1 (Koc, 2022).

Algorithm 1. The pseudo code of SMA method

Procedure SMA (population size Npop, maximum iterations MaxIter, X)
 Initialize randomly slime mould population (X)
 iter=1
while iter < MaxIter
 Evaluate the fitness values of all the slime mould
 Update the best fitness, X_{best}
 Calculate the W
for each search portion
 Update p, vb, and vc
 Update positions
end for
 t=t+1;
end while
return X_{best}
end procedure

2.2. Archimedes optimization algorithm (AOA)

The AOA method is a new optimization algorithm in which the population consists of embedded objects. Similar to other metaheuristic algorithms, AOA begins the search process by creating an initial population of objects with random volumes, densities, and accelerations (Koc, 2022; Hashim et al., 2021). The density and volume of each object is updated in every loop. The acceleration of the objects is recalculated and updated, taking into account the collision situation with other adjacent objects. The new position of the object is computed from the reorganized volume, density, and acceleration (Desuky et al., 2021). The pseudo code of AOA is presented in Algorithm 2 (Koc, 2022).

Algorithm 2. The pseudo code of AOA method

Procedure AOA (population size Npop, maximum iterations MaxIter, C₁, C₂, C₃, C₄)
 Generate the initial population randomly
 Calculate the fitness values of the population
 Select the individual with the best fitness in the population
 iter=1
while iter < MaxIter
 for i=1 to Npop
 Update density and volume values of object_i
 Update transfer operator named TO and density
 If TO < 0.5 // **Exploration phase**
 Update acceleration according to the exploration equation and normalize acceleration
 Update position
 else // **Exploitation phase**
 Update acceleration according to the exploitation equation and normalize acceleration
 Update direction flag
 Update position of object_i
 end
 end for
 Calculate the fitness value for each object in the population and choose the best object
 iter= iter+1;
end while
return the best object
end procedure

2.3. Arithmetic Optimization Algorithm (AROA)

AROA is a population based optimization method that depends on the use of arithmetic operations, which can solve optimization problems without computing derivatives (Abualigah et al., 2021). The arithmetic operators used in the AROA method are addition, subtraction, multiplication, and division operators, and these operators are used to obtain the optimal solution from a set of possible solutions. The pseudo code of AROA is presented in Algorithm 3 (Koc, 2022).

Algorithm 5. The pseudo code of AROA method

Procedure AROA (population size Npop, maximum iterations MaxIter, X)
 Initialize randomly population (Npop)
 iter=1
while t < MaxIter
 Evaluate fitness values of Npop
 Set X_{best} as the location of the best solution
 Update MOA (Acceleration ratio) and MOP (probability ratio) values
for i=1 to Npop
 for j=1 to DimSize
 Generate random values between [0, 1] for r1, r2 and r3
 if r1 > MOA // **Exploration Phase**
 if r2 > 0.5
 (1) Apply the division math operator
 Update the ith solutions' jth position using the first rule
 else
 (2) Apply the multiplication math operator
 Update the ith solutions' jth position using the second rule
 end if
 else
 if r3 > 0.5 // **Exploitation Phase**
 (1) Apply the subtraction math operator
 Update the ith solutions' jth position using the first rule
 else
 (2) Apply the addition math operator

```

Update the  $i^{\text{th}}$  solutions'  $j^{\text{th}}$  position using the second rule
end if
end if
end for
end for
t=t+1;
end while
return Xbest
end procedure

```

3. Test Suits

Benchmark problems are frequently used to compare the performance of optimization algorithms. Therefore, in order to show the effectiveness of the SMA, AROA, and AOA methods, in experiments five different unimodal or multimodal benchmark problems, such as the sphere, rosenbrock, restring, ackley, and griewank problems are used (Surjanovic & Bingham, 2013). The explanation of the test problems employed in the study is shown in Table 1.

Table 1. The benchmark problems used in experiments

FN	Function	LB and UB	Mathematical model
F1	Sphere	$[-100,100]^D$	$F(x) = \sum_{i=1}^N x_i^2$
F2	Rosenbrock	$[-30,30]^D$	$F(x) = \sum_{i=1}^{N-1} [100 (x_{i+1} - x_i^2)^2 + (x_i - 1)^2]$
F3	Rastrigin	$[-5.12,5.12]^D$	$F(x) = \sum_{i=1}^N x_i^2 - 10 \cos(2\pi x_i) + 10 * \text{DimSize}$
F4	Ackley	$[-32,32]^D$	$F(x) = 20 + e + -20 \exp \left(-0.2 \sqrt{\frac{1}{N} \sum_{i=1}^N x_i^2} \right) - \exp \left(\frac{1}{N} \sum_{i=1}^N \cos(2\pi x_i) \right)$
F5	Griewank	$[-600,600]^D$	$F(x) = \sum_{i=1}^N \frac{x_i^2}{4000} - \prod_{i=1}^N \cos \left(\frac{x_i}{\sqrt{i}} \right) + 1$

Where, LB represents the lower bound of the related problem, and UB represents the upper bound of the related problem. FN shows the index of the problem, and the mathematical model shows the function of the benchmark problem.

4. Experimental Results

In this study, three different metaheuristic methods such as SMA, AOA and AROA methods are implemented on the benchmark problems with different criteria. SMA, AOA and AROA methods were coded in MATLAB platform. Experiments are performed to compare the AOA, SMA, and AROA methods according to the population (Npop), the problem dimensionality (DimSize), and the stopping criterion (MaxIter). Besides, the compared methods are executed with 30 independent run on the test problems for each criterion. The algorithmic parameters of the AOA, SMA, and AROA methods have been selected in accordance with the original studies. The experiments are reported as the Best, Worst, Mean and Standard Division (Std.) of the fitness values for 30 independent runs.

Table 2. The analysis of population size for compared algorithms

FN Criterion	Npop=10			Npop=30			Npop=50			Npop=100			
	SMA	AOA	AROA	SMA	AOA	AROA	SMA	AOA	AROA	SMA	AOA	AROA	
F1	Best	0.00E+00	2.25E-272	1.30E-109	0.00E+00	7.25E-239	5.19E-279	0.00E+00	5.56E-243	0.00E+00	0.00E+00	4.11E-246	0.00E+00
	Worst	0.00E+00	1.13E-163	3.86E-18	0.00E+00	8.36E-173	1.41E-59	0.00E+00	3.33E-172	4.60E-61	0.00E+00	1.70E-179	0.00E+00
	Mean	0.00E+00	3.87E-165	1.29E-19	0.00E+00	3.31E-174	4.69E-61	0.00E+00	1.11E-173	1.53E-62	0.00E+00	5.67E-181	0.00E+00
	Std.	0.00E+00	0.00E+00	7.05E-19	0.00E+00	0.00E+00	2.57E-60	0.00E+00	0.00E+00	8.41E-62	0.00E+00	0.00E+00	0.00E+00
F2	Best	2.62E+01	2.87E+01	2.79E+01	2.66E+01	2.85E+01	2.75E+01	2.66E+01	2.86E+01	2.68E+01	2.65E+01	2.86E+01	2.63E+01
	Worst	2.84E+01	2.90E+01	2.89E+01	2.79E+01	2.90E+01	2.88E+01	2.76E+01	2.89E+01	2.89E+01	2.75E+01	2.89E+01	2.86E+01
	Mean	2.73E+01	2.89E+01	2.84E+01	2.71E+01	2.88E+01	2.82E+01	2.71E+01	2.88E+01	2.82E+01	2.70E+01	2.88E+01	2.77E+01
	Std.	6.40E-01	6.91E-02	3.36E-01	3.39E-01	1.09E-01	3.49E-01	2.49E-01	9.70E-02	5.06E-01	2.47E-01	1.04E-01	5.05E-01
F3	Best	0.00E+00	0.00E+00	0.00E+00	0.00E+00	0.00E+00	0.00E+00	0.00E+00	0.00E+00	0.00E+00	0.00E+00	0.00E+00	0.00E+00
	Worst	0.00E+00	1.68E+02	0.00E+00	0.00E+00	1.25E+02	0.00E+00	0.00E+00	0.00E+00	0.00E+00	0.00E+00	0.00E+00	0.00E+00
	Mean	0.00E+00	3.03E+01	0.00E+00	0.00E+00	8.02E+00	0.00E+00	0.00E+00	0.00E+00	0.00E+00	0.00E+00	0.00E+00	0.00E+00
	Std.	0.00E+00	6.19E+01	0.00E+00	0.00E+00	3.06E+01	0.00E+00	0.00E+00	0.00E+00	0.00E+00	0.00E+00	0.00E+00	0.00E+00
F4	Best	8.88E-16	8.88E-16	8.88E-16	8.88E-16	8.88E-16	8.88E-16	8.88E-16	8.88E-16	8.88E-16	8.88E-16	8.88E-16	8.88E-16
	Worst	8.88E-16	4.44E-15	8.88E-16	8.88E-16	4.44E-15	8.88E-16	8.88E-16	4.44E-15	8.88E-16	8.88E-16	4.44E-15	8.88E-16
	Mean	8.88E-16	1.24E-15	8.88E-16	8.88E-16	1.24E-15	8.88E-16	8.88E-16	1.95E-15	8.88E-16	8.88E-16	2.66E-15	8.88E-16
	Std.	0.00E+00	1.08E-15	0.00E+00	0.00E+00	1.08E-15	0.00E+00	0.00E+00	1.66E-15	0.00E+00	0.00E+00	1.81E-15	0.00E+00
F5	Best	0.00E+00	0.00E+00	1.95E-02	0.00E+00	0.00E+00	7.03E-04	0.00E+00	0.00E+00	3.90E-03	0.00E+00	0.00E+00	1.97E-10
	Worst	0.00E+00	0.00E+00	7.00E-01	0.00E+00	0.00E+00	2.00E-01	0.00E+00	0.00E+00	2.51E-01	0.00E+00	4.15E-02	8.81E-02
	Mean	0.00E+00	0.00E+00	3.09E-01	0.00E+00	0.00E+00	8.70E-02	0.00E+00	0.00E+00	7.71E-02	0.00E+00	1.38E-03	3.02E-02
	Std.	0.00E+00	0.00E+00	1.96E-01	0.00E+00	0.00E+00	5.55E-02	0.00E+00	0.00E+00	5.14E-02	0.00E+00	7.58E-03	2.63E-02

The first analysis is made for determining the population size criterion. Table 2 presents the Best, Worst, Mean and Std. values of 30 independent runs for the AOA, AROA and SMA algorithms. The population size is analyzed for four different values such as 10, 30, 50, and 100. Furthermore, for this analysis, the DimSize and MaxIter values are set to 30 and 1000, respectively. When Table 2 is examined, it can be seen that for F1, F3, and F5 problems, the SMA methods obtain the best results for each value of the population size. In addition, for the F2 problems, the best fitness value is obtained by the SMA method when the population size is chosen to be 10. However, the best mean and the worst results are obtained by the SMA method when the population size is selected as 100. For F4 problem, all compared algorithms have the same fitness value for each population size value with respect to the best criteria. But when all population size values are taken into account, the comparison methods have their best results when Npop is selected as 100. As a result, the population size is set to 100 for further analysis.

Table 3. The analysis of dimension size for compared algorithms

FN Criterion	DimSize=10			DimSize=30			DimSize=50			DimSize=100			
	SMA	AOA	AROA	SMA	AOA	AROA	SMA	AOA	AROA	SMA	AOA	AROA	
F1	Best	0.00E+00	3.97E-303	0.00E+00	0.00E+00	4.11E-246	0.00E+00	0.00E+00	8.00E-230	1.15E-296	0.00E+00	7.09E-218	8.51E-13
	Worst	0.00E+00	8.66E-228	0.00E+00	0.00E+00	1.70E-179	0.00E+00	0.00E+00	2.92E-167	4.71E-07	0.00E+00	9.55E-155	2.24E-02
	Mean	0.00E+00	2.89E-229	0.00E+00	0.00E+00	5.67E-181	0.00E+00	0.00E+00	9.72E-169	1.57E-08	0.00E+00	3.18E-156	1.12E-02
	Std.	0.00E+00	0.00E+00	0.00E+00	0.00E+00	0.00E+00	0.00E+00	0.00E+00	0.00E+00	8.60E-08	0.00E+00	1.74E-155	6.17E-03
F2	Best	3.94E+00	8.11E+00	3.90E+00	2.65E+01	2.86E+01	2.63E+01	4.76E+01	4.86E+01	4.75E+01	9.80E+01	9.87E+01	9.78E+01
	Worst	4.83E+00	8.86E+00	5.22E+00	2.75E+01	2.89E+01	2.86E+01	4.82E+01	4.89E+01	4.89E+01	9.88E+01	9.89E+01	9.89E+01
	Mean	4.38E+00	8.55E+00	4.57E+00	2.70E+01	2.88E+01	2.77E+01	4.79E+01	4.88E+01	4.84E+01	9.84E+01	9.88E+01	9.87E+01
	Std.	2.28E-01	1.61E-01	3.31E-01	2.47E-01	1.04E-01	5.05E-01	1.61E-01	9.17E-02	2.99E-01	1.53E-01	7.05E-02	2.61E-01
F3	Best	0.00E+00	0.00E+00	0.00E+00	0.00E+00	0.00E+00	0.00E+00	0.00E+00	0.00E+00	0.00E+00	0.00E+00	0.00E+00	0.00E+00
	Worst	0.00E+00	8.28E+00	0.00E+00	0.00E+00	0.00E+00	0.00E+00	0.00E+00	0.00E+00	0.00E+00	0.00E+00	0.00E+00	0.00E+00
	Mean	0.00E+00	2.76E-01	0.00E+00	0.00E+00	0.00E+00	0.00E+00	0.00E+00	0.00E+00	0.00E+00	0.00E+00	0.00E+00	0.00E+00
	Std.	0.00E+00	1.51E+00	0.00E+00	0.00E+00	0.00E+00	0.00E+00	0.00E+00	0.00E+00	0.00E+00	0.00E+00	0.00E+00	0.00E+00
F4	Best	8.88E-16	8.88E-16	8.88E-16	8.88E-16	8.88E-16	8.88E-16	8.88E-16	8.88E-16	8.88E-16	8.88E-16	8.88E-16	8.88E-16
	Worst	8.88E-16	4.44E-15	8.88E-16	8.88E-16	4.44E-15	8.88E-16	8.88E-16	4.44E-15	8.88E-16	8.88E-16	4.44E-15	8.88E-16
	Mean	8.88E-16	1.36E-15	8.88E-16	8.88E-16	2.66E-15	8.88E-16	8.88E-16	2.78E-15	8.88E-16	8.88E-16	3.02E-15	8.88E-16
	Std.	0.00E+00	1.23E-15	0.00E+00	0.00E+00	1.81E-15	0.00E+00	0.00E+00	1.80E-15	0.00E+00	0.00E+00	1.77E-15	0.00E+00
F5	Best	0.00E+00	0.00E+00	0.00E+00	0.00E+00	0.00E+00	1.97E-10	0.00E+00	0.00E+00	1.07E-01	0.00E+00	0.00E+00	3.28E+00
	Worst	0.00E+00	6.08E-01	0.00E+00	0.00E+00	4.15E-02	8.81E-02	0.00E+00	0.00E+00	5.31E-01	0.00E+00	0.00E+00	1.04E+02
	Mean	0.00E+00	8.24E-02	0.00E+00	0.00E+00	1.38E-03	3.02E-02	0.00E+00	0.00E+00	3.10E-01	0.00E+00	0.00E+00	3.46E+01
	Std.	0.00E+00	1.61E-01	0.00E+00	0.00E+00	7.58E-03	2.63E-02	0.00E+00	0.00E+00	9.89E-02	0.00E+00	0.00E+00	2.77E+01

The second analysis is made for determining the value of DimSize. The Best, Worst, Mean and Std. values of 30 independent runs for the AOA, AROA and SMA methods are given in Table 3. The DimSize value is analyzed for four different values such as 10, 30, 50, and 100. In addition, for this analysis, the Npop and MaxIter values are set to 100 and 1000, respectively. Looking at Table 3, we can see that for F1, F3, and F5 problems, the SMA methods give the best results for each value of the DimSize. Furthermore, the best mean and the worst results for the F2 problem are obtained by the SMA method when the DimSize value is set to 10. However, for the F2 problems, the best fitness value is obtained by the AROA method when the DimSize value is selected as 10. For F4 problem, all compared algorithms have the same fitness value for each DimSize value with respect to the best criteria. However, when all DimSize values are considered, the comparison methods have their best results when DimSize is set to 10.

The final analysis is performed to determine the value of the MaxIter parameter. The Best, Worst, Mean and Std. values of 30 independent runs for the AOA, AROA and SMA methods are presented in Table 4. The MaxIter parameter is analyzed for four different values such as 100, 500, 1000, and 10000. In addition, for this analysis, the Npop and DimSize parameters are set to 100 and 30, respectively. According to the Table 4, it is seen that for F1, F3, and F5 problems, the SMA methods obtain the optimal results for each value of the MaxIter. In addition, for F2 problem, the best, mean, worst results are obtained by the SMA method when the MaxIter parameter is set to 10000. On the F4 problem, all compared algorithms obtain the same fitness value on each MaxIter parameter in terms of the best criterion. However, when all MaxIter values are considered, the comparison methods have their best results when MaxIter parameter is selected as 10000.

Table 4. The analysis of the stopping criterion for compared algorithms

FN	Criterion	MaxIter=100			MaxIter=500			MaxIter=1000			MaxIter=10000		
		SMA	AOA	AROA	SMA	AOA	AROA	SMA	AOA	AROA	SMA	AOA	AROA
F1	Best	0.00E+00	1.75E-21	7.85E-99	0.00E+00	3.89E-125	0.00E+00	0.00E+00	4.11E-246	0.00E+00	0.00E+00	0.00E+00	0.00E+00
	Worst	0.00E+00	8.15E-15	7.35E-15	0.00E+00	2.63E-89	3.85E-81	0.00E+00	1.70E-179	0.00E+00	0.00E+00	0.00E+00	0.00E+00
	Mean	0.00E+00	7.99E-16	2.46E-16	0.00E+00	1.53E-90	1.28E-82	0.00E+00	5.67E-181	0.00E+00	0.00E+00	0.00E+00	0.00E+00
	Std.	0.00E+00	1.92E-15	1.34E-15	0.00E+00	5.88E-90	7.03E-82	0.00E+00	0.00E+00	0.00E+00	0.00E+00	0.00E+00	0.00E+00
F2	Best	2.81E+01	2.85E+01	2.79E+01	2.72E+01	2.86E+01	2.67E+01	2.65E+01	2.86E+01	2.63E+01	2.24E+01	2.81E+01	2.46E+01
	Worst	2.89E+01	2.89E+01	2.89E+01	2.81E+01	2.89E+01	2.85E+01	2.75E+01	2.89E+01	2.86E+01	2.33E+01	2.89E+01	2.67E+01
	Mean	2.86E+01	2.87E+01	2.86E+01	2.76E+01	2.87E+01	2.80E+01	2.70E+01	2.88E+01	2.77E+01	2.29E+01	2.87E+01	2.54E+01
	Std.	1.55E-01	1.00E-01	2.33E-01	2.26E-01	9.27E-02	3.78E-01	2.47E-01	1.04E-01	5.05E-01	1.98E-01	1.68E-01	4.91E-01
F3	Best	0.00E+00	0.00E+00	0.00E+00	0.00E+00	0.00E+00	0.00E+00	0.00E+00	0.00E+00	0.00E+00	0.00E+00	0.00E+00	0.00E+00
	Worst	0.00E+00	2.19E+02	0.00E+00	0.00E+00	0.00E+00	0.00E+00	0.00E+00	0.00E+00	0.00E+00	0.00E+00	2.25E+01	0.00E+00
	Mean	0.00E+00	4.51E+01	0.00E+00	0.00E+00	0.00E+00	0.00E+00	0.00E+00	0.00E+00	0.00E+00	0.00E+00	7.51E-01	0.00E+00
	Std.	0.00E+00	7.23E+01	0.00E+00	0.00E+00	0.00E+00	0.00E+00	0.00E+00	0.00E+00	0.00E+00	0.00E+00	4.11E+00	0.00E+00
F4	Best	8.88E-16	1.08E-11	8.88E-16	8.88E-16	8.88E-16	8.88E-16	8.88E-16	8.88E-16	8.88E-16	8.88E-16	8.88E-16	8.88E-16
	Worst	8.88E-16	1.72E-08	8.88E-16	8.88E-16	7.99E-15	8.88E-16	8.88E-16	4.44E-15	8.88E-16	8.88E-16	4.44E-15	8.88E-16
	Mean	8.88E-16	1.49E-09	8.88E-16	8.88E-16	3.97E-15	8.88E-16	8.88E-16	2.66E-15	8.88E-16	8.88E-16	1.01E-15	8.88E-16
	Std.	0.00E+00	3.22E-09	0.00E+00	0.00E+00	1.54E-15	0.00E+00	0.00E+00	1.81E-15	0.00E+00	0.00E+00	6.49E-16	0.00E+00
F5	Best	0.00E+00	0.00E+00	2.09E-02	0.00E+00	0.00E+00	8.95E-08	0.00E+00	0.00E+00	1.97E-10	0.00E+00	0.00E+00	0.00E+00
	Worst	0.00E+00	1.42E-01	7.73E-01	0.00E+00	0.00E+00	2.83E-01	0.00E+00	4.15E-02	8.81E-02	0.00E+00	0.00E+00	7.84E-02
	Mean	0.00E+00	8.55E-03	2.68E-01	0.00E+00	0.00E+00	6.85E-02	0.00E+00	1.38E-03	3.02E-02	0.00E+00	0.00E+00	1.15E-02
	Std.	0.00E+00	3.27E-02	1.73E-01	0.00E+00	0.00E+00	7.61E-02	0.00E+00	7.58E-03	2.63E-02	0.00E+00	0.00E+00	1.69E-02

5. Conclusions

This study is concerned with the comparison of some newly proposed metaheuristic methods such as SMA, AOA and AROA methods in terms of different criteria. SMA, AOA and AROA methods are population-based stochastic optimization algorithms. Typically, the first version of metaheuristic algorithms is proposed to solve continuous optimization problems. Hereby, SMA, AOA and AROA methods were proposed in literature for solving continuous optimization problems. Benchmark problems are often used to compare the performance of optimization algorithms. Therefore, in this study, five different unimodal or multimodal benchmark problems are used in experiments to show the effectiveness of the SMA, AROA, and AOA methods. In experiments, SMA, AOA, and AROA algorithms are compared in terms of various criteria such as population size, problem dimensionality, and stopping criterion. The SMA, AOA, and AROA algorithms are executed 30 independent runs for each problem, and the algorithms are compared in terms of the Best, Worst, Mean and Standard Division (Std.) criteria. According to the experimental results, continuously increasing the number of individuals in the population did not have much effect on the performance of the algorithms after a certain point. In addition, When the dimensionality of the problems is taken into account, the optimal solution becomes more difficult to find as the number of dimensions of the problem increases. Finally, when the stopping criterion values are evaluated, increasing the number of iterations allows more search operations to be performed in the search space, thus increasing the likelihood of finding better solutions. When all experiments and analysis are considered, it can be seen that SMA method provides a better performance than the AOA and AROA methods in terms of the solution quality and robustness.

References

- Aslan, M. (2017). *An approach based on shuffled frog leaping algorithm for vertex coloring problem in graphs*, Selcuk University].
- Karaboğa, D. (2011). *Yapay Zekâ Optimizasyon Algoritmaları* (pp. 244). Nobel Yayın Dağıtım.

- Mahmoudi, S., & Lotfi, S. (2015). Modified cuckoo optimization algorithm (MCOA) to solve graph coloring problem. *Applied Soft Computing*, 33, 48-64.
- Djelloul, H., Sabba, S., & Chikhi, S. (2014). Binary bat algorithm for graph coloring problem. (Ed.),^(Eds.). Complex Systems (WCCS), 2014 Second World Conference on.
- Aslan, M., Gunduz, M., & Kiran, M. S. (2020). A Jaya-based approach to wind turbine placement problem. *Energy Sources, Part A: Recovery, Utilization, and Environmental Effects*, 1-20.
- Beşkirli, M., Koç, İ., Haklı, H., & Kodaz, H. (2018). A new optimization algorithm for solving wind turbine placement problem: Binary artificial algae algorithm. *Renewable energy*, 121, 301-308.
- Beşkirli, M., Koc, I., & Kodaz, H. (2019). Optimal placement of wind turbines using novel binary invasive weed optimization. *Tehnički vjesnik*, 26(1), 56-63.
- Aslan, M., & Beşkirli, M. (2022). Realization of Turkey's energy demand forecast with the improved arithmetic optimization algorithm. *Energy Reports*, 8, 18-32.
- Özdemir, D., Dörterler, S., & Aydın, D. (2022). A new modified artificial bee colony algorithm for energy demand forecasting problem. *Neural Computing and Applications*, 34(20), 17455-17471.
- Saglam, M., Spataru, C., & Karaman, O. A. (2022). Electricity Demand Forecasting with Use of Artificial Intelligence: The Case of Gokceada Island. *Energies*, 15(16), 5950.
- Koc, I., Atay, Y., & Babaoglu, I. (2022). Discrete tree seed algorithm for urban land readjustment. *Engineering Applications of Artificial Intelligence*, 112, 104783.
- Koc, I., & Babaoglu, I. (2021). A comparative study of swarm intelligence and evolutionary algorithms on urban land readjustment problem. *Applied Soft Computing*, 99, 106753.
- Kucukmehmetoglu, M., & Geymen, A. (2016). Optimization models for urban land readjustment practices in Turkey. *Habitat international*, 53, 517-533.
- Kong, X., Gao, L., Ouyang, H., & Li, S. (2015). A simplified binary harmony search algorithm for large scale 0–1 knapsack problems. *Expert Systems with Applications*, 42(12), 5337-5355.
- Rizk-Allah, R. M., & Hassanien, A. E. (2018). New binary bat algorithm for solving 0–1 knapsack problem. *Complex & Intelligent Systems*, 4(1), 31-53.
- Xiang, W.-l., An, M.-q., Li, Y.-z., He, R.-c., & Zhang, J.-f. (2014). A novel discrete global-best harmony search algorithm for solving 0-1 knapsack problems. *Discrete Dynamics in Nature and Society*, 2014, 1-12.
- Zhang, X., Huang, S., Hu, Y., Zhang, Y., Mahadevan, S., & Deng, Y. (2013). Solving 0-1 knapsack problems based on amoeboid organism algorithm. *Applied Mathematics and Computation*, 219(19), 9959-9970.
- Desuky, A. S., Hussain, S., Kausar, S., Islam, M. A., & El Bakrawy, L. M. (2021). EAOA: an enhanced archimedes optimization algorithm for feature selection in classification. *IEEE Access*, 9, 120795-120814.
- Emary, E., Zawbaa, H. M., & Hassanien, A. E. (2016). Binary grey wolf optimization approaches for feature selection. *Neurocomputing*, 172, 371-381.
- Hancer, E., Xue, B., Karaboga, D., & Zhang, M. (2015). A binary ABC algorithm based on advanced similarity scheme for feature selection. *Applied Soft Computing*, 36(Supplement C), 334-348. <https://doi.org/https://doi.org/10.1016/j.asoc.2015.07.023>
- Qiao, L.-Y., Peng, X.-Y., & Peng, Y. (2006). BPSO-SVM wrapper for feature subset selection. *ACTA ELECTONICA SINICA*, 34(3), 496.
- Atay, Y., Aslan, M., & Kodaz, H. (2018). A swarm intelligence-based hybrid approach for identifying network modules. *Journal of computational science*, 28, 265-280.
- Koc, I. (2022). A fast community detection algorithm based on coot bird metaheuristic optimizer in social networks. *Engineering Applications of Artificial Intelligence*, 114, 105202.
- Ahmed, Z. H. Genetic Algorithm for the Traveling Salesman Problem using Sequential Constructive Crossover Operator. *International Journal of Biometrics & Bioinformatics (IJBB)*, 3(6).

- Ouaarab, A., Ahiod, B., & Yang, X.-S. (2014). Discrete cuckoo search algorithm for the travelling salesman problem. *Neural Computing and Applications*, 24(7-8), 1659-1669.
- Gunduz, M., & Aslan, M. (2021). DJAYA: A discrete Jaya algorithm for solving traveling salesman problem. *Applied Soft Computing*, 105, 107275.
- Aslan, M., Gunduz, M., & Kiran, M. S. (2019). JayaX: Jaya algorithm with xor operator for binary optimization. *Applied Soft Computing*, 82, 105576.
- Akyol, S., & Alataş, B. (2012). Güncel Sürü Zekâsı Optimizasyon Algoritmaları. *Nevşehir Üniversitesi Fen Bilimleri Enstitü Dergisi*, 1, 36-50.
- Alataş, B. (2007). *Kaotik Haritalı Parçacık Sürü Optimizasyon Algoritmaları Geliştirme*, Fırat Üniversitesi].
- Li, S., Chen, H., Wang, M., Heidari, A. A., & Mirjalili, S. (2020). Slime mould algorithm: A new method for stochastic optimization. *Future Generation Computer Systems*, 111, 300-323.
- Abualigah, L., Diabat, A., Mirjalili, S., Abd Elaziz, M., & Gandomi, A. H. (2021). The arithmetic optimization algorithm. *Computer methods in applied mechanics and engineering*, 376, 113609.
- Hashim, F. A., Hussain, K., Houssein, E. H., Mabrouk, M. S., & Al-Atabany, W. (2021). Archimedes optimization algorithm: a new metaheuristic algorithm for solving optimization problems. *Applied Intelligence*, 51(3), 1531-1551.
- Surjanovic, S., & Bingham, D. (2013). Virtual library of simulation experiments: test functions and datasets. *Simon Fraser University, Burnaby, BC, Canada, accessed May, 13, 2015.*

AI-BASED ANALYSIS OF SOCIOECONOMIC AND ETHNIC INFLUENCES ON STUDENT PERFORMANCE

Mahmut DİRİK

Faculty of Engineering, Department of Computer Engineering, Sirnak University, Şırnak, Türkiye

ABSTRACT

This research article addresses the construction of a machine learning model to study and improve student academic performance, examining the role of demographic variables. The article highlights the need for data-centered approaches in educational analysis and policy formulation. It emphasizes the potential of machine learning in identifying and mitigating factors that are detrimental to academic success, thus promoting equitable educational practices. Furthermore, the article emphasizes the importance of predictive analytics in tailoring educational experiences and highlights the revolutionary impact of technological advancement in the education sector.

Keywords: Academic Performance, Educational Equity, Student Success Monitoring, Educational Outcomes

1. Introduction

In the evolving landscape of educational advancement, the transformative role of machine learning and data-driven strategies is revolutionizing our approach to enhancing student academic performance. This article delves into a comprehensive case study employing machine learning models to dissect and interpret the myriad of variables impacting students' academic outcomes. By harnessing the robust capabilities of data analytics, the study not only elucidates the factors detrimentally affecting student success but also paves the way for the establishment of more equitable and personalized educational methodologies [1]–[3] [4], [5].

Embracing Data-Driven Education

Central to this exploration is the meticulous construction of a state-of-the-art machine learning model, specifically tailored to scrutinize and bolster student academic performance. Utilizing the extensive data encapsulated in the “StudentsPerformance.csv” file, the study meticulously analyzes a spectrum of demographic variables, including gender, race/ethnicity, and parental education levels. These variables are pivotal, offering profound insights into the intricate nexus between diverse demographic attributes and academic achievement. The research emphasizes the quintessence of a data-centric approach in crafting educational strategies and policies. It champions the integration of comprehensive data analysis, aiming to reveal underlying patterns and trends critically influencing student success [1], [6]–[8].

Harnessing Predictive Analytics for Tailored Education

Predictive analytics stands at the forefront of this narrative, transcending beyond merely mapping the current educational terrain to envisaging future educational trajectories and necessities. The machine learning model emerges as an instrumental tool in personalizing educational experiences, meticulously calibrated to resonate with the distinct needs and potential of each student. This paradigm shift is vital in transcending conventional, uniform teaching methodologies, ushering in a learning environment that is more adaptable, responsive, and efficacious [6], [7], [9].

Practical Applications and Futuristic Outlook

The capabilities of the model extend to providing actionable insights, enabling educators to proactively and effectively shape educational interventions. This integration of machine learning into educational frameworks exemplifies the potential of technology in revolutionizing learning experiences, making them more inclusive and attuned to the varied needs of a diverse student population [10], [11].

Conclusively, this study not only reaffirms the pivotal impact of technological advancements, particularly machine learning and advanced analytics, in the education sector but also heralds a future where education is intrinsically interlinked with innovation. The ramifications of this technology transcend the traditional boundaries of educational settings, heralding a new epoch marked by inclusivity, adaptability, and heightened efficacy. Standing at the threshold of this educational revolution, the integration of machine learning models, as exemplified in this article, signifies a crucial stride towards a more informed, data-driven, and equitable educational future.

2. Material and Methods

2.1 Data Source

The primary data source for this study is the data set [12], which includes a variety of variables related to student academic performance. This data set includes demographic information, parents' education level, lunch type, test preparation courses, and students' maths, reading, and writing scores.

2.2 Data Description

In order to effectively convey the characteristics of the data set used in this study, a structured table is presented. This table methodically describes the key attributes of the data and provides essential information about each variable. Included in this presentation are the names of the variables, their respective types (categorical or numeric) and brief descriptions for each variable. This format ensures a clear and comprehensive understanding of the data elements underlying the analysis.

Table 1. Data Description Table [12]

<i>Variable Name</i>	<i>Type</i>	<i>Description</i>
Gender	Categorical	The gender of the student (Male/Female).
Race/Ethnicity	Categorical	Categorized into groups (e.g., Group A, Group B, etc.).
Parental Level of Education	Categorical	Includes categories like bachelor's degree, some college, etc.
Lunch	Categorical	Type of lunch (Standard or Free/Reduced).
Test Preparation Course	Categorical	Indicates if the student completed a test preparation course.
Math Score	Numerical	Numeric score in the mathematics test.
Reading Score	Numerical	Numeric score in the reading test.
Writing Score	Numerical	Numeric score in the writing test.

2.3 Software and Tools

The analyses were carried out using statistical software and programming languages suitable for data analysis, such as Python with libraries like pandas, NumPy and scikit-learn.

By utilizing these methods, the study aimed to provide a comprehensive insight into the factors that influence student achievement and provide evidence-based recommendations for educational strategies and policies.

2.4 Data Visualization

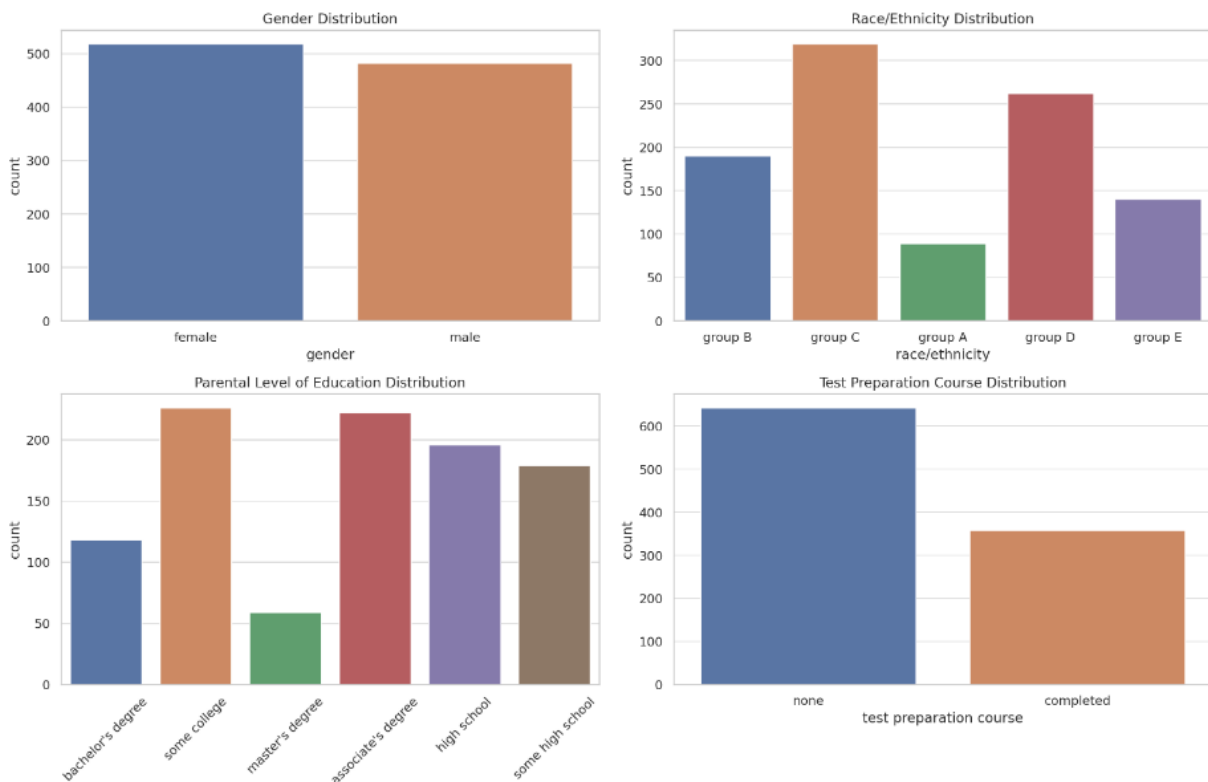


Figure 1. The visualizations of a revealing overview of the attributes of the dataset

The visualizations above provide an insightful overview of the dataset's attributes:

- **Gender Distribution:** This chart shows the distribution of students by gender, providing a clear visual representation of the male-to-female ratio in the dataset.
- **Race/Ethnicity Distribution:** This graph depicts the diversity of the student population in terms of race/ethnicity, categorized into different groups.
- **Parental Level of Education Distribution:** This chart illustrates the range of parental education levels, from high school to master's degree, offering insight into the educational background of the students' families.
- **Test Preparation Course Distribution:** This plot reveals the proportion of students who completed a test preparation course versus those who did not, highlighting the engagement in preparatory activities for the tests.

These visualizations form a crucial part of the data analysis, as they provide a foundational understanding of the demographic and academic landscape within which the student performance is evaluated.

2.5 Data Correlation Analysis

The correlation matrix is an important tool for understanding the relationships between the various academic outcomes within the data set, with a focus on student outcomes in math, reading and writing. This matrix represents a statistical analysis that quantifies the extent to which these academic outcomes are related. Each cell in the matrix shows the correlation coefficient between two subjects and provides insight into how one outcome might predict or be related to another. A higher correlation coefficient indicates a stronger relationship between the scores, meaning that a high performance in one subject is often reflected by a high performance in another subject. A lower coefficient, on the other hand, indicates a weaker correlation. Such a matrix is helpful in identifying patterns and potential areas for targeted educational intervention.

Table 2. Correlation Matrix of Student Score

The key findings from this matrix are as follows:

Math and reading achievement: There is a moderately strong positive correlation between math and reading scores. This suggests that students who perform well in math also perform well in reading, even if the correlation is not extremely strong.

Results in math and writing: A similar moderately strong positive correlation is observed between math and writing scores. This indicates that students who perform well in math also perform well in writing.

Results in reading and writing: There is a very strong positive correlation between results in reading and writing. This is the strongest correlation observed in the data set, suggesting that students' performance in reading and writing are closely linked, with high-performing students in one subject likely to perform well in the other.

These correlations are important as they suggest that the skills required for success in these subjects may be linked. For example, strong reading skills could contribute to better performance in writing and vice versa. The moderate correlation between math and the other two subjects (reading and writing) could indicate a different set of skills or abilities that influence performance in math compared to reading and writing.

2.6 Kernel Density Estimate (KDE)

Kernel density estimation (KDE) [13] is a basic statistical tool for estimating the probability density function of a continuous random variable. In the context of analyzing student achievement data, KDE provides a smooth, continuous visualization of the distribution of grades in subjects such as mathematics, reading and writing.

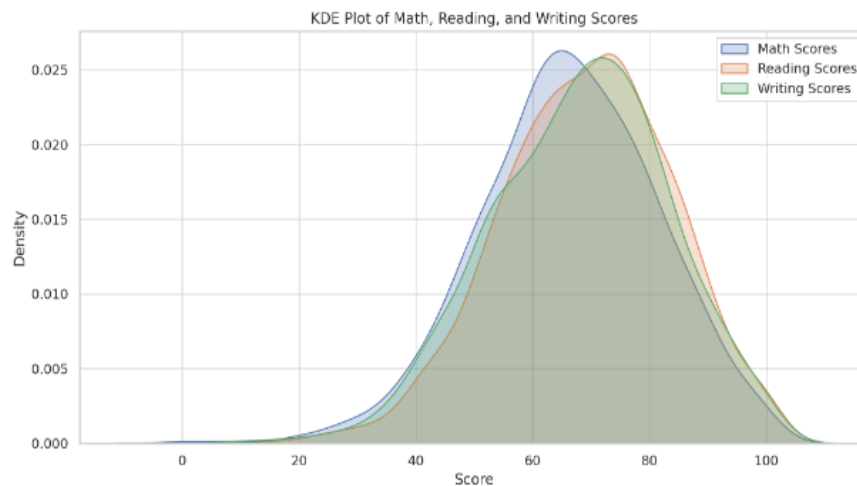


Figure 2. Kernel Density Estimate plot.

Figure 2 visualizes the distribution of math, reading and writing scores among students in the data set:

- **Math Scores:** The distribution of math results shows a reasonably normal distribution with a peak indicating the most common range of results. There appears to be a slight skew towards the lower range.
- **Reading results:** The reading results also show a near normal distribution. Compared to the math results, the peak in reading results is slightly higher, indicating a concentration of students in this area.
- **Writing results:** Similar to the reading results, the writing results also show a normal distribution with a clear peak. The distribution of the writing results is very similar to that of the reading results, which emphasizes the strong correlation between these two subjects found in the correlation analysis.

These KDE charts provide a visual representation of the distribution of student results in math, reading and writing. They show that while there is a general tendency for students to cluster around certain score ranges in each subject, there are also notable differences as shown by the breadth of the distributions. The similarity in the distribution patterns of the results for reading and writing is consistent with the high correlation between these two subjects.

3. Results and Findings

From the extensive analysis conducted in this study, several important conclusions can be drawn regarding the effectiveness of different machine learning algorithms in predicting and classifying student performance in math. In the study, a robust dataset was used to critically evaluate five different machine learning models: Logistic Regression, Random Forest Classifier, Naive Bayes, Gradient Boosting Classifier and MLP Classifier. Each model was thoroughly analyzed for its efficiency in classifying high and low performing students in mathematics.

The results resulting from the application of different machine learning models in this study are presented in a series of tables and diagrams. These visual representations play a crucial role in communicating the effectiveness and comparative performance of the models in classifying students based on their mathematical ability.

3.1. Performance Metrics

Table 3. Performance Metrics Table

Model	Accuracy	Precision	Recall	F1 Score	ROC AUC Score	Specificity
Logistic Regression	77.67%	72.97%	68.64%	70.74%	76.08%	83.52%
Random Forest Classifier	78.33%	76.24%	65.25%	70.32%	76.03%	86.81%
Naive Bayes	78.33%	70.87%	76.27%	73.47%	77.97%	79.67%
Gradient Boosting Classifier	79.33%	77.45%	66.95%	71.82%	77.16%	87.36%
MLP Classifier	64.00%	52.55%	87.29%	65.61%	68.09%	48.90%

This table systematically lists the key performance indicators such as accuracy, precision, recall, F1 score, ROC, [14], [15] score and specificity for each model. It provides a clear, numerical representation of each model's performance in relation to these metrics and allows for easy comparison between models.

Accuracy: Determined by $(TP + TN) / (TP + TN + FP + FN)$. It represents the overall correctness of the model [16].

Precision: Given by $TP / (TP + FP)$. It indicates the accuracy of the positive predictions [15].

Recall (sensitivity): Calculated as $TP / (TP + FN)$. It indicates the ability of the model to identify all relevant instances [17].

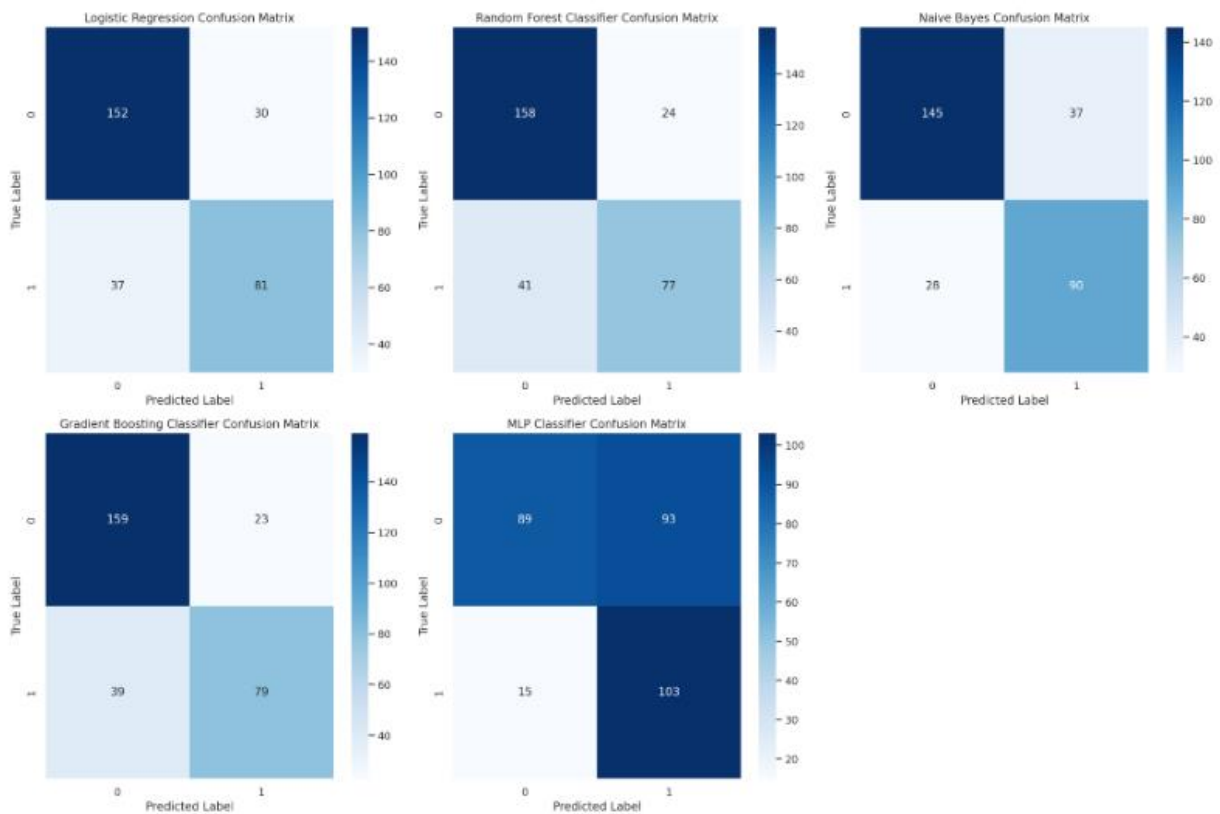
Specificity: Measured as $TN / (TN + FP)$. It reflects the ability of the model to identify negative instances [18].

F1 score: The harmonic means of precision and recall. It represents a balance between the precision and recall of the model [19].

3.2. Confusion Matrix

Confusion matrices [20] are an important tool for evaluating the performance of classification models. They provide a detailed breakdown of the predictions made by a model and thus enable a differentiated assessment of the model's accuracy. In the context of this study, where different machine learning models were used to classify students as high or low achievers in math, confusion matrices play a crucial role in understanding the effectiveness of each model.

In this study, the confusion matrices obtained for each machine learning model are listed below. These matrices provide a detailed overview of the performance of each algorithm in classifying students as high or low performers in math.

Table 4. Confusion Matrix Table

A confusion matrix for a binary classification problem usually consists of four components:

True Positives (TP): The number of instances correctly predicted to perform.

True Negatives (TN): The number of instances correctly predicted as low performers.

False Positives (FP): The number of instances that were incorrectly predicted as high performers (also known as Type I errors).

False Negatives (FN): The number of instances incorrectly predicted as low performers (also known as Type II errors).

3.3. ROC Curves Analysis

Analyzing the Receiver Operating Characteristic (ROC) [14] curve is an essential aspect of evaluating the performance of classification models, especially in studies such as ours that focus on predicting and classifying student performance. ROC curves provide a graphical representation of a model's diagnostic capabilities and show the trade-off between the rate of true positives and the rate of false positives at different thresholds.

As part of our research, the ROC curves for each model studied are carefully analyzed to evaluate their ability to differentiate between high and low academic performance, as shown in the next graph.

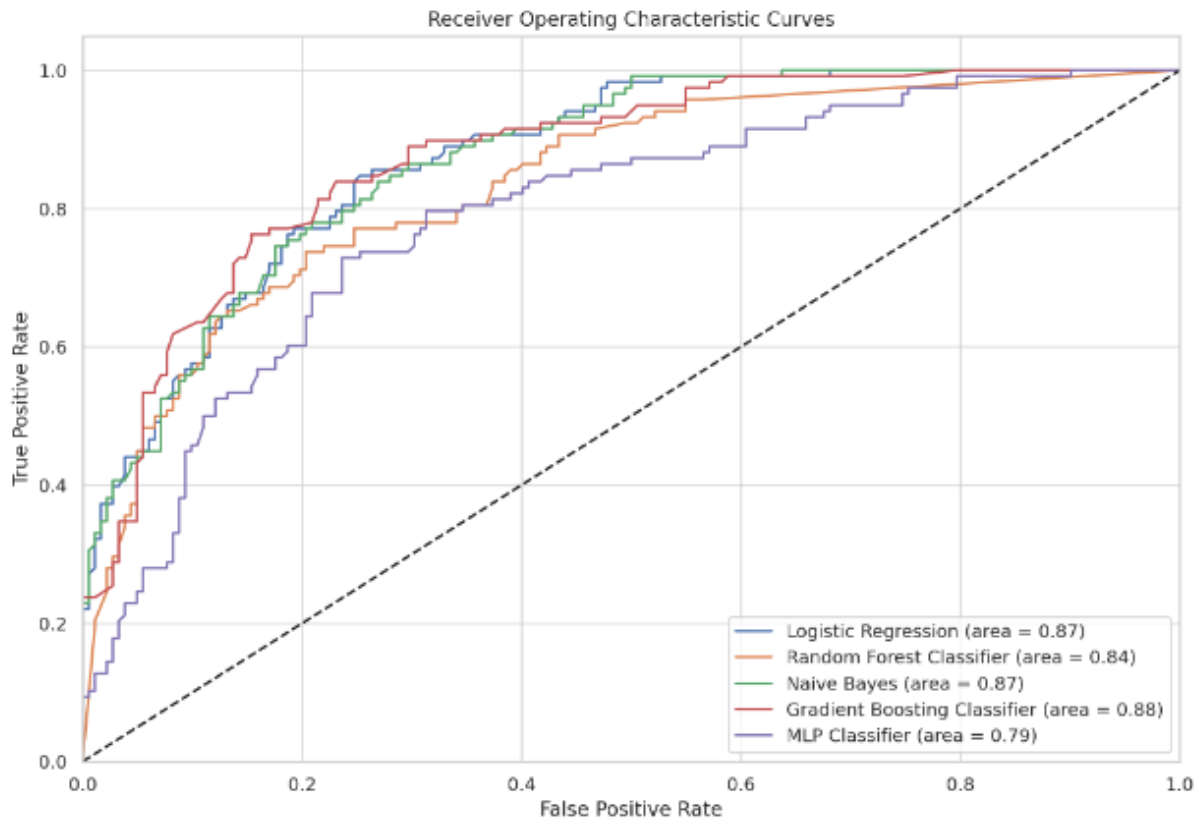


Figure 3. ROC Curves

Models that have higher values in the Area Under the Curve (AUC) [21] are considered better in this discrimination. Such models are considered more reliable in predicting student performance and prove invaluable in the educational context to initiate early interventions and provide targeted support.

In this comprehensive study, we embarked on an analytical journey to evaluate the effectiveness of different machine learning models in predicting and categorizing students' academic performance. Using a robust set of performance metrics — including accuracy, precision, recall, F1 score, ROC AUC score and specificity — the performance of each model in predicting academic outcomes was thoroughly evaluated. This multi-faceted approach to performance assessment allowed for a thorough understanding of each model's strengths in discriminating between high- and low-performing students.

Key observations:

Variability in model performance: our investigation revealed significant differences in the abilities of each model. Certain models exhibited higher accuracy and precision, suggesting that they correctly identified students' achievement levels.


Model-specific strengths and weaknesses: The study showed that each machine learning model has its own advantages and limitations. While some models excelled in accuracy, they could compromise in other areas, such as recall or specificity. This emphasizes the need to select a machine learning model that is tailored to the specific goals and constraints in the educational context.

Results of predictive analytics: The predictive power of these models proved to be considerable and provided valuable insights into student performance. This aspect is crucial for the early identification of students who may need additional academic support so that teachers can intervene in a timely and targeted manner.

4. Conclusion

In summary, this study provides a comprehensive assessment of machine learning models in the educational context and highlights their ability to revolutionize educational strategies and policy decisions. The insights gained not only contribute to the advancement of personalized learning, but also highlight the growing importance of data-driven approaches in the ever-evolving educational landscape. The integration of these models promises to be an important step towards a more informed, efficient and equitable educational future.

References

- [1] S. Batool, J. Rashid, M. W. Nisar, J. Kim, H. Y. Kwon, and A. Hussain, "Educational data mining to predict students' academic performance: A survey study," *Education and Information Technologies 2022 28:1*, vol. 28, no. 1, pp. 905–971, Jul. 2022, doi: 10.1007/S10639-022-11152-Y.
- [2] S. Bhutto, I. F. Siddiqui, Q. A. Arain, and M. Anwar, "Predicting Students' Academic Performance Through Supervised Machine Learning," *ICISCT 2020 - 2nd International Conference on Information Science and Communication Technology*, Feb. 2020, doi: 10.1109/ICISCT49550.2020.9080033.
- [3] O. Ojajuni *et al.*, "Predicting Student Academic Performance Using Machine Learning," *Lecture Notes in Computer Science (including subseries Lecture Notes in Artificial Intelligence and Lecture Notes in Bioinformatics)*, vol. 12957 LNCS, pp. 481–491, 2021, doi: 10.1007/978-3-030-87013-3_36.
- [4] F. A. Orji and J. Vassileva, "Machine Learning Approach for Predicting Students Academic Performance and Study Strategies based on their Motivation," Oct. 2022, Accessed: Dec. 21, 2023. [Online]. Available: <https://arxiv.org/abs/2210.08186v1>
- [5] M. Yağcı, "Educational data mining: prediction of students' academic performance using machine learning algorithms," *Smart Learning Environments*, vol. 9, no. 1, pp. 1–19, Dec. 2022, doi: 10.1186/S40561-022-00192-Z/TABLES/14.
- [6] A. Khan and S. K. Ghosh, "Student performance analysis and prediction in classroom learning: A review of educational data mining studies," *Educ Inf Technol (Dordr)*, vol. 26, no. 1, pp. 205–240, Jan. 2021, doi: 10.1007/S10639-020-10230-3/TABLES/11.
- [7] E. Alyahyan and D. Düşteğör, "Predicting academic success in higher education: literature review and best practices," *International Journal of Educational Technology in Higher Education*, vol. 17, no. 1, pp. 1–21, Dec. 2020, doi: 10.1186/S41239-020-0177-7/TABLES/15.
- [8] S. S. Ganorkar, N. Tiwari, and V. Namdeo, "Analysis and Prediction of Student Data Using Data Science: A Review," *Smart Innovation, Systems and Technologies*, vol. 182, pp. 443–448, 2021, doi: 10.1007/978-981-15-5224-3_44/COVER.
- [9] M. Kurni, M. S. Mohammed, and K. G. Srinivasa, "Predictive Analytics in Education," *A Beginner's Guide to Introduce Artificial Intelligence in Teaching and Learning*, pp. 55–81, 2023, doi: 10.1007/978-3-031-32653-0_4.
- [10] T. Susnjak, G. S. Ramaswami, and A. Mathrani, "Learning analytics dashboard: a tool for providing actionable insights to learners," *International Journal of Educational Technology in Higher Education*, vol. 19, no. 1, pp. 1–23, Dec. 2022, doi: 10.1186/S41239-021-00313-7/FIGURES/3.
- [11] M. Kurni, M. S. Mohammed, and K. G. Srinivasa, "Predictive Analytics in Education," *A Beginner's Guide to Introduce Artificial Intelligence in Teaching and Learning*, pp. 55–81, 2023, doi: 10.1007/978-3-031-32653-0_4.
- [12] "Student Academic Performance Analysis  | Kaggle." Accessed: Dec. 21, 2023. [Online]. Available: <https://www.kaggle.com/code/bhartiprasad17/student-academic-performance-analysis>
- [13] Y. J. Kang, Y. Noh, and O. K. Lim, "Kernel density estimation with bounded data," *Structural and Multidisciplinary Optimization*, vol. 57, no. 1, pp. 95–113, Jan. 2018, doi: 10.1007/S00158-017-1873-3/TABLES/12.

- [14] T. Fawcett, "An Introduction to ROC Analysis," *Pattern Recognit Lett*, vol. 27, no. 8, pp. 861–874, Jun. 2006, doi: 10.1016/j.patrec.2005.10.010.
- [15] J. Davis and M. Goadrich, "The Relationship Between Precision-Recall and ROC Curves."
- [16] A. A. Syntetos and J. E. Boylan, "The accuracy of intermittent demand estimates," *Int J Forecast*, vol. 21, no. 2, pp. 303–314, 2005, doi: 10.1016/j.ijforecast.2004.10.001.
- [17] D. M. W. Powers, "Evaluation: From Precision, Recall and F-Measure to ROC, Informedness, Markedness & Correlation," *Journal of Machine Learning Technologies*, vol. 2, no. 1, pp. 37–63, 2011, Accessed: Mar. 17, 2022. [Online]. Available: <https://api.semanticscholar.org/CorpusID:55767944#id-name=S2CID>
- [18] C. Catal, "Performance Evaluation Metrics for Software Fault Prediction Studies," *Acta Polytechnica Hungarica*, vol. 9, no. 4, pp. 2012–193.
- [19] D. Chicco and G. Jurman, "The advantages of the Matthews correlation coefficient (MCC) over F1 score and accuracy in binary classification evaluation," *BMC Genomics*, vol. 21, no. 1, pp. 6-1-6–13, Jan. 2020, doi: 10.1186/s12864-019-6413-7.
- [20] M. Makhtar, D. C. Neagu, and M. J. Ridley, "Comparing multi-class classifiers: On the similarity of confusion matrices for predictive toxicology applications," *Lecture Notes in Computer Science (including subseries Lecture Notes in Artificial Intelligence and Lecture Notes in Bioinformatics)*, vol. 6936 LNCS, pp. 252–261, 2011, doi: 10.1007/978-3-642-23878-9_31.
- [21] J. A. Hanley and B. J. McNeil, "The meaning and use of the area under a receiver operating characteristic (ROC) curve," *Radiology*, vol. 143, no. 1, pp. 29–36, 1982, doi: 10.1148/radiology.143.1.7063747.

COMPARATIVE ANALYSIS OF SWARM ROBOTICS DESIGN THROUGH REINFORCEMENT LEARNING AND PARTICLE SWARM OPTIMIZATION

ALAA ISKANDAR

University of Miskolc Miskolc, Hungary

Dr. Bela Kovacs

University of Miskolc Miskolc, Hungary

ABSTRACT

This research paper explores automatic design methods that facilitate the development of collective behaviors in swarm robotic systems, allowing multiple robots to autonomously collaborate and perform complex tasks. The focus of the study is on two primary methodologies: particle swarm optimization (PSO) and reinforcement learning (RL). We conducted a comparative analysis to evaluate the effectiveness of these methods in guiding a group of mobile robots in diverse and challenging environments. The aim was to develop a navigation system that enables the swarm to efficiently traverse unknown areas, which vary in complexity from open spaces to more cluttered ones. Key metrics for comparison included the time efficiency of each robot and the swarm as a whole, their adaptability in pathfinding, and their capacity to generalize solutions to novel environments.

Experiments conducted using the Webots simulator with a Python controller revealed distinct strengths and weaknesses of both methodologies. RL showed commendable performance in scenarios similar to its training conditions, achieving quicker completion times and better coordination among robots. However, its effectiveness decreased in unfamiliar situations, requiring extensive retraining or modifications for improved adaptability. On the other hand, PSO demonstrated consistent performance across various environments. Despite its relatively slower pace, PSO maintained robustness and did not require reconfiguration to adapt to new challenges. These findings provide insightful comparisons between RL and PSO in the context of swarm robotics, highlighting their respective advantages and limitations in dynamic environments.

Keywords: Reinforcement Learning, Proximal Policy Optimization algorithm, Sparse rewards, Shaping rewards, Webots simulator, E-puck robot

REWARD DESIGN STRATEGIES IN REINFORCEMENT LEARNING FOR COLLECTIVE BEHAVIOR GENERATION

ALAA ISKANDAR

University of Miskolc Miskolc, Hungary

Dr. Bela Kovacs

University of Miskolc Miskolc, Hungary

ABSTRACT

This paper delves into the intricate realm of reward design within Reinforcement Learning (RL), with a specific focus on generating collective behavior in multi-agent systems. The essence of RL lies in its ability to guide agents' actions through rewards, thus shaping desired behaviors. In this context, we explore the implications and methodologies of reward shaping, sparse rewards, multi-objective tasks, and inverse reinforcement learning (IRL) in crafting effective collective behaviors.

Reward shaping emerges as a crucial technique, involving the addition of supplementary rewards to facilitate learning. This method accelerates convergence and encourages specific behaviors in agents, proving especially beneficial in complex, multi-agent scenarios. However, the challenge lies in designing these additional rewards without inadvertently altering the optimal policy. Sparse rewards, characterized by infrequent feedback, present another interesting paradigm. While they pose a significant challenge due to limited learning signals, we investigate techniques to circumvent these obstacles, such as using intrinsic motivation and curiosity-driven exploration.

This research discusses approaches to harmonize these objectives, ensuring efficient collective decision-making. IRL, on the other hand, focuses on understanding and replicating behaviors by observing experts. We examine how IRL can be utilized to derive reward functions that align with desired collective behaviors, particularly in scenarios where explicitly defining rewards is challenging.

Overall, this research contributes to the understanding of reward design in RL for multi-agent systems, offering insights into how different strategies can be leveraged to induce cooperative and coordinated behaviors among agents.

Keywords: Reinforcement Learning, Reward Shaping, Sparse Rewards, Multi-Objective RL, Inverse Reinforcement Learning.

EXAMINATION OF THE ALBEDO PARAMETER ON SOME ELEMENTS WITH ATOMIC NUMBER VARIING BETWEEN 4 AND 30

Ahmet TURŞUCU

*Assoc. Prof. Dr., Sirnak University, Faculty of Engineering, Department of Electric-Electronic, Şırnak-Türkiye
(Responsible Author) ORCID: 0000-0002-4963-697X*

ABSTRACT

The albedo factor, one of the radiation shielding parameters, has become widespread in the field of X-ray spectroscopy as a subject that attracts much attention from researchers. The albedo factor parameter, which has been frequently mentioned recently, includes albedo number, albedo dose and albedo energy components. By calculating these components, the scattering coefficient of radiation over the target material is determined. Based on this information, we have discussed the calculation of albedo values of some elements used in radiation shielding processes in this study. To carry out this study, we were helped by a radiation source and a detector used to collect and evaluate the resulting rays. The parameters thus calculated are plotted as a function of atomic number. As a result, according to the data obtained, it was observed that the scattering values obtained with increasing atomic number increased, and the albedo values increased.

Keywords: XRF, Albedo Factor, Albedo Number, Albedo Dose, Albedo Energy.

Introduction

X-ray fluorescence spectrometry (XRF), which is frequently used in non-destructive testing studies, is also frequently used by researchers in different areas, such as calculating shielding parameters. Similarly, energy-dispersive X-ray fluorescence spectroscopy is a very important technique for analyzing mixtures or compounds formed by combining different elements in different proportions. Thanks to this important feature of X-ray fluorescence spectroscopy, its use as a guide in the development, examination and production of materials and materials used in industry and scientific research comes to the fore. In addition, x-ray fluorescence spectroscopy has a wide operating range regardless of the chemical composition of the material to be examined. In our study, using the technique we mentioned, the scattering values of Compton and coherently scattered photons from the target samples were determined, and calculations were made.

Depending on the change in photon energy after the collision, it is possible to divide collision events into elastic and inelastic. With this classification, it is possible to understand the flexibly emitted photons and the possibility of rebounding from the target in case of scattering. From here, adding all the events of flexible photon emission and backscattering from the target to the elastic scattering category would be correct. We can give examples of inelastic scattering types such as photoelectric, Compton and pair formation processes. Unlike inelastic scattering, Rayleigh scattering, nuclear Thomson scattering, Delbrück scattering, and nuclear resonance events are types of flexible scattering.

This study will calculate albedo factor parameters, which means the ratio of the intensity values of elastic and inelastic scatterings mentioned above. It would also be correct to state that the calculation of the albedo parameter is used to determine the ability of compounds composed of one element or different compositions of different elements to scatter photons. To reiterate, albedo values have three components, which are only one of the radiation shielding parameters.

Many researchers have carried out backscatter measurement and albedo factor parameter studies. Alajerami et al., 2024 synthesized two new glass series in the form of $10\text{Bi}_2\text{O}_3\text{-}20\text{BaO}\text{-}(70\text{-x})\text{B}_2\text{O}_3\text{-xTeO}_2$ and $10\text{MoO}_3\text{-}20\text{SrO}\text{-}(70\text{-x})\text{B}_2\text{O}_3\text{-xTeO}_2$ using the melting method. The physical and radiation shielding properties of the glass samples obtained by this method were investigated. As expressed in the formulas, an increase in density was achieved by adding TeO_2 into the melt. The shielding capacities of the produced materials for different radiation types such as alpha, beta, gamma and neutron were investigated using SRIM and Phy-X/PSD software. Negm et al., 2024 have conducted research on the radiation protection properties of the ATP

structure by changing the magnetite concentration in the structure called Attapulgit (ATP), which consists of nano magnetite and different copper oxides (CuO). Additionally, different nanocomposites were synthesized from ATP combined with different concentrations of copper oxide (CuO) and nano magnetite (Fe₃O₄) and their effects on radiation shielding were investigated. Tamam et al., 2024 have studied the lead-free, thermally stable, transparent and chemical structure $(29.5-0.4x) \text{CaO} + 10\text{CaF}_2 + (60-0.6x) \text{B}_2\text{O}_3 + x\text{TeO}_2 + 0.5\text{Yb}_2\text{O}_3$ (x) was found, which has important optical properties for technological applications. They conducted research on glasses with 10, 16, 22, 31 and 54 mol (%). In this way, the protection values of TeO₂ against different types of radiation on the developed glass material were examined. Calculations made with XCOM (Gerward, L., et al., 2001) were also simulated using the FLUKA code. Kavun et al., 2024 have used the melt quenching technique, glass systems containing 42.5P₂O₅, 42.5B₂O₃ and $(15-x) \text{Li}_2\text{O}-x\text{V}_2\text{O}_5$ (x values 0, 2.5, 5, 10 and 15) were produced. These materials were then irradiated using ¹³³Ba and ⁶⁰Co point sources with an activity of 1 mCi. Gamma spectra and absorbed values with energies of 384 keV, 1173 keV and 1333 keV emitted from the source with 1mCi activity were measured using a NaI(Tl) detector.

In this study, the albedo factor parameters of some elements used in the production of materials used in radiation protection were calculated under a scattering angle of 168 degrees, using a ²⁴¹Am source with 5Ci power, emitting photons with 59.54 keV energy.

Experimental Details and Calculation Method

Experimental Management

In our research, which will be carried out using the X-ray fluorescence spectroscopy technique, an HPGe semiconductor detector and radioactive source emitting gamma rays were used. The setup diagram of the experimental setup and the layout of the components are shown in Figure 1. Additionally, there is a specially prepared chamber in the experimental setup, which surrounds the sample and the source. The features of this chamber are given in Figure 2. Thanks to this chamber surrounding the sample and the source, firstly, it is ensured that the researcher is minimally affected by harmful rays, and secondly, external factors that cause scattering in the chamber are minimized. The sample chamber shown in Figure 2 is designed in a conical shape and its walls are coated with lead. In this way, it is aimed that the characteristic rays emitted from the sample and other scattered photons reach the detector in a monochromatic pattern. The rays, which are directed within this entire system and are quite monochromatic, are ensured to reach the counting system at an angle of 168 degrees. At this scattering angle, it is protected from unwanted scattering that may occur on the existing system.

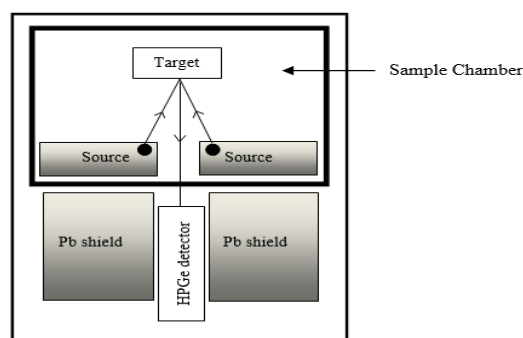


Figure 1. Experimental setup (radius of collimator is 0.53 cm). This figure is only a schematic diagram of experimental setup.

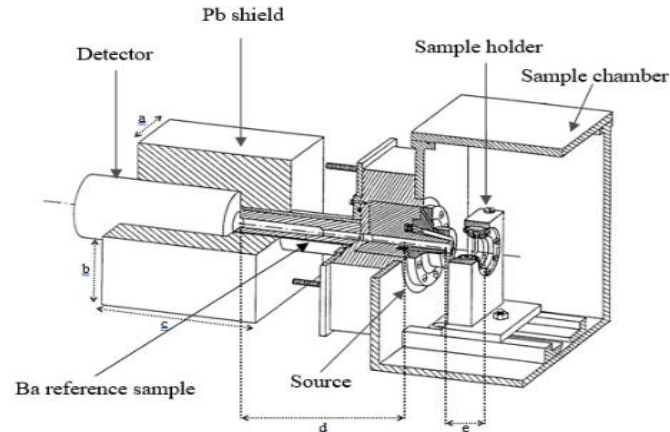


Fig. 2. Sample chamber

(a=6.5 cm, b=6.3 cm, c=13.5cm, d=11 cm, e=5 cm).

Albedo Factor Calculations

The experimental setup used in the study consists of a semiconductor detector used to collect photons and a multi-channel analyzer to which this detector is connected. The multi-channel analyzer was operated in connection with a computer and the Genie-2000 program, which provides control via the computer. Thanks to this program, characteristic peaks were detected depending on the energy of the photons counted by the detector. The Origin 7.5 program was used to use the area values under these characteristic hills in the calculations. In the calculations, the terms N_{bs} and N_i were used to represent the incident and scattered photon components [7]. These terms are used in the equation given below in calculating the albedo number (Figure 3),

$$A_N = \left[\frac{N_{bs}/\varepsilon(E_{bs})}{(N_i/\varepsilon(E_i))(1/d\Omega)(1/2)} \right] \quad (1)$$

The terms $\varepsilon(E_{bs})$ and $\varepsilon(E_i)$ of equation (1) express the number of backscattered photons arriving at the detector and the detector efficiency for backscattered photons, respectively. The solid angle is also expressed with the term $(d\Omega)$ used in the same equation. The solid angle is defined as the angle between the center of the target material causing scattering and the collimator aperture to the detector. Finally, $(1/2)$ used in the denominator is the regulation factor used to express that half of the photons emitted by the source reach the detector.

After calculating the albedo number, we can calculate the albedo energy (Figure 4) with the value obtained. The equation for this calculation is presented below,

$$A_E = \left[\frac{E_{bs}}{E_i} \right] A_N \quad (2)$$

The terms E_i and E_{bs} that appear in this equation also represent incoming and backscattered photons. The albedo energy (Figure 5) term obtained by using this equation is directly proportional to the albedo dose component that we will finally calculate and is calculated using the equation given below,

$$A_D = \left[\frac{\sigma_a(E_{bs})}{\sigma_a(E_i)} \right] A_E \quad (3)$$

Equation (3), which we used in the last calculation, unlike the others, includes air absorption correction for backscattered and incident photons. These coefficients were calculated from the XCOM (Gerward, L., et al., 2001) database using the density values of the elements in the air and used in the equation. Different elements present in the air and their percentages are given in Table 1.

Table 1. Table of gaseous composition of dry air.

Constituent	Chemical symbol	Mole percent
Nitrogen	N ₂	78.084
Oxygen	O ₂	20.947
Argon	Ar	0.934
Carbon dioxide	CO ₂	0.0350
Neon	Ne	0.001818
Helium	He	0.000524
Methane	CH ₄	0.00017
Krypton	Kr	0.000114
Hydrogen	H ₂	0.000053
Nitrous oxide	N ₂ O	0.000031
Xenon	Xe	0.0000087
Ozone	O ₃	0.00000001

Findings and Discussion

In this part of our study, we will make a general evaluation based on the values we obtained. Generally speaking, we have obtained data that will support radiation shielding studies. Namely, in our study, experiments were carried out with entirely pure samples and values were obtained. Based on the obtained values, an increase in all albedo parameters was observed, as expected with increasing atomic numbers of pure samples. This result is also expected theoretically. Although we must prove the theoretically expected results through experimental studies, the materials to be produced from pure materials used in different proportions and hand mixtures must be tested separately.

To conduct a broader range of studies and test the reliability of the data obtained, we consider our study as a beginning for other studies that we will carry out in the future, and the values obtained with the pure materials used in this study will be used to obtain, develop and test armoring structures containing different mixtures to be made in the future. We hope it will help with the process.

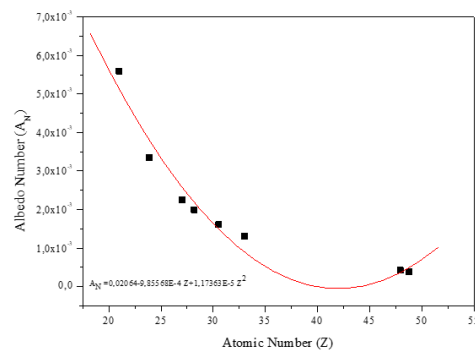


Figure-3. The albedo number distribution of target samples as a function of the atomic number.

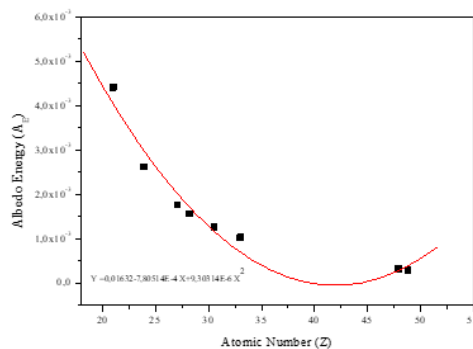


Figure-4. The albedo energy distribution of target samples as a function of the atomic number.

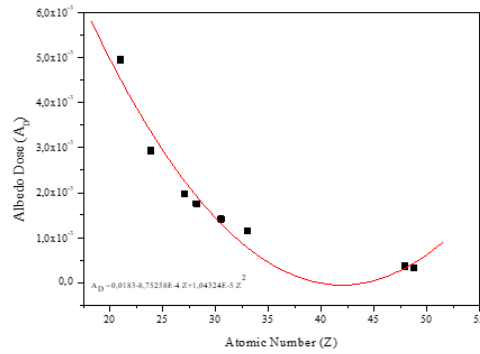


Figure-5. The albedo dose distribution of target samples as a function of the atomic number.

References

- Alajerami, Y. S. M., Mhareb, M. H. A., Sayyed, M. I., Hamad, M. Kh., Abuelhia, E., Alshamari, A., Alqahtani, M. Y., & Imheidat, M. A. (2024). Physical and radiation shielding properties for borate, boro-tellurite, and tellurite glass system modified with different modifiers: Comparative study. *Optical Materials*, 147, 114558. <https://doi.org/10.1016/j.optmat.2023.114558>
- Kavun, Y., Eskalen, H., Kavgacı, M., Yaykaşlı, H., & Bahşi, M. (2024). A novel vanadium pentoxide doped glasses characterization for radiation shielding applications. *Applied Radiation and Isotopes*, 203. <https://doi.org/10.1016/j.apradiso.2023.111086>
- Negm, H. H., Allam, E. A., Abdeltwab, E., Mostafa, M., Mahmoud, M. E., & El-Taher, A. (2024). A new nanocomposite of copper oxide and magnetite intercalated into Attapulgitte clay to enhance the radiation shielding. *Radiation Physics and Chemistry*, 216, 111398. <https://doi.org/10.1016/j.radphyschem.2023.111398>
- Tamam, N., Al Huwayz, M., Alrowaili, Z. A., Alwadai, N., Katubi, K. M., Alqahtani, M. S., Olarinoye, I. O., & Al-Buriah, M. S. (2024). Radiation attenuation of boro-tellurite glasses for efficient shielding applications. *Applied Radiation and Isotopes*, 203. <https://doi.org/10.1016/j.apradiso.2023.111080>
- Gerward, L., et al., 2001. "X-ray absorption in matter. Reengineering XCOM." *Radiat. Phys. Chem.*, 60(1-2): 23-24.

AN ASSESSMENT OF PULSE WIDTH MODULATION METHODS FOR DC-DC MODULAR MULTILEVEL CONVERTERS

Abdurrahim ERAT

*Lec., Şırnak University, Vocational School of Şırnak, Department of Electricity and Energy, Şırnak-Türkiye
Ph.D. Student, Gaziantep University, Faculty of Engineering, Department of Electrical and Electronics Engineering, Gaziantep-Türkiye, (Responsible Author) ORCID: 0000-0003-0606-9132*

Ahmet Mete VURAL

*Prof. Dr., Gaziantep University, Faculty of Engineering, Department of Electrical and Electronics Engineering, Gaziantep-Türkiye
ORCID: 0000-0003-2543-4019*

ABSTRACT

Due to its unique characteristics consisting of remarkable levels of modularity, scalability to higher power and voltage levels, non-isolated functionality, high efficiency, and enhancement of power quality, DC-DC Modular Multilevel Converter (MMC) technology which is derived from AC-DC or its inverse counterpart, DC-AC MMC technology has attracted the fascination of many researchers in more recent years. The implementation of present-day asynchronous AC power networks as well as the interconnection of modern DC power networks both internally and externally with conventional AC networks depend substantially upon DC-DC MMC technological advances. In the recently created new generation DC-DC MMC technology as well as in conventional DC-DC converter structures, the Pulse Width Modulation (PWM) techniques are critically important. The ability of DC-DC MMC technology to the aforementioned critical operational duties largely depends on a well-designed PWM technique. PWM technology incorporates particular techniques to transform a firsthand signal into impulses that take place at predetermined timings. Using this approach, the width of the pulse delivered to the power switch from the reference source can be changed to turn the power switch on or off based on the transmitted signal. This paper presents the fundamental role that PWM technology plays in the DC-DC MMC technologies and the overall operating system. An insightful assessment of the PWM methods employed in modern DC-DC MMC systems has been provided.

Keywords: PWM Techniques, DC-DC Power Converter, DC-DC MMC, Power Systems Control.

Introduction

Power electronics-based converter systems are used at various stages of the electrical energy supply chain, from power plants to load centers and ultimately to end users. These converter systems include both future-oriented modern converter systems and conventional converter systems that operate on AC-DC, DC-AC, AC-AC, and DC-DC. Power electronics-based modular multilevel converter (MMC) (Marquardt, 2001) technology, which has become the focus of attention of many researchers, especially in the last twenty years, plays a critical role in modern power networks. MMC technology provides excellent prospects in both classic and modern power systems applications because of its properties, which include efficiency, high quality of voltages and currents, high effectiveness output, high modularity, straightforward scalability, low voltage and current rating requirements for the power switches, excellent reliability, high-quality output waveforms, transformerless operation capability, high quality of output, high availability, easy implementation, excellent harmonic performance, and reliability (Bashir et al., 2023; F. Deng et al., 2020; Erat & Vural, 2022; Liu et al., 2021; Perez et al., 2021; Priya et al., 2019; Wang et al., 2020; Xiao et al., 2023). MMC technology provides worthwhile solutions in a variety of fields, including vehicles powered by electricity, solar photovoltaic energy structures, medium voltage variable-speed motor drive systems, battery charging infrastructures, power transmission systems, battery energy storage systems, power quality improvement systems, DC-DC MMC architecture which has been created using MMC technology has a tremendous value in integrating recently designed contemporary direct current (DC) power systems with existing alternative current (AC) power networks that have varying voltage levels. Both conventional converter systems and the latest DC-DC MMC Technologies which are based on power electronics and are efficiently employed in

power systems need an efficient power switching system to perform an efficient power conversion process. Pulse Width Modulation (PWM) technology is the best approach for this power-switching procedure. With PWM technology, a signal can be generated at its intended venue by modifying the width of the resulting impulses. Stated differently, PWM technology is a means of transforming an input signal toward impulses at predetermined intervals utilizing certain technologies. In essence, power switching is what PWM technology does. By varying the width of the pulse sent from the reference source to the power switch in this manner, the power switch is switched on or off based on this signal width.

Many PWM approaches have recently found a position in DC-DC MMC technology, due to the efficient advancements in power electronics and semiconductor technology. Many researchers have preferred different PWM techniques to develop many DC-DC MMC topologies. In this study (Sha et al., 2021), a cascaded H-bridge and MMC-based DC transformer construction is proposed. The PWM approach has been used in three distinct scenarios which are equal and unequal carrier-phase-shift PWM (CPS-PWM), the quasi-square-wave-modulation method, and extended-phase-shift (EPS) modulation for the suggested design to show efficient performance. While an uneven five-level voltage waveform is proposed to be produced via unequal CPS-PWM control, MMC's equal CPS-PWM can generate an equal five-level voltage waveform. The intermediate AC side of the transformer's insulation design challenge and the voltage tension on the AC side can be significantly decreased by using the quasi-square wave modulation approach, which has a broad gain range. To significantly reduce backflow power and current stress, the EPS control has been implemented in this study. This article (Dey & Bhattacharya, 2021) proposes a DC-DC MMC approach that can be used to provide an efficient interconnect for power transfer between a voltage source converter-based high voltage direct current (HVDC) grid of various voltage levels and a line commutated converter (LCC)-based HVDC network. In the present study, the submodule (SM) switching frequency has been reduced for simulation objectives by the application of hybrid modulation, which combines nearest level control (NLC) with PWM. On the other hand, because the experimental version requires fewer power switches, phase-shifted PWM technology has been used. To rapidly charge numerous electric vehicles (EVs), this study (Sarkar & Das, 2023b) suggests an isolated single input-multiple output DC-DC MMC. By using an intermediary medium-frequency transformer which offers galvanic isolation, the suggested design allows for high-voltage ratios for converting from medium voltage direct current (MVDC) to low voltage direct current (LVDC). The suggested design in this article significantly lowers the dv/dt tension by utilizing the sinusoidal level-shifted PWM (LS-PWM) approach. To link two distinct DC voltage levels, a hybrid DC-DC MMC converter is proposed in this study (Elserougi et al., 2023). putting out a hybrid DC-DC MMC converter that uses a single bidirectional HV valve, i.e., fewer HV valves than other hybrid DC-DC MMCs already on the market. A technique that lowers switching losses is described for operating the concerned HV valve under soft switching. To achieve the intended functionality, the phase disposition PWM (PD-PWM) approach in association with the soft-switching operating method has been employed in the suggested DC-DC MMC architecture. A multiport DC-DC MMC for connecting several HVDC systems is proposed in this study (Qin et al., 2020). The suggested design not only inherits the benefits of traditional MMC but also offers various additional advantages, such as lower size, more appealing investment expenses, and less SM quantity. In this study, the PSC-PWM technique has been used to produce switching signals for the planned design. Every SM is separately regulated in the PSC-PWM method. The relevant SM switching impulses are then obtained by comparing the triangle carriers with the SM modulation reference. An optimization approach centered on finite control set model predictive control has been provided in this research (Akbar et al., 2020) to address malfunctioning SMs or enhance the functionality of an isolated DC-DC MMC throughout tapping change. The present study examines a two-level modulation technique and demonstrates that when elevation parameters are modified to accommodate malfunctioning SMs or tap altering that yields a result other than the desired output voltage, SMs are unable to swiftly modify their final output voltage. The present paper (Chen et al., 2022) reveals the connection between the switching signal waveforms and the MVDC side current ripples. By modifying the phase-shifted ratios for every SM's generating signals, an offline genetic algorithm-based optimum PS-PWM technique is suggested to mitigate the MVDC side current ripple. By integrating the suggested modulation technique with a suggested online progressive energy control plan, a restricted set of ideal phase-shifted proportions can handle all imbalanced scenarios. For upcoming MVDC rail traction applications, a bidirectional DC-DC MMC architecture is suggested in this study (Sarkar & Das, 2023a). The level shift pulse width modulation (LS-PWM) method is applied in MMC. The primary transformer's waveform is exceptionally sinusoidal thanks to the LS-PWM technology. The hybrid DC-DC

MMC presented in this study (Diab et al., 2023) effectively addresses the problem of capacitor voltage imbalance throughout DC-DC transformation. In this study, the number of SMs to be incorporated into the upper arm is determined by using Phase Disposition PWM (PD-PWM) technique. The number of SMs in the lower arm that need to be triggered is determined by the upper arm's obtained quantity. Arm currents, capacitor voltages, and the total amount of arms SMs to be activated have been used to apply the capacitor voltage balancing method. In the present article (ERAT & VURAL, n.d.), a unique DC-DC MMC design has been described. The main goal of this design is to offer an efficient means of combining modern HVDC power systems with HVAC power systems that are presently in use, each with a distinct voltage level. An individual PD-PWM approach is used for the upper arm and lower arm SMs in the proposed DC-DC MM architecture in order to transfer power efficiently.

This paper offers a significant assessment of the PWM methods applied in several significant DC-DC MMC structures that have appeared in the literature. The fundamental concepts of PWM technology and some of the different varieties of PWM technology are then highlighted.

Fundamentals of PWM Technology

In essence, PWM technology is a form of power switching (Insulated Gate Bipolar Transistor (IGBT), Metal Oxide Semiconductor Field Effect Transistor (MOSFET) etc.). Using this approach, the width of the pulse delivered to the power switch from the reference source is adjusted to turn the power switch on or off based on this signal width. Figure 1 shows three different PWM signals with duty cycle rates of 30%, 50%, and 70%. The percentage of a period during which a signal or system is active is called a duty cycle or power cycle. Under these circumstances, the power switch will be open or active. The PWM method calculates a signal's period by integrating the active and inactive portions of the duty cycle. The following equation can be used to quantitatively describe this statement:

$$\text{Period of the pulse} = \text{duty cycle}_{\text{active}} + \text{duty cycle}_{\text{inactive}} \quad (1)$$

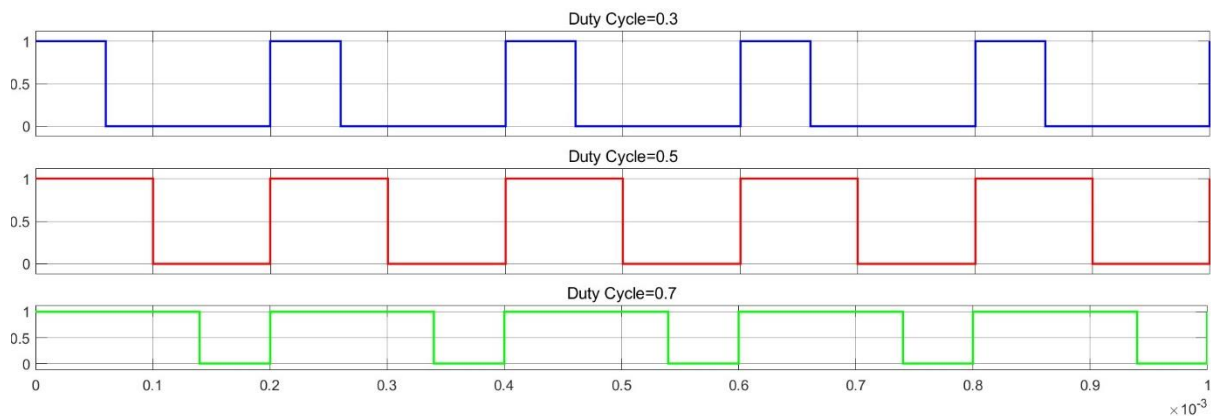


Figure 1. Three PWM signals, 30%, 50%, and 70% duty cycle values.

The goal of the approach to modulation is to minimize the need for filtration by producing the desired signal with the least amount of distortion in low-order harmonics while moving the inevitable distortions to bigger levels (Raju et al., 2019). High operating frequency semiconductor power components such as MOSFETs or IGBTs are commonly used in PWM technology. PWM approaches have been divided into three categories based on switching frequency: low switching frequency PWM modulation, high switching frequency PWM modulation, and fundamental switching frequency PWM modulation structures as shown in Figure 2.

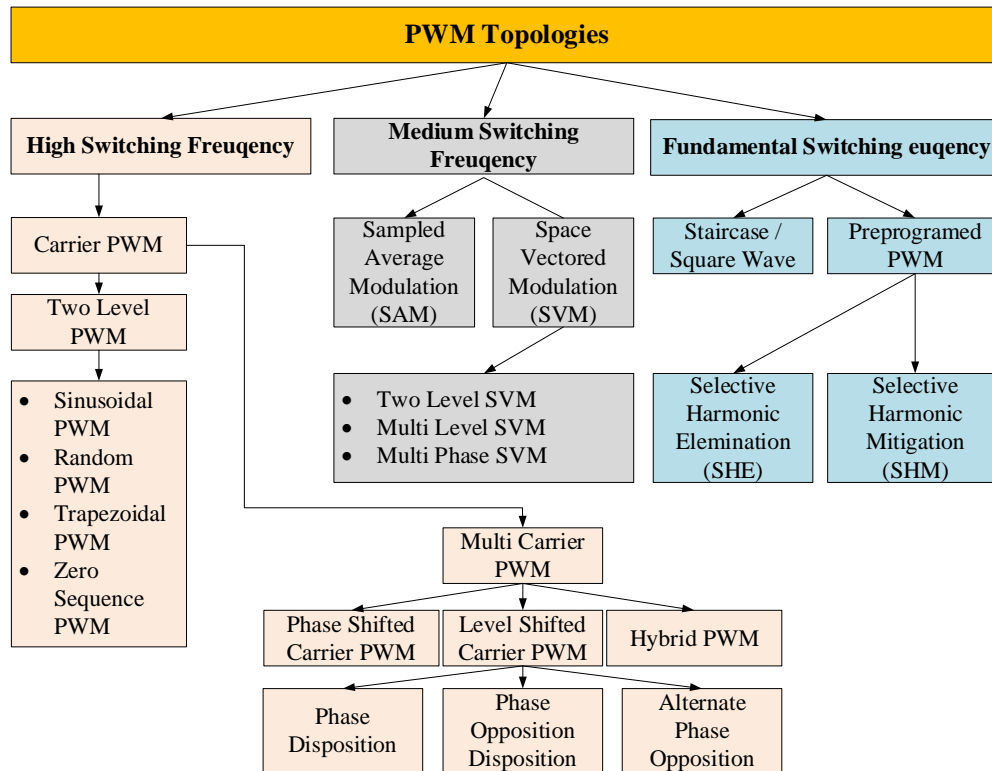


Figure 2. PWM modulation architectures (Raju et al., 2019).

Specific PWM techniques are preferred over others for power switching in conventional and DC-DC MMC setups. The modulation techniques aim to achieve several regulating objectives, such as voltage adjustment, common-mode voltage enhancement, equipment switching frequency reduction, power distortion minimizing, and current ripple mitigation. PWM approaches allow for more exact control of the output voltage's frequency and level while producing an output voltage with exceptional features. The two primary classifications used for categorizing the multilevel PWM approaches are carrier-based modulation (CBM) and space vector modulation (SVM). Researchers prefer specific PWM approaches for DC-DC MMC systems, as has been demonstrated in the introduction section above. Following is a quick explanation of a number of these PWM methods. PSC-PWM is a modulation approach powered by high-frequency carrier signals. Using the PSC-PWM PWM technique, an output signal is generated through the comparison of N SMs in the phase arms of DC-DC MMC architectures and N signals with a distinct triangular carrier pattern of the identical magnitude and frequency to a reference signal with a sine pattern. As seen in Figure 3, the triangle carrier signals in PSC-PWM are oriented horizontally and have the same amplitude. This method requires N identical triangular carriers, each for every SM, spaced N degrees away from one another.

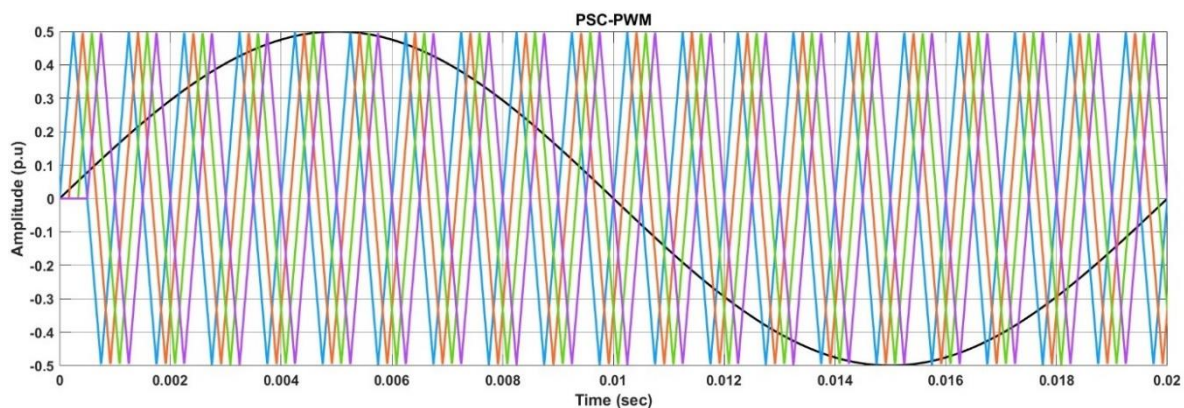


Figure 3. PSC-PWM arrangement (Four carrier signals).

Similar to the PSC-PWM method, LSC-PWM is a high-frequency carrier signal-based modulation approach. In the LSC-PWM technique, reference sinusoidal waveform and high-frequency carrier waves are compared between themselves as shown in Figure 4. For the SM power switches that are utilized in MMC configurations, the comparison that results produces an output signal. By dividing the amplitude of the reference signal by the number of SMs, the magnitude of each carrier signal for the LSC-PWM technique is calculated. Increasing the intensity of the carrier signals modifies their position, allowing them to be divided into many ranges.

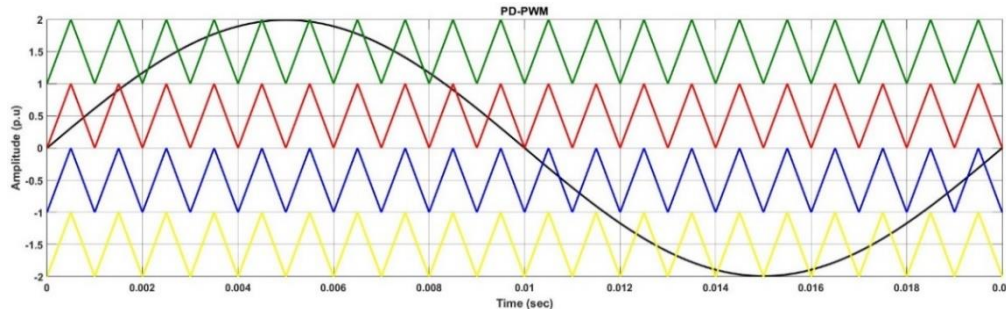


Figure 4. PD-PWM structure (Four carrier carriers).

The LSC-PWM methodology is subdivided into three distinct categories: phase-disposition (PD-PWM), phase-opposition-disposition (POD-PWM), and alternate phase opposition-disposition (APOD-PWM). The carrier signals used in a carrier constructed in the PD-PWM technique all have the same frequency and phase sequences. This modulation technique considers the reference signal's amplitude while calculating the carrier signal magnitudes, as shown in Figure 4. Another level-shifted method similar to the PD-PWM structure is POD-PWM. In the POD-PWM approach, the upper arm carrier signals of the MMC have a 180-degree phase shift concerning the lower arm carrier signals of the MMC. The configuration of the four carrier signals used in the POD-PWM approach is shown in Figure 5. In the APOD-PWM approach, the carrier signals are in phase for carriers above the zero axis and 180 degrees out of phase for carriers beneath the zero axis. Stated differently, the carrier signals are 180° shifted in alternating fashion for each pair of signals. Figure 6 shows the APOD-PWM approach's carrier signals. In addition to the PWM methods listed above for DC-DC MMC systems, researchers also favor other methods of PWM.

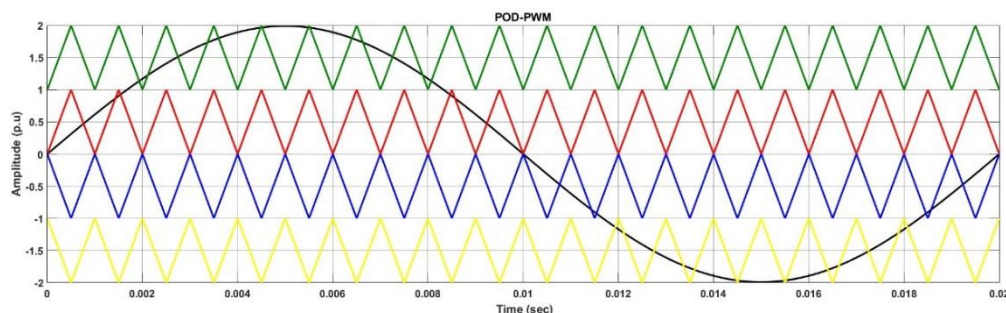


Figure 5. POD-PWM structure (Four carrier carriers).

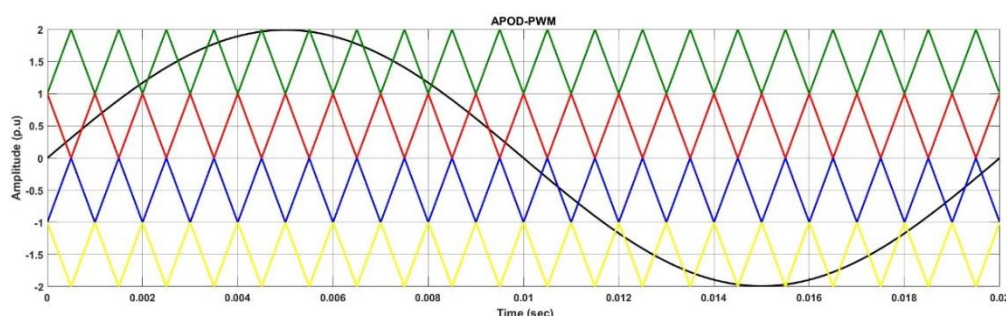


Figure 6. The construction of the APOD-PWM method carriers (Four carrier carriers).

In addition to the PWM methods listed above for DC-DC MMC systems, researchers also favor other methods of PWM such as hybrid PWM techniques, Selective Harmonic Elimination (SHE) PWM, Nearest Level Modulation (NLM), and Space Vector Pulse Width Modulation (SV-PWM). To maximize the efficiency of new-generation power systems and achieve effective power transfer appropriate with the waveform of the resultant signal utilized in conventional and innovative DC-DC MMC designs, new types of hybrid PWM techniques have been developed by combining or modifying traditional PWM techniques in several ways. This study (Ronanki et al., 2018) proposes a novel hybrid PWM technique that combines the best features of PD-PWM and PSC-PWM. In comparison to traditional PWM strategies, the suggested hybrid approach to PWM offers several benefits: higher output voltage, lower intensity of circulating currents, and smaller fluctuations in capacitor voltage regardless of low-frequency operation; it also reduces the problem of inconsistent power distribution and switch usage; it lessens low-order harmonics in circulating current frequencies; it reduces harmonics encompassing the switching frequency; it lowers converter losses; and it lowers the value of arm inductance. SHE-PWM is a low-frequency switching-based PWM approach that allows the output voltage's basic and many lesser harmonics to be neutralized at lower frequencies. The goal of the SHE PWM technique is to provide an output voltage waveform that is roughly sinusoidal, with the main component that can be adjusted as necessary below a defined range of values and with selected harmonics removed. The nearest level modulation (NLM) modulation technique is appealing for MMC architectures with a large number of SMs. The NLM approach uses no trapezoidal carrier signal and computes the switching states and operating rates for every stage of the MMC architectures immediately (Moranchel et al., 2015). Unlike carrier-based modulation, which uses triangle carrier waves, the NLM uses just one, offering more flexibility and ease of use for digital realization (Y. Deng et al., 2015; Moranchel et al., 2015). SV-PWM is a more effective carrierless modulation approach than carrier-based PWM techniques because it uses reduced DC link voltage, has better harmonic characteristics, is easier to apply in digital configurations, and has redundancy modes of operation available. A popular and extremely effective modulation structure for traditional and DC-DC MMC applications is SV-PWM.

Conclusion

This paper presents a critical assessment of PWM technology, which is the backbone of DC-DC MMC systems based on power electronics. A significant comparison of PWM methods that are favored by several researchers has been provided, particularly concerning the management of recently developed DC-DC MMC systems. Furthermore, a key categorization of PWM approaches utilized in both conventional and DC-DC MMC systems, as well as the fundamental operating principles of PWM technology, have been described. Significant analyses of the architectures and operating systems of the PWM methods covered by this categorization have been provided.

References

- Akbar, S. M., Hasan, A., Watson, A., Wheeler, P., & Odhano, S. (2020). Finite Control Set Model Predictive Control of Isolated DC/DC Modular Multilevel Converter. *IECON 2020 The 46th Annual Conference of the IEEE Industrial Electronics Society*, 5282–5289. <https://doi.org/10.1109/IECON43393.2020.9254434>
- Bashir, S. B., Ismail, A. A. A., Elnady, A., Farag, M. M., Hamid, A.-K., Bansal, R. C., & Abo-Khalil, A. G. (2023). Modular Multilevel Converter-Based Microgrid: A Critical Review. *IEEE Access*, 11, 65569–65589. <https://doi.org/10.1109/ACCESS.2023.3289829>
- Chen, P., Liu, J., Xiao, F., Zhu, Z., Huang, Z., & Ren, Q. (2022). Optimal Phase-Shifted Modulation Method for Suppressing the Current Ripple of Modular Multilevel Converter-Bidirectional DC–DC Converter Under Unbalanced Operation. *IEEE Journal of Emerging and Selected Topics in Power Electronics*, 10(1), 690–703. <https://doi.org/10.1109/JESTPE.2021.3106159>
- Deng, F., Lü, Y., Liu, C., Heng, Q., Yu, Q., & Zhao, J. (2020). Overview on submodule topologies, modeling, modulation, control schemes, fault diagnosis, and tolerant control strategies of modular multilevel converters. *Chinese Journal of Electrical Engineering*, 6(1), 1–21. <https://doi.org/10.23919/CJEE.2020.000001>
- Deng, Y., Saeedifard, M., & Harley, R. G. (2015). An improved nearest-level modulation method for the

- modular multilevel converter. *2015 IEEE Applied Power Electronics Conference and Exposition (APEC)*, 1595–1600. <https://doi.org/10.1109/APEC.2015.7104560>
- Dey, S., & Bhattacharya, T. (2021). A Transformerless DC–DC Modular Multilevel Converter for Hybrid Interconnections in HVDC. *IEEE Transactions on Industrial Electronics*, 68(7), 5527–5536. <https://doi.org/10.1109/TIE.2020.2994889>
- Diab, M., Elserougi, A. A., & Abdel-Khalik, A. S. (2023). A hybrid DC-DC modular multilevel converter with capacitors parallel connectivity for arm energy balancing. *Alexandria Engineering Journal*, 83, 286–297. <https://doi.org/https://doi.org/10.1016/j.aej.2023.10.050>
- Elserougi, A., Abdelsalam, I., & Massoud, A. (2023). A hybrid half-bridge submodule-based DC–DC modular multilevel converter with a single bidirectional high-voltage valve. *IET Generation, Transmission & Distribution*, 17(18), 4146–4160.
- Erat, A., & Vural, A. M. (2022). DC/DC Modular Multilevel Converters for HVDC Interconnection: A Comprehensive Review. *International Transactions on Electrical Energy Systems*.
- ERAT, A., & VURAL, A. M. (n.d.). *An Innovative DC-DC Modular Multilevel Converter Topology for Interconnection Asynchronous High Voltage Direct Current Power Grids*.
- Liu, J., Dong, D., & Zhang, D. (2021). A Hybrid Modular Multilevel Converter Family With Higher Power Density and Efficiency. *IEEE Transactions on Power Electronics*, 36(8), 9001–9014. <https://doi.org/10.1109/TPEL.2021.3055690>
- Marquardt, R. (2001). Stromrichterschaltungen mit verteilten energiespeichern. *German Patent DE10103031A1*, 24, 40.
- Moranchel, M., Bueno, E. J., Rodriguez, F. J., & Sanz, I. (2015). Implementation of nearest level modulation for Modular Multilevel Converter. *2015 IEEE 6th International Symposium on Power Electronics for Distributed Generation Systems (PEDG)*, 1–5. <https://doi.org/10.1109/PEDG.2015.7223079>
- Perez, M. A., Ceballos, S., Konstantinou, G., Pou, J., & Aguilera, R. P. (2021). Modular Multilevel Converters: Recent Achievements and Challenges. *IEEE Open Journal of the Industrial Electronics Society*, 2, 224–239. <https://doi.org/10.1109/OJIES.2021.3060791>
- Priya, M., Ponnambalam, P., & Muralikumar, K. (2019). Modular-multilevel converter topologies and applications—a review. *IET Power Electronics*, 12(2), 170–183.
- Qin, F., Hao, T., Gao, F., Xu, T., Niu, D., & Ma, Z. (2020). A Multiport DC-DC Modular Multilevel Converter for HVDC Interconnection. *2020 IEEE Applied Power Electronics Conference and Exposition (APEC)*, 520–524. <https://doi.org/10.1109/APEC39645.2020.9124277>
- Raju, M. N., Sreedevi, J., P Mandi, R., & Meera, K. S. (2019). Modular multilevel converters technology: a comprehensive study on its topologies, modelling, control and applications. *IET Power Electronics*, 12(2), 149–169. <https://doi.org/10.1049/iet-pel.2018.5734>
- Ronanki, D., Azeez, N. A., Patnaik, L., & Williamson, S. S. (2018). Hybrid multi-carrier PWM technique with computationally efficient voltage balancing algorithm for modular multilevel converter. *2018 IEEE International Conference on Industrial Electronics for Sustainable Energy Systems (IESES)*, 224–229. <https://doi.org/10.1109/IESES.2018.8349878>
- Sarkar, S., & Das, A. (2023a). A DC-DC Modular Multilevel Converter Topology with Single Arm for MVDC Railway Application. *2023 IEEE 32nd International Symposium on Industrial Electronics (ISIE)*, 1–6. <https://doi.org/10.1109/ISIE51358.2023.10227946>
- Sarkar, S., & Das, A. (2023b). An Isolated Single Input-Multiple Output DC–DC Modular Multilevel Converter for Fast Electric Vehicle Charging. *IEEE Journal of Emerging and Selected Topics in Industrial Electronics*, 4(1), 178–187. <https://doi.org/10.1109/JESTIE.2022.3221006>
- Sha, G., Duan, Q., Sheng, W., Ma, C., Zhao, C., Zhang, Y., & Tian, J. (2021). Research on Multi-Port DC-DC Converter Based on Modular Multilevel Converter and Cascaded H Bridges for MVDC Applications. *IEEE Access*, 9, 95006–95022. <https://doi.org/10.1109/ACCESS.2021.3072161>

Wang, Y., Aksoz, A., Geury, T., Ozturk, S. B., Kivanc, O. C., & Hegazy, O. (2020). A Review of Modular Multilevel Converters for Stationary Applications. In *Applied Sciences* (Vol. 10, Issue 21). <https://doi.org/10.3390/app10217719>

Xiao, Q., Jin, Y., Jia, H., Tang, Y., Cupertino, A. F., Mu, Y., Teodorescu, R., Blaabjerg, F., & Pou, J. (2023). Review of Fault Diagnosis and Fault-Tolerant Control Methods of the Modular Multilevel Converter Under Submodule Failure. *IEEE Transactions on Power Electronics*, 38(10), 12059–12077. <https://doi.org/10.1109/TPEL.2023.3283286>

CUBESAT TRACKING CONTROL USING SLIDING MODE CONTROLLER AND FUZZY SLIDING MODE CONTROLLER

Onur SİLAHTAR

Dr. Research Assistant, Van Yüzüncü Yıl University, Faculty of Engineering, Department of Electric-Electronic Engineering, Van-Türkiye, (Responsible Author) ORCID: 0000-0002-9654-8008

Özkan ATAN

Associate Professor Dr., Van Yüzüncü Yıl University, Faculty of Engineering, Department of Electric-Electronic Engineering, Van-Türkiye, ORCID: 0000-0001-6443-9600

ABSTRACT

In this study, a sliding fuzzy controller (FSMC) was designed to track the position of two cube satellites moving in the Line of Sight (LOS) coordinate plane. For this purpose, the dynamic models of two CubeSat defined as chaser and non-cooperative target were obtained in the LOS coordinate plane. Then, firstly, Lyapunov criteria were applied and a sliding mode controller (SMC) design was made to ensure the stability of the system. Since the chased target CubeSat was a non-cooperative target, the control process was applied only to the chaser CubeSat. Then, the system was simulated with the MATLAB/Simulink program and efficiency criteria such as settling time, steady-state error and maximum overshoot were obtained. This time, a designed fuzzy sliding mode controller (FSMC) was applied to the same system under the same initial conditions. Efficiency criteria obtained from FSMC were compared with the system under SMC. Accordingly, although both systems reached stability in approximately the same time, it was observed that the steady-state error of the system under FSMC was approximately 27% less. In addition, it was observed that the maximum overshoot amount was approximately 12.3 times higher in the SMC system than in the FSMC system. This high amount of overshoot causes the risk of de-orbiting the chaser cube satellite in the space environment and means quite high energy consumption. In addition, considering the controller outputs, it was observed that the switching was quite hard in the SMC system, while the switching was relatively soft in FSMC system. Considering all these results, it is concluded that the FSMC controller is more efficient and applicable than the SMC controller for the proposed system.

Keywords: Sliding Mode Control (SMC), Fuzzy Sliding Mode Control(FSMC), Line of Sight (LOS) Coordinates, Cubesat Tracking Control, Lyapunov Criteria.

TARGET DETECTION AND TRACKING USING IMAGE PROCESSING AND INTUITIONISTIC FUZZY CONTROLLER

Onur SİLAHTAR

Dr. Research Assistant, Van Yüzüncü Yıl University, Faculty of Engineering, Department of Electric-Electronic Engineering, Van-Türkiye, (Responsible Author) ORCID: 0000-0002-9654-8008

Özkan ATAN

Associate Professor Dr., Van Yüzüncü Yıl University, Faculty of Engineering, Department of Electric-Electronic Engineering, Van-Türkiye, ORCID: 0000-0001-6443-9600

ABSTRACT

In this study, detection and tracking of a target object was achieved by using image processing and an intuitionistic fuzzy controller (IFC). For this purpose, a 15cmx15cm blue square object was determined as the target and a camera was integrated into the gyroscope testing set, which can move in two axes. Using gyroscope, which can be moved up and down thanks to two brushless DC motors attached to it, the exact middle point of the target was detected and then was tracked. Firstly, using image processing algorithms, the color and size information of the object was transferred to the "RaspberryPi" development board integrated into the gyroscope and data input was provided. Then, via IFC embedded in the RaspberryPi board and designed within the scope of this study, "Pulse Width Modulation (PWM) signals" were generated to activate the motors. In order to increase the rotational inertia of the gyroscope, reaction wheels produced from a 3D printer were attached to the shaft of the motors. In addition, thanks to the RaspberryPi tools in the MATLAB/Simulink program, the fast wireless communication feature of the RaspberryPi and the efficiency of the designed IFC, the data obtained from the camera was quickly evaluated and the engines reacted quickly. Moreover, the output parameters of the system were observed in real time in the MATLAB/Simulink program. When the results obtained were examined, it was seen that the system reached stability in a short time and the maximum overshoot was determined to be at an acceptable value. When designing the controller of such a complex system, aerodynamic effects, weight, gravity, internal and external disturbances, etc. were not taken into account. Despite this, the fact that the system is stable and has a robust structure reveals the importance of IFC.

Keywords: Intuitionistic Fuzzy Controller (IFC), Image processing, Target Detection and Tracking, Embedded System.

ELECTRON SPIN RESONANCE STUDY ON SPIN SUSCEPTIBILITY OF GRAPHITE NANOPARTICLES

Özgül KARATAŞ

*Assist. Prof. Dr., Konya Technical University, Vocational School of Technical Sciences, Department of Electricity and Energy,
Konya – Türkiye, ORCID: 0000-0003-3848-5800*

ABSTRACT

In recent years, many theoretical and experimental research have been carried out on carbon-based materials due to their possible applications such as electronic and spintronic devices, etc. Generally, experimental studies have focused on transport properties, but research on magnetic properties is quite lacking. The structure of graphitic particles at the nanoscale is highly defective with influences on their physical and chemical properties. Electron spin resonance (ESR) is a sensitive technique that can be used to detect paramagnetic species. By analysing the ESR signal, different contributions to the sample's overall magnetism can be identified, coming from defects and conduction electrons.

Herein, the spin susceptibility of graphite nanoparticles in carbon-based pencil was investigated by means of ESR technique in the 20 – 300 K temperature range. According to the obtained ESR measurements, a narrow and sharp Lorentz line was observed at all temperatures. Moreover, the spin sensitivity decreased with increasing temperature, and a Curie-like behaviour was clearly evident. This was attributed to localized defect states in the sample. The temperature-dependent changes in Lande g-factor and line width were also analysed. The g-factor was calculated to be around 2.003, which was very close to the free electron spin g-value and the line widths exhibited a significant linear temperature dependence, decreasing as temperature increased.

Keywords: ESR, Graphite, Spin Susceptibility, Nanoparticle

EDGE COMPUTING ASSISTED INTELLIGENT HEALTHCARE MONITORING SYSTEM FOR ELDERLY PEOPLE

S. Satheeskumaran

Department of Electronics and Communication Engineering Anurag Univerity, Hyderabad, India

K. Sasikala

Department of Electrical and Electronics Engineering Vels Univerity, Chennai, India

N. Sharath Babu

Department of Electronics and Communication Engineering Anurag Univerity, Hyderabad, India

Kumar Neeraj

Department of Electronics and Communication Engineering Anurag Univerity, Hyderabad, India

ABSTRACT

Many healthcare devices have been developed in the past for elderly people by continuous monitoring. Elderly care and monitoring can be accomplished by collecting physiological data and proper analysis. Fall detection can be identified with the help of motion sensors and health condition is monitored by various sensors in the wearable device. These sensors generate huge amount of data and it is highly impossible to analyze the data within the wearable device. Hence it is mandatory to opt for cloud storage and analysis to deal with the enormous amount of data generated in continuous monitoring. To avoid the delay in processing, edge computing framework is proposed.

Though elderly people health deteriorates due to variety of chronic diseases, heart disease risk detection and prediction are focused in this work. To perform fall detection and prediction is also focused in this work to initiate some preventive steps. Fall detection is also linked with heart rate sensors to improve the reliability and accuracy. Careful analysis of these generated data is highly important to take necessary decision, hence deep learning based approaches are utilized in the edge computing framework.

Keywords: Internet of Things, Edge analytics, Intelligent Healthcare, Fall detection, smart communication

HUMIDITY AND TEMPERATURE SENSING LAUNDRY RACK

Kelven Kenn Simon

Keningau Vocational College, Electrical Technology Department, Keningau, Sabah

Mohd Hairul Izhan Jubberin

Keningau Vocational College, Electrical Technology Department, Keningau, Sabah

Abstract

Automated laundry rack is a self-adjusting light and water sensitive rack for apartment residents. It is equipped with several electronic components. It is easy, quick and safe. Apartments residents often feel frustrated to return homes and find their clothes wet and dripping with water on drying racks outside their houses. The unpredictable nature of weather and limited space for drying racks make it harder for apartment tenants to dry their clothes outside their homes.

Keywords: humidity, temperature, laundry rack

SCALAR CONTROL BASED ON INTERVAL TYPE-2 FUZZY LOGIC OF DUAL STAR INDUCTION MACHINE

HELLALI Lallouani

Department of Electrical Engineering, Faculty of Technology, University of Msila, Algeria

MOUSSA Oussama

Department of Automatics and Electromechanical, Faculty of science and technology, Ghardia, Algeria

Saad Belhamdi

Department of Electrical Engineering, Faculty of Technology, University of Msila, Algeria

AKKA Ali

Department of physics sciences, Higher Normal School of Boussada, Boussada, 28001, Algeria

ABSTRACT

Today, the six-phase induction machine instead of traditional three-phase induction machine is used in many applications (such as compressors, rolling mills, pumps, fans, cement mills....) for there advantages in power segmentation, electromagnetic torque pulsation minimization and precision.

Since the last of 20s years, the researchers concentrate their efforts to develop the techniques of control. Several techniques are developed as vector control or scalar control. The main difficulty in the dual star induction machine (DSIM) control resides in the fact that complex coupling exists between machine input variables, output variables and machine intern variables as the field, torque or speed. The scalar control ensures the decoupling between field and torque and made the control of the double stator induction machine similar to that of a DC motor, where there exists a natural decoupling between field and torque.

Fuzzy logic is a scheme used in artificial intelligence and widely utilized in different areas including the control and the automation. The application of interval type-2 fuzzy logic has been a success and it is able to control machines with measurement uncertainties. Fuzzy regulators (IT2FLC) have been successfully used for a few numbers of non linear and complex processes, IT2FLC are robust and their performances are insensible to parameter variations contrary to conventional regulators. Recently several researchers make efforts to improve the robustness and performances of the IT2FLC by using neuron and genetic algorithms.

In the aim to improve the performance of the electrical drives based on scalar control, fuzzy logic regulators attracts more and more the attention of many scientists the configuration and design of the interval type-2 fuzzy Logic regulators for the scalar control of dual star induction machine. The purpose of this work is to provide a scalar control interval type-2 fuzzy logic for dual star induction machine. The suggested interval type-2 fuzzy logic regulators out performs the type-1 fuzzy logic and PI regulators, according to the simulation study for high-performance control of the dual star induction machine drive.

Keywords: Dual star induction machine, Inverter, scalaire control, Interval type-2 fuzzy logic.

AN ASSESSMENT OF THE STATUS OF WOMEN IN STEM FIELDS IN TURKEY

Dicle ÖZCAN ELÇİ

*Assist. Prof., Şırnak University, Faculty of Health, Department of Social Work, Şırnak-Türkiye
(Responsible Author) ORCID: 0000-0003-0493-4428*

ABSTRACT

Becoming competent in STEM (science, technology, engineering and mathematics) fields has become increasingly important in the world and especially in Turkey since the early 2010s in order to catch up with the requirements of the age. Indeed, we are witnessing an era in which the level of development and progress of societies is coordinated with the progress in science and technology. In this context, studies on STEM fields in Turkey continue to be carried out through institutions such as the Ministry of National Education, Ministry of Industry and Technology, Universities and TÜBİTAK. Today, despite the rapidly closing gender gaps between women and men in education and employment, it is a fact that fields or sectors such as science, technology, engineering and mathematics are still dominated by men. Women's representation in these disciplines, which are seen as masculine fields, is still insufficient and gender stereotypes and prejudices persist. In this context, the subject of this study is an assessment of the situation of women and girls in STEM fields in Turkey. The aim is to analyze the education and employment conditions of girls and women in science, technology, engineering and mathematics in line with specific reports. The study is a review of some reports on the representation and status of women in STEM fields in Turkey. As a result, it was revealed that the participation of women and girls in relevant fields is considerably lower than that of men, which is mostly related to the values attributed to gender roles.

Keywords: STEM, women, gender roles, gender inequality.

AUDIOVISUAL ENGINEERING FOR EDUCATIONAL INNOVATION

Jose A. R. CEMBRANOS

Prof. Dr., Jose A. R. Cembranos Universidad Complutense de Madrid, Facultad de Ciencias Físicas, Departamento de Física Teórica, Madrid-Spain, (Responsible Author) ORCID: 0000-0002-4526-7396

ABSTRACT

This work explores the transformative role of audiovisual engineering in fostering educational innovation. In present dynamic learning environments, traditional educational methods are evolving to embrace technology and multimedia resources. Audiovisual engineering, at the intersection of technology and pedagogy, plays a pivotal role in enhancing the educational experience. We examine the current landscape of education, highlighting the challenges and opportunities presented by the digital era. It then delves into the key principles of audiovisual engineering, discussing how it integrates advanced technologies, such as virtual reality, augmented reality, and interactive multimedia, to create immersive and engaging educational content.

The impact of audiovisual engineering on student engagement and knowledge retention is a focal point, with insights into how educators can leverage these technologies to cater to diverse learning styles. We also discuss the importance of adaptability and scalability in designing audiovisual educational solutions that can evolve with the changing needs of students and educators. Moreover, case studies and examples showcase successful implementations of audiovisual engineering in various educational settings at Universidad Complutense de Madrid (Spain), from traditional classrooms to online platforms. The article concludes by emphasizing the ongoing evolution of audiovisual engineering and its potential to shape the future of education through continuous innovation and strategic integration of cutting-edge technologies. As education embraces the digital age, audiovisual engineering stands as a cornerstone for unlocking new dimensions of learning, collaboration, and knowledge dissemination.

Keywords: audiovisual content, university teaching, student engagement, learning outcomes, mixed methods.

A MOVE TOWARDS CASHLESS ECONOMY: A CASE OF CONTINUOUS USAGE OF MOBILE WALLETS IN INDIA

Dr. C. Vijai

Associate Professor, Department of Commerce and Business Administration, Vel Tech Rangarajan Dr. Sagunthala R&D Institute of Science and Technology, INDIA. ORCID: 0000-0003-0041-7466

M. Elayaraja

Assistant Professor, Department of Commerce, St.Peter's Institute of Higher Education and Research, Tamil Nadu, INDIA.

ABSTRACT

The smartphone is used everywhere in this modern world. The technological advancement has made the smartphone as devices where mobile users can make money transactions or payment by using an application installed on the phone. This paper aims to study the mobile wallet and also study customer risk, satisfaction, security and awareness regarding the functionality of mobile wallets. It also explains mobile wallet importance and scope for the customer. A structured questionnaire was prepared and data were collected from 260 respondents and a factor affecting the adoption and usage of the mobile wallets was analyzed by using ANOVA and frequency analysis. SPSS was used to perform statistical analysis.

Keywords: Mobile wallet, Cashless Transaction, E-Commerce, Virtual cash, Smart phones, Micro payments.

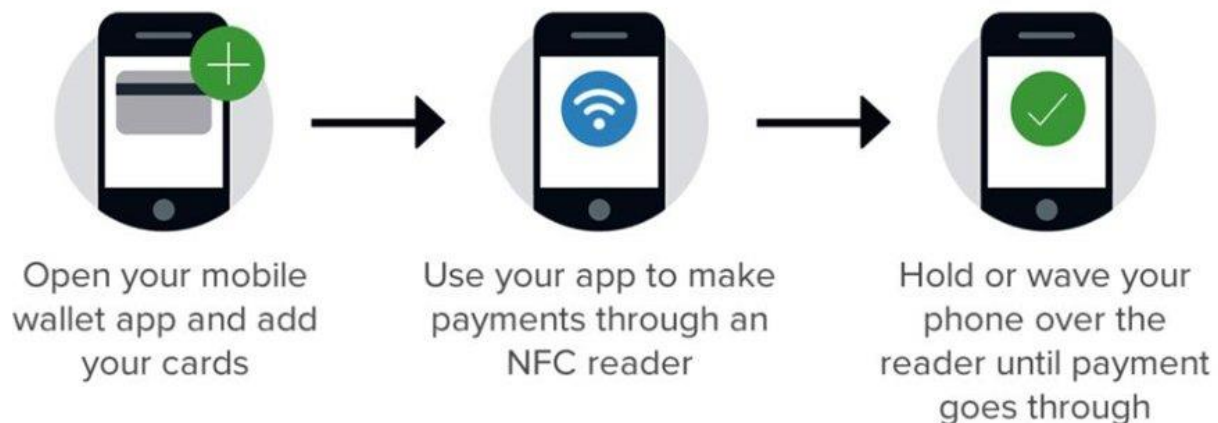
INTRODUCTION

Digital Wallets or mobile wallets (e-wallets) refer to a device or service that lets you carry out monetary transactions electronically. Cashless payments for monetary transactions can be done through a Digital Wallet. And you can also link your digital wallet with your mobile phone number. India has seen a phenomenal increase in the number of digital wallet users. The nation is slowly moving towards being a cashless economy. A Digital Wallet or a Mobile Wallet (e-wallet) makes your life easier by helping you to carry out transactions in a quick and easy way.¹ A mobile wallet, in simple terms, is a virtual mobile-based wallet where one can store cash for making mobile, online or offline payments. There are various types of mobile wallets in India, such as open, semi-open, semi-closed and closed - depending on the type of usage and payments that can be made. Wallets are growing rapidly as they help in increasing the speed of transaction, especially for e-commerce companies and all e-commerce marketplaces have integrated with such mobile wallets too.²

¹ "Digital Wallets In India | Go Cashless with these TOP 20" <https://www.sumhr.com/digital-wallets-india-list-online-payment-gateway/>. Accessed 21 Oct. 2019.

² "Top 10 Mobile Wallets in India | Best money Transfer App in" 29 Nov. 2018, <https://www.socialbeat.in/blog/top-10-mobile-wallets-in-india/>. Accessed 21 Oct. 2019.

What is a Mobile Wallet?



Source: <https://magnetoitsolutions.com/blog/year-of-mobile-wallets-in-india>

Mobile Wallet, or sometimes known as Digital Wallet, is an electronic device or online service that allows an individual to make electronic transactions. These electronic transactions include purchasing items online or buying something from the store with the help of smartphones.³

GLOBAL MOBILE WALLET MARKET

The major key players operating in the global mobile wallet market are Apple Inc., Amazon.com Inc., American Express, Microsoft Corp. Inc, Visa Inc., Paytm, Alipay, MasterCard Inc, BlackBerry Ltd., Samsung Electronics Co., Ltd., and Google Inc, among others.⁴

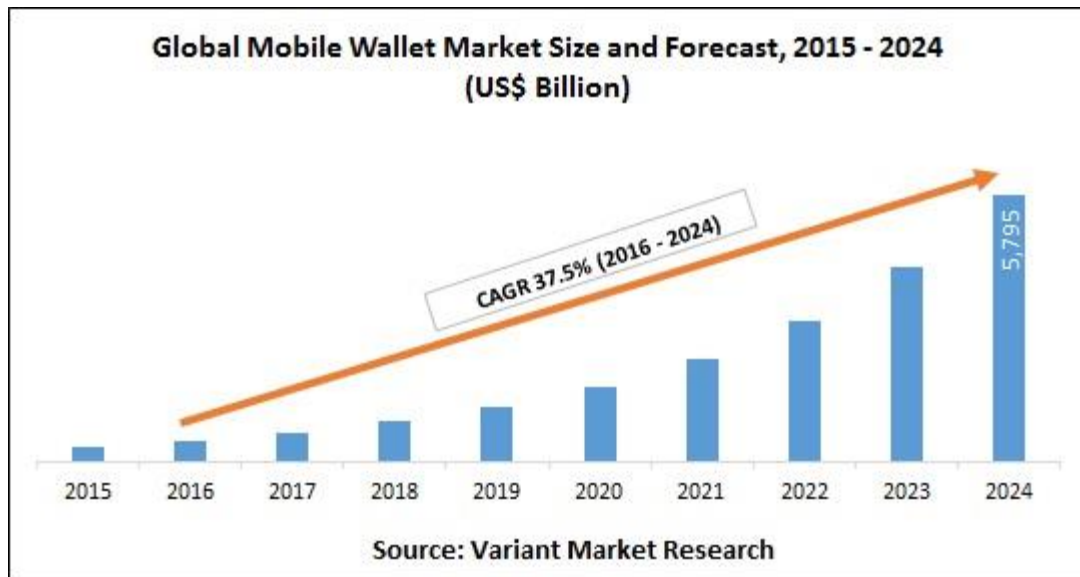
According to the report, the global mobile wallet market was valued at approximately USD 594.00 billion in 2016 and is expected to reach approximately USD 3,142.17 billion by 2022, growing at a CAGR of around 32% between 2017 and 2022.

Worldwide adoption of smartphones and technological advancements are influencing the growth of mobile wallet market. The mobile wallet is a type of payment service by which anyone can receive and send money via mobile devices. A mobile wallet is a form of e-commerce model that is made to be used with mobile devices and offers convenience and easy access. It provides service of the online transaction for every single operation in a routine. Mobile wallet offers various facilities such as debit, credit and online transaction from a bank account.⁵

³ "2019: Year of Mobile Wallets in India - Magneto IT Solutions." 20 May. 2019, <https://magnetoitsolutions.com/blog/year-of-mobile-wallets-in-india>. Accessed 17 Oct. 2019.

⁴ "Mobile Wallet Market - Variant Market Research." <https://www.variantmarketresearch.com/report-categories/information-communication-technology/mobile-wallet-market>. Accessed 17 Oct. 2019.

⁵ "Global Share of Mobile Wallet Market to Surpass \$3,142.17" 10 Jul. 2019, <http://www.globenewswire.com/news-release/2019/07/10/1880730/0/en/Global-Share-of-Mobile-Wallet-Market-to-Surpass-3-142-17-Billion-by-2022-Zion-Market-Research.html>. Accessed 17 Oct. 2019.



GLOBAL MOBILE WALLET MARKET SHARE BY REGION

Based on geography, global mobile wallet market is segmented into North America, Europe, Asia- Pacific, and Rest of the World (RoW). North America is further bifurcated into U.S., Canada, and Mexico whereas Europe segment consist of UK, Germany, France, Italy, and others. Asia-Pacific is segmented into India, China, Japan, South Korea, and others while RoW is bifurcated into South America, Middle East, and Africa.⁶

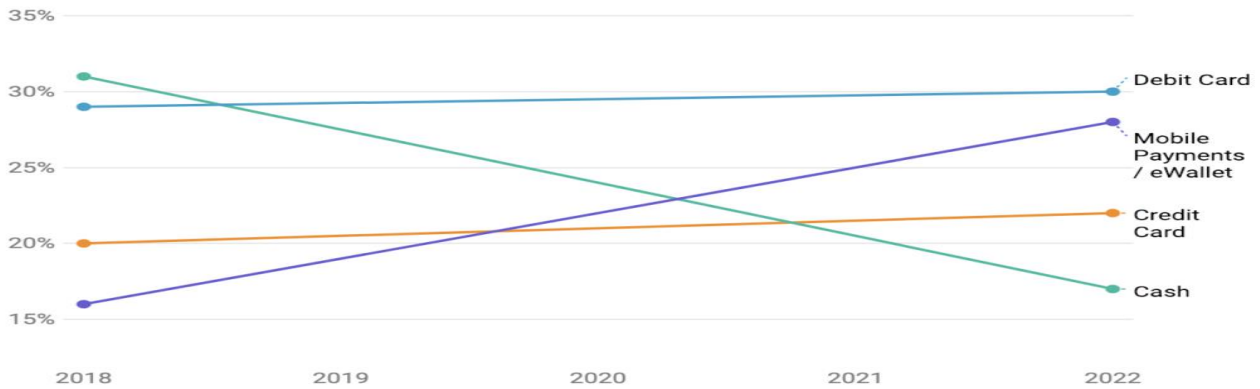


GLOBAL USE OF MOBILE PAYMENTS FORECAST

According to Worldpay's 2018 Global Payment Report the use of mobile payments is set to continue its inexorable rise and become the second most common payment method after debit cards by 2022. Global Use of Mobile Payments Forecast To Increase To 28% In 2022 And Surpass Credit Cards And Cash (2018)⁷

⁶ "Mobile Wallet Market - Variant Market Research." <https://www.variantmarketresearch.com/report-categories/information-communication-technology/mobile-wallet-market>. Accessed 17 Oct. 2019.

⁷ "30 Global Mobile Payment Stats & Trends - Merchant Savvy." <https://www.merchantsavvy.co.uk/mobile-payment-stats-trends/>. Accessed 17 Oct. 2019.



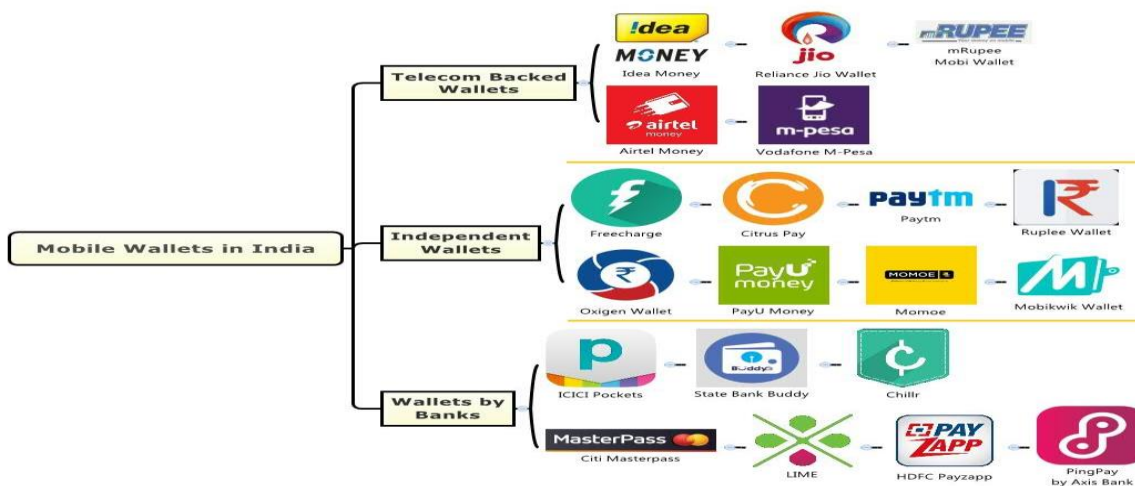
Source: World pay's 2018 Global Payment Report

SCENARIO OF INDIAN MOBILE WALLET MARKET

According to “India Mobile Wallet Market Size & Analysis, Forecast & Opportunities, 2018-2023”, mobile wallet market registered whopping double digit value growth, with a CAGR of 67.10% during review period of 2013-17 despite headwinds like mandatory KYC. The market advanced on the back of rising digital awareness, increasing smartphone ownership coupled with surging internet penetration, and convenience associated with such services. The market is forecast to gain immensely during forecast period of 2018-23 to reach around USD 7 Billion by 2023, on account of Government’s increased focus to make India a cashless and digital economy. This will help the industry and directly benefit companies like Paytm, Mobikwik, FreeCharge, Oxigen and many others.⁸

MOBILE WALLET ECOSYSTEM IN INDIA

- ❖ Telecom-operated mobile wallets
- ❖ Mobile wallets offered by banks
- ❖ Independent mobile wallet



Source: <https://www.techinasia.com/talk/mobile-wallet-wars-india>

⁸ "India Mobile Wallet Market Size & Analysis, 2018-2023" 22 Aug. 2018, <https://www.prnewswire.com/news-releases/india-mobile-wallet-market-size--analysis-2018-2023-market-registered-double-digit-value-growth-with-a-cagr-of-67-10-during-review-period-of-2013---2017--300700990.html>. Accessed 17 Oct. 2019.

TYPES OF WALLETS

There are three types of mobile wallets in India – open, semi-closed and closed.

- **Open wallets** can only be issued by the banks. They allow you to purchase goods and services, cash withdrawal at ATMs and to transfer funds.
- **Semi-closed wallets** have a specific contract with the issuer to accept the payment instruments. They will allow you to buy goods and services or perform financial services at clearly identified merchant locations.
- **Closed wallets** are accounts issued by a company to a consumer for buying goods and services exclusively from that company. Here a certain amount of money is locked with the company in case of a cancellation or return of the order, or gift cards.⁹

RESEARCH METHODOLOGY

The study is based on the primary data collected from 260 respondents from the different parts of Chennai. By using a structured questionnaire. A five-point Likert scale was used in the questionnaire for obtaining responses. SPSS was used to do statistical analysis.

HYPOTHESIS OF THE STUDY

H0-Null Hypothesis: There is no significant relationship between gender and aware regarding the functionality of mobile wallets.

H0-Null Hypothesis: There is no significant relationship between gender and continue using mobile wallet.

H0-Null Hypothesis: There is no significant relationship between Education and aware regarding the functionality of mobile wallets.

H0-Null Hypothesis: There is no significant relationship between Occupation and Mobile wallet services allow for a faster usage of mobile applications

H0-Null Hypothesis: There is no significant relationship between Occupation and Money loaded in M-wallet on a monthly.

DATA INTERPRETATION AND ANALYSIS

Table 1 Aware regarding the functionality of mobile wallets

Gender	Maybe	No	Yes	Total	X2	P Value	H0 Accepted/ Rejected
Male	7	5	80	92	2.1383	0.343	Accepted
	5.9	0.8	-5.5	1.2			
	6	8	154	168			
Female	-4.0	-0.8	5.7	0.8			
Total	13	13	234	260			
	1.8	0.1	0.1	2.0			

Sources: collected and computed through Questionnaire.

H0-Null Hypothesis: There is no significant relationship between gender and aware regarding the functionality of mobile wallets.

Significant at 5% (P<0.05) –Rejected, Non Significant at 0.05–(P>0.05)-Accepted.

⁹ "Types of Mobile Wallets and Leaders in India - TutorialsPoint." 26 Dec. 2016, <https://www.tutorialspoint.com/articles/types-of-mobile-wallets-and-leaders-in-india>. Accessed 18 Oct. 2019.

Table 1 indicates that P-value is 0.343. Since P-value is more than 0.05, the null hypothesis is accepted at a 5% level of significance. Hence, it is concluded that there is no significant association between gender and aware regarding the functionality of mobile wallets.

Table 2 Want to continue using mobile wallet

Gender	Maybe	No	Yes	Total	X2	P Value	H0 Accepted/ Rejected
Female	15	0	77	92	1.8047	0.406	Accepted
	2.5	0.0	-0.3	2.2			
Male	24	3	141	168			
	-2.3	2.6	0.3	0.6			
Total	39	3	218	260			
	0.2	2.6	0.0	2.8			

Sources: collected and computed through Questionnaire.

H0-Null Hypothesis: There is no significant relationship between gender and continue using mobile wallet.
Significant at 5% (P<0.05) –Rejected, Non Significant at 0.05–(P>0.05)-Accepted.

Table 2 indicates that P-value is 0.406. Since P-value is more than 0.05, the null hypothesis is accepted at a 5% level of significance. Hence, it is concluded that there is no significant association between gender and continue using the mobile wallet.

Table 3 Aware regarding the functionality of mobile wallets

Education	Maybe	No	Yes	Total	X2	P Value	H0 Accepted/ Rejected
Degree	4	0	15	19	17.5646	0.002	Rejected
	11.5	0.0	-3.9	7.6			
P.G and above	8	13	217	238			
	-6.4	2.3	5.6	1.6			
Up to H.Sc	1	0	2	3			
	3.8	0.0	-1.2	2.6			
Total	13	13	234	260			
	8.9	2.3	0.5	11.7			

Sources: collected and computed through Questionnaire.

H0-Null Hypothesis: There is no significant relationship between Education and aware regarding the functionality of mobile wallets.

Significant at 5% (P<0.05) –Rejected, Non Significant at 0.05–(P>0.05) - Accepted.

Table 3 indicates that P-value is 0.002. Since P-value is less than 0.05, the null hypothesis is rejected at a 5% level of significance. Hence, it is concluded that there is a significant association between Education and awareness regarding the functionality of mobile wallets.

Table 4 Mobile wallet services allow for a faster usage of mobile applications

Occupation	Maybe	No	Yes	Total	X2	P Value	H0 Accepted/ Rejected
Business	6	1	8	15	26.0699	0.000	Rejected
	16.2	4.3	-8.2	12.3			
Employed	12	1	100	113			
	0.5	0.3	-0.8	0.0			
Profession	8	0	79	87			
	-1.9	0.0	3.4	1.5			
Student and housewife	1	0	44	45			
	-3.1	0.0	8.4	5.3			
Total	27	2	231	260			
	11.7	4.6	2.9	19.2			

Sources: collected and computed through Questionnaire.

H0-Null Hypothesis: There is no significant relationship between Occupation and Mobile wallet Services allow for a faster usage of mobile applications.

Significant at 5% (P<0.05) –Rejected, Non Significant at 0.05–(P>0.05) - Accepted.

Table 4 reveals that high-level perception observed among Mobile wallet services allows for a faster usage of mobile applications. As the calculated P-value is less than 0.000 and the result is highly significant at a 5% level. Hence, the null hypothesis is rejected. There is a significant association between Occupation and Mobile wallet services that allow for a faster usage of mobile applications.

Table 5 Money loaded in M-wallet on a monthly

Occupation	1001 - 2000	2001- 3000	3001- 4000	Above 4000	Less than 1000	X2	P Value	H0 Accepted/ Rejected
Business	8	0	7	0	0	83.8028	0.000	Rejected
	9.6	0.0	25.2	0.0	0.0			
Employed	35	21	2	22	33			
	4.1	-0.6	-5.9	17.5	-4.3			
Profession	27	10	11	12	27			
	3.2	-9.9	10.9	1.3	-0.2			
Student and housewife	6	18	0	0	21			
	-9.4	27.1	0.0	0.0	17.0			
Total	76	49	20	34	81			
	7.5	16.6	30.3	18.8	12.5			

Sources: collected and computed through Questionnaire.

H0-Null Hypothesis: There is no significant relationship between Occupation and Money loaded in M-wallet on a monthly.

Significant at 5% (P<0.05) –Rejected, Non Significant at 0.05–(P>0.05) - Accepted.

Table 5 reveals that high-level perception observed among money loaded in M-wallet on a monthly as the calculated P-value is less than 0.000 and the result is highly significant at a 5% level. Hence, the null hypothesis is rejected. There is a significant association between Occupation and money loaded in M-wallet on a monthly.

FINDINGS AND CONCLUSION

Technology can modification everything, and it pays the approach for future services, particularly in money areas. Mobile billfold usage awareness as unfolding among the client in Chennai town thanks to a government policy of termination and this as forcefully evoked the usage of the mobile wallets. And accountable towards digital payments, and a conducive in some or the opposite approach towards growth and success of constructing India digital. In spite of many security problems, the client is inclined towards e-payments due to its convenience, easy use, fast service, and availability. The future of mobile wallets would be bright in India and with the emergence of technology; mobile wallets will provide more value-added services to the customer.

REFERENCES

1. Poonam P and Shalu R, Mobile Wallet: An upcoming mode of business transactions, International Journal in Management and Social Science, Vol. 4, Issue no.5
2. <https://www.google.co.in/wallet/>
3. <https://www.phonepe.com/en/>
4. <https://www.rbi.org.in/>
5. <https://www.investopedia.com/terms/m/mobile-wallet.asp>
6. <https://www.socialbeat.in/blog/top-10-mobile-wallets-in-india/>
7. <https://magnetoitsolutions.com/blog/year-of-mobile-wallets-in-india>
8. www.money-on-mobile.net
9. <https://www.digitalindia.gov.in/>

THE IMPACT OF USING AI CHATGPT ON DIGITAL MARKETING

Ihor PONOMARENKO

*Assoc. Prof., State University of Trade and Economics, Faculty of Trade and Marketing, Department of Marketing, Kyiv-Ukraine
(Responsible Author) ORCID: 0000-0003-3532-8332*

Dmytro PONOMARENKO

*PhD Student, International University of Business and Law, Kyiv-Ukraine
ORCID: 0009-0002-2904-3904*

ABSTRACT

The evolution of modern information technologies has led to the intensification of the development of Data science approaches, first of all, it is necessary to pay attention to the prospects of using artificial intelligence, which is based on high-performance machine learning algorithms. In the digital environment, there are opportunities to collect big data continuously and accumulate information on specialized servers for further processing through the use of various models. Neural networks have gained considerable popularity in modern conditions, which, thanks to the flexibility of choosing architectures and the ability to configure various activation functions, allow the processing of heterogeneous data and obtaining optimal results. There are a large number of different products based on neural networks on the market, among which it is advisable to pay attention to ChatGPT. This product from OpenAI functions based on artificial intelligence and allows companies to create extended text responses on a significant number of topics based on requests. The presence of a significant level of competition in the digital environment encourages companies to introduce various innovative technologies to secure leading positions. Establishing effective communications with the target audience involves the use of modern digital marketing tools. The formation and implementation of an effective digital marketing strategy allows companies to segment the audience by scientific principles and apply specialized models of interaction with each group of consumers. Thanks to the use of artificial intelligence, companies have the opportunity to build personalized communication with each client, which contributes to increasing the level of loyalty. The use of ChatGPT allows companies to create high-quality content for interaction with the target audience and optimize the use of available resources. ChatGPT provides an opportunity to interact with users on social media on an ongoing basis, stimulating interest in the company and its products.

Keywords: ChatGPT, communications, content, digital marketing, information, target audience.

Introduction

Technological transformations and the introduction of innovations contribute to the active development of various machine learning algorithms. IT companies compete with each other and develop advanced technologies that allow optimizing business processes in various areas of activity. Thanks to the large amount of data that accumulates in the process of interaction between various participants of the business environment on the Internet, it has become possible to test machine learning algorithms and identify effective ways of transforming various products. In modern conditions, a large number of products are presented in digital form and represent specialized software that makes it possible to make changes on a permanent basis in order to optimize the functioning of the relevant modules. Machine learning algorithms are an effective tool for improvement, which make it possible to identify various hidden relationships between indicators in the database. Technological giants with significant financial resources and the ability to attract the best specialists in the industry have taken machine learning to a qualitatively new level. One of the applied directions in the field of data processing is the technology of artificial intelligence, which involves interaction with various users through text messages. At this stage, the chatbot with artificial intelligence ChatGPT, which was developed by the OpenAI company, gained the most popularity. The effectiveness of the presented product was evaluated by various groups of consumers, in particular, specialists in the field of marketing,

who were given the opportunity to increase the effectiveness of the development and implementation of marketing campaigns in the digital environment.

Materials and Methods

The presented work involves the study of specialized scientific and practical sources regarding the peculiarities of the use of ChatGPT by companies to increase the level of profitability and ensure the appropriate level of communications. The implementation of the GPT-3 model in the form of a scheme allows you to monitor the execution of relevant processes and obtain the optimal result, which is advisable to increase the effectiveness of the use of digital marketing tools (Floridi et al., 2020).

Findings and Discussion

Cloud computing has significantly expanded the possibilities of using machine learning algorithms, because powerful equipment that has access to servers with information that accumulates 24/4 is used in the process of implementing algorithms for processing large data sets. Modern machine learning algorithms can use structured, semi-structured, and unstructured data to build various models and identify relationships. It should be noted that digital data, text, audio, and video content, as well as various images, can be used as valuable information (Janiesch et al., 2021).

When implementing neural networks in practical applications, the following approaches are put into practice:

1. **Classification:** This algorithm employs a set of metrics to identify segments within a population that share specific characteristics. Through the discerned relationships, grouping is facilitated. Each cluster exhibits distinct behavior influenced by social, economic, psychological, and demographic factors (Radhakrishnan et al., 2023).
2. **Recommender Systems:** By utilizing a metric framework, neural networks establish clusters for recommender systems. This aids in selecting pertinent recommendations for new segments of the population, aligning with their particular activities (Shrivastava et al., 2023).
3. **Predictive Models:** Leveraging the connections unearthed by neural networks, predictive models enable the anticipation of user behavior. Drawing from identified relationships and trends, causal connections can be established, allowing for the projection of subject behavior in upcoming time frames based on key influencing factors (Gehlot et al., 2023).

The perspective of using text information when interacting with artificial intelligence, which is based on complex neural networks, is explained by the relative ease of consumers creating thematic queries thanks to the use of relevant sets of words. The interaction of the user and artificial intelligence thanks to the use of a specialized chat allows to creation of a human-oriented dialogue and achieves a high level of mutual understanding. Based on the presented principles, such products as ChatGPT (text content generation) and DALL-E (high-quality image generation) were created (Fulton, 2023).

Chatbot with artificial intelligence ChatGPT should be classified as a model that solves the problem of classification. Based on the query, keywords are identified and relationships between them are searched to determine the meaningful component. By the identified relationships, the relevant text is searched in the databases to which the presented chat has access. It should be noted that in this case a set of complex calculations is implemented based on numerical information by converting a text query into numbers. Calculations and implementation of an algorithm based on artificial intelligence involve the involvement of neural networks with complex architectures and their implementation on servers with high power. Improvement of the algorithms integrated into the chatbot leads to the appearance of new versions of ChatGPT (Wu et al., 2023).

Figure 1 shows how ChatGPT works from the user's initial text query to the generated keyword response.

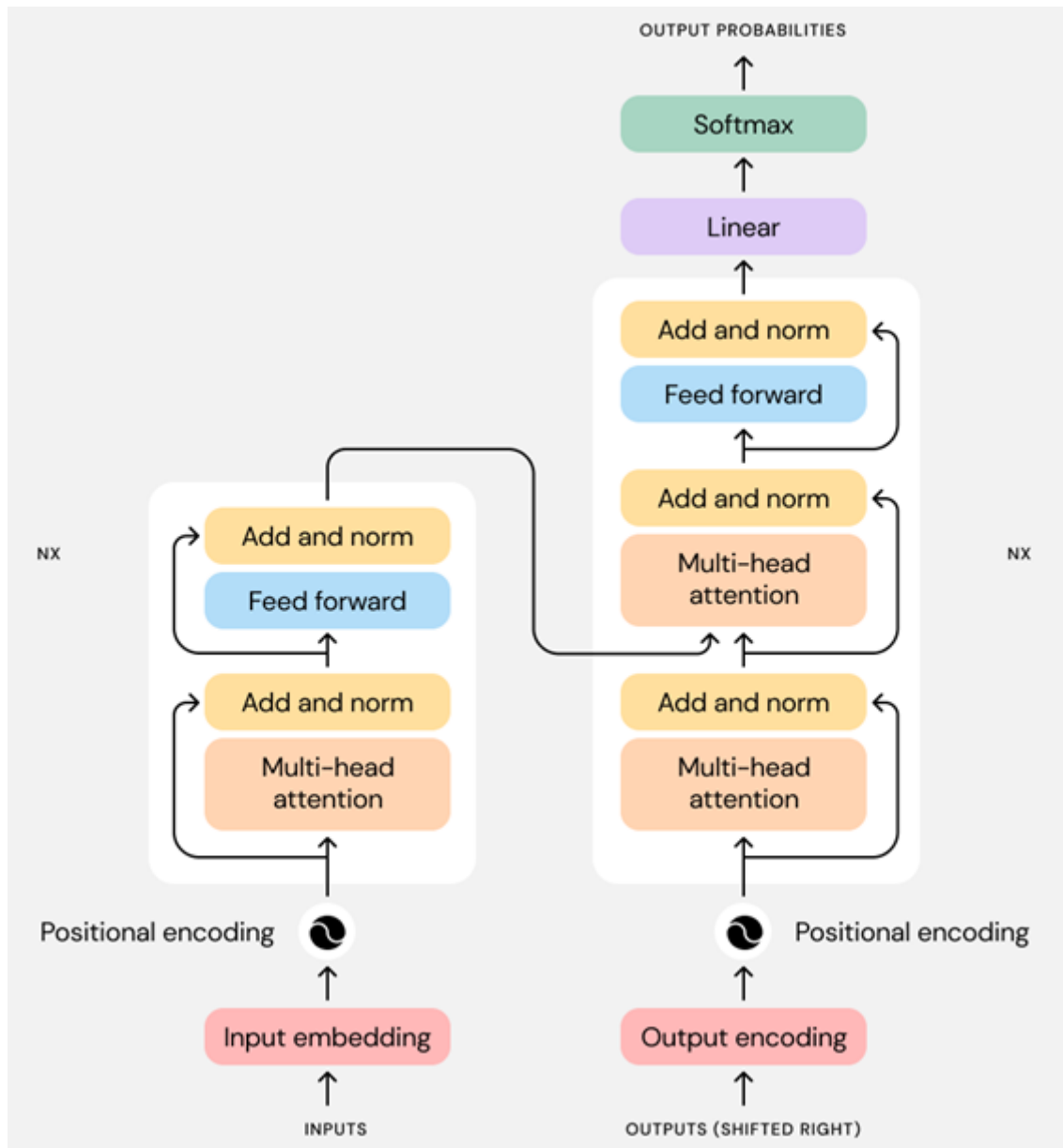


Figure 1. GPT-3 model (SINCH, 2022)

Companies constantly improve their marketing strategies in offline and online environments to ensure high competitive positions in the functioning markets. Digitalization processes force modern brands to actively reorient themselves to the Internet, as demographic changes lead to the gradual replacement of older generations by representatives of Generation Z, and soon, the activation of the alpha generation. Each of the demographic groups is characterized by certain distinctive characteristics, but the company's interaction with any customers involves the use of relevant content. Modern users are focused primarily on video content and photos, which allows companies to receive the necessary information in a visualized form. In many cases, textual information is also in demand among consumers, but the description should be concise and stimulate attention thanks to intriguing titles. The presented principles regarding the formation of active text content are used by companies when applying various digital marketing tools (Ariffin et al., 2023).

Among the key directions of using ChatGPT in the process of improving the digital marketing strategy of companies, it is advisable to highlight the following:

1. Increasing the SEO efficiency of the company's resources on the Internet. Thanks to the constant search for relevant keywords, it is possible to achieve high positions for the company's resources in search results,

which significantly affects the level of attracting new users. The effectiveness of ChatGPT allows to create lists of keywords for company pages in various social media according to the specifics of their operation. Along with this, it is possible to implement various strategies for the formation of specialized dictionaries and markup of pages according to the specifics of various groups of potential customers (Cutler, 2023).

2. Creation of unique texts. Modern users appreciate unique and concise texts that allow them to get information about the relevant products or services of the company. Thanks to the use of ChatGPT, it is possible to create relevant textual content that will be interesting to the relevant groups of consumers. For each of the groups, it is possible to generate a text that will be perceived with the highest possible level of interest (Lancaster, 2023).

3. Communication with users in social networks. The process of interacting with the target audience in various social networks involves not only posting test information but also communicating with users. Subscribers appreciate prompt and competent answers to their questions (Koyuturk et al., 2023). To motivate users to engage in dialogue and discuss issues related to brands, it is advisable to use ChatGPT, which allows to quickly generate answers to questions from various visitors to the company's social media resources.

Conclusion and Recommendations

The development of various technologies similar to ChatGPT is an objective reality of today and is actively used by various companies in the process of implementing complex marketing strategies in the digital environment. Along with the generation of text content, other approaches are also implemented that can be used to establish communications with the target audience. One of the examples of the potential use of innovations in the field of content generation is Microsoft's integration of the Paint graphic editor into Windows 11, which, based on specialized algorithms, will generate images based on text requests from users (Bowden, 2023). The development of artificial intelligence in the future will allow companies to create personalized content for each of their customers, increasing the level of interpersonal communication between the brand and consumers. Over time, users will perceive communication with artificial intelligence as communication with alive people. Accordingly, companies will receive more effective marketing tools for promoting their products in the digital environment and increasing the level of loyalty of the target audience.

References

- Floridi, L., & Chiriatti, M. (2020). GPT-3: Its nature, scope, limits, and consequences. *Minds and Machines*, 30, 681-694. <https://doi.org/10.1007/s11023-020-09548-1>
- Janiesch, C., Zschech, P., & Heinrich, K. (2021). Machine learning and deep learning. *Electronic Markets*, 31(3), 685-695. <https://doi.org/10.1007/s12525-021-00475-2>
- Radhakrishnan, A., Belkin, M., & Uhler, C. (2023). Wide and deep neural networks achieve consistency for classification. *Proceedings of the National Academy of Sciences*, 120(14), e2208779120.
- Shrivastava, R., Sisodia, D. S., & Nagwani, N. K. (2023). Deep neural network-based multi-stakeholder recommendation system exploiting multi-criteria ratings for preference learning. *Expert Systems with Applications*, 213, 119071.
- Gehlot, A., Ansari, B. K., Arora, D., Anandaram, H., Singh, B., & Arias-González, J. L. (2022, July). Application of Neural Network in the Prediction Models of Machine Learning Based Design. In *2022 International Conference on Innovative Computing, Intelligent Communication and Smart Electrical Systems (ICSSES)* (pp. 1-6). IEEE.
- Fulton, J. S. (2023). Authorship and ChatGPT. *Clinical Nurse Specialist*, 37(3), 109-110. DOI: 10.1097/NUR.0000000000000750
- Wu, T., He, S., Liu, J., Sun, S., Liu, K., Han, Q. L., & Tang, Y. (2023). A brief overview of ChatGPT: The history, status quo and potential future development. *IEEE/CAA Journal of Automatica Sinica*, 10(5), 1122-1136. doi: 10.1109/JAS.2023.123618.

- SINCH. GPT-3: What is it, and what's the hype about? (2022). Access Address (19.11.2023): <https://www.sinch.com/blog/gpt-3-what-is-it-and-whats-the-hype-about/>
- Ariffin, S. K., Hilmawan, H., & Zhang, Q. (2023). Consumers Consumption Values and Consumer Satisfaction toward Continuous Intention to View Digital Video Content. *Journal of Entrepreneurship, Business and Economics*, 11(2), 81-129.
- Cutler, K. (2023). ChatGPT and search engine optimisation: The future is here. *Applied Marketing Analytics*, 9(1), 8-22.
- Lancaster, T. (2023). Artificial intelligence, text generation tools and ChatGPT—does digital watermarking offer a solution?. *International Journal for Educational Integrity*, 19(1), 10. <https://doi.org/10.1007/s40979-023-00131-6>
- Koyuturk, C., Yavari, M., Theophilou, E., Bursic, S., Donabauer, G., Telari, A., ... & Ognibene, D. (2023). Developing Effective Educational Chatbots with ChatGPT prompts: Insights from Preliminary Tests in a Case Study on Social Media Literacy. arXiv preprint arXiv:2306.10645.
- Bowden Z. Microsoft may bring AI capabilities to apps like Paint and Photos on Windows 11 (2023). Access Address (19.11.2023): <https://www.windowscentral.com/software-apps/windows-11/microsoft-may-bring-ai-capabilities-to-apps-like-paint-and-photos-on-windows-11>

APPLICATION OF ROBOTIC MILKING OF COWS IN THE FUNCTION OF SUSTAINABLE FARM DEVELOPMENT IN THE REPUBLIC OF SERBIA

Suzana KNEŽEVIĆ

*Academy of Applied Studies Šabac, Unit for Agricultural and Business Studies and Tourism,
Orcid: orcid.org/0000-0002-7983-8169*

Milena MILOJEVIĆ

*Academy of Applied Studies Šabac, Unit for Agricultural and Business Studies and Tourism,
Orcid: orcid.org/0000-0001-6997-1532*

Maja DOŠENOVIĆ MARINKOVIĆ

*Academy of Applied Studies Šabac, Unit for Agricultural and Business Studies and Tourism,
Orcid: orcid.org/0009-0007-8904-0197*

Goran STANIŠIĆ

*Academy of Applied Studies Šabac, Unit for Agricultural and Business Studies and Tourism,
Orcid: orcid.org/0000-0001-8584-287X*

ABSTRACT

The concept of sustainable agriculture development involves the application of sustainable technical and engineering systems on farms. One such solution, increasingly applied in the Republic of Serbia, is the use of robotic milking systems on dairy farms. The goal of implementing robotic milking is to enhance milk production and quality, as well as to ensure the welfare and protection of the animals. Some of the solutions used on farms in Serbia are designed with cows wearing pedometers around their legs, signaling any changes for each individual cow. Cows are trained to independently go to the robotic milking system when they feel the need, exhibiting lower levels of stress and agitation. Milking with robots can be organized three to four times a day, allowing cows to enter the robot every 6 to 8 hours. The robot stops milking when the milk flow ceases, contributing to udder health preservation.

The use of robotic milking also contributes to a balanced animal diet and early detection of diseases such as mastitis. The system selectively directs cows to different parts of the barn, following the "resting, milking, feeding" principle. From the perspective of sustainable development, robotic milking contributes to the survival of livestock farms. The Ministry of Agriculture is involved in the entire process, providing subsidies for the purchase of milking robots and various other incentives to increase milk production.

Keywords: robotic milking, cows, sustainable development, farm, Republic of Serbia



THE INVESTIGATION OF DIRECT DYE SORPTION ON LINEN FABRIC

Milena Nikodijević

University of Niš, Faculty of technology, Department of textile science, Leskovac, Republic of Serbia

Nemanja Vučković

International university of Novi Pazar, Department of art, Novi Pazar, Republic of Serbia

ABSTRACT

This paper presents the investigation of direct dye adsorption on linen fabric. The prepared linen fabric was subjected to dyeing by a standard process, varying in concentration and time of dyeing. The used fabric is 100% natural cellulose fabric derived from linen fabrics. The samples of linen fabric had linear density 73 tex of warp and 63 tex of weft and surface mass $238 \text{ g}\cdot\text{m}^{-2}$. Flax, an ancient and natural cellulose fiber, stands as a testament to the enduring legacy of human ingenuity in fabric production. Flax is one of the oldest materials utilized for crafting textiles, meeting the diverse needs of clothing and beyond. Direct dyes, characterized by their chemical composition primarily consisting of sulfonated azo compounds, trace their origins to benzidine, its derivatives, or amines such as diaminostilbene. These water-soluble dyes, universally known for their solubility in aqueous solutions, exhibit a notable subset that further dissolves in low-alcohol solutions, showcasing the versatility inherent in their molecular structure. Samples of fabric were dyed at temperature of $60 \text{ }^{\circ}\text{C}$. The concentration of dye on the fiber is the dependent variable and independent variables are temperature, time, additives and salts and dye selection. The degree of dye exhaustion decreases as the dye concentration increases during dyeing, whereas the degree of dye exhaustion increases with longer dyeing times. As beginning concentrations and times grow, so does the variation in the amount of adsorbate adsorbed. An increased amount of dye is adsorbed per unit mass of linen fabric when the dyeing process is prolonged. The maximum absorption happened at the dye concentrations and dyeing times that are higher. The modeling of fabric dyeing identified the efficacy of *Freundlich* nonlinear and linear isotherms in simulating isothermal adsorption. Parameters in the *Freundlich* model vary with adsorbent quantity and temperature.

Keywords: linen fabric, dyeing, direct dye, *Langmuir* isotherm, *Freundlich* isotherm

DEVELOPMENT OF AN INTERACTIVE MODULE FOR DESIGNING ADDRESSABLE CLOTHING

Yulia KOBERNIK

Graduate student Russian State University named after A.N. Kosygin (Technology, Design, Art). Department of Art Modeling, Design and Technology of Clothing. Moscow Russia

Varvara GETMANTSEVA

PhD in Engineering, Russian State University named after A.N. Kosygin (Technology, Design, Art). Department of Art Modeling, Design and Technology of Clothing. Moscow Russia, ORCID № 0000-0003-0441-3198

ABSTRACT

Clothing today is acquiring new functionality. Many scientists propose to control and regulate the physiological and emotional state of the person wearing the garment. It is also proposed to endow clothes with information and communicative functionality (charging of smartphones, signalling functions, etc.). All this is very important for human life activity. But in order to provide all this functionality in clothes it is necessary to collect in the information base and organise consistency of all characteristics and properties of the product, including, characteristics of materials and ways of technical solution of the product as a functional product.

In the framework of this work, a hypothesis is put forward about the possibility of organising an interactive digital module that would include a database of clothing characteristics, properties, place and way of its use and other positions. By selecting these positions it will be possible to regulate the functionality of the product, adjusting it to the needs of the consumer.

The developed interactive model assumes certain stages of actions in the development of the product. The developed scheme of the interactive model is the author's and describes the process of designing a garment according to the given parameters and characteristics.

Keywords: interactive module, clothing, clothing design, construction, database.

With the development of innovative technologies and artificial intelligence (AI), manufacturing processes in various fields of activity are being transformed. The fourth industrial revolution is characterised by the application of robotics and digital control technologies, which increases the efficiency of industrial production.

Artificial intelligence is a system that is capable of imitating human intellectual and creative activity, the purpose of which is to create non-material things. AI is characterised by learning, making decisions, determining conclusions and much more.

AI is divided into three main groups:

1. Weak or limited. A human-created programme that is capable of handling a limited set of individual tasks better than a human being
2. General. A programme can solve any intellectual task as well as a human. For example, painting a picture or chatting with a human, composing a song or creating a new scientific theory. An AI that can successfully mimic human thinking, but no more.
3. Strong or super-intelligent. Such a programme should perform absolutely all tasks of intellectual and creative nature better than a human and even surpass it.

The ability of artificial intelligence to make a decision independently is based on three aspects: the algorithm given when the program is written, the data set, and the conditions on which the program can rely to make a decision.

Machine learning is an AI tool built on the processing of large amounts of data. It involves algorithms that can categorize, evaluate information and produce the most appropriate solution. There are three types of machine learning:

1. "With a teacher". A method where the correct result is prescribed in the program in advance.
2. "Without a teacher". A method when there is a lot of different information and the program has to build connections between the data by itself.
3. "Deep learning" - neural network, some mathematical model built on the principle of organization and functioning of biological neural networks. Artificial neural networks consist of modeling nodes, which are connected by links to transfer information according to various algorithms. In this scheme, while maintaining dependency, the output data of one node becomes the input data for another node. The neural network is trained by the difference between the processed data and the desired result[1].

Areas such as marketing and design are, to date, the first to apply AI to customer interactions. With the help of BIG DATE and machine learning, it's easy to predict the design at the consumer's request without the need for a designer. One example is the Tommy Hilfiger brand. In 2018, the American company announced a collaboration with IBM and the Fashion Institute of Technology (FIT) to develop an artificial intelligence that would create collections instead of a designer and be a source of inspiration for retailers. In this collaboration, the task of the AI was to collect data and analyze it, predicting consumer preferences. The partnership resulted in new colors, fabric prints and shapes for a new clothing collection[2,3].

The authors of this paper proposed to develop an interactive module with neural network properties. The subject of research is winter sportswear.

Considering the database design process in a mass production environment, 4 main blocks shaping the development are identified:

- block one "Input Data", which includes information on the product, such as product type and its characteristics; gender and age; type of sport; region of use; and time of year; protective functions and individual sensations of the consumer.
- Block two "Material Package" including data on materials for the product depending on the selected or labeled functions[4,5].
- Block three "Design Solution", including product design options and transformations of certain elements depending on the "input data".
- Block four "Technological solution", including data on technological processing of products depending on the selected design and material package.
- Block five "Output data", including design and construction documentation for the manufacture of the product.

For each block of the interactive model of databases a set of operations is defined, displaying the stage-by-stage process of product design. Blocks in the database are interconnected by systems. Each subsequent block depends on the previous one, which allows us to speak about the sequential development of technical solution of the set on the basis of synthesis and analysis of the previous information (Fig. 1).

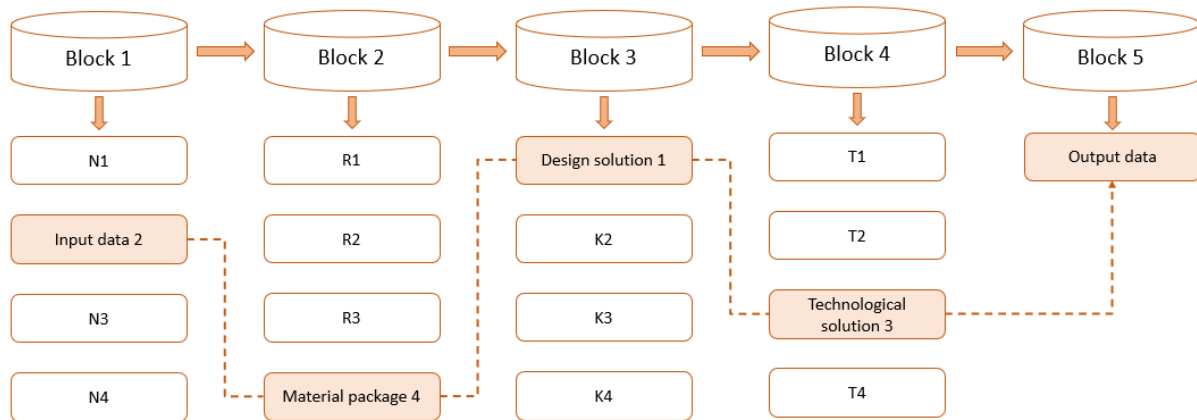


Figure 1 - Links between blocks of the interactive module

User interaction with the program (interactive module) is built according to certain rules. In the start window there are 4 main sections (Fig. 2). By the example of the first block let's consider the stages of interaction. In this block the information on the product is filled in, the so-called "Input Data" for the manufacturer.

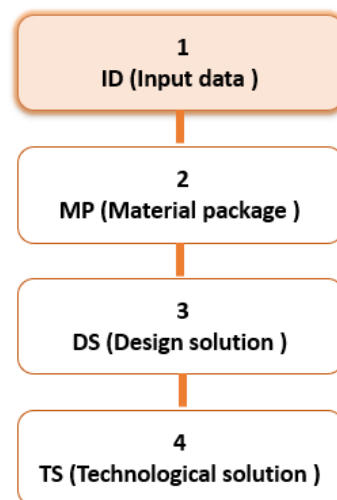


Figure 2 - Start window of the program

Having analyzed the elements and descriptions of products for active winter sports recreation, the structure of the first section was developed, where the type of product and its characteristics, gender and age, type of sport, region of operation and time of year are defined.

To start filling in the input data in the program, you need to click on the button of the selected section and go to the window with a list of all levels and sub-levels. For example, select the section "1 ID". We get to the window with the list of all levels of this section:

1. Select the first level "Sex/Age" (Fig. 3), a list of sublevels opens, in which it is necessary to select the sex and age group of the person for whom the costume will be designed.

Figure 3 - First level "Gender/Age"

2. Clicking the "Next" button we go to the second level "Type of sport" (Fig.4), a list of sub-levels opens, in which it is necessary to select a group of winter sports.

Figure 4 - "Type of sport" level

3. In the section "product operation region" in the interactive module, it is necessary to specify the place where the product is planned to operate.
4. On the fourth level select the protective functions of the product (Fig. 5). The program provides three options:
 - Light and high level of protection - these packages contain already selected protective functions for certain areas of the body. You do not need to choose them. They are ready-made packages with selected protection functions.
 - Select protection - the program user selects individual protection for each area of the body.



Figure 5 - Level Four. Protective functions in clothing

After completing all levels in the first section, the program analyzes the information and passes it to the second level for selection of the material package. Accordingly, after selecting the data in the second block, the program again analyzes the data and transfers it to the third level for design selection, etc. As a final result in the last fifth block we get a ready package of design and technological documentation for sewing the first sample of the product.

The interactive module is a digital tool in the product development process. Its main function is to provide manufacturers with up-to-date information on a permanent basis[6]. The interactive model of the addressable garment database being developed will allow:

- to process information according to specified algorithms;
- use the arrays to develop new models of products according to the selected functions;
- store large amounts of information.

Bibliography

1. Artificial intelligence empowers designers at IBM, Tommy Hilfiger, and FIT Collaboration. [Electronic resource] URL: <https://www.forbes.com/sites/rachelarthur/2018/01/15/ai-ibm-tommy-hilfiger/?sh=7304eaf478ac> (accessed 01.12.2023)
2. Gaidai, M. O. Revolution in the fashion industry / M. O. Gaidai, K. V. Zbykovsky // Spring Days of Science of Higher School of Economics : Collection of reports of the international conference of students and young scientists, Ekaterinburg, April 17-19, 2019. - Yekaterinburg: LLC "Publishing house UMC UPI", 2019. - C. 337-339
3. Tukhanova, V. Yu. Designing the quality of garments using artificial intelligence / V. Yu. Tukhanova // Kostyumologiya. - 2021. - T. 6, № 2
4. Cherunova I.V. Physico-biological conditions for the design of protective clothing against human cooling in the air and water // Engineering Herald of the Don. 2017, №3. - 13 c
5. Smirnova D.S., Kryuchkova A.A., Getmantseva V.V. The study of design features of the suit for protection from the cold in the Arctic and the Arctic shelf / In the Proceedings of the All-Russian Conference of young researchers with international participation: Social and humanitarian problems of education and professional self-realization (Social Engineer - 2019). - 2019. - C. 325-327.
6. Kobernik Y.O. Development of a method to intellectualize the design process of winter sportswear with adjustable features/ Y.O. Kobernik, V.V. Getmanceva// International Cappadocia scientific research congress: Full Text Book-II. - Cappadocia-Nevşehir 17 December 2021. – p.311-313

ENERGY SPECTRUM OF NON RELATIVISTIV SHRODINGER EQUATION FOR NONLINEAR POTENTIAL

Khalid Reggab

Ziane Achour university, Faculty of exact sciences and informatic, Departement of physics. Djelfa, Algeria
ORCID ID: <https://orcid.org/0002-9283-9035>

ABSTRACT

In this work, we represent one of several method for solving the nonlinear system like the Schrodinger equation, the numerical method, which is called the semi-inverse variation method, the method was applied to solve the Schrodinger equation for different cases and values of constants and, the method gives satisfied results and agreed with the previous works. The main objective of this work is to give the variation numerical formulation to search solutions in the quantum domain using the semi-inverse variation method [2] which is based to resolute the Schrodinger equation and therefore to find the wave function and the energy eigenvalues. This method was applied the radial part of Schrodinger equation. In order to determine the wave functions and accompanying energy, this study is based on the solution of the radial Schrödinger equation. The semi-inverse variational approach, an approximation method, is presented in this work. This approach is applied to different potentials into the most well-known equations which are the Schrodinger, Klein Gordon, and Dirac equations, to determine the solution of the energy eigenvalues and associated wave functions. To demonstrate the accuracy of the computation and the viability of the method, we provided specific instances. The semi-inverse approach of building generalized variational principles is provided here, demonstrating a novel theoretical foundation and new, diverse methods for constructing generalized variational principles of different fluid and elasticity issues. The semi-inverse approach will have a significant impact not only on fluid mechanics, but also on elasticity theorems.. Comparing the results of the study with those from other power ways, the information gathered demonstrates the efficacy and precision of the procedure. We reviewed the semi-inverse technique findings by comparing them to the results obtained by using the related Laguerre polynomials to solve the radial Schrödinger equation. The semi-inverse variational approach is a strong mathematical tool for developing a variational formulation for a wave type differential problem. So far, this method provides an effective and best strategy for establishing variational principles for a wide range of physical issues.

Keywords: Shrodinger equation, semi inverse, variation method, energy eigenvalues.

ZEMİNLERİN SIVILAŞMA POTANSİYELLERİNİN BELİRLENMESİNDE KULLANILAN YÖNTEMLERİN KARŞILAŞTIRILMASI

Prof. Dr. M. Tahir NALBANTÇILAR

Ankara Hacı Bayram Veli Üniversitesi, Coğrafya Bölümü, Ankara - Türkiye

Öğr. Gör. Yakup ANIT

Şırnak Üniversitesi, Şırnak Meslek Yüksekokulu, Şırnak - Türkiye

ÖZET

Sıvılaşma, suya doygun kohezyonsuz zeminlerin deprem, patlama veya sarsıntılara bağlı olarak gelişen tekrarlı yükler etkisiyle, zemin taneleri arasındaki boşluk suyu basıncının artması, boşluk suyu basıncının yeterince drene olamaması ve benzeri nedenlerle; zemindeki efektif gerilmenin sıfıra yaklaşması yani zeminin taşıma gücünün azalmasına bağlı olarak; zeminin gösterdiği tepki ve/veya olgudur. Literatürde, sıvılaşma nedeniyle taşıma gücünü kaybeden zeminlerde; i) üstteki yapıların zemine gömülmesi, ii) üstteki yapıların devrilmesi/yan yatması, iii) yapıların yana eğilmesi, iv) gömülü yapıların zemin yüzeyine çıkması, v) istinat yapıları ve şevlerin yanal yer değiştirmesi vb. hasarların oluştuğu kaydedilmiştir.

Araştırmacılar, sıvılaşma mekanizmasını anlamak ve zeminlerin sıvılaşma potansiyelini belirlemek için gerilme, birim deformasyon ve enerjiye dayalı yöntemleri önermişlerdir. Zeminlerin sıvılaşma potansiyeli, gerilme yaklaşımını kullanan SPT, CPT gibi arazi yöntemleri ve dinamik üç eksenli kesme, burulmalı kesme, rezonant kolon, bender eleman gibi laboratuvar deneyleri ile belirlenmektedir. Sıvılaşma potansiyelini laboratuvar tekniklerini kullanarak belirlemede son zamanlarda enerji kavramı da kullanılmaya başlanmıştır.

Bu çalışmada, zeminlerin sıvılaşma potansiyelini belirlemek için önerilmiş yöntemlerden bazılarının karşılaştırılması yapılarak; enerji temeline dayanan ve üç yönlü dinamik hareket uygulayabilen Dinamik Basit Kesme Deney (DBKD) düzeneği kullanılarak zeminlerin sıvılaşma potansiyeli ve sıvılaşma enerjisinin hesaplanması hakkında bilgi verilmektedir.

Anahtar Kelimeler: Sıvılaşma, Sıvılaşma Analizi, Sıvılaşma Deneyleri, Dinamik Basit Kesme Deneyi.

COMPARATIVE EVALUATION OF METHODS USED IN DETERMINING THE LIQUEFACTION POTENTIAL OF SOILS

ABSTRACT

Liquefaction is the inability of saturated, loose, cohesionless soils to be drained due to the increasing pore water pressure of saturated, loose, cohesionless soils that are subjected to repeated loads due to the shaking of earthquakes, and the water behaves like a liquid. Soils that rapidly lose their bearing capacity due to liquefaction cause damage such as the structures on them sinking into the ground, tilting sideways, or lateral displacement of retaining structures and slopes. Researchers have proposed methods based on stress, strain and energy to understand the liquefaction mechanism and determine the liquefaction potential of soils. The liquefaction potential of soils is determined by field methods such as SPT and CPT, which use the stress approach, and laboratory experiments such as dynamic triaxial shear, torsional shear, resonant column and bender element. Recently, the concept of energy has started to be used to determine the liquefaction potential using laboratory techniques.

In this study, by comparing some of the methods proposed to determine the liquefaction potential of the ground; based on energy and capable of applying three-way dynamic movement; Information is given about the liquefaction potential of soils and the calculation of liquefaction energy using the Dynamic Simple Shear Test (DBKD) apparatus.

Key Words: Liquefaction, Liquefaction Analysis, Liquefaction Experiments, Dynamic Simple Shear Test

1. GİRİŞ

Sıvılaşma, suya doymun kohezyonsuz zeminlerin deprem, patlama veya sarsıntılara bağlı olarak gelişen tekrarlı yükler etkisiyle, zemin taneleri arasındaki boşluk suyu basıncının artması, boşluk suyu basıncının yeterince drene olamaması ve benzeri nedenlerle; zemindeki efektif gerilmenin sıfıra yaklaşması yani zeminin taşıma gücünün azalmasına bağlı olarak; zeminin gösterdiği tepki ve/veya olgudur.

Suya doymun gevşek kumlarda, statik veya dinamik yükleme koşullarında gelişen aşırı boşluksuyu basıncı nedeniyle dayanımları hızla azalmakta ve üzerinde bulunan mühendislik yapılarında ciddi hasarlar oluşabilmektedir. Bu hasarlar, binaların zemine gömülmesi, gömülü yapıların zemin yüzeyine çıkması, yapıların yan yatması veya istinat yapılarının ve şevlerin yanal olarak yer değiştirmesi şeklinde görülmektedir (Towhata, 2008).

Tarihsel süreçte yaşanan sıvılaşma örneklerine ilk olarak 1964 ABD’de Alaska depremi (M_w 9,2) ve Japonya’da Niigata ($M_w=7,5$) depreminde fark edilmiştir. Son yıllarda sıvılaşmanın olumsuz etkileri, 11 Mart 2011 tarihinde Tohoku Körfezinde ($M_w=9.0$) görülmüştür (Bhattacharya ve ark. 2011). Ülkemizde 6 Şubat 2023 tarihinde merkez üssü sırasıyla Pazarcık (Kahramanmaraş) ve Elbistan (Kahramanmaraş) olan 7,7 ve 7,6 büyüklüğündeki depremler; başta Kahramanmaraş, Hatay ve Adıyaman illeri olmak üzere 11 il merkezi ve ilçelerini etkilemiştir. Bu alan içerisinde, Kahramanmaraş, Hatay il merkezleri ile Pazarcık, Gölbaşı, İskenderun başta olmak üzere birçok lokasyonda deprem sonucunda deprem zeminde meydana gelen sıvılaşmaya bağlı olarak yapılarda büyük hasarlar meydana geldiği gözlenmiştir.

Son yıllarda sıvılaşma konusunda kapsamlı araştırmalar gerçekleştirilmiştir. Bunlar genel olarak;

- i) laboratuvar yöntemleri (DeAlba vd., 1976; Ladd vd., 1989),
- ii) arazi yöntemleri (Davis ve Berrill, 2001; Çetin vd., 2004) ve
- iii) sayısal teknikler (Chen vd., 2005; Baziar ve Jafarian, 2007; Zhang vd., 2015; Kokusho vd., 2015; Kokusho ve Mimori, 2015)

şeklinde gruplandırılabilir.

Kohezyonsuz zeminler olarak adlandırılan kumlu zeminlerin sıvılaşma potansiyelinin değerlendirilmesi karmaşık bir jeoteknik problemidir. Sıvılaşmayı birçok faktör etkilemektedir. Bu faktörler; depremin büyüklüğü, iç merkez-sıvılaşan alan uzaklığı, zemin tipi, zeminin sismik sönümlenme karakteristiği, yayılım yolu etkileri, çevre basıncı, zemin katmanlarının geometrisi ve sahaya özgü diğer koşullardır (Law vd., 1990).

Sıvılaşma mekanizmasını anlamak ve zeminlerin sıvılaşma potansiyelini belirlemek amacıyla birçok farklı teknik ve yöntem üzerinde çalışmalar sürdürülmektedir. Bunlar genel olarak arazi ve laboratuvar yöntemleri olarak iki ana gruba ayrılabilir. Bu çalışmada, dinamik yükleme koşulları için geliştirilen laboratuvar tekniklerine değinilecektir. Bunlardan bazıları:

- i. Bender elemanları deneyi,
- ii. Rezonant kolonu deneyi,
- iii. Dinamik üç eksenli basınç deneyi,
- iv. İçi boş silindirik burulmalı kesme deneyi,
- v. Tekrarlı basit kesme deneyi ve
- vi. Laboratuvar model deneyleridir.

Bu laboratuvar yöntemlerini ilke edindikleri yaklaşımlara göre üç ana grupta toplamak mümkündür (Green, 2001). Bunlar; i) Gerilmeye Dayalı Yöntem, ii) Birim Deformasyona Dayalı Yöntem ve iii) Enerjiye Dayalı Yöntem olarak gruplandırılabilir.

1.1. Gerilmeye Dayalı Yöntem

Bu yöntem genellikle arazi ve laboratuvar deney sonuçlarını kullanarak geliştirilmiş bu yaklaşım yaygın kullanılan sıvılaşmayı değerlendirme yöntemidir (Seed ve Idriss, 1971). Ancak, yöntem depremin

büyüklüğü, yüzeydeki maksimum yatay yer ivmesi ve kaynak mesafesi gibi birtakım belirsizlikleri barındırmakta ve yeni çalışmalarla sürekli güncellenmektedir (Youd ve Idriss, 2001). Bu yöntemdeki esas ölçüt, döngü sayısı ve kesme gerilmesi düzeyidir. Seed ve Idriss (1971) tarafından basitleştirilmiş yöntemde, gerçek deprem hareketin laboratuvar koşullarında harmonik yükleme ile ilişkilendirmek amacıyla eşdeğer gerilme değeri ve döngü sayısının tanımlanması önerilmiştir. Gerilmeye dayalı yaklaşımın, meydana gelen sıvılaşma olaylarından elde edilen verilerle sürekli olarak iyileştirilmesine ve güncellenmesine rağmen, rastgele yükleme ile ilgili belirsizlikleri halen devam etmektedir (Green, 2001, Baziar ve Jafarian, 2007).

1.2. Birim Deformasyona Dayalı Yöntem

İki etkileşimli ideal hale getirilmiş kum tanesinin mekaniğinden türetilip daha sonra doğal zeminler için genelleştirilmiştir (Green, 2001; Baziar ve Jafarian, 2007). Bu yöntem esas itibariyle boşluk suyu basıncına, kum türüne, rölatif sıklığa, başlangıç efektif gerilme değerine ve örnek hazırlama yöntemine bakılmaksızın, yaklaşık %0.01 gösterilen eşik kesme birim deformasyonu değerini aşması durumunda, gelişmeye başladığı hipotezine dayanmaktadır. Birim deformasyona dayalı yaklaşım teorik olarak mümkün olsa da sıvılaşmanın meydana gelmesi için gerekli boşluksuyu basıncı artışının başladığı noktayı tahmin etmesi sebebiyle daha az kullanılmaktadır ve mutlaka sıvılaşmanın meydana geleceğini ifade etmemektedir. Bu yöntemin ana eksikliği, döngüsel kesme gerilmesine kıyasla kesme birim deformasyonunun tahmin edilmesindeki güçlüğüdür (Seed, 1980, Zhang vd., 2015).

1.3. Enerjiye Dayalı Yöntem

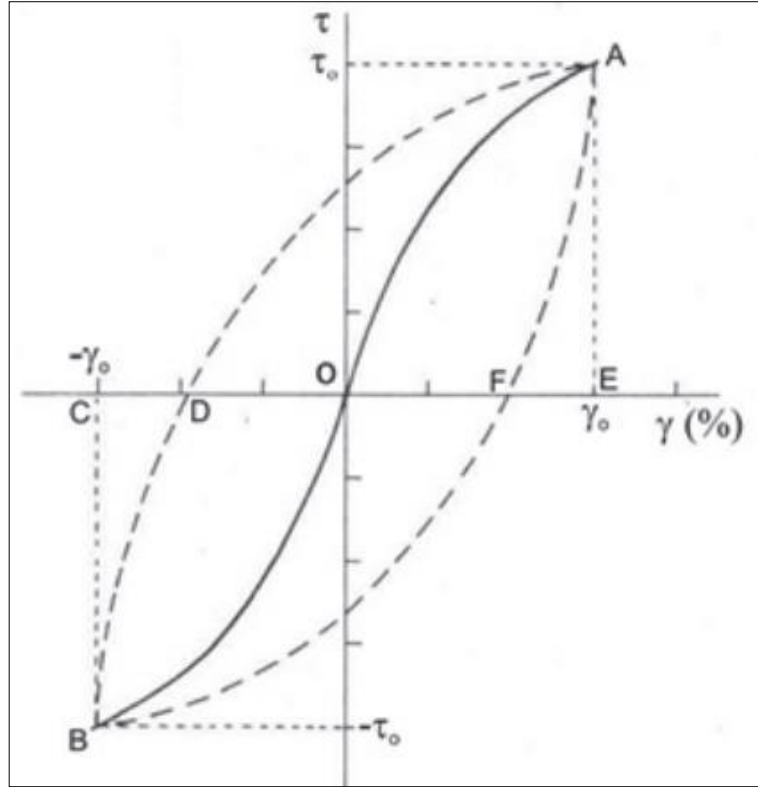
Enerji kavramı kumu sıkılaştırma ve sıvılaşma analizinde ilk olarak Nemat-Nasser ve Shokooh (1979) tarafından ortaya atılmıştır. Bu yaklaşımda kullanılan başlıca parametreler, zeminin rölatif sıklığı (D_r) ve efektif gerilmedir (σ'). Deneylerden elde edilen sıvılaşma enerjisini, numuneye uygulanan frekans (f) ve öteleme miktarının (kesme birim deformasyon oranının- γ) da etkilediği kabul edilmektedir. Kum parçacıklarının kalıcı olarak yeniden düzenlenmesiyle ilişkilendirilen, sıvılaşmaya yol açan belli koşullar altında enerji sabit bir değerdir. Parçacıklarının kalıcı olarak yeniden düzenlenmesiyle ilişkilendirilen birim hacimde biriken enerji (J/m^3), bir döngü sırasında gelişen histerez çevrimi içindeki alan olarak verilir (Hardin ve Drenevich, 1972; Şekil 1).

Numune tarafından sıvılaşmaya kadar absorbe edilen, birim hacimde biriken enerji (δW) aşağıdaki şekilde verilir (Figuroa vd., 1994; Liang vd., 1995):

$$\delta W = \sum_{i=1}^{n-1} 0,5((\tau_i + \tau_{i+1})(\gamma_{i+1} - \gamma_i)) \quad (\text{Eşitlik 1})$$

Burada; τ =kesme gerilmesi, γ =kesme birim deformasyonu ve n =sıvılaşma için kaydedilen döngü sayısıdır.

Bu yaklaşımda, yükleme sürecinde birim hacimde biriken enerji aşırı boşluksuyu basıncının gelişmesiyle doğrudan ilişkilidir. Taneciklerinin kalıcı olarak yeniden düzenlenmesiyle ilişkilendirilen birim hacimde biriken enerji (J/m^3), bir döngü sırasında geliştirilen histerez çevrimi içinde kalan alan olarak ifade edilmektedir (Hardin ve Drenevich, 1972; Figuroa vd., 1994; Liang vd., 1995). Sıvılaşma enerjisi, uygulanan kesme gerilmesi ve kesme birim deformasyonunun büyüklüğüne bağlı olarak ifade edilebildiği için sıvılaşmayı tanımlamada birim enerjinin kullanılması uygundur (Amini ve Noorzad, 2018).



Şekil 1. Tipik bir gerilme-birim deformasyon histerez döngüsü (Hardin ve Drenevich, 1972'den uyarlanmıştır).

Kayabalı vd. (2018)'e göre, anakaya seviyesindeki a_{max} değerini zemin seviyesindeki a_{max} değerine dönüştürmek için aşırı sadeleştirilmiş bir varsayım veya yer tepki analizi gerçekleştirilmelidir. Zemin içinden geçen ve yayılan toplam enerji değişmediği için, enerji temelli yöntemde ne anakaya seviyesindeki a_{max} ne de zemin seviyesindeki a_{max} değerini hesaplamaya gerek vardır. Bu durum diğer iki sıvılaşma değerlendirme yöntemine kıyasla enerji temelli yaklaşımın en belirgin üstünlüğünü oluşturmaktadır.

1. SIVILAŞMA AMAÇLI BAZI LABORATUVAR DENEYLERİ

Literatürde, sıvılaşma potansiyelinin veya enerjisinin belirlenmesine yönelik olarak geliştirilen birçok yöntem bulunmaktadır. Bu çalışmada yaygın olarak kullanılan bazı deney düzeneklerine değinilmiştir.

Bu çalışmada, bazı laboratuvar yöntemleri tanıtıldıktan sonra özellikle "Tekrarlı (Devirsel) Basit Kesme Düzeneği" ile ilgili olarak detay bilgi verilecektir. Bu cihaz, Ankara Üniversitesi Mühendislik Fakültesi Jeoloji Mühendisliği bölüm laboratuvarında bulunmaktadır. Yatay ve düşey yönde tekrarlı yükleme yapılabilmesi en önemli avantajıdır. Diğer sıvılaşma deney düzeneklerine göre gelişmiş özelliklere sahiptir. Sıvılaşma potansiyelinin laboratuvarında sadece rölatif sıkılık ve efektif gerilme ile bulunabiliyor olması, fazla sayıda belirsizlik içeren ve gerilme yöntemine dayanan arazi teknikleri için önemli bir alternatiftir.

i) Dinamik Üç Eksenli Deney

Seed (1980)'in gerçekleştirdiği ilk çalışmalardan günümüze kadar, dinamik üç eksenli deneyler oldukça geliştirilmiş, birçok ülkede kullanımı yaygınlaşmıştır. Taneli zeminlerin gerilme-şekil değiştirme özelliklerinin belirlenebilmesi için en çok tercih edilen deneylerden birisidir (Sweere, 1990). Dinamik üç eksenli deneyler ile hem kohezyonsuz (iri taneli) zeminlerin hem de kohezyonlu (ince taneli) zeminlerin, "Esneklik modülü" ve "Plastik şekil değiştirme" belirlenebilmektedir.

Dinamik üç eksenli basınç deney düzeneğinde (Şekil 2) çapı 50-75 mm arasında ve boyu 100-150 mm arasında değişen ebatlarda numune hazırlanabilmektedir. Deney sistemi pnömatik gerilme kontrollü olup, 0.001-2 Hz aralığındaki frekanslarda devirsel gerilme üretebilmektedir. Deney sisteminde; düşey yük, düşey yer değiştirme, boşluk suyu basıncı ve numunenin hacim değişimi ölçülebilmekte ve kaydedilebilmektedir. Zemin numunelerindeki gerilme-şekil değiştirme ilişkileri, sinüzoidal yükler uygulanarak izotropik ve anizotropik koşullar altında belirlenebilmektedir. Üç eksenli hücrenin üzerine bağlanan sensörlerle 10^{-5} - 10^{-6} düşey deformasyon seviyesinde başlangıç elastisite modülü hesaplanabilmektedir.

Dinamik üç eksenli deney uzun zaman alması, pahalı bir deney olması nedeniyle daha çok araştırma amaçlı kullanılmaktadır. Dinamik üç eksenli deneye paralel olarak dinamik basit kesme deneyi de yapılmaktadır. Bu deney yöntemiyle; dinamik kesme gerilmesi, toplam düşey gerilme, dinamik kesme uzaması, boşluk suyu basıncı elde edilebilmektedir. Dinamik basit kesme deneyi, dinamik üç eksenli deneye göre doğal sıvılaşma olgusunu daha gerçekçi olarak açıklayabilmektedir. Bu deneyde zemin numunesine uygulanan kesme gerilmesinin üniform olarak dağılmadığı kabul edilmektedir (Seed ve Idriss, 1971). Deney sisteminin sadece tek yönde kuvvet veya dinamik etki uyguladığı için (özellikle düşey yönde kuvvet/yük/gerilme uyguladığı için) arazi yükleme koşullarını tam olarak modelleyemediği kabul edilmektedir.



Şekil 2. Dinamik Üç Eksenli Deney Düzeneği

ii) Silindirik Burulmalı Kesme Deneyi

“Ishihara ve Li (1972) tarafından çeşitli K_0 değerlerinde silindirik kum numunelerinin konsolidasyonuna ve devirsel burulma kayma gerilmeleri ile kesmeye izin veren üç eksenli bir burulma kesme aparatı kullanılmıştır. Eksenel yük pistonu, numuneyle aynı yatay kesit alanına sahip olacak şekilde tasarlanmıştır, böylece boşluk suyu hacmindeki herhangi bir değişiklik sınırlandırılarak numune üzerindeki yanal gerilme önlenmiştir. Buna bağlı olarak, düzlemsel şekil değiştirme koşulları altında tekrarlı kesme gerilmeleri uygulanabilmektedir. Burulma kesme testleri, içi dolu veya içi boş silindirik düzeneklerde gerçekleştirilebilir. Ancak, içi dolu silindirlerin burulmasında; numune boyunca düzgün olmayan bir gerilme dağılımı oluşmaktadır. İçi boş silindirlerin kullanılmasıyla bu durum önlenmiştir” (Ishihara, 2006).

Hücre içerisine yerleştirilen silindir bir numuneye belirli frekanslarda üst başlıktan tork uygulanmaktadır. Uygulanan burulma etkisiyle numunede kayma gerilmeleri ortaya çıkmaktadır. Sıvılaşmaya veya tekrarlı yumuşamaya karşı meydana gelen kayma gerilmeleri bazı ampirik formüller kullanılarak tahmin edilebilmektedir.

Burulmalı kesme deneyinde (Şekil 3) zeminlerin deformasyon özellikleri araştırılırken drenaj ve gerilmelerin kontrolünü ve arazi yükleme koşullarını iyi modelleyebilmektedir. Ancak, numune hazırlama güçlüğü, hacmine göre yüzey alanının yüksek olması, numune üzerinde üniform olmayan radyal birim deformasyon uygulaması ve uzun numune yüksekliği (Kammerer ve Pestana, 2002) gibi sebeplerden dolayı bu sistem pratik amaçlar için çok uygun olmamaktadır.



Şekil 3. Silindirik Burulmalı Kesme Deney Düzeneği

iii) Rezonant Kolon Deneyi

Sismik zemin büyütmesi ve makine temelleri başta olmak üzere dinamik kuvvetlerin söz konusu olduğu yerlerde zeminlerin küçük birim deformasyonlardaki kesme modülünü (G_{max} veya G_0) ve sönümleme karakteristiklerini (D) belirlemek için kullanılır. Yakın geçmişteki araştırmalar, bu deneyin sonuçlarının küçük birim deformasyonlardaki ($10^{-8} > d$) statik yüklere uygulanabileceğini göstermiştir (Burland, 1989).

Hazırlanan silindirik numuneler özel bir üç eksenli hazneye yerleştirilir ve arazideki koşullara uygun şekilde konsolide edilir. Numunenin elektromanyetik ekipman ile donanımlı özel yükleme başlığı içeren bir ucuna çok düşük genlikli burulmalı titreşimler uygulanır. Hareket transdüserleri yardımıyla rezonant frekansı, sönümlemesi ve birim deformasyon genlikleri ölçülür (Woods, 1994).

Rezonant kolon deneyi (Şekil 4) yüksek kalibreli, frekans bazlı özel bakım ve kalibrasyon gerektiren laboratuvar düzeneği ile yapılır (spektrum analizörü vb. gibi). Kesme dalgası hızının (V_s) ölçülmesiyle kesme birim deformasyon modülü bulunur.

Kuyudan-kuyuya, kuyu-aşağı, yüzey dalgası ve süspansiyon loglama teknikleri gibi arazi yöntemleri ile doğrudan V_s ölçümleri alınabilse de, rezonant kolon deneyinin artan kesme birim deformasyonu (γ_s) ile G_{max} 'daki değişimin (azalmanın) yanında, γ_s ile birlikte artan sönümlenmeyi (D) verme gibi bir avantajı söz konusudur. Aynı zamanda malzeme özellikleri kesme birim deformasyonlu burulma yüklemesi sırasında değişmez. Bu durum, aynı numunenin farklı çevre basınçlarında test edilmesine imkan sağlamaktadır. Ancak, arazideki gerçek zemin özelliklerinden daha farklı zemin özellikleri bu testin en önemli dezavantajıdır.

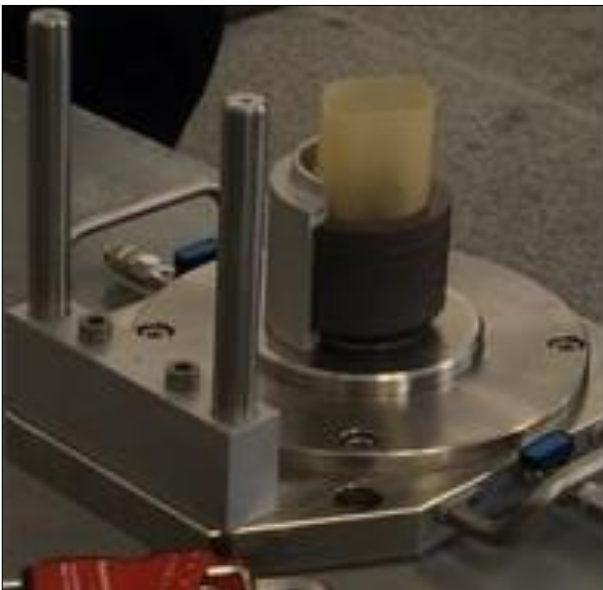


Şekil 4. Rezonant kolon deney düzeneği

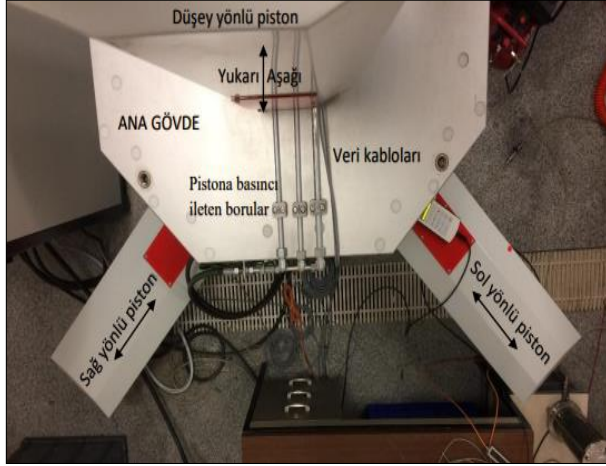
iv) Dinamik Basit Kesme Deneyi (DBKD)

Bu deney düzeneğinde, üç yönde gerçek deprem verisi girilerek deney yapılabilmesi mümkündür. Zeminlerin sıvılaşma potansiyelinin belirlenmesi için geliştirilen bu düzeneğin diğer yöntemlerden daha güvenilir olduğu kabul edilmektedir. Sadece düşey yönde tekrarlı yük uygulayan cihazlardan farklı olarak, yatayda iki yönde dinamik kesme kuvveti, düşey yönde ise dinamik yük uygulayabilmektedir. Yatay ve düşey yöndeki yükleme kapasitesi 10 kN olan cihazın dinamik koşullardaki yükleme hızı her yönde 10 Hz'e kadar çıkabilmektedir. Cihaz, harmonik veya rasgele yüklemeye izin vermektedir. Cihaz, dinamik pistonlarla birlikte hareket eden ve 50 mm'ye kadar ölçüm alabilen deformasyon ölçerlerle teçhiz edilmiştir. Boşluk suyu basıncına ve ölçümüne olanak veren sistemde basınç ölçüm kapasitesi 1 MPa'dır (Beyaz vd., 2021).

Kum numuneleri deney boyunca latex membranlar içerisine yerleştirilerek testler gerçekleştirilmektedir. Deney sırasında kesme işlemi, numuneyi saran 1 mm kalınlığında teflon kaplı bilezikler tarafından yapılmaktadır (Şekil 5 ve Şekil 6).



Cihaz tarafından üç yönde monte edilmiş pistonlar aracılığıyla; numuneye yatayda birbirine dik iki yönde (x ve y yönlerinde), düşeyde ise tek yönde (z yönünde; yataydakilere dik konumda) hareket (sarsıntı) uygulanabilmektedir (Kahraman, 2021; Şekil 7). Cihaza yerleştirilen bir numune, yatayda hareket edebilen bir tablanın üzerine yerleştirilmektedir, üstüne yatay yönde hareket etmeyen bir başlıkla düşey gerilme veya dinamik hareket uygulanabilmektedir (Şekil 8).

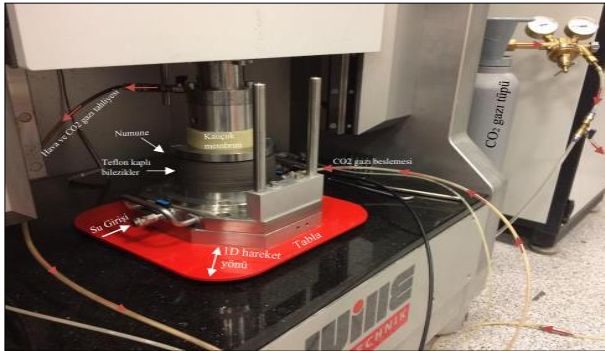


Şekil 7. Dinamik basit kesme deney düzeneğinin üstten görünüşü (Kahraman, 2021)

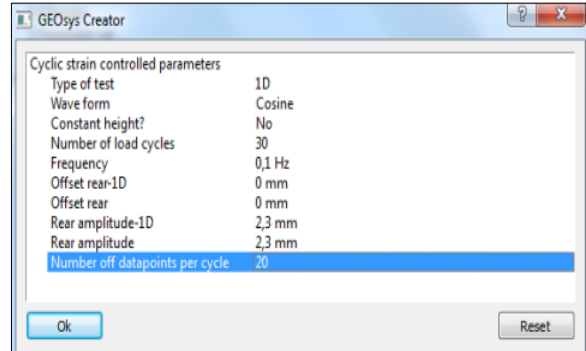


Şekil 8. Dinamik basit kesme deney düzeneğinin karşıdan görünüşü (Kahraman, 2021)

Deneylerden, suya doyurma işlemine başlamadan önce, numunelerden CO₂ gazı geçirilerek, ortamdaki havanın CO₂ gazı ile yer değiştirmesi bir nevi CO₂ gazı ile doyurma işlemi gerçekleştirilmektedir (Şekil 9). Deney düzeneği için hazırlanmış yazılım üzerinden deney yöntemi ve deney uygulama parametreleri/değerleri sisteme tanıtılabilmektedir (Şekil 10). Deney, efektif gerilmenin sifıra ulaştığı yani sıvılaşmanın gerçekleştiği anda, bitmiş kabul edilerek sonlandırılır.



Şekil 9. Dinamik basit üç eksenli deney düzeneği (CO₂ gazı ile doyurma işlemi)



Şekil 10. Deney yöntemi ve parametrelerinin sisteme tanıtıldığı ekran görüntüsü

Dinamik basit kesme deneyi, diğer dinamik deneylere göre birçok üstün yönere ve çeşitli avantajlara sahiptir. Dinamik basit kesme deneyi, arazi koşullarının laboratuvar ortamında gerçeğe en yakın modellenebildiği deney düzeneklerinden biridir. Dinamik basit kesme deneyi, rezonant kolon deneyiyle karşılaştırıldığında, dinamik basit kesme deneyi değerlerinin oldukça geniş bir aralıkta yer aldığı görülmektedir. Rezonant kolon deneyinde kayma deformasyonları %10⁻³-%1 arasında değişirken, dinamik basit kesme deneyinde bu aralık %10⁻²-%5 olmaktadır. Dinamik basit kesme deneyinde elde edilen deformasyon aralığı sismik olaylar sırasında zeminde meydana gelen deformasyon aralığına karşılık gelir (Das, 1993).

Dinamik basit kesme testi, üç eksenli testle karşılaştırıldığında, dinamik basit kesme deneyinde, kesme esnasında, numunenin düzlem deformasyon altında sabit kalmakta olup, asal gerilmelerin dönmesine olanak tanınmasından dolayı birçok avantaja sahip olması üç eksenli deney sistemine üstünlük sağlamaktadır. Bu durum birçok geoteknik problem için daha gerçekçi bir yükleme durumu sağlamaktadır (Erşan, 2005).

2. SONUÇLAR

Zeminlerin sıvılaşma potansiyeli, arazi ve laboratuvar yöntemleriyle belirlenebilmektedir. Sıvılaşma potansiyeli, zeminin özelliklerine dayalı olarak kısmen tahmin edilebilmekteyken bir depremde sıvılaşmanın gerçekleşip-gerçekleşmeyeceği laboratuvar yöntemleriyle ve ampirik formüllerle daha kuvvetle tahmin edilebilmektedir. Zemin türünü, yoğunluğunu ve yer altı su seviyesinin derinliğini belirleyerek, zemin sıvılaşma olasılığı öngörülebilmektedir.

Kohezyonsuz zeminlerin sıvılaşma potansiyelini değerlendirmek için çeşitli yöntemler geliştirilmiştir. Bunlar, gerilme temelli yöntemler, birim deformasyon temelli yöntemler ve enerji temelli yöntemler olmak üzere üç ana gruba ayrılabilir.

Sıvılaşma potansiyelinin laboratuvarda rölatif sıklık ve efektif gerilme gibi bazı parametrelerle belirlenebilmesi; çok sayıda belirsizlik içeren ve gerilme yöntemine dayanan arazi teknikleri için önemli bir alternatiftir.

Hem gerilme hem de birim deformasyon temelli yaklaşımlarda derinlik düzeltme faktörü (r_d) kullanılırken, enerjiye dayalı yöntemde bu yaklaşıma ihtiyaç duyulmaz.

Zemin içinden geçen ve yayılan toplam enerji değişmediği için, enerji temelli yöntemde ne anakaya seviyesindeki a_{max} ne de zemin seviyesindeki a_{max} değerini hesaplamaya gerek vardır. Bu durum diğer iki sıvılaşma değerlendirme yöntemine kıyasla enerji temelli yaklaşımın en belirgin üstünlüğünü oluşturmaktadır.

Enerji temeline dayanan ve üç yönlü dinamik hareket sağlayabilen "Devirsel Basit Kesme Deneyi (DBKD)" düzeneği, arazi koşullarını laboratuvar ortamında gerçeğe en yakın modelleyebilen yöntemdir.

Dinamik basit kesme deneyini (DBKD) rezonant kolon deneyiyle kıyaslandığında, DBKD değerlerinin oldukça geniş bir aralıkta yer aldığı görülmektedir. Elde edilen deformasyon aralığı sismik olaylarda zeminde meydana gelen deformasyon aralığına karşılık gelmektedir.

Devirsel basit kesme deneyi, dinamik üç eksenli deneyiyle kıyaslandığında; DBKD düzeneğinde kesme uygulanırken, asal gerilmelerin dönmesine olanak tanıdığından dolayı dinamik üç eksenli deney sistemine üstünlük sağlamaktadır. Böylece birçok geoteknik problem için daha gerçekçi bir yükleme durumu sağlamaktadır.

Devirsel basit kesme deneyi, zeminlerin sıvılaşma enerjisini belirlemede, arazi şartlarını daha gerçekçi ve güvenilir olarak yansıttığı için diğer deneylere alternatif olarak önerilmektedir.

KAYNAKÇA

Amini, P.F., Noorzad, R., 2018. Energy-based evaluation of liquefaction of fiber-reinforced sand using cyclic triaxial testing. *Soil Dynamics and Earthquake Engineering*, 104, 45-53.

Baziar, M.H., Jafarian, Y., 2007. Assessment of liquefaction triggering using strain energy concept and ANN model, capacity energy. *Soil Dynamics and Earthquake Engineering*, 27, 1056–1072.

Beyaz T., Kayabalı, K., Sönmezer, Y.B., 2021. Kumların sıvılaşmasında rölatif sıklık ve kesme birim deformasyonu etkisinin incelenmesi. *Pamukkale Univ Muh Bilim Derg*, 27(3), 431-440.

Bhattacharya, S., Hyodo, M., Goda, K., Tazoh, T., Taylor, C.A., 2011. Liquefaction of soil in the Tokyo bay area from the 2011 Tohoku (Japan) earthquake. *Soil Dynamics and Earthquake Engineering*, 31, 1618–1628. <https://doi.org/10.1016/j.soildyn.2011.06.006>.

- Burland, J.B., 1989. Small is beautiful: The stiffness of soils at small strains. *Canadian Geotechnical Journal*, 26 (4), 499-516.
- Chen, Y.R., Hsieh, S.C., Chen, J.W., Shih, C.C., 2005. Energy-based probabilistic evaluation of soil liquefaction. *Soil Dynamics and Earthquake Engineering*, 25(1):55-68.
- Çetin, K.O., Seed, R.B., Der-Kiureghian, A., Tokimatsu, K., Harder, Jr. L.F., Kayen, R.E., Moss, R.E.S., 2004. Standard penetration test-based probabilistic and deterministic assessment of seismic soil liquefaction potential. *Journal of Geotechnical and Geoenvironmental Engineering*, ASCE, 130(12),1314–1340.
- Das, B.M., 1993. *Principles of soil dynamics*, PWS-KENT Publishing Company, Boston.
- Davis, R.O., Berrill, J.B., 2001. Pore pressure and dissipated energy in earthquakes-Field verification. *Journal of Geotechnical and Geoenvironmental Engineering*, ASCE, 127(3), 269-274.
- DeAlba, P.S., Seed, H.B., Chan, C.K., 1976. Sand liquefaction in large-scale simple shear tests. *Journal of Geotechnical Engineering Division*, ASCE, 102(GT9): 909–927.
- Erşan, H., 2005. Tekrarlı yüklemeler etkisi altında zeminlerin konsolidasyonu, Doktora Tezi, İTÜ Fen Bil Enst., 247 s. İstanbul.
- Figuroa, J.L., Saada, A.S., Liang, L., Dahisaria, M.N., 1994. Evaluation of soil liquefaction by energy principles. *Journal of Geotechnical Engineering*, ASCE, 120(9): 1554–1569.
- Green R.A., 2001. Energy-Based evaluation and remediation of liquefiable soils. Ph Dissertation, Virginia Polytechnic Institute and State University, Blacksburg, VA.
- Hardin, B.O., Drenevich, V.P., 1972. Shear modulus and damping in soils—design and curves. *ASCE Journal of the Soil Mechanics and Foundations Division*, 94 (SM3), 689-708.
- Ishihara, K., 2006. Liquefaction of Subsurface Soils During Earthquakes. *Journal of Disaster Research*. 1 (2), 245-261.
- Jafarian, Y., Towhata, I., Baziar, M.H., Noorzad, A., Bahmanpour, A., 2012. Strain energy based evaluation of liquefaction and residual pore water pressure in sands using cyclic torsional shear experiments. *Soil Dynamics and Earthquake Engineering*, 35, 13-28.
- Kahraman G., 2021. Tek tip kumda artan ince tane yüzdesinin sıvılaşma enerjisine etkisinin araştırılması. Yük Lis Tezi, PAÜ Fen Bil Enst., Denizli.
- Kammerer, A., Pestana, J.M., 2002. Undrained response of monterey 0/30 sand under multidirectional cyclic simple shear loading conditions. University of California, Geotechnical Engineering Report No: UCB/GT/02-01, Berkeley, USA.
- Kayabalı, K., Yılmaz, P., Fener, M., Aktürk, Ö., Habibzadeh, F., 2018, Zemin sıvılaşmasının enerji yaklaşımıyla değerlendirilmesi. *MTA Dergisi*, 156: 195-206.
- Kokusho, T., Mimori, Y., 2015. Liquefaction potential evaluations by energy-based method and stress-based method for various ground motions. *Soil Dynamics and Earthquake Engineering*, 75, 130-146.
- Kokusho, T., Mimori, Y., Kaneko, Y., 2015. Energy-based liquefaction potential evaluation and its application to a case history, 8th Int. Conf. on Earthquake Geotechnical Engineering, New Zealand.
- Ladd, R.S., Dobry, R., Yokel, F.Y., Chung, R.M., 1989. Pore water pressure buildup in clean sands because of cyclic straining. *ASTM Geotechnical Testing Journal*, 12(1), 2208-2228.
- Law, K.T., Cao, Y.L., He, G.N., 1990. An energy approach for assessing seismic liquefaction potential. *Canadian Geotechnical Journal*, 27, 320–329.
- Liang, L., 1995. Development of an energy method for evaluating the liquefaction potential of a soil deposit. PhD dissertation, Case Western Reserve University, Department of Civil Engineering, Cleveland, OH.
- Nemat-Nasser, S., Shokooh, A.A., 1979. Unified approach to densification and liquefaction of cohesionless sand in cyclic shearing. *Can Geotech J.*, 16(4), 659-678.

- Seed, H.B., Idriss, I.M., 1971. Simplified procedure for evaluating soil liquefaction potential. *Journal of the Soil Mechanics and Foundations Division*, 97(8), 1249-1274.
- Seed, H.B., 1980. Closure to soil liquefaction and cyclic mobility evaluation for level ground during earthquakes. *Journal of Geotechnical and Geoenvironmental Engineering*, ASCE, 106(GT6), 720-724.
- Sweere, G.T.H., 1990. *Unbound granular bases for roads*. delft university of technology, Delft-Netherlands, 431 pp.
- Towhata, I., 2008. *Geotechnical Earthquake Engineering*. 1st ed. Berlin, Heidelberg, Germany, Springer-Verlag.
- Woods, R.D., 1994. Laboratory measurement of dynamic soil properties. *Dynamic Geotechnical Testing II (STP 1213)*, ASTM, West Conshohocken, PA, 165-190.
- Youd, T.L., Idriss, I.M., 2001. Liquefaction resistance of soils: summary report from the 1996-NCEER and 1998-NCEER/NSF workshops on evaluation of liquefaction resistance of soils. *Journal of Geotechnical and Geoenvironmental Engineering*, 127(4), 297-313.
- Zhang, W., Goh, A.T.C., Zhang, Y., Chen, Y., Xiao, Y., 2015. Assessment of soil liquefaction based on capacity energy concept and multivariate adaptive regression splines: *Engineering Geology*, 188, 29- 37.

ESTIMATION OF GROUND MOTION DURATION DURING THE BOUMERDES EARTHQUAKE OF MAY 21, 2003 IN THE NORTH OF ALGERIA

AOUARI Issam

Civil Engineering department, University of Bouira

BENAHMED Baizid

Civil Engineering department, University of Djelfa

MEHMET Palanci

Civil Engineering department, Arel Istanbul University

ROUABEH Aïcha

Civil Engineering department, University of Bouira

ABSTRACT

The duration of the earthquake plays a very important role in the estimation of the seismic risk in civil construction. Several authors have shown the effect of the duration of an earthquake on the seismic behaviour of buildings. In this paper, the estimation of the strong motion duration of the earthquake of May 21, 2003 in Boumerdes region in the north of Algeria is presented. The ground motion database used in this study consists of 20 reel horizontal acceleration time histories recorded during the Boumerdes earthquake. The duration of the strong phase will be calculated by different approaches in order to make a comparison between these models. The results show a difference between the values of the ground motion duration proposed by these authors.

Word keys: Boumerdes earthquake, significant duration, uniform duration.

1. Introduction

Several various parameters, including peak amplitudes, frequency contents, duration, etc., have been specified to show the damage potential of earthquake. Usually, the seismic design of structures according to seismic design codes is based on peak ground motion parameters. However, recent studies shown that the response of a structure in the event of an earthquake depends very strongly not only on the amplitude of the ground motion but also in some cases on the duration of the ground motion (Yaghmaei, Shaghayegh and Mohammad, 2022). Whilst there are many studies that directly and indirectly show correlation between earthquake duration and structural damages. For example Chai and Fajfar (Chai and Fajfar, 2000) suggest that inelastic design base shear should increase for buildings subjected to longer duration earthquake. Yaghmaei-Sabegh and Makaremi (2017) studied ground motion duration effects to construct damage-based inelastic response spectra. The results of this study revealed that ground motion duration is an effective parameter in the energy dissipation of structures (Yaghmaei-Sabegh and Makaremi, 2017). Wang et al. (2016) proposed integrated duration of horizontal and vertical components and investigated their effect on concrete dams. It was found that integrated duration has higher correlation and more significant influence on the peak displacement of concrete dams (Wang *et al.*, 2016).

2. Methodology

Data used in this study

In this study, The Boumerdes May 21, 2003 earthquake data of the main shock was used to calculate the emphasized ground motion duration. The data was recorded by several stations of the national accelerograph network piloted by the CGS (Laouami, Slimani, Bouhadad, J. L. Chatelain, *et al.*, 2006). Ten stations (10 accelerographs) are used to characterize the seismic motion, the closest of which is located at 20 km (Keddara

station) from the source determined by the national network of accelerographs, and the most distant is located at 165 km (Ain Defla station). The **Table 1** show the Hypocentral distance, the maximum accelerations recorded (PGA), the maximum displacement (PGD), and the maximum velocity (PGV) according to the horizontal components (E-W, N-S) by different stations during the main shock of the Boumerdes earthquake of May 21, 2003. Figure 1 shows the location and types of recording stations (Bouhadad *et al.*, 2004).

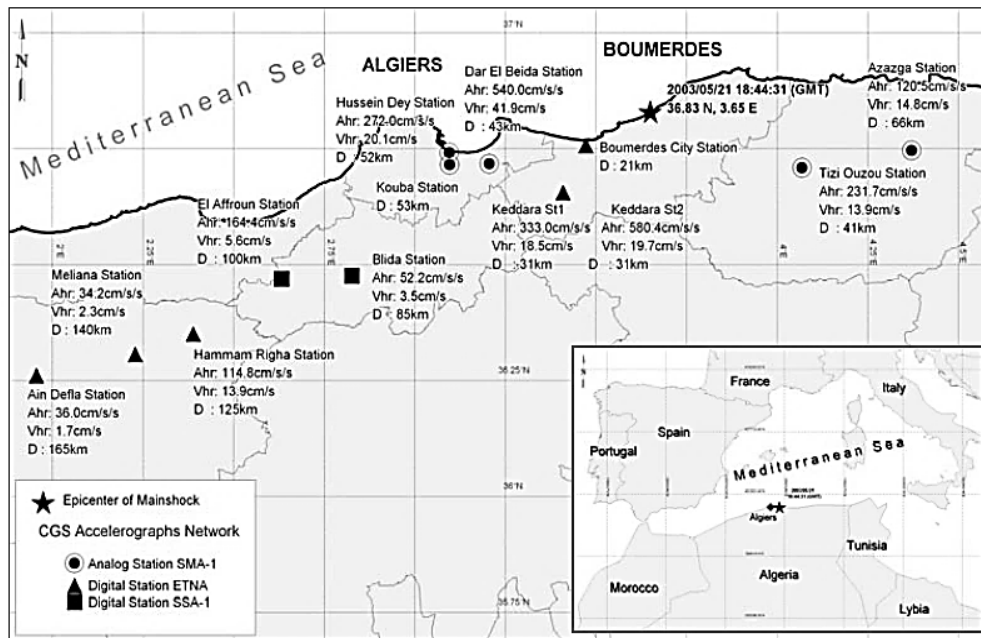


Figure 1 (*) Location of the 2003 Boumerdes earthquake. Ahr and Vhr are the maximum resultants of the horizontal acceleration and velocity, respectively. D is the hypocentral distance. (Meslem *et al.*, 2008)

Table 1 Seismic parameters of the main shock of the May 21th, 2003 of Boumerdes earthquake.

Champ	Station	Distance Hyp (Km)	Composante	PGA (g)	PGV (cm/s)	PGD (cm)	RMSa (g)
Champ Proche	Keddara 01	31	E-W	0,33	14,68	04,27	0,03
			N-S	0,26	11,02	04,84	0,04
Champ Moyen	Tizi Ouzou	41	E-W	0.50	27.50	9.20	-
			N-S	0,20	13,98	09,76	0,03
	Dar El Beida	43	E-W	0,19	06,89	01,76	0,04
			N-S	0,54	38,79	15,86	0,07
Champ Lointain	Hussien Dey	52	E-W	0,27	18,29	09,73	0,04
			N-S	0,23	17,63	09,25	0,03
	Azazga	66	E-W	0.12	13,85	03,98	0,02
Champ Lointain	Blida	85	E-W	0,05	03,70	01,04	0,01
			N-S	0,04	03,05	01,01	0,00
	Afroune	100	E-W	0.16	04,95	0,140	0,01
			N-S	0,09	05,28	0,320	0,01
	Hammam Righa	125	E-W	0,11	12,05	07,33	0,02
			N-S	0,07	09,73	03,46	0,02
	Meliana	140	E-W	0,03	02,22	01,50	0,01
			N-S	0,03	01,89	0,470	0,01
Ain Defla	165	E-W	0,03	01,54	01,88	0,01	
		N-S	0,02	01,32	02,93	0,01	

Analyses of earthquakes records showed that the period of strongest motion parts taken approximately 10 seconds (see Figure 2) and the frequencies were concentrated in the band of 4 to 10 Hz. In some locations, acceleration of 0.54 g (Dar El-Beida station) for the horizontal component was recorded (see Table 1). The most affected prefectures were Boumerdes and Algiers. Officially, 2,278 people died, 11,450 suffered injuries, and more than 180,000 were made homeless. Some 10,280 constructions collapsed, resulting in direct economic loss amounting to 5 billion US\$ at a first estimation (Bechtoula and Ousalem, 2005).

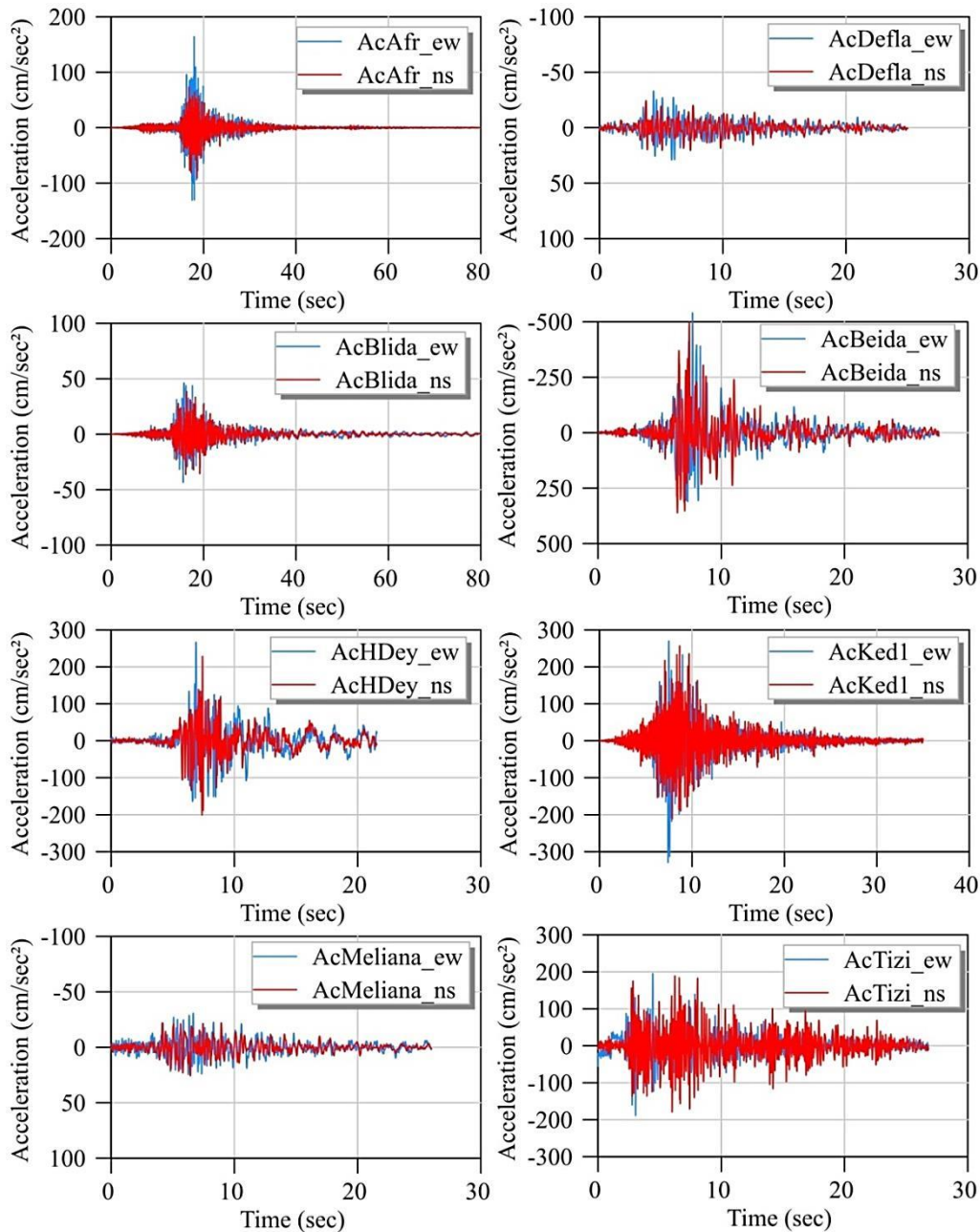


Figure 2 Accelerograms for Boumerdes earthquake of May 21, 2003.

Ground motion duration estimation

a reading in the literature we find that more than 40 definitions of duration are available, most of them are summarized by (Bommer and Marytínez pereira, 1999). Each of these definitions identifies that only the part of an earthquake record which has acceptably high acceleration amplitude, energy content, intensity or other

seismic parameters significantly affects structure response. The methods to calculate the duration of strong motion of an earthquake can be grouped into four main categories:

- 1) **Bracketed duration:** are defined as the entire time elapsed between the first and last overshoot of a fixed level of acceleration a_0 . This definition is given by (Bolt, 1973), (Kawashima and Aizawa, 1989).

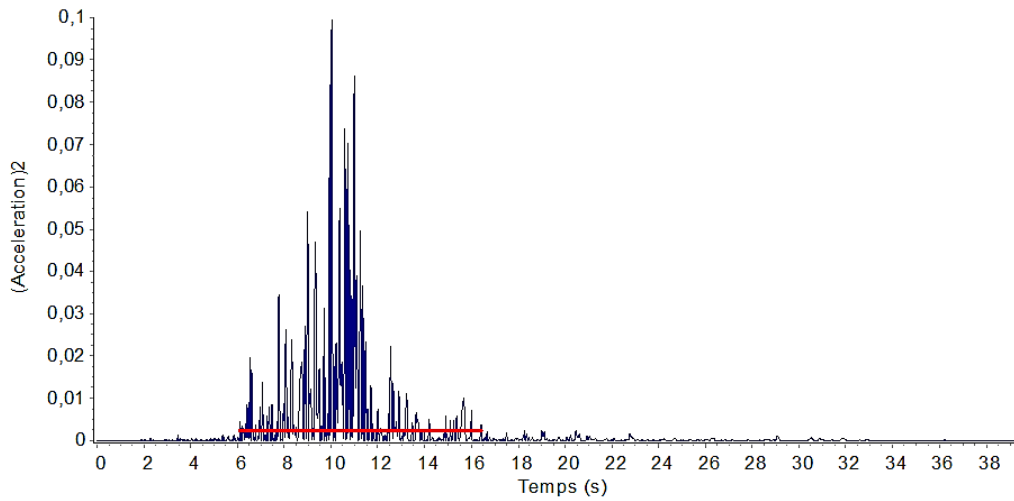


Figure 3 estimation de la durée entre crochets pour le séisme de Imperial Valley d'El-Centro 1940 (DB=10.48s avec un niveau d'accélération = 0.05g).

- 2) **Uniform duration:** is defined by a bound level of acceleration, a_0 , the duration is defined as the sum of the time intervals during which the acceleration is greater this boundary (Sarma and Casey, 1990).

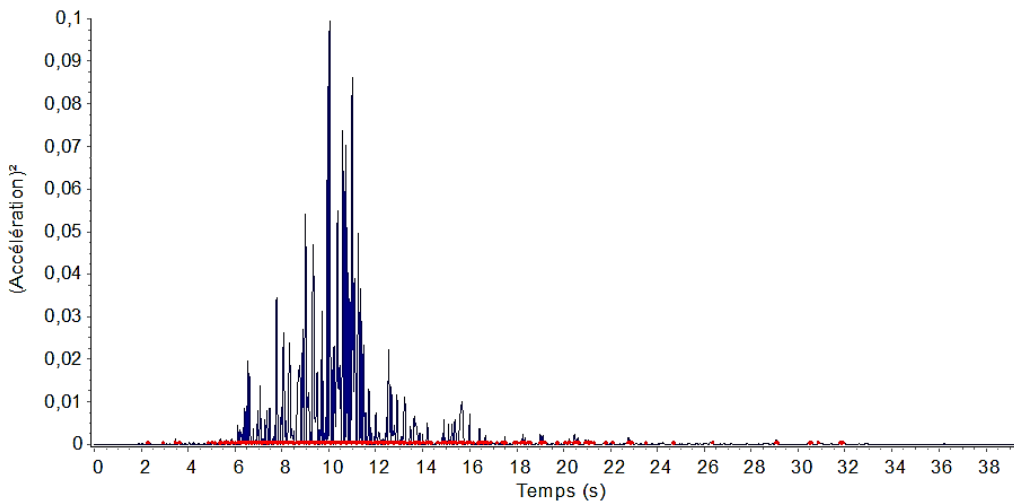


Figure 4 Durée uniforme (DU) estimée pour le séisme de Imperial Valley d'El-Centro 1940 (DU=10.48s avec un niveau d'accélération = 0.02g).

- 3) **Effective or Structural duration:** this definition is proposed by (Bommer and Maryt nez pereira, 1999) and defined as interval time between tow level of Arias intensity (0.06 and 1.2).

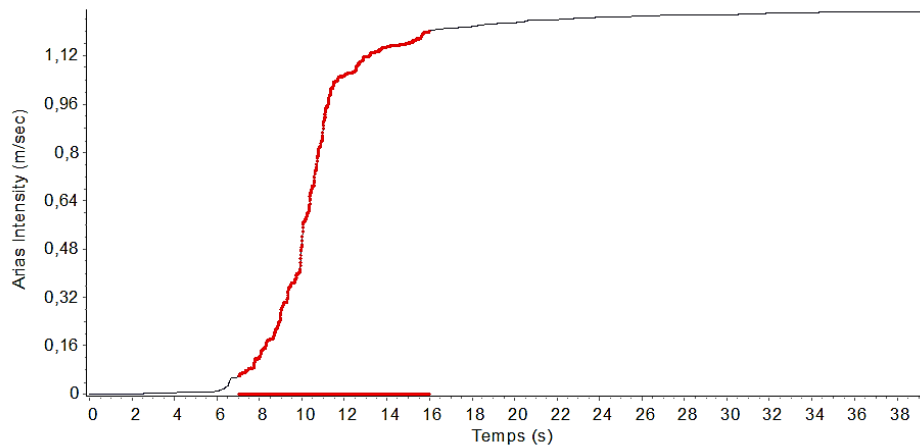


Figure 5 Dur e effective (DE) estim e pour le s isme de Imperial Valley d'El-Centro 1940 (DE=8.93s avec une valeur estim e entre 0.06 et 1.2 le l'intensit  d'Arias).

- 4) **Significant duration:** is based on the accumulation of energy in the accelerograms represented by the integral of the square of the ground acceleration, velocity or displacement. These definitions are given by (Trifunac and Brady, 1975), (McCann and Shah, 1979), (Vanmarcke and Lai, 1980). Figure 4 illustrates the approach of the method for the El-Centro, 1940 earthquake.

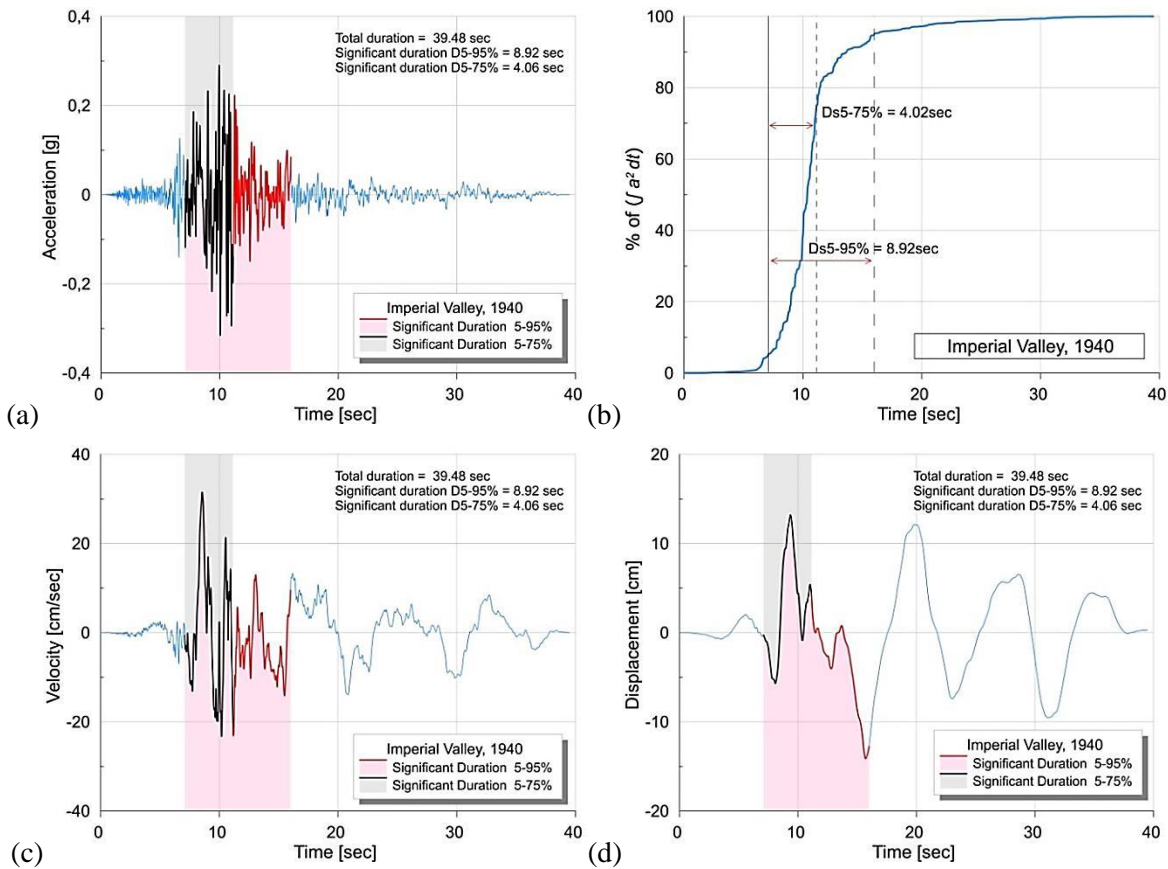


Figure 6 (a) Acc el ration (b) Intensit  d'Arias (c) Vitesse, (d) D placement du s isme d'El-Centro (1940). La r gion rouge repr sente la dur e significative du pour un niveau de 5   95 % et la r gion grise pour un niveau de 5   75 %. ($D_{s,5-95\%}=8.92s$ et $D_{s,5-75\%}=4.06s$).

3. Results and discussion

Applying the four definitions of strong motion duration given in previous section to the accelerograms data of the Boumerdes earthquake, we use the SeismoSignal software to calculate the values of the durations presented in section 2.2.

Table 2 Ground motion duration of the records for Boumerdes earthquake.

Record station	Uniform duration (sec)	Bracketed duration (sec)	Significant duration (sec)	Effective duration (sec)	Total duration (sec)
AcAfr_ew	9,81	22,23	9,62	7,93	79,98
AcAfr_ns	13,92	33,3	10,67	0,0	79,98
AcAinDefla_ew	15,99	24,57	13,3	0,0	24,97
AcAinDefla_ns	18,03	24,9	14,54	0,0	24,97
AcBlida_ew	21,01	65,42	18,63	0,0	79,98
AcBlida_ns	22,69	72,35	21,78	0,0	79,98
AcDeBeida_ew	26,98	23,45	10,62	10,68	27,65
AcDeBeida_ns	10,11	23,18	9,55	9,54	27,65
Achammam_ew	17,25	29,49	13,25	13,96	29,49
Achammam_ns	21,01	29,49	14,97	16,03	29,49
AcHDEY_ew	11,02	18,07	11,8	12,14	21,53
AcHDEY_ns	11,1	17,8	10,57	10,44	21,53
AcKed1cl_ew	9,17	22,61	9,87	10,6	34,97
AcKed1cl_ns	13	27,43	10,6	10,77	34,97
AcMeliana_ew	19,3	25,91	16,15	0,0	25,79
AcMeliana_ns	18,19	25,82	13,63	0,0	25,79
AcTIZI_ew	14,99	26,72	14,41	14,29	26,8
AcTIZI_ns	18,02	26,73	16,61	16,64	26,8
Mean duration(sec)	16,199	29,971	13,365	7,390	39,018

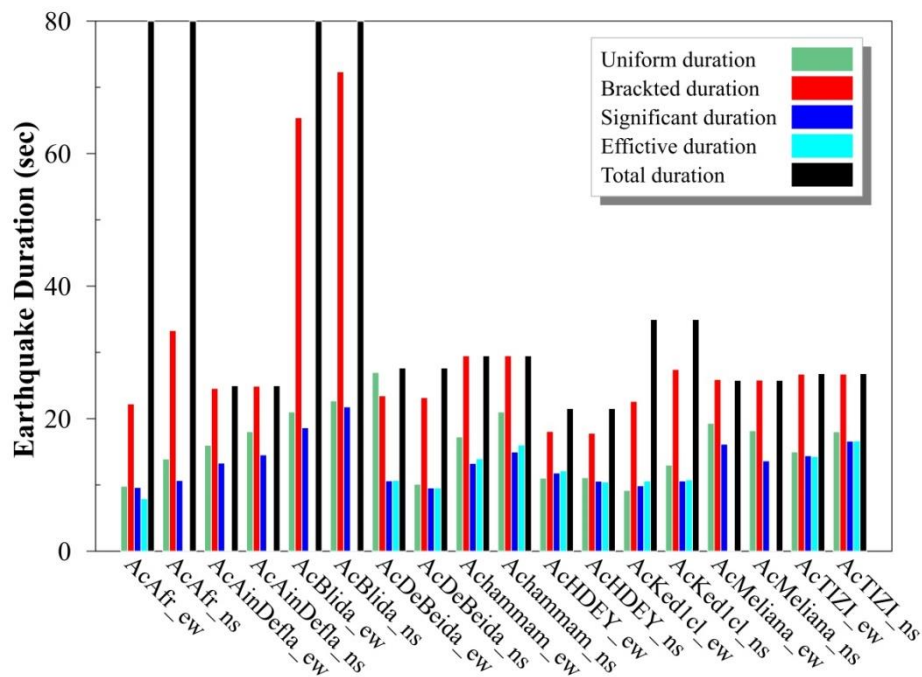


Figure 7 Bar plot of proposed duration computation for Boumerdes earthquake of May 21, 2003.

Figure 7 show the computed duration with different definition given in previous section. It can be observed that, the bracketed duration is very similar to total duration. The values are in order of 30sec. we see also; the significant and effective definitions are very close (a round 10 sec). The maximum ground motion duration (red line) value (26.98sec) is observed in Dar EL-Beida station, this value is given by the Bracketed definition. If we consider the means duration values of all records for each definitions, the results are; (16,20; 29,97; 13,36; 7,39; 39,02) sec for uniform, bracketed, significant, and effective duration respectively.

4. Conclusion

In conclusion, the duration of strong part of the accelerograms records by May 21, 2003 Boumerdes earthquake are computed by several definition given in literature. The ground motion database used in this study consists of 20 reel horizontal acceleration time histories recorded during Boumerdes earthquake. It can be seen that the values are different from one definition to another. In many studies, the significant duration is the parameter most used by researchers to quantify the energy released during the earthquake (here the mean of significant duration for Boumerdes earthquake equal to 13.36sec).

References

- Bechtoula, H. and Ousalem, H. (2005) 'The 21 May 2003 Zemmouri (Algeria) earthquake: Damages and disasterr responses', *Journal of Advanced Concrete Technology*. doi: 10.3151/jact.3.161.
- Bolt, B. A. (1973) 'Duration of strong ground motion', in *5th World Conference on Earthquake Engineering*. Rome, pp. 1304–1313.
- Bommer, J. J. and Marytínez pereira, A. (1999) 'The effective duration of earthquake strong motion', *Journal of Earthquake Engineering*, 3(2), pp. 127–172. doi: 10.1080/13632469909350343.
- Bouhadad, Y. *et al.* (2004) 'The Boumerdes (Algeria) earthquake of May 21, 2003 (Mw = 6.8): Ground deformation and intensity', *Journal of Seismology*. doi: 10.1007/s10950-004-4838-0.
- Chai, Y. H. and Fajfar, P. (2000) 'A procedure for estimating input energy spectra for seismic design', *Journal of Earthquake Engineering*, 4(4), pp. 539–561. doi: 10.1080/13632460009350382.
- Kawashima, K. and Aizawa, K. (1989) 'Bracketed and normalized durations of earthquake ground acceleration', *Earthquake Engineering & Structural Dynamics*, 18(7), pp. 1041–1051. doi: 10.1002/eqe.4290180709.
- Laouami, N., Slimani, A., Bouhadad, Y., Chatelain, J. L., *et al.* (2006) 'Evidence for fault-related directionality and localized site effects from strong motion recordings of the 2003 Boumerdes (Algeria) earthquake: Consequences on damage distribution and the Algerian seismic code', *Soil Dynamics and Earthquake Engineering*. doi: 10.1016/j.soildyn.2006.03.006.
- Laouami, N., Slimani, A., Bouhadad, Y., Chatelain, J.-L., *et al.* (2006) 'Evidence for fault-related directionality and localized site effects from strong motion recordings of the 2003 Boumerdes (Algeria) earthquake: Consequences on damage distribution and the Algerian seismic code', *Soil Dynamics and Earthquake Engineering*, 26(11), pp. 991–1003. doi: 10.1016/j.soildyn.2006.03.006.
- McCann, M. W. J. and Shah, H. C. (1979) 'Determining strong-motion duration of earthquakes', *Bulletin of the Seismological Society of America*, 69(4), pp. 1253–1265.
- Meslem, A. *et al.* (2008) 'Strong Motion Distribution and Microtremor Observation Following the 21 May 2003 Boumerdes , Algeria Earthquake', in *The 14 World Conference on Earthquake Engineering*. Beijing, China, pp. 10–17.
- Sarma, S. K. and Casey, B. J. (1990) 'Duration of Strong Motion in Earthquakes', in *9th European Conference on Earthquake Engineering*. Moscow, pp. 10A, 174–183.
- Trifunac, M. D. and Brady, A. G. (1975) 'A study on the duration of strong earthquake ground motion', *Bulletin of the Seismological Society of America*, 65(3), pp. 581–626. doi: 10.1016/0148-9062(76)90487-3.

- Vanmarcke, E. H. and Lai, S.-S. P. (1980) 'Strong-motion duration and RMS amplitude of earthquake records', *Bulletin of the Seismological Society of America*, 70(4), pp. 1293–1307.
- Wang, G. *et al.* (2016) 'A general definition of integrated strong motion duration and its effect on seismic demands of concrete gravity dams', *Engineering Structures*, 125, pp. 481–493. doi: 10.1016/j.engstruct.2016.07.033.
- Yaghmaei-Sabegh, S. and Makaremi, S. (2017) 'Development of duration-dependent damage-based inelastic response spectra', *Earthquake Engineering & Structural Dynamics*, 46(5), pp. 771–789. doi: 10.1002/eqe.2830.
- Yaghmaei, S., Shaghayegh, S. and Mohammad, K. (2022) 'A new region - specific empirical model for prediction of ground motion significant duration in Turkey', *Bulletin of Earthquake Engineering*. Springer Netherlands, (0123456789). doi: 10.1007/s10518-022-01417-9.

**EFFECTS OF UNCERTAINTIES IN SOIL AND STRUCTURAL PROPERTIES ON LATERAL
LOAD DISTRIBUTION ALONG A PILE IN PROXIMITY TO AN UNDRAINED SLOPE**

Amira Chekrit

Department of civil Engineering, Badji Mokhtar University, Annaba, Algeria

Abdelmadjid Hacene Chaouche

Department of civil Engineering, Badji Mokhtar University, Annaba, Algeria

ABSTRACT

The study presented concerns the analysis of piles placed close to a crest and laterally loaded; the crest is characterized by an alpha slope and is clayey in nature.

Bi-dimensional finite element analyses are realized on piles with different parameters, such as length and diameter, installed at different distances from the crest with varying slopes.

The results of these analyses are used to model the distribution of lateral load along the length of the pile depending on slope inclination; the distance between the pile and the crest.

P-Y curves are then plotted for the cases presented above; cases for which such curves rarely exist in the bibliography.

The P-Y curves obtained are used to perform a series of numerical analyses.

This study shows that the present results for piles near slopes with P-Y curves already existing in some research are in agreement.

KEYWORDS – Piles, Lateral loads, Clayly slope, Finite element method, Numerical analysis, Soil-pile interactions, Slopes

IMPORTANCE OF RESOURCE ALLOCATION TO MAINTAIN HEALTH AND SAFETY AT CONSTRUCTION SITE

Subhojit Chattaraj

Assistant Professor, Department of Civil Engineering, Greater Kolkata College of Engineering and Management, JIS Group, West Bengal, India

Sandeepan Saha

Assistant Professor, Department of Civil Engineering, Greater Kolkata College of Engineering and Management, JIS Group, West Bengal, India

Sandip Sarkar

Assistant Professor, Department of Civil Engineering, Greater Kolkata College of Engineering and Management, JIS Group, West Bengal, India

Dipak Paul

Student, Department of Civil Engineering, Greater Kolkata College of Engineering and Management, JIS Group, West Bengal, India

ABSTRACT

Construction sites are dynamic environments characterized by numerous hazards and risks, making them one of the most accident-prone industries. Health and safety concerns in construction demand vigilant attention and effective resource allocation to safeguard the well-being of workers and prevent accidents. This study explores the Importance of effective resource allocation as it plays a significant role in maintaining health and safety in constructionsites. Construction sites are inherently complex and hazardous environments, where multiple resources, including personnel, time, equipment, and finances, are involved. Effectively managing and allocating these resources to prioritize health and safety initiatives is crucial formitigating risks and ensuring the well-being of workers and the surrounding community. Inadequate resource allocation for health and safety in construction sites can lead to a range ofnegative consequences that compromise the well-being of workers and the overall safety performance of the project. The current study will navigate both the aspects of Effective Resource allocation and its effect on the construction business.

Keyword: Construction, Health and Safety Issues, Resource Allocation, Strategy

IMPORTANCE OF STRATEGIES TO AVOID CONSTRUCTION SITE FATALITIES: A REVIEW APPROACH

Sandeepan Saha

Assistant Professor, Department of Civil Engineering, Greater Kolkata College of Engineering and Management, JIS Group, West Bengal, India

Subhojit Chattaraj

Assistant Professor, Department of Civil Engineering, Greater Kolkata College of Engineering and Management, JIS Group, West Bengal, India

Sahali Halder

Student, Department of Civil Engineering, Greater Kolkata College of Engineering and Management, JIS Group, West Bengal, India

Trishita Giri

Student, Department of Civil Engineering, Greater Kolkata College of Engineering and Management, JIS Group, West Bengal, India

ABSTRACT

The construction business is renowned for its inherent risks and hazards, making the implementation of effective strategies for health and safety paramount. This paper explores the significance of such strategies in construction sites and highlights the benefits they bring in terms of worker well-being, regulatory compliance, project efficiency, and overall productivity by reviewing past works. It emphasizes key elements of these strategies, including hazard identification, risk assessment, regulatory compliance, training and education, communication, and continuous improvement. By understanding and implementing these strategies, construction companies can create a safe and secure working environment that protects workers, minimizes accidents, and fosters a culture of safety.

Keyword: Construction, Health and Safety Issues, Strategy

SUSTAINABLE CONCRETE: USING MARBLE WASTES AS AN ENVIRONMENTALLY FRIENDLY AGGREGATE

Mohammed KHATTAB

University Mohamed Khider Biskra, Department of Civil Engineering and hydraulics, Biskra, Algeria

Oday Jaradat

University Mohamed Khider Biskra, Department of Civil Engineering and hydraulics, Biskra, Algeria

Samya HACHEMI

University Mohamed Khider Biskra, Department of Civil Engineering and hydraulics, Biskra, Algeria

Hicham BENZETTA

Université Ziane Achour – Djelf, Laboratoire de Développement en Mécanique et Matériaux, Department of Civil Engineering, Djelfa, Algeria

ABSTRACT

Using Marble Wastes (MW) as potential substitutes for natural aggregates in new construction can achieve significant benefits in saving natural resources, reducing greenhouse gas emissions and costs. In the present research, MW was used as a total substitute (100%) to natural aggregates (coarse, fine or both) in concrete to study its ecological aspect. For this reason, four environmental impact categories for all concrete studied were evaluated including global warming Potential (GWP), acidification Potential (AP), eutrophication Potential (EP), abiotic depletion and photochemical oxidant creation Potential (POCP). Furthermore, the compressive strength of concrete made with RMA was evaluated and compared with conventional concrete made with 100% of coarse and fine natural concrete. According to the results obtained, the replacement of NA (coarse, fine or both) by 100% of RMA exerted the greatest impact on GWP, AP, EP, and POCP evaluation results.

Keywords: Sustainable construction, Environmental impacts, Marble wastes, Recycled aggregates

1. Introduction

Concrete is one of the popular construction materials around the world and is employed in both structural and non-structural applications. The construction, renovation and demolition activities generate large amount of concrete waste. The disposal of this waste is a challenging issue for all big cities in the world [1]. Untreated construction waste, which may be transported to suburban areas for open disposal or placement in landfills, occupies a large amount of land.

The construction sector has the potential to incorporate wastes either to produce new materials or to improve the properties of existing materials. In this context, the potential benefits of using construction and demolition wastes to improve the mechanical properties of concrete have been demonstrated in several studies [2-5].

Among the construction and demolition wastes, Recycled Marble Aggregates (RMA) can be used in concrete in the form of aggregates (coarse and fine) or additions (powder) to improve concrete performance. In this regard, about 40% of marble waste is small pieces that are usually dumped in landfills [6]. Using RMA as fine aggregates, several researchers have found that RMA could be used as fine aggregates in production of concrete [7, 8] and mortars [9, 10]. Additionally, RMA was used as coarse aggregates. The results obtained by authors such as [11-13] indicate that RMA could be used as coarse aggregates to improve concrete performance.

Environmental impact assessment-based research aimed at identifying the potential environmental impact of each aggregate in advance must also be conducted to determine the applicability of recycled and by-product aggregates [14].

This study thus aims to evaluate the environmental impact when they are used as aggregates in concrete. To this end, the six potential environmental impacts (i.e., global warming potential, acidification potential, photochemical oxidant creation Potential and eutrophication potential) of the manufacture and production of conventional concrete and recycled aggregates concrete. Also, the compressive strength of concrete made with RMA was evaluated.

2. Methodology and experimental details

2.1 Materials employed

The cement employed for the production of all concrete mixes was Portland-Pozzolana cement (CEMI/A-P 42.5 N). Natural Aggregates (NA) used in this research were calcareous sand and calcareous crushed stone as fine and coarse aggregates, respectively. Recycled Marble Aggregates (RMA) were used as coarse and fine recycled aggregates. The RBA used in this study was obtained from a marble quarry in Jerash /Jordan (Fig.1).



Fig.1. Marble waste used in this study

2.2. Mix proportion

Four concrete mixtures were developed as a part of this research programme in two separate families: For the first family, conventional concrete (which considered as reference concrete RC), the one control mixture with cement dosage of 370 kg/m³ (w/c=0.5) was made only of 100% coarse and fine NA. RC formulation was determined according to Dreux and Festa method [15]. For the second family, three concrete mixtures (CRMA, FRMA and CFRMA), with the same cement dosage and w/c of RC were prepared by replacing 100% (by weight) of NA (coarse, fine or both) with marble wastes. Notation: the symbol “C” Coarse, “F” Fine, “CF” Coarse and Fine, “RMA” Recycled Marble Aggregate.

2.3. Testing procedure

To assess the sustainability of the concretes prepared with RMA in this study, the environmental impact associated with the production of 1 m³ of concrete was evaluated. Cement and aggregates are the main components for the emission of carbon dioxide in concrete production Devi et al. [42]. For the environmental study, four environmental impact categories were selected in this study, namely global warming (GWP), acidification (AP), eutrophication (EP) and photochemical oxidant formation (POCP). The values of GWP, AP, EP and POCP for each raw material of concrete (cement, natural aggregates and water) were taken from the previous literature [16,17] and mentioned in Table 1.

Table 1. Characterization value of raw materials for concrete [16,17].

Concrete ingredients	GWP	AP	EP	POCP
	kg CO ₂ eq	kg SO ₂ eq	kg PO ₄ ⁻³	kg C ₂ H ₄ eq
C	0.898	1.48×10 ⁻³	2.211×10 ⁻⁴	1.42×10 ⁻⁴
NA	0.0052	0.011	0.00192	0.000107
W	0.01258	0.000194	0.0006557	0.000209

The symbol “C” Cement, “NA” Natural Aggregates “W” Water.

To study the effect of coarse, fine or both RMA on the compressive strength of concrete mixtures, three cubic samples were tested for each type of concrete mixture according to the NF EN 12390-3 [18]. About 24 samples were tested after the 7 and 28- days curing period.

1. Results and discussion

3.1. Compressive strength

Figure 2 presents the Compressive strength of the cubic samples tested at 14 and 28 days. It can be seen from the figure that concretes containing RMA (CRMA, FRMA and CFRMA) had a lower Compressive strength value in comparison with RC. The Compressive strength of CRMA, FRMA and CFRMA concretes is affected by the type of RMA used (coarse, fine or both). The lowest strength was measured in the case of CRMA and FRMA concrete mixtures at the age of 14 and 28 days. As seen in Figure 2, the Compressive strength of CRMA concrete mixture, due to the replacement of 100% coarse RMA, declined by 22% and 17% at the age of 14 and 28 days compared to RC, respectively. Moreover, the replacement of 100% of fine RMA in FRMA concrete mixtures has reduced compressive strength by 19% and 13% at the age of 14 and 28 days, respectively.

Authors such as Kore and Vyas, [19] and Uygunoğlu et al. [20] found that the main reasons for the reduction in Compressive strength were attributed to the RMA having a flakier shape than natural aggregates, resulting in higher fraction in marble aggregates during mixing. In contrast, the highest Compressive strength of recycled concrete was obtained for the CFRMA concrete mixture (see Figure 8). The results declared that the Compressive strength of the CFRMA concrete mixture, which simultaneously contained coarse and fine RMA, was reduced by about 11% and 9% at the age of 14 and 28 days, respectively.

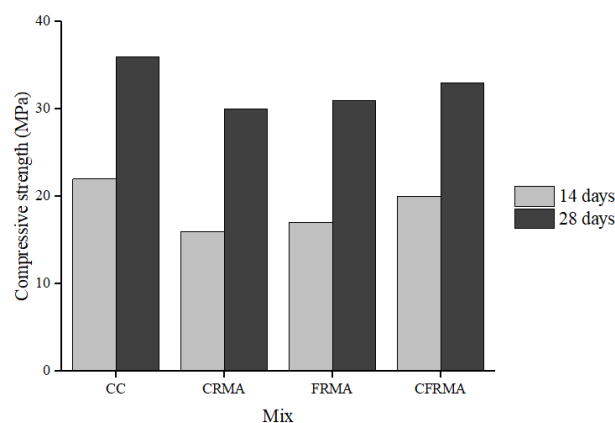


Fig.2. Effects of marble aggregates (coarse, fine or both) on the compressive strength of concrete.

3.2. Environmental Impact Assessment

Table 2 shows the results of the evaluation of the four environmental impacts. As can be seen in Table 5, GWP had the highest contribution to the environmental impact. In other words, the GWP evaluation results for RC

was 343.02 (kg CO₂eq). However, a comparison between the mixes with RMA (CRMA, FRMA and CFRMA) and RC showed that the replacement of NA (coarse, fine or both) by 100% of RMA had a lower effect on the GWP. For instance, the GWP of recycled concrete was 338.04 (kg CO₂eq) for CRMA, 339.60 (kg CO₂eq) for FRMA and 334.60 (kg CO₂eq) for CFRMA. It is clear according to Table 2 that the inclusion of RMA reduced the GWP due to a reduction in aggregate content.

In particular, the AP, EP and POCP of the control mixture were evaluated to be 18.44 (kg SO₂eq), 3.32 (kg PO₄-3) and 0.26 (kgC₂H₄eq), respectively. However, the AP, EP and POCP evaluation results for CRMA, FRMA and CFRMA concrete mixtures were lower than that of the RC. The AP, EP and POCP evaluation results for CRMA concrete mixture were 7.88 (kg SO₂eq), 1.42 (kg PO₄-3) and 0.16 (kgC₂H₄eq), respectively. However, in the case of FRMA concrete mixture in which the total of the fine NA was replaced with RMA, the AP, EP and POCP evaluation results were higher than that of the CRMA concrete mixture (see Table 5). On the other hand, a comparison between the mixture of CFRMA and RC showed that the replacement of coarse and fine NA by 100% of RMA had a significant influence on the AP, EP and POCP. For instance, the AP, EP and POCP of mix CFRMA were 0.58 (kg SO₂eq), 0.20 (kg PO₄-3) and 0.09 (kgC₂H₄eq), respectively

As a conclusion, the results showed that the replacement of NA (coarse, fine or both) by RMA exerted the greatest impact on AP, EP, and POCP evaluation results. In contrast, the replacement of NA by RMA did not seem to have a significant influence on GWP. Alzard et al., [21] reported similar results in the literature.

Table 2. Environmental impact assessment of different concrete mixes.

	RC	CRMA	FRMA	CFRMA
GWP (KgCO ₂ eq)	343.02	338.04	340.02	334.60
AP(kg SO ₂ eq)	18.44	7.88	11.14	0.58
EP(kg PO ₄ ⁻³)	3.32	1.48	2.05	0.20
POCP(kgC ₂ H ₄ eq)	0.26	0.16	0.19	0.09

3. Conclusions

According to the research carried out in this study, the following results are presented as research achievements:

1. The inclusion of RMA as a total replacement for NA in concrete negatively affects its compressive strength. A decrease was from 17% to 22% for the CRMA concrete mixture and from 13% to 19% for the FRMA concrete mixture. Interestingly, the use of 100% of coarse and fine RMA results in decrease in compressive strength of approximately 9% after 28 days of curing.
2. The GWP, AP, EP and POCP evaluation results for all the recycled concrete mixtures proportions investigated in this study were lower to those of the reference mixture.
3. The substitution of NA (coarse, fine or both) by RMA leads to contributes more intensely to reducing the AP, EP, and POCP.
4. It can be concluded that the combined use of RMA may lead to the fact that recycled aggregate is an environmentally friendly material.
5. Finally, it is recommended to use 100% of RMA in the production of concrete in non-structural elements.

References

- [1]. M. M. Rafi, T. Aziz, (2022). Experimental testing of fly ash containing recycled aggregate concrete exposed to high temperatures. *Sustainable and Resilient Infrastructure*, 7(1), 1-16.
- [2]. Vardhan, K., Siddique, R., Goyal, S. (2019). Influence of marble waste as partial replacement of fine aggregates on strength and drying shrinkage of concrete. *Construction and Building Materials*, 228, 116730.

- [3]. Khattab, M., Jaradat, O., Hachemi, S., Suleiman, H., & Benzetta, H. Mechanical, physical and environmental performance of sustainable concrete containing marble wastes.
- [4]. Khattab, M., S. Hachemi, and H. Benzetta. "Assessment of quality of recycled brick concrete using Ultrasonic pulse velocity." In ASPS Conference Proceedings, First International Conference on Energy, Thermofluids and Materials Engineering, ICETME 2021.
- [5]. Hachemi, S., Khattab, M., & Benzetta, H. (2022). The Effects of Recycled Brick and Water/Cement Ratios on the Physical and Mechanical Performance of Recycled Aggregates Concrete. *Innovative Infrastructure Solutions*, 7, Article No. 270.
- [6]. Ural, N., Yakş, G. (2020). Utilization of marble piece wastes as base materials. *Open Geosciences*, 12(1), 1247-1262.
- [7]. Kırgız, M. S. (2016). Fresh and hardened properties of green binder concrete containing marble powder and brick powder. *European Journal of Environmental and Civil Engineering*, 20(sup1), s64-s101.
- [8]. Hebhouh, H., Aoun, H., Belachia, M., Houari, H., Ghorbel, E. (2011). Use of waste marble aggregates in concrete. *Construction and Building Materials*, 25(3), 1167-1171.
- [9]. Buyuksagis, I. S., Uygunoglu, T., Tatar, E. (2017). Investigation on the usage of waste marble powder in cement-based adhesive mortar. *Construction and Building Materials*, 154, 734-742.
- [10]. Keleştemur, O., Yıldız, S., Gökçer, B., Arici, E. (2014). Statistical analysis for freeze–thaw resistance of cement mortars containing marble dust and glass fiber. *Materials & Design*, 60, 548-555.
- [11]. Kore, S. D., Vyas, A. K. (2016). Impact of marble waste as coarse aggregate on properties of lean cement concrete. *Case studies in construction materials*, 4, 85-92.
- [12]. Binici, H., Shah, T., Aksogan, O., Kaplan, H. (2008). Durability of concrete made with granite and marble as recycle aggregates. *Journal of materials processing technology*, 208(1-3), 299-308.
- [13] Andre, A., de Brito, J., Rosa, A., Pedro, D. (2014). Durability performance of concrete incorporating coarse aggregates from marble industry waste. *Journal of Cleaner Production*, 65, 389-396.
- [14]. Xia, B.; Ding, T.; Xiao, J. Life cycle assessment of concrete structures with reuse and recycling strategies: A novel framework and case study. *Waste Manag.* 2020, 105, 268–278.
- [15]. Dreux G, Festa J. *New guide to concrete and its constituents*. Edition Eyrolles, Paris; 1998: Vol. 8, pp. 205–284.
- [16]. Devi, K., Saini, B., Aggarwal, P. (2021). Economic and Ecological Feasibility of Marble Powder in Cement Mortar. In: Kalamdhad, A.S. (eds) *Integrated Approaches Towards Solid Waste Management*. Springer, Cham.
- [17]. Kim, T. H., Tae, S. H. (2016). Proposal of environmental impact assessment method for concrete in South Korea: An application in LCA (life cycle assessment). *International journal of environmental research and public health*, 13(11), 1074.
- [18]. European Standard NF EN 12390-3. (2003). Test for hardened concrete Part 3: Compressive strength of test specimens. ISSN 0335-3931. The French Association of Standardization (AFNOR). 11 avenue Francis de Pressens' e France 93571 SaintDenis La Plaine Cedex.
- [19]. Kore, S. D., Vyas, A. K. (2016). Impact of marble waste as coarse aggregate on properties of lean cement concrete. *Case studies in construction materials*, 4, 85-92.
- [20]. Uygunoğlu, T., Topçu, İ. B., Çelik, A. G. (2014). Use of waste marble and recycled aggregates in self-compacting concrete for environmental sustainability. *Journal of cleaner production*, 84, 691-700.
- [21]. Alzard, M. H., El-Hassan, H., El-Maaddawy, T. (2021). Environmental and economic life cycle assessment of recycled aggregates concrete in the United Arab Emirates. *Sustainability*, 13(18), 10348.

APPLICATION OF SINGLE-VALUED NEUTROSOPHIC-DEMATEL TO INVESTIGATE CAUSAL EFFECTS OF CRITERIA OF SUSTAINABLE URBAN TRANSPORT

Lazim ABDULLAH

*Faculty of Ocean Engineering Technology and Informatics, Universiti Malaysia Terengganu Kuala Nerus, Malaysia,
ORCID: 0000-0002-6646-4751*

ABSTRACT

Rapid development in national economy and urbanization process have led to a renewed interest in sustainable urban transport. There are multiple criteria to be considered to create a sustainable urban transport atmosphere. In this paper, a multi-criteria decision-making method combined with an indeterminacy theory is applied to investigate the relationships between criteria of urban transport. Specifically, this paper aims to investigate the relationship among twelve criteria of sustainable urban transport development using the single-valued neutrosophic-DEMATEL (SVN-DEMATEL). The SVN-DEMATEL allows us to identify the most influential criteria, a list of cause criteria and a list of effect criteria of sustainable urban transport development. In addition, the method also suggests unidirectional relationship among the criteria where the cause-and-effect criteria can be clearly visualised. The computational result shows that Transport productivity and efficiency (C2) as the most important influential criterion. On the other hand, Economic Attractiveness (C12) is the most affected criterion in creating a sustainable urban transportation development. The results would be a great significance for the practical implementation in initiating sustainable urban transportation.

Keywords: Urban transport; Neutrosophic sets; decision making; cause-effect relationship

Introduction

The majority of developing country cities have seen a sharp increase in the problems associated with transportation, including pollution, accidents, a lack of public transportation, environmental degradation, climate change, and accessibility issues for the impoverished in the city. According to Pojani et al. (2015), certain cities in Denmark, Ireland, and the United Kingdom have seen a trend of reclaiming urban space from the automobile by outlawing cars from large portions of downtown areas and restricting them in other ways. This trend has been observed in more developed countries, specifically in Northern Europe. These days, these locations are often regarded as leading instances of sustainable urban development, as numerous cities worldwide work to meet urban sustainability criteria by enhancing public transportation, promoting non-motorized modes of transportation, establishing pedestrian zones, restricting the use of private vehicles, and also attempting to reverse the changes to cities brought about by the dominance of the automobile. To achieve a sustainable urban transport, policy makers may face major challenges in their attempts to identify sustainable transportation alternatives. Not only the above challenges, it is said that in many cities, public transport remains unsustainable, unsafe, inaccessible and also unaffordable, which particularly affecting the poor (Cuomo, 2019; Plano, 2022). Apart from these negative effects to poor people, unsustainable urban transport also poses other negative effects such as an increase in inequality regarding accessibility and congestion (Banister, 2008), and unsustainable resource use (Gösslin, et al., 2018). To delve into these issues, Loo (2018) also investigates various transport sustainability issues in developing countries by exploring the key issues, problems and potential solutions for improving transport sustainability. The study concludes with deep concerns on sustainable transport in smart cities and how to move towards a holistic sustainable transport plan.

In order to ensure that public health, ecosystems, and generational equity are all respected, the Council of the European Union (CEU, 2001) suggested several conditions for a sustainable transport system. These objectives include meeting the basic needs and access of individuals, enterprises, and the community in a secure and consistent manner. Second requirement is to provide alternatives for transport modes and

promotes competitive economy, and balanced regional development, in other words, being affordable, efficient, and fair. Last but not least, minimising waste and damaging emissions to the extent that the planet can absorb them, using renewable resources at a rate lower than their replenishment, lessening noise pollution and the impact on the environment, and using less resources that deplete the environment until appropriate renewable alternatives are created. These requirements are factors or criteria that need to be considered in supporting sustainable urban transport. It is known that state of sustainability depends on several intertwined factors. By considering these complicated factors, one thing for sure is sustainable urban transport must integrate the perspective social, economic, and environmental aspects of city (Bibri, 2020, Al-Thani et al., 2022). However, in some big cities, the success of transport development has not been evenly distributed among the population, thus sustainability is not fully achieved.

Nevertheless, the concept of sustainability in general and sustainable urban transport in particular are still vague, uncertain and indeterminacy (Izadikhah et al., 2021). Due to the difficulty in defining sustainable urban transport, Gillis et al., (2015) conducted a literature review in an effort to propose a framework of creating a set of criteria or indicators for sustainable mobility in cities. This set of criteria is believed to satisfy and fulfil the goal of sustainable urban transport. Kraus, & Proff, (2021) proposed thirty three criteria of sustainable transport based on the three dimensions of sustainability; environmental, social and economic. It is presumed that these criteria are interrelated. For instance, air pollution must be related to people's health. Under the economic dimension, for example, operating cost may affect affordability. However, these relationships are not easily established due to vagueness and intangibility of criteria. However, few research have been able to draw on any systematic research into the relationship among criteria. To bridge this knowledge gap, this paper aims to establish cause-effect relationship among criteria of sustainable urban transport. In addition, this paper also aims to construct unidirectional relationships among criteria. On top of this relationship, the most influential criteria can be identified. All these aims can be achieved using the computational method single-valued neutrosophic-DEMATEL (SVN-DEMATEL). The DEMATEL is an abbreviation of Decision making trial and evaluation laboratory which is considered as an effective method for the identification of cause-effect relationship (Fontella and Gabus, 1976). On the other hand, single valued neutrosophic set (SVNS) is an extension of fuzzy set, which characterised by memberships of truth, indeterminacy, and falsity information (Wang et al., 2010). Details of SVNS and DEMATEL will be elucidated in the Section 3.

Materials and Methods

This section discusses the way this research is conducted. The materials such as information about decision makers and criteria used in this study are elucidated in this section. This section also presents the computational procedures used in this study.

2.1 Data Collection and Decision Makers

In order to establish which criteria of the urban transport development is the most important and to rank them based on their importance, data elicited from four decision makers are collected. Personal communication with decision makers was conducted where evaluation of interrelationship between criteria and weight of criteria are sought. The degree of importance or weight of decision makers is made based on their work experience and knowledge in sustainability and development of transportation. Brief biodata of decision makers (DMs) is summarised in Table 1.

Table 1 Profile of Decision Makers (DMs)

	DM 1 (D₁)	DM 2 (D₂)	DM 3 (D₃)	DM 4 (D₄)
Designation	Senior Civil Engineer	Civil Engineer	Senior Lecturer	Assistant Secretary
Years of experience	15	6	12	8
Employer	Municipal City Council	Municipal City Council	Government- Funded University	Ministry of Transport

The information provided by these decision makers are considered as subjective judgments that makes the information uncertain or indeterminacy (Paramanik et al., 2022; Büyüközkan et al., 2018).

2.2 Criteria

In the first subsection, decision makers (D₁, D₂, D₃, and D₄) are asked to assess how the twelve criteria relate to one another. The criteria are adopted from Do and Chen (2013) which research was about analysing stakeholder consensus for sustainable transport development decision. The criteria are Equality (C₁), Transport productivity and efficiency (C₂), Service quality (C₃), Accident frequency (C₄), Accident severity (C₅), Air Pollution(C₆), Noise Pollution (C₇), Energy Consumption (C₈), Space Usage (C₉), Transport cost (C₁₀), Travel time (C₁₁), and Economic attractiveness (C₁₂). The criteria and their brief descriptions are summarised in Table 2.

Table 2 Criteria and their description

Criteria	Descriptions
Equality (C ₁):	The equal right and opportunity to use a transport area is the main focus of this criterion. Everyone in society should be able to use the urban transport property, including those with disabilities, kids, seniors, and those with low incomes.
Transport productivity and efficiency (C ₂):	This criterion shows how well the transport property can be used, including the total number of passengers transported and the number of passengers per hour on each available road.
Service quality (C ₃):	This criterion is present to guarantee that the transport property offers services that satisfy user needs.
Accident frequency (C ₄):	By removing the most likely places for conflict in the traffic flow, this criterion shows the ability to prevent conflicts.
Accident severity (C ₅):	The capacity of the transport property to stop or lessen the likelihood of mass fatality incidents.
Air Pollution(C ₆):	This criterion shows how well the transport property can keep dirty cars out of the urban transport system.
Noise Pollution (C ₇):	The capacity of the transport property to keep raucous cars out of the urban transport network.
Energy Consumption (C ₈):	The transportation characteristic aids in lowering the usage of high energy usage
Space Usage (C ₉):	Reduced use of highly space-consuming transport modes is made possible by the transport property.
Transport cost (C ₁₀):	This illustrates the transport property's ability to lower transportation expenses.
Travel time (C ₁₁):	This is the ability to shorten the time and distance travelled by both passengers and cargo.
Economic attractiveness (C ₁₂):	This characteristic denotes the capacity to raise the degree of regional economic competitiveness by, for example, generating new income and employment that are brought about either directly or indirectly by urban transport projects.

Decision makers are requested to make judgements on the degree of influence of one criterion with respect to other criteria. Linguistic variable ‘influence’ and its respective single valued neutrosophic numbers (SVNNs) are given in Table 3.

Table 3 Linguistic variable and its corresponding SVNNs (Sahin and Yigider , 2016)

Integer	Linguistic Variable	SVNNs
0	No Influence	$\langle 0.00, 1.00, 1.00 \rangle$
1	Low Influence	$\langle 0.20, 0.85, 0.80 \rangle$
2	Medium Influence	$\langle 0.40, 0.65, 0.60 \rangle$
3	High Influence	$\langle 0.60, 0.35, 0.40 \rangle$
4	Very High Influence	$\langle 0.80, 0.15, 0.20 \rangle$

The collected information is then become the input to the computational tool SVN-DEMATEL method. The following next subsection elucidates the computational procedures of the method.

3.3 Computational Procedures of SVN-DEMATEL method

The computational procedures of SVN-DEMATEL method are retrieved from Awang et al., (2019) with some modifications to fit with the framework of this study. Despite using the SVNS as a basis in defining linguistic variable, Awang et al., (2019) integrated AHP-DEMATEL because they interested to find not only relationship among criteria but also weight of criteria. In the current research, the objectives are just limited to establish relationship among criteria. The procedures are given as follows.

Step 1: Construct Initial Direct-Influence matrix

Linguistic rating in the form of SVNNs are used to construct direct influence matrix. The list of criteria affecting the sustainable urban transport development are defined. The set of n criteria is denoted by $C = \{C_1, C_2, \dots, C_n\}$.

$$A^k = [a_{ij}^k] = \begin{matrix} c_1 \\ c_2 \\ \dots \\ c_n \end{matrix} \begin{bmatrix} a_{11}^k & a_{12}^k & \dots & a_{1n}^k \\ a_{21}^k & a_{22}^k & \dots & a_{2n}^k \\ \vdots & \vdots & \ddots & \vdots \\ a_{m1}^k & a_{m2}^k & \dots & a_{mn}^k \end{bmatrix} \quad (1)$$

where $a_{ij}^k = [T, I, F]$, $i = 1, 2, \dots, m$, $j = 1, 2, \dots, n$ the rating by decision makers, k in the evaluation of the interrelationship among criteria.

Step 2: Calculate weights of decision makers.

To determine the level of significance among decision makers, the weight of decision makers is also important. A decision maker's level of significance is determined by their background and expertise in sustainability and transportation development. Linguistic variable ‘importance’ and their respective SVNNs are given in Table 4.

Table 4 Linguistic variable ‘importance’ and its corresponding SVNNS

Integer	Linguistic Variable	SVNNS
0	Very unimportant (VU)	$\langle 0.1, 0.8, 0.9 \rangle$
1	Unimportant (U)	$\langle 0.35, 0.6, 0.7 \rangle$
2	Medium (M)	$\langle 0.5, 0.4, 0.45 \rangle$
3	Important (I)	$\langle 0.8, 0.2, 0.15 \rangle$
4	Absolutely important (AI)	$\langle 0.9, 0.1, 0.1 \rangle$

Different weights are given to each decision maker based on their experience and expertise in sustainable urban transportation. The relative importance of the k -th decision maker is determined using the priority equation developed by Boran et al. (see equation (2)).

Let $A_k = (T_k, I_k, F_k)$ be the SVNNS for rating of k -th expert. Then, the weight of k -th expert, λ_k can be obtained as follows:

$$\lambda_k = \frac{\left(T_k + F_k \left(\frac{T_k}{T_k + I_k} \right) \right)}{\sum_{k=1}^l \left(T_k + F_k \left(\frac{T_k}{T_k + I_k} \right) \right)}, \text{ where } \sum_{k=1}^l \lambda_k = 1. \quad (2)$$

Step 3: Construct Aggregated Initial Direct-Influence Matrix

As in Eq (3), the initial direct-influence matrices of each individual expert are combined using the SVNWA aggregation operator.

$$a_{ij} = \text{SVNWA}(a_{ij}^1, a_{ij}^2, \dots, a_{ij}^l) = \sum_{k=1}^l \lambda_k a_{ij}^k$$

$$= \left[1 - \prod_{k=1}^l (1 - T_{ij}^k)^{\lambda_k}, \prod_{k=1}^l (I_{ij}^k)^{\lambda_k}, \prod_{k=1}^l (1 - T_{ij}^k)^{\lambda_k} - \prod_{k=1}^l (I_{ij}^k)^{\lambda_k} \right] \quad (3)$$

where $i, j \in \{1, 2, 3, \dots, n\}$

The neutrosophic aggregated direct-influence matrix, A , is denoted as below:

$$A = \begin{bmatrix} a_{11} & a_{12} \cdots & a_{1n} \\ \vdots & \ddots & \vdots \\ a_{n1} & a_{n2} & \cdots a_{nm} \end{bmatrix},$$

where a_{ij} is SVNNSs with the form of $\langle T_{ij}, I_{ij}, F_{ij} \rangle$, and indicates the influence degree of criteria i on criteria j .

Step 4. Transform Aggregated SVNNSs Matrix into Aggregated Crisp Matrix.

The following equation is used to convert the aggregated SVNNSs relation matrix into Real Number Matrix, X' .

$$X' = \frac{(3+T-2I-F)}{4} \quad (4)$$

Step 5. Construct normalized direct-influence matrix, X .

Eqs. (5) and (6) can be used to obtain the normalised direct-influenced matrix, (X).

$$X = k \times X' \quad (5)$$

where

$$k = \min \left[\frac{1}{\max \sum_{j=1}^n a_{ij}}, \frac{1}{\max \sum_{i=1}^n a_{ij}} \right] \quad (6)$$

Step 6. Find Total Direct-Influence Matrix, B .

The following formulas can be used to get the matrix B .

$$B = X(I - X)^{-1} \text{ when } \lim_{k \rightarrow \infty} X^k = [0]_{n \times n} \quad (7)$$

where $B = [b_{ij}]_{n \times n} = \begin{bmatrix} b_{11} & \cdots & b_{1n} \\ \vdots & \ddots & \vdots \\ b_{n1} & \cdots & b_{nn} \end{bmatrix}$ and I is the neutrosophic identity matrix with diagonal entries of $\langle 1, 1, 1 \rangle$ and non-diagonal entries of $\langle 0, 0, 0 \rangle$.

Step 7: Find Sum of Row (R), Sum of Column (C), $R+C$, $R-C$ of Total Relation Matrix.

Calculate the sums of rows and columns. From the deneutrosophied matrix B , the prominence and relation of each criterion can be derived using eq (10).

$$\left. \begin{aligned} R &= \left[\sum_{i=1}^n a_{ij} \right]_{1 \times n} = [a_i]_{n \times 1} \\ C &= \left[\sum_{j=1}^n a_{ij} \right]_{1 \times n} = [a_j]_{n \times 1} \end{aligned} \right\} \quad (8)$$

The horizontal axis vector ($R + C$) values indicate "Prominence" represents the importance of each criterion while the vertical axis vector ($R - C$) named as "Relation".

Step 8: Construct Causal diagram.

The horizontal axis, called "Prominence," and the vertical axis, called "Relation," are used to construct the causal diagram. The value of $(R + C)$ indicates each criterion's relative importance, and the value of $(R - C)$ indicates the net effect of all the criteria added to the system. A criterion belongs to the causal category if $(R - C)$ is positive, while if the $(R - C)$ value is negative, the criterion belongs to effect group.

Step 9: Determine threshold value, α and draw the network relationship map (NRM).

By mapping the coordinates (R+C, R-C), an NRM can be created that clearly expresses the relationships between the criteria, the extent of influences, and the impacts of each criterion. This provides an intelligible structure. If a criterion is positive, it is regarded as belonging to the cause group. The criterion is regarded as the effect group if is negative. Matrix B's minor influences are eliminated by setting the threshold value, α .

The threshold value is determined by averaging the entries in Total Relation Matrix. Eq (8) is used to find α .

$$\alpha = \frac{\sum_i^m \sum_i^n b_{ij}}{m \times n} \quad (8)$$

where b_{ij} is the Total Direct-Influence Matrix and $m \times n$ is the size of matrix.

The above nine-step computational procedures are implemented with the data of sustainable urban transport.

Computation and Results

It is recalled that the aim of this study is to establish relationships among multiple criteria of sustainable urban transport. Evaluation about degree of influence of one criterion to other criteria is elicited from a group of decision makers using the linguistic variable 'influence'. This information is translated into SVNN prior to implementing computation. In short, the information in the form of SVNN is used as the input to the SNN-DEMATEL. Detailed computations and results are presented as follows,

Step 1: Construct Initial Direct-Influence matrices.

Linguistic judgments by decision makers are collected to construct Initial Direct-Influence matrices.

Step 2: Calculate weights of decision makers.

Weight for each decision maker is calculated using Eq (1).

For example,

$$D_1: 1 - \sqrt{[(1-0.9)^2 + (0.1)^2 + (0.1)^2]}/3 = 0.9$$

$$D_2: 1 - \sqrt{[(1-0.9)^2 + (0.1)^2 + (0.1)^2]}/3 = 0.9$$

$$D_3: 1 - \sqrt{[(1-0.5)^2 + (0.4)^2 + (0.45)^2]}/3 = 0.548152$$

$$D_4: 1 - \sqrt{[(1-0.8)^2 + (0.2)^2 + (0.15)^2]}/3 = 0.815158$$

Summation of weights

$$\Sigma 0.9 + 0.9 + 0.54812 + 0.815158 = 3.15331$$

Therefore, weight of Decision Maker 1:

$$W_1 = \frac{0.9}{3.16331} = 0.28451$$

Similar weights are calculated for other decision makers.

Step 3: Construct aggregated initial direct-influence matrix

The SVNWA aggregation operator is used to aggregate the initial direct-influence matrices of each decision maker (see eq (2)).

For example,

$$a_{11} = a_{22} = a_{33} = a_{44} = a_{55} = a_{66} = a_{77} = a_{88} = a_{99} = a_{10,10} = a_{11,11} = a_{12,12} : \langle 0, 1, 1 \rangle$$

$$1 - \prod_{p=1}^q (1 - T_{ij}^{(p)})^{W_q} = 1 - ((1 - 0)^{0.28451} * (1 - 0)^{0.28451} * (1 - 0)^{0.173284} * (1 - 0)^{0.257691}) = 0.000$$

$$\prod_{p=1}^q (I_{ij}^{(p)})^{W_q} = (1.0^{0.28451}) * (1.0^{0.28451}) * (1.0^{0.173284}) * (1.0^{0.257691}) = 1.0$$

$$\prod_{p=1}^q (F_{ij}^{(p)})^{W_q} = (1.0^{0.28451}) * (1.0^{0.28451}) * (1.0^{0.173284}) * (1.0^{0.257691}) = 1.0$$

The remaining entries of the matrix are calculated similarly.

Step 4: Transform aggregated matrix to aggregated crisp matrix, X'

Eq (3) is used to transform the aggregated initial direct-influence matrix to the aggregated initial direct-influence matrix with entries are real numbers.

For example, criteria

C_1 :

$$a_{21} = \frac{3 + 0.760887 - (2 * 0.186602) - 0.239113}{4} = 0.7871$$

$$a_{31} = \frac{3 + 0.496198 - (2 * 0.497792) - 0.503802}{4} = 0.4992$$

...

$$a_{12,1} = \frac{3 + 0.358983 - (2 * 0.638003) - 0.641017}{4} = 0.3605$$

The remaining entries are calculated similarly. The aggregated direct-influence matrix with real numbers is shown as Matrix X' .

$$X' = \begin{pmatrix} 0.0000 & 0.698283 & 0.825 & \dots & 0.128669 & 0.530686 \\ 0.7871 & 0.0000 & 0.782755 & \dots & 0.782755 & 0.375 \\ 0.4992 & 0.692041 & 0.0000 & \dots & 0.730184 & 0.566842 \\ 0.1038 & 0.460169 & 0.566842 & \dots & 0.237666 & 0.381407 \\ 0.1038 & 0.460169 & 0.566842 & \dots & 0.237666 & 0.381407 \\ 0.0533 & 0.05335 & 0.375 & \dots & 0.0000 & 0.032849 \\ 0.0533 & 0.05335 & 0.375 & \dots & 0.0000 & 0.032849 \\ 0.4739 & 0.344201 & 0.290303 & \dots & 0.236645 & 0.032849 \\ 0.6445 & 0.625 & 0.671533 & \dots & 0.457977 & 0.194874 \\ 0.8004 & 0.800377 & 0.757129 & \dots & 0.825 & 0.457977 \\ 0.8004 & 0.800377 & 0.757129 & \dots & 0.0000 & 0.457977 \\ 0.3605 & 0.194874 & 0.250481 & \dots & 0.328653 & 0.0000 \end{pmatrix}_{12 \times 12}$$

Step 5: Construct normalized direct-relation matrix.

The matrix in Step 4 is normalised using eq (5) and eq (6).

The normalized direct-influence matrix, X is given as

$$X = \begin{pmatrix} 0.00000 & 0.09243 & 0.10921 & \dots & 0.01703 & 0.07025 \\ 0.10419 & 0.00000 & 0.10361 & \dots & 0.10361 & 0.04964 \\ 0.06608 & 0.09161 & 0.00000 & \dots & 0.09665 & 0.07503 \\ 0.01374 & 0.06091 & 0.07503 & \dots & 0.03146 & 0.05049 \\ 0.01374 & 0.06091 & 0.07503 & \dots & 0.03146 & 0.05049 \\ 0.00706 & 0.00706 & 0.04964 & \dots & 0.00000 & 0.00435 \\ 0.00706 & 0.00706 & 0.04964 & \dots & 0.00000 & 0.00435 \\ 0.06272 & 0.04556 & 0.03843 & \dots & 0.03132 & 0.00435 \\ 0.08531 & 0.08273 & 0.08889 & \dots & 0.06062 & 0.02580 \\ 0.10595 & 0.10595 & 0.10022 & \dots & 0.10921 & 0.06062 \\ 0.10595 & 0.10595 & 0.10022 & \dots & 0.00000 & 0.06062 \\ 0.04772 & 0.02580 & 0.03316 & \dots & 0.04350 & 0.00000 \end{pmatrix}_{12 \times 12}$$

Step 6: Find Total Relation Matrix, B using Eq (7).

Table 4.12 show the result of Total Relation Matrix, B .

$$B = \begin{pmatrix} 0.0969287 & 0.1869427 & 0.2131374 & \dots & 0.1049480 & 0.1344074 \\ 0.2349207 & 0.1516349 & 0.2650092 & \dots & 0.2154913 & 0.1475390 \\ 0.2022241 & 0.2364863 & 0.1754243 & \dots & 0.2112546 & 0.1711645 \\ 0.1028692 & 0.1541498 & 0.1807726 & \dots & 0.1112379 & 0.1135458 \\ 0.1023505 & 0.1533727 & 0.1798612 & \dots & 0.1106771 & 0.1129734 \\ 0.0421627 & 0.0436371 & 0.0882084 & \dots & 0.0309545 & 0.0273138 \\ 0.0427238 & 0.0442178 & 0.0893824 & \dots & 0.0313665 & 0.0276773 \\ 0.1200352 & 0.1090090 & 0.1158296 & \dots & 0.0824390 & 0.0491894 \\ 0.1887518 & 0.1949761 & 0.2171013 & \dots & 0.1522426 & 0.1041067 \\ 0.2131605 & 0.2195589 & 0.2281655 & \dots & 0.1995300 & 0.1398503 \\ 0.2157151 & 0.2217017 & 0.2307478 & \dots & 0.1027551 & 0.1407118 \\ 0.0812534 & 0.0633968 & 0.0739351 & \dots & 0.0714662 & 0.0264133 \end{pmatrix}_{12 \times 12}$$

Step 7: Find Sum of Row (R), Sum of Column (C), $R+C$ and $R-C$ of the total relation matrix, B

Eq (8) is used to calculate R and C followed by $R+C$ and $R-C$.

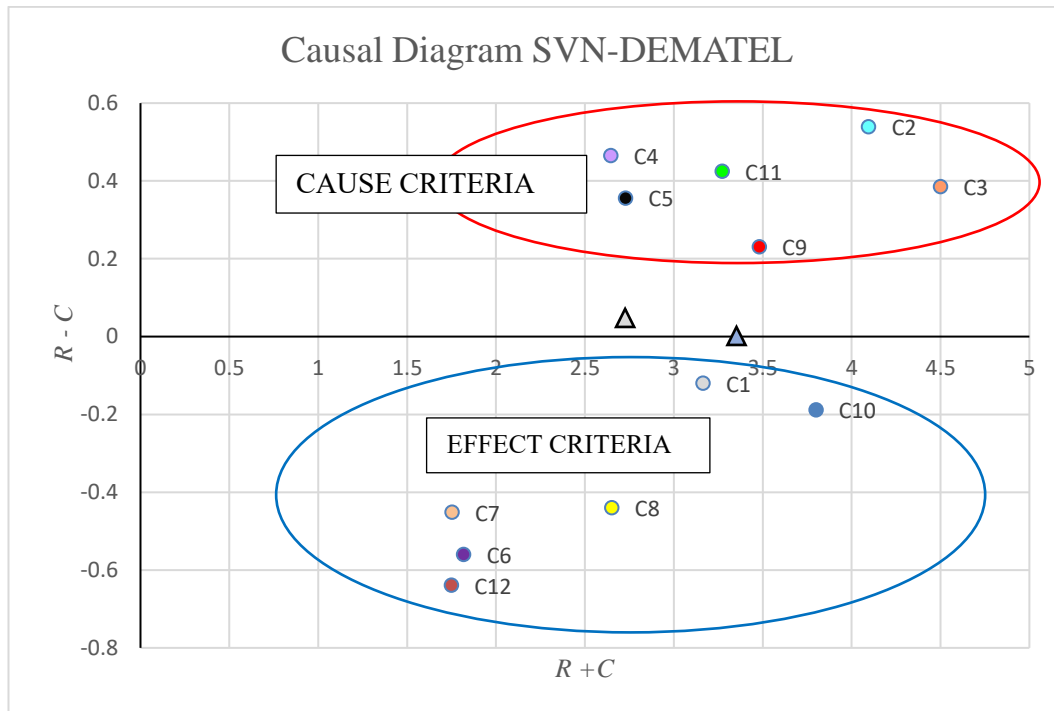
Table 5 shows R , C , $R+C$ and $R-C$ of criteria.

Table 5 Values of R , C , $R+C$ and $R-C$

Criteria	R	C	$R+C$	$R-C$
C_1	1.522774148	1.643095597	3.165869745	-0.120321449
C_2	2.317755148	1.779083992	4.09683914	0.538671156
C_3	2.442828459	2.057574822	4.50040328	0.385253637
C_4	1.555361479	1.090632056	2.645993535	0.464729423
C_5	1.542478752	1.186915973	2.729394725	0.355562779
C_6	0.629422323	1.18945904	1.818881363	-0.560036717
C_7	0.65110918	1.10280187	1.75391105	-0.45169269
C_8	1.106194684	1.546224951	2.652419635	-0.440030267
C_9	1.855892779	1.625443111	3.481335891	0.230449668
C_{10}	1.805592915	1.99335641	3.798949324	-0.187763495
C_{11}	1.848891017	1.424362633	3.27325365	0.424528383
C_{12}	0.555542312	1.194892741	1.750435053	-0.639350429

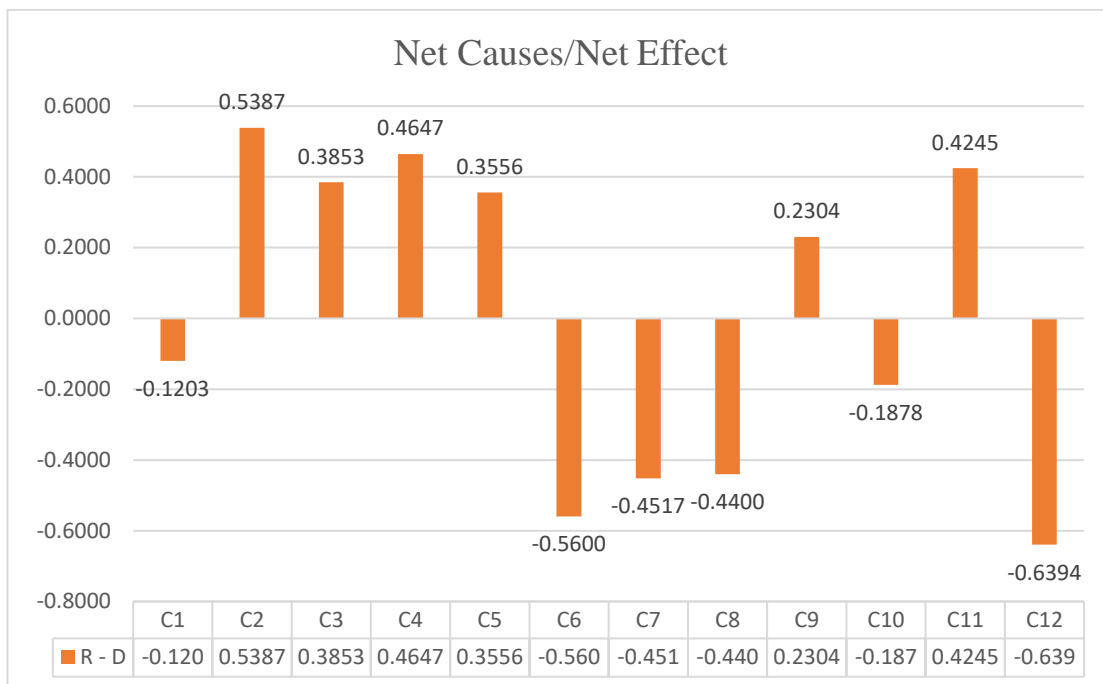
Step 8: Construct Causal diagram.

The causal diagram is constructed by horizontal axis ($R + C$) named as “Prominence” and the vertical axis ($R - C$) named as “Relation”. The causal diagram is depicted in Figure 1.

Fig 1 The causal diagram

From the figure, there are two groups of criteria. Transport productivity and efficiency (C_2), Service quality (C_3), Accident frequency (C_4), Accident severity (C_5), Space Usage (C_9), and Travel time (C_{11}) are the criteria under the Cause Group. These criteria are believed to have a strong influence in sustainable urban transportation. On the other hand, Equality (C_1), Air Pollution (C_6), Noise Pollution (C_7), Energy Consumption (C_8), Transport cost (C_{10}), and Economic attractiveness (C_{12}) are the criteria under the Effect Group in which these criteria receive effect from the Cause Group. In other words, the criteria under Effect Group have no influence on sustainable urban transport.

Apart from the clusters of cause-effect criteria, analysis of the criteria is further enhanced by having the strength of criteria regardless the group which they belong. The strength of influence (net cause) and strength of effect (net effect) of each criterion from each group is illustrated in Figure 2.

Fig 2 Net Causes/Effect Graph SVN

It can be seen that the criteria Transport productivity and efficiency (C_2) is the most influential cause criteria while Economic attractiveness (C_{12}) is the most affected criteria. However, the above figure has no information on which criteria in the cause group that may influence which criteria in the effect group. To see the illustration of unidirectional relationship between among criteria, a network relationship map (NRM) is drawn.

Step 9: Determine threshold value, α and draw the NRM.

A threshold value must be established in order to draw NRM. Using equation (8), the threshold value α is equal to 0.1238461. If the values in matrix B are less than the threshold, they are indicated by '0,' and if the values are equal to or greater than the threshold, they are indicated by '1'. The goal of drawing and visualising the NRM is to observe a network of relationships or direction of influence among criteria based on the information that is either '0' or '1'. Figure 3 shows the NRM.

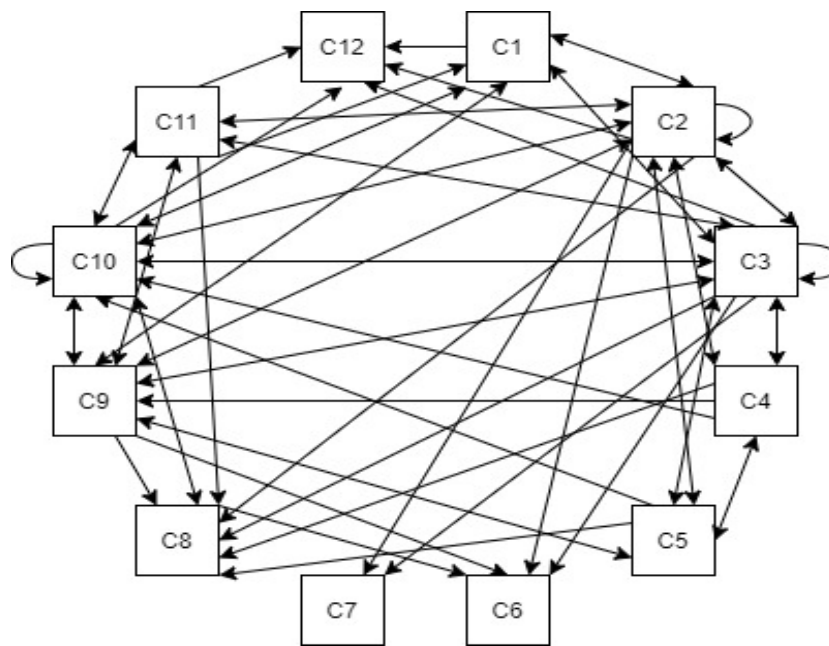
Fig 3 Network Relationship Map

Figure 3 indicates that some of the criteria are interrelated. It can be seen that the criterion C_{10} is easily affected and influenced by the other nine criteria including itself. Furthermore, it can also be seen that the criterion 'Transport productivity and efficiency' (C_2) plays its role in influencing the other criteria. The best strategy for sustainable urban transport is to pay close attention to the criterion C_2 as this criterion has stronger influential power compared to other cause criteria. This result conflicts with research by Do and Chen (2013) on the selection problem of sustainable urban transport, where "having support from relevant agencies" is the most challenging task in the implementation and "safety" is the most important criterion of the future expected impacts. The multi-criteria method fuzzy analytic hierarchy process was applied instead of SVN-DEMATEL might explain the inconsistency between two results.

Conclusion and Recommendations

The present study was designed to establish the causal relationship among criteria of sustainable urban transport. This study was conducted via decision makers linguistic judgments by using the method SVN-DEMATEL. This study has found that generally the twelve criteria can be separated into cause group and effect group. There are six criteria that can be called as cause criteria, and six criteria are grouped as effect criteria. The second finding was the recognition of 'transport productivity and efficiency' as the most influential criterion. In other words, this criterion has potential to influence other criteria. The results of this investigation also show the unidirectional relationship where cause criteria affect one or more other criteria in the effect group. The findings of this study suggest that efficiency of urban transport must be given extra attention in managing sustainable urban transport as this factor may amplify ripple effect to other factors. From the perspective of the method used, this research extends our knowledge of the SVN-DEMATEL method. The method can be further modified by introducing weight of criteria instead of just solely weight of the decision makers.

Thanks and Information Note

Special thanks to research student Nazreena Izzani Ishak for assisting personal communication sessions with group of decision makers and also data analysing.

References

- Al-Thani, H., Koç, M., Isaifan, R. J., & Bicer, Y. (2022). A Review of the Integrated Renewable Energy Systems for Sustainable Urban Mobility. *Sustainability*, 14(17), 10517.
- Awang, A., Aizam, N.A.H., & Abdullah, L. (2019). An Integrated Decision-Making Method Based on Neutrosophic Numbers for Investigating Factors of Coastal Erosion. *Symmetry*, 11(3): 328.
- Banister, D. (2008). The sustainable mobility paradigm. *Transport Policy*, 15, 73–80
- Bibri, S. E. (2020). Advances in the leading paradigms of urbanism and their amalgamation: compact cities, eco-cities, and data-driven smart cities. Springer Nature.
- Büyüközkan, G., Feyzioglu, O., & Göçer, F. (2018). Selection of sustainable urban transportation alternatives using an integrated intuitionistic fuzzy Choquet integral approach. *Transportation Research Part D: Transport and Environment*, 58, 186-207.
- CEU, C. (2001). Council Resolution on the Integration of Environment and Sustainable Development into the Transport Policy.
- Cuomo, C.K. (2019). The Case for Sustainable Urban Transportation for Malaysia. <http://jeffreysachs.center/columns-op-eds/The-Case-for-Sustainable-Urban-Transportation-for-Malaysia> [20 November 2019].
- Do, Q. H., & Chen, J. F. (2013). Establishing the index system for sustainable urban transport project selection: an application of group MCDM based on the fuzzy AHP approach. *International Journal of Business and Management Invention*, 2(6), 47-57.
- Fontela, E., & Gabus, A. (1976). The DEMATEL observer.
- Gillis, D., Semanjski, I., & Lauwers, D. (2015). How to monitor sustainable mobility in cities? Literature review in the frame of creating a set of sustainable mobility indicators. *Sustainability*, 8(1), 29.
- Gössling, S., Cohen, S., Higham, J., Peeters, P., & Eijgelaar, E. (2018). Desirable transport futures. *Transportation Research Part D: Transport and Environment*, 61, 301-309.
- Izadikhah, M., Azadi, M., Toloo, M., & Hussain, F. K. (2021). Sustainably resilient supply chains evaluation in public transport: A fuzzy chance-constrained two-stage DEA approach. *Applied soft computing*, 113, 107879.
- Kraus, L., & Proff, H. (2021). Sustainable urban transportation criteria and measurement—a systematic literature review. *Sustainability*, 13(13), 7113.
- Loo, B.P.Y. (2018). Unsustainable Transport and Transition in China, <http://www.scopus.com/inward/record.url?partnerID=x8ErFbHU&eid=2-s2.0-85041922852>.
- Pojani D & Stead D. (2015). Sustainable Urban Transport in the Developing World: Beyond Megacities. *Sustainability* 7(6):7784-7805.
- Plano, C. (2022). Improving paratransit service: Lessons from transport management companies in Nairobi, Kenya and their transferability. *Case Studies on Transport Policy*, 10(1), 156-165.
- Paramanik, A. R., Sarkar, S., & Sarkar, B. (2022). OSWMI: An objective-subjective weighted method for minimizing inconsistency in multi-criteria decision making. *Computers & Industrial Engineering*, 169, 108138.
- Şahin, R. & Yigider, M. (2016). A Multi-Criteria Neutrosophic Group Decision Making Method Based TOPSIS for Supplier Selection. *Applied Mathematics & Information Sciences*. 10. 1843-1852. 10.18576/amis/100525.
- Wang, H., Smarandache, F., Zhang, Y., & Sunderraman, R. (2010). Single valued neutrosophic sets. *Infinite study*, 12.

DEVELOPMENT OF A SOLID CATALYST DERIVED FROM SARDINE SCALES AND EGGSHELLS FOR BIODIESEL SYNTHESIS

Amina OUAHBI

Laboratory of Physical-Chemistry, Materials and Catalysis (LCPMC), Faculty of Sciences Ben M'Sik, HASSAN II University, Casablanca, Morocco.

Youness BOUHAIJ

Laboratory of Physical-Chemistry, Materials and Catalysis (LCPMC), Faculty of Sciences Ben M'Sik, HASSAN II University, Casablanca, Morocco.

Abdeslam EL BOUARI

Laboratory of Physical-Chemistry, Materials and Catalysis (LCPMC), Faculty of Sciences Ben M'Sik, HASSAN II University, Casablanca, Morocco.

Omar TANANE

Laboratory of Physical-Chemistry, Materials and Catalysis (LCPMC), Faculty of Sciences Ben M'Sik, HASSAN II University, Casablanca, Morocco.

ABSTRACT

The world is facing an energy crisis due to growing energy demand, resource depletion and global warming. It is therefore essential to develop sustainable alternative fuels with characteristics similar to those of conventional fuels. Biodiesel is widely studied as a sustainable fuel and has proven to be efficient, sustainable, economic and environmentally friendly. With this in mind, a novel catalyst has been prepared by mixing eggshells and sardine scales in order to synthesize biodiesel from waste frying oil (WFO) by transesterification reaction. The catalysts were characterized by SEM, DRX and IR and the catalytic activity of the calcined catalysts at different temperatures was assessed. The results confirmed that the main components of calcined eggshells and sardine scales were calcium oxide (CaO), β Tricalcium Phosphate (β TCP) and hydroxyapatite (HAP) respectively. Moreover, the best biodiesel yield and the strongest catalytic activity were obtained at a calcination temperature of 900 °C for 3h. The optimal experimental conditions of the transesterification reaction allowing a maximum yield of 89% were obtained under the following conditions: methanol to oil molar ratio of 15:1, 2.5 wt.% catalyst concentration at 65 °C during 4h30. The catalytic activity of the catalyst after hydration (moisture contamination) for 60 days shows no significant loss of activity. The physicochemical properties of the produced biodiesel were investigated and compared with the EN14214 and ASTM D-6751 standards for biodiesel specifications. Consequently, the natural wastes such as eggshells and fish scales, used as heterogeneous catalysts, proved their effectiveness, sustainability and their contribution to reduce the abundant wastes since they can be reused for 4 cycles in the transesterification reaction with slight loss of activity.

Keywords: Biodiesel, Transesterification, Heterogeneous catalyst, CaO, HAP, Btcp

Z-SCHEME PHOTOCATALYTIC SYSTEMS FOR PHOTOELECTROCHEMICAL WATER SPLITTING

Fatih ARLI

*Dr., Sirnak University, Faculty of Engineering, Department of Energy systems engineering, Sirnak- Türkiye
ORCID: 0000-0002-0899-3460*

ABSTRACT

With the continued consumption of fossil energy, solar energy is predicted to play a vital role in meeting future energy demands and reducing environmental problems. Photobiological water splitting, thermochemical water splitting, photocatalytic (PC WS), and photoelectrochemical water splitting (PEC WS) technology are all available for producing hydrogen from solar energy. Among these, PEC WS is a promising technology for a renewable, sustainable, and environmentally friendly natural world. PEC technology research in hydrogen production employing solar energy and WS into hydrogen and oxygen has recently increased significantly. Research into Z-scheme heterojunction structures has increased in the last few decades, as it is an innovative approach to architecting various heterostructures to improve PEC performance. It shows outstanding performance and is an artificial imitation of photosynthesis. The Z-scheme system's working principle includes two photocatalysts, and an electron shuttle is used in this system. Photons are captured by Z-order materials, which leads to the formation of electrons and holes within the material. The resulting electrons are transferred to the shuttle, which is an electron carrier. This electron shuttle initiates electrochemical reactions in photocatalysts, producing compounds such as H₂ and O₂, enabling water splitting. Here, the applications of the Z scheme in PEC will be reviewed, and the productive findings obtained from recent studies will be evaluated. Information about challenges and potential advances in Z-scheme architectures and their future development directions will also be presented.

Keywords: Solar energy, Photoelectrochemical technology, Water splitting, Hydrogen production, Z-scheme heterojunction.

Introduction

Rapid economic and industrial developments have rapidly increased the consumption of fossil fuels today, resulting in severe energy and environmental problems. Since coal, natural gas, and oil are non-renewable, it has become inevitable to develop alternative green energy sources (J. Li et al., 2022; Wei et al., 2023). Hydrogen gas has a high gravimetric energy density ($\approx 140 \text{ MJ kg}^{-1}$) and zero carbon emissions, creating a clean economy and eliminating environmental problems (Zhao et al., 2023). Photocatalysis, electrolysis, thermocatalysis, and photoelectrochemical (PEC) systems are technologies designed to produce hydrogen by splitting water. PEC WS has significant advantages over others in hydrogen production (H. Liu et al., 2023). The aim of hydrogen production by water splitting using PEC WS sunlight and photocatalyst is to develop not only an environmentally friendly technology but also an economic strategy. Moreover, this technology will reduce the excessive consumption of fossil energy. However, solar-to-hydrogen (STH) efficiencies are still far from meeting some requirements for solar-driven applications. Photocatalysts with the properties required to improve STH efficiency should be able to absorb visible light radiation, rapidly utilize photonic energy to generate charge carriers, prevent heat losses, and promote PEC WS and organic reformation (Clarizia et al., 2023). Also, In the overall PEC WS system, efficient light harvesting, accelerated surface redox reactions with the design and fabrication of viable photoelectrodes, and promoted charge separation play a vital role in achieving a high STH (Bian et al., 2015; Celebi & Salimi, 2022). Constructing a suitable heterojunction between two semiconductors with a suitable band gap is a very effective way of boosting charge separation performance (Celebi et al., 2021; Zhang et al., 2020). Recently, it has been determined that Z-scheme heterojunctions are more efficient than type II heterojunctions due to accelerated electron-hole separation and unique band positions (Celebi et al., 2021; Guo et al., 2020). Figure 1 demonstrates the number of publications in PEC WS and Z-scheme PEC WS reported in the Web of Science between 2020 and 2023.

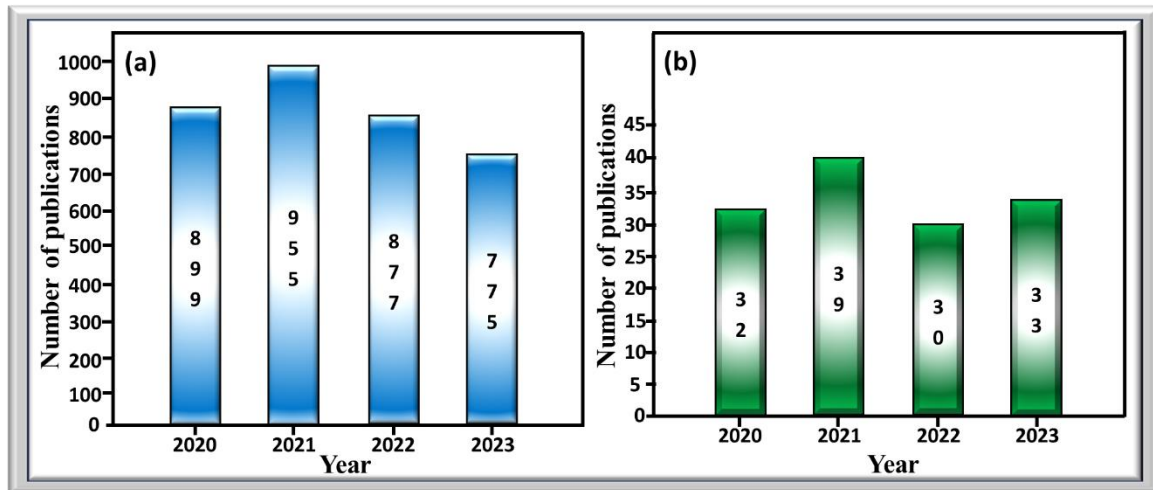


Figure 1. Number of publications reported in Web of Science between 2020-2023: a) PEC WS, b) Z-scheme PEC WS

The primary research objective is to examine the functional mechanism of Z-scheme heterojunction structures and compare their efficacy with one-component and two-component structures in PEC WS technologies.

Basic principle of PEC WS

PEC WS is a highly promising technology for utilizing solar energy. It employs semiconductors to convert sunlight and water into hydrogen fuel (Qiu et al., 2019). Solar water splitting is a thermodynamically uphill reaction with a Gibbs free energy of 237 kJ mol^{-1} . Therefore, the materials employed in the solar water-splitting process must fulfill specific criteria. The material's band gap should be approximately 1.5 eV (more than 1.23 eV) to absorb a significant portion of the incident light. The valence band (VB) edge potential should be more positive to allow water oxidation than the $\text{O}_2/\text{H}_2\text{O}$ redox potential of 1.23 V vs. NHE ($\text{pH} = 0$). In addition, water reduction requires the conduction band (CB) to be more negative than the H^+/H_2 redox potential of 0 V vs. NHE . When exposed to light, the material absorbs photons with energies greater than the band gap, resulting in photoexcited electrons and holes delivered to the surface to carry out water oxidation and reduction processes, as illustrated in Figure 2a. PEC WS is a method that uses materials as photoelectrodes (photoanode or photocathode), producing H_2 and O_2 on distinct electrode surfaces, ideally in separate chambers (Figure 2b) (Kalanoor et al., 2018; Qiu et al., 2019).

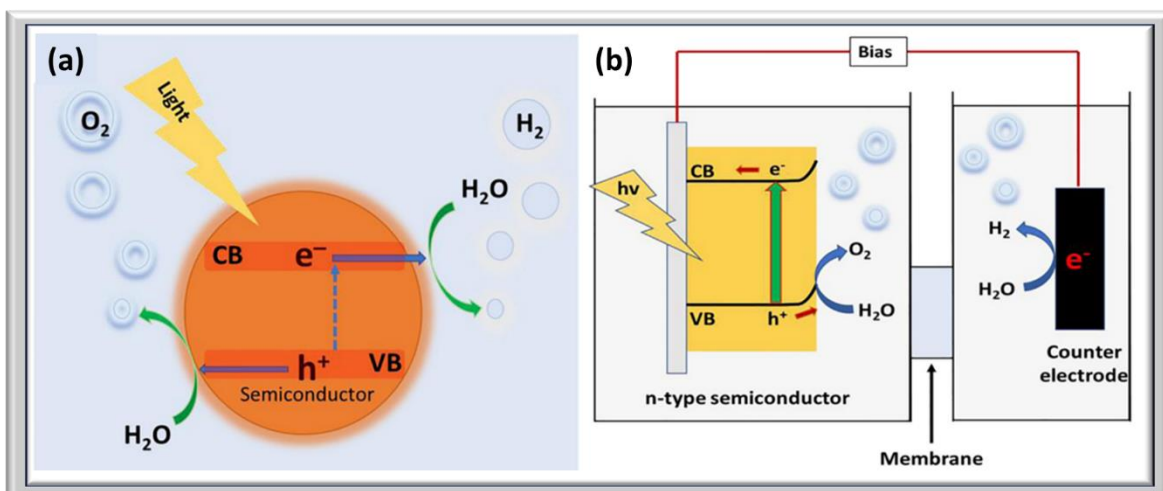


Figure 2. a) Solar WS systems in semiconductors and b) n-type PEC WS (Kalanoor et al., 2018).

In addition, water reduction requires the conduction band (CB) to be more negative than the H^+/H_2 redox potential of 0 V vs. NHE. When exposed to light, the material absorbs photons with energies greater than the band gap, resulting in photoexcited electrons and holes delivered to the surface to carry out water oxidation and reduction processes, as illustrated in Figure 2a. PEC WS is a method that uses materials as photoelectrodes (photoanode or photocathode), producing H_2 and O_2 on distinct electrode surfaces, ideally in separate chambers (Figure 2b) (Kalanoor et al., 2018; Qiu et al., 2019).

PC WS by one-step photoexcitation

PEC WS has enormous potential for converting solar energy into hydrogen on a massive scale (Abe, 2010; Wen et al., 2020). The road to high photoconversion performance depends on designing and developing low-cost semiconductor electrodes with high light harvesting capabilities, efficient separation of photogenerated electron-hole pairs, and strong redox for WS (Abe, 2010). The one-step photoexcitation method processes the water reduction and oxidation reactions on a single semiconductor photocatalyst. Figure 3 illustrates a schematic representation of the charge transfer method for single-component photocatalysts in WS (Maeda, 2013; Ng et al., 2020). Although several semiconductor materials have been constructed, it is difficult for a single-component material to fulfill all criteria simultaneously (C. Liu et al., 2019; Wen et al., 2020). As an illustration, metal oxides have been extensively investigated. As a result of the investigations, high quantum performances of 10% were obtained in some of them. However, the material's band gap will expand (to more than 3 eV) if the lower half of the conduction band of metal oxides is located at a more negative potential than the water reduction potential (Abe, 2011; Wei et al., 2023). As another example, some metal chalcogenides, including CdS and CdSe, appear to be suitable photocatalysts for general WS because they have a small band gap and suitable potential for water reduction and oxidation. Since S^{2-} and Se^{2-} anions are more susceptible to oxidation than water, they cause oxidation and degradation of the CdS or CdSe catalyst, meaning that these metal chalcogenides are unstable in the water oxidation reaction to form O_2 (Abe, 2011; Maeda, 2013).

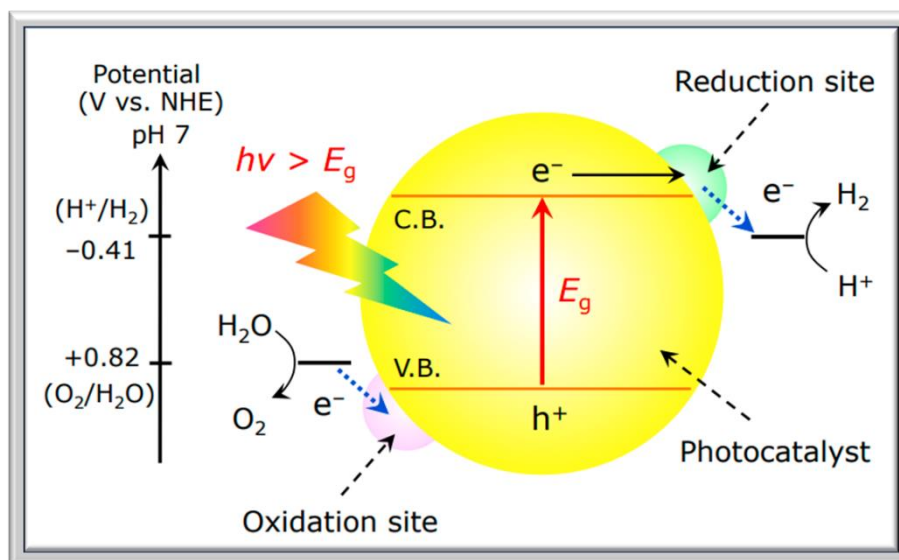


Figure 3. Graphical illustration of photocatalysts in single components (Maeda, 2013).

PC WS by two-step photoexcitation

As a result of single-component photocatalytic systems failing to meet the desired needs, researchers conducted detailed research to solve this problem. In particular, they aimed to increase the photocatalytic performance and the charge separation efficiency. Then, they investigated utilizing both different semiconductors to create type II heterojunction nanocomposites. By designing appropriate heterojunction structures, electrons and holes can be isolated in separate regions, increasing the lifetime of photogenerated

carriers. As demonstrated in Figure 4, gas formation occurs in two separate photocatalysts: HER (HEP) in H_2 evolution photocatalysts and OER (OEP) in O_2 evolution photocatalysts. Although this system also facilitated charge separation, it weakened the redox ability because of the movement of electrons and holes towards the more electropositive CB and electronegative VB potential, attributed to the nature of charge transfer.

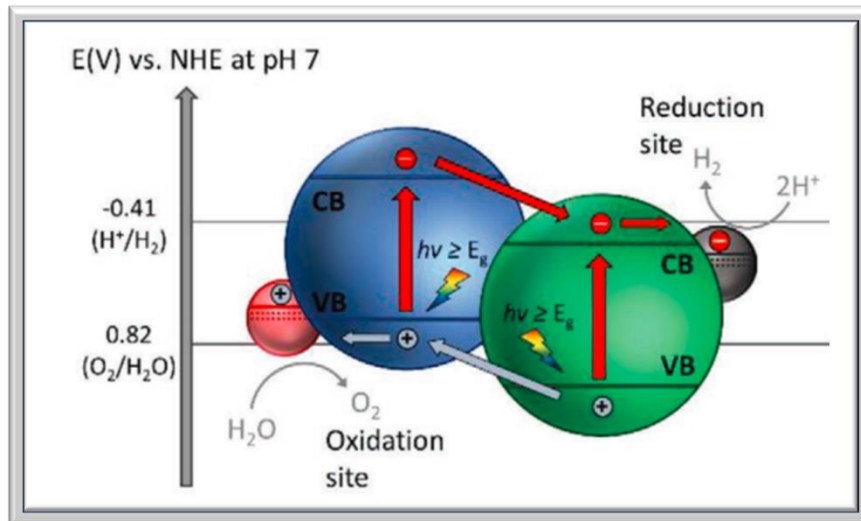


Figure 4. The diagram of type-II heterojunction photocatalysts (Ng et al., 2020).

Basic principles of Z-scheme materials

Two approaches to PC WS have been studied so far. The first approach uses a single-component photocatalyst, known as one-step photoexcitation (Abe et al., 2018; Maeda, 2013; Ng et al., 2020). Due to the abovementioned limitations, some (oxy)nitrites, (oxy)sulfides, metal oxides, and chalcogenides have been reported in the literature for general WS. Problems such as low STH performance and poor stability under oxidative/reductive photo corrosion have restricted the utilization of single-component photocatalysts in WS (Abe et al., 2018; Maeda, 2013). The second approach uses a two-photocatalyst, known as a Z-scheme photocatalytic system. WS reduction and oxidation processes take place on spatially divided photocatalysts in the Z scheme system (Figure 5).

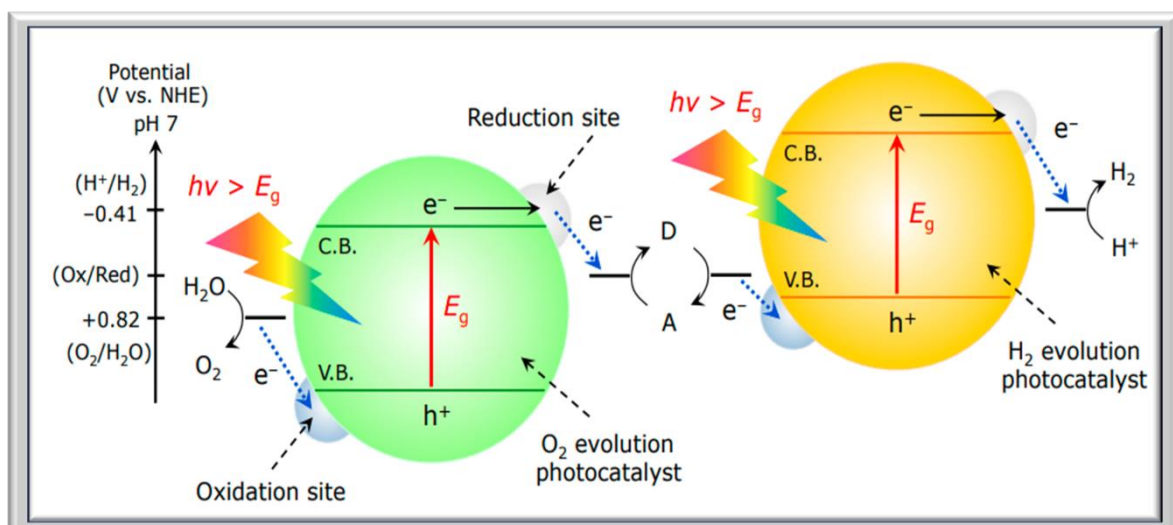


Figure 5. Energy diagram demonstrating the PC WS process using a two-step photoexcitation system (Maeda, 2013).

Thanks to this situation, the possibility of recombination of spatially separated H₂ and O₂ is significantly reduced. The redox shuttling cycle consumes photoinduced electrons from the CB of the OEP and holes from the VB of the HEP. Thus, the holes in the OEP and the electrons in the HEP are utilized for the oxidation and reduction of water, respectively (Wei et al., 2023). In establishing the Z-schemes that are fundamental for general water dissociation, a critical role is played by the oxidized redox mechanism, the reduction of OEP by CB electrons, and the reduced redox mechanism, the oxidation of HEP by holes, VB, from the H₂O/H₂ potential to a more positive CB or Semiconductors that are thermodynamically inadequate for one-step WS with a VB more negative than the H₂O/O₂ potential can be easily used in Z-order WS (Ng et al., 2020; Wei et al., 2023). The energy band configuration of HEP and OEP must be staggered to obtain high efficiency from the Z-scheme system. Moreover, the light-induced electrons in the CB of HEP and the substantial holes in the VB of OEP should remain in the starting bands without migrating to the other photocatalyst. There are disadvantages in a typical Z-order photocatalytic system with redox shuttles (electron acceptors and electron donors shown as A/D) because they are particle suspensions (Ng et al., 2020; Wei et al., 2023). These are:

- A/D can only be implemented in liquid phase reactions of the Z scheme due to its chemical structure.
- The distinctive structural characteristics of redox shuttled Z-order systems have a minimal effect on the transport of charge carriers, as there is a spatial separation between HEP and OEP, which discourages close interaction.
- Due to the obstruction of light by A/D, the light absorption capacity of HEP and OEP is reduced.
- The reaction pH of the aqueous solution is significant for the activity of A/D.
- Side reactions unavoidably accompany ionic redox shuttles.

Despite these disadvantages mentioned above, the disadvantages of the Z-scheme can be offset by its advantages, such as low cost, simple technology, and a relatively wide selection of semiconductors that can be exploited to achieve overall WS (Wei et al., 2023). The Z-scheme of the photocatalytic system can be inferred from the historical pathway in Figure 6, which shows that a great deal of effort has been made over the years to develop a photosynthesis-like light-harvesting system to achieve full performance from solar energy. In 1979, Bard reported a breakthrough approach in his work by designing the concept of an electron mediator as a charge transport mediator between two photosystems for reduction and oxidation processes, respectively (Ng et al., 2020).

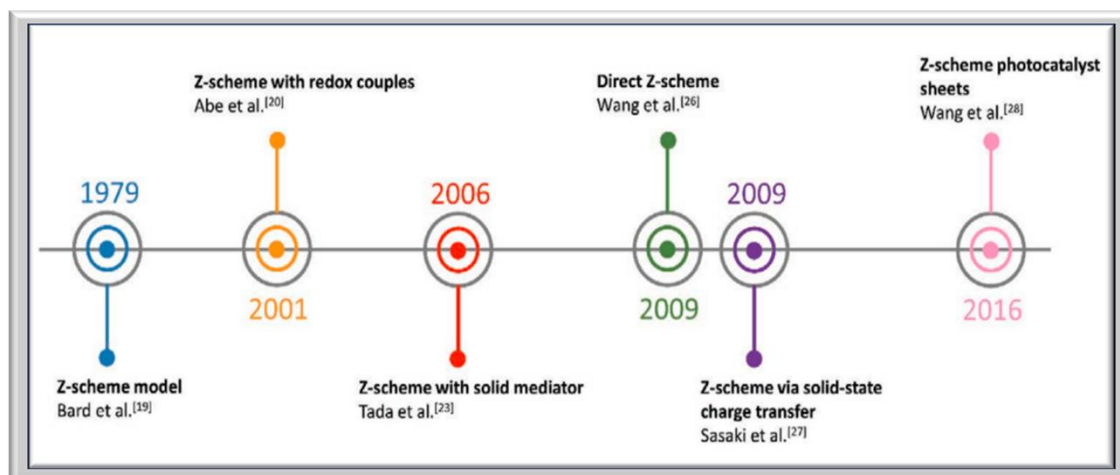


Figure 6. Roadmap for the Z-scheme's development (Ng et al., 2020).

Figure 7 depicts the electron-mediator Z-scheme configuration. This system's fundamental principle is that when stimulated by illumination, electrons from the VB of both PS I and II are excited to the CB, leaving photogenerated holes in the VB. The photogenerated electrons in PS II will subsequently be transferred to the VB of PS I by means of an electron-mediator Ohmic contact (Abdul Nasir et al., 2021; Ng et al., 2020).

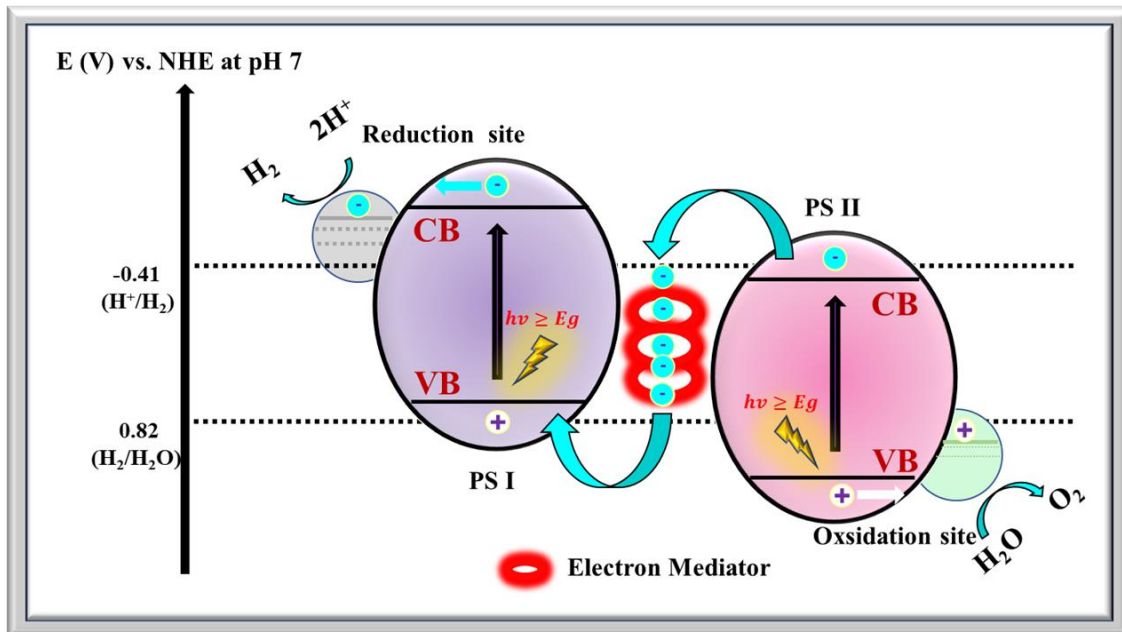


Figure 7. Z-scheme photocatalytic system via electron mediator (Ng et al., 2020).

The following are the advantages of this method above others.

- This system is an electron transfer type, where the electrons and holes to be accommodated in two separate photocatalysts also preserve their strong redox capabilities.
- It requires a lower change in Gibbs free energy to drive each photosystem.
- With a reasonably substantial overpotential sufficient to manage the excellent redox reaction, the Z-scheme system grants an effective charge separation in separated locations (Abdul Nasir et al., 2021; Ng et al., 2020).

Table 1. Performance evaluation of various type II and Z-scheme heterojunction catalysts.

Catalyst	Type of junction	Application area	Current density @ potential	Light/ source	Ref. /Pub years
ZnO@PDA/CeO ₂	Z-scheme het.	WS	0.25 $\mu\text{A}/\text{cm}^2$ @ 0.25 V vs. RHE	30 mW/cm ² / LED	(Celebi et al., 2021)
CeO ₂ /ZnO	Type II het.	WS	0.3 mA/cm ² @0.5V	200mW/cm ²	(Xiao et al., 2019)
WO _{3-x} /TiO ₂	Z-scheme het.	WS	4.25 mA/cm ² @ 0.28 V	300 W Xe.	(Lin et al., 2021)
BiVO ₄ /g-C ₃ N ₄	Z-scheme het.	WS	1.14 mA/cm ² @ 0.39 V vs. RHE	300 W Xe.	(Mane et al., 2022)
WO ₃ /BiVO ₄	Type II het.	WS	1.21 mA/cm ² @ 1.23 V vs. RHE	500 W Xe.	(SU et al., 2021)
InN/PM6	Z-scheme het.	WS	4.82 mA/cm ² @ 1.45 vs. RHE	100 mW cm ² / AM 1.5 G	(Xie et al., 2023)
Ti-Fe ₂ O ₃ /In ₂ O ₃	Z-scheme het.	WS	2 mA/cm ² @ 1.23 vs. RHE	300 W Xe.	(Y. Li et al., 2021)

Conclusion

PEC WS is a promising technology for sustainable hydrogen production, and the following components are required for this system.

- catalyst
- visible light absorber
- sacrificial electron donor

In these systems, WS occurs at the interface of the semiconductor, and the potential required for WS can be generated at the interface between the semiconductor and the liquid. PEC WS systems, the semiconductor is required to be photostable in an aqueous solution, to be cheap, and the band gap should be suitable for WS (Ayodhya, 2023). Here, a brief description of PEC WS is given. Then, information about the single component, type II heterojunction, and the Z-scheme designed by the researchers for use in solar hydrogen production systems is presented to the reader. As a result of the research, it is concluded that the Z-scheme is more efficient in hydrogen production compared to others.

References

- Abdul Nasir, J., Munir, A., Ahmad, N., Haq, T. ul, Khan, Z., & Rehman, Z. (2021). Photocatalytic Z-Scheme Overall Water Splitting: Recent Advances in Theory and Experiments. *Advanced Materials*, 33(52). <https://doi.org/10.1002/adma.202105195>
- Abe, R. (2010). Recent progress on photocatalytic and photoelectrochemical water splitting under visible light irradiation. *Journal of Photochemistry and Photobiology C: Photochemistry Reviews*, 11(4), 179–209. <https://doi.org/10.1016/j.jphotochemrev.2011.02.003>
- Abe, R. (2011). A two-step photoexcitation system for photocatalytic water splitting into hydrogen and oxygen under visible light irradiation. *Solar Hydrogen and Nanotechnology VI*, 8109, 81090B. <https://doi.org/10.1117/12.893146>
- Abe, R., Maeda, K., Abdul Nasir, J., Munir, A., Ahmad, N., Haq, T. ul, Khan, Z., Rehman, Z., Wang, Q., Domen, K., Wang, Y. Y., Suzuki, H., Xie, J., Tomita, O., Martin, D. J., Higashi, M., Kong, D., Abe, R., Tang, J., ... Zhou, Z. (2018). C₂N/WS₂ van der Waals type-II heterostructure as a promising water splitting photocatalyst [Review-article]. *Chemical Reviews*, 1(1), 5201–5241. <https://doi.org/10.1039/c8na00084k>
- Ayodhya, D. (2023). Semiconductors-based Z-scheme materials for photoelectrochemical water splitting: A review. *Electrochimica Acta*, 448(December 2022), 142118. <https://doi.org/10.1016/j.electacta.2023.142118>
- Bian, J., Li, Q., Huang, C., Li, J., Guo, Y., Zaw, M., & Zhang, R. Q. (2015). Thermal vapor condensation of uniform graphitic carbon nitride films with remarkable photocurrent density for photoelectrochemical applications. *Nano Energy*, 15, 353–361. <https://doi.org/10.1016/j.nanoen.2015.04.012>
- Celebi, N., Arlı, F., Soysal, F., & Salimi, K. (2021). Z-scheme ZnO@PDA/CeO₂ heterojunctions using polydopamine as electron transfer layer for enhanced photoelectrochemical H₂ generation. *Materials Today Energy*, 21, 100765. <https://doi.org/10.1016/j.mtener.2021.100765>
- Celebi, N., & Salimi, K. (2022). Yolk-shell ZnO@C-CeO₂ ternary heterostructures with conductive N-doped carbon mediated electron transfer for highly efficient water splitting. *Journal of Colloid and Interface Science*, 605, 23–32. <https://doi.org/10.1016/j.jcis.2021.07.052>
- Clarizia, L., Nadagouda, M. N., & Dionysiou, D. D. (2023). Recent advances and challenges of photoelectrochemical cells for hydrogen production. *Current Opinion in Green and Sustainable Chemistry*, 41, 1–12. <https://doi.org/10.1016/j.cogsc.2023.100825>
- Guo, F., Chen, J., Zhao, J., Chen, Z., Xia, D., Zhan, Z., & Wang, Q. (2020). Z-scheme heterojunction g-C₃N₄@PDA/BiOBr with biomimetic polydopamine as electron transfer mediators for enhanced visible-light driven degradation of sulfamethoxazole. *Chemical Engineering Journal*, 386(January), 124014. <https://doi.org/10.1016/j.cej.2020.124014>

- Kalanoor, B. S., Seo, H., & Kalanur, S. S. (2018). Recent developments in photoelectrochemical water-splitting using WO₃/BiVO₄ heterojunction photoanode: A review. *Materials Science for Energy Technologies*, 1(1), 49–62. <https://doi.org/10.1016/j.mset.2018.03.004>
- Li, J., Yuan, H., Zhang, W., Jin, B., Feng, Q., Huang, J., & Jiao, Z. (2022). Advances in Z-scheme semiconductor photocatalysts for the photoelectrochemical applications: A review. *Carbon Energy*, 4(3), 294–331. <https://doi.org/10.1002/cey2.179>
- Li, Y., Wu, Q., Chen, Y., Zhang, R., Li, C., Zhang, K., Li, M., Lin, Y., Wang, D., Zou, X., & Xie, T. (2021). Interface engineering Z-scheme Ti-Fe₂O₃/In₂O₃ photoanode for highly efficient photoelectrochemical water splitting. *Applied Catalysis B: Environmental*, 290, 120058. <https://doi.org/10.1016/j.apcatb.2021.120058>
- Lin, S., Ren, H., Wu, Z., Sun, L., Zhang, X.-G., Lin, Y.-M., H. L. Zhang, K., Lin, C.-J., Tian, Z.-Q., & Li, J.-F. (2021). Direct Z-scheme WO₃-nanowire-bridged TiO₂ nanorod arrays for highly efficient photoelectrochemical overall water splitting. *Journal of Energy Chemistry*, 59, 721–729. <https://doi.org/10.1016/j.jechem.2020.12.010>
- Liu, C., Zhou, J., Su, J., & Guo, L. (2019). Turning the unwanted surface bismuth enrichment to favourable BiVO₄/BiOCl heterojunction for enhanced photoelectrochemical performance. *Applied Catalysis B: Environmental*, 241(August 2018), 506–513. <https://doi.org/10.1016/j.apcatb.2018.09.060>
- Liu, H., Fan, X., Li, Y., Guo, H., Jiang, W., & Liu, G. (2023). Hematite-based photoanodes for photoelectrochemical water splitting: Performance, understanding, and possibilities. *Journal of Environmental Chemical Engineering*, 11(1), 109224. <https://doi.org/10.1016/j.jece.2022.109224>
- Maeda, K. (2013). Z-scheme water splitting using two different semiconductor photocatalysts. *ACS Catalysis*, 3(7), 1486–1503. <https://doi.org/10.1021/cs4002089>
- Mane, P., Bae, H., Burungale, V., Lee, S. W., Misra, M., Parbat, H., Kadam, A. N., & Ha, J. S. (2022). Interface-engineered Z-scheme of BiVO₄/g-C₃N₄ photoanode for boosted photoelectrochemical water splitting and organic contaminant elimination under solar light. *Chemosphere*, 308(P1), 136166. <https://doi.org/10.1016/j.chemosphere.2022.136166>
- Ng, B. J., Putri, L. K., Kong, X. Y., Teh, Y. W., Pasbakhsh, P., & Chai, S. P. (2020). Z-Scheme Photocatalytic Systems for Solar Water Splitting. *Advanced Science*, 7(7). <https://doi.org/10.1002/advs.201903171>
- Qiu, Y., Pan, Z., Chen, H., Ye, D., Guo, L., Fan, Z., & Yang, S. (2019). Current progress in developing metal oxide nanoarrays-based photoanodes for photoelectrochemical water splitting. *Science Bulletin*, 64(18), 1348–1380. <https://doi.org/10.1016/j.scib.2019.07.017>
- SU, X., LIU, C., LIU, Y., YANG, Y., LIU, X., & CHEN, S. (2021). Construction of BiVO₄ nanosheets@WO₃ arrays heterojunction photoanodes by versatile phase transformation strategy. *Transactions of Nonferrous Metals Society of China*, 31(2), 533–544. [https://doi.org/10.1016/S1003-6326\(21\)65515-2](https://doi.org/10.1016/S1003-6326(21)65515-2)
- Wei, Y., Zhang, Z., Wang, W., Song, Z., Cai, M., & Sun, S. (2023). Photocatalytic Z-scheme Overall Water Splitting: Insight into Different Optimization Strategies for Powder Suspension and Particulate Sheet Systems. *ChemPhysChem*, 24(16). <https://doi.org/10.1002/cphc.202300216>
- Wen, P., Sun, Y., Li, H., Liang, Z., Wu, H., Zhang, J., Zeng, H., Geyer, S. M., & Jiang, L. (2020). A highly active three-dimensional Z-scheme ZnO/Au/g-C₃N₄ photocathode for efficient photoelectrochemical water splitting. *Applied Catalysis B: Environmental*, 263(April 2019). <https://doi.org/10.1016/j.apcatb.2019.118180>
- Xiao, Y., Yu, H., & Dong, X. ting. (2019). Ordered mesoporous CeO₂/ZnO composite with photodegradation concomitant photocatalytic hydrogen production performance. *Journal of Solid State Chemistry*, 278(May), 120893. <https://doi.org/10.1016/j.jssc.2019.120893>
- Xie, S., Liang, J., Liu, Q., Liu, P., Wang, J., Li, J., Wu, H., Wang, W., & Li, G. (2023). Core-shell InN/PM6 Z-scheme heterojunction photoanodes for efficient and stable photoelectrochemical water splitting. *Journal of Materials Chemistry A*, 11(46), 25671–25682. <https://doi.org/10.1039/D3TA04656G>
- Zhang, Q., Zhao, X., Duan, L., Shen, H., & Liu, R. (2020). Controlling oxygen vacancies and enhanced visible light photocatalysis of CeO₂/ZnO nanocomposites. *Journal of Photochemistry and Photobiology A:*

Chemistry, 392(May 2019), 112156. <https://doi.org/10.1016/j.jphotochem.2019.112156>

Zhao, Y., Niu, Z., Zhao, J., Xue, L., Fu, X., & Long, J. (2023). Recent Advancements in Photoelectrochemical Water Splitting for Hydrogen Production. In *Electrochemical Energy Reviews* (Vol. 6, Issue 1). Springer Nature Singapore. <https://doi.org/10.1007/s41918-022-00153-7>

USE OF SOLAR DRYING SYSTEMS IN DIFFERENT INDUSTRIAL SECTORS

Hakan DUMRUL

Dr., Sirnak University, Faculty of Engineering, Department of Energy systems Engineering, Sirnak-Türkiye
ORCID: 0000-0003-1122-3886

Edip TAŞKESEN

Dr., Sirnak University, Faculty of Engineering, Department of Energy systems Engineering, Sirnak-Türkiye
ORCID: 0000-0002-3052-9883

Ali BULUT

Mr., Sirnak University, Postgraduate Education Institute, Department of Energy Science and Technologies, Sirnak-Türkiye
(Responsible Author) ORCID: 0000-0002-9335-710X

ABSTRACT

The moisture content of materials can be a disadvantage in terms of use. To use some materials more efficiently, their moisture content must be reduced. Moisture content can be reduced by drying. In everyday life and a variety of industries, drying is essential. Fossil fuels provide the thermal energy required for drying. Solar energy, a renewable energy, is considered an alternative to fossil fuels and a way to reduce the resulting environmental factors. In this study, the classification of solar dryer systems is shown. The use of solar drying systems in automobile, food and agriculture, rubber, paper, sugar cane, lignite and wastewater treatment industries are investigated, and the results are discussed.

Keywords: Solar dryer, Industrial solar drying, Solar drying systems, Performance.

1. Introduction

Today, the main objective of energy research is to reduce consumption by increasing energy efficiency. In this direction, alternative sources have been sought, and renewable energy has gained importance. Using renewable energy sources in daily life and industrial regions should be promoted since they help lessen the greenhouse gas effect (Lingayat, Balijepalli, et al., 2021). Solar energy is preferred in domestic and industrial areas due to its abundant availability and low cost for maintenance and repair of technologies using this energy. Today, solar energy is used in drying, heating, cooling, water distillation, and freezing systems. Drying is widely used in various sectors. As a result of drying, the material's moisture is reduced. Bacterial diversity of the material with reduced moisture content is prevented, and storage and transportation costs are reduced by providing dimensional gain. It is the thermal heat from fossil fuels that is needed for drying. In developed countries, the amount of thermal energy used for drying makes up between 12% and 40% of all industrial energy usage (Bennamoun & Belhamri, 2003), which in turn accounts for 20% to 70% of production costs depending on the type of industries (Pirasteh et al., 2014). To reduce the emission rate of fossil fuels and to take measures against increasing energy costs, the use of solar drying systems in the drying process should be expanded. In this way, a clean, economical, and sustainable use of resources can emerge. Depending on a country's environmental, economic and geographical conditions, solar thermal energy for various industries can provide hot water, hot air or steam at high temperatures. (Tasmin et al., 2022). The solar dryer collectors help increase the thermal heat needed for drying. Table 1 shows the temperature range of some collectors (Kalogirou, 2013).

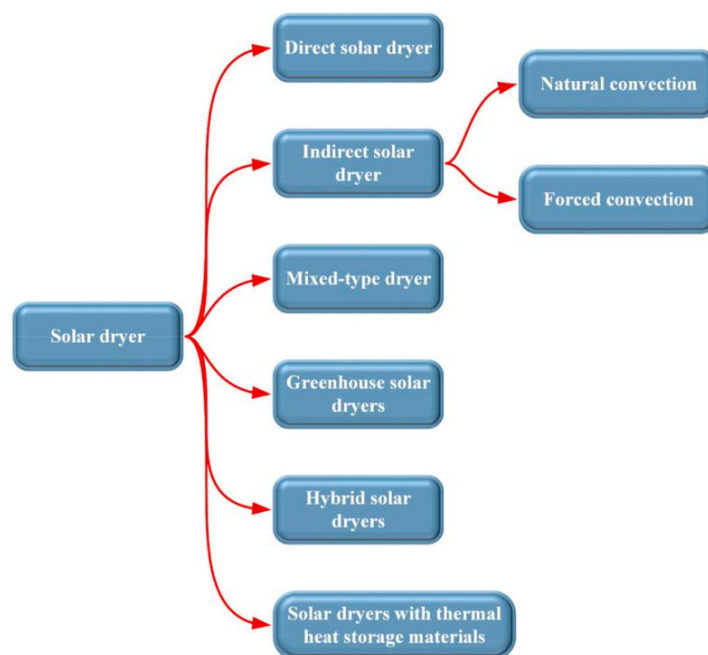
Table 1. Operating temperature range of some solar collectors (Kalogirou, 2013)

Collector Type	Temperature Range (°C)
Flat-plate collector (FPC)	30–80
Evacuated tube collector (ETC)	50–200
Stationary compound parabolic collector (CPC)	60–240
Cylindrical trough collector (CTC)	60–300

The traditionally used open sun drying system has several disadvantages. For this reason, many studies have been carried out to make more efficient use of solar energy in the drying process. As a result of these studies, more efficient solar drying systems have been examined, and their usage areas have been expanded. This study reviews the use of solar drying systems, which are widely used in the agricultural sector and other industrial sectors. Systems for solar drying are categorized, and the importance of solar energy for the drying process is emphasized.

2. Classification of Solar Drying Systems

Solar dryers help us to control the temperature, humidity, speed, etc., which are essential parameters for drying. Direct and indirect solar dryers are the two categories separating these controlled solar dryers. These can be natural or forced convection species (Lingayat, VP et al., 2021). The overall efficiency of natural convection dryers ranges between 20% and 40% (Udomkun et al., 2020). It is advised to use forced convection dryers since they provide more controlled drying conditions and improved efficiency (Mustayen et al., 2014). Figure 2 shows examples of solar dryers in various designs. Various dryers have been discussed in the studies. Dryers can generally be classified according to their design, the supporting heat source used etc. (Lingayat, Balijepalli, et al., 2021). In Figure 1, solar drying systems are generally classified.

**Figure 1.** Different types of solar dryers (EL-Mesery et al., 2022)

2.1. Direct Solar Dryers

Open sun drying is a primitive system widely used around the world. In this method, the product to be dried is placed on the ground and subject to solar radiation (Mühlbauer, 1986). Since the drying process is unprotected, the product is exposed to environmental factors, and the drying efficiency is low. This method uses transparent glass to store materials in a space exposed to solar radiation. According to their design and construction, they can be classified as cabin and greenhouse species. Cabinet species solar dryers are used for low volume drying. Greenhouse solar dryers are used for extensive volume bulk drying (El Hage et al., 2018). These dryers can provide temperatures between 30 °C and 60 °C (Mezrhab et al., 2010). A schematic representation of the direct solar dryer is given in Figure 2.

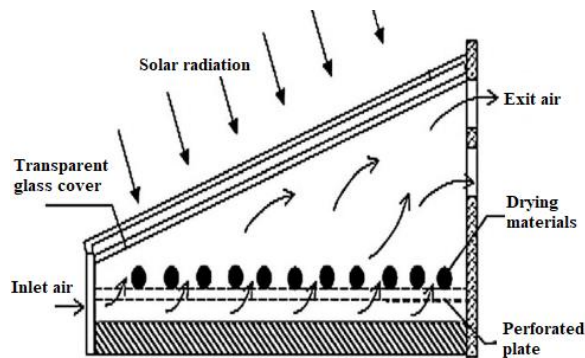


Figure 2. Visualization of the direct sun dryer (Prakash & Kumar, 2013)

2.2. Indirect Solar Dryers

This system uses heated air to remove moisture and protect the product from sunlight. (Abhay et al., 2018). Compared to direct solar dryers, the moisture removal and heat transfer rate can be more precisely regulated. Indirect solar dryers can operate in forced and natural convection mode (EL-Mesery et al., 2022). The schematic representation of the indirect solar dryer system is given in Figure 3.

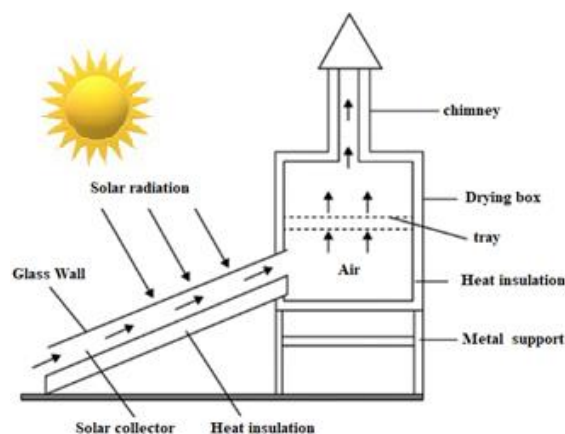


Figure 3. Schematic of indirect solar dryer system (Geete et al., 2021)

2.3. Mixed Type Solar Dryers

The theory behind mixed mode drying systems is integrating direct and indirect solar drying systems. The system generates hot air using a solar air heater and a transparent drying chamber. (Dhalsamant et al., 2018).

2.4. Hybrid Solar Dryers

Hybrid solar drying systems, integrating the product drying process without the reliance on natural sunlight, serve as auxiliary heating systems. This system integrates LPG heaters, mechanical heat pumps, electric heaters, and biomass heaters into the solar system (Mishra et al., 2021). An illustration of a hybrid solar dryer can be seen in Figure 4.

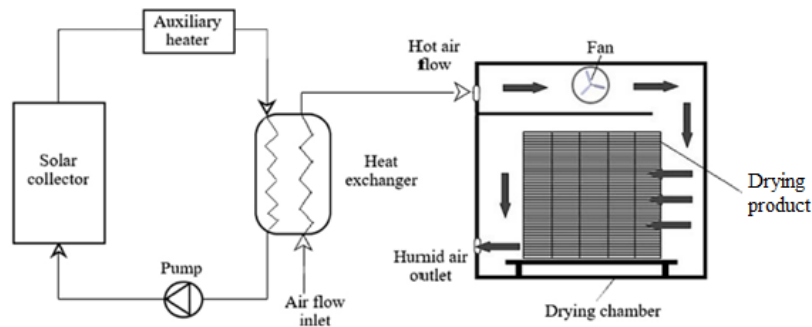


Figure 4. Hybrid solar dryer (Kamarulzaman et al., 2021)

3. Solar Drying Systems in Different Industries

The rapid depletion of fossil fuels, the rising costs and the damage to the environment caused by the increase in consumption have led industrial sectors to turn to renewable sources of energy in recent years. Solar energy is used directly or as an aid in industry in most countries where there is sufficient solar radiation for solar drying. Solar drying systems for industrial applications are an important area of research. Solar drying systems used in various industries are discussed and illustrated below (Luthra et al., 2015).

3.1. Agriculture and Food Industry

The water in food materials causes harmful micro-organisms to multiply over time. These micro-organisms and bacteria cause the food material to rot. One of the ways to prevent decay is drying. The drying process can reduce the amount of moisture in the material. Drying also saves transportation costs by reducing the volume and mass of the food material (Chandramohan, 2016). The use of fossil fuels is reduced by using solar energy for drying. There have been many studies on using solar dryers for drying in agriculture and the food industry. A natural convection solar dryer was integrated with sodium chloride and sodium sulphate decahydrate materials to dry red peppers by Ndukwu et al., (2017). They found that integrating sodium sulphate decahydrate, a thermal energy storage material, with the solar dryer prevented the emission of 602 tonnes of carbon dioxide into the atmosphere per year compared to a diesel engine dryer.

3.2. Maritime Industry

In the marine industry, solar energy is crucial for drying seafood. Murali et al., (2020) developed a solar dryer with a thermal energy storage system for drying shrimps. LPG was used as an auxiliary heat source in the dryer. By drying 50 kg of shrimp for 6 hours, the moisture content was reduced from 76.71% to 15.38%. During this process, the sun provided 73.93% of the heat. Since seafood is a sensitive food, its moisture content should be between 15% and 20% to be consumed (Rahman, 2006). To control this balance, it is recommended that solar dryers should be designed as hybrids (Rizal & Muhammad, 2018).

3.3. Tea Industry

Tea is a widely consumed beverage. China and India account for about 2/3 of tea production (Chang, 2015). Drying is the cornerstone of the tea industry. India uses 85% of thermal and 15% of electrical energy for tea

production processes (A. Sharma et al., 2019). Ozturk & Dincer, (2020) conducted an exergo-economic analysis of a solar dryer integrated with a photovoltaic unit for drying tea leaves. In the study, the moisture content of 100 kg of fresh tea was reduced from 80% to 3% in four days. Amer et al., (2018) dried chamomile leaves with an electric heater-assisted solar drying system. As a result of the process, the moisture content was reduced to 6%, and it was reported that 27-30 hours of drying time was saved compared to the open solar drying process.

3.4. Automobile Industry

Paint drying is an essential process for the automotive industry. This process is mainly carried out using hot air in the temperature range of 80 °C - 150 °C (Lingayat, Balijepalli, et al., 2021). Instead of obtaining this heat energy from fossil fuels, turning to solar energy will be beneficial in terms of economic and environmental factors. Solar air collectors can achieve the 80°C - 150°C temperature required for the sector (Orsato & Wells, 2007).

3.5. Rubber Industry

The drying process is crucial for preserving the quality of the rubber sheet that is ultimately produced from the raw material. The final product is obtained after 10-20 days of drying by drying rubber sheets naturally and in the open sun. The drying of raw rubber sheets by inappropriate systems results in 80% of products being of poor quality (Brey Mayer et al., 1993). The rubber is dried with hot air from 45 °C to 60 °C (Tanwanichkul et al., 2013). This temperature can be easily achieved with solar dryer systems. Brey Mayer et al., (1993) dried 320 kg of rubber sheets in the temperature range of 45 °C - 60 °C with the solar air collector-assisted drying system they developed. The moisture content decreased from 60% to 0.5% during this process, which lasted for five days. In 8.8 hours at 100 °C, Pratoto et al., (1998) successfully lowered the moisture content of rubber sheets from 60% to 0.5% using an indirect solar dryer powered by an electric air heater system.

3.6. Sugar Cane Industry

In the sugarcane industry, the crushed fibers, the waste material after processing, are called bagasse. Bagasse can be used for electricity generation, biomethane production, fuel and feed (Rabelo et al., 2011). The moisture content should be reduced to increase the combustion efficiency of the bagasse used as fuel. Drying in the open sun contains factors that will reduce the combustion efficiency of the product (Lingayat, Balijepalli, et al., 2021). According to certain studies, wet bagasse can be effectively dried using a solar drying system (Phadkari et al., 2017; Subahana & Natarajan, 2019). Forced convection solar dryers reduced the moisture content of 1 kg bagasse from 48% to 16.77% (Phadkari et al., 2017). Another study proposed a solar dryer system to obtain SiO₂ from sugarcane ash. The SiO₂ obtained because of the process can be used as an alternative to cement (Embong et al., 2016).

3.7. Paper Industry

There are different production processes in the paper industry. One of these processes is drying in the temperature range of 60 °C - 150 °C (Gemechu et al., 2012). In a study, 80% drying efficiency was achieved with a solar dryer system supported by a water heater and air-water exchanger (Hjort & Thomas, 2014). Using solar energy as process heat in the paper industry reduces carbon dioxide emissions (A. K. Sharma et al., 2016).

3.8. Sewage Industrial Waste Industry

Sludge and sewage sludge, which are mixtures of industrial and municipal wastes, can be dried for volumetric gain to lower the cost of storage and evacuation. Wastewater treatment results in sludge that is 95% water (Lingayat, Balijepalli, et al., 2021). Mechanical systems for water reduction are not suitable for pathogen

reduction. Therefore, it is recommended to use solar energy for thermal heat, which plays a vital role in pathogen reduction (Lingayat, Balijepalli, et al., 2021). The water sludge was dried in direct and indirect solar dryers. As a result of the study, it was determined that the indirect solar drying system was more efficient (Ameri et al., 2020). Salihoglu et al., (2007) conducted a study to reduce the moisture content of sludge subjected to mechanical dewatering. In this study, they reduced the weight of the sludge by 60% by using a greenhouse solar dryer. The same study determined that the pathogen rate decreased by adding 15% lime to the sludge before drying.

3.9. Lignite Coal Industry

When producing electricity in thermal power plants, lignite coal is crucial. Lignite, with an average moisture content of 30% to 70%, faces challenges during combustion. Liu et al., (2017) analysed the drying of lignite coal by solar drying systems. The analysis concluded that the boiler efficiency of dried lignite increased and provided a 34% electricity gain. Reducing the moisture content before combustion improves combustion performance (Nikolopoulos et al., 2015). Compared to other drying products, lignite has large dimensional amounts. Turning to solar energy for drying these amounts of lignite will provide significant gains.

3.10. Clay Brick and Ceramic Industry

Materials such as bricks, ceramics and pottery from clay go through shaping, drying and firing processes after the clay is mixed with water and thickened (Lingayat et al., 2022). The wet bricks are subjected to pre-drying before being put into the kiln. The moisture content is reduced for quality bricks from 20%-25% to 8%-12% in the pre-drying process (Maheshwari & Jain, 2017). The moisture removal process accounts for 15% of the total energy in the production process (Maithel, 2013). In the ceramic industry, the moisture content must be reduced from 65% to 5% during drying. This process uses traditional resources that are harmful to the environment (Ciaccio et al., 2017). Renewable energy sources can meet this energy consumption. Solar energy has been proposed to meet this demand (El Hage et al., 2018)(Maheshwari & Jain, 2017) and several studies have been conducted to develop solar drying systems. Bououd et al., (2018) and Murugesan et al., (2001) have designed a solar dryer system to make the drying of clay bricks more efficient. Ceramic drying was carried out in the solar-biomass integrated solar dryer developed for ceramic production. In the research, the moisture content was reduced from 25% to 5% and a 12% saving in drying time compared to drying in the open sun was reported (Del Mundo, 2000). The schematic diagram of the developed hybrid solar dryer is shown in Figure 5.

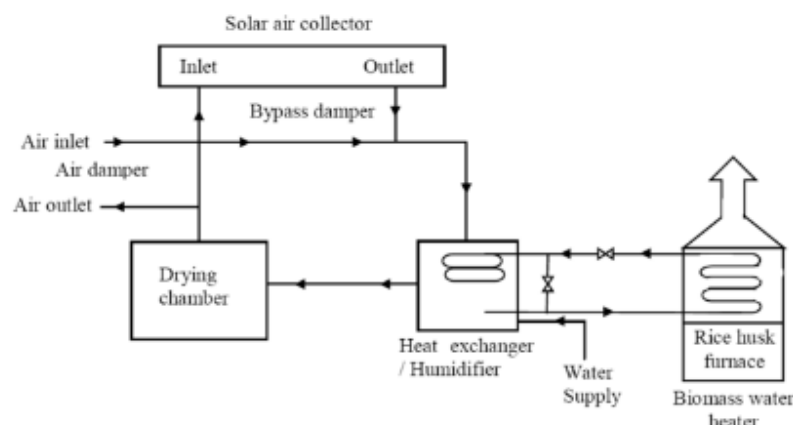


Figure 5. Schematic representation of the solar dryer developed for ceramic drying (Del Mundo, 2000).

3.11. Biomass Industry

The biological component known as biomass is derived from living things or organic matter, including waste from city farms and forestry residues. An alternate energy source for producing heat and electricity is biomass. It can aid in lowering CO₂ emissions and is typically inexpensive (Holmberg & Ahtila, 2005; Yahya et al., 2017). Animals such as chickens and cattle can be fed dried biomass waste. Joardder et al., (2014) suggested a solar-assisted biomass pyrolysis system that could reduce CO₂ emissions and fuel costs by approximately 32% and 33%, respectively, at an outlet temperature of up to 162°C. Figure 6 shows the hybrid solar dryer for paddy drying. In the system integrated with the biomass oven, the moisture content was reduced from 20% to 14% at an average temperature of 70 °C. The drying time of the paddy was shortened in the designed dryer system (Yahya et al., 2017).

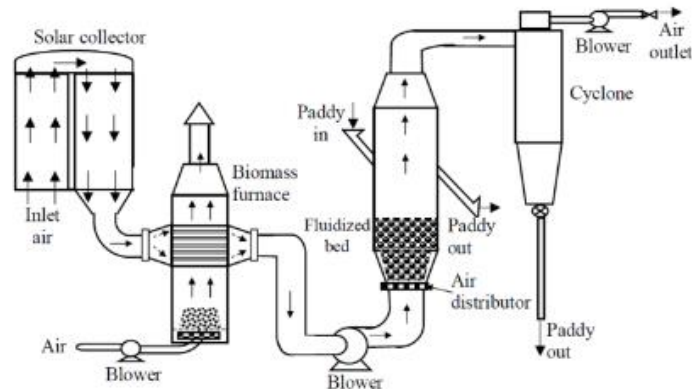


Figure 6. Diagram for a hybrid fluidized bed dryer that combines solar and biomass for drying paddy (Yahya et al., 2017).

4. Conclusions

Solar drying systems are a technology open to development in many industrial fields, especially agriculture. In this study, we analysed the various contributions of solar drying systems in the industrial sector in-depth and drew the following conclusions.

- Hybrid solar dryer systems are more effective in reducing drying time than other solar dryer systems.
- It has been found that forced convection solar dryer systems exhibit higher efficiency than natural convection solar dryers.
- Solar dryers are an effective tool for reducing the CO₂ emissions associated with mechanical dryers powered by fossil fuels and saving electricity.
- It is essential for countries to use solar thermal energy to reduce fossil fuel consumption in the future and develop sustainable industrial systems.
-

5. References

- Abhay, L., Chandramohan, V. P., & Raju, V. R. K. (2018). Numerical analysis on solar air collector provided with artificial square shaped roughness for indirect type solar dryer. *Journal of Cleaner Production*, 190, 353–367.
- Amer, B. M. A., Gottschalk, K., & Hossain, M. A. (2018). Integrated hybrid solar drying system and its drying kinetics of chamomile. *Renewable Energy*, 121, 539–547.
- Ameri, B., Hanini, S., & Boumahdi, M. (2020). Influence of drying methods on the thermodynamic parameters, effective moisture diffusion and drying rate of wastewater sewage sludge. *Renewable Energy*, 147, 1107–1119.

- Bennamoun, L., & Belhamri, A. (2003). Design and simulation of a solar dryer for agriculture products. *Journal of Food Engineering*, 59(2–3), 259–266. [https://doi.org/10.1016/S0260-8774\(02\)00466-1](https://doi.org/10.1016/S0260-8774(02)00466-1)
- Bououd, M., Hachchadi, O., Janusevicius, K., Mechaqrane, A., & Martinaitis, V. (2018). Energy performance of a clay tiles solar drying system. *AIP Conference Proceedings*, 2056(1).
- Breymayer, M., Pass, T., Mühlbauer, W., Amir, E. J., & Mulato, S. (1993). Solar-assisted smokehouse for the drying of natural rubber on small-scale Indonesian farms. *Renewable Energy*, 3(8), 831–839.
- Chandramohan, V. P. (2016). Numerical prediction and analysis of surface transfer coefficients on moist object during heat and mass transfer application. *Heat Transfer Engineering*, 37(1), 53–63.
- Chang, K. (2015). World tea production and trade: Current and future development. *Food and Agriculture Organization of the United Nations, Rome*, 3–4.
- Ciacco, E. F. S., Rocha, J. R., & Coutinho, A. R. (2017). The energy consumption in the ceramic tile industry in Brazil. *Applied Thermal Engineering*, 113, 1283–1289.
- Del Mundo, R. R. (2000). A hybrid solar-biomass drying system for ceramic wares. *World Renewable Energy Congress VI*, 1091–1093.
- Dhalsamant, K., Tripathy, P. P., & Shrivastava, S. L. (2018). Heat transfer analysis during mixed-mode solar drying of potato cylinders incorporating shrinkage: Numerical simulation and experimental validation. *Food and Bioprocesses Processing*, 109, 107–121.
- EL-Mesery, H. S., EL-Seesy, A. I., Hu, Z., & Li, Y. (2022). Recent developments in solar drying technology of food and agricultural products: A review. *Renewable and Sustainable Energy Reviews*, 157(December 2021), 112070. <https://doi.org/10.1016/j.rser.2021.112070>
- El Hage, H., Herez, A., Ramadan, M., Bazzi, H., & Khaled, M. (2018). An investigation on solar drying: A review with economic and environmental assessment. *Energy*, 157, 815–829.
- Embong, R., Shafiq, N., Kusbiantoro, A., & Nuruddin, M. F. (2016). Effectiveness of low-concentration acid and solar drying as pre-treatment features for producing pozzolanic sugarcane bagasse ash. *Journal of Cleaner Production*, 112, 953–962.
- Geete, A., Singh, Y., & Rathore, S. (2021). Energy and exergy analyses of fabricated solar drying system with smooth and rough surfaces at different conditions: A case study. *Heat Transfer*, 50. <https://doi.org/10.1002/htj.22171>
- Gemechu, E. D., Butnar, I., Llop, M., & Castells, F. (2012). Environmental tax on products and services based on their carbon footprint: a case study of the pulp and paper sector. *Energy Policy*, 50, 336–344.
- Hjort, M., & Thomas, D. E. (2014). Performance of a solar paper drier for small-scale paper sheet production. *Journal of Mechanical Engineering*, 44(1), 6–9.
- Holmberg, H., & Ahtila, P. (2005). Evaluation of energy efficiency in biofuel drying by means of energy and exergy analyses. *Applied Thermal Engineering*, 25(17–18), 3115–3128.
- Joardder, M. U. H., Halder, P. K., Rahim, A., & Paul, N. (2014). Solar assisted fast pyrolysis: a novel approach of renewable energy production. *Journal of Engineering*, 2014.
- Kalogirou, S. A. (2013). *Solar energy engineering: processes and systems*. Academic press.
- Kamarulzaman, A., Hasanuzzaman, M., & Rahim, N. A. (2021). Global advancement of solar drying technologies and its future prospects: A review. *Solar Energy*, 221, 559–582.
- Lingayat, A., Balijepalli, R., & Chandramohan, V. P. (2021). Applications of solar energy based drying technologies in various industries—A review. *Solar Energy*, 229, 52–68.
- Lingayat, A., VP, C., & VRK, R. (2021). Drying kinetics of tomato (*Solanum lycopersicum*) and Brinjal (*Solanum melongena*) using an indirect type solar dryer and performance parameters of dryer. *Heat and Mass Transfer*, 57, 853–872.
- Lingayat, A., Zachariah, R., & Modi, A. (2022). Current status and prospect of integrating solar air heating

- systems for drying in various sectors and industries. *Sustainable Energy Technologies and Assessments*, 52, 102274.
- Liu, M., Wang, C., Han, X., Li, G., Chong, D., & Yan, J. (2017). Lignite drying with solar energy: Thermodynamic analysis and case study. *Drying Technology*, 35(9), 1117–1129.
- Luthra, S., Kumar, S., Garg, D., & Haleem, A. (2015). Barriers to renewable/sustainable energy technologies adoption: Indian perspective. *Renewable and Sustainable Energy Reviews*, 41, 762–776.
- Maheshwari, H., & Jain, K. (2017). Carbon footprint of bricks production in fixed chimney Bull's trench kilns in India. *Indian J. Sci. Technol*, 10(16), 1–11.
- Maithel, S. (2013). Evaluating energy conservation potential of brick production in India. *SAARC Energy Centre, Islamabad, Pakistan*.
- Mezrhab, A., Elfarh, L., Naji, H., & Lemonnier, D. (2010). Computation of surface radiation and natural convection in a heated horticultural greenhouse. *Applied Energy*, 87(3), 894–900.
- Mishra, S., Verma, S., Chowdhury, S., & Dwivedi, G. (2021). Analysis of recent developments in greenhouse dryer on various parameters-a review. *Materials Today: Proceedings*, 38, 371–377.
- Mühlbauer, W. (1986). Present status of solar crop drying. *Energy in Agriculture*, 5(2), 121–137.
- Murali, S., Amulya, P. R., Alfiya, P. V., Delfiya, D. S. A., & Samuel, M. P. (2020). Design and performance evaluation of solar-LPG hybrid dryer for drying of shrimps. *Renewable Energy*, 147, 2417–2428.
- Murugesan, K., Suresh, H. N., Seetharamu, K. N., Narayana, P. A. A., & Sundararajan, T. (2001). A theoretical model of brick drying as a conjugate problem. *International Journal of Heat and Mass Transfer*, 44(21), 4075–4086.
- Mustayen, A., Mekhilef, S., & Saidur, R. (2014). Performance study of different solar dryers: A review. *Renewable and Sustainable Energy Reviews*, 34, 463–470.
- Ndukwu, M. C., Bennamoun, L., Abam, F. I., Eke, A. B., & Ukoha, D. (2017). Energy and exergy analysis of a solar dryer integrated with sodium sulfate decahydrate and sodium chloride as thermal storage medium. *Renewable Energy*, 113, 1182–1192.
- Nikolopoulos, N., Violidakis, I., Karampinis, E., Agraniotis, M., Bergins, C., Grammelis, P., & Kakaras, E. (2015). Report on comparison among current industrial scale lignite drying technologies (A critical review of current technologies). *Fuel*, 155, 86–114.
- Orsato, R. J., & Wells, P. (2007). The automobile industry & sustainability. In *Journal of cleaner production* (Vol. 15, Issues 11–12, pp. 989–993). Elsevier.
- Ozturk, M., & Dincer, I. (2020). Exergoeconomic analysis of a solar assisted tea drying system. *Drying Technology*, 38(5–6), 655–662.
- Phadkari, S., Patil, S., & Deokar, S. U. (2017). Design and Modeling of Solar Bagasse Dryer. *International Conference on Ideas, Impact and Innovation in Mechanical Engineering (ICIIME 2017)*, 662–668.
- Pirasteh, G., Saidur, R., Rahman, S. M. A., & Rahim, N. A. (2014). A review on development of solar drying applications. *Renewable and Sustainable Energy Reviews*, 31, 133–148.
- Prakash, O., & Kumar, A. (2013). Historical review and recent trends in solar drying systems. *International Journal of Green Energy*, 10(7), 690–738.
- Pratoto, A., Daguinet, M., & Zeghami, B. (1998). A simplified technique for sizing solar-assisted fixed-bed batch dryers: application to granulated natural rubber. *Energy Conversion and Management*, 39(9), 963–971.
- Rabelo, S. C., Fonseca, N. A. A., Andrade, R. R., Maciel Filho, R., & Costa, A. C. (2011). Ethanol production from enzymatic hydrolysis of sugarcane bagasse pretreated with lime and alkaline hydrogen peroxide. *Biomass and Bioenergy*, 35(7), 2600–2607.
- Rahman, M. S. (2006). Drying of fish and seafood. *Handbook of Industrial Drying*, 547–559.
- Rizal, T. A., & Muhammad, Z. (2018). Fabrication and testing of hybrid solar-biomass dryer for drying fish.

Case Studies in Thermal Engineering, 12, 489–496.

Salihoglu, N. K., Pinarli, V., & Salihoglu, G. (2007). Solar drying in sludge management in Turkey. *Renewable Energy*, 32(10), 1661–1675.

Sharma, A., Dutta, A. K., Bora, M. K., & Dutta, P. P. (2019). Study of energy management in a tea processing industry in Assam, India. *AIP Conference Proceedings*, 2091(1).

Sharma, A. K., Sharma, C., Mullick, S. C., & Kandpal, T. C. (2016). Carbon mitigation potential of solar industrial process heating: paper industry in India. *Journal of Cleaner Production*, 112, 1683–1691.

Subahana, K. R., & Natarajan, R. (2019). Theoretical modelling and experimental investigation of the convective drying kinetics of biomass in an improved solar tunnel dryer. *Biofuels*, 10(3), 279–286.

Tanwanichkul, B., Thepa, S., & Rordprapat, W. (2013). Thermal modeling of the forced convection Sandwich Greenhouse drying system for rubber sheets. *Energy Conversion and Management*, 74, 511–523.

Tasmin, N., Farjana, S. H., Hossain, M. R., Golder, S., & Mahmud, M. A. P. (2022). Integration of solar process heat in industries: a review. *Clean Technologies*, 4(1), 97–131.

Udomkun, P., Romuli, S., Schock, S., Mahayothee, B., Sartas, M., Wossen, T., Njukwe, E., Vanlauwe, B., & Müller, J. (2020). Review of solar dryers for agricultural products in Asia and Africa: An innovation landscape approach. *Journal of Environmental Management*, 268, 110730.

Yahya, M., Fudholi, A., & Sopian, K. (2017). Energy and exergy analyses of solar-assisted fluidized bed drying integrated with biomass furnace. *Renewable Energy*, 105, 22–29.

THERMAL INSULATION AND MATERIALS IN BUILDINGS

Ojlan OĞUZ

*St, Sirnak University, Faculty of Engineering, Department of Civil Engineering, Sirnak-Türkiye
(Responsible Author) ORCID: 0009-0006-3703-7490*

Edip TAŞKESEN

*Dr., Sirnak University, Faculty of Engineering, Department of Energy systems Engineering, Sirnak-Türkiye
ORCID: 0000-0002-3052-9883*

Hamza ALAHMAD

*Mr., Sirnak University, Postgraduate Education Institute, Department of Energy Science and Technologies, Sirnak-Türkiye
(Responsible Author) ORCID: 0000-0002-6261-3449*

ABSTRACT

To meet our growing energy demand, it will be more typical to protect nature by saving energy rather than polluting our world more, and this approach reduces energy costs. This study focuses on the world scope of heat dissipation with the provision of energy saving with eco-friendly and convenient method and its developments in Turkey, details of its layers in the structure, financial materials, the study of programming methods, the study of the relevant laws, regulations and standards. As a result of the examination, it was seen that the thermal insulation used in the structures has a significant effect on energy saving.

Keywords: Energy Saving, Thermal Insulation, Energy costs, Civil

Introduction

Today, when energy resources are increasingly consumed, energy expenditures cause the deterioration of both economic and ecological order. However, the amount of energy needed in the places where we try to provide comfort and living conditions increases greatly with the development of technology. Considering the costs paid to obtain the need for energy and energy, it becomes necessary to get the most efficiency with the least energy. The best choice that can be made in this direction is energy saving.

Considering that most of the energy consumed in buildings is used for heating and cooling purposes, it is more clearly understood that thermal insulation plays a big role in energy saving. In particular, compared to developed countries, thermal insulation is becoming more important in our country (Bektaş et al., 2017).

TS 1998 Standard for Thermal Insulation in Buildings, which came into force in 2000 , and which required thermal insulation in buildings since 825, was an important indicator of the importance of thermal insulation started in our country (Bayraktar & Bayraktar, 2016; Candan, 2007).

Building envelope material minimizes thermal energy transfer (Qin et al., 2021). Although primarily for thermal purposes, insulation encompasses acoustic, fire, and impact resistance (e.g., damping industrial vibrations). Insulation selection often considers multitasking capabilities (Building Insulation, n.d.).

Investing in insulation is vital economically and environmentally (Qin et al., 2021). It curtails energy consumption, enhancing thermal stability for occupants. Reinforcing insulation is crucial for climate change mitigation (Bicycle Infrastructure, 2020; Wilson, 2010), especially in oil, gas, or coal-heated structures. Governments and utilities incentivize insulation through regulations, aiming to optimize efficiency, diminish grid energy usage, and cut environmental and infrastructure costs in new and revamped buildings.



Figure 1. Example of thermal insulation for buildings: Thermal wall (Building Insulation, n.d.)

In this study, an overview of thermal insulation was provided, and an analysis of the materials and characteristics employed in construction for thermal insulation was conducted.

Heat Insulation

The processes applied to restrict the passage of heat between two environments of different temperatures are called "Heat Insulation. Exterior facade of buildings, window windows, joinery, roofs, in order to reduce the energy we spend to warm up in winter and cool down in summer and to live a more comfortable life, measures are taken to reduce the laying and the heat passage in transmission installations. People need environments with a temperature of 20-22°C to live a comfortable life. In many regions of Turkey, winters are quite cold and summers are hot. In cold climates, insulation materials are considered thicker, while in hot areas thicknesses may be less. Thermal insulation is important not only against cold, but also for protection from heat. It should not be forgotten that the cost of cooling in summer is much higher than the cost of heating in winter (Yaman et al., 2015).

Heat, which is an energy form of nature, is always transferred from hot environment to cold environment according to natural laws. This transfer can not be stopped, but it can be controlled by thermal insulation. The heat inside the building causes heat loss by moving towards the external environment, while in summer the heat in the external environment can heat the environment by moving into the building. While the impact of architectural design is great, the biggest heat losses in most buildings usually occur on exterior walls (Figure 2) (Yaman et al., 2015).

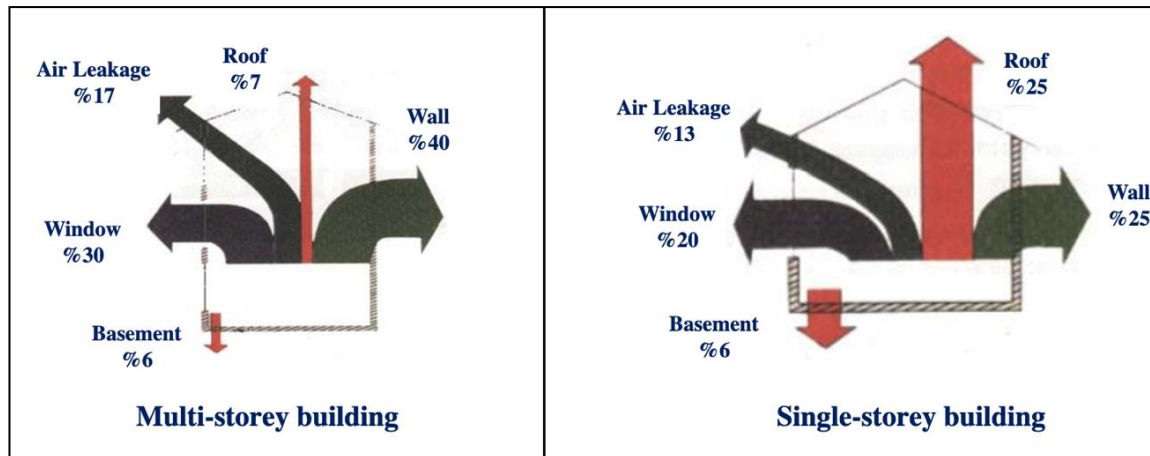


Figure 2. Heat losses in multi- and single-storey buildings (Dağsöz et al., n.d.).

Exterior wall insulation

It is the insulation applied to the elements such as wall, pole, beam, cantilever flooring that cause heat loss in the outer shell of the structure. The construction exterior insulation can be realized from the outside (coating), between the walls and from the inside. Individuals have become more sensitive to thermal insulation due to increased energy costs and environmental sensitivity, and they learn about the thermal insulation status of new or old buildings and use their preferences in this direction (Benallel et al., 2022; Guo, 2012; Yaman et al., 2015).

Roof temperature insulation

%Roofs with 7% to 25% heat loss are observed; It is dissolved in two different ways as a heated (roof living area) between the roof and an unheated roof.

- Roof-to-Roof Heated Roofs,
- Roof Non-heated Roofs,
- Terrace Roofs (Tariku et al., 2023).

Window heat insulation

Depending on the architectural design, they are the building elements where significant heat losses are experienced according to the external facade joinery dimensions. In particular, heat losses in glass fronts of buildings such as business centers, shopping malls and exhibition halls reach the highest rates. In addition to the use of double glazing or even triple glazing, the joinery (aluminum, pvc, wood, etc.) must also be heat-insulated. Insulating glass is formed by combining two or more glass plates between them to contain dry air or argon gas. Heat glasses can reduce heat transitions even more by coating their surfaces if desired (Yaman et al., 2015).

Thermal insulation materials

In order for thermal insulation materials to be compliant with ISO and CEN standards, the Thermal Conductivity Coefficient (0,065 W/mK) must be lower than 0.065 W/mK. The lower the coefficient of thermal conductivity of the insulating material, the higher the resistance to heat passage. The thermal conductivity calculation values specified in the TS825 standard (h); 23°C temperature and 80% relative humidity environment. The water vapor diffusion resistance factor (ab) is an important feature in thermal insulation materials. The water vapor formed in the internal environment tries to reach the external

environment by passing through the pores of the building element. In this process, it is undesirable for water vapor to condense inside the structure, since this can damage the concrete and reinforcement. Therefore, caution should be exercised in the selection and calculation of thermal insulation materials (Tariku et al., 2023; Yaman et al., 2015).

Various thermal insulation materials used in Turkey:

- Extruded Polystyrene Foam (XPS) is a foam material produced for the purpose of thermal insulation, with homogeneous cell structure. XPS, which can be produced at different densities, has a heat conductivity calculation value and the fire response class is D or E,
- Ekspande Polystyrene Foam (EPS) is a material produced in the form of blocks or sheets as a result of pre-inflation of polystyrene raw material,
- EPS has a heat conductivity calculation value of a given range in density, and the fire response class is D or E,
- Glass Wool is a material created by melting and fiberizing silica sand under high pressure. The heat conductivity calculation value of glass wool, which can be produced at different intensities, is within a certain range and is a non-combustible material in class A1 or A2,
- Rock Wool is a material created by melting and fiber of basalt and diabase stones at a certain temperature. The heat conductivity calculation value of rock wool, which can be produced at different densities, is within a certain range and is a fireproof material in class A1 or A2,
- Polyurethane Rigid Foam (PUR) is a material that expands as a result of the mixture of polyol system and isocyanate in certain proportions. The thermal conductivity calculation value of PUR used at a certain density is within a certain range and the fire response class is D, E or F.
- Phenol Foam (PF) is a material obtained by adding inorganic inflators and hardeners to phenol-formaldehyde bakelite. The thermal conductivity calculation value of PF, which can be produced at different densities, is within a certain range, and the fire response class varies depending on the specific coatings (Tariku et al., 2023; Yaman et al., 2015).

Other thermal insulation materials can also be examined similarly, and according to the application, the properties to be sought are: Heat Transmission Coefficient, Density, Fire Class, Temperature Resistance, Mechanical Strength, Vapor Diffusion Resistance, etc, Water Absorption and Dimensional Stability.

Advantages of Heat Insulation

There is an extremely close relationship between the development of a country and the economy of the country. One of the applications that directly affect the country's economy is thermal insulation application. We can consider the advantages of thermal insulation at the individual and country level. For countries, increasing economic development and a healthy environment with energy savings can be shown as an example of a budget and better comfort conditions that grow with fuel savings for individuals (Yaman et al., 2015). The main advantages of thermal insulation are:

- Serious waste occurs in buildings without insulation. This situation directly harms the country's economy. Although the geographical features and the region we live in have easy access to energy resources, it is a great necessity to prevent waste in energy consumption,
- Thermal insulation applications in buildings, the amount of energy used can be reduced, therefore energy-saving buildings can be produced,
- With correct thermal insulation applications, the amount of energy consumed decreases every year.
- Thermal insulation prevents the formation of thermal bridges that occur in buildings,
- In houses where thermal insulation is applied, heat spreads evenly. In this way, undesirable situations such as condensation and drafts do not occur, and a comfortable life is ensured,

- Thermal insulation provides a healthy living comfort by preventing formations such as moisture and mold that affect the comfort of life in buildings (Yaman et al., 2015).

Conclusion and Recommendations

Sustainable living necessitates insulation. Additionally, the increasing energy expenses in economies heavily reliant on external energy sources, such as Turkey, make insulation imperative for both the national economy and household budgets. The fact that insulation-related expenditures can be recovered within 3-5 years, that insulation increases building costs by a maximum of 5%, and the enforcement of relevant regulations, all indicate that insulation-related efforts will further advance globally and in our country. It is inevitable that research and development activities will lead to the enhancement of existing products and the discovery of new ones. Insulation constitutes a holistic approach; merely insulating the external facade does not suffice to consider a building insulated. An insulated structure encompasses the insulation of its external facade, roof, basement, windows, doors, mechanical installations, and, if applicable, ventilation systems.

References

- Bayraktar, D., & Bayraktar, E. (2016). Mevcut Binalarda Isı Yalıtımı Uygulamalarının Değerlendirilmesi. Mehmet Akif Ersoy Üniversitesi Fen Bilimleri Enstitüsü Dergisi, 7(1), 59–66.
- Bektaş, V., Çerçevik, A. E., & Kandemir, S. Y. (2017). Binalarda Isı Yalıtımının Önemi ve Isı Yalıtım Malzemesi Kalınlığının Yalıtıma Etkisi. Bilecik Şeyh Edebali Üniversitesi Fen Bilimleri Dergisi, 4(1), 36–42.
- Benallel, A., Tilioua, A., Mellaikhafi, A., & Hamdi, M. A. A. (2022). Thickness optimization of exterior wall insulation for different climatic regions in Morocco. Materials Today: Proceedings, 58, 1541–1548.
- Bicycle Infrastructure. (2020, February 6). Project Drawdown . <https://drawdown.org/solutions/bicycle-infrastructure>
- Building insulation. (n.d.). Wikipedia. Retrieved December 5, 2023, from [https://en.wikipedia.org/wiki/Building_insulation#:~:text=In%20a%20narrow%20sense%2C%20insulation%20fiber%20\(sheep's%20wool\)%2C](https://en.wikipedia.org/wiki/Building_insulation#:~:text=In%20a%20narrow%20sense%2C%20insulation%20fiber%20(sheep's%20wool)%2C)
- Candan, N. (2007). Isı Yalıtım Sistemleri ve Özelliklerinin Karşılaştırılması [Yüksek Lisans Tezi]. Sakarya Üniversitesi.
- DAĞSÖZ, A. K., BAYRAKTAR, K. G., & ÜNVEREN, H. H. (n.d.). ISI YALITIMI VE KALORİFER TESİSATI STANDARTLARI ÜZERİNE GÖRÜŞLER.
- Guo, S. R. (2012). The application and developmental trend of exterior wall external insulation. Applied Mechanics and Materials, 174, 1367–1371.
- Qin, Z., Li, M., Flohn, J., & Hu, Y. (2021). Thermal management materials for energy-efficient and sustainable future buildings. Chemical Communications, 57(92), 12236–12253.
- Tariku, F., Shang, Y., & Molleti, S. (2023). Thermal performance of flat roof insulation materials: A review of temperature, moisture and aging effects. Journal of Building Engineering, 107142.
- Wilson, A. (2010, January 1). Avoiding the Global Warming Impact of Insulation. Building Green . <https://www.buildinggreen.com/feature/avoiding-global-warming-impact-insulation#:~:text=The%20bottom%20line%20is%20that,in%20the%20green%20building%20industry.>
- Yaman, Ö., Şengül, Ö., Selçuk, H., Çalikuş, O., Kara, İ., Erdem, Ş., & Özgür, D. (2015). Binalarda Isı Yalıtımı ve Isı Yalıtım Malzemeleri. Türkiye Mühendislik Haberleri (TMH), 487(4), 62–75.

HYDROELECTRIC POWER PLANTS AND THEIR IMPACT ON ENERGY

Yusuf DEĞİŞMAN

Institute of Graduate Studies, Energy Science and Technology, Şırnak University, 73000, Şırnak, Turkey

Regaib DİRİK

Institute of Graduate Studies, Energy Science and Technology, Şırnak University, 73000, Şırnak, Turkey

Serdal DAMARSEÇKİN

Şırnak University, Faculty of Engineering, Department of Energy Systems Engineering, 73000 Şırnak, Turkey

ABSTRACT

Hydroelectric power plants play an important role in energy production and their impact on the environment. In this study, we will present a broad assessment of the functioning, advantages, disadvantages and impacts of hydroelectric power plants in the energy sector.

Hydropower plays an important role in the energy sector. As a clean and sustainable source, it is increasingly preferred due to growing energy demand and environmental concerns. In addition, hydropower plants allow for more efficient use of renewable energy sources by meeting energy storage and balancing needs. This increases energy security and can stabilize the volatility of energy demand.

In conclusion, the energy generation and environmental impacts of hydroelectric power plants are of great importance. Although they play an important role in terms of clean energy production and balancing energy demand, their environmental impacts should be taken into account and sustainability strategies should be used. In the future, hydropower will remain an important player in the energy sector, but environmentally friendly practices need to be promoted. Turkey's hydropower potential offers a great opportunity to achieve sustainable development and clean energy goals. However, it is important to manage this potential effectively and be sensitive to environmental impacts. Turkey is taking an important step towards transforming its energy sector through hydropower generation.

Key Words: Hydropower, Water Resources, Energy, Fossil Fuels, Greenhouse Gases

1. INTRODUCTION

Hydroelectric power is a method of energy generation that converts the kinetic energy of water into electrical energy. This method uses the gravitational flow of water from a high to a low level. Hydroelectric power plants generate electricity by turning turbines during this flow of water. This clean and sustainable source of energy takes advantage of nature to keep greenhouse gas emissions to a minimum.

Hydroelectric power generation uses infrastructure elements such as water reservoirs, dams and waterways. As water flows from a high point to a low point, this energy drives turbines to turn. The rotating turbines are converted into electricity by generators.

1.1. Hydroelectric Power Plants and Environmental Impact

Hydroelectric power plants are considered clean and renewable energy sources and use the kinetic energy of water to generate electricity. Such plants generate electricity by converting the flow and gravitational potential of water into energy. However, the construction and operation of hydropower plants can cause some impacts on the environment. To explain these impacts in more detail, we can examine the following headings:

1.1.1. Waterbed and Ecosystem Changes: Hydropower plants are often associated with large dams. These dams collect water from rivers and release it in a controlled manner. This changes the water regime of rivers and can affect the natural flow of water. The construction of dams can lead to the flooding of the land

below them, which can lead to the inundation of forests and ecosystems. This can lead to habitat loss and loss of habitat for local plant and animal species.

1.1.2. Flood and Drought Regulation: Hydropower plants can control flood waters and regulate water supply during dry periods. This can be seen as an environmentally positive impact because it can reduce damage from flooding and support the sustainable use of water resources.

1.1.3. Silt Transport and Embankment: Dams can trap silt and sediment from rivers and deposit it in the river bed. This can cause siltation of waterbeds over time and can have negative environmental impacts. This can make erosion control of rivers more difficult and affect ecosystems downstream.

1.1.4. Migratory Fish Pathways: Hydropower dams can prevent migratory fish species from moving up rivers. This can lead to declining fish populations and damage local fishing industries. However, modern hydropower plants are designed to provide specialized passages and facilities for fish to migrate.

1.1.5. Methane Gas Release: Hydro power dam scan produce methane gas due to the decay of organic matter. Methane has the potential to create a greenhouse effect and it is important to monitor and control the release of this gas to reduce environmental impacts.

As a result, hydro power plant scan causes environmental impacts, but these impacts are largely dependent on project design, operation and maintenance. Modern hydropower plants strive to minimize environmental impacts by adopting environmentally friendly technologies and practices. This emphasizes the importance of hydropower as a sustainable energy source and encourages its use as part of environmental protection efforts.

1.2. Structure of Hydroelectric Power Plants

Hydroelectric power plants are complex systems that function to convert the kinetic energy of water into electrical energy. The structure of these plants includes a number of important components that enable the generation of electricity:

1.2.1. Dam: The central component of a hydropower plant is a dam, where water is stored and released. Dams are built to control the flow of rivers and utilize the kinetic energy of water. Dams can be built using concrete, rock, earth or fill materials. Dams raise the water table to create a large reservoir of water and the height of this reservoir increases the potential energy.

1.2.2. Water Eye and Control Structures: At the top of the dam is a water intake where water is released into the river bed and the intake of water to the power plant is controlled. This control structure regulates the flow of water and directs it to the turbines for power generation. The water from the water intake reaches the turbines, usually through large pipes or canals.

Turbines are the main components that convert the kinetic energy of water into mechanical energy. Turbines rotate depending on the speed and pressure of the water and drive a generator to generate electricity. Different types of turbines can be used in hydroelectric power plants, for example, Francis, Pelton or Kaplan turbines. Each turbine type is selected to suit different water conditions and energy demands.

Generators: The rotational motion of turbines drives a generator. Generators convert mechanical energy into electrical energy. This electrical energy is then distributed to consumption areas through transmission lines.

1.2.3. Electricity Transmission System: Electricity generated from hydroelectric power plants is transported to consumption areas by transmission lines or power transmission lines. These transmission systems ensure that electricity is transported safely and over long distances.

Floodplain Dams provide protection against flash floods. When large amounts of water are stored, the floodplain of the dam allows excess water to be released safely, thus minimizing the danger of flooding.

Hydroelectric power plants offer a clean and environmentally friendly option for power generation. They require effective management of water resources and ensure sustainable use of water. Furthermore, hydropower plants may have high installation costs, but offer the advantages of low operating costs and sustainable power generation in the long term. Therefore, hydro power plants play an important role in power generation portfolios and are an important source to meet clean energy demands [1], [2].

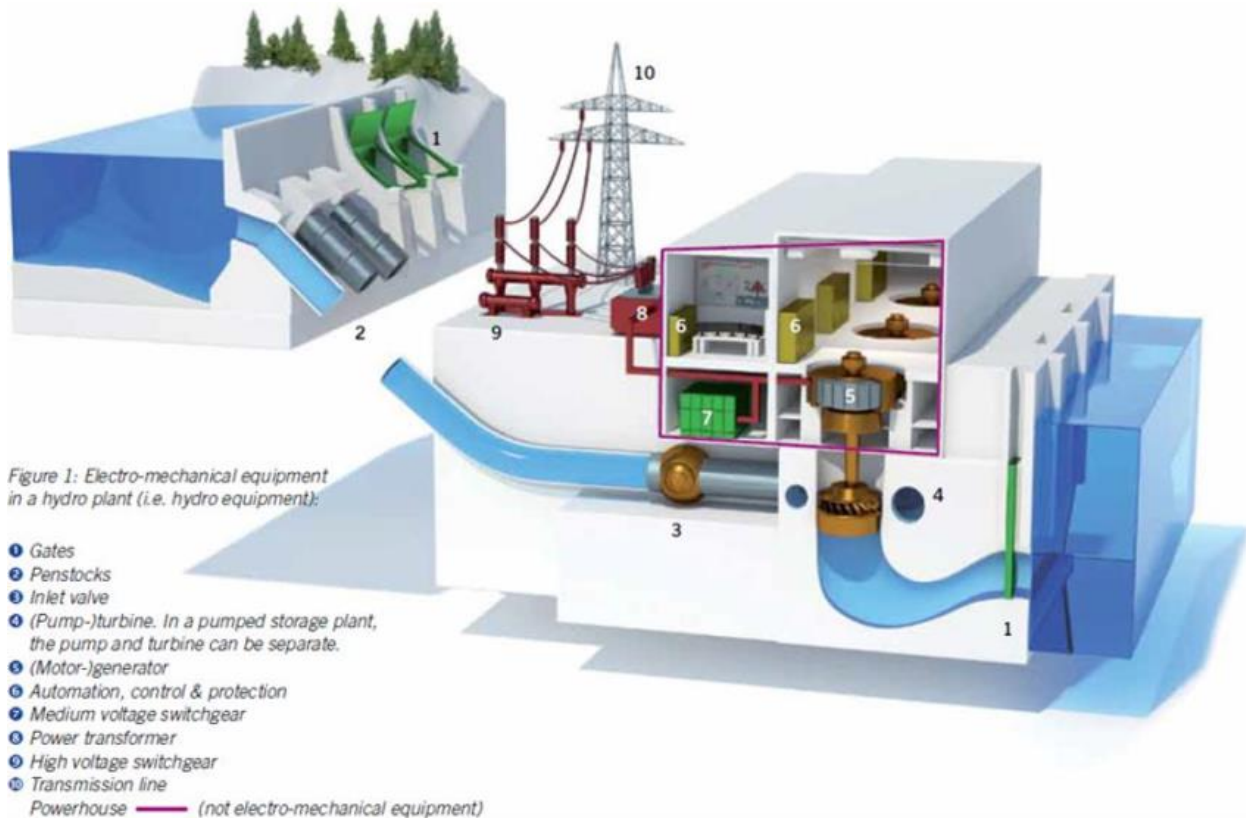


Figure 1: Hydroelectric Power Plant Structure [3]

1.3. Working Principles of Hydroelectric Power Plants

Hydroelectric power plants are power generation facilities that operate on the basis of converting the potential energy of water into kinetic energy and then into electrical energy. The working principles of hydroelectric power plants are explained in more detail below:

1.3.1. Water Storage: Hydroelectric power plants start with a reservoir or dam where water is stored. This storage area is designed to accumulate and control water. The height of the water reservoir determines the amount of potential energy, because gravity will turn into potential energy as the water will fall from high to low.

1.3.2. Water Flow: Controlled by opening the gates or valves of the dam, the water flows downward from the reservoir under the influence of gravity. At this point, the speed and kinetic energy of the water increases.

Turbines The flow of water is directed into mechanical devices called turbines. The blades inside the turbines resist against the flow of water and as the water hits the blades, the turbines start to rotate. This rotation represents the conversion of the kinetic energy of water into mechanical energy.

1.3.3. Generators: Rotating turbines provide mechanical energy to turn a generator. Generators produce electrical energy using magnetic fields and coils of wire. The rotating motion causes the magnetic fields in the generator to change and this results in the creation of electric current.

1.3.4. Electricity Generation: Electric energy generated by generators is transferred to transmission lines by adjusting the voltage level through a transformer. This electrical energy is transported along the transmission lines to the electricity grid or local distribution system. It is then transmitted to the points of electricity consumption, i.e. homes, businesses and industrial facilities.

Hydroelectric power plants are a sustainable and environmentally friendly source of energy. Water resources are usually renewable and abundant, so hydropower provides long-term energy production. Furthermore, hydropower plants do not contribute to greenhouse gas emissions and can increase energy security. However,

the environmental and ecological impacts of large dam projects must be considered and these facilities must be carefully planned [1], [4], [5].

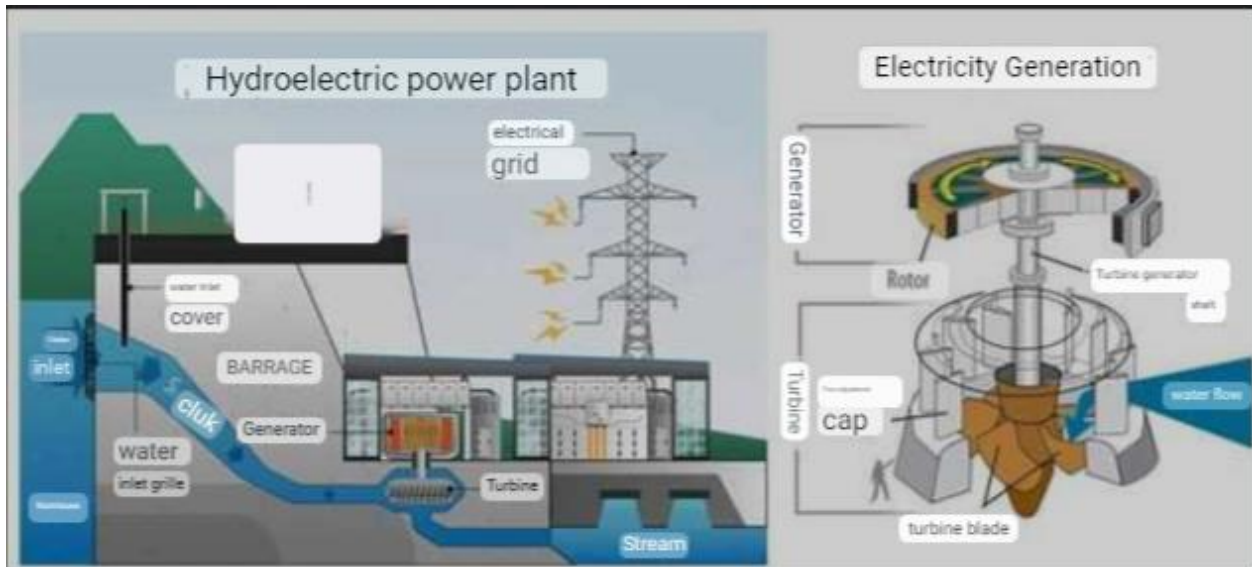


Figure2: Basic Operating Principle of Hydroelectric Power Plant [6]

2. TYPES OF HYDROELECTRIC POWER PLANTS

Hydroelectric power plants include various types that convert the kinetic energy of water into electrical energy. [7] These types have different design and operational characteristics. Here are the hydroelectric

Basic types of power plants:

2.1. Hydroelectric Power Plants with Dams:

- In this type of power plant, a large dam or reservoir is built. The dam stores water with high gravity potential.
- The water is controlled using dam gates or valves. When these gates are opened, the water is released and flows downwards under the influence of gravity.
- The speed and quantity of the flow can be adjusted depending on the size and design of the dam.
- Water is directed to turbines, and the turbines capture the kinetic energy of the water. The turbines generate mechanical energy with their rotating blades.
- This mechanical energy is used to turn generators. Generators produce electrical energy.
- The obtained electrical energy is transported to consumption areas via transmission lines.

2.2. Fluidized Bed Hydroelectric Power Plants:

- Fluidized bed hydro power plants use the natural flow of rivers and don't require a large dam or reservoir.
- The water flow is controlled and the kinetic energy of the water is captured using fluidized bed channels or tunnels.
- This type of power plant is a sustainable option that generally impacts the environment less and preserves the natural flow regime.

2.3. Pumped Storage Hydroelectric Power Plants (PDS):

- PDS is used to store energy and balance energy demand.
- Storage reservoirs with two different height levels are used.
- During periods of low demand, water is pumped from high to low with excess electrical energy.
- During periods of high demand, water is released and electricity is generated by driving turbines.

2.4. Navigable Hydroelectric Power Plants:

- Such power plants are used to overcome the natural barriers of rivers or to raise or lower the level of water to generate energy through gradient changes.
- The water level can be controlled to allow ships or other vehicles to pass.

2.5. Tidal Hydroelectric Power Plants:

- It exploits differences in the height of ocean water caused by tides.
- They are built in coastal areas and convert the kinetic energy created by tidal movements into electrical energy.

2.6. Micro Hydroelectric Power Plants:

- They are small-scale hydro power plants and are usually used to meet local energy needs.
- They are designed as fluidized bed or small dam hydroelectric power plants.

Each type of hydroelectric power plant is selected considering local conditions, water resources and energy demands and offers different advantages. All of these types have the ability to convert water kinetics into electrical energy, but their application areas and environmental impacts are different [5], [8], [9].

3 ADVANTAGES AND DISADVANTAGES OF HYDROELECTRIC POWER PLANTS

3.1. Plants Advantages:

3.1.1. Clean and Green Energy Production: Hydropower is an environmentally friendly energy source. Water kinetics is a natural process and hydroelectric power plants do not contribute to greenhouse gas emissions, do not cause air pollution and do not pollute the environment.

3.1.2. Sustainability: Water resources are generally renewable and abundant. Hydropower plants ensure long-term energy production and use water resources in a sustainable way.

3.1.3. Energy Storage and Balancing: Pumped storage hydropower plants (PDS) are used to store energy and balance energy demand. Energy can be stored during periods of low demand and released during periods of high demand to generate electricity.

3.1.4. High Efficiency: Hydroelectric power plants are highly efficient and provide a continuous source for electricity generation.

3.1.5. Water Resources and Water Regulation: Hydropower plants can help control water resources, support flood control and provide water for irrigation.

3.1.6. Low Operating Costs: Hydroelectric power plants generally have low operating costs and no fuel costs.

3.2. Disadvantages:

3.2.1. Environmental Impacts: Hydropower plants with dams can cause environmental impacts as they create large reservoirs of water. Aquatic ecosystems may change, wetlands may disappear and local fauna may be affected.

3.2.2. Soil Loss: Dam construction often results in large soil loss. This can lead to the destruction of natural areas.

3.2.3. Displacement of Villages and Communities: Dam construction may require some settlements to be flooded, which may lead to the displacement of villages and communities.

3.2.4. Geological Risks: Dams can be vulnerable to geological risks and must be earthquake resistant.

3.2.5. Infrastructure Cost: Hydropower plants with dams can be expensive to build and maintain. In addition, land ownership may be required for large reservoirs.

3.2.6. Sensitivity to Climate Change and Rainfall Irregularity: Hydropower plants are sensitive to precipitation levels and irregularity of water resources. Climate change can affect the stability of water resources.

Each hydropower project is unique and its advantages and disadvantages may differ depending on local conditions, project size and design. Each project therefore requires a careful environmental and economic assessment [10] - [12]

4. ENVIRONMENTAL IMPACTS OF HYDROELECTRIC POWER PLANTS

Although hydroelectric power plants are a sustainable and clean source of energy generation, they can cause some impacts on the environment. These impacts can vary depending on the type and size of the hydroelectric power plant and local conditions. Here are the impacts of hydroelectric power plants on the environment:

4.1. Aquatic Ecosystems and Fish Migration:

- Hydropower plants with dams create large reservoirs of water and this can affect river ecosystems. Reservoirs change the flow of water and can affect plant and animal species in aquatic ecosystems.
- Fish breeding and migration routes may be interrupted. This can have negative impacts on fish populations.

4.2. Affecting Wetlands:

- Dams can cause wetlands to be flooded. This can lead to the destruction of wetlands and inundation of forests.

4.3. Loss of Land:

- Dam construction can lead to loss of land. Forested areas and agricultural lands maybe flooded.

4.4. Declining Biodiversity:

- Creating reservoirs and changing the flow of water can affect the habitats of local plant and animal species. This can lead to a reduction in biodiversity.

4.5. Water and Water Resources Changes:

- Dams can alter local water regimes. The use and availability of local water resources can be affected.

4.6. Geological Risks:

Dams can be vulnerable to geological risks and must be resistant to earthquakes.

4.7. Displacement:

- During dam construction, residential areas may be flooded, resulting in the displacement of villages and communities.

4.8. Infrastructure Cost:

- Construction and maintenance of hydroelectric power plants with dams can be expensive. Additionally, land ownership may be required for large reservoirs.

4.9. Sensitivity to Climate Change and Precipitation Irregularity:

- Hydro power plants are sensitive to rainfall levels and their regularity of water supplies. Climate change can affect the stability of water resources.

These impacts can vary depending on the local conditions, project size and design of hydropower plants. Well-planned hydropower projects can take various measures to minimize or compensate for these impacts. Environmental impact assessments and sustainability strategies are used to enhance the environmental sustainability of hydropower projects [4], [13], [14].

5. MODERN APPLICATIONS OF HYDROELECTRIC POWER PLANTS

Hydropower plants have various applications to meet modern energy needs and ensure sustainable power generation. Here are modern applications of hydropower plants:

5.1. Clean Energy Production: Hydropower plants play an important role in clean and green energy production. Growing global energy demand and environmental concerns have increased the importance of hydroelectric power plants in modern energy portfolios.

5.2. Energy Storage and Balancing: Pumped storage hydropower plants (PDS) are used to store energy and balance energy demand. Energy can be stored during periods of low demand and electricity is generated during periods of high demand. This helps to stabilize the fluctuation of energy demand.

5.3. Integration with Renewable Energy Sources: Hydropower plants can be integrated with other renewable energy sources such as wind and solar power. This stabilizes energy supply and ensures uninterrupted energy production.

5.4. Tidal Power Generation: Tidal hydroelectric power plants, which take advantage of tidal movements in coastal areas, are used to generate tidal power. This converts the kinetic energy resulting from height differences in the sea into electrical energy.

5.5. Micro Hydropower Plants: Small-scale hydropower plants are referred to as micro or mini hydropower plants. Such plants are used to meet local energy needs and provide electricity in remote areas.

5.6. Water Management: Hydropower plants can help manage water resources. Dams help to store and control water, which affects flood control, irrigation and water supply.

5.7. Environmental Impact Mitigation: Modern hydropower projects use sustainability strategies and environmental impact assessments to minimize environmental impacts. This seeks to protect aquatic ecosystems and natural habitats.

5.8. Combating Climate Change: Hydroelectric power plants play an important role in combating climate change with low carbon emissions and clean energy production.

Hydropower plants are finding more and more applications today as a clean, sustainable and environmentally

friendly energy source that meets modern energy needs. This increases energy security while supporting the environmental and sustainability goals of the energy sector [15]

6. THE FUTURE OF HYDROPOWER

Hydropower will continue to play an important role in the energy sector in the future. As a clean, sustainable and low-carbon energy source, hydropower has great potential for environmentally friendly energy production. The importance of hydropower in the future is based on factors such as combating climate change and increasing energy demand. In addition, the energy storage and stabilization capabilities of hydroelectric power plants will facilitate their integration with renewable energy sources and increase energy security. The development of modern technologies will enable hydropower projects to be made more efficient while reducing their environmental impact. Therefore, hydropower will continue to play an important role in the future in terms of meeting energy needs and ensuring environmental sustainability [8], [16.]

EVALUATION AND RESULTS

In this study, an evaluation was made by considering the operating principle of our country's hydroelectric power plants, their impact on the environment, the structure of the power plants, power plants types, their future, advantages and disadvantages.

Hydroelectric power plants in turkey are 709 as of 2023, and the number of ongoing power plants is 23. The total installed capacity is 31,555 MWe. The ratio of production to consumption is 26.14%. [17]

In this period when the need for energy is increasing every year and foreign dependency is increasing, using domestic energy resources will move us forward as a country and will also reduce our foreign dependency. Considering the geographical location and geopolitical structure of our country, it is clear that the potential power of hydroelectric power plants is not used 100% and in the areas where they are used, studies that will increase the efficiency of appropriate technological tools and instilling environmental awareness will ensure more production and move our counter forward in the field of energy.

REFERENCES

- [1] F. University, E. Faculty, and E.-E.M. Department, "Modeling of Hydroelectric Power Plants Ebru ÖZBAY Muhsin Tunay GENÇOLU."
- [2] G. Tarihi *et al.*, "AN ENVIRONMENTAL PERSPECTIVE ON HYDROELECTRIC POWER PLANT (HPP) APPLICATIONS IN TURKEY."
- [3] "Hydroelectric Power Plant and Working Principle | MÜHENDİS." Accessed: Nov. 05,2023.[Online].Available:<https://muhendis.web.tr/hydroelectric-power-plant-operating-principle/>
- [4] O. Üçüncü and Ö. Demirel, "PRECAUTIONS AND PROTECTION ACTIONS TO BE TAKEN ON THE NEGATIVE ENVIRONMENTAL EFFECTS OF HEPP PROJECTS, THE CASE OF KILIÇLI REGULATOR AND HEPP PROJECT."
- [5] M. Şekkelî and Öf. Keçecioğlu, "Development of Hydroelectric Power Plants in Turkey and Case Study of Kahramanmaraş Region," 2011.
- [6] "Project Ensuring Sustainability in Hydroelectric Power Plants: MİLHES." Accessed:Nov.05,2023.[Online].Available: <https://www.frmtr.com/bilim-ve-teknoloji/8189147-hidroelektrik-santrallerinde-surdurulebilirlik-saglayan-proje- milhes.html>
- [7] M. S. Güney and k. Kaygusuz "Hydrokinetic energy conversion systems: A technology status review" <https://doi.org/10.1016/j.rser.2010.06.016>
- [8] İ. GÜZEL and A. BENLİ, "Investigation of Rainwater Harvesting and Hydroelectric PotentialonStateRoadsNearBingölCityCenter,"*DUMFEngineeringJournal*,vol. 11, no. 1, pp. 405-417, Mar. 2020, doi: 10.24012/dumf.565949.

- [9] M. Semih ÖZDEMİR, A. Dalcalı, C. OCAK Bandırma Onyedi Eylül University, E. and Faculty of Natural and Applied Sciences, T. Gazi University, and T. Vocational Sciences "Corresponding Author/Corresponding Author Run of river Hydroelectric Power Plants and Turbine-Generators Used In These Power Plants Article history," 2020.
- [10] "Advantages and Disadvantages of Hydroelectric Power-Enerjiday." Accessed: Nov. 05, 2023. [Online]. Available: <https://www.enerjiday.com/hydroelectric-energy-advantages-and-disadvantages/1005/>
- [11] "Benefits and Harms of Hydroelectric Power Plants." Accessed: Nov. 05, 2023. [Online]. Available: <https://www.ekolojist.com/faydali-bilgiler/hes-nedir-faydalari-ve-zararlari-what/>
- [12] "What is Hydroelectric Energy and Hydroelectric Power Plant? What are the Advantages and Disadvantages? Machinery and Technology Center. "Accessed: Nov. 05, 2023 [Online]. Available: <https://www.maktoloji.com/2017/07/hidroelektrik-enerji-ve-hydroelectric.html>
- [13] "THE REALITY OF HYDROELECTRIC POWER PLANTS AND THEIR ENVIRONMENTAL IMPACT TMMOB Chamber of Mechanical Engineers." Accessed: Nov. 05, 2023. [Online]. Available: <https://www.mmo.org.tr/denizli/haber/hidroelektrik-santraller-gercegi-ve-cevresel-effects>
- [14] H. Nautiyal and V. Goel "Sustainability assessment of hydropower projects" <https://doi.org/10.1016/j.jclepro.2020.121661>
- [15] H. TIRYAKI and A. GÜN, "Frequency Control in a Hydroelectric Power Plant with Modern Optimization Methods," *International Journal of Engineering Research and Development*, pp. 266-274, Jan. 2019, doi: 10.29137/umagd.427027.
- [16] İ. Çolak *et al.*, "TURKEY'S ENERGY FUTURE," 2008.
- [17] Türkiye Energy Atlas Available: <https://www.enerjiatlasi.com/hidroelektrik/>

AN UPDATED REVIEW ON BLENDS OF FUEL BASED ON BIOMASS AS A POTENTIAL REPLACEMENT FOR THE FORTHCOMING RENEWABLE ENERGY SYSTEM

K.R.Padma

*Assistant Professor, Department of Biotechnology, SriPadmavatiMahilaVisvaVidyalayam (Women's) University, Tirupati, AP
(Corresponding Author) Orcid no:0000-0002-6783-3248*

K.R.Don

*Reader, Department of Oral Pathology and Microbiology, Sree Balaji Dental College and Hospital, Bharath Institute of Higher Education and Research (BIHER) Bharath University, Chennai, Tamil Nadu, India.
Orcid No: 0000-0003-3110-8076.*

ABSTRACT

The search for renewable fuels with efficiency levels on par with current conventional fuels has been sparked by growing concerns over the depletion of fossil fuels. The possibilities and chances for using alternative fuels in diverse applications are covered in the current article. This study investigates the current trends in the use of biomass-based fuels as a feasible alternative for heavy-duty transportation. It also covers the fuels' costs and technological readiness levels, with a focus on using them as drop-in fuels in heavy-duty engines to reduce the possibility of greenhouse gas emissions and harmful gas emissions. In terms of sustainability, cost, and emission reduction, this study's extended research suggests that ethanol would be the greatest option for use in heavy-duty transportation. High percentages of ethanol can be added to traditional diesel, which is still the primary fuel for heavy-duty vehicles, or combined with it. Nevertheless, a few issues need to be fixed before ethanol-diesel fuel mixes may be fully adapted for heavy-duty transportation. However, biomass and other renewable energy sources are already widely used, so their place in the system going forward is certain. Even so, there is a need to find new strategies because the considerable increase in biomass usage raises severe questions regarding its sustainability. The authors of this paper attempted to review the properties of alternative fuels as well as the applications and manufacturing prospects associated with them. The researchers analyzed several suggested alternative fuels and their benefits and cons to determine the best use for each fuel and to arrive at the best options.

Keywords: Greenhouse gas, Emission reduction, Heavy-duty engines, Sustainability, Renewable fuels.

INVESTIGATING THE PERFORMANCE OF A WATER-BASED PV/T SYSTEM

Mariem Zaghdoudi

Laboratory of Nanomaterials and Renewable Energy Systems (LANSER), Research and Technology Center of Energy (CRTE_n), Tunisia, ORCID: 0000-0001-8245-7407

Issam Attar

Majdi hazam and Hatem Oueslati, Laboratories of Thermal Processes, Research and Technology Center of Energy, Hammam-Lif, Tunis, Tunisia ORCID: 0000-0003-3165-7104

ABSTRACT

A PV/T collector with the capability to produce thermal energy and electrical energy simultaneously has attracted the attention of farmers in Tunisia particularly in terms of reducing the cost of heating greenhouses in the cold period of the year because the temperature under greenhouse is very low at night. Consequently, the heating of the greenhouses is essential. Our research was based on the problem caused and so developed to give a solution about the last one and reduce the electrical cost specially in winter. The simulation of the HSWHS behavior was developed by using TRNSYS 16 program which is a transient system simulation program used to simulate the instantaneous and the long-term thermal performances of the HSWHS by introducing the meteorological data of the city region of Borj Cédria, located at the south of Tunis capital, Tunisia. The experimental study of the performance of the PV/T collector was carried out before and after its thermal insulation and the efficiency (η) was calculated. It was observed that the efficiency of the collector was increased after its thermal insulation. The efficiency difference reached a maximum of 10 % compared to the uninsulated collector and the electric efficiency of the collector was decreased from 11 a.m. to 1:30 p.m.

Keywords: PV/T, Greenhouse, HSWHS, Solar Energy

Introduction

The problem of temperature inversion is one of solar origin principal problems about which the cultures under shelters complain [1]. Indeed, for the winter period, farmers found many problems in their agriculture field, because the temperature under greenhouse is very low at night. Consequently, the heating of the greenhouses is essential. To overcome these problem, some searcher focused their research on the PV/T collector with the capability to produce thermal energy and electrical energy respectively. The last one has attracted the attention of farmers in Tunisia [2], particularly in terms of reducing the cost of heating greenhouses agricultural in the cold period of the year [3-4]. Based on the previous results, we continue to study the PV/T collector, after cleaning and isolating the last one, in the goal of improving the thermal efficiency and the thermal performance.

Materials and Methods

Before the study of the electrical and thermal properties of the PV/T collector, the last one was placed outside, firstly, must be cleaned and isolated in the goal to improve its thermal efficiency (Fig. 1). Secondly, an internal cleaning was done before connecting the thermocouples to measure the temperature at different levels of the galvanized steel plate. Third, a glass wool was used, one and two layers were placed respectively and covered with a second layer formed by polystyrene sheets, to improve the thermal performance of PV/T collector.

Finally, the experimental study of the performance of the PV/T collector was carried out before and after its thermal insulation and the efficiency values were given.



Figure 1: The PV/T collector isolation

Findings and Discussion

The simulation of the HSWHS behavior was developed by using TRNSYS 16 program and the simulation results are grouped in Table 1. We note that the efficiency of the collector was increased after its thermal insulation, and the difference was nearly 10 % compared to unisolated collector. So the electric efficiency of the collector was decreased, this behavior was related to the temperature rise of the PV/T collector. The electrical efficiency difference attended a percentage nearly 1% after insulation collector (Figure 2).

Table 1: Energy study of HSWHS

Month	E_{supplied} (kWh)	$E_{\text{collected}}$ (kWh)	r (%)
December	2201	701	89
January	2186	811	90
February	2050	980	103
March	2035	1379	141
April	1588	1801	241

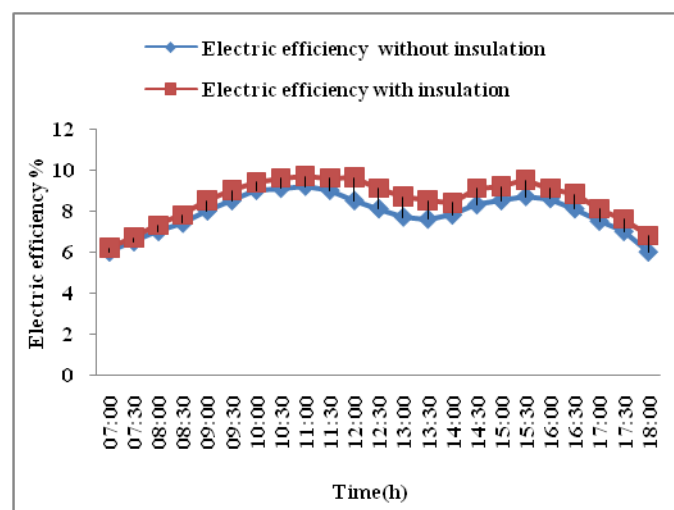


Figure 2 : Electrical efficiency versus time

We note that $\Delta T = (T_s - T_e)$ is inversely proportional to the flow rate, for a constant pump inlet temperature.

Conclusion and Recommendations

Results given by the PV/T collector before and after its thermal insulation were very interesting, the efficiency of the collector was increased after its thermal insulation, and the difference was nearly 10 % compared to unisolated collector. So, that the performance of the heating system were strongly varied under the inlet flow rate affect. A significant economic result were given by the heating system efficiency. Values varied from 89 % in December to 241% in April for a 10 m³ greenhouse.

References

- [1] Fraisse, G., Menezo, C., Johannes, K., 2007. Energy performance of water hybrid PV/T collectors applied to combisystems of direct solar floor type. *Sol. Energy* 81, 1426–1438.
- [2] I.Attar, N. Naili, N. Khalifa, M. Hazami, A. Farhat., 2013. Parametric and numerical study of a solar system for heating a greenhouse equipped with a buried exchanger. *Energ. Convers. Manage*,70, 163-173.
- [3] Chow, T., Ji, J., He, W., 2007. Photovoltaic–thermal collector system for domestic application. *J. Sol.Energy Eng.* 129, 205–209.
- [4] Barbu, M.; Darie, G.;,2020. A Parametric Study of a Hybrid Photovoltaic Thermal (PVT) System Coupled with a Domestic Hot Water (DHW) Storage Tank. *Energies*, 13, 64-81.

**THE ECOLOGICAL RISK OF CONTAMINATION WITH TOXIC METALS IN THE SOILS,
WASTE AND ASH, AROUND THE "TREPÇA" COMPLEX, THE "KOSOVO" THERMAL
POWER PLANTS AND THE NEW FERRONICKEL COMPLEX**

Islam Zuzaku

University of Pristina, "HASAN PRISHTINA", Faculty of Mathematical-Natural Sciences, Department of Chemistry- Pristine-Kosovo!

Skender Demaku

University of Pristina, "HASAN PRISHTINA", Faculty of Mathematical-Natural Sciences, Department of Chemistry- Pristine-Kosovo!

Donika Sylejmani

University of Pristina, "HASAN PRISHTINA", Faculty of Mathematical-Natural Sciences, Department of Chemistry- Pristine-Kosovo!

ABSTRACT

Samples of toxic waste, soil and ash, were collected in the landfill (solid environmental hot-spots) near the "Trepça" Complex, "New Ferronickel" and Kosovo "Thermal Power Plants", and analyzed by the ICP-OES method to measure the concentration of 10 toxic metals (Pb, Cd, Cr, Ni, Zn, Cu, As, Co, Mn, and Fe). The pollutant with the highest mean concentration (in acidic medium) was Fe (36400.00 mg/kg), followed by the Mn (8683.00 mg/kg), Cr (6575.00 mg/kg), As (4739.00 mg/kg), Pb (3364.00 mg/kg), Zn (2394.00 mg/kg), Ni (922.60 mg/kg), Cu (297.60 mg/kg), Co (46.60 mg/kg) and Cd (61.8mg/kg). To analyze the level of heavy metal pollution in an area, more than one pollution index analysis is needed, so in this study 3 pollution indices were used, namely the geoaccumulation index (I_{geo}), contamination factor (CF_i), and the pollution load index (PLI). The CF_i (contamination factor) values determined for Fe, Mn, Cr, As, Pb, Zn, Ni, Cu, Co and Cd indicated a high degree of contamination in all samples. In all soil samples the PLI values indicated the presence of soil pollution.

Keywords: Trepça, Ferronickel, thermal power plant, toxic metals, ecology risk, soil, waste, ash

MODELING AND CONTROL WITH MPPT SPEED FOR WIND ENERGY CONVERSION SYSTEM (WECS) BASED ON PERMANENT MAGNET SYNCHRONOUS GENERATOR (PMSG)

Hicham Sayhi

Electricals Engineering Laboratory of Biskra LGEB, University of Biskra, Biskra, Algeria

Amor Bourek

Electricals Engineering Laboratory of Biskra LGEB, University of Biskra, Biskra, Algeria

Abdelkarim Ammar

Signals and Systems Laboratory (LSS), Institute of Electrical and Electronic Engineering, University of M'hamed BOUGARA of Boumerdes, Boumerdes, Algeria

Ilyes Dahnoun

Electricals Engineering Laboratory of Biskra LGEB, University of Biskra, Biskra, Algeria

ABSTRACT

This paper introduces a thorough model for wind energy systems, with a specific emphasis on the Maximum Power Point Tracking (MPPT) control method implemented in a variable-speed wind energy conversion system based on a Permanent Magnet Synchronous Generator (PMSG). The model comprehensively covers the aerodynamic characteristics of the wind turbine, along with the electrical and mechanical components. The simulation and analysis processes are conducted through the Matlab/Simulink interface. The results obtained from a variety of simulations conclusively illustrate the dynamic performance and effectiveness of the proposed control strategy.

Keywords: wind turbine, permanent magnet synchronous generator (PMSG), MPPT, control, wind energy, uncontrolled rectifier, filter.

**RELATIVISTIC ELASTIC SCATTERING OF A HYDROGEN ATOM ($2S-2S$) BY ELECTRON
IMPACT IN THE PRESENCE OF A CIRCULARLY POLARIZED LASER FIELD**

ABARAGH Mouloud

*Polydisciplinary Faculty, Laboratory of Research in Physics and Engineering Sciences
Sultan Moulay Slimane University, Superior School of Technology of Beni Mellal*

Elmostafa HROUR

*Polydisciplinary Faculty, Laboratory of Research in Physics and Engineering Sciences
Sultan Moulay Slimane University, Superior School of Technology of Beni Mellal*

Jamal GUERROUM

*Polydisciplinary Faculty, Laboratory of Research in Physics and Engineering Sciences
Research Team in Theoretical Physics and Materials (RTTPM)
Sultan Moulay Slimane University, Polydisciplinary Faculty of Khouribga*

ABSTRACT

Within the framework of the first Born approximation, we have investigated the elastic scattering of hydrogen atoms by electron impact in the presence of a circularly polarized monochromatic laser field. The incident and scattered electron wave functions modified by the laser are described using Volkov solutions, while the target is defined by the exact relativistic wave function of the hydrogen atom in the metastable state $2s_{1/2}$. Various Relativistic Differential Cross Sections were obtained under different conditions: in the absence of a laser field and with the influence of a single circularly polarized laser field. By considering selected geometrical conditions, we explored the dependence of differential cross sections on the incident electron energy and the impact of laser field parameters. The Kroll-Watson sum rule is verified for the single circularly polarized laser field based on the number of exchanged photons.

Keywords: Laser-assisted, QED calculations, Differential cross section, relativistic scattering, Hydrogen atom.

FREE VIBRATION ANALYSIS OF STEPPED BEAM WITH VARYING CROSS-SECTION WITH A CRACK

Mehmet HASKUL

*Assoc. Prof. Dr. Şırnak University, Faculty of Engineering, Department of Mechanical Engineering, Şırnak-Türkiye,
(Responsible Author)*

Murat KISA

Prof. Dr. Harran University, Faculty of Engineering, Department of Mechanical Engineering, Şanlıurfa-Türkiye

ABSTRACT

In this study, a numerical method is proposed for the free vibration analysis of a stepped cracked beam with linearly varying cross-section. A computer program was written using the finite element method to calculate the natural frequencies and mode shapes of the cracked stepped beam. In the applied method the beam is divided into elements at certain locations, including the crack section. System matrices, stiffness and mass were obtained, and the free vibration of the cracked beam was done. The crack in the beam was considered and modeled as a massless spring. The stiffness of the crack was determined by utilizing the principles of linear elastic fracture mechanics. Numerical data were obtained from natural frequencies and mode shapes of different crack depth ratios and various crack locations of the stepped beam. The results are presented in graphical form. The results, presented graphically, have shown that, the crack location, crack ratio and taper ratio have significant effects on the natural frequencies and mode shapes of the cracked beam.

Keywords: Free vibration, crack, stepped beam, varying cross section.

Introduction

Engineering structures are constantly exposed to external loads, and these loads cause damage to the structure over time. The most common of these damages are cracks. Cracks reduce the stiffness of the structure and accordingly change its dynamic properties. Identifying and eliminating such problems beforehand is an essential step in preventing further damage that may arise. The suitable and usable method for crack is vibration analysis. The application of vibration analysis is both easy and more cost-effective than other methods.

Many studies are in the literature on vibration analysis of cracked beams, columns, and frame structures. They studied beams, bars, and shells containing cracks (Salawu, 1997; Dimarogonas, 1996; Wauer, 1990; Gasch 1993; Krawczuk & Ostachowicz, 1996; Jassim et al., 2013). Du et al. (2021) used the transfer matrix method for the free vibration analysis of an axially loaded variable cross-section Euler-Bernoulli beam with many fixed members. Haskul and Kisa (2021a, 2021b) used the finite element method and component mode synthesis method to calculate the natural frequencies and mode shapes of varying cross-section beams with crack. Kisa and Brandon (2000) developed a finite element scheme to calculate the eigensystem of a broken beam for different degrees of closure. Feldman (2011) has produced an instructive guide on converting Hilbert applications to mechanical vibration. Choi (2003) developed the finite element-transfer stiffness coefficient method to efficiently conduct free vibration analysis of 2D structures such as plate structures. Using the dynamic transfer coefficient of the stiffness method, they formulated a free and forced vibration analysis algorithm for frame structures. The method is based on the concept of transferring the dynamic stiffness coefficient associated with the force and displacement vector at each node from the left end to the right end of the structure. Kisa (2004) modeled the problem using finite elements and component mode synthesis methods to examine the effect of cracks on the dynamic properties of a cantilever composite beam made of graphite fiber reinforced polyamide. Moon and Choi (2000) compared the numerical results obtained by the transfer dynamic stiffness coefficient method for a space frame structure with the results obtained by the finite element method and experiment. Using the dynamic stiffness method, Boscolo and Banerjee (2011) investigated the in-plane free vibration behavior of plates. Mehmood (2015) used the finite element method

and numerical time integration method (new signal method) in vibration analysis to understand the dynamic response of the frame subjected to moving point loads. Koohestani and Kaveh (2010) presented a method for the buckling and free vibration analysis of cyclically iterated space lattice structures. Ramu and Mohanty (2012) used Kirchhoff plate theory for finite element analysis to obtain the natural frequencies of a simply supported rectangular plate. Ranjbaran et al (2008) presented a mathematical formula for buckling analysis of a column and vibration analysis of a beam. The beam and column are assumed to be non-uniform and cracked. The problem is expressed as an optimization problem using variational calculus. An optimization technique is used for the analysis of the buckling load. Considering the similarity between the fundamental equation for buckling and free vibration, the beam's fundamental frequency and mode shape were calculated by the same method. Shabani and Cunedioğlu (2020) performed a free vibration analysis of a non-uniform symmetrical beam with edge cracks made of functionally graded material. Timoshenko beam theory was used for the multilayer sandwich beam's finite element analysis, and the cantilever beam was modeled with 50 layers of material. Yendhe et al. (2016) investigated the vibration behavior of beams both experimentally and using the SEM software ANSYS. This study analyzed vibration on different cantilever beams with transverse cracks and boundary conditions. Orhan (2007) investigated the free and forced vibration analysis of cracked beams using a finite element program to determine the crack in a cantilever beam. In the study, single and double-sided crack conditions were evaluated. Ranjbaran (2014) investigated the effect of stiffeners on the free vibration analysis of structural frameworks in performing free vibration analysis of cracked elements. Saavedra and Cuitino (2001) presented the theoretical and experimental dynamic behavior of different multi-beam systems containing a transverse crack. Yoon et al. (2007) investigated the effect of two open cracks on the dynamic behavior of a double-cracked simply supported beam, both analytically and experimentally. In this study, free vibration analysis of a cracked stepped beam with linearly varying cross-section supported at both ends was carried out. Many studies have been carried out on the free vibration analysis of cracked beams (Kisa 2011, 2012; Kisa and Gürel 2006, 2007; Kisa et al. 1998; Kisa and Brandon 2000).

Materials and Methods

In this study, the beam shown in Figure 1 is divided into sub-elements. Free vibration analysis was carried out by obtaining the stiffness and mass matrices of a beam element with two nodes and three degrees of freedom at each sub-element.

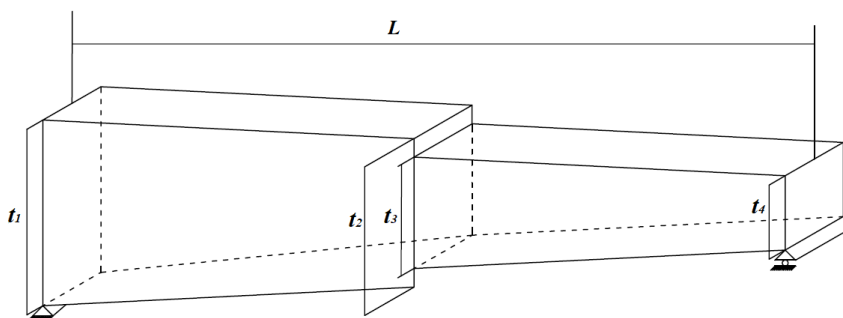


Figure 1. Sketch of non linear stepped beam

The $EI_{zz}(x)$ and $EA(x)$ equations for the beam at a distance x :

$$EI_{zz}(x) = EI_{zz1} \left(1 + \alpha \left(\frac{x}{L} \right) \right)^3 \quad (1)$$

$$EA(x) = EA_1 \left(1 + \alpha \left(\frac{x}{L} \right) \right) \quad (2)$$

where I_{zz1} and A_1 represent the left end's area moment of inertia and cross-sectional area, respectively.

α is stated as:

$$\alpha = \frac{t_2 - t_1}{t_1} = \frac{t_4 - t_3}{t_3} \quad (3)$$

A beam element's stiffness matrix is shown below (Haskul 2010).

$$K = \begin{bmatrix} \frac{1}{C} & 0 & 0 & \frac{-1}{C} & 0 & 0 \\ 0 & \frac{A_1}{D_1} & \frac{A_2}{D_1} & 0 & \frac{-A_1}{D_1} & \frac{A_1L - A_2}{D_1} \\ 0 & \frac{A_2}{D_1} & \frac{A_3}{D_1} & 0 & \frac{-A_2}{D_1} & \frac{A_2L - A_3}{D_1} \\ \frac{-1}{C} & 0 & 0 & \frac{1}{C} & 0 & 0 \\ 0 & \frac{-A_1}{D_1} & \frac{-A_2}{D_1} & 0 & \frac{A_1}{D_1} & \frac{A_2 - A_1L}{D_1} \\ 0 & \frac{A_1L - A_2}{D_1} & \frac{A_2L - A_3}{D_1} & 0 & \frac{A_2 - A_1L}{D_1} & \frac{A_1L^2 - 2A_2L + A_3}{D_1} \end{bmatrix} \quad (4)$$

where; A_1, A_2, A_3, D_1 and C are given as:

$$A_i = \int_0^L \frac{x^{(i-1)}}{EI_{zz}(x)} dx, \quad i = 1, 2, 3, \quad (5)$$

$$D_1 = A_1 \cdot A_3 - A_2^2 \quad (6)$$

$$\frac{1}{C} = \frac{EA_1}{L} \left[\frac{\alpha}{\ln(\alpha + 1)} \right] \quad (7)$$

A beam element's mass matrix is given below (Haskul 2010):

$$[M] = \begin{bmatrix} m_{11}^A & 0 & 0 & m_{12}^A & 0 & 0 \\ 0 & m_{11}^B & m_{12}^B & 0 & m_{13}^B & m_{14}^B \\ 0 & m_{21}^B & m_{22}^B & 0 & m_{23}^B & m_{24}^B \\ m_{21}^A & 0 & 0 & m_{22}^A & 0 & 0 \\ 0 & m_{31}^B & m_{32}^B & 0 & m_{33}^B & m_{34}^B \\ 0 & m_{41}^B & m_{42}^B & 0 & m_{43}^B & m_{44}^B \end{bmatrix}_{6 \times 6} \quad (8)$$

where m_{ij}^A and m_{ij}^B ;

$$[m]^A = \begin{bmatrix} \frac{1}{12} \rho A_1 L (4 + \alpha) & \frac{1}{12} \rho A_1 L (2 + \alpha) \\ \frac{1}{12} \rho A_1 L (2 + \alpha) & \frac{1}{12} \rho A_1 L (4 + 3\alpha) \end{bmatrix} \quad (9)$$

$$[m]^B = \begin{bmatrix} \frac{1}{35} \rho A_1 L (13+3\alpha) & \frac{1}{420} \rho A_1 L^2 (22+7\alpha) & \frac{9}{140} \rho A_1 L (2+\alpha) & -\frac{1}{420} \rho A_1 L^2 (13+6\alpha) \\ & \frac{1}{840} \rho A_1 L^3 (8+3\alpha) & \frac{1}{420} \rho A_1 L^2 (13+7\alpha) & -\frac{1}{280} \rho A_1 L^3 (2+\alpha) \\ & & \frac{1}{35} \rho A_1 L (13+10\alpha) & -\frac{1}{420} \rho A_1 L^2 (22+15\alpha) \\ \text{Simetrik} & & & \frac{1}{840} \rho A_1 L^3 (8+5\alpha) \end{bmatrix} \quad (10)$$

The amount of energy required for the unit strain occurring in front of the crack, the strain energy release rate, J for plane strain is as given below (Tada et al. 1985):

$$J = \frac{1-\nu^2}{E} K_I^2 + \frac{1-\nu^2}{E} K_{II}^2 + \frac{1+\nu}{E} K_{III}^2 \quad (11)$$

The strain energy release rate is always positive and includes three independent strain modes.

Reexpressing J using the superposition principle, we get

$$J = \frac{1-\nu^2}{E} (K_{I1} + K_{I2} + \dots + K_{In})^2 + \frac{1-\nu^2}{E} (K_{II1} + K_{II2} + \dots + K_{IIn})^2 + \frac{1+\nu}{E} (K_{III1} + K_{III2} + \dots + K_{III3})^2 \quad (12)$$

The flexibility coefficients resulting from cracks in the structure can be calculated using Castigliano's theorem and the stress concentration factor. However, if the amount of strain energy released is treated according to the Griffith-Irwin theory (Irwin, 1960), the flexibility coefficient is obtained as:

$$c_{ij} = \frac{\partial u_i}{\partial P_j} = \frac{\partial^2}{\partial P_i \partial P_j} \int_A J(P_i, A) dA \quad (13)$$

The flexibility coefficients c_{11} , c_{13} , c_{22} and c_{33} are given as:

$$\left. \begin{aligned} c_{11} &= \frac{2\pi}{E^* b^2 d} \int_0^a \xi F_1^2 \left(\frac{\xi}{b} \right) d\xi \\ c_{13} &= c_{31} = \frac{12\pi}{E^* b^3 d} \int_0^a \xi F_1 \left(\frac{\xi}{b} \right) F_2 \left(\frac{\xi}{b} \right) d\xi \\ c_{22} &= \frac{2\pi \kappa^2}{E^* b^2 d} \int_0^a \xi F_2^2 \left(\frac{\xi}{b} \right) d\xi \\ c_{33} &= \frac{72\pi}{E^* b^4 d} \int_0^a \xi F_3^2 \left(\frac{\xi}{b} \right) d\xi \end{aligned} \right\} \quad (14)$$

where the the crack stiffness matrix is given as;

$$[C]^{-1} = \begin{bmatrix} \frac{c_{33}}{-c_{13}^2 + c_{11}c_{33}} & 0 & \frac{c_{13}}{c_{13}^2 - c_{11}c_{33}} \\ 0 & \frac{1}{c_{22}} & 0 \\ \frac{c_{13}}{c_{13}^2 - c_{11}c_{33}} & 0 & \frac{c_{11}}{-c_{13}^2 + c_{11}c_{33}} \end{bmatrix}_{3 \times 3} \quad (15)$$

For a beam with two nodes and three degrees of freedom at each node, the stiffness matrix caused by the crack in the crack region is:

$$K_{cr} = \begin{bmatrix} [C]^{-1} & -[C]^{-1} \\ -[C]^{-1} & [C]^{-1} \end{bmatrix}_{(6 \times 6)} \quad (16)$$

where, K_{cr} represent to the stiffness matrix occurring in the beam due to the crack.

Cracks within the structure are known to lead to reduced stiffness (Irwin, 1960). The stiffness matrix $[K]_{wcr}$ of the cracked beam is:

$$[K]_{wcr} = [K] + [K]_{cr} \quad (17)$$

The free vibration equation in matrix notation can be given as:

$$([K]_{wcr} - \lambda[M])\varphi = 0 \quad (18)$$

By using of equation 18, the dynamic characteristics of a tapered beam containing crack were obtained.

Findings and Discussion

Free vibration analysis of a cracked beam with linearly varying thickness and pinned-pinned at both ends was performed. A computer program was prepared using the finite element method for vibration analysis, natural frequencies and mode shapes were calculated for different crack location and crack depth ratios of the beam.

Geometric properties of the varying cross-section one-step cracked beam shown in Figure 2; $L=0.2$ m, $t_2/t_1=t_4/t_3$ thickness ratio varies linearly. Mechanical properties are the elasticity modulus is $E=216 \times 10^9 \text{N/m}^2$, Poisson's ratio is $\nu=0.3$ and density is $\rho=7850 \text{kg/m}^3$.

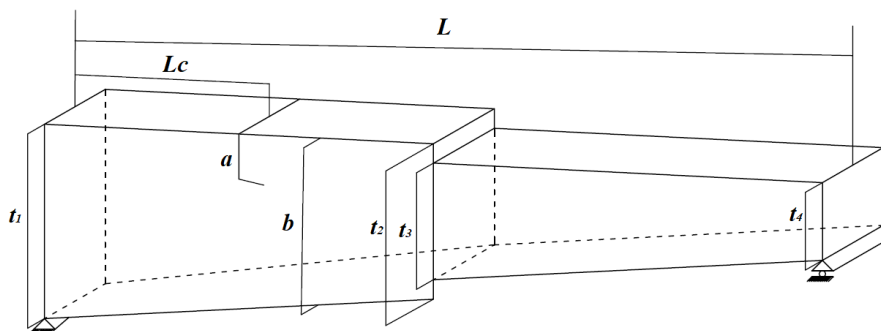


Figure 2. Sketch of stepped beam with a crack

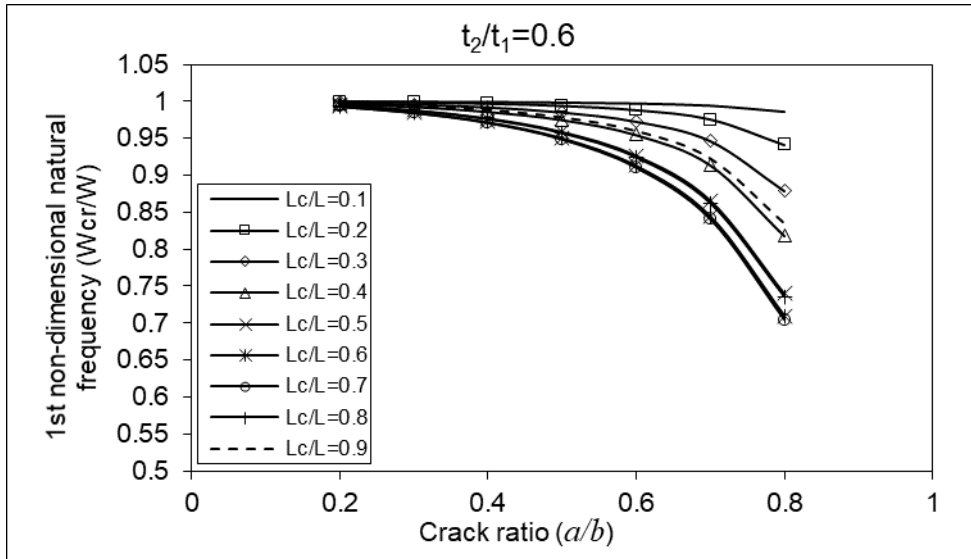


Figure 3. First non-dimensional natural frequencies of pinned–pinned one-stepped cracked beam for taper ratio $t_2/t_1=0.6$, crack locations $L_c/L=0.1-0.9$ and crack depth ratios $a/b=0.2-0.8$

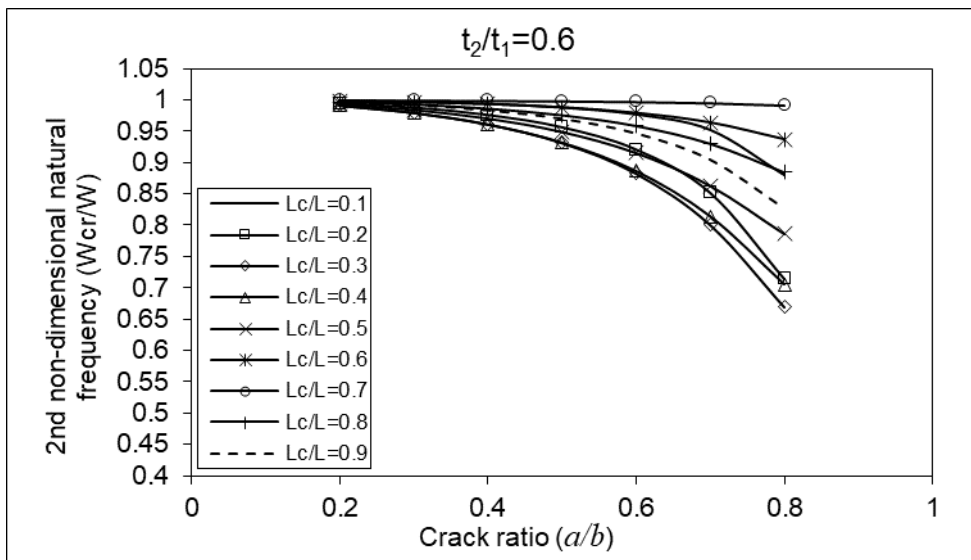


Figure 4. Second non-dimensional natural frequencies of pinned–pinned one-stepped cracked beam for taper ratio $t_2/t_1=0.6$, crack locations $L_c/L=0.1-0.9$ and crack depth ratios $a/b=0.2-0.8$

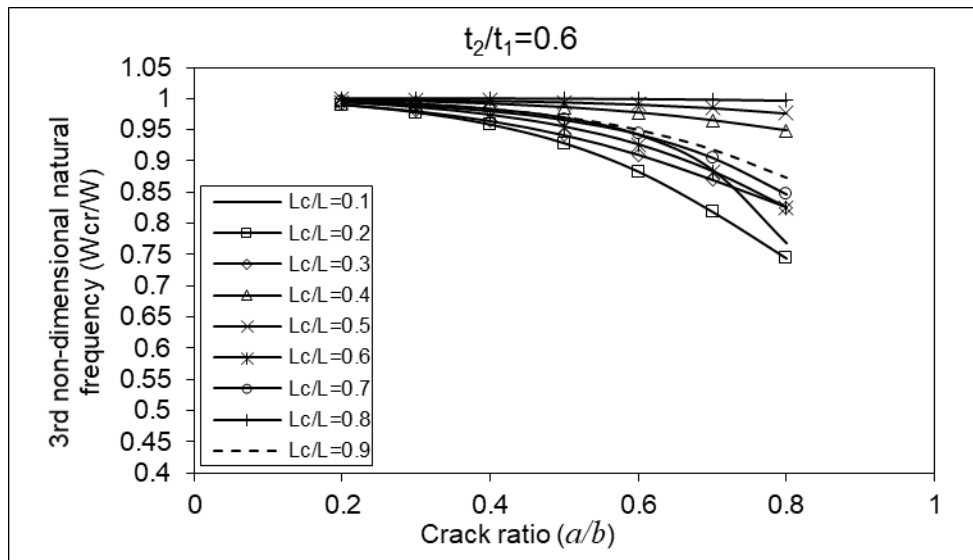


Figure 5. Tird non-dimensional natural frequencies of pinned–pinned one-stepped cracked beam for taper ratio $t_2/t_1=0.6$, crack locations $L_c/L=0.1-0.9$ and crack depth ratios $a/b =0.2-0.8$

In the Figures 3,4 and 5 the change of the first, second and third non-dimensional natural frequencies of the beam with pinned at both ends, with a taper ratio $t_2/t_1=0.6$ and crack locations $L_c/L=0.1-0.9$, depending on the crack depth ratio, is given. As seen from the figures, the maximum decrease in the first natural frequency occurred where the crack was located at $L_c/L=0.7$. The maximum frequency decrease in the second natural frequency occurred where the crack was at $L_c/L=0.3$, and the maximum decrease in the third natural frequency occurred when the crack location was $L_c/L=0.2$.

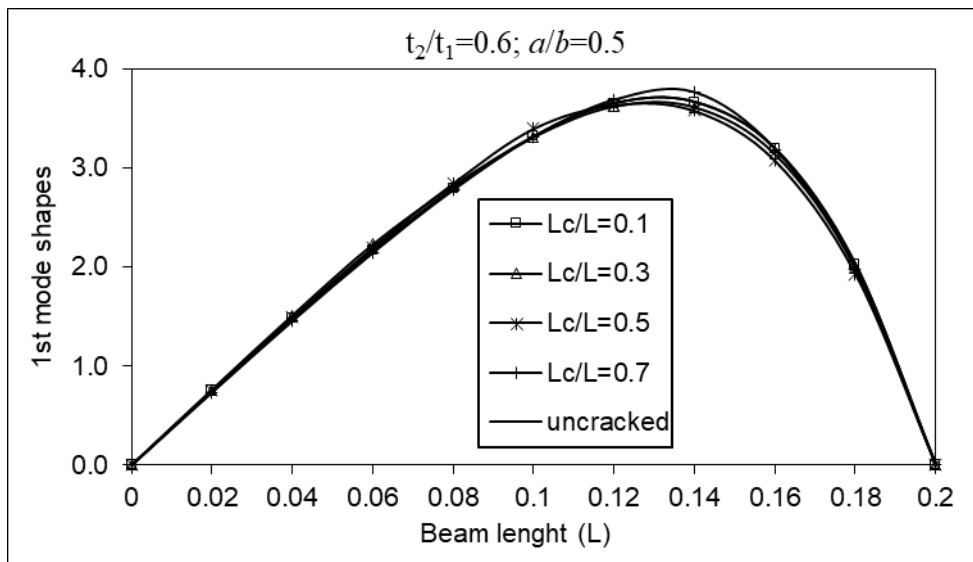


Figure 6. First mode shapes of pinned–pinned cracked one-stepped beam for crack depth ratio $a/b = 0.5$ and taper ratio $t_2/t_1 = 0.6$

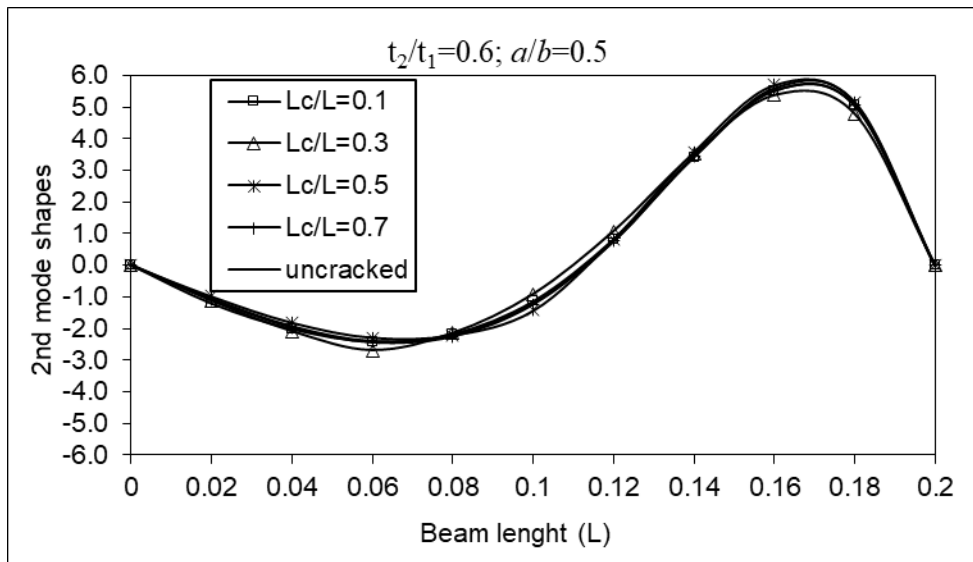


Figure 7. Second mode shapes of pinned–pinned cracked one-stepped beam for crack depth ratio $a/b = 0.5$ and taper ratio $t_2/t_1 = 0.6$

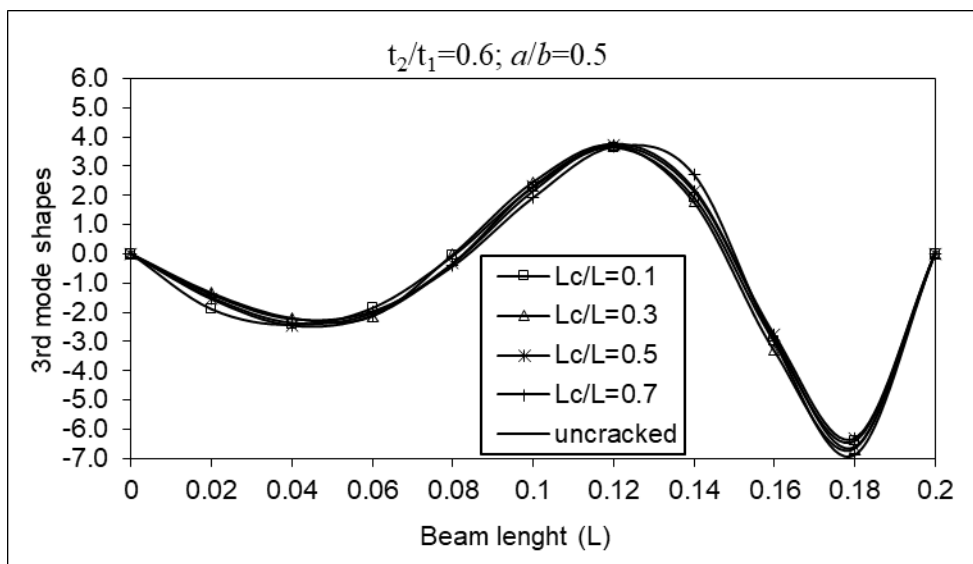


Figure 8. Third mode shapes of pinned–pinned cracked stepped beam for crack depth ratio $a/b = 0.5$ and taper ratio $t_2/t_1 = 0.6$

Figures 6, 7 and 8 shows the changes of the first, second and third mode shapes depending on the crack locations for the taper ratio $t_2/t_1 = 0.6$ and crack depth ratio $a/b = 0.5$. As can be seen from the figures, the first mode shape is most affected when the crack location is at $Lc/L = 0.7$, the second mode shape is at the crack location $Lc/L = 0.3$, and the third mode shape is most affected when the crack location is at $Lc/L = 0.5$.

It can be seen that the mode shapes change in parallel with the natural frequencies given in the Figure 3, 4 and 5.

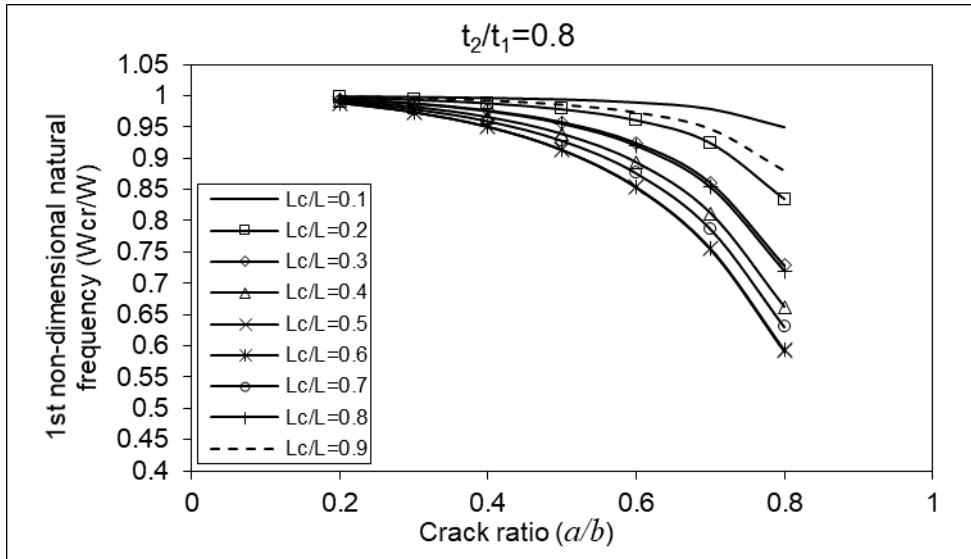


Figure 9. First non-dimensional natural frequencies of pinned-pinned one-stepped cracked beam for taper ratio $t_2/t_1 = 0.8$, crack locations $Lc/L = 0.1-0.9$ and crack depth ratios $a/b = 0.2-0.8$

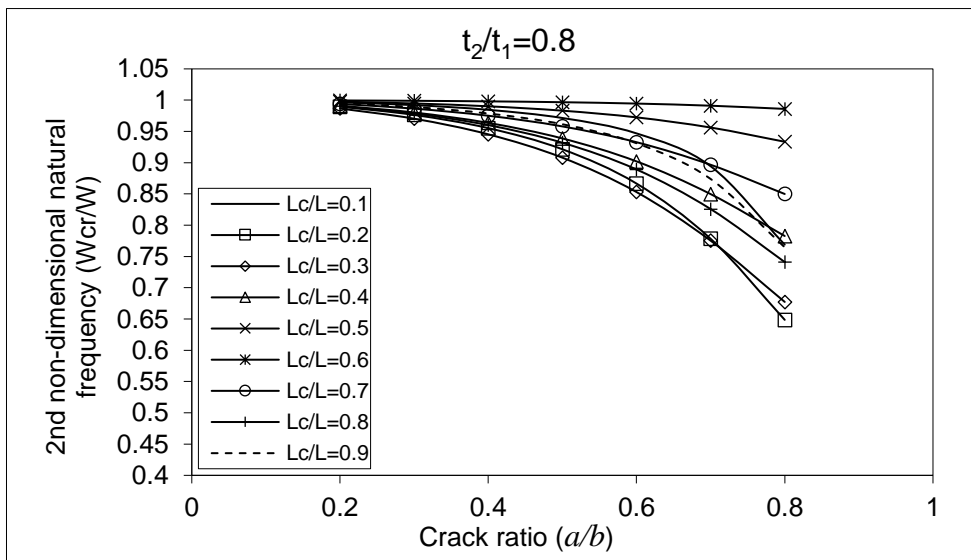


Figure 10. Second non-dimensional natural frequencies of pinned-pinned one-stepped cracked beam for taper ratio $t_2/t_1 = 0.8$, crack locations $Lc/L = 0.1-0.9$ and crack depth ratios $a/b = 0.2-0.8$

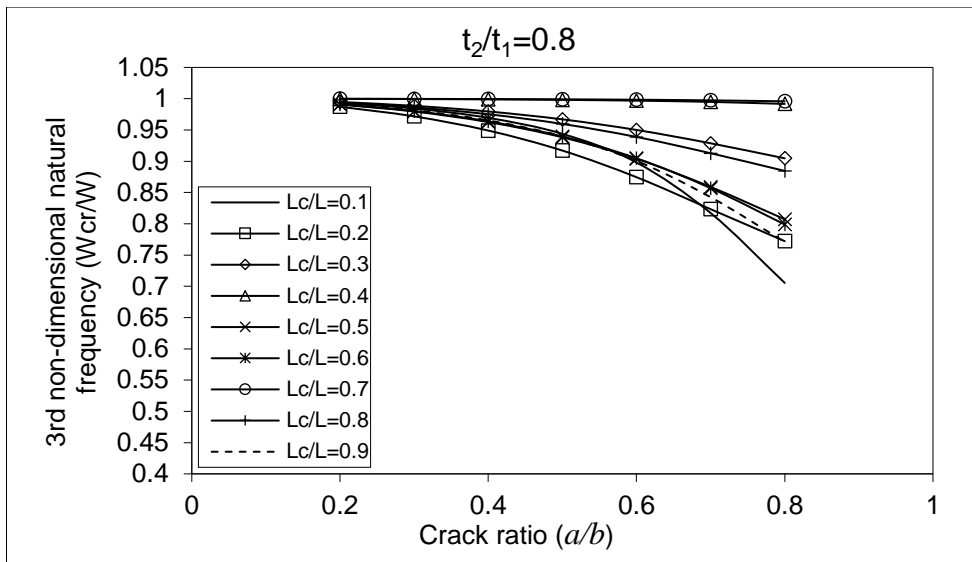


Figure 11. Third non-dimensional natural frequencies of pinned–pinned one-stepped cracked beam for taper ratio $t_2/t_1 = 0.8$, crack locations $L_c/L = 0.1–0.9$ and crack depth ratios $a/b = 0.2–0.8$

In the Figures 9,10 and 11 the change of the first, second and third non-dimensional natural frequencies of the beam with pinned at both ends, with a taper ratio $t_2/t_1 = 0.8$ and crack location $L_c/L = 0.1-0.9$, depending on the crack depth ratio, is given. As seen from the figures, the maximum decrease in the first natural frequency occurred where the crack was $L_c/L = 0.6$. The maximum frequency decrease in the second natural frequency occurred where the crack was $L_c/L = 0.2$, $L_c/L = 0.1$ and $L_c/L = 0.9$, and the maximum decrease in the third natural frequency occurred when the crack location was $L_c/L = 0.1$ and $L_c/L = 0.9$.

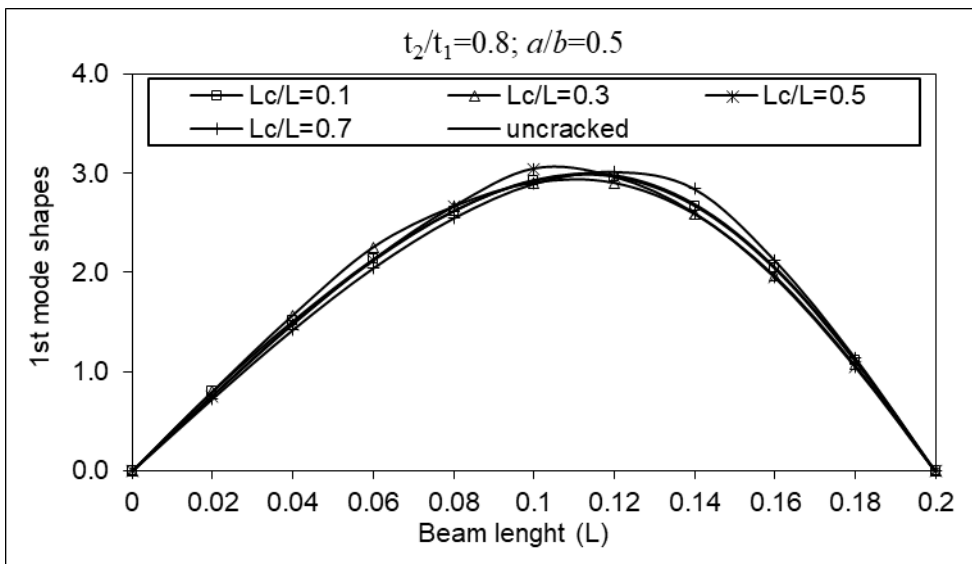


Figure 12. Third mode shapes of pinned–pinned cracked stepped beam for crack depth ratio $a/b = 0.5$ and taper ratio $t_2/t_1 = 0.8$

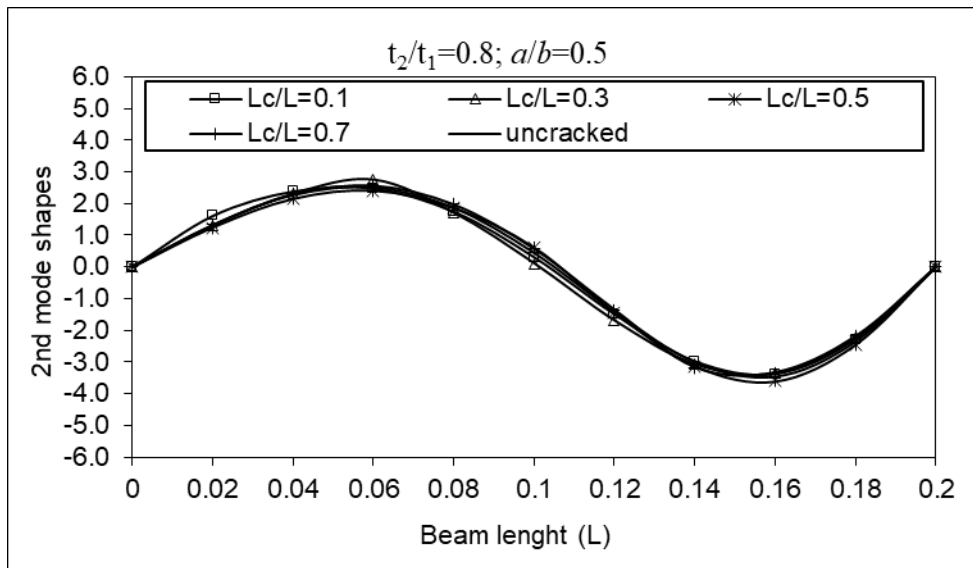


Figure 13. Third mode shapes of pinned–pinned cracked stepped beam for crack depth ratio $a/b = 0.5$ and taper ratio $t_2/t_1 = 0.8$

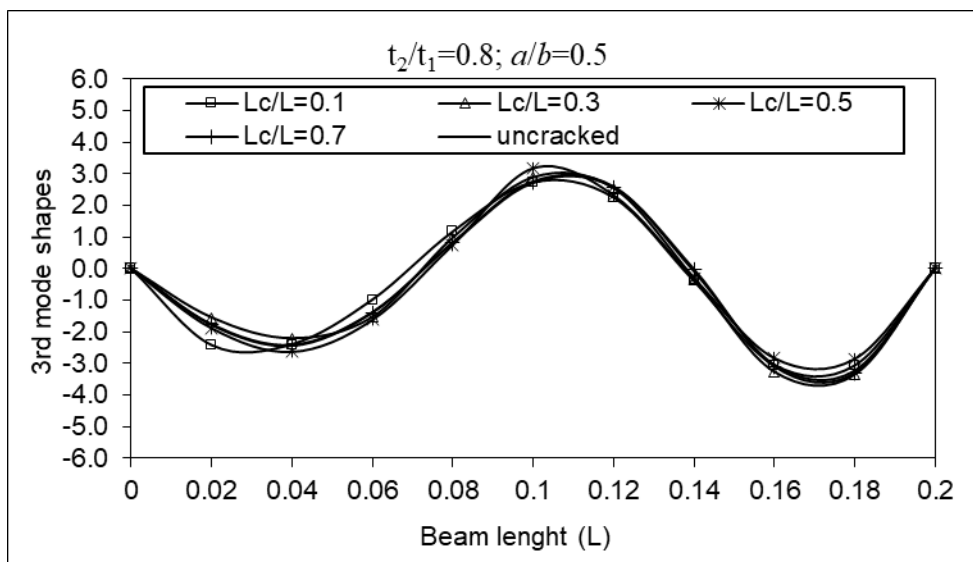


Figure 14. Third mode shapes of pinned–pinned cracked stepped beam for crack depth ratio $a/b = 0.5$ and taper ratio $t_2/t_1 = 0.8$

Figures 12, 13 and 14 shows the changes of the first, second and third mode shapes depending on the crack locations for the taper ratio $t_2/t_1=0.8$ and crack depth ratio $a/b=0.5$. It can be seen that the natural vectors change in parallel with the natural frequencies given in the Figure 9, 10 and 11.

Conclusion and Recommendations

In this study, free vibration analysis of single-stepped cracked beam and linearly varying thickness was performed using the finite element method. The one-stepped beam was discussed as pinned-pinned both ends. The effects of taper ratio, crack location and crack depth ratios on vibration parameters are given in figures. It was observed that the crack located near the midpoint of the beam caused significant changes in the first natural frequency and mode shape of the beam. A crack located close to the supports of the beam affects the second natural frequency and mode shape, while a crack located at 0.3 and 0.7 of the beam length affects the

third natural frequency and mode shape. The maximum decreases in the first, second and third natural frequencies occur when the crack is located in different positions of the beam, and this is due to the fact that the cracks in these regions cause maximum energy loss in the beam vibrating in the relevant mode.

References

- Salawu, O. S. (1997). Detection of structural damage through changes in frequency: a review. *Engineering structures*, 19(9), 718-723.
- Dimarogonas, A. D. (1996). Vibration of cracked structures: a state of the art review. *Engineering fracture mechanics*, 55(5), 831-857.
- Wauer, J. R. (1990). On the dynamics of cracked rotors: a literature survey. *Applied Mechanics Reviews* 43 (1) 13–17.
- Gasch, R. (1993). A survey of the dynamic behaviour of a simple rotating shaft with a transverse crack. *Journal of sound and vibration*, 160(2), 313-332.
- Krawczuk, M., & Ostachowicz, W. (1996). Damage indicators for diagnostic of fatigue cracks in structures by vibration measurements—a survey. *Journal of Theoretical and Applied Mechanics*, 34(2), 307-326.
- Jassim, Z. A., Ali, N. N., Mustapha, F., & Jalil, N. A. (2013). A review on the vibration analysis for a damage occurrence of a cantilever beam. *Engineering Failure Analysis*, 31, 442-461.
- Du, Y., Cheng, P., & Zhou, F. (2022). Free vibration analysis of axial-loaded beams with variable cross sections and multiple concentrated elements. *Journal of Vibration and Control*, 28(17-18), 2197-2211.
- Haskul, M., & Kisa, M. (2021). Free vibration of the double tapered cracked beam. *Inverse Problems in Science and Engineering*, 29(11), 1537-1564.
- Haskul, M., & Kisa, M. (2021). Free-vibration analysis of cracked beam with constant width and linearly varying thickness. *Emerging Materials Research*, 11(1), 125-137.
- Kisa, M., & Brandon, J. (2000). The effects of closure of cracks on the dynamics of a cracked cantilever beam. *Journal of sound and vibration*, 238(1), 1-18.
- Feldman, M. (2011). Hilbert transform in vibration analysis. *Mechanical systems and signal processing*, 25(3), 735-802.
- Choi, M. S. (2003). Free Vibration Analysis of Plate Structures Using Finite.
- Kisa, M. (2004). Free vibration analysis of a cantilever composite beam with multiple cracks. *Composites Science and Technology*, 64(9), 1391-1402.
- Moon, D. H., & Choi, M. S. (2000). Vibration analysis for frame structures using transfer of dynamic stiffness coefficient. *Journal of Sound and Vibration*, 234(5), 725-736.
- Boscolo, M., & Banerjee, J. R. (2011). Dynamic stiffness method for exact inplane free vibration analysis of plates and plate assemblies. *Journal of Sound and Vibration*, 330(12), 2928-2936.
- Mehmood, A. (2015). Using finite element method vibration analysis of frame structure subjected to moving loads. *International Journal of Mechanical Engineering and Robotics Research*, 4(1), 50-65.
- Koohestani, K., & Kaveh, A. (2010). Efficient buckling and free vibration analysis of cyclically repeated space truss structures. *Finite Elements in Analysis and Design*, 46(10), 943-948.
- Ramu, I., & Mohanty, S. C. (2012). Study on free vibration analysis of rectangular plate structures using finite element method. *Procedia engineering*, 38, 2758-2766.
- Ranjbaran, A., Hashemi, S., & Ghafarian, A. (2008). A new approach for buckling and vibration analysis of cracked column.
- Shabani, S., & Cunedioğlu, Y. (2020). Free vibration analysis of cracked functionally graded non-uniform beams. *Materials Research Express*, 7(1), 015707.

- Yendhe, V. S., Kadlag, P. V. L., & Shelke, P. R. S. (2016). Vibration analysis of cracked cantilever beam for varying crack size and location. *International Research Journal of Engineering and Technology*, 3(8), 1913-1919.
- Orhan, S. (2007). Analysis of free and forced vibration of a cracked cantilever beam. *Ndt & E International*, 40(6), 443-450.
- Ranjbaran, A. (2014). Free-vibration analysis of stiffened frames. *Journal of Engineering Mechanics*, 140(9), 04014071.
- Saavedra, P. N., & Cuitino, L. A. (2001). Crack detection and vibration behavior of cracked beams. *Computers & Structures*, 79(16), 1451-1459.
- Yoon, H. I., Son, I. S., & Ahn, S. J. (2007). Free vibration analysis of Euler-Bernoulli beam with double cracks. *Journal of mechanical science and technology*, 21, 476-485.
- Kisa, M. (2011). Vibration and stability of multi-cracked beams under compressive axial loading. *International Journal of the Physical Sciences*, 6(11), 2681-2696.
- Kisa, M. (2012). Vibration and stability of axially loaded cracked beams. *Structural engineering and mechanics: An international journal*, 44(3), 305-323.
- Kisa, M., & Gurel, M. A. (2006). Modal analysis of multi-cracked beams with circular cross section. *Engineering Fracture Mechanics*, 73(8), 963-977.
- Kisa, M., & Gurel, M. A. (2007). Free vibration analysis of uniform and stepped cracked beams with circular cross sections. *International Journal of Engineering Science*, 45(2-8), 364-380.
- Kisa, M., Brandon, J., & Topçu, M. (1998). Free vibration analysis of cracked beams by a combination of finite elements and component mode synthesis methods. *Computers & structures*, 67(4), 215-223.
- Kisa, M., & Brandon, J. A. (2000). Free vibration analysis of multiple open-edge cracked beams by component mode synthesis. *Structural engineering and mechanics: An international journal*, 10(1), 81-92.
- Haskul, M. (2010). *Çatlak içeren değişken kesitli kirişlerde titreşim probleminin sonlu elemanlar metoduyla modellenmesi/Finite element method for the vibration of cracked beams with varying cross section* (Doctoral dissertation).
- Tada, H., Paris, P. C., & Irwin, G. R. (1973). The stress analysis of cracks. *Handbook, Del Research Corporation*, 34(1973).
- Irwin, G. (1960). *Fracture Mechanics*, Editors JN Goodier and NJ Hoff.

OPTIMIZATION OF FDM PARAMETERS TO INCREASE THE COMPRESSIVE STRENGTH OF ABS PARTS

Mehmet Said Bayraklılar

Department of Civil Engineering, Siirt University, Siirt, 56100, Türkiye

Muhammed Tayyip Koçak

Department of Electrical and Electronics Engineering, Siirt University, Siirt, 56100, Türkiye

Department of Software Engineering, Istanbul Health and Technology University, Istanbul, 34000, Türkiye

ABSTRACT

Additive manufacturing (AM) shows a great proficiency in modeling in industry and a wide variety in product shape and size. With the development of EI technology came many challenges, some of which were the fulfillment of the technical requirements of the parts, such as compressive strength, tensile strength, flexural strength, surface finish, and dimensional accuracy. To solve these problems, Acrylonitrile Butadiene Styrene (ABS) materials are being developed, and at the same time, the relevant process parameters are optimized by machine learning methods to achieve the optimal technical requirements of these materials. In this study, the compressive strength of ABS specimens produced by melt stacking modeling (MSM), one of the ML methods, was investigated. Three printing parameters, such as layer thickness, fill ratio, and scanning angle, were used to produce the samples. Taguchi methodology was used to reduce the experimental procedures, and the analysis of variance (ANOVA) method was used to investigate the process parameters to obtain the optimum compressive strength. In the optimization process, the artificial neural network technique was used to determine the best compression parameter values.

Keywords: Additive Manufacturing (AM), Melt Masonry Modeling (MMM), ABS

ANALYZING THE IMPACT OF FLOW FIELD CHANNEL DESIGN VARIATIONS ON PEMFC PERFORMANCE: A COMPUTATIONAL FLUID DYNAMICS (CFD) STUDY WITH CONSTRICTION AND ENLARGEMENT CONFIGURATIONS

Dr. BRAKNI Oumaima

*University of Science and Technology Houari Boumediene (USTHB), Algiers, Algeria.
ORCID NO: 0000-0002-6765-7950*

Dr. Amrouche Fethia

Centre de Développement des Énergies Renouvelables, CDER, 16340 Algiers, Algeria

Dr. Abdallah Mohammedi

Department of Mechanical Engineering, Faculty of Technology, University of Batna 2, Algeria

Prof. KERBOUA ZIARI Yasmina

University of Science and Technology Houari Boumediene (USTHB), Algiers, Algeria,

ABSTRACT

Fuel cell technology, particularly Proton Exchange Membrane Fuel Cells (PEMFCs), plays a pivotal role in the quest for clean and efficient energy solutions. The intricate interplay of fluid dynamics within the flow field channels significantly influences the overall performance of PEMFCs. This study employs Computational Fluid Dynamics (CFD) with Gambit and Fluent to meticulously examine the impact of flow field channel design variations, specifically focusing on constriction and enlargement configurations. Through a systematic analysis, we explore the nuanced effects of these geometric alterations on key performance metrics, including mass transport, water management, and overall cell efficiency. The study employs a multi-dimensional approach, considering diverse operational conditions and electrode configurations. The findings not only shed light on the underlying mechanisms governing PEMFC behavior but also provide valuable insights for optimizing flow field designs to enhance overall cell performance. This research contributes to the ongoing efforts to advance the understanding and efficiency of PEMFCs for a sustainable energy future.

Keywords: PEMFC - Fluent - Fluid dynamics - Fuel cell designs.

STUDY THE EFFECT OF DOPING WITH SILVER NANOPARTICLES ON THE PROPERTIES OF ZIRCONIUM DIOXIDE MEMBRANES AND THEIR EFFECT ON IT AS A GAS SENSOR

Radhiyah M. Aljarrah

Iraq/University of Kufa/ Faculty of Science/ Department of Physics

Ali M. Aljawdah

Iraq/University of Babilon/ Faculty of Science/ Department of Physics

ABSTRACT

In this research, zirconium dioxide ZrO_2 thin films were prepared by pulsed laser deposition method. The deposition process was carried out on glass bases at a temperature of 300°C and a vacuum pressure of 10^{-3} mbar.

The structural, optical and sensitive properties of the prepared films were studied.

The structural properties were studied using X-ray diffraction and finding structural parameters. It was found that the prepared films were of a quaternary phase. It was also found that the process of adding impurities led to improving the crystalline structure of the prepared films. When calculating the structural parameters such as lattice constants and crystal size, it was observed that there was an increase in the grain size from (30 – 100 nm) after adding impurities (nano-silver), also it was found that the preferred plane for crystal growth is (011).

The surface topography was also studied through the results of the scanning electron microscope, where the results showed that the surfaces of all the membranes were uniform, homogeneous, and free of cracks, in addition to the presence of spherical-shaped grains on the surface, and that the doping process led to an increase in the surface roughness. The results of the atomic force microscope showed that the doping process led to an increase in the surface roughness rate.

The optical measurements showed that the transmittance value of the membranes reached 95% and decreased when increases the impurities ratio to 15% at a doping percentage of 9%. There was also an increase in optical absorbance when doping percentages increased. After studying the optical energy gap, it was found that its 4.31 eV for pure films and it was decreased when impurities were added to reach (2.9 eV) at a doping rate of 9%.

Gas sensor for NH_3 gas was prepared from pure and doped (ZrO_2) films, and the sensitivity of the films was studied and found that the maximum sensitivity for pure films was (20 %) and the maximum sensitivity of the ZrO_2 impregnated films was (56 %) at an operating temperature of 250°C when the film was 9% impregnated.



INVESTIGATION OF SOIL AGGRESSIVITY TO UNDERGROUND STORAGE PIPES AND TANKS: IMPLICATIONS OF CORROSION CONTROL

Woyengitonye Butler Abadani

Department of Science Laboratory Technology (Physics Unit), School of Applied Sciences, Federal Polytechnic, Ekowe, Bayelsa State, Nigeria.

ABSTRACT

Corrosion can be as the degradation or deterioration of physical properties of a material due to reaction with its environment. Buried steel tanks and pipelines throughout the world often suffer from soil corrosion; because this relatively benign environment is easily overlooked. This study investigates soil aggressivity to underground storage pipes and tanks, with a focus on implications of corrosion control. Surface geoelectrical sounding method of geophysical survey was used to determine soil aggressivity to buried metallic structures. This method is fast and less expensive compared to the usual approach of soil borings and experimentally measuring soil properties to determine aggressivity. The depth to which pipelines (water mains) and fuel storage tanks are laid is 0 – 10m; which is moderately aggressive in stations 1, 2,7,9, 10 and mildly or non aggressive in stations 3,4,5,6,8. The study recommends the need for government to make available an aggressivity map for the respective states, while soil electrical resistivity survey should be carried out before installation of metal pipes and fuel storage tanks in the subsurface, due to the complex nature of the subsurface in Bayelsa State. the study also recommends that metal pipes and fuel storage tanks to be installed be custom designed based on the respective aggressivity for each station.

KEYWORDS: Soil aggressivity, underground storage, storage pipes, underground tanks, corrosion control

INTRODUCTION

Soil corrosion is the deterioration of metal(s) or other materials brought about by chemical, mechanical and biological process by soil environment. In Nigeria and most part of the world, water mains, the oil, gas and chemical industries primarily rely on underground structures to transport and store their products. These structures include; pipelines for transportation and underground tanks for storage both at the operation, production and retail stations or centres. These facilities generate significant social and economic growth from taxes and creation of thousands of permanent jobs to operate and maintain them. Corrosion is one of the main bones of contention when it comes to environmental issues, and is continually a critical issue for the utility boards, petroleum and chemical industries.

A vast majority of pipelines and storage tanks are made of cast iron and coated to prevent corrosion and contamination of products stored. But all coatings manifest flaws that expose the bare pipe or tank to the soil environment; hence undergoes various types or forms of corrosion which includes; general corrosion, pitting corrosion, filiform corrosion, etc (Okiongbo and Akpefure, 2012). Corrosion reduces the expected life span of pipelines and fuel storage tanks which often results in ruptures. Rupture of these structures (i.e underground pipelines and storage tanks) can result in the fuel leaks and seepage into the ground which have devastating ecological consequences. Given the implication of such rupture and that which corrosion plays, it is imperative that the prediction of potential aggressivity of soil and thus the application of proper corrosion control measures be taken not only to protect the environment from spillage(s) but also avert cost of repair, replacement clean up, lost and of lives and properties.

The control and effective minimization of corrosion is possible by proper understanding of the characteristics of the material and the environmental condition(s) in which they are to be used or seated. This enhances the design of the cast iron. Soil aggressivity is not a measurable parameter. Therefore, in the evaluation of aggressivity, a list of critical parameters is usually employed. These include; moisture content, PH value, Redox potential, etc (Okiongbo and Akpefure, 2012). Soil borings and experimentally measuring these properties provides the principal source of information for determining soil aggressivity (Okiongbo and

Ogobiri, 2012). The electrical resistivity is highly significant in cases in-situ determination if the degree of soil aggressivity of soil. Also it is an indicator of soil aggressivity; as the rate of aggressivity is a function of the electrical conductivity (Khare and Nahar, 1997).

Evidence pertaining the subsurface soil types, its moisture content, and aggressivity can be determined from surface resistivity measurements, the vertical electrical sounding (VES) method of geophysical investigation is a non-invasive, relatively cheap technique that provides data for the diagnosis of corrosion of buried fuel storage tanks and pipelines (Okiongbo and Akpefure, 2012).

The intent of this project is to create a public awareness of soil related risks and hazards that may not be really apparent in this way; users will be able to use this information to assess the risks assets, either as means of prioritising maintenance and liability of improving design new installations.

DESCRIPTION OF THE STUDY AREA

Yenagoa, the capital of Bayelsa state is one rapidly growing urban centre in Nigeria. Yenagoa is surrounded by major communities such as; Tombia, Emeyal, Oloibiri, Otuoke, Ogbia, Elebele, etc. It has a total mass of over 70km² bounded by longitude 4°38'N, latitude 6°3' and 6°40'E. There are two climatic seasons; the wet (raining) and the dry season. There are various perennial streams and rivers in the area which form a network that empties into the Atlantic Ocean. As such most of its terrain is marshy.

GEOLOGY OF THE STUDY AREA

The geology of the study area is same as that of the Niger Delta. The formation of the present day started during the early Palaeocene and resulted mainly from the build-up of fine grained sediments eroded and transported by the river Niger and its tributaries. The subsurface geology of the Niger Delta consists of three lithostratigraphic units (Akata, Agbada and Benin Formations) which are in turn overlain by various types Quaternary deposits.

The Benin formation (2100m) is made up of over 90% massive, porous coarse sands with localised clay/shale interbeds (Allen, 1965). The Quaternary deposits (40 to 150m thick) generally consists of rapidly alternating sequences of sand and silt/clay with the latter becoming increasingly more prominent seawards. Benin formation is where all boreholes sunk.

Agbada formation (paralic clastics), this formation forms the hydrocarbon prospective sequence in the Niger Delta. It is represented by an alternation of sands, silt and clays in various proportions and thickness representing cyclic sequence of offlap units. Most exploration wells in the Niger Delta have bottomed in this lithofacies, which reaches a thickness of more than 3000m.

Akata formation is composed of shales, clays and silts at the base of the known delta sequence. They contain a few streaks of sand, possibly of tubidic origin and were deposited in holomarine (Delta front to deep marine) environments (Short and Stauble, 1967).

AIMS OF THE STUDY

The aims of this study are to;

- i. Determine the aggressiveness of the soil in Yenagoa and its environs to buried metallic utility pipes and fuel storage tanks.
- ii. Provide detailed underground management information (soil aggressivity in Yenagoa and its environs).
- iii. Examine the mitigation measures in the light of the degree of corrosivity.

SCOPE OF THE STUDY

The scope of this study is to;

- i. To acquire Vertical Electrical Sounding (VES) data
- ii. Process and interpret the VES data acquired in (i) above
- iii. Classify the soil electrical resistivity obtained from (ii) above in terms of soil aggressivity/corrosivity.

LITERATURE REVIEW

Corrosion can be as the degradation (i.e deterioration of physical properties of the material) of a material due to reaction with its environment. Buried steel tanks and pipelines throughout the world often suffer from soil corrosion; because this relatively benign environment is easily overlooked. The economic consequences of this oversight thus come in the form of repairing and replacing of so many such structures. Long term corrosion results in loss of products, contamination of the soil environment and accidents that cause loss of properties and lives (Jones and Denny, 1996).

THE NATURE OF THE SOIL

Soil is a naturally unconsolidated deposit of materials that cover the surface of the earth; whose chemistry is capable of supporting life growth. Soil is a product of natural decomposition, chemical and physical weathering of materials acting upon rocks, vegetation and animal matters over some geologic time.

The factors involving the formation of soil are:

- i. Living matter
- ii. Climate
- iii. Relief,
- iv. Parent materials

Soil is a habitat of the plant; as such its chemical, physical and biological properties affect or influence soil aggressivity rate.

This study focuses on the physical properties, which are:

- i. Pore space
- ii. Size.

The pore space has a direct effect on the movement of water; which determines the rate of corrosion of a soil. The size of grains determines the rate at which soil can retain water which also affect corrosivity.

CORROSION AS AN ELECTROCHEMICAL PROCESS

If a piece of bare iron is left outside where it is exposed to moisture, it will rust quickly. It will do so more quickly if the moisture is salt water. The corrosion rate is enhanced by an electrochemical process in which a water droplet becomes a voltaic cell (i.e electrochemical cell that derives electrical energy from spontaneous redox reaction taking place within the cell) in contact with metal, oxidising the iron.

Underground environment contains moisture and the first step in the occurrence of corrosion is the formation of a soluble chemical compound containing the metal which is corroding. Iron does this fairly readily whereas more resistant metals such as copper corrode slowly (Corcoran et al, 1977).

When iron pipes are buried in the soil, the nature and result of the chemical properties of the pipe changes, depending on the spatial characteristics of both metal and soil conditions. For example, the structure of the metal varies, stress can be induced, moisture content and composition of the soil may change and the degree of aeration may fluctuate. Due to this variation at certain points on the metal or pipe surface, the metal atoms pass more readily into solution than those at other points or places.

Neutral metal atoms leave the metallic structure and become positively charged ions and thus corrosion proceeds. Such affected area constitutes the anode and a corresponding cathode is on an adjacent area of the metal which is not corroding.

An electric circuit is established via the soil and metal electrolyte.

Thus corrosion proceeds until the entire metal is consumed or some constraining influence stops the process. Figure 1 below shows corrosion taking place as a result of differential aeration. Also the chemical reaction of corrosion is expressed as thus;

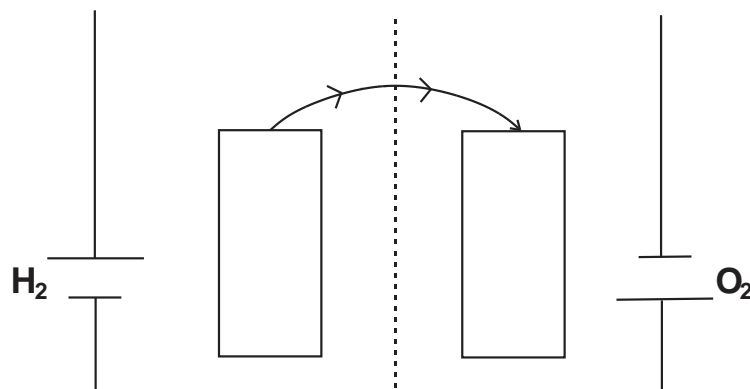
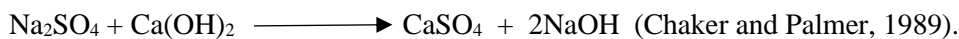


Figure 1: A DIAGRAM OF ANODE – CATHODE REACTION (Khare and NAhar, 1996)

TYPES OF CORROSION

The effect of the reaction of a metal with its environment may take variety of forms according to the nature of the attack on the metal and of the reaction product (Khare and Nahar, 1996).

Below are the various types of corrosion

- i. Uniform corrosion
- ii. Pitting corrosion
- iii. Filiform corrosion

UNIFORM CORROSION

When the reaction between the metal and the environment extends over the entire surface of the metal; it is referred to as “general or uniform corrosion”. In uniform corrosion, the anodic and cathodic sites or positions cannot be distinguished. Actual anodic current density (i_a) and cathodic current density (i_c) are equal ($i_a = i_c$) (Khare and Nahar, 1996).

PITTING CORROSION

When the reaction between the metal and the environment is confined over a localised area; it is called Pitting Corrosion”. In this case, different area of the metal surface are predominantly “anodic or cathodic”. The

attack is therefore localised and frequently intense. In Pitting Corrosion, the anodic current density (i_a) is greater than the cathodic current density (i_c) ($i_a > i_c$) (Khare and Nahar, 1996).

FILIFORM CORROSION

This type of corrosion occurs under painted or plated surfaces when moisture permeates the coating lacquers and “quick-dry” paints are most susceptible to the problem. The use of such (quick-dry) paints should be avoided unless on the absence of an adverse effect that has been proven by field experience.

When coating is required, it should exhibit low water vapour transmission characteristics and excellent adhesion. Zinc rich coatings should also be considered for coating carbon steel(s) because of their cathodic protection quality. Filiform corrosion normally starts at small, some microscopic defects in the coating.



SOIL PROPERTIES AFFECTING CORROSION

The following are the factors affecting the degree of corrosion in ferrous metal (cast iron).

Electrical Resistivity

The corrosion of ferrous metals in the soil is essentially an electrochemical process and it depends upon the presence of an electrolyte. This can be accessed by measuring the electrical resistivity which is proportional to the concentration of soil electrolyte (Khare and Nahar, 1996); it is the main indicator of corrosivity.

Electrical resistivity depends on soil moisture content and concentration of current carrying soluble ions (Palmer, 1989).

Table 1.0: Classification of Soil Aggressivity (Okiongbo and Ogobiri, 2012)

S/NO	RESISTIVITY (Ohm-m)	SOIL AGGRESSIVITY
1.	Up to 10	Very Strongly Aggressive (VSA)
2.	10 -60	Moderately Aggressive (MA)
3.	60 – 180	Slightly Aggressive (SA)
4.	180 – above	Practically non- Aggressive (PNA)

Oxidation Reduction Potential

The oxidation reduction potential of a soil is significant because sulphate reducing bacteria can live only under anaerobic conditions. These bacteria(s) can reduce sulphate to sulphide and the corresponding oxidation of elemental hydrogen involves them in the corrosion mechanism.

Below is a table for the criteria of (ORP) in terms of corrosivity.

Table 2.0: The relationship between ORP and Soil Aggressivity (Khare and Nahar, 1996)

S/NO	RANGE OF SOIL ORP (Mv)	CLASSIFICATION OF SOIL AGGRESSIVITY
5.	<100	Severely Aggressive
6.	100 – 200	Moderately Aggressive
7.	200 – 400	Slightly Aggressive
8.	>400	Non Aggressive

Moisture Content

A moisture content of more than twenty percent (>20%) is likely to increase soil aggressiveness. A moisture content of twenty percent (20%) is the value at which the whole of a metal surface is in contact with the soil and may be regarded as electrochemically active (Khare and Nahar, 1996).

pH

pH expresses an energy level of protons present in the soil. As the pH value increases, the degree of aggressiveness decreases. For a pH of 4, it becomes constant. The degree of aggressiveness of iron between pH of 4 and pH of 9 is virtually unchanged except when sulphate reducing bacteria(s) are present.

Table 3.0: Classification of Soil Aggressivity in relation to pH values (Khare and Nahar, 1996)

S/NO	pH values	Classification of Soil Aggressivity
1.	≥8	Most Aggressive
2.	7	Very Severely Aggressive
3.	< 4	Severely Aggressive
4.	6.5 – 7.5	Moderately Aggressive

Although soil corrosivity potential can be estimated using resistivity, pH value, redox potential, etc. traditionally, appropriate information to estimate corrosivity is obtained by obtaining soil borings and experimentally determining the above soil properties. But the above procedure requires considerable laboratory resources and it is very expensive.

Since electrical resistivity is the dominating parameter in causing corrosion to buried iron water main and fuel storage tanks. Then, we can use electrical resistivity method to categorise the aggressiveness of a soil.

SURFACE RESISTIVITY METHOD

Surface electrical resistivity survey is based on the principle that the distribution of electric potential in the ground around a current electrode depends on the electrical resistivity distribution of the surrounding soil and rocks. The traditional practice is to apply a direct current (D.C) between two electrodes implanted in the ground and to measure the potential difference (p.d) between two additional electrodes that do not carry current (Wightman, et al, 2003).

Mineral grains comprise of soil and rocks which are essentially nonconductive except in some materials (such as metallic ores), the resistivity of soil and rocks is governed by the amount of moisture content, its resistivity, etc (Okiongbo and Ogobiri, 2012). To the extent, difference in lithologies are accompany by difference in resistivity. Electrical resistivity survey is useful in determining soil corrosivity, estimating depth of bee rocks, etc (Wightman et al, 2003).

Generally, resistivity of a soil or rock is controlled primarily by the moisture content. Hence, there are wide ranges in resistivity for any particular soil or rock type and resistivity values cannot be interpreted directly in terms of soil type or lithology (Wightman et al, 2003).

Electrical method has inherent limitations that affect accuracy that is expected. Like every other method, the value of a measurement obtained at any location represents a weighted average of the effects produced over a large volume of material, with the nearby portion contributing most heavily (Wightman et al, 2003).

Resistivity survey data are represented in the form of values of apparent resistivity (ρ_a). Apparent resistivity is the resistivity of an electrically homogenous and isotropic half space that would yield the measured relationship between the applied current and the potential difference for a particular arrangement and spacing of electrodes.

In addition to current electrodes, figure 1 shows a pair of potential electrodes M and N.

From figure 1, the potential difference may be written as:

$$V = U_M - U_N \\ = \frac{\rho I}{2\pi r} \left\{ \frac{1}{AM} - \frac{1}{BM} + \frac{1}{BN} - \frac{1}{AN} \right\} \dots\dots\dots(1)$$

Where;

U_M and U_N are the potential at M and N

To investigate resistivity variation with depth, we use the schlumberger array configuration. The apparent resistivity (ρ_a) is affected by materials at increasingly great depth as the electrode spacing is increased. Because of this effect, a plot ρ_a against electrode spacing may be used to indicate vertical variation in resistivity (Wightman *et al.*, 2003).

TYPES OF ARRAY CONFIGURATION

Schlumberger Array

The electrodes M and N are fixed and A and B are moved outwards symmetrically in steps. At some point, the capability of the measuring device generally falls down in which case MN (potential electrodes) distance is increased to compensate for the fall in potential. Bearing in mind that $MN \ll \frac{AB}{2}$. It is advisable to repeat readings at these points.

The apparent resistivity may sometimes differ significantly at these points (i.e the repeated values). If these results are plotted as ρ_a against $\frac{AB}{2}$, each step of ρ_a value obtained in these points will be found to lie on a separate curve segments displaced from each other.

The different segments must be suitably merged to obtain a single smooth sounding curve. However, the predominant contributions to shift come from the differing effect of local inhomogeneities at the old and new points of MN (Parasnis, 1997).

Furthermore, from figure 2, geometry factor (K) arising from the schlumberger array configuration is expressed as;

$$K = \frac{\pi a^2}{b} \left\{ 1 - \frac{b^2}{4a^2} \right\} \dots\dots\dots(2)$$

Where

$$a = \frac{AB}{2}$$

$$b = MN$$

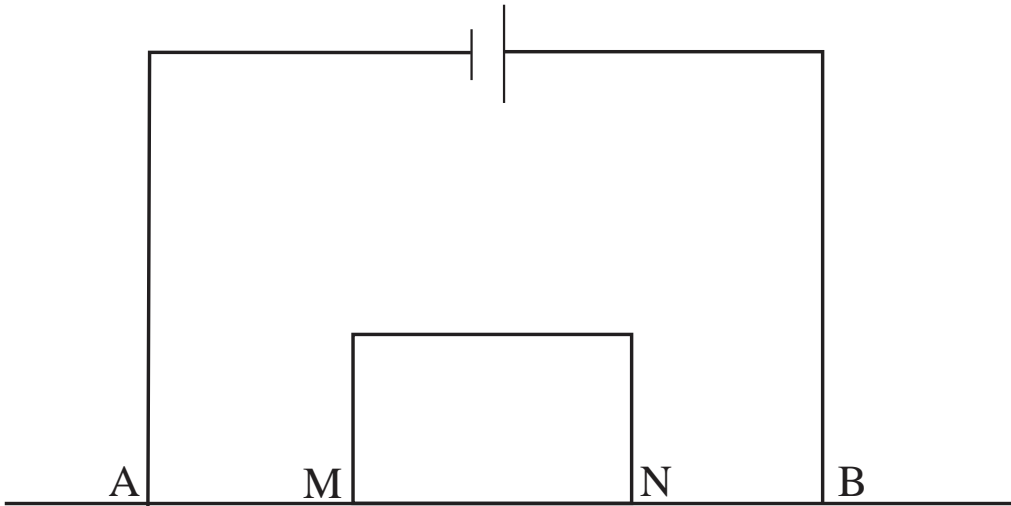


Figure 4.0: Schlumberger Array Configuration

From Figure 1, the apparent resistivity in terms of the applied current, distribution of potential and arrangement of electrodes is given below through examination of potential distribution due to a single electrode. The effect of an electrode pair is found by superposition.

Consider a single point electrode located on the boundary of a semi-finite electrically homogeneous medium, which represents a fictitious earth. If the electrode carries current I, the potential at any point in the medium is given by

$$U = \frac{\rho I}{2\pi r} \dots\dots\dots(3)$$

Where;

U is potential V

P is resistivity of medium

R is electrode(s) distance

For an electrode pair with current I at electrode A and -I at electrode B in figure 1; the potential at a point is given by the algebraic sum of the individual contributions.

$$U = \frac{\rho I}{2\pi r_A} - \frac{\rho I}{2\pi r_B}$$

$$= \frac{\rho I}{2\pi} \left\{ \frac{1}{r_A} - \frac{1}{r_B} \right\} \dots\dots\dots(4)$$

Where r_A and r_B is the separation between A and B.

The quantity inside the bracket in equation (1) is a function of the various electrode spacing and it is denoted by $\frac{1}{K}$ which allows the rewriting of the expression as;

$$V = \frac{\rho I}{2\pi K} \dots\dots\dots(5)$$

Where K is the geometric factor from the Schlumberger array configuration

$$\therefore \rho = 2\pi K \frac{V}{I} \dots\dots\dots(6)$$

N/B: when the measurements are made in a heterogeneous earth, the ρ is replaced with ρ_a . Hence

$$\rho_a = K \frac{\Delta V}{I} \dots\dots\dots(7)$$

WENNER ARRAY

the Wenner Array configuration also consists of four electrodes which are equally spaced. Setting $r_1 = r_4$ and $r_2 = r_3$. Below is a diagram showing a typical Wenner Array configuration.

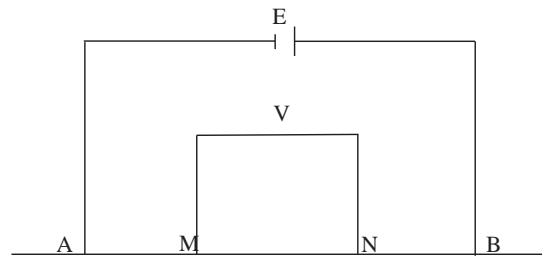


Figure 5.0 A diagram of Wenner Array Configuration

From the above figure 3;

$$K = 2\pi a$$

$$P = 2\pi a \frac{V}{I} \dots\dots\dots(8)$$

For depth exploration, using the Wenner configuration, the electrodes are expanded about a fixed central point. Increasing the spacing “a” in steps for lateral exploration or mapping the spacing remains constant and all four electrodes are moved out equally.

METHODS AND MATERIALS

Instrumentation

The instruments used in carrying out the electrical resistivity survey are;

- i. ABEM TERRAMETER (SAS 1000): This is used in measuring the resistivity variation of the subsurface
- ii. CAR BATTERY: A 12 volt car battery was used in powering the Abem Terrameter .
- iii. FIVE ELECTRODE(S): Two electrodes were used as current electrodes (C1 & C2) in sending current to the subsurface and two electrodes were used as the potential electrodes (P1 & P2), while the remaining one electrode was used as a central point.
- iv. FOUR HAMMERS: These hammers were used in implanting the electrodes into the subsurface.
- v. GLOBAL POSITIONING SYSTEM (GPS): This was used to locate survey site and also to measure the site elevation.
- vi. MEASURING TAPES: These measuring tapes were used in measuring point(s) of move out.
- vii. CABLES: Four reels of flexible electrical cables of diameter 2.11mm were used in the survey; two for current electrodes and the remaining two for potential electrodes.
- viii. RECORDING SHEET: This was used in recording measured resistivity value(s) that were displayed by the Abem Terrameter and also the elevation and coordinates recorded by the GPS.

Data Acquisition

A total of VES stations were occupied in various communities in Yenagoa and its environ. The variation of resistivity with depth also known as Vertical Electrical Sounding (VES), reflecting more or less horizontal stratification of the earth materials. The schlumberger array configuration was used in the data acquisition.

It is required that $\frac{AB}{2} \geq 5MN$.

In data acquisition, expanding $\frac{AB}{2}$ while MN is fixed, the process yields a rapid decreasing potential difference across MN which ultimately exceeds the measuring capability of the Terrameter. At this point MN is increased typically 2 to 4 times larger than the preceding value and the survey is continued.

A table showing the recording sheet and the manner in which field measurement(s) are commonly taken at $\frac{AB}{2}$ and MN is presented in appendix A.

Data Analysis

In processing the data, the geometric factor $K = \frac{\pi a^2}{b} \left\{ 1 - \frac{b^2}{4a^2} \right\}$ was used.

Apparent resistivity was determined by simply multiplying the resistance measured by the Abem Terrameter with geometric factor. The results obtained from the above operation was plotted on a log -log graph with electrode spacing $\frac{AB}{2}$, and outliers were filtered using IPI2WIN (1D resistivity sounding interpretation software). This constitutes the field curve. Afterwards, we put these values into Interpex (1D resistivity Data inversion software) which was further subjected to computer assisted iterative interpretation. This software was used to perform a qualitative analysis and interpretation of the field curves.

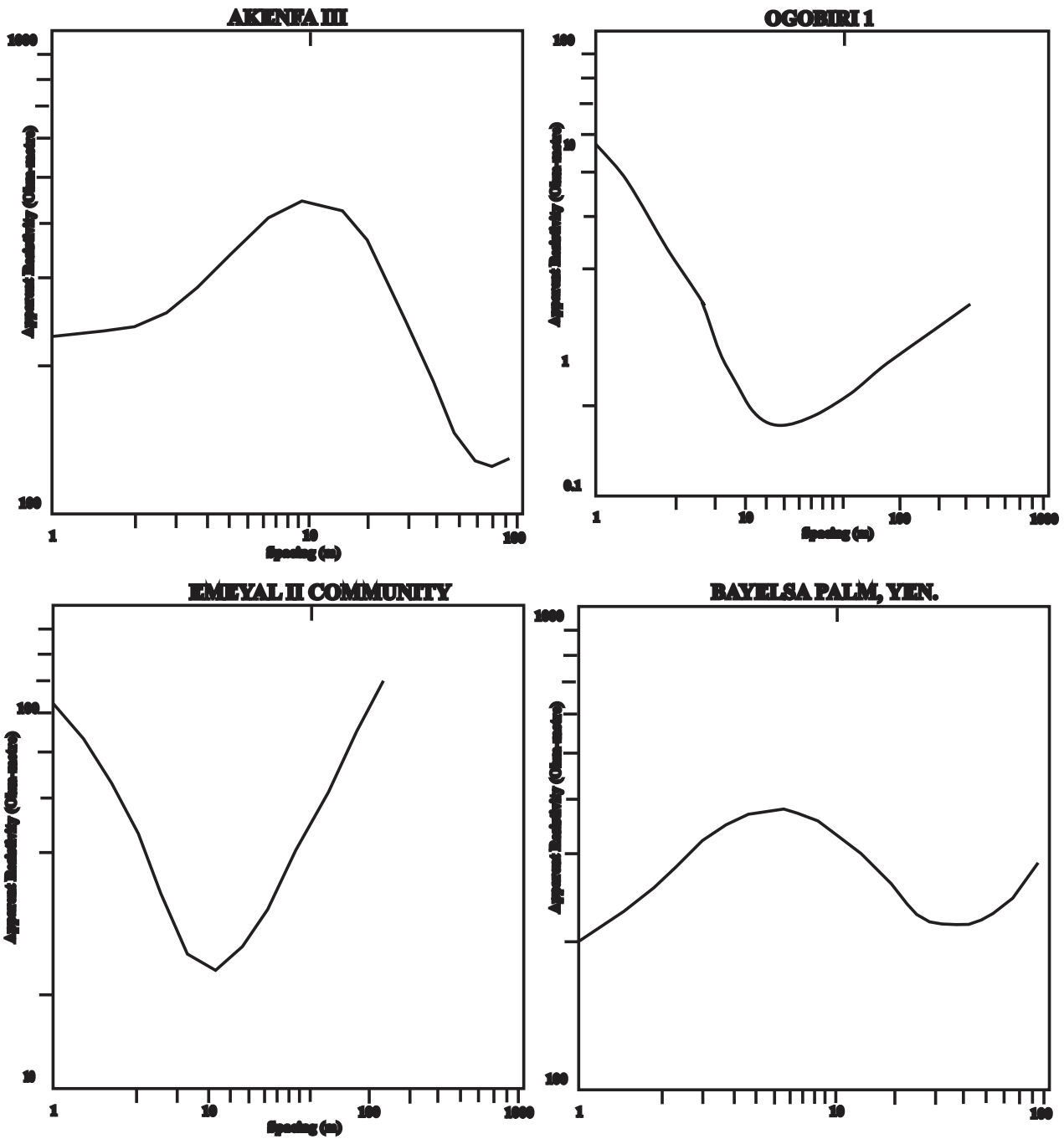
The software requires that the user introduces the thickness, and resistivity of the subsurface layers. The theoretical curve for initial input parameters is then compared with the field curve. The method of iteration was then performed until a fit error between field and synthetic curve is of the range 0 to 2.5% and is constant.

Thus, the software yields the thickness and resistivity of the various layers. The model parameters for each VES station, as well as the percentage rms error are presented in chapter four.

PRESENTATION AND DISCUSSION OF RESULTS

Presentation of Results

The form of geoelectrical sounding curves vary considerably throughout the study area, but having more of the HA, KH, HK a A type curves with 3 – 4 interpretable geoelectric layers shown in figure 5.0



The model parameters for each VES station. Was well as the percentage root mean square (rms) error which provide a quantitative and qualitative assessment of the interpretation is presented in table 4.0

Table 4.0: Summary of Modelled Results for All Sounding.

VES NO	RESISTIVITY (Ω m)				LAYER THICKNESS (m)				FITTING ERRON (%)
	1	2	3	4	1	2	3	4	
1	311.93	57.37	24.76		0.68	2.46	10.76		2.01
2	221.00	87.95	48.67		1.02	4.27	7.43		1.05
3	610.21	16.03	82.05		0.50	2.00	18.00		1.90
4	189.72	36.11	689.48		1.34	2.08	1.44		2.60
5	229.07	193.57	2168.70	78.96	1.80	0.83	2.50	36.60	1.75
6	1152.30	6243.60	1130.80	20377.00	0.90	3.00	35.75	139.4	0.7
7	91.80	49.50	15.1		0.50	1.20	11.70		1.11
8	202.43	49.40	1573.80		0.60	8.00	7.600		1.56
9	16.70	28.50	36.25		1.50	9.14	25.77		0.8
10	220.80	91.92	43.44		0.94	5.00	13.40		0.3

DISCUSSION OF RESULTS

Most of the sounding curves obtained were of HA-type ($\rho_1 > \rho_2 < \rho_3 > \rho_4$), i.e a bowl shaped curved with a steeply descending left branch and a gently ascending right branch representing the presence of four geoelectric layers (Fig. xxxx). The terminal branch of many of the HA curves rose steeply into positive slopes that made inclination angle 45° with the abscissa. Such a steep rise in a sounding curve is a reflection of highly resistive sedimentary rocks at depth. The descending left branch indicates a resistive top soil underlain by a conductive in material could possibly be wet clays (Okiongbo and Ogobiri, 2012).

From the interpretation of these data, we have seen that resistivity generally increases with depth in the Niger Delta corroborating the findings of the results reveal wide irregular variation in resistivity both vertically and laterally. This supports the complex depositional environment of the study area. Since pipelines and fuel storage tanks are expected to be buried in the subsurface within the depth of 0 – 10m; therefore we restrict our interpretation to the top ten metres only. The first unit corresponding to a depth of 0 – 10m 9 (table 4.0), representing the surface soil resistivity of 92 - 312 Ω m. The variation of surface soil resistivity is attributed to local conditions prevailing at the points. The relatively higher values of resistivity indicates dry soils and the presence of coarse sand, and relatively lower values indicates wet grains of finer sizes and different mineralogical composition such as fine sands, salt and clays. The finer the size of the grains, the greater the specific surface area per unit bulk volume, grain volume, or pore volume which enables the grains to absorb charged ions at their surfaces and thus, the conduction of electric current will be easier (Okiongbo and Ogobiri, 2012). The depth range of 1.0 to 2.5m represents the aeration zone above the water table and exhibits resistivity range of 28 to 6243 Ω m.

Generally, resistivity variations are as a result of changes in lithology, size, shape of grains, pore water salinity and clay content. The formations of large aggressive cells that lead to severe corrosion failures are associated with low resistivities. A low resistivity is classified as a very severely aggressive soil which is an indicator of aeration and excess wetness in the soil. For resistivity exceeding 180 Ω m, the medium is moderately aerated; hence corrosion cells may not form. However, there are stations where soil resistivity is very low (in stations 1, 2, 7, 9 and 10); these stations are considered strongly aggressive to moderately aggressive to buried steel water mains and fuel storage tanks. Five points out of the ten stations occupied is considered to be mildly aggressive to non aggressive to buried metallic structures.

IMPLICATIONS FOR CORROSION CONTROL

Since the corrosiveness of soil may change on a yearly basis; there is no prediction as to how long the service life of buried metal(s) can last before failure.

PROTECTIVE COATING

Most at times when coating is used as a preventive tool against corrosion; the metal or steel is coated to reduce the cathode and anode surface area ratio. Thus decreasing aggressivity rate. Buried metal materials act both as anode and cathode. Because the region of metal acting as cathode is not always known, it is best to coat the entire material and use some method of cathodic protection (Kuan et al, 2006).

CATHODIC PROTECTION

Cathodic protection is a way of reducing the corrosion potential to decrease the corrosion rate of a metallic material. The most common types are impressed current cathodic protection and sacrificial anode cathodic protection.

SACRIFICIAL ANODE CATHODIC PROTECTION

Sacrificial anode protection occurs when a metal is coupled to a more reactive (anodic) metal. This connection is referred to as galvanic couple. In order to effectively transfer corrosion from the metal structure, the anode material must have a large enough natural voltage difference to produce an electric current flow. The sacrificial anode cathodic protection system provides the driving potential from a natural electromotive force difference between the anode (grounded) and the metal to be protected; therefore it is used in areas of very low resistivity.

Effective application of cathodic protection can provide complete protection to any exposed areas for the life of the metallic structure. The combination of an external coating and cathodic protection provides most economical and effective choice for protection of buried pipelines (water mains) and fuel storage tanks. For bare ineffective coated existing pipeline, cathodic protection often becomes the only practical alternative for corrosion protection. Three metals are commonly used for cathodic protection of steels. The choice of selection is based on the resistivity and electrolyte. A general application guide is provided below

- i. Magnesium : This is applicable to fresh water and soil
- ii. Zinc: This is applicable to low resistivity soil and saltwater
- iii. Aluminium: This is applicable to saltwater and limited fresh water.

One important feature of the sacrificial anode system is the minimal maintenance required for these systems to function (Francis, 2003).

IMPRESSED CURRENT CATHODIC PROTECTION

The buried pipes and fuel storage tanks receive current from a D.C power source via an auxiliary inert electrode buried in the ground. The pipe becomes the cathode and the auxiliary electrode the anode. In this case the iron will dissolve from the anode by the reaction given below;



and the electrode is described as a consumable electrode. If the anode is an electrochemical inert material (metal), the surrounding will be oxidised and water reaction will occur.



In saline solution, however, chlorine may be produced at the anode. Magnetite, carbonaceous material (graphite), lead oxide are the materials commonly used for the anode, etc. This is because of their high resistance to corrosion. One important feature of the impressed current cathodic protection (ICCP) system is that it is constantly monitored for the electrical potential of the soil or sea water in order to carefully adjust the output anodes (voltage) (Francis, 2003).

CAOTING – CATHODIC PROTECTION

Coating is often applied to prevent corrosion. But all coating contain flaws that expose the bare pipeline and fuel storage tanks to the subsurface environment and thus undergoes corrosion at these coating flaws. Therefore, the most effective method for preventing corrosion is to use coating in conjunction with cathodic protection (Beaver et al.).

An important consideration in cathodic protection is the location and nature of the site where the anode(s) is placed (groundbed). For the anodes of groundbed system discharge useful amount of current, the contact resistance between the anodes and the earth must be low. The groundbed resistance is expressed as

$$R_A = \frac{\rho}{2\pi l} \left[\ln \frac{4l}{r} - 1 \right] \dots\dots\dots(9)$$

Where,

R_A is the groundbed resistance

ρ is the soil resistivity

l is the length of the active bed

r is the radius of the active bed.

The above expression indicates that high soil resistivity would require low bed resistance required for optimum cathodic-coating protection system (Okiongbo and Ogobiri, 2012).

CONCLUSION AND RECOMMENDATIONS

Surface geoelectrical sounding method of geophysical survey was used to determine soil aggressivity to buried metallic structures. This method is fast and less expensive compared to the usual approach of soil borings and experimentally measuring soil properties to determine aggressivity. The depth to which pipelines (water mains) and fuel storage tanks are laid is 0 – 10m; is moderately aggressive in stations 1, 2,7,9, 10 and mildly or non aggressive in stations 3,4,5,6,8.

The following are the recommendations based on the findings of the study.

- i. Due to the complex nature of the subsurface in Bayelsa State; soil electrical resistivity survey should be carried out before installation of metal pipes and fuel storage tanks in the subsurface.
- ii. The metal pipes and fuel storage tanks to be installed be custom designed based on the aggressivity determined from (i) for each station.
- iii. The government should provide or produce an aggressivity map for the state.

REFERENCES

- Allen JRL (1965), Late Quaternary Niger Delta and Adjacent Areas: Sedimentary Environment and Lithofacies. American Association of Petroleum Geologists, Bulletin 2: 429 – 431.
- Butlin, K.r and W.H.J. Vernor (1949), Institute of Water Engineers, London, p. 3, 627.
- Corcoran, Jarvis, Mackney, Stebens (1977), Soil Corrosiveness in South Oxfordshire. Soil science, Vol. 28, p.473 – 484.
- Corfield, G, (1930), Method of determining soil corrosivity. L.A Gas and Electric Corporation, U.S.A.
- Chaker, Victor Ed (1972), Corrosion forms and control for infrastructure. American Society for testing and materials, ASTM International, p.81.
- D.S Parasnis (1997), Principles of Applied Geophysics. Fifth Edition, Chapman and Hall, London, p.127 – 133.

- J.A. Beavers, and N.G. Thompson (2006), External Corrosion of Oil and Natural Pipelines. American Society of Engineers Handbook 13c.
- J.E.A. Osemeikhian, M.B. Asokhia (1997), Applied Geophysics for Engineers and Geophysicists. First Edition, p.96 – 103.
- Kuan Jung (Calvin) Chen, Nicholas Paravasquez, Hsien Cheng Pu (2006), Corrosion in soil and concrete, University of California, U.S.A.
- K.S. Okiongbo and G. Ogobiri (2012), Predicting Soil Corrosivity Along a Pipeline Rout in the Niger Delta Basin using geoelectrical method; Implications for Corrosion Control. Journal of Geotechnical and Geological Engineering.
- M. Khare and S.N. Nahar (1996), Soil Aggressiveness towards buried water pipes. Environmental Technology, Vol. 18, p.187 – 192
- Robinson, W.C (1993), Testing for Corrosiveness; environmental effects, U.S.A
- Smith, W.H (1968), Soil Evaluation in Relation to Cast Iron Pipes. JAWWA, p.60, 221 – 227.
- Wightman, W. E. JAlinos, F. Sirles, P. Hanna (2003), Application of Geophysical Methods for Highway Related problems. Federal Highway Administration, Central Federal Lands Highway Division, Lakewood, Co Publication No. FHWA-IF-04-021
- [http://www.cflhd.gov/resources/agm\(2003\)](http://www.cflhd.gov/resources/agm(2003))
- [http://www.corrosionsource.com\(2003\)](http://www.corrosionsource.com(2003))
- [http://www.contechsystems.com\(2001\)](http://www.contechsystems.com(2001))
- [http://www.mesaproducts.com\(2005\)](http://www.mesaproducts.com(2005))
- [http://www.coninstitute.sc\(2001\)](http://www.coninstitute.sc(2001))

**SENSORLESS MAXIMUM POWER EXTRACTION CONTROL USING PERTURB AND
OBSERVE (P&O) METHOD FROM PERMANENT MAGNET SYNCHRONOUS GENERATOR
(PMSG) BASED WIND ENERGY CONVERSION SYSTEM (WECS)**

Hicham Sayhi

Electricals Engineering Laboratory of Biskra LGEB, University of Biskra, Biskra, Algeria

Amor Bourek

Electricals Engineering Laboratory of Biskra LGEB, University of Biskra, Biskra, Algeria

Abdelkarim Ammar

*Signals and Systems Laboratory (LSS), Institute of Electrical and Electronic Engineering, University of M'hamed BOUGARA of
Boumerdes, Boumerdes, Algeria*

Ilyes Dahnoun

Electricals Engineering Laboratory of Biskra LGEB, University of Biskra, Biskra, Algeria

ABSTRACT

By adjusting the wind turbine's rotational speed, wind energy conversion systems (WECS) can maximize power extraction. For the purpose of improving maximum power extraction, This study proposes a sensorless maximum power extraction control from WECS using a permanent magnet synchronous generator (PMSG). The proposed technique does not require information about wind speed or turbine characteristics necessary to calculate the duty cycle of the boost converter. Whereas it uses the output voltage and current of a rectifier. To achieve quick convergence, the duty cycle's step size is adaptively adjusted based on the variation between the rectifier's output power and its previous duty cycle, up until the maximum power point is reached. SIMPower simulations are used to assess the effectiveness of the proposed sensorless maximum power extraction control.

Keywords: maximum power point tracking (MPPT), permanent magnet synchronous generator (PMSG), wind energy conversion system (WECS), perturbation and observation, simpower, Boost Converter, uncontrolled rectifier, sensorless.

A TECHNICAL SURVEY ON ENERGY POTENTIALS OF POINT FOCUS SOLAR COLLECTOR SYSTEM: A SUSTAINABLE RESOURCE FOR ENERGY MIX AUGMENTATION

Imoh Ime Ekanem

*Department of Mechanical Engineering, Akwa Ibom State Polytechnic, Ikot Osurua, PMB. 1200, Nigeria.
ORCID ID: 0000-0002-8973-9260*

Aniekan Essienubong Ikpe

*Department of Mechanical Engineering, Akwa Ibom State Polytechnic, Ikot Osurua, PMB. 1200, Nigeria.
ORCID ID: 0000-0001-9069-9676*

ABSTRACT

The increasing demand for energy and the need to reduce greenhouse gas (GHG) emissions, has led to a growing interest in exploring alternative energy sources. Point focus solar collector (PFSC) systems, have emerged as a promising technology for harnessing solar energy and converting it into electricity or heat. This survey was conducted on the energy potentials of PFSCs including their efficiency, cost-effectiveness, environmental impact, and potentials for integration into the existing energy infrastructure. Findings revealed that PFSC systems involves zero GHG emissions, making them a clean and sustainable energy option that contributes to the reduction of GHG emissions. It was observed that the levelized cost of electricity (LCOE) from PFSC systems has become competitive with conventional energy sources, such as coal and natural gas. This cost-effectiveness, combined with the potential for long-term savings on fuel costs, makes PFSC systems an attractive option for energy mix augmentation. Considering their power potentials, PFSC systems can be integrated into the grid to provide electricity during peak demand periods or to supplement the energy supply during periods of low solar radiation. Also, they can be combined with thermal energy storage technologies to provide a continuous and reliable energy supply. Conventional studies indicated that the efficiency of PFSC systems depends on various factors, including the type of collector, the concentration ratio, and the tracking mechanism. The high efficiency, cost-effectiveness, and minimal environmental impact make PFSC systems a viable option for large-scale energy production. Thus, with PFSC systems, the energy mix can be augmented to reduce the reliance on conventional energy sources while contributing to a more sustainable and secured energy future.

Keywords: Energy potential, Solar collectors, Energy mix, GHG emissions, sustainability.

DESIGNING A PROTOTYPE FOR BOTH TRANSMITTER AND RECEIVER SECTIONS OF MORSE CODE COMMUNICATION USING ARDUINO UNO

Husain M. Ahmad

M College of Engineering and Technology, American University of the Middle East, Eqaila, Kuwait

Ahmad B. Alazmi

M College of Engineering and Technology, American University of the Middle East, Eqaila, Kuwait

Muammer Catak

M College of Engineering and Technology, American University of the Middle East, Eqaila, Kuwait

ABSTRACT

Assistive devices enable people to take part in education, the labour market and civil life so they can achieve their own quality of life. People are often disconnected, isolated, and imprisoned in poverty in the absence of assistive technology, compounding the burden of disease and disability on an individual, their families, and the community. Because of its simplicity and applicability, Morse code is one of the ways utilized in assistive technology. Individuals with severe motion difficulties can send the code as long as they retain some motor control. The objective this study is to build up and test a prototype that utilizes laser signals to send Morse code. The laser would send pulses of light that correspond with the “dots” and “dashes” in Morse code. When the laser falls on the LDR, it changes its value. These changes in the LDR value are used to decode the laser signals into readable text. The results show that the prototype can print certain letters successfully.

Keywords: Morse code, Encoding, Decoding, Microcontroller

1. Introduction

The telegraph made history in 1844 when it transmitted the first message, which was entitled "What hath God Wrought" (telling "What God has done") [1, 2, 3]. The telegraph's operator works based on Morse code that is presented in a series of dots and dashes that will be combined together to generate numbers and letters [4, 5]. One of the most fascinating features of this Morse code is that it has two symbols (on- or off-keying) in its representation, which is similar to binary encoding. This means that it can transmit and receive wireless text messages in conditions of noise or fading [5].

During the 19th century, new technologies are based on the same principles as those used in the telegraph system to construct again the future by offering widespread usage, especially in assistive technology [6, 7]. Assistive products are used to improve or maintain an individual's independence and function. In the present work, a communication system based on Morse code is going to be designed to be used by disabled people as an assistive method to communicate wirelessly. Further information will be provided in the following sections. In today's world, gaining access to the internet and information has never been easier because of personal computers and smart phones. It is one of the main ways of obtaining information and communicating with others. However, disabled people with severe physical impairments cannot use this technology, which is designed for abled people. This hinders them from functioning independently and improving their social opportunities. Assistive technology is “any device that allows a person with a disability to perform the tasks that nondisabled people are able to do without it” [8]. Morse code is one of the approaches used in assistive technology because of its simplicity and practicality. Individuals with severe motion disabilities can send the code as long as they have slight motor control.

2. Literature Review

In this section, three different available approaches will be provided to solve the problem along with presenting their advantages and disadvantages.

2.1. Eye Tracker Device

As the name suggests, an eye tracker or gaze interaction device, which uses the movement of the eyes to navigate and control a computer or smart device. This functions similarly to a PC keyboard or mouse. This is a perfect solution for people with disabilities such as spinal cord injuries, paralysis, and motor disabilities [9]. Users can surf the web, play computer games, and send messages and much more. A typical eye tracker would consist of invisible infrared light and extremely high-quality camera sensors. The infrared light is used to illuminate the eyes and the camera sensors capture the reflection of the retina and the cornea to move the cursor around.

2.2. Switch Access

Switch access is when switches are used to navigate through computers and devices instead of using keyboards and computers. People who suffer from cognitive or physical impairments mainly use this. For instance, a wrist switch (right) and a foot switch (left), which give an input to the computer upon tap. This makes for a 2-input system that can be used to navigate through apps.

2.3. Morse Code using a Laser

Since the code consists of only two inputs: dots and dashes, it can be easily implemented using a switch. This switch can be activated using any body part the person is able to move whether it is the head, elbow, knees, or fingers. Adaptive Design Association has implemented this, which is an organization that builds custom adaptations for disabled children [10]. The organization has worked with Google to develop a solution that uses Morse code. Using Morse code is faster than switch access scanning, especially when typing on a keyboard. This is because the user does not have to make many steps to choose a specific character. One can immediately input the Morse code of that character.

Instead of using switches, Morse code can be sent using visual signals like a laser. The laser signals can represent a dot and dash by varying the time that the laser is turned ON. A microcontroller will be used to translate the laser signals sent in Morse code to text on a computer monitor.

2.4. Advantages and Disadvantages of the Solutions

Table 1 evaluates the three solutions by providing the pros and cons for each of them.

Table 1 Evaluating the three solutions

Solution	Advantage	Disadvantage
Eye Tracker	Precise and accurate; requires almost no motor movement except for eye movement	Expensive; not suitable for blind people
Switch Access	Reliable	Slow; causes fatigue because of constant clicking
Morse Code Using Laser	Cheap; easy to implement; fast	Not as reliable as other solutions

3. Material and Method

3.1. International Morse Code

Morse code is a technique of text transmission as a series of on-off states or lights to be simply interpreted by a listener/observer with no intellectual equipment. The technique is used, in telecommunication, to encode text characters in a standardized manner presented by two distinct signal durations referred as dots (.) and dashes (-). The code is dubbed after Samuel Morse, who was one of the telegraph's early inventors [11]. The International Morse Code includes the A-Z letters, and the 0-9 Arabic numerals besides a few various sets of punctuation marks and arithmetic signs, e.g., \$, !, +, =, etc. The code encodes these various types of letters and numbers by processing short and long series of signals, which are the dots and dashes. A special string of dots and dashes in Morse code denotes a symbol, which is a text letter or number. The unit of time measurement used in code transmission is the dot duration. The dash's duration is three times greater than the dot's duration.

Table 2 Timing and binary code of Morse code

Feature	Timing	Binary Code
A dot	1 unit	1
A dash	3 units	111
Space between dots/dashes	1 unit	0
Space between characters	3 units	000
Space between words	7 units	0000000

The letters of a word are separated by a space of three dots (a dash), while the words are segregated by a space of seven dots [12]. In addition, since Morse code is transmitted utilizing only two states, which are on and off, it can be interpreted as a binary code [12]. Table 2 presents both timing and the binary code corresponding to each feature in Morse code.

The length of each Morse letter goes inversely with the frequency of its occurrence in English, which helps boost communication speed. The most used letter in the English language is "E," and thus, it has the fastest code denoted by a dot only (i.e., E="•") [13].

3.2. The Proposed Solution

In this section, a simple block diagram for the Morse code communication system is introduced. As shown in Fig. 1, the transmission block, labeled by Tx, uses either a LED or a laser diode, both work, to convert from electrical- to light-energy so that high-intensity coherent light will be produced. Once the laser diode blinks, the receiving block, labeled by Rx, is designed to receive that blinking coming from the laser via a light-dependent resistor (LDR). LDR is a variable resistance that can change its resistance when the light intensity, fallen upon it, changes. Then, at the serial monitor block, a user can get transmission results that will be displayed on a screen based on the Morse code algorithm. This communication system is designed to transmit and receive data wirelessly. The data is sent from the transmitter to the receiver end, and then, it will be displayed on the screen. The user can insert data (e.g., English alphabet) to be sent via a keypad. For the presented system, a computer is attached to the USB port of a microcontroller, at the transmission side, so that the user can insert the text.

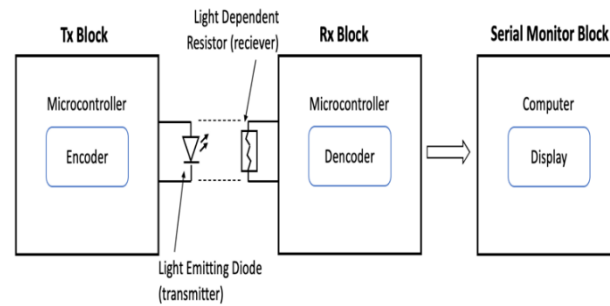


Figure 1 Block diagram for Morse code communication system

Fig. 2 presents the circuit diagrams for both the transmitter, shown in (a), and the receiver, shown in (b). Starting with the transmitter circuit, a laser diode module is used to send a character. It is controllable via an Arduino microcontroller. The laser module is programmed to switch on/off according to the Morse Code Standard's encoding systems. A sequence of both dashes and dots denotes the A-Z alphabetic letters. The binary format is the representation of those dashes and dots in order to be understood by Arduino. This means whenever a sign exists, the binary "1" is represented, while if there is no sign, then it means "0." For that reason, the signal side (S) of the laser module is connected to pin 12 at the digital port of the Arduino, while the GND side is connected to the GND of the Arduino.

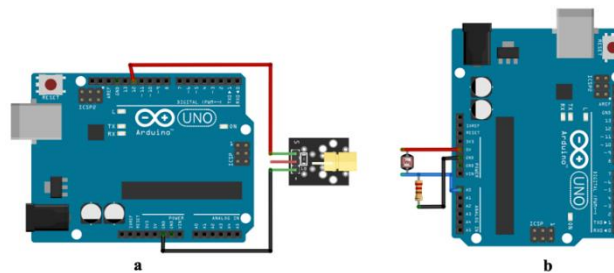


Figure 2 Circuits Diagram: (a) the transmitter circuit, (b) the receiver circuit

Ending with the receiver circuit, an LDR, which is sensitive to light intensity, is used to read the value of the signal sent by the laser module. The LDR is connected in series with a 10K resistor to form a voltage divider circuit. Doing so helps to read the change in voltage value rather than the resistance value because reading the voltage is much easier in circuits and especially with microcontrollers. Thus, the voltage divider circuit is applied by 5V delivered from the Arduino so that the voltage value will vary from 0 to 5V depending on the resistance values of both the LDR and the resistor. To read this change in voltage by the Arduino, the serial connection node of the LDR and the resistor is connected to pin A0 at the analog port, while the other side of the resistor is grounded. Once the Arduino reads the analog voltage, it can realize what code has been transmitted by evaluating the light intensity based on its frequency. As soon as the code is received, a serial monitor will be used to view the character assigned for that code.

As shown in Fig. 3, the transmitter and the receiver circuits are active and physically separated to bypass any interferences. For over-the-air transmission, the LDR and the laser diode are aligned horizontally and placed away from any reflectable surfaces. The prototype can transmit and receive data wirelessly. The data will be sent from the transmitter to the receiver end, and then, it can be displayed on a computer.

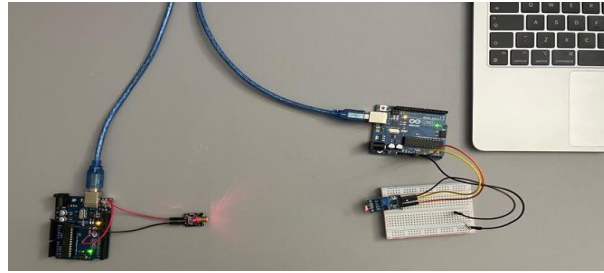


Figure 3 Hardware experimental setup

The transmitter circuit does encoding based on Morse Code Standard. The unique code of each character from a to z is held in the microcontroller's memory database. When a particular dots and dashes combination is sent and the receiver decodes the code, the system will start searching for the corresponding character in the database. The resulting character will be printed on the computer screen if the input signal follows the database entry.

For instance, the character "A" will be processed in this form if the character is to be sent. The input "Dot-Dash" is used to represent the character. The following action, in the transmission section, is performed:

- Pulse is produced for the first one second so that the binary "1" is generated.
- No pulse is produced for the next one second so that the binary "0" is generated.
- Pulse is produced for the following three seconds so that the binary "111" is generated.

These digital pulses make the laser to be blinking accordingly transmitting the "A" character to the receiver section where the LDR will be changing its resistance to match the frequency of the transmitted signal. Meanwhile, the analog voltage of the character will be read from the microcontroller so that it can realize the corresponding code. Thus, the letter "A" will be displayed on the screen based on the Morse code algorithm. The receiver code is relatively simple when compared to other receiver codes in different DIY projects. The tradeoff is that not all the letters can be printed using this code algorithm. To understand the reason, we need to explain the code algorithm first.

The LDR sensor has a reading of less than 1000 when there is no laser signal. Once the laser falls onto it, its value exceeds 1000. These values can be quantized to 0's and 1's. When the sensor value is < 1000 the code interprets it as a 0 and when the sensor value is > 1000 it interprets it as a 1. The code will enter a loop to count the 1's and store them in the variable "a" and count the 0's and store them in the variable "f". Based on the number of "a" and "f" the letter will be printed.

For example, if the letter "a" was sent this would correspond to 101110000000. The counter "a" is going to be equal to 4 and the counter "f" is going to be equal to 10. This will print the letter "a" on the serial monitor.

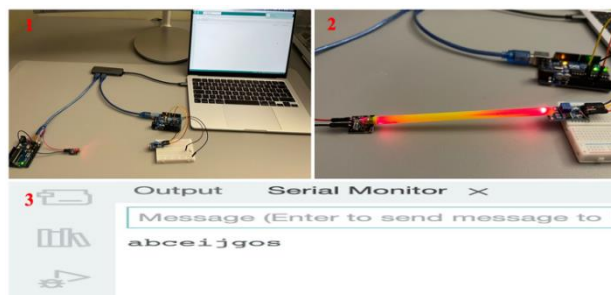


Figure 4 Experimental processes: (1) making the connections, (2) adding a straw, (3) obtaining the results

4. Findings

In this section, a test of transmitting and receiving alphabetic data was carried out. Fig. 4 shows the experimental processes for sending and receiving alphabetic letters. In this experiment, some random letters “a, b, c, e, I, j, g, o, and s” were inserted by the authors to be sent to the receiver section and display the transmission results there. The letters were encoded, based on the Morse Code algorithm, and then sent using the laser module. The receiver received these proposed encoding signals using the LDR and then compared them against the database Morse code where the number of dots/dashes is saved for each letter. A straw was used to align the LDR and the laser diode horizontally and avoid reflection coming from near flat surfaces. The serial monitor program was then utilized to analyze the receiver's ability to obtain the correct number of characters. As shown in Fig. 11, the transmitted letters were received successfully at a certain distance.

However, there were other letters sent, but unfortunately, the wrong results were obtained. The problem arises when there are letters that have the same number of 1's and 0's. This is true for the letters “a” and “n”. For example, the letter “n” is represented by 11101000000000 which makes a = 4 and f = 10 exactly like the letter “a”. With this limitation, the code can only print the letters “a, b, c, e, i, j, g, o, and s”. Although the code has this limitation, it makes it simple to understand [16].

Besides, the letters that had been received incorrectly had a delay, and thus the receiver side was affected. Another issue was that the laser module was not in the exact line of sight with the LDR sensor. This means that the sensor was not able to detect whether the laser module is on or off. Also, the condition of the room can affect the results. For instance, if the room is dark, the results should be better. All these issues were expected because the Morse code algorithm used in programming and controlling is too simple, and it can be developed to reach accurate results in further works.

5. Conclusion

The developed prototype permits users to wirelessly transmit and receive alphabetic data at a distance by using communication-based Morse code. On the transmission side, the data is inserted using the keypad, and then it is encoded according to the Morse code algorithm. The laser module does transmission by producing high-intensity coherent light. On the receiver end, the light is detected by the LDR, and then it does decoding on the transmitted data to be displayed on the serial monitor.

The prototype was able to send some of the alphabetic letters “a, b, c, e, i, j, g, o, and s” successfully to the receiver side. However, there was an error in sending the other letters. This is because of the simplicity of the code used, and the delay caused by light intensity. Therefore, although the transmission of data is achieved, its accuracy is not 100%. In future development, the Morse code will be developed and improved to reach 100% accuracy in transmission. In addition, the audio feature will be added by adding a buzzer to the receiver section.

References

- [1]. Newsroom, "Key characters in the development of the telecommunications industry," Feb 2020. [Online]. Available: <https://impactotic.co/en/characters-in-the-history-of-the-telecommunications-industry/>. [Accessed Dec 2022].
- [2]. M. E. Leach, "The growth of the electric telegraph on the railways of Britain," Papers Presented at the Sixteenth I.E.E. Week-End Meeting on the History of Electrical Engineering, pp. 98-109, 1988.
- [3]. S. Coggeshall, "A Critique of Communication at the Centennial of the Telegraph," in Proceedings of the IRE., vol. 32, no. 8, pp. 445-448, 1944.
- [4]. M. S. a. D. Hochfelder, "Two controversies in the early history of the telegraph," IEEE Communications Magazine., vol. 48, no. 2, pp. 28-32, 2010.
- [5]. R. F. Pocock, "The first radio-telegraph transmission," Electronics and Power, vol. 15, no. 9, pp. 327-329, 1969.

- [6]. M. H. L. e. al., "A new observation of strain-induced slow traps in advanced CMOS technology with process-induced strain using random telegraph noise measurement," 2009 Symposium on VLSI Technology, pp. 52-53, 2009.
- [7]. e. a. E. Oh, "Methodology to Predict Random Telegraph Noise Induced Threshold Voltage Shift Using Machine Learning," 2020 4th IEEE Electron Devices Technology & Manufacturing Conference (EDTM), pp. 1-4, 2020.
- [8]. D. K. Anson, Assistive technology for people with disabilities, Colorado: Green Wood, 2018.
- [9]. Abilities , "Eye-control Empowers People with Disabilities," 2 April 2022. [Online]. Available: <https://www.abilities.com/community/assistive-eye-control.html>. [Accessed 29 November 2022].
- [10].Google, "Imagining new ways to learn Morse code's dots and dashes," 3 December 2018. [Online]. Available: <https://blog.google/outreach-initiatives/accessibility/imagining-new-ways-learn-morse-codes-dots-and-dashes/>. [Accessed 30 November 2022].
- [11].101computing.net, "Morse Code using a Binary Tree," Nov 2021. [Online]. Available: <https://www.101computing.net/morse-code-using-a-binary-tree/>. [Accessed Dec 2022].
- [12].e. a. Paparao Nalajala, "Morse code Generator Using Microcontroller with Alphanumeric Keypad," IEEE explore, pp. 762-766, 2016.
- [13].L. S. Howeth, textsHistory of communications-electronics in the United States Navy, U.S: Washington : U.S. Government Printing Office, 1963.
- [14].D. HERRES, "Morse code, the first serial communication protocol," Oct 2019. [Online]. Available: <https://www.testandmeasurementtips.com/morse-code-the-first-serial-communication-protocol/>. [Accessed Dec 2022].
- [15]. S. Silva, "Morse code translator using the Arduino platform: Crafting the future of microcontrollers," SAI Computing Conference, pp. 675-680, 2016.
- [16]. "Communication Using Morse Code," [Online]. Available: <https://www.instructables.com/Communication-Using-Morse-Code/>. [Accessed Dec 2022].

SEMI-AUTONOMOUS MILITARY EQUIPMENT TRANSPORT VEHICLE WITH TARGET TRACKING

Uzuner S.

*Department of Mechatronics, Faculty of Engineering, University of Duzce, Duzce, Marmara, TÜRKİYE, 81620,
ORCID: 0000-0002-9099-1324*

Tok A.

*Department of Electronics and Automation, Dr. Engin PAK Cumayeri Vocational School, University of Duzce, Duzce, Marmara,
TÜRKİYE, 81620*

ABSTRACT

Migration and terrorist attacks represent significant challenges in our contemporary world. One of Turkey's primary objectives today is to counteract illicit activities perpetrated by terrorists. It is well-known that many terrorists infiltrate our country through rural areas characterized by difficult terrain conditions. In such demanding landscapes, soldiers are burdened with the arduous task of carrying heavy equipment on their backs and wielding cumbersome weapons during extended deployments and operations. Consequently, soldiers experience increased fatigue, leading to decreased combat effectiveness. Moreover, the transportation of military equipment to critical locations during conflicts and the safe evacuation of wounded soldiers for medical treatment remain persistent issues that military initiatives strive to address and overcome. In this study, the aim is to design a semi-autonomous transport vehicle equipped with sensors.

As the focus of this study was not on the vehicle itself, a lightweight RC off-road vehicle without a controller and sensors was procured in a ready-made state, capable of traversing challenging terrain conditions. However, a transport cabin that aligns with the dimensions of the all-terrain vehicle and minimizes the risk of tipping over was designed using SolidWorks software. Two infrared sensors and one ultrasonic sensor were integrated into the off-road vehicle to enable semi-autonomous tracking of a target in front of the vehicle. These sensors provide essential input for the tracking mechanism. The vehicle's power requirements were fulfilled by employing a lithium battery. The system's control was facilitated by Arduino UNO, which processed the data received from the sensors. The software was developed to ensure seamless motor control, enabling the vehicle to follow the target object without complications.

This study successfully developed a transport mechanism capable of carrying a 1 kg payload on an existing mobile off-road vehicle. The designed vehicle was equipped with the capability to semi-autonomously follow a target positioned ahead, even in challenging terrain conditions. A prototype of the vehicle was created, and the functionality of the developed software was observed, demonstrating its ability to relay distance information from sensors and send appropriate speed commands to the engines. An ultrasonic distance sensor measured the distance between the military personnel positioned ahead and the all-terrain vehicle, maintaining a constant range of 1-2 meters. This sensor ensured a consistent distance between the personnel and the vehicle. In practical terms, when the military personnel needed to accelerate, the vehicle accelerated accordingly, and when they needed to decelerate, the vehicle slowed down accordingly. If the personnel stopped, the vehicle also came to a halt. To facilitate the detection of the military personnel, two infrared and light sources were mounted on the sides of the ultrasonic sensor. These sources emitted signals towards the personnel and were subsequently detected by infrared sensors. The purpose of these dual sensors was to sense the response from the personnel. When the personnel performed a turn to the right or left, the sensor receiving a greater number of infrared beams caused the respective engine on the right or left side to rotate faster, thereby affecting the turn of the off-road vehicle.

Studies in literature focusing on enhancing military technological capabilities and security are of paramount importance in the strategic planning of nations. Given the prolonged struggle against terrorist activities, these studies hold significant priority for our country. The Ministry of Defense places great emphasis on these strategic endeavours. The literature demonstrates that the concept of IoT plays a pivotal role in controlling semi-autonomous military equipment from secure remote locations. However, it is important to acknowledge

that connecting devices to the Internet also introduces security risks. Therefore, the work conducted with domestic resources holds tremendous value. It highlights the criticality of safeguarding military data from third-party access and underscores the need to assess the risk of potential control of military equipment by foreign entities. Simultaneously, the system designed in the present study for the transportation of heavy materials in civilian life and the transportation of patients in the healthcare field has the potential to provide a broader vision. Through such efforts, the accomplishments attained can extend beyond meeting military needs to influencing civilian life. This approach enables the utilization of manpower and resources in diverse ways, catering to military requirements and civilian applications.

MICROBIOLOGICAL QUALITY PARAMETERS OF PICKLED SORYAZ SAMPLES COLLECTED FROM SALES POINTS IN ŞIRNAK

Mehmet Emin ERKAN

*Prof. Dr. Dicle University Faculty of Veterinary Medicine, Department of Food Hygiene and Technology, Diyarbakır, Türkiye
(Responsible Author), ORCID: 0000-0001-5581-3867*

Aydın VURAL

*Prof. Dr. Dicle University Faculty of Veterinary Medicine, Department of Food Hygiene and Technology, Diyarbakır, Türkiye
ORCID: 0000-0002-6232-2131*

ABSTRACT

There are many functional foods with functional properties that are traditionally produced and offered for consumption. There are many functional foods with functional properties that are traditionally produced and consumed in Şırnak such as gurız, pırtığa bige, mende, helis, siyabu, revas, kevzan and soryaz.

Allium kharputense, regionally called "Soryaz", is one of 179 *Allium* species. Antimicrobial, antifungal, antioxidant, anticoagulant, antihypertensive, anticancer effects of *Allium* species have been reported by many researchers.

In this study, microbiological quality parameters of 30 salted soryaz samples collected from Şırnak city centre and its districts in different periods were investigated. Samples were analysed for Total Mesophilic Aerobic Bacteria (TMAB), Coliform bacteria, *Escherichia coli*, *Staphylococcus-Micrococcus* spp., *Listeria monocytogenes*, *Salmonella* spp., *Yersinia enterocolitica*, *Lactobacillus* spp., mould, yeast, and sulphite reducing anaerobic bacteria.

Salmonella spp., *Listeria monocytogenes* and *Yersinia enterocolitica* could not be detected in soryaz samples, while *Escherichia coli*, Coliform bacteria and Sulphide reducing anaerobic were detected in 40 %, 60 % and 80 % of samples, respectively. It was determined that the microbiological quality of soryaz samples offered for sale in Şırnak was very low and this situation posed a potential health risk.

Key words: Soryaz, *A. kharputense*, Food Hygiene, Prebiotic

Introduction

As globalization progresses, consumers are readily exposed to many foods from various cultures. The need for studying specialty and unique food products, sometimes known as traditional, authentic, ethnic, or exotic foods, is increasing to accommodate consumers' growing demands. However, the number of studies conducted on these types of products with microbiologic and physicochemical quality test is limited (1). There are many foods with functional properties that are traditionally produced and consumed. There are many foods with potential functional properties such as gurız, pırtığa bige, mende, helis, siyabu, revas, kevzan and soryaz which are traditionally produced and consumed by the people in Şırnak. There is no scientific literature on some locally produced and consumed foods.

The concept of "traditional" food is that of foods that represent a group of people, knowledge, and even local resources (2). This uniqueness often is referred to as "authenticity", which may be more often used for cultural products, rather than those that are part of our daily routines (3). Authenticity can be defined simply as something that is original and comes from the past (4). Cities with a five-hundred-year history of authentic clothing have a deeper history and culture than many countries. However, as social life becomes more individualized and has negative effects on authentic culture, the value of everything authentic increases. Food from different regions or countries can provide "unique" and "exotic" characteristics to individuals from other cultural backgrounds (5). Human beings are in search of getting to know new tastes and seeing and knowing the differences.

Approximately 800.000 plant species in the world have been used by human beings as food, medicine, paint and ornamental plants (6). Although nearly 10.000 plant species grow naturally in our country, they cannot be utilized sufficiently (7) or they are not known. A plant that is widely used in one region does not grow in other regions. Different climates and altitudes also increase plant diversity. There are many foods with functional properties that are traditionally produced and consumed in this region. soryaz is one of these traditional foods that are consumed in the region of Şırnak. *A. kharputense*, locally called "soryaz", is one of 179 species of *Allium*. (8) Researchers have reported that soryaz has antibacterial and antimicrobial (9, 10), antifungal (11), anticoagulant, antihypertensive and anticancer (12, 13) activities.

The aim of this study was to investigate the hygienic quality of pickled soryaz which is consumed in Şırnak and to increase the recognition of this traditional food.

Material and methods

Microbiological analysis

The soryaz samples were brought to the laboratory in cold chain with bags equipped with ice packs. 10 g of the samples were taken under aseptic conditions and homogenized with 0.85% sterile physiological saline. Serial dilutions were prepared from homogenized (1/10) to 10⁹ steps and cultured on appropriate media. All microbiological analyses were performed in two parallel runs. The media and incubation conditions used in the analyses are shown in Table 1 (14-22).

Table 1. Medias and incubation conditions used in microbiologic analysis

Microorganisms	Methods
Total Mesophilic Aerobic Bacteria	ISO 4833-1:2013
Coliforms	ISO 4832:2006
<i>Escherichia coli</i>	ISO 16649-2: 2001
Staphylococcus-Micrococcus spp.	Harrigan WF. (1998)
<i>Listeria monocytogenes</i>	ISO 11290
<i>Salmonella spp.</i>	ISO 6579:2002
<i>Yersinia enterocolitica</i>	EN ISO 10273:2017
Lactobacillus spp.	Harrigan WF. (1998)
Mould spp.	ISO 7954:1987
Yeast spp.	ISO 7954:1987
Sulphite Reducing Anaerobic Bacteria	Speck ML. (1976)

Results and Discussion

In this study, microbiological quality parameters of 30 salted soryaz samples collected from Şırnak city centre and its districts in different periods were investigated. Samples were analysed for Total Mesophilic Aerobic Bacteria (TMAB), Coliform bacteria, *Escherichia coli*, *Staphylococcus-Micrococcus* spp., *Listeria monocytogenes*, *Salmonella* spp., *Yersinia enterocolitica*, *Lactobacillus* spp., mould, yeast, and sulphite reducing anaerobic bacteria.

Salmonella spp., *Listeria monocytogenes*, *Yersinia enterocolitica* could not be detected in soryaz samples, while *Escherichia coli*, Coliform bacteria and Sulphide reducing anaerobic were detected in 40 %, 60 % and 80 % of samples, respectively. The results of microbiological analysis of soryaz samples offered for sale in Şırnak are given in Table 2.

Table 2. Microbiological Quality Parameters of soryaz samples (log₁₀ CFU/g)±SS*

Microorganism (n:30, Log ₁₀ CFU/g)	min.	max.	mean+SD	contamination rate %
Total Mesophilic Aerobic Bacteria	4.23	8.82	8.41+1.76	100
Coliforms	1	7.99	6.87+0.98	60
<i>Escherichia coli</i>	1	5.57	3.87+1.07	40
Staphylococcus-Micrococcus spp.	1	4.36	3.13+1.37	40
<i>Listeria monocytogenes</i>	ND	ND	ND	0
<i>Salmonella spp.</i>	ND	ND	ND	0
<i>Yersinia enterocolitica</i>	ND	ND	ND	0
Lactobacillus spp.	2.47	4.23	3.21+0.61	100
Mould spp.	2	4.68	3.44+1.00	90
Yeast spp.	2	5.83	3.94+1.29	90
Sulphite Reducing Anaerobic bacteria	2	2.48	1.63+0.53	80

Fresh vegetables can be contaminated with pathogenic bacteria in any steps of all the process from cultivation to consuming. These bacteria cause major public health concern worldwide in terms of human illnesses (23). No study was found on the microbiological quality of soryaz. In one study, it was reported that soryaz (*Allium kharputense*) was antimicrobial against *B. cereus*, *B. subtilis*, *E. faecalis*, *E. coli* and *S. Typhimurium* (24).

The high presence of mould and yeast can be considered as indicators of rapid spoilage of a product. Salt tolerant yeasts cause spoilage of pickled and salted foods by consuming lactic acid, yeasts make the pickles less acidic—and more hospitable to spoilage microbes. Halotolerant yeast are capable of causing spoilage of fermented vegetables due to gas formation (bloating) and film formation (25) and also off-flavours and off-odours, although spoilage caused by yeasts does not usually results in human diseases as yeasts are rarely pathogenic and do not produce toxins (26).

Conclusion

In conclusion, considering the public health, fresh vegetables are common sources for various microorganisms and also pathogenic bacteria. Therefore, it is essential to ensure applying good agricultural practices and good manufacturing practices during production. Producers be informed about the sources of microbial contamination and should be trained in hygienic production. These products, which are likely to be authentic and functional, must undergo a pasteurization or sterilization process before consumption. To determine the microbiological and physicochemical properties of *Allium kharputense* and to increase its recognition more work needs to be done.

References

1. Yang J, Lee J. Application of Sensory Descriptive Analysis and Consumer Studies to Investigate Traditional and Authentic Foods: A Review. *Foods*. 2019; 8(2):54.
2. D'Antuono, L.F.; Bignami, C. Perception of typical Ukrainian foods among an Italian population. *Food Qual. Preference* 2012, 25, 1–8.
3. Groves, A.M. Authentic British food products: A review of consumer perceptions. *Int. J. Consumer Stud.* 2001, 25, 246–254.
4. Heitmann, S. (2011). Authenticity in tourism. P. Robinson S. Heitmann ve P. Dieke (ed.) *Research Themes for Tourism içinde* (ss.45- 58). Wallingford: CABI.
5. Jang, S.S.; Ha, J.; Park, K. Effects of ethnic authenticity: Investigating Korean restaurant customers in the US. *Int. J. Hosp. Manag.* 2012, 31, 990–1003. [Google Scholar] [CrossRef]
6. Öztürk, M., Özçelik H.(1991). *Doğu Anadolu'nun Faydalı Bitkileri*, Siirt İlim Vakfı Yay., Ankara.

7. Baytop, T.(1984). Türkiye’de Bitkiler ile Tedavi, İstanbul Üniversitesi Eczacılık Fak.Yay., İstanbul.
8. Yabalak E, Gizir A. Evaluation of Total Polyphenol Content, Antioxidant Activity and Chemical Composition of Methanolic Extract from *Allium Kharputense* Freyn et. Sint. and Determination of Mineral and Trace Elements. JOTCSA. 2017 Jun;4(3):691–708.
9. Fritsch RM, Keusgen M. Occurrence and taxonomic significance of cysteine sulphoxides in the genus *Allium* L. (Alliaceae). Phytochemistry. 2006; 67(11): 1127-35.
10. Panomket P, Wanram S, Srivorasmas T, Pongprom N. Bioactivity of plant extracts against *Burkholderia pseudomallei*. Asian Biomed. 2012; 6(4):619-23.
11. Corea G, Fattorusso E, Lanzotti V. Saponins and flavonoids of *Allium triquetrum*. J Nat Prod. 2003; 66(11): 1405-11.
12. Kimbaris AC, Siatis NG, Daferera DJ, Tarantilis PA, Pappas CS, Polissiou MG. Comparison of distillation and ultrasound-assisted extraction methods for the isolation of sensitive aroma compounds from garlic (*Allium sativum*). Ultrason Sonochem. 2006; 13(1): 54-60.
13. Banerjee SK, Mukherjee PK, Maulik SK. Garlic as an antioxidant: The good, the bad and the ugly. Phyther Res. 2003; 17(2): 97-106.
14. Microbiology of the Food Chain - Horizontal Method for the Enumeration of Microorganisms - Part 1: Colony Count at 30oC by the Pour Plate Technique. International Organization of Standardization, Geneva, Switzerland.
15. Microbiology of food and animal feeding stuffs – Horizontal method for the enumeration of coliforms – Colony-count technique. International Organization of Standardization, Geneva, Switzerland.
16. Horizontal Method for the Enumeration of β - glucuronidase Positive *E. coli* - Colony Count Technique at 44 °C Using. International Organization of Standardization, Geneva, Switzerland.
17. Laboratory Methods in Food Microbiology. Academic Press, New York, 1998.
18. Microbiology of food and animal feeding stuffs — Horizontal method for the detection and enumeration of *Listeria monocytogenes*. ISO 11290, International Organization for Standardization, Geneva, 1996.
19. Microbiology of Food and Animal Feeding Stuff—Horizontal Method for the Detection of *Salmonella* spp. ISO 6579:2002, International Organization for Standardization, Geneva, Switzerland, 2002.
20. Microbiology of the food chain horizontal method for the detection of pathogenic *Yersinia enterocolitica*, Geneva, Switzerland Int. Org. for Standardization; 2017
21. Microbiology of food and animal feeding stuffs. Enumeration of yeasts and mould. ISO 7954:1987, International Organization for Standardization, Geneva, Switzerland, 1987.
22. Speck ML. (1976). Compendium of Methods for the Microbiological Examination of Foods. American Public Health Association, Washington DC, USA.
23. Serkan Kemal Buyukunal, Ghassan Issa, Filiz Aksu, Aydin Vural. Microbiological Quality of Fresh Vegetables and Fruits Collected from Supermarkets in Istanbul, Turkey. Journal of Food and Nutrition Sciences. Vol. 3, No. 4, 2015, pp. 152-159.
24. Teğın İ, Fidan M, Hallaç B. Siirt Eruh Bölgesinde Yetişen *Allium Kharputense* Ekstraktinin Kuru Madde, Renk, Antimikrobiyal Etkilerinin Belirlenmesi. International Siirt scientific resource congress.18-19 November 2022. Pp: 608-620.
25. Franco W, Pérez-Díaz IM, Johanningsmeier SD, McFeeters RF. Characteristics of spoilage-associated secondary cucumber fermentation. Appl Environ Microbiol. 2012; 78(4):1273-84.
26. Stratford M. Food and beverage spoilage yeasts. Yeasts in food and beverages. Berlin, Germany: Springer, 2006:335-79.

ASSESSMENT OF PRECIPITATION AND TEMPERATURE GRIDDED DATASET FOR NIGERIA

Bashir Tanimu

Department of Water Resources and Environmental Engineering, Ahmadu Bello University Zaria, Nigeria

Al-Amin Danladi Bello

Department of Water Resources and Environmental Engineering, Ahmadu Bello University Zaria, Nigeria

Sule Argungu Abdullahi

Department of Water Resources and Environmental Engineering, Ahmadu Bello University Zaria, Nigeria

Morufu Ajibola Ajibke

Department of Water Resources and Environmental Engineering, Ahmadu Bello University Zaria, Nigeria

ABSTRACT

Climate data is essential for assessing the environment and hydrologic cycle over time and space. Data collection in developing nations is difficult due to restrictions. For the first time, this study used advanced time series similarity algorithms and short time series distance (STS) to evaluate, compare, and rank five gridded climate datasets: the Climate Research Unit (CRU), Terra Climate (TERRA), Climate Prediction Centre (CPC), European Reanalysis V.5 (ERA5), and climatologies at high resolution for Earth's land surface areas (CHELSA) based on their ability to replicate in-situ rainfall and temperature data. The approaches were tested by comparing compromise programming (CP) rankings based on four statistical criteria for duplicating in-situ rainfall, maximum temperature, and lowest temperature at 26 locations across Nigeria. CRU was Nigeria's finest gridded climate dataset, followed by Chelsa, Terra, ERA5, and CPC. The group decision-making technique integrated STS values for CRU rainfall, maximum and lowest temperature were 17, 10.1, and 20.8, respectively. CP based on traditional statistical metrics validated STS and CCD results. CRU's Pbias was 0.5–1, KGE 0.5–0.9, NSE 0.3–0.8, and NRMSE -30–68.2, which were better than the other products. The findings show that STS can analyse climatic data without sophisticated and time-consuming multi-criteria decision procedures based on various statistical indicators.

Introduction

Climate data is very vital in evaluating the environment and hydrologic cycle across various periods and geographical regions (Lawal et al. 2021). Comprehending the geographical and temporal dynamics is vital for practical applications in agriculture, water resources, river basin management, and disaster prevention (Beck et al., 2019; Sehad et al., 2017). The two most important variables in climate impact and eco-hydrological studies are Rainfall and temperature (Xu et al., 2023). Accurate weather data is crucial for understanding environmental changes. Collecting data in less developed nations faces substantial challenges due to constraints (Hassan et al. 2020). These challenges encompass the scarcity or total absence of radar networks and rain gauges, limited resources, insufficient infrastructure (Ibrahim et al. 2022; Waseem et al. 2022).

Studies have proposed an alternative to overcome the limitations, employing gridded datasets which merged gauge and satellite data. These are increasingly used in hydrological and climate change research (Ren et al., 2018). Gridded data's reliability differs according to the temporal and geographic climatic factors (Bai & Liu, 2018), so evaluating gridded data's applicability is crucial for specific locations. Addressing uncertainty is vital, prompting significant research to assess dataset performance within regions (Nashwan et al., 2019). The findings of statistical metrics sometimes need to be more consistent, which complicates the process of making decisions based on the obtained data (Beck et al., 2019; Salman et al., 2019). Inaccurate findings and conclusions might arise from evaluating gridded product performances only using correlation and error

measures (Ahmed et al. 2019b; Hassan et al. 2020). To address the constraints associated with depending solely on error analysis, multi-criteria decision making (MCDM) tools are currently utilized. Compromise programming (CP) is one such MCDA based on the results obtained from distinct metrics (Muhammad et al., 2019; Zeleny, 2011). It has been widely applied in reliable assessment of gridded data performance based on several statistical metrics (Salman et al., 2019; Muhammad et al., 2019; Salehie et al., 2021). This method has some drawbacks including time consuming, complexity and difficulty in data handling.

Similarity is a modern technique that measures how similar two items or entities are in a variety of fields (Liao, 2005). Time series analysis uses this concept to evaluate how similar two sets of temporal data are to one another (Liao, 2005; Nashwan & Shahid, 2019). Time series similarity analysis has been applied various in fields, including medicine, environmental sciences energy etc. Short time series distance (STS) is a shape-based similarity metric developed to capture the differences in the shape of two noisy time series (Benítez & Díez, 2022). Given the irregular and uneven rainfall time series data features, this piecewise slope transformation distance similarity measure can effectively measure how the gridded rainfall series is similar to in-situ observation (Li et al., 2012; Zhang & Pi, 2017). The study aimed in assessing the applicability of STS in evaluating the performance of gridded rainfall and temperature data products in reproducing observed data in Nigeria.

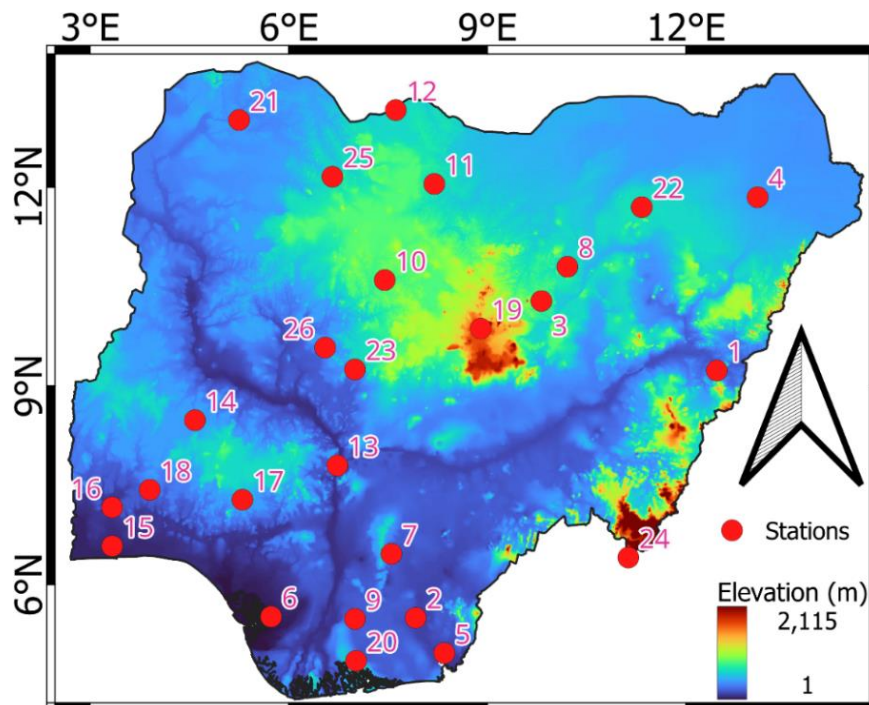


Figure 1. Map of Nigeria showing the location and elevation of the selected observed stations

Study Area

Nigeria, located in West Africa, spans latitudes 4° to 14°N and longitudes 2.50° to 14°E (Bala et al., 2023). Bounded by the Atlantic Ocean, Sahara Desert, Benin Republic, and Cameroon, its diverse geography covers 925,796 km², featuring lowlands, highlands, and plateaus (Abatan et al., 2016). Elevation ranges from sea level at 0 metre to 2419 m in Chappal Waddi within the North-Eastern region of the nation. Nigeria experiences a two-season climate, with a rainy period from March to October and a dry season from November to March, influenced by the north-south movement of the inter-tropical discontinuity and coastal effects from the Atlantic Ocean (Lawal et al. 2021).

Data and sources

Observation data

The study collected observed data on monthly rainfall, maximum temperature (T_{max}) and minimum temperature (T_{min}) from 27 stations spanning (1980-2015) across Nigeria. The observed data were acquired from the Nigerian Meteorological Agency (NIMET). The stations were chosen based on complete records, geographical and temporal distribution, and longevity life span for climate analysis.

Table 1 Stations used in this study

Station No	Name	longitude	Latitude	Station No	Name	longitude	Latitude
1	Yola	12.47	09.23	15	Ilorin	04.58	08.48
2	Akwa Ibom	07.92	05.50	16	Ikeja	03.33	06.58
3	Anambra	06.78	07.50	17	Ogun	03.33	07.17
4	Bauchi	09.82	10.28	18	Ondo	05.30	07.28
5	Maiduguri	13.08	11.85	19	Oyo	03.90	07.43
6	Cross River	08.35	04.97	20	Plateau	08.90	09.87
7	Delta	05.73	05.52	21	Rivers	07.02	04.85
8	Enugu	07.55	06.47	22	Sokoto	05.25	13.02
9	Dadin Kowa	10.21	10.80	23	Yobe	11.33	11.70
10	Imo	07.00	05.48	24	FCT Abuja	07.00	09.25
11	Kaduna	07.45	10.60	25	Gembu	11.13	06.41
12	Kano	08.20	12.05	26	Gusau	06.66	12.16
13	Katsina	07.62	13.17	27	Minna	06.55	09.58
14	Kogi	06.73	07.80				

Gridded Datasets

The CPC, CRU, ERA5 V.5, CHELSA and TERRA provided the monthly gridded rainfall, T_{max}, and T_{min} data products used in the study. Table 2 briefly describes the gridded dataset used in the study.

Table 2. Summary of the Gridded dataset used in the study

Product	Variable	Spatial Extent	Temporal Resolution	Spatial Resolution	Source
CPC	P, T _{max} and T _{min}	Global	Daily (1979-2020)	0.5°	https://psl.noaa.gov/data/gridded/data.cpc.globalprecip.html
CRU	P, T _{max} and T _{min}	Global	Monthly (1901-2020)	0.5°	https://crudata.uea.ac.uk/cru/data/hrg/cru_ts_4.07/cruts
CHELSA	P, T _{max} and T _{min}	Global	Monthly (1979-2013)	0.0083°	https://envicloud.wsl.ch/#/?prefix=chelsa%2Fchelsa_V2%2F
ERA5	P, T	Global	Hourly (1979-2020)	0.1°	https://cds.climate.copernicus.eu/cdsapp#!/dataset/reanalysis-era5-single-levels
TERRA	P, T _{max} and T _{min}	Global	Monthly (1958-2020)	0.04°	https://www.climatologylab.org/terraclimate.html

Methodology

Procedure

The main steps followed in this study for assessment of the gridded dataset are;

1. Monthly observed station data were collected from the NIMET, URBA and GHCN
2. Gridded datasets were downloaded from the provider's websites (Table 2) in a raster (.tif) or nc format.
3. The gridded datasets were extracted using R and interpolated for the study area using the bilinear interpolation technique.
4. STS was estimated between the gridded and observed data at each location.
5. A group decision-making method was used to rank the gridded dataset for Nigeria based on STS at each location for rainfall and temperatures.
6. Compromise programming was used to validate the result obtained by employing statistical metrics.

Short Time Series distance (STS)

STS quantifies the dissimilarity across time series by evaluating the disparities in the slopes of their respective piecewise linear functions (Möller-Levet et al., 2005; Benítez and Díez, 2022; Zhang and Pi, 2017).

The STS distance is defined as the distance between two time series, $X_T = (x_1, x_2, \dots, x_T)$, $Y_T = (y_1, y_2, \dots, y_T)$, the STS distance is defined as (Möller-Levet et al., 2005):

$$d_{STS}(X, Y) = \sqrt{\sum_{k=0}^{N-1} \left(\frac{y_{k+1} - y_k}{t_{k+1} - t_k} - \frac{x_{k+1} - x_k}{t'_{k+1} - t'_k} \right)^2} \quad (1)$$

where t and t' represent the time-related indicators of series X and Y , respectively. Although their temporal indices may begin in various time contexts, x and y are required to be of similar length and every increment has to be equal:

$$t_{k+1} - t_k = t'_{k+1} - t'_k, \quad (2)$$

Compromise Programming

Compromise programming (Freimer & Yu, 1976) is a technique used in MCDM. It belongs to distance-based MCDM techniques (Momeni et al., 2021). The concept involves identifying solutions near an ideal point (Ardil, 2021). Compromise index (CPI) can be calculated by quantifying the distance in the equation below:

$$CPI = \left[\sum_{i=1}^n |x_i - x_i^*|^p \right]^{\frac{1}{p}} \quad (3)$$

where x_i represents normalised indicator i for gridded data product, x_i^* represents the normalised ideal value of the index i and p is the parameter to measure the distance between a solution and the ideal point. For linear distance, p is taken as 1. The CPI values are consistently positive, and the model performs better when the CPI values are lower.

The STS results was validated using CP. It was based on the performances of four statistical metrics. Table 3 depicts the metrics and their formulas applied and their optimal values. The terminologies employed to

illustrate statistical measures; x_g , x_{obs} , and n are the gridded dataset, observed station data, and number of recorded data, respectively.

Table 3 Equations of the statistical metrics employed

Statistical metric	Optimal value
$NRMSE = \frac{\left[\frac{1}{n} \sum_{i=1}^n (x_{g,i} - x_{obs,i})^2 \right]^{1/2}}{\frac{1}{n \sum_{i=1}^n x_{g,i}}}$	0
$Pbais = \left[\frac{\sum_{i=1}^n (x_{obs} - x_g)}{\sum_{i=1}^n x_{obs}} \right] \times 100$	0
$NSE = 1 - \frac{\sum_{i=1}^n (x_{g,i} - x_{obs,i})^2}{\sum_{i=1}^n (x_{obs,i} - x'_{obs})^2}$	0
$KGE = 1 - \sqrt{(R-1)^2 + \left(\frac{\mu_g}{\mu_0} - 1 \right)^2 + \left(\frac{\sigma_g/\mu_g}{\sigma_0/\mu_0} - 1 \right)^2}$	1

Multi Criteria Group Decision Making (MCGDM): STS evaluate the performance of the gridded dataset and ranked them at each location based on rainfall and temperature. This study employed Multi Criteria Group Decision Making (MCGDM) for final ranking. In this method, an overall index (R_r) was computed by assigning weights based on gridded dataset performance at stations. The highest-weighted dataset held the top rank. The weight assigned to rank positions was calculated as the reciprocal of the rank value (R_r) = $rank^{-1}$. if a gridded dataset attained ranks 1st, 2nd, 3rd, 4th, and 5th at Y_1, Y_2, Y_3, Y_4 and Y_5 stations, the overall score of each gridded dataset was calculated to be:

$$The\ GDMA = R_m = Y_1 \left(\frac{1}{R_{r1}} \right) + Y_2 \left(\frac{1}{R_{r2}} \right) + Y_3 \left(\frac{1}{R_{r3}} \right) + Y_4 \left(\frac{1}{R_{r4}} \right) + Y_5 \left(\frac{1}{R_{r5}} \right) \quad (4)$$

Results

Assessment of gridded datasets using Short time series

The performance of each gridded data set in replicating rainfall, Tmax and Tmin at each station was first estimated using STS (Eq. 1). The obtained results for the five gridded datasets at 25 stations in Nigeria are shown in Table 4. The values were used to rank the gridded data product with the lowest value as 1st and the highest values as 5th.

The ranks obtained by different rainfall datasets using STS are presented in Figure 3. A similar procedure is followed for Tmax and Tmin to rank the gridded data products. The ranking of the gridded datasets for Tmax and Tmin is provided in Figures 4 and 5. A deep green to red color ramp is used to show the rank of the data products in different stations in the figure, where the deep green indicates the best performance (rank 1) while red represents the worst performance (rank 5).

Figure 3 shows that most gridded datasets could not stimulate the observed data ideally, but CRU performed best in most stations in replicating the observed precipitation. TERRA and CHELSA are ranked second and third in replicating the station data. CPC performed worst as it performed very poorly in most of the stations. CHELSA outperformed other dataset products by replicating the observed Tmax, ranking first in most stations (Figure 4). CRU performed best in some stations in the Southwest but poorly in the entire north. CPC is ranked worst as it performed poorly in most stations, especially within the northern region. TERRA performed better than ERA5 and CPC, especially in replicating observed Tmax in the south. Finally, CRU outperformed other dataset products by replicating the observed Tmax in most of the stations within the study

area, as shown in Figure 5. CHELSA performed best in some stations in the south. CPC and TERRA performed poorly, but TERRA was better than CPC in replicating most of the station's Tmax. ERA5 is ranked worst as it performed poorly in most stations.

Group Decision Making

STS showed different performances of different gridded datasets at different locations for rainfall and temperature. MCGDM was employed to choose the most suitable dataset from the contradicting results obtained at different locations. The R_m of each gridded dataset for each variable is estimated using Eq. 4. The obtained results for five gridded datasets and three variables for STS is presented in Tables 6. The ranking of each data product for rainfall and temperatures based on this is also provided in the tables. The results show CRU is the best product for replicating rainfall in terms of STS followed by TERRA and CHELSA. CRU also showed the best performance in replicating Tmin, while CHELSA showed the best performance for Tmax. The results show that STS identified CRU as the best product for Nigeria, followed by CHELSA, TERRA, and ERA5

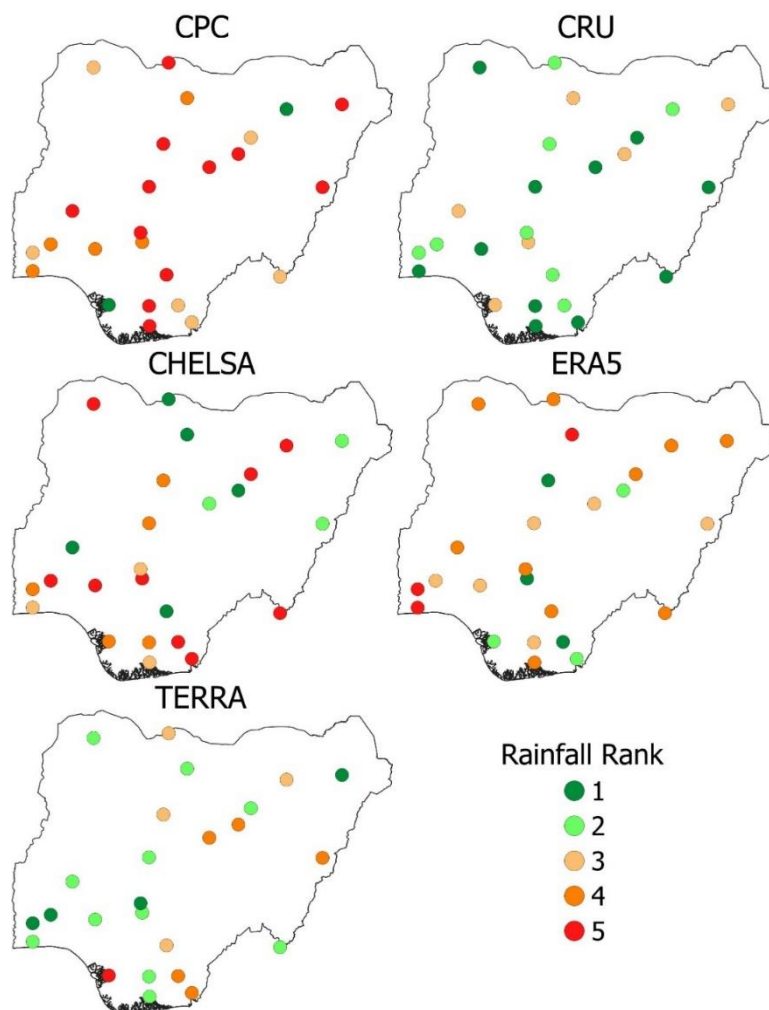


Figure 3. Rank of different gridded data products based on short time distance method in replicating rainfall at different stations. The color ramp indicates the rank at different observation stations.

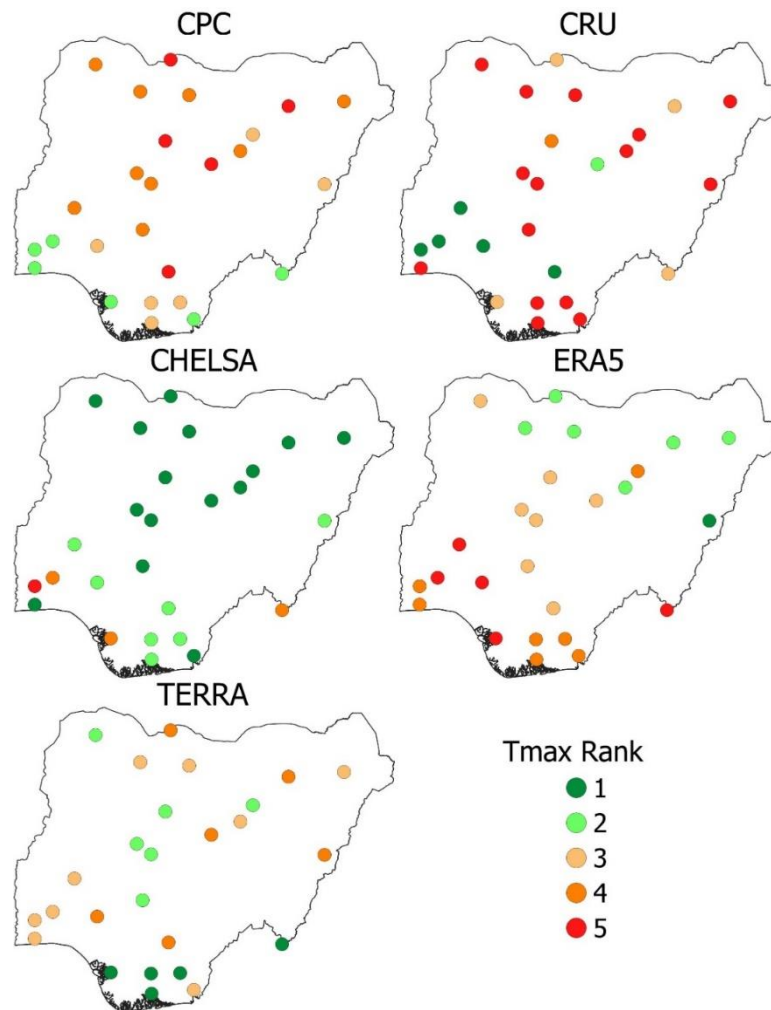


Figure 4. Rank of different gridded data products based on short time distance method in replicating maximum temperature at different stations. The color ramp indicates the rank at different observation stations.

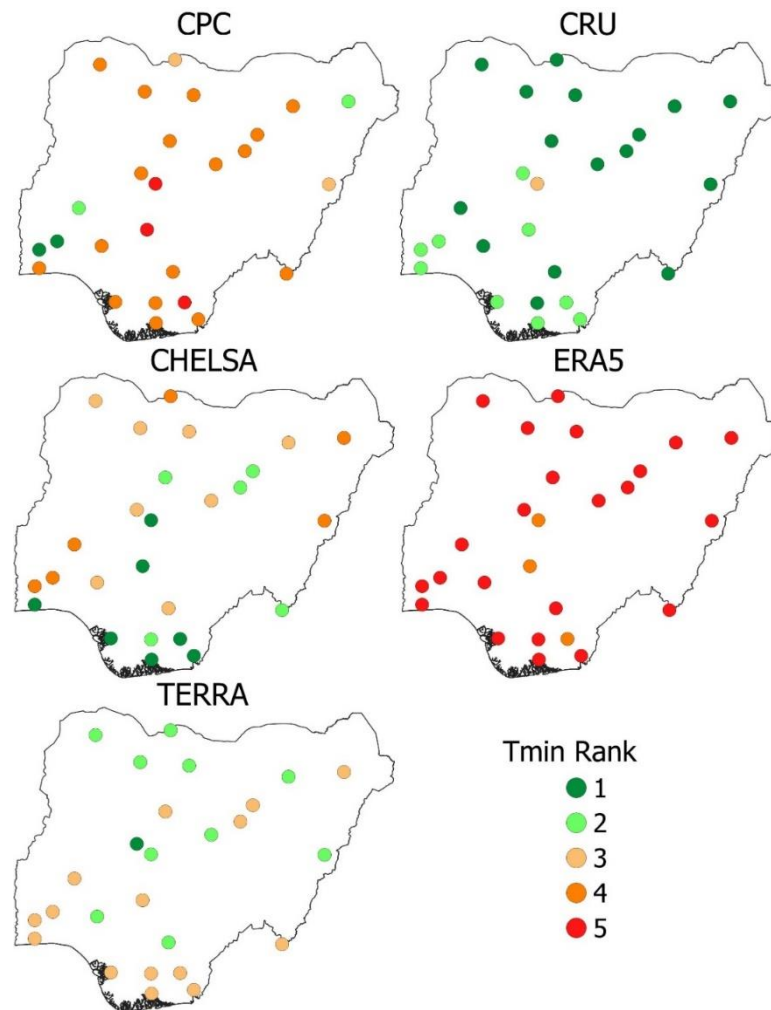


Figure 5. Rank of different gridded data products based on short time distance method in replicating minimum temperature at different stations. The color ramp indicates the rank at different observation stations.

Table 4. Group decision index and the ranking of five gridded datasets for rainfall, maximum and minimum temperature based on short time series distance

Dataset	Rainfall		Max Temperature		Min Temperature		R_m	Final Rank
	R_m	Rank	R_m	Rank	R_m	Rank		
CPC	7.7	5	8.2	5	8.5	4	0.65	5
CRU	17	1	10.1	3	20.8	1	2.33	1
CHELSA	10.6	3	19.4	1	13.7	2	1.83	2
ERA	9.6	4	9.1	4	5.4	5	0.70	4
TERA	12.3	2	12.5	2	11	3	1.33	3

Validation using Compromise Programming

The ranking of the five gridded datasets obtained by STS was validated by CP. Four statistical indices, KGE, NSE, NRSME, and Pbias, were employed as part of the assessment based on CP. These four metrics can assess a product's capacity to accurately reproduce the observed data's distinct characteristics. The heatmaps in Figure 6 present the performance of different gridded dataset products in all locations based on the statistical metrics. The blue color in the heatmap indicates better performance, while red represents bad performance. The cyan colour in the heat map indicates higher capabilities, while the magenta-purple represents less ability in different metrics.

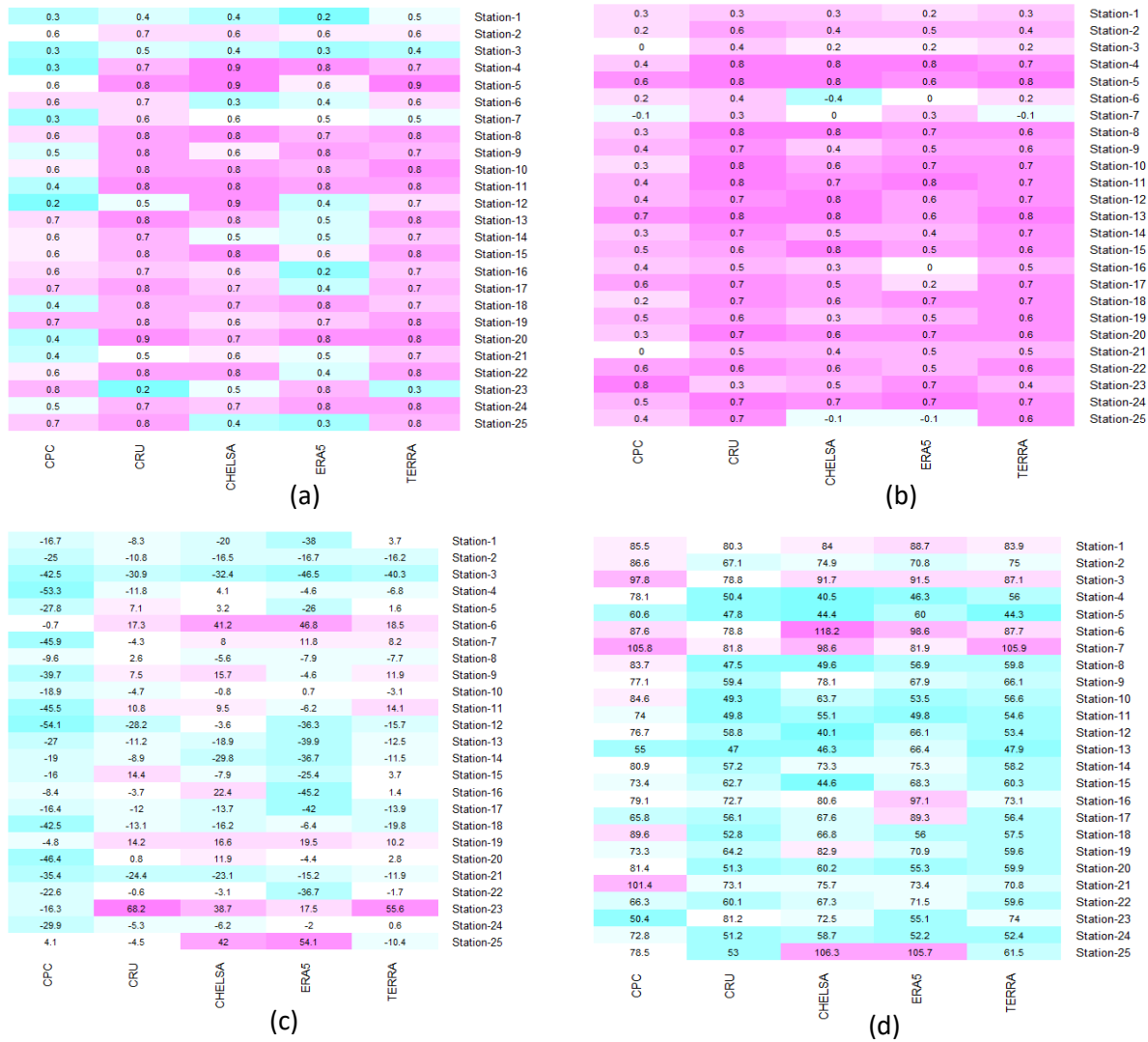


Figure 6. The performance of the gridded rainfall data based on (a) KGE, (b) NSE, (c) NRSME, and (d) Pbias at 25 stations in Nigeria. Blue color indicates better performance, while red represents bad performance

CPI was estimated using Eq. 3 based on the results of the statistical metrics presented in Figure 6. Figure 7 shows the CPI values estimated for different gridded rainfall datasets at 25 stations using a heat map. Since a lower CPI value represents good performance, the cyan colour in the heat map indicates higher capabilities. Similarly, the magenta-purple colour represents less ability. Figure 4 depicts many cells with colours ranging from blue, cyan, white, and sky purple. The figure shows CRU as the superior dataset product, followed by Terra Climate, Chelsa, ERA5 and CPC. The results show that the CRU gridded dataset and TERRA performed better than other datasets in most stations ranked by CPI.

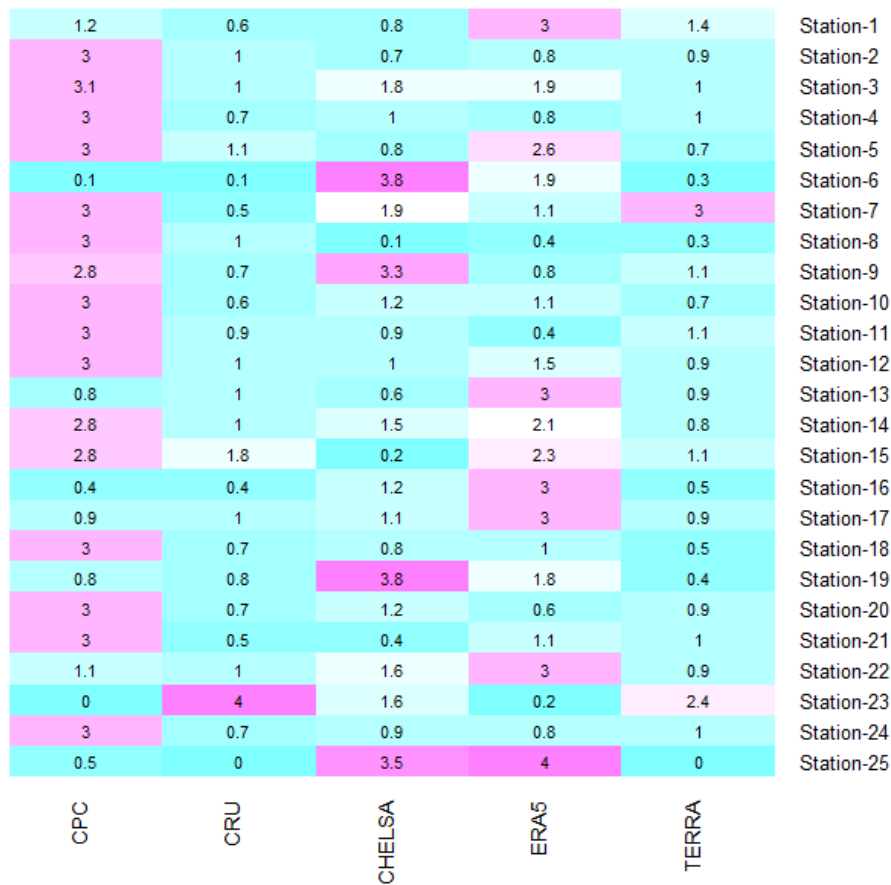


Figure 7. Heat map showing the CPI values of all gridded rainfall datasets employed in this study. Blue color indicates better performance, while red represents bad performance.

The spatial distribution of the ranks obtained using CPI for rainfall, Tmax and Tmin are presented in Figures 8 to 10. The figure shows that CRU excelled as the top or second-best gridded rainfall product, aligning closely with observed values in most locations, making it the superior choice for observation. TERRA performed best in some stations in the Southwest and North-West regions. CPC performed worst in most stations.

Figure 9 shows that CHELSA excelled in estimating Tmax, aligning closely with observed values in most locations, making it the superior choice for observation. CPC performed second best while CRU and ERA5 performed worst in a number of the stations within the designated study area. Figure 10 shows that CRU excelled as the top best-gridded Tmin product, aligning closely with observed values in most locations, making it the superior choice for observation.

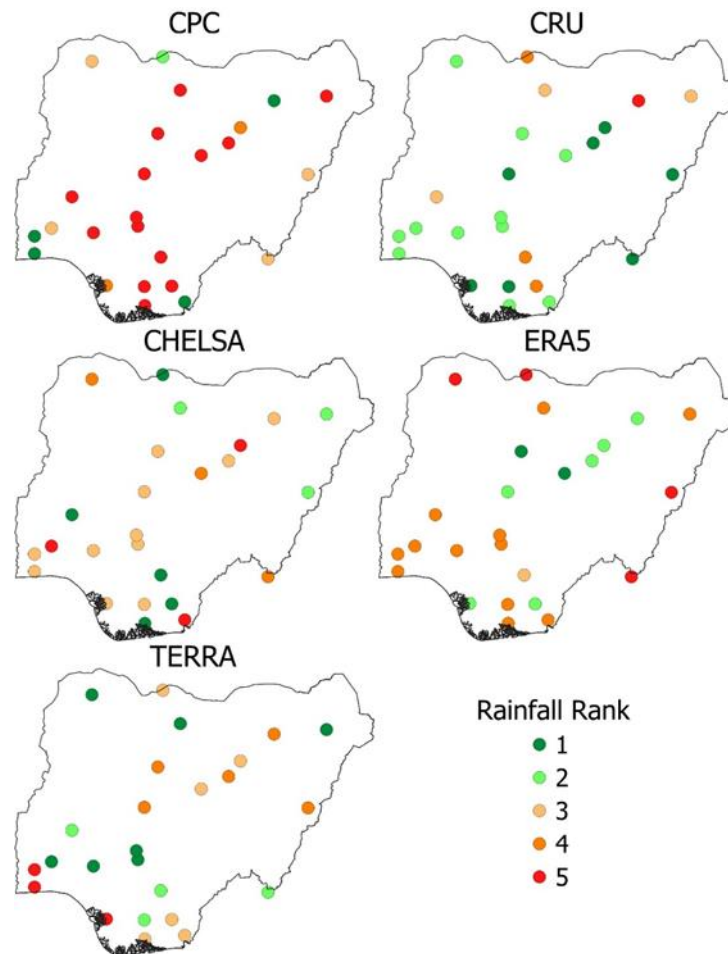


Figure 8. The rank of different gridded data products based on the compromise programming approach in validating replicating rainfall at different stations. The color ramp indicates the rank at different observation stations

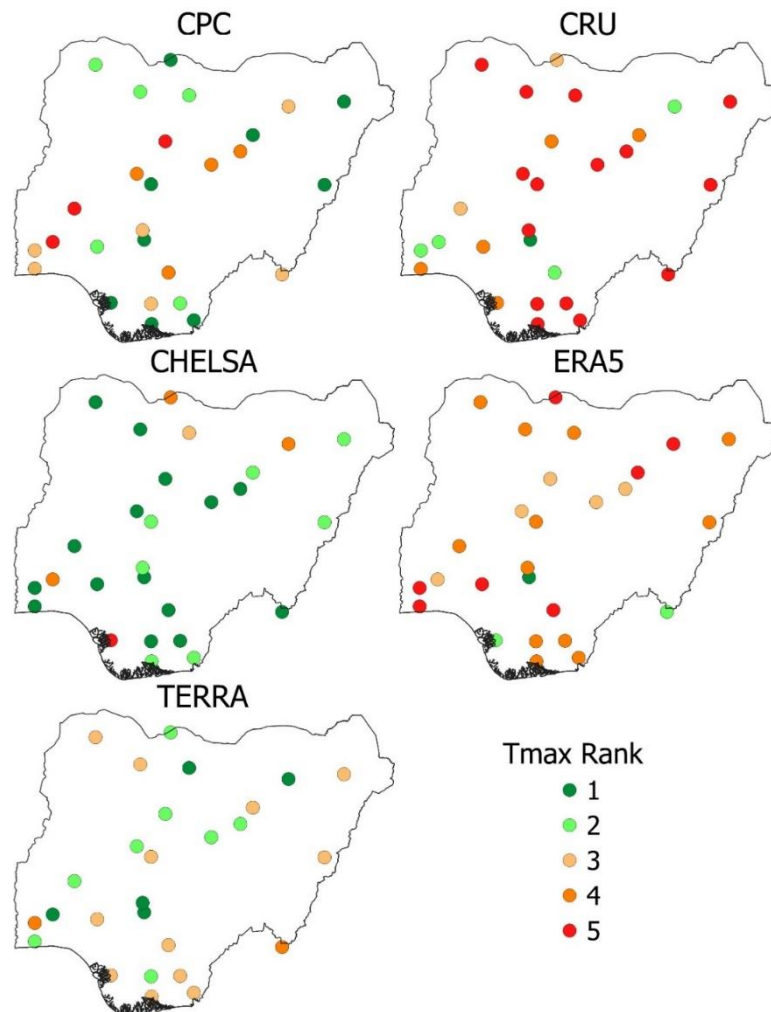


Figure 9. The rank of different gridded data products based on the compromise programming approach in validating replicating maximum temperature at different stations. The color ramp indicates the rank at different observation stations.

Group decision index was also applied in compromise programming method in order to rank the gridded dataset based CPI ranking. Table 7 shows the ranking of the gridded datasets based on the rainfall, maximum and minimum temperature ranking. The results shows clearly agreed with the result obtained from the STS .

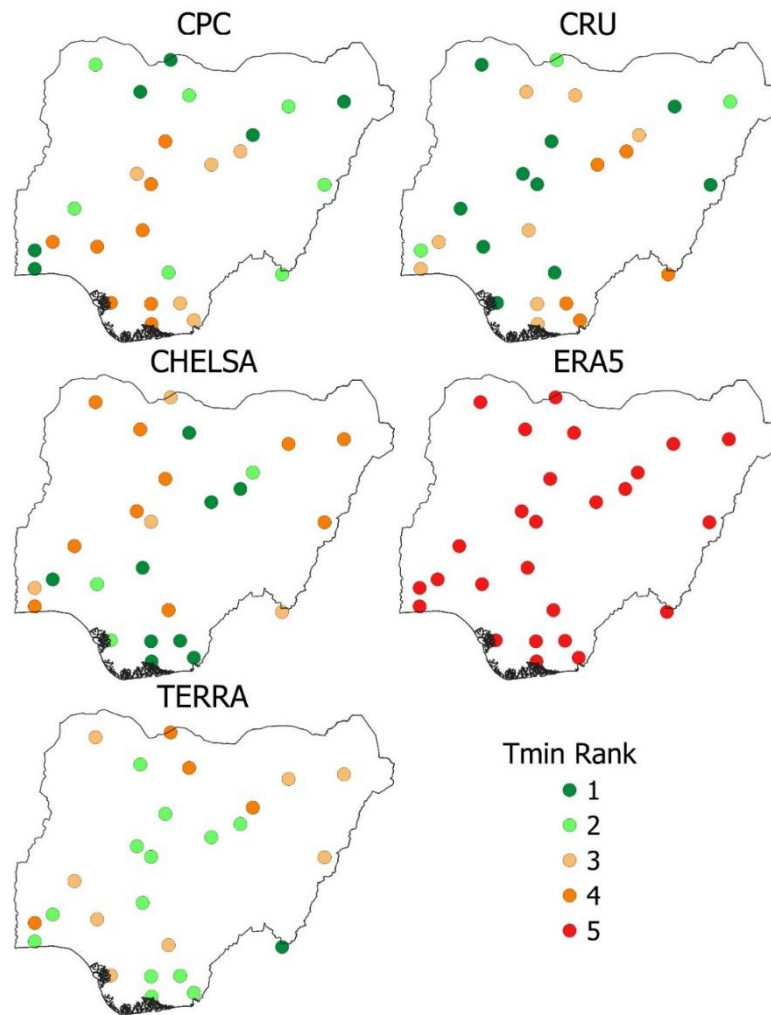


Figure 10. The rank of different gridded data products based on the compromise programming approach in validating replicating minimum temperature at different stations. The color ramp indicates the rank at different observation stations.

Table 5. Group decision index and the ranking of five gridded datasets for rainfall, maximum and minimum temperature-based compromise programming method

Dataset	Rainfall		Max Temperature		Min Temperature		R_m	Final Rank
	R_m	Rank	R_m	Rank	R_m	Rank		
CPC	9.1	4	14.1	2	13.2	3	1.07	4
CRU	14.5	1	6.9	4	15.4	1	2.25	1
CHELSA	11.5	3	18.8	1	14.3	2	1.83	2
ERA	9.1	4	7.1	5	5.2	5	0.65	5
TERA	12.9	2	12.5	3	11.2	4	1.08	3

Discussion and Conclusion

This study assessed the performance of five different temperature and rainfall gridded data products at 25 observed stations on a monthly scale across Nigeria using STS. The study utilised a minimum data period of 35 years (1980–2015), exceeding the World Meteorological Organization's (WMO) recommended 30 years for analysing climatic trends. In this study, the best gridded data product was chosen for both rainfalls, Tmax and Tmin, as choosing different datasets might result in highly significant errors in providing interrelated indices. The results show that the time series similarity method can be employed in ranking the gridded

dataset based on their performance in selecting a suitable dataset for impact studies. The STS revealed the CRU data product as Nigeria's most appropriate gridded dataset and also the result based on validation using compromise programming agreed with the results from the time series, i.e. ranking the CRU dataset as the most suitable gridded dataset for replicating the observation station data performance in selecting a suitable dataset for impact studies. Findings from studies in some regions within Nigeria have proved consistent with the present findings. The CRU performed best in the Niger Delta region (Lawal et al., 2021). Also, Salaudeen et al. (2021) validated CPC and CRU temperature data products for the Upper Benue River Basin. CRU proved superior and was chosen for water resource assessment. The CRU gridded datasets can be confidently used to replace measured station data for climatic studies in Nigeria. Future research studies can be undertaken to evaluate the effectiveness of the methods in evaluating gridded data with a high temporal resolution (daily datasets). The reliability of CRU gridded data to replicate precipitation and temperature extremes in the study area can also be evaluated by employing it in various hydro-climatic studies, like droughts and aridity.

References

- Abatan, A. A., Abiodun, B. J., Lawal, K. A., & Gutowski, W. J. (2016). Trends in extreme temperature over Nigeria from percentile-based threshold indices. *International Journal of Climatology*, 36(6), 2527–2540. <https://doi.org/10.1002/joc.4510>
- Abdourahamane, Z. S. (2021). Evaluation of fine resolution gridded rainfall datasets over a dense network of rain gauges in Niger. *Atmospheric Research*, 252(July 2020), 105459. <https://doi.org/10.1016/j.atmosres.2021.105459>
- Ahmed, K., Shahid, S., Wang, X., Nawaz, N., & Khan, N. (2019). Evaluation of gridded precipitation datasets over arid regions of Pakistan. *Water*, 11(2), 210.
- Ahmed, K., Shahid, S., Wang, X., Nawaz, N., & Najeebullah, K. (2019). Evaluation of gridded precipitation datasets over arid regions of Pakistan. *Water (Switzerland)*, 11(2). <https://doi.org/10.3390/w11020210>
- Akande, A., Costa, A. C., Mateu, J., & Henriques, R. (2017). Geospatial Analysis of Extreme Weather Events in Nigeria (1985-2015) Using Self-Organizing Maps. *Advances in Meteorology*, 2017. <https://doi.org/10.1155/2017/8576150>
- Ardil, C. (2021). *Comparison of Composite Programming and Compromise Programming for Aircraft Selection Problem Using Multiple Criteria Decision Making Analysis Method*. December.
- Bai, P., & Liu, X. (2018). Evaluation of five satellite-based precipitation products in two gauge-scarce basins on the Tibetan Plateau. *Remote Sensing*, 10(8), 1316.
- Bala, A., Aliu, A. M., & Salihu, L. (2023). Evaluation of CMIP6 Models Skill in Representing Annual Extreme Precipitation over Northern. 27(2), 49–61. <https://doi.org/10.9734/JGEESI/2023/v27i2670>
- Beck, H. E., Pan, M., Roy, T., Weedon, G. P., Pappenberger, F., Van Dijk, A. I. J. M., Huffman, G. J., Adler, R. F., & Wood, E. F. (2019). Daily evaluation of 26 precipitation datasets using Stage-IV gauge-radar data for the CONUS. *Hydrology and Earth System Sciences*, 23(1), 207–224. <https://doi.org/10.5194/hess-23-207-2019>
- Benítez, I., & Díez, J.-L. (2022). Automated Detection of Electric Energy Consumption Load Profile Patterns. *Energies*, 15(6), 2176.
- Freimer, M., & Yu, P. L. (1976). Some New Results on Compromise Solutions for Group Decision Problems. *Management Science*, 22(6), 688–693. <https://doi.org/10.1287/mnsc.22.6.688>
- Hassan, I., Kalin, R. M., White, C. J., & Aladejana, J. A. (2020). Evaluation of daily gridded meteorological datasets over the Niger Delta region of Nigeria and implication to water resources management. *Atmospheric and Climate Sciences*, 10(1), 21–39.
- He, W., Ma, L., Yan, Z., & Lu, H. (2023). Evaluation of advanced time series similarity measures for object-based cropland mapping. *International Journal of Remote Sensing*, 44(12), 3777–3800.

- Ibrahim, A. H., Molla, D. D., & Lohani, T. K. (2022). Performance evaluation of satellite-based rainfall estimates for hydrological modeling over Bilate river basin, Ethiopia. *World Journal of Engineering*, June. <https://doi.org/10.1108/WJE-03-2022-0106>
- Lawal, I. M., Bertram, D., White, C. J., Jagaba, A. H., Hassan, I., & Shuaibu, A. (2021). Multi-criteria performance evaluation of gridded precipitation and temperature products in data-sparse regions. *Atmosphere*, 12(12), 1597.
- Lawal, Y. B., Ojo, J. S., & Falodun, S. E. (2021). Variability and trends in rain height retrieved from GPM and implications on rain-induced attenuation over Nigeria. *Heliyon*, 7(10), e08108. <https://doi.org/10.1016/j.heliyon.2021.e08108>
- Li, H., Fang, L., Wang, P., & Liu, J. (2012). An algorithm based on piecewise slope transformation distance for short time series similarity measure. *Proceedings of the 10th World Congress on Intelligent Control and Automation*, 691–695.
- Liao, T. W. (2005). Clustering of time series data—a survey. *Pattern recognition*, 38(11), 1857–1874.
- Möller-Levet, C. S., Klawonn, F., Cho, K.-H., Yin, H., & Wolkenhauer, O. (2005). Clustering of unevenly sampled gene expression time-series data. *Fuzzy sets and Systems*, 152(1), 49–66.
- Momeni, M., Behzadian, K., Yousefi, H., & Zahedi, S. (2021). A Scenario-Based Management of Water Resources and Supply Systems Using a Combined System Dynamics and Compromise Programming Approach. *Water Resources Management*, 35(12), 4233–4250. <https://doi.org/10.1007/s11269-021-02942-z>
- Muhammad, M. K. I., Nashwan, M. S., Shahid, S., Ismail, T. bin, Song, Y. H., & Chung, E. S. (2019). Evaluation of empirical reference evapotranspiration models using compromise programming: A case study of Peninsular Malaysia. *Sustainability (Switzerland)*, 11(16). <https://doi.org/10.3390/su11164267>
- Nashwan, M. S., & Shahid, S. (2019). Symmetrical uncertainty and random forest for the evaluation of gridded precipitation and temperature data. *Atmospheric Research*, 230(July), 104632. <https://doi.org/10.1016/j.atmosres.2019.104632>
- Nashwan, M. S., Shahid, S., & Chung, E. S. (2019). Development of high-resolution daily gridded temperature datasets for the central north region of Egypt. *Scientific Data*, 6(1), 1–13. <https://doi.org/10.1038/s41597-019-0144-0>
- Ogbu, K. N., Hounguè, N. R., Gbode, I. E., & Tischbein, B. (2020). Performance evaluation of satellite-based rainfall products over Nigeria. *Climate*, 8(10), 103.
- Ren, P., Li, J., Feng, P., Guo, Y., & Ma, Q. (2018). Evaluation of multiple satellite precipitation products and their use in hydrological modelling over the Luanhe River Basin, China. *Water (Switzerland)*, 10(6). <https://doi.org/10.3390/w10060677>
- Salaudeen, A., Ismail, A., Adeogun, B. K., & Ajibike, M. A. (2021). Validating Gauge-based Spatial Surface Atmospheric Temperature Datasets for Upper Benue River Basin, Nigeria. *Nigerian Journal of Environmental Sciences and Technology*, 5(1), 173–190. <https://doi.org/10.36263/nijest.2021.01.0259>
- Salehie, O., Ismail, T., Shahid, S., Ahmed, K., Adarsh, S., Asaduzzaman, M., & Dewan, A. (2021). Ranking of gridded precipitation datasets by merging compromise programming and global performance index: a case study of the Amu Darya basin. *Theoretical and Applied Climatology*, 144(3–4), 985–999. <https://doi.org/10.1007/s00704-021-03582-4>
- Salman, S. A., Shahid, S., Ismail, T., Al-Abadi, A. M., Wang, X. jun, & Chung, E. S. (2019). Selection of gridded precipitation data for Iraq using compromise programming. *Measurement: Journal of the International Measurement Confederation*, 132, 87–98. <https://doi.org/10.1016/j.measurement.2018.09.047>
- Sehad, M., Lazri, M., & Ameer, S. (2017). Novel SVM-based technique to improve rainfall estimation over the Mediterranean region (north of Algeria) using the multispectral MSG SEVIRI imagery. *Advances in Space Research*, 59(5), 1381–1394.
- Shiru, M. S., Shahid, S., Chung, E.-S., Alias, N., & Scherer, L. (2019). A MCDM-based framework for selection of general circulation models and projection of spatio-temporal rainfall changes: a case study of

Nigeria. *Atmospheric Research*, 225, 1–16.

Wang, Z., Shang, P., & Mao, X. (2023). Ordinal network-based affine invariant Riemannian measure and its expansion: powerful similarity measure tools for complex systems. *Nonlinear Dynamics*, 111(4), 3587–3603.

Waseem, S., Muhammad, I., Rehan, L., Shahzada, A., & Muhammad, A. (2022). Performance evaluation and comparison of observed and reanalysis gridded precipitation datasets over Pakistan. *Theoretical and Applied Climatology*, 0123456789, 4100.

Xu, X., Zhang, X., & Li, X. (2023). Evaluation of the Applicability of Three Methods for Climatic Spatial Interpolation in the Hengduan Mountains Region. *Journal of Hydrometeorology*, 24(1), 35–51.

Zeleny, M. (2011). Multiple Criteria Decision Making (MCDM): From Paradigm Lost to Paradigm Regained? *Journal of Multi-Criteria Decision Analysis*, 18(1–2), 77–89. <https://doi.org/10.1002/mcda.473>

Zhang, M., & Pi, D. (2017). A novel method for fast and accurate similarity measure in time series field. *2017 IEEE International Conference on Data Mining Workshops (ICDMW)*, 569–576.

PASTRY PRODUCTS WITH A LOW SUGAR CONTENT THROUGH THE USE OF SUBSTITUTES

Huțu Dana

Faculty of Food Engineering, Stefan cel Mare University of Suceava, Country Romania

Amariei Sonia

Faculty of Food Engineering, Stefan cel Mare University of Suceava, Country Romania

ABSTRACT

In recent decades, people's interest in adopting a healthy lifestyle, characterized by low sugar consumption, has seen a significant increase. This change in attitude comes in response to the many scientific studies that highlight the negative impact of excessive sugar consumption on human health. Aspects such as the alarming increase in the rate of obesity, type 2 diabetes and other metabolic conditions have prompted more and more people to reevaluate and adjust the nutritional content of their diet. Substituting sugar (with apple puree, oligofructose, stevia, inulin, date syrup) in pastry and bakery products is a healthy alternative, but this alternative can change the properties of the pastry batter. The purpose of this study was to analyze the textural properties (Hardness, Adhesiveness, Stickiness, Cohesivity, Gumminess and Chewiness) of the muffin batter, the humidity and the specific weight of the batter. The specific weight increased along with the water content and varied from 0.93 (PC) to 1.03 (P100). The water content of the muffin dough increased as the percentage of brown sugar was raised, respectively the percentage of apple puree, which has a higher humidity than sugar. The sample with the textural properties closest to those of the control sample was P60, in which 60% of the amount of sugar was substituted with apple puree. Based on the results obtained, apple puree can be a substitute for sugar in baked goods due to the natural sweetness it adds, the ability to maintain moisture and the possibility to reduce the total sugar intake.

Key words: sugar, apple puree, muffins, texture, specific gravity, moisture content

ENVIRONMENTAL PROTECTION AS A RECOGNIZED NECESSITY FOR HUMAN SOCIETY

Assoc. prof. M. As. Michailov

PhD – SWU “Neofit Rilski” – Bulgaria

ABSTRACT

The position of some structures in the Society regarding the idea of environmental protection is incomprehensible, including and through the intervention of political and ideological approaches.

In the proposed material, some ideas regarding these activities are offered for discussion, paying attention to the ecologically sound use of nature, which will contribute to a more distinct economic effect in production and consumption, i.e., the benefit of environmental protection will be realized not only through NGO-campaigns, but through fuller engagement of all structures in Society.

Keywords: environmental protection, environmental protection activities, anthropogenic impact, economic development

EXPLORING CHAT-GPT'S PIVOTAL ROLE IN SHAPING THE LANDSCAPE OF INDUSTRY 4.0

Zohaib Hassan Sain

Superior University, Faculty of Business & Management Sciences, Pakistan
ORCID ID: <https://orcid.org/0000-0001-6567-5963>

ABSTRACT

This research delves into the transformative role of Chat-GPT in Industry 4.0, exploring its profound impact on communication dynamics within the Fourth Industrial Revolution. Chat-GPT, an advanced language model, plays a pivotal role in optimizing efficiency, refining decision-making processes, and fostering collaboration across diverse industrial sectors. The study rigorously investigates the challenges and opportunities associated with integrating Chat-GPT, emphasizing critical factors such as data security, ethical considerations, and scalability. By shedding light on Chat-GPT's implications in Industry 4.0, this research contributes to our nuanced understanding of how language models drive innovation, influencing human-machine collaboration and communication dynamics in the continually evolving technological landscape.

Keywords: Chat-GPT, Industry 4.0, Innovation in Communication, Human-Machine Interaction, Technological Advancements.

EXPLORING THE TRANSFORMATIVE IMPACT: AI'S INFLUENCE ON ADVANCEMENTS IN INDUSTRIAL RESEARCH

Zohaib Hassan Sain

Superior University, Faculty of Business & Management Sciences, Pakistan
ORCID ID: <https://orcid.org/0000-0001-6567-5963>

ABSTRACT

This research investigates the transformative influence of artificial intelligence (AI) on the landscape of industrial research. AI, as a powerful tool, plays a pivotal role in shaping and advancing research methodologies within diverse industrial sectors. The study delves into the specific ways AI is revolutionizing data analysis, pattern recognition, and decision-making processes in industrial research. It also explores the challenges and opportunities associated with the integration of AI, addressing ethical considerations, data privacy, and the overall impact on research outcomes. By examining the multifaceted role of AI in industrial research, this research contributes to a deeper understanding of the evolving dynamics between technology and scientific inquiry.

Keywords: Artificial Intelligence (AI), Data Analysis, Industrial Research, Pattern Recognition, Research Methodologies.

POLYPYRROLE- EMBEDDED PHOSPHATE NANOPARTICLES: AN EFFICIENT APPROACH FOR HEAVY METAL REMOVAL IN WASTEWATER TREATMENT

Hamid Zouggari

Laboratory of Materials and Environment, Faculty of Sciences, Ibn Zohr University, Agadir, Morocco.

Mahir Fatima-Zahra

*Laboratory of Materials and Environment, Faculty of Sciences, Ibn Zohr University, Agadir, Morocco.
Organic Chemistry and Physical Chemistry Laboratory, Faculty of Sciences, Ibn Zohr University, Agadir, Morocco.*

Albourine Abdallah

Laboratory of Materials and Environment, Faculty of Sciences, Ibn Zohr University, Agadir, Morocco.

ABSTRACT

Heavy metals have become an issue of extreme concern across the globe as a result of its harmful effects, Herein, we report the elaboration of polypyrrole-embedded phosphate nanoparticles composite for the Cr(VI) ions removal from water. The adsorption capability of as-synthesized composite towards Cr(VI) ions has been evaluated under several experimental conditions, such as the adsorbent dosage, initial dye concentration, contact time under agitation, pH of dye solution and temperature. Thermodynamics parameters such as free energy (ΔG°), entropy (ΔS°), and enthalpy (ΔH°) were also calculated and suggested that the adsorption process is spontaneous and endothermic in nature. The kinetics data revealed that the adsorption of Cr(VI) ions onto the composite follows the pseudo-second order kinetics model. The maximum adsorption capacity was found to be $53.74 \text{ mg}\cdot\text{g}^{-1}$. Moreover, the composite surface displayed a Langmuir-like adsorption isotherm, in contrast to a Freundlich isotherm, owing to its homogeneous active site distribution. Regeneration investigation showed the excellent reusability of the composite during the cleaning up of solution containing Cr(VI) ions. Hence, we may assert that the polypyrrole-embedded phosphate nanoparticles composite has a potential application prospect as an efficient adsorbent for Cr(VI) ions adsorption.

Keywords: Wastewater treatment, polypyrrole-embedded phosphate nanoparticles, Cr(VI) ions removal, regeneration.



THE EFFECT OF SYNTHETIC MATERIALS ON A BIOLOGICAL SYSTEM

Irina Nikolayevna Ivashchenko

Candidate of Technical Sciences, Associate Professor, KUBGU "Kuban State University", Krasnodar, Russia

Sivoplyasova Alina Olegovna

Student, KUBGU "Kuban State University", Krasnodar, Russia

ABSTRACT

The article discusses the impact of synthetic materials on health. Scientific facts and simple solutions to minimize the negative impact.

Keywords: synthetic, textile, health, fabrics, materials, influence, biological system.

Introduction

Modern industrial technology has long since brought to the forefront the use of synthetic materials in various areas of our lives. From clothing and bedding to furniture and car seats, synthetics are all around us. Synthetic textile materials are widely used in everyday life and have many advantages. However, their impact on the human body as a biological system is an undeniable fact.

The study of a biological system represents a wider interaction of the human organism, both with the properties of the product and with the surrounding external environment, taking into account the changes occurring in the ratios of components of the internal environment of the organism not only at the biological and psychophysiological level, but also in their integrity and unity with regulatory functions.

Investigating the effects of synthetic textiles on body thermoregulation is a significant challenge in the current scientific field, especially in the context of their interaction with the human body as a biosystem. According to the results of many studies, synthetic materials have properties that can affect the body's functioning and its ability to maintain an optimal temperature.

One of the most important characteristics of synthetic materials that affects body temperature is their ability to retain heat. Unlike natural materials, synthetics do not have direct breathability abilities, which can affect the body's thermoregulation. Some synthetics, such as Nitron, have good thermal insulation properties, which can inhibit the natural escape of heat.

Synthetic textile materials have a number of characteristics that can affect the human body.

Given the specific properties of synthetic materials, it should be noted that they have low permeability to air. This can negatively affect the respiratory system of a person, especially for those who suffer from allergic reactions or have hypersensitivity to irritants. Synthetic materials do not have the same ability to absorb moisture as natural materials, resulting in increased sweating and moisture in the undergarment.[1]

A further aspect is the ability of synthetic materials to accumulate static electricity. When such materials are used, micro-particles, including dust and contaminants from the environment, may be attracted. This situation can cause discomfort on the skin and can be a source of irritation. In addition, many synthetic textile materials are used with added chemicals such as dyes and various drug treatments. Some of these substances can cause allergic reactions or have potentially harmful effects on the human body with individual characteristics, which can lead to the development of various respiratory diseases such as bronchitis or asthma.

One of the most popular synthetic materials is polyester. Studies show that when wearing products with polyester fibers, static electricity builds up on the skin, which can cause discomfort. In addition, polyester does not allow the skin to breathe, which can cause sweating and discomfort. [1]

Another important aspect of the effect of synthetic fabrics on the body is the toxicity of some of them. For example, synthetic fabrics containing formaldehyde or azo dyes can cause allergic reactions and skin irritation [3]. When producing materials, it is necessary to strictly adhere to the regulatory documentation in terms of free formaldehyde content.

According to SanPiN 2.1.2.2.1078-01 "Hygienic requirements for textile and yarn fibers and threads, as well as finished textile products" of the Ministry of Health of the Russian Federation, the formaldehyde content in textile products should not exceed 30 mg/kg. However, some synthetic fabrics may contain insignificant but still present amounts of formaldehyde that can cause allergic reactions in children.

Thus, the effect of synthetic materials on the skin and the body as a whole should be taken into account when choosing clothing and other textiles for everyday use, especially for children and adolescents, as well as for the elderly. In the former, the thermoregulation system is not yet perfect, only in the development is, and in the latter - its functions are declining. According to all normative documents it is recommended to give preference to natural materials, in the fiber composition of which prevail components of cotton, linen or wool and silk, which allow the skin to breathe and minimize the risk of various pathologies and strictly comply with the proposed percentage of synthetic fibers by type of material.

A harmonious combination of synthetic fibers in fabrics can minimize the number of negative factors of their use. And at preservation of the best properties of natural fibers to provide in combination with synthetic fibers the necessary strength characteristics, wear resistance, stretchability, elasticity, thermoplasticity.

List of references used

1. Health Harms of Synthetic Fabrics: URL: http://zdravnic_a.net/health/healthy-lifestyle/health-and-beauty/1160-damage-synthetic-fabric-for-health
2. Orlenko L. B., Gavrilova N. I. Konfeksionirovanie materialovaniy for clothes: Study guide. -M.: FORUM: INFRA-M, 2006. -288.c
3. Mesyachenko V.T. Synthetic fabrics. - Moscow : Economics, 1965. - 158 c. : ill. ; 20 cm. - Bibliography: p. 155-156.

EXPLORING THE CAPABILITIES OF UNITY 3D GAMING SOFTWARE

Dhruv Kohli

Chitkara University Institute of Engineering and Technology Chitkara University, Punjab, India

Devang Khurana

Chitkara University Institute of Engineering and Technology Chitkara University, Punjab, India

Barinder Singh

Chitkara University Institute of Engineering and Technology Chitkara University, Punjab, India

Amanpreet Kaur

Chitkara University Institute of Engineering and Technology Chitkara University, Punjab, India

Paras Sachdeva

Chitkara University Institute of Engineering and Technology Chitkara University, Punjab, India

ABSTRACT

Unity 3D game engine is a great platform to build different kinds of game easily and efficiently, which is very useful to develop the game of your own kind. It consists of many different types of assets which are helpful for building up designed and interactive games. It consists of concepts of physics like box collider, gravity, rigidbody, etc. which are provided with the help of the C# scripting language used in unity deployed with the help of the Visual Studio Code Editor. Unity has made the game development process much easier for the developer which provides access to different types of gaming experience also used with Virtual Reality, which is an amazing feature of this Software.

Keywords: Innovation, Learning Opportunities, Practical Training, Knowledge Sharing, Research and Development, Gaming, Scripting, Assets, Interactive

I. INTRODUCTION

Some of the most played video games were made with the help of the Unity 3D game engine, including super Mario Bros. It is used to create games for all major platforms, including Windows, Mac OS, iOS, Android, Xbox, PlayStation, and Nintendo. Unity 3D is a game engine released in 2005 by Unity Technologies. It is a comprehensive game engine that includes a powerful rendering engine, physics engine, animation system, and scripting language [1].

The Unity 3D game engine is designed to be easy to use, and has learning opportunities with a simple user interface and powerful tools for creating high-quality 3D graphics. It also includes a variety of tools for creating realistic environments, character models, and complex scenes. The Unity 3D game engine is also used for AR and VR development applications. It enables developers to create high-quality experiences that can be used on a variety of platforms. Unity gives a successful entrepreneurship journey to students who want to pursue their career in the gaming sector.

This software allows developers to create sharable 3D experiences on the web. It is also used by a wide range of developers, from professionals creating AAA titles to indie developers creating casual games. It is an ideal platform for creating mobile games that can be used to create some of the most popular mobile titles, such as Angry Birds and Temple Run [2].

II. UNITY EDITOR

It contains windows like inspector, toolbar, game view, etc. as shown in Fig. 1. Assets of these windows and

their properties have been brought into solidarity. It is accessible whenever intelligent and vivid encounters can be created progressively. Windows, Linux, or Macintosh can be chosen as a working framework.

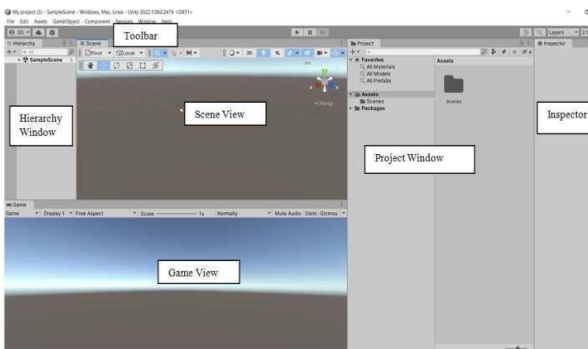


Fig: 1 Affiliates in unity 3d

GAME AND SCENE VIEW:

During game development, the game view assists clients in reviewing the overall look and feel of the game. It enables developers to change variables and allows them to test the modified changes repeatedly. This implies that the developer doesn't need to gather or send the project for each opportunity to experience the changes.

In game development, game view shows the player's perspective of the game world, while the scene view shows the developer's perspective. The game view allows for testing game play mechanics and visuals, while the scene view is used for editing and manipulating the game's components. The scene and game view are shown in Fig. 2 below to understand both the views simultaneously [3].

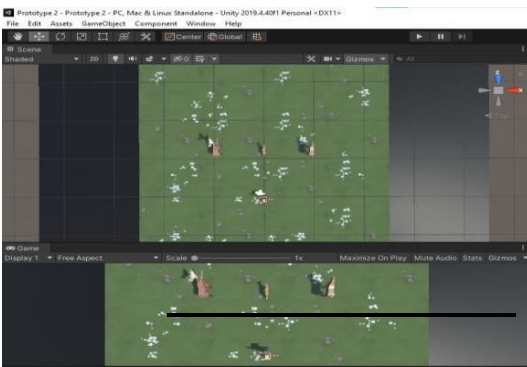


Fig: 2 Game and Scene view

A. INSPECTOR

Utilizing inspector, every component of a game item can be changed. A designer can change the properties of objects available in the scene view to obtain the right look and feel. Sound, physical science, contents, and colliders are parts combined with an object. These parts can be seen in the' Fig.3 given below.

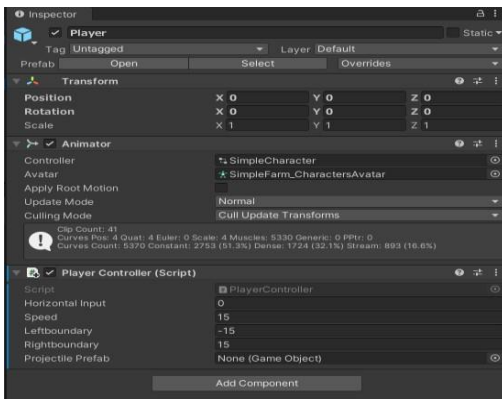


Fig: 3 Inspector window

B. 'HIERARCHY':

Hierarchy panel displays a hierarchical view of all game objects in a scene, organized by their parent-child relationships. This allows for easy manipulation and management of game objects. An engineer can put together items on top of each other like a parent-youngster ordered progression as displayed in Fig. 4.'

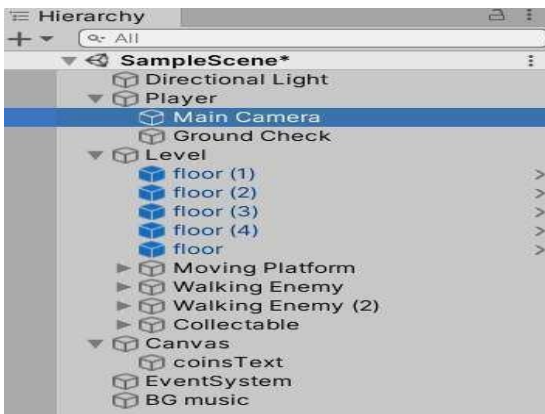


Fig: 4 Hierarchy Window

➤ ESTABLISHING SCENES OF UNITY

The process of loading a game in Unity 3D is fairly straight forward. Firstly, the user must create a new scene in the unity editor and then add the required game objects. Then, they must create scripts to control the game objects and assign them to the relevant game objects. After that, they must add the required assets and textures to the project, set up the physics, lighting, and audio components. Once it is done, the user can then add the user interface elements like menus, scoreboards, etc. Finally, the user has to test the game for bugs and errors, compile and build the game for the target platform and publish [4].

III. UNITY ASSET STORE

The Unity Asset Store is a marketplace for 3D models, audio, textures, graphics, scripts, and more, all built by a thriving community of Unity developers. It allows developers to find the right assets for their projects quickly and easily, and also provides an easy way to make money by selling their own creations. With a wide variety of content and regular sales, the unity asset store is a great place for game developers to get the content they need [5].

SCRIPTING

Scripting in unity 3D is an important part of creating immersive, interactive experiences in games which need practical training. Unity, as a powerful game engine, has all the tools necessary to create complex, but it all comes down to how you use them. Scripting is the process of creating scripts to control games 'objects, their behavior, and the overall logic of the game. It is done using C# programming language that is simple to learn, making it a great choice for scripting in unity [6]. It is also a cross-platform language, so you can write scripts once and deploy them to all platforms that unity supports. Unity provides several tools to help you with scripting, such as the Visual Studio Code editor and the MonoDevelop IDE. These editors provide a compiler, debugger, and other helpful tools to help you write scripts more efficiently. While writing scripts, the unity API can be used to access features of the engine. The Unity API allows you to access components and objects in your scene, modify their properties, and manage their behavior. The API can be used to create custom components and objects shown in Fig. 5.

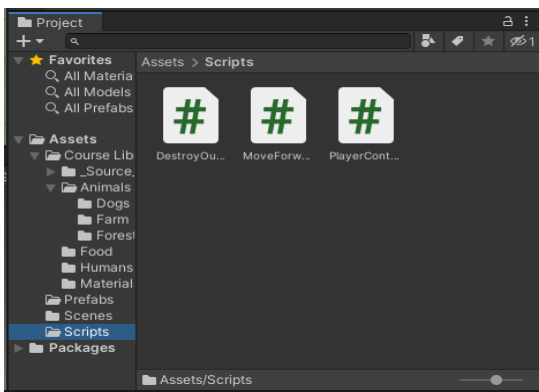


Fig: 5 Types of Scripts in Unity

Table -1 Different characteristics of ' Unity 3D'

'Navigating the Interface'	Object Manipulation	'Import & Export Assets'	Scene Setup	Physics	Assets Combinations
Framework [8]	selection	assets	adding component* to a game object*	'rigid bodies & collider	texture
'Scene'	moving	'importing' 3d models	scene border*	physics material	materials
Hierarchy	rotating	importing scripts	adding meshes	no relation	scene building
Project	scaling	asset packages	asset usage	moving forward	assets folder downloaded here
Inspector	modify attributes	customizing the ground	editing properties	scripting	adding component

The ' MonoBehaviour class that allows the content to run in the game circle. When the content is in running mode, unity provides default strategies that are automatically requested in the unit. Some common strategies are being characterized below :

Start (): This tactic is used once, before the material receives the most recent update.

Update (): This method activates each edge when the game is in running mode and the contents are empowered.

‘**OnDestroy ()**: This technique destroys MonoBehaviour. It stops before hand dynamic game articles.’

OnCollisionEnter (): This technique is activated when rigid bodies or colliders collide [7].’

‘Inspector can be used to’ proclaim factors, ‘and the client can see factors in the monitor window.’

IV. SPECIFIC FEATURES OF UNITY

a) *Configuration*: - The interface consists of essential panels like the Scene view for designing game environments, the Game view for real-time previews, and the Hierarchy view for managing game objects. The Project view organizes assets, while the Inspector view provides detailed control over selected elements. Unity's intuitive drag-and-drop functionality enhances workflow efficiency. Additionally, customizable layouts empower developers to tailor their workspace, fostering a seamless experience as shown in Fig 6.

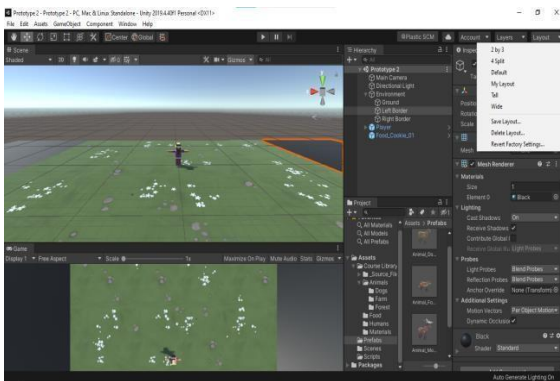


Fig: 6 Types of Layout

b) *Modifying the Objects*:-.

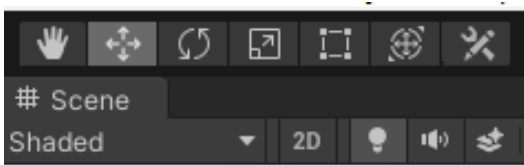


Fig: 7 Different Tools used for movement

With the click of a mouse, you can easily move, rotate, and scale objects in 2D and 3D space as shown above in Fig. 7. The software also allows you to assign materials to objects, adjust lighting, and modify physics. It includes a variety of tools to help you create complex 3D environments or objects that are realistic and detailed. You can also use Unity 3D to create interactive games and experiences, such as virtual reality and augmented reality [9].

c) *Assets*:

Unity Assets are packages of pre-built game objects, scripts, textures, models, sounds, and other game-related materials that can be used to create a complete game. Unity assets can be used to quickly create games with a high level of customization and polish [10]. Assets are available on its website and can be downloaded and transferred to the Assets folder as shown in Fig. 8. Unity Assets are a great way to speed up the research and development process [11].

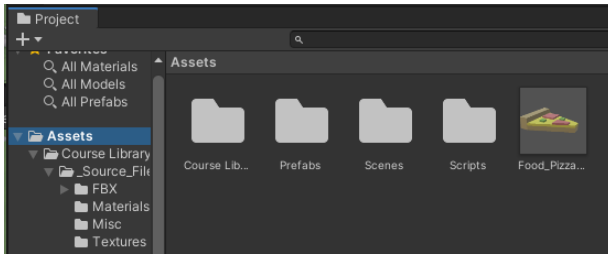


Fig: 8 Assets in Unity

d) *Physics:*

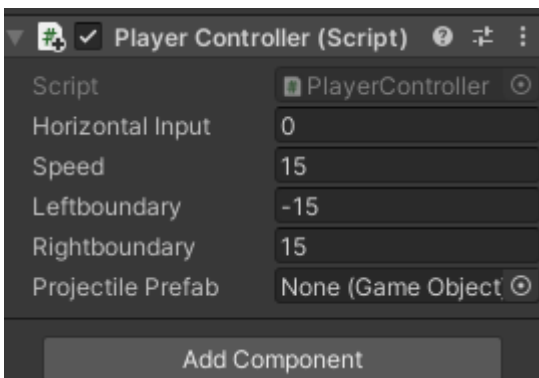


Fig: 9 Player Controlling Script

As shown in Fig 9, these elements of Leftboundary and Rightboundary are applied so that the player should not move out of the border area of the ground [12].

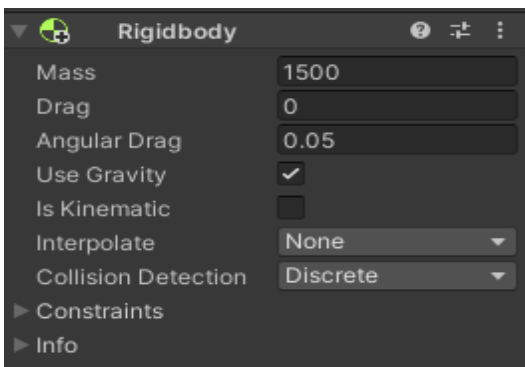


Fig: 10 Rigidbody window

As shown in Fig: 10, that Rigidbody has numerous options. Firstly, there are settings to control the mass drag and angular drag of the game object. The mass of the object affects how collisions are treated with the object. 'Game objects with higher mass will react less when colliding with lower mass game object. The drag of a game object affects how quickly it will slow down without other interactions and angular drag effects'. If you are adding torque to the object to rotate it, the angular drag would create resistance to this force.

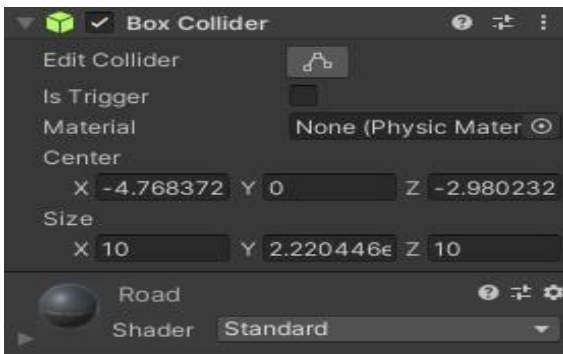


Fig: 11 Box collider

As shown in Fig: 11 box 'colliders are a component that permits the game object to react with other colliders. These are the components that 'define the shape of a game object for the purpose of collisions'. It is undetectable, and does not need to be in exact state.'

There are two types of box colliders:-

- i. **Primitive:** - It further includes a Box collider, capsule collider and sphere colliders in 2D or 3D form.
- ii. **Non – Primitive:** - It further contains Mesh colliders in 3D and Polygon colliders in 2D form.

Triggers: - Triggers don't have actual collision but they detect if one collider enters the space of another collider by creating a physical collision.

e) *Consolidating Assets:*

Consolidating assets for the Unity 3D gaming software is a great way to streamline development time, create a unified look and feel for all game assets, and reduce code bloat. Not only does consolidating assets streamline development time, it also helps reduce the memory footprint of the game, allowing for smoother performance. Additionally, it allows developers to quickly update and replace assets without needing to rewrite any code, saving precious time and money.

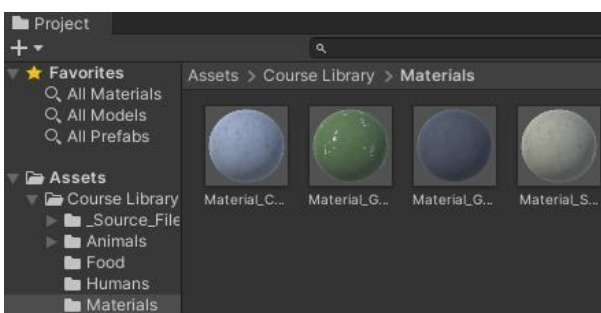


Fig: 12 Materials used in Unity scene view

Fig. 12 above shows the consolidating assets for Unity 3D that ensures that all game assets look consistent, reducing the need for complex coding solutions. This allows the users to customize the background, surface and the scene according to their interests.

V. APPLICATIONS DEVELOPED

USING UNITY

Unity is a powerful gaming engine that allows developers to create immersive and interactive 3D experiences for players. It is one of the most versatile game engines available and can be used to develop for a variety of platforms including mobile, console, and PC. Unity also provides an extensive development environment that allows developers to create and test their projects quickly [13].

A. CAR DRIVING:

The game comprises a scene view sandbox. Unity 3D's car driving simulation offers realistic smooth controls and immersive graphics. Create custom car models, design tracks, implement AI traffic, and simulate real-world driving scenarios for engaging gameplay experiences [14]. Scene and game view are displayed in Fig. 13 below.

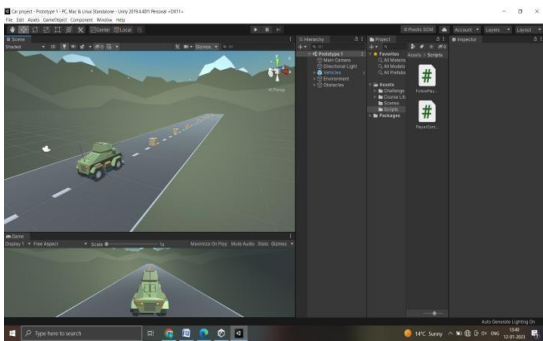


Fig: 13 Car Driving game views

B. FOOD FLIGHT:

The experience could involve the user flying through a 3D environment, collecting food items such as fruits and vegetables and avoiding obstacles as shown in Fig. 14.

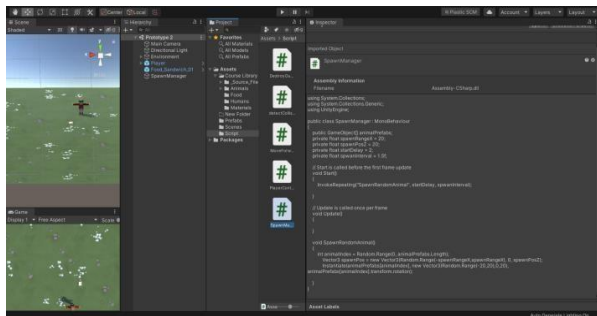
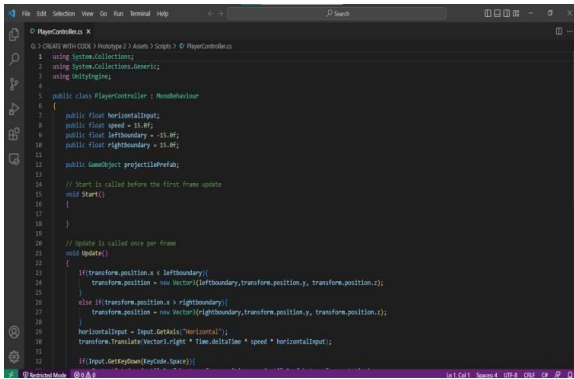


Fig: 14 Food Flight and script view

As shown in Fig. 15, the Food Flight script can be used in Unity to create a game where the player must control a food delivery plane and navigate it through dangerous obstacles and enemies [15]. The player will use the arrow keys to move the plane and the space bar to shoot enemies. The script will control the plane's speed, the obstacles, and enemies, as well as the score and other elements of the game. The script can also be used to create power-ups and bonus levels. With the Food Flight script, developers can create an exciting and challenging game that will keep players engaged for hours.



```

1  CREATE WITH CODE > Package 2 > Asset > Script > PlayerController
2  using System.Collections;
3  using System.Collections.Generic;
4  using UnityEngine;
5
6  public class PlayerController : MonoBehaviour
7  {
8      public float horizontalInput;
9      public float speed = 15.0f;
10     public float leftBoundary = -15.0f;
11     public float rightBoundary = 15.0f;
12
13     public GameObject projectilePrefab;
14
15     // Start is called before the first frame update
16     void Start()
17     {
18     }
19
20     // Update is called once per frame
21     void Update()
22     {
23         if (transform.position.x < leftBoundary)
24             transform.position = new Vector3(leftBoundary, transform.position.y, transform.position.z);
25
26         else if (transform.position.x > rightBoundary)
27             transform.position = new Vector3(rightBoundary, transform.position.y, transform.position.z);
28
29         horizontalInput = Input.GetAxis("Horizontal");
30         transform.Translate(Vector3.right * Time.deltaTime * speed * horizontalInput);
31
32         if (Input.GetKeyDown(KeyCode.Space))

```

Fig: 15 Scripts in VS code studio

C. PLAY FETCH:

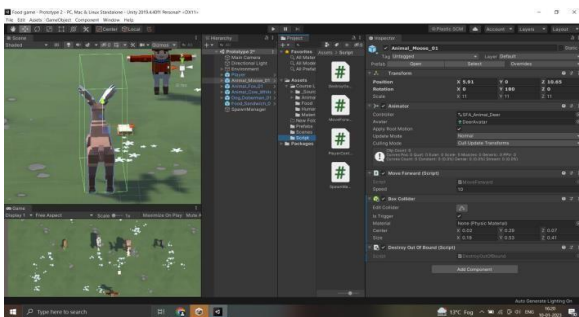


Fig: 16 Final view of Food Flight Game

Play fetch is a great way to get your virtual dog or pet to interact with the environment in Unity. This can be implemented by creating a script that includes a random vector to specify the location of the thrown item and then track the item when thrown. This could be done by attaching a tag to the item, and then having the dog chase the item by tracking its tag which is clearly visible in Fig. 16.

Overall, Unity is an excellent choice for developers looking to create games for laptops. It provides powerful tools, a low learning curve, and a wide range of features and add-ons. With Unity, developers can quickly create projects that are optimized for gaming and can be customized to meet specific needs [16].

VI. CONCLUSION

Unity 3D is one of the leading gaming software solutions with its powerful visuals and versatile capabilities. With its wide range of features and support, Unity 3D is the perfect choice for creating high quality 3D games for mobile, desktop, and console. The robust engine and vast asset library make it an ideal tool for gaming experiences [17]. Use of Unity 3D helps in the knowledge sharing of the gaming world. It is the best option for developers looking to quickly create and deploy stunning 3D games with minimal effort.

Unity 3D is the ultimate choice and innovation for all aspiring game developers.

REFERENCES

1. Hu, J., Gen Wan, W. and Yu, X., 2012, July. A pathfinding algorithm in real-time strategy game based on Unity3D. In *2012 International Conference on Audio, Language and Image Processing* (pp. 1159-1162). IEEE.

2. Yang, C.W., Lee, T.H., Huang, C.L. and Hsu, K.S., 2016, November. Unity 3D production and environmental perception vehicle simulation platform. In *2016 International Conference on Advanced Materials for Science and Engineering (ICAMSE)* (pp. 452-455). IEEE.
3. Miles, J., 2016. *Unity 3D and PlayMaker Essentials: Bringing it together*. Taylor & Francis, CRC Press.
4. Kumar, A., Mantri, A. and Dutta, R., 2021. Development of an augmented reality-based scaffold to improve the learning experience of engineering students in embedded system course. *Computer Applications in Engineering Education*, 29(1), pp.244-257.
5. Young, C.J., Nieborg, D.B. and Joseph, D.J., 2020. "Bringing Your Vision to Life": Production Platforms And Industry Unity. *AoIR Selected Papers of Internet Research*.
6. Creighton, R.H., 2010. *Unity 3D game development by example: A Seat-of-your-pants manual for building fun, groovy little games quickly*. Packt Publishing Ltd.
7. Singh, S. and Kaur, A., 2022, November. Game Development using Unity Game Engine. In *2022 3rd International Conference on Computing, Analytics and Networks (ICAN)* (pp. 1-6). IEEE.
8. https://www.tutorialspoint.com/unity/unity_introduction.htm (10th February 2023)
9. Anwar, H., Pebrianto, A., Sya'rawi, H., Novyanti, R. and Rahmawati, N., 2022, November. Designing Promotional Tools on Banjarmasin State Polytechnic. In *Proceeding of International Conference On Economics, Business Management, Accounting and Sustainability* (Vol. 1, pp. 59-67).
10. Dutta, R., Mantri, A., Singh, G., Malhotra, S. and Kumar, A., 2020. Impact of flipped learning approach on students motivation for learning digital electronics course. *Интеграция образования Integration of Education*, 24(3), pp.453-464.
11. Harshfield, Nicholas, and Dar-jen Chang. "A Unity 3D framework for algorithm animation." In *2015 Computer Games: AI, Animation, Mobile, Multimedia, Educational and Serious Games (CGAMES)*, pp. 50-56. IEEE, 2015.
12. X. Liu, Y.-H. Sohn and D.-W. Park, "Application development with augmented reality technique using unity 3D and vuforia," *International Journal of Applied Engineering Research*, vol. 13, no. 21, pp. 15068-15071, 2018.
13. Lee, M.J., 2013. A Study on Game Production Education through Recent Trend Analysis of 3D Game Engine. *Journal of the Korea Convergence Society*, 4(1), pp.15-20.
14. Richards, Deborah, et al. "Evaluating the models and behaviour of 3D intelligent virtual animals in a predator-prey relationship." *Proceedings of the 11th International Conference on Autonomous Agents and Multiagent Systems- Volume 1*. 2012.
15. <https://medium.com/@pat.x.guillen/challenge-2-play-fetch-c96298b387b4> (25 Jan 2023)
16. <https://unity.com/solutions/game> (25 Jan 2023)
17. Sun, H., Fan, M. and Sharma, A., 2021. Design and implementation of construction prediction and management platform based on building information modelling and three-dimensional simulation technology in industry 4.0. *IET collaborative intelligent manufacturing*, 3(3), pp.224-232.



THE IMPACT OF USING AI CHATGPT ON DIGITAL MARKETING

Ihor PONOMARENKO

*Assoc. Prof., State University of Trade and Economics, Faculty of Trade and Marketing, Department of Marketing, Kyiv-Ukraine
(Responsible Author) ORCID: 0000-0003-3532-8332*

Dmytro PONOMARENKO

*PhD Student, International University of Business and Law, Kyiv-Ukraine
ORCID: 0009-0002-2904-3904*

ABSTRACT

The evolution of modern information technologies has led to the intensification of the development of Data science approaches, first of all, it is necessary to pay attention to the prospects of using artificial intelligence, which is based on high-performance machine learning algorithms. In the digital environment, there are opportunities to collect big data continuously and accumulate information on specialized servers for further processing through the use of various models. Neural networks have gained considerable popularity in modern conditions, which, thanks to the flexibility of choosing architectures and the ability to configure various activation functions, allow the processing of heterogeneous data and obtaining optimal results. There are a large number of different products based on neural networks on the market, among which it is advisable to pay attention to ChatGPT. This product from OpenAI functions based on artificial intelligence and allows companies to create extended text responses on a significant number of topics based on requests. The presence of a significant level of competition in the digital environment encourages companies to introduce various innovative technologies to secure leading positions. Establishing effective communications with the target audience involves the use of modern digital marketing tools. The formation and implementation of an effective digital marketing strategy allows companies to segment the audience by scientific principles and apply specialized models of interaction with each group of consumers. Thanks to the use of artificial intelligence, companies have the opportunity to build personalized communication with each client, which contributes to increasing the level of loyalty. The use of ChatGPT allows companies to create high-quality content for interaction with the target audience and optimize the use of available resources. ChatGPT provides an opportunity to interact with users on social media on an ongoing basis, stimulating interest in the company and its products.

Keywords: ChatGPT, communications, content, digital marketing, information, target audience.

Introduction

Technological transformations and the introduction of innovations contribute to the active development of various machine learning algorithms. IT companies compete with each other and develop advanced technologies that allow optimizing business processes in various areas of activity. Thanks to the large amount of data that accumulates in the process of interaction between various participants of the business environment on the Internet, it has become possible to test machine learning algorithms and identify effective ways of transforming various products. In modern conditions, a large number of products are presented in digital form and represent specialized software that makes it possible to make changes on a permanent basis in order to optimize the functioning of the relevant modules. Machine learning algorithms are an effective tool for improvement, which make it possible to identify various hidden relationships between indicators in the database. Technological giants with significant financial resources and the ability to attract the best specialists in the industry have taken machine learning to a qualitatively new level. One of the applied directions in the field of data processing is the technology of artificial intelligence, which involves interaction with various users through text messages. At this stage, the chatbot with artificial intelligence ChatGPT, which was developed by the OpenAI company, gained the most popularity. The effectiveness of the presented product was evaluated by various groups of consumers, in particular, specialists in the field of marketing,

who were given the opportunity to increase the effectiveness of the development and implementation of marketing campaigns in the digital environment.

Materials and Methods

The presented work involves the study of specialized scientific and practical sources regarding the peculiarities of the use of ChatGPT by companies to increase the level of profitability and ensure the appropriate level of communications. The implementation of the GPT-3 model in the form of a scheme allows you to monitor the execution of relevant processes and obtain the optimal result, which is advisable to increase the effectiveness of the use of digital marketing tools (Floridi et al., 2020).

Findings and Discussion

Cloud computing has significantly expanded the possibilities of using machine learning algorithms, because powerful equipment that has access to servers with information that accumulates 24/4 is used in the process of implementing algorithms for processing large data sets. Modern machine learning algorithms can use structured, semi-structured, and unstructured data to build various models and identify relationships. It should be noted that digital data, text, audio, and video content, as well as various images, can be used as valuable information (Janiesch et al., 2021).

When implementing neural networks in practical applications, the following approaches are put into practice:

1. **Classification:** This algorithm employs a set of metrics to identify segments within a population that share specific characteristics. Through the discerned relationships, grouping is facilitated. Each cluster exhibits distinct behavior influenced by social, economic, psychological, and demographic factors (Radhakrishnan et al., 2023).
2. **Recommender Systems:** By utilizing a metric framework, neural networks establish clusters for recommender systems. This aids in selecting pertinent recommendations for new segments of the population, aligning with their particular activities (Shrivastava et al., 2023).
3. **Predictive Models:** Leveraging the connections unearthed by neural networks, predictive models enable the anticipation of user behavior. Drawing from identified relationships and trends, causal connections can be established, allowing for the projection of subject behavior in upcoming time frames based on key influencing factors (Gehlot et al., 2023).

The perspective of using text information when interacting with artificial intelligence, which is based on complex neural networks, is explained by the relative ease of consumers creating thematic queries thanks to the use of relevant sets of words. The interaction of the user and artificial intelligence thanks to the use of a specialized chat allows to creation of a human-oriented dialogue and achieves a high level of mutual understanding. Based on the presented principles, such products as ChatGPT (text content generation) and DALL-E (high-quality image generation) were created (Fulton, 2023).

Chatbot with artificial intelligence ChatGPT should be classified as a model that solves the problem of classification. Based on the query, keywords are identified and relationships between them are searched to determine the meaningful component. By the identified relationships, the relevant text is searched in the databases to which the presented chat has access. It should be noted that in this case a set of complex calculations is implemented based on numerical information by converting a text query into numbers. Calculations and implementation of an algorithm based on artificial intelligence involve the involvement of neural networks with complex architectures and their implementation on servers with high power. Improvement of the algorithms integrated into the chatbot leads to the appearance of new versions of ChatGPT (Wu et al., 2023).

Figure 1 shows how ChatGPT works from the user's initial text query to the generated keyword response.

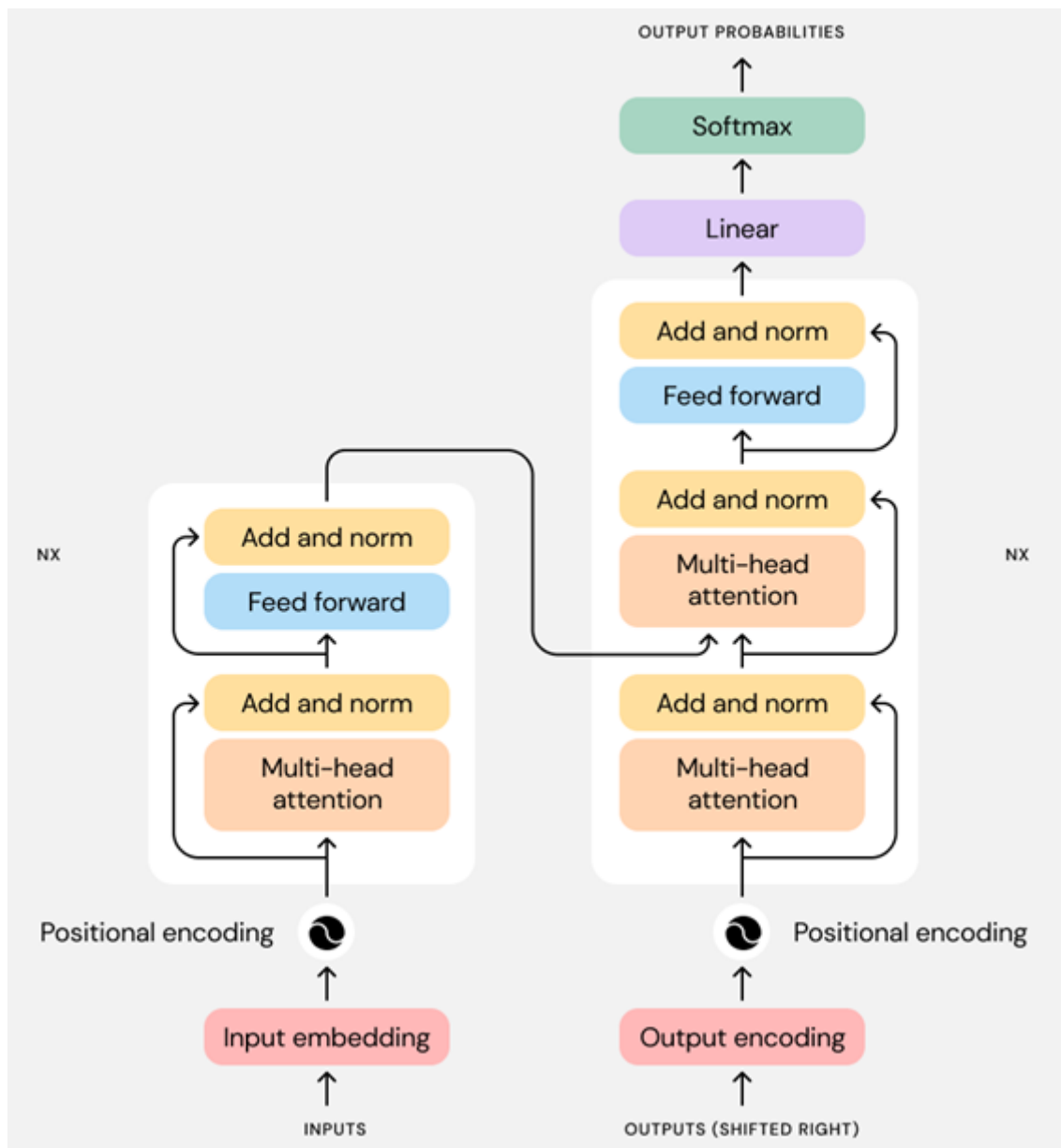


Figure 1. GPT-3 model (SINCH, 2022)

Companies constantly improve their marketing strategies in offline and online environments to ensure high competitive positions in the functioning markets. Digitalization processes force modern brands to actively reorient themselves to the Internet, as demographic changes lead to the gradual replacement of older generations by representatives of Generation Z, and soon, the activation of the alpha generation. Each of the demographic groups is characterized by certain distinctive characteristics, but the company's interaction with any customers involves the use of relevant content. Modern users are focused primarily on video content and photos, which allows companies to receive the necessary information in a visualized form. In many cases, textual information is also in demand among consumers, but the description should be concise and stimulate attention thanks to intriguing titles. The presented principles regarding the formation of active text content are used by companies when applying various digital marketing tools (Ariffin et al., 2023).

Among the key directions of using ChatGPT in the process of improving the digital marketing strategy of companies, it is advisable to highlight the following:

1. Increasing the SEO efficiency of the company's resources on the Internet. Thanks to the constant search for relevant keywords, it is possible to achieve high positions for the company's resources in search results,

which significantly affects the level of attracting new users. The effectiveness of ChatGPT allows to create lists of keywords for company pages in various social media according to the specifics of their operation. Along with this, it is possible to implement various strategies for the formation of specialized dictionaries and markup of pages according to the specifics of various groups of potential customers (Cutler, 2023).

2. Creation of unique texts. Modern users appreciate unique and concise texts that allow them to get information about the relevant products or services of the company. Thanks to the use of ChatGPT, it is possible to create relevant textual content that will be interesting to the relevant groups of consumers. For each of the groups, it is possible to generate a text that will be perceived with the highest possible level of interest (Lancaster, 2023).

3. Communication with users in social networks. The process of interacting with the target audience in various social networks involves not only posting test information but also communicating with users. Subscribers appreciate prompt and competent answers to their questions (Koyuturk et al., 2023). To motivate users to engage in dialogue and discuss issues related to brands, it is advisable to use ChatGPT, which allows to quickly generate answers to questions from various visitors to the company's social media resources.

Conclusion and Recommendations

The development of various technologies similar to ChatGPT is an objective reality of today and is actively used by various companies in the process of implementing complex marketing strategies in the digital environment. Along with the generation of text content, other approaches are also implemented that can be used to establish communications with the target audience. One of the examples of the potential use of innovations in the field of content generation is Microsoft's integration of the Paint graphic editor into Windows 11, which, based on specialized algorithms, will generate images based on text requests from users (Bowden, 2023). The development of artificial intelligence in the future will allow companies to create personalized content for each of their customers, increasing the level of interpersonal communication between the brand and consumers. Over time, users will perceive communication with artificial intelligence as communication with alive people. Accordingly, companies will receive more effective marketing tools for promoting their products in the digital environment and increasing the level of loyalty of the target audience.

References

- Floridi, L., & Chiriatti, M. (2020). GPT-3: Its nature, scope, limits, and consequences. *Minds and Machines*, 30, 681-694. <https://doi.org/10.1007/s11023-020-09548-1>
- Janiesch, C., Zschech, P., & Heinrich, K. (2021). Machine learning and deep learning. *Electronic Markets*, 31(3), 685-695. <https://doi.org/10.1007/s12525-021-00475-2>
- Radhakrishnan, A., Belkin, M., & Uhler, C. (2023). Wide and deep neural networks achieve consistency for classification. *Proceedings of the National Academy of Sciences*, 120(14), e2208779120.
- Shrivastava, R., Sisodia, D. S., & Nagwani, N. K. (2023). Deep neural network-based multi-stakeholder recommendation system exploiting multi-criteria ratings for preference learning. *Expert Systems with Applications*, 213, 119071.
- Gehlot, A., Ansari, B. K., Arora, D., Anandaram, H., Singh, B., & Arias-González, J. L. (2022, July). Application of Neural Network in the Prediction Models of Machine Learning Based Design. In *2022 International Conference on Innovative Computing, Intelligent Communication and Smart Electrical Systems (ICSSES)* (pp. 1-6). IEEE.
- Fulton, J. S. (2023). Authorship and ChatGPT. *Clinical Nurse Specialist*, 37(3), 109-110. DOI: 10.1097/NUR.0000000000000750
- Wu, T., He, S., Liu, J., Sun, S., Liu, K., Han, Q. L., & Tang, Y. (2023). A brief overview of ChatGPT: The history, status quo and potential future development. *IEEE/CAA Journal of Automatica Sinica*, 10(5), 1122-1136. doi: 10.1109/JAS.2023.123618.

- SINCH. GPT-3: What is it, and what's the hype about? (2022). Access Address (19.11.2023): <https://www.sinch.com/blog/gpt-3-what-is-it-and-whats-the-hype-about/>
- Ariffin, S. K., Hilmawan, H., & Zhang, Q. (2023). Consumers Consumption Values and Consumer Satisfaction toward Continuous Intention to View Digital Video Content. *Journal of Entrepreneurship, Business and Economics*, 11(2), 81-129.
- Cutler, K. (2023). ChatGPT and search engine optimisation: The future is here. *Applied Marketing Analytics*, 9(1), 8-22.
- Lancaster, T. (2023). Artificial intelligence, text generation tools and ChatGPT—does digital watermarking offer a solution?. *International Journal for Educational Integrity*, 19(1), 10. <https://doi.org/10.1007/s40979-023-00131-6>
- Koyuturk, C., Yavari, M., Theophilou, E., Bursic, S., Donabauer, G., Telari, A., ... & Ognibene, D. (2023). Developing Effective Educational Chatbots with ChatGPT prompts: Insights from Preliminary Tests in a Case Study on Social Media Literacy. arXiv preprint arXiv:2306.10645.
- Bowden Z. Microsoft may bring AI capabilities to apps like Paint and Photos on Windows 11 (2023). Access Address (19.11.2023): <https://www.windowcentral.com/software-apps/windows-11/microsoft-may-bring-ai-capabilities-to-apps-like-paint-and-photos-on-windows-11>

FORWARD HUNTING FOR MALWARE AND RANSOMWARE DETECTION TO DECREASE RISK

Avinash Kumar

Department of Computer Science and Engineering, Mangalayatan University, Beswan, Aligarh

ABSTRACT

The business and the individual life when get hit by malware or ransomware make huge loss. The malware and ransomware may sniff the victim data and hence will lead to breach of personal and sensitive data. Therefore, it's very important to prevent the malware and ransomware attack rather than mitigating it. The use of forward hunting may help to diagnose the target and analyses the weakness in the target before the actual attack take place. This will highly depend upon the way that InfoSec Team is going to detect the vulnerabilities and also detecting when the attack is on process. This will help to reduce risk on the system and hence finally reducing the loss of funds, prestige in business and penalty by government that may occur due to cyber-attack.

Keywords- Malware, Ransomware, Risk Analysis, Forward Hunting

A NOVEL PERIODONTAL DISEASE GRADE CLASSIFICATION METHODOLOGY USING CONVOLUTIONAL NEURAL NETWORK

Saptadeepa Kalita

Department of Computer Science and Engineering, Sharda University, Greater Noida

ABSTRACT

With the advancement of artificial intelligence, the demand of automated assistance in the field of medical imaging has become important to reduce time and inaccuracy in physical examination. Modern lifestyle choices are resulting in a variety of dental diseases which led to multiple research challenges which are carried out for pre-emptive detection in order to deal with these diseases within time. Periodontal diseases (PD) are a type of dental disorder which is rapidly increasing and being the major cause of early teeth loss. The convolutional neural network (CNN) method is implemented in the detection and grade wise classification of the periodontal disease. A dataset containing 350 dental images in radio visio graphy (RVG) format belonging to an age group of 18-75 years is used for both training as well as testing. This method has successfully detected mild periodontitis, moderate periodontitis and severe periodontitis by achieving a satisfactory accuracy of as high as 94% with minimum loss, precision value, recall and F1 score of 0.41, 0.93-0.95 and 0.91-0.94 respectively for all the three classes of Periodontitis.

Keywords: Artificial Intelligence, Convolutional neural network, Dental diseases, Performance parameters, Periodontal Diseases, RVG Images

ENHANCING NETWORK SECURITY: AN INTRUSION DETECTION AND PREVENTION APPROACH

Oyewale Mustapha Akinola

Dept. of Computer Engineering, The Federal Polytechnic Ilaro, Ogun State, Nigeria.

Adaramola Ojo Jayeola

Dept. of Computer Engineering, The Federal Polytechnic Ilaro, Ogun State, Nigeria.

ABSTRACT

The field of cyber security is constantly evolving, and protecting networks from cyber-attacks is more crucial than ever. There is a need to demonstrate the effectiveness of IDPS in detecting and preventing intrusions on a network system. Therefore, this research focuses on the implementation of an Intrusion Detection and Prevention System (IDPS) that uses Snort and pfSense as a mechanism for network intrusion detection and prevention to create a cost-effective, efficient, and reliable IDPS. The pfSense was deployed on a virtual machine (VM) alongside a Windows 10 operating system. The configuration facilitated the configuration of firewall settings and Snort rule sets via the pfSense web GUI, offering a user-friendly interface. The IDPS's efficacy was tested utilizing malicious websites to generate network traffic. However, the combined capabilities of the snort and pfSense provide real-time intrusion detection, comprehensive threat prevention, and adaptable security policies, making them invaluable tools for enterprises of all scales. By leveraging the strengths of these two softwares, organizations can safeguard their networks and sensitive data from a wide spectrum of cyber threats.

Keywords: Cyber-attacks, IDPS, PfSense, Security, Snort.

A CASE STUDY ON CISCO PACKET TRACER AND GNS3 SIMULATORS: A PRACTICAL VIEWPOINT

Muktha D S

Department of Computer Science, CHRIST University

Sagaya Aurelia

Department of Computer Science, CHRIST University

ABSTRACT

Cisco Packet Tracer and GNS3 are both network simulation and emulation tools used for designing and testing network configurations. However, Cisco Packet Tracer is designed primarily for educational purposes and offers a simplified user interface, making it more accessible to beginners. GNS3, on the other hand, is intended for more advanced users and offers more flexibility and scalability. While Cisco Packet Tracer is ideal for learning networking concepts, GNS3 is more suitable for professionals who need to simulate and test complex network scenarios.

In today's complex network environment, network simulation and emulation tools are essential for network design, testing, and troubleshooting. Cisco Packet Tracer and GNS3 are two such tools that have become popular among network engineers, students, and IT professionals. Cisco Packet Tracer offers a simplified user interface and limited set of devices and features, making it a perfect choice for beginners who want to learn networking concepts. In contrast, GNS3 offers more flexibility and scalability, enabling users to simulate complex network topologies and connect to a wider range of real or virtual devices. In this article, we will compare and contrast these two tools and help you understand their similarities and differences.

Keywords: Cisco Packet Tracer, GNS3, CN simulators

**A FREE DATA REDUNDANCY METHOD FOR SENTIMENT CLASSIFICATION IN
MOVIEREVIEW USING ENSEMBLE MACHINE LEARNING APPROACH**

Usman Mahmud

Al-Qalam University, Katsina

Mohammed Hassan

Bayero University, Kano

Abubakar Ado

Yusuf Maitama Sule University, Kano

Abubakar Abdulkadir Bichi

Yusuf Maitma Sule University, Kano

Armaya'u Zango Umar

Al-Qalam University, Katsina

ABSTRACT

Sentiment Analysis is a Natural Language Processing domain related to the identification or extraction of user sentiments or opinions from written language. Although, there is a continued interests in understanding people's interest through the contents they share online. However, the features generated from the sentiment dataset are of very high-dimension, characterized by irrelevant and redundant features that do not contribute to analyzing sentiment or opinion value. The existing approaches utilizes dimensional reduction techniques to minimize the features size by maintaining a subset of informative features. However, the existing feature reduction methods in cooperated into the sentiment analysis framework are still inefficient. Thus, a new approach should be investigated for efficient and effective sentiment analysis. Therefore, this paper proposed an approach that combines the techniques of Feature Selection based-Information Gain and Feature Hashing to overcome the drawbacks of the existing approaches. Experimental results show that the proposed approach outperformed the baseline and existing method (s) compared in almost all the analyzed cases.

Keywords: Sentiment analysis, Feature selection, Feature hashing, Information gain

**SOLUTION TO SUPPORTING WOMEN'S INTEGRATION AND DIGITAL
TRANSFORMATION IN INDUSTRY 4.0**

Nguyen THỊ HANG

*Thai Nguyen University, University of Information and Communication Technology, Vietnam
ORCID: 0000-0003-2777-7023*

Nguyen MANH HUNG

Thai Nguyen high School for the Gifted

Pham Thi THU THUY

Women's Union Thai Nguyen Province

Nguyen HONG NHUNG

Khanh Hoa high School

Nguyen KHANH LINH

Iris School

ABSTRACT

Supporting women's integration and digital transformation in the Industry 4.0 is one of the urgent and strategically long-term tasks for agencies and organizations to achieve sustainable development goals and international economic integration. Assisting women in integrating and embracing digital transformation within the Industry 4.0 not only benefits women but also significantly contributes to the sustainable development of society, aiming towards comprehensive economic growth. This requires active participation from both the social community and businesses to establish a fair and sustainable environment for women participating in the Industry 4.0 revolution. The article explores the establishment of support networks and encourages women's involvement in communities, organizations, and business networks, enabling them to share experiences, learn, and create new business opportunities. Therefore, ensuring that they have the opportunities and resources to adapt and thrive in the digital technology environment is crucial. This will generate substantial value by equipping women with the necessary knowledge and skills to adapt to new technologies, ensuring gender equality, and encouraging women's participation in STEM fields (Science, Technology, Engineering, Mathematics) so that they can contribute actively to the Industry 4.0.

Keywords: Industry 4.0 revolution, digital transformation, women's integration, digital economy.

ENHANCING EFFICIENCY: THE INTEGRATION OF BLOCKCHAIN TECHNOLOGY WITH INTERNET OF THINGS

Yassir Soulainani

Institute of Information Science, University of Miskolc, Miskolc-Egyetemváros, Hungary

Nehéz Károly

Institute of Information Science, University of Miskolc, Miskolc-Egyetemváros, Hungary

ABSTRACT

The convergence of Blockchain technology with the Internet of Things (IoT) has emerged as a transformative paradigm with the potential to reshape industries, enhance security, and foster innovation. This research paper delves into the intricate interplay between these two dynamic domains, elucidating the multifaceted dimensions of their integration. In an era marked by the proliferation of IoT devices and the ever-growing need for secure and efficient data management, Blockchain technology offers a compelling solution. Its core attributes, including immutability, transparency, and decentralization, position it as a formidable ally in addressing the inherent security and trust challenges embedded within IoT ecosystems. This paper embarks on a comprehensive journey, guided by empirical analysis, discussions, and user feedback. It scrutinizes the performance metrics, scalability implications, and security enhancements introduced by the integration. It presents tangible evidence of the advantages of Blockchain-IoT synergy through real-world use cases, ranging from supply chain management and healthcare data integrity to smart city traffic optimization. Scalability, privacy concerns, and energy efficiency demand innovative solutions. Regulatory frameworks must evolve to accommodate this emerging convergence, safeguarding data privacy, and security.

Keywords: Blockchain, Internet of things, Data

DEEP LEARNING IN THE DIAGNOSIS OF EAR DISEASES: EFFECTIVE AND RAPID SOLUTIONS

Murat CANAYAZ

*Assoc. Prof. Dr., Van Yuzuncu Yil University, Faculty of Engineering, Department of Computer Engineering, Van-Türkiye,
(Responsible Author)*

ABSTRACT

Deep learning represents an alternative approach to conventional diagnostic methods in the diagnosis of ear diseases and offers the potential to achieve more effective and faster results. Deep learning algorithms are known for their ability to analyze large datasets and recognize complex patterns. These algorithms, used in the diagnosis of ear diseases, can recognize and classify symptoms by learning from the data rather than relying on predefined features. This enables a more precise identification of the characteristic features of different ear diseases and increases the potential for improving treatment processes. Especially in ear imaging procedures, such as otoacoustic emissions or intracavitary cameras, deep learning serves as a valuable aid for physicians to accurately diagnose and create appropriate treatment plans. Otoscopic examination is particularly important for the diagnosis of diseases such as myringosclerosis, earwax, and chronic otitis media. In this study, EfficientNet models were employed to classify these diseases, and the results showed a remarkable success rate of 99% on the validation data during training. The test data also exhibited an impressive accuracy rate of 95%. In the research, the dataset consists of training images from 160 patients and test images from 20 patients, totaling 720 images across 4 classes. In future studies, it is planned to work on new models by increasing the disease classes.

Keywords: deep learning, diagnosis of ear diseases, Efficient Net

REALIZATION OF MILK QUALITY CLASSIFICATION WITH C4.5 DECISION TREE ALGORITHM: PERFORMANCE MEASUREMENT ACCORDING TO F1 SCORE and MCC METRICS

Ahmet ÇELİK

Assist. Prof. Dr. Ahmet ÇELİK, Kütahya Dumlupınar University, Tavşanlı Vocational School, Department of Computer Technology Kütahya-Türkiye, (Responsible Author) ORCID: 0000-0002-6288-3182

ABSTRACT

Milk and dairy products are an important building block among food products. In addition to being an important source of calcium, milk is recommended to be consumed by everyone from young to old because it contains many vitamins in its structure. Therefore, it is of great importance to determine the quality correctly. Milk quality is measured by looking at very few criteria in many companies. Most quality control processes are carried out by employees through observation, which leads to erroneous determinations. When low quality milk and high quality milk, which cannot be determined correctly, are mixed, the substance also causes losses. As in many areas, it will be beneficial for milk quality to be made by smart, autonomous systems. In this case, it will be possible to determine the milk quality quickly by looking at many parameters. Machine learning algorithms can be used for classification applications in many areas. One of the commonly used machine learning algorithms is the C4.5 decision tree algorithm. F1 score and MCC (Matthews Correlation Coefficient), which are suitable for data sets containing unbalanced class records, were used as classification success metrics. In the study, the Milk Quality Prediction dataset shared in the Kaggle open source data repository was used. The dataset contains 1059 records. Each of these records has 7 attribute values. These attributes are; pH, Temperature, Taste, Odor, Oil, Turbidity and Color are the data. In this data set, milk quality is divided into 3 classes as low, medium and high. According to the results obtained, 0.991 success was achieved according to the F1 score metric and 0.986 success was achieved according to the MCC metric.

Keywords: Classification, Machine Learning, Milk Quality Control, Success Metric, F1 Score, Matthews Correlation Coefficient

Introduction

The quality of milk consumed or sold is often rapidly affected by various contaminants (Kumari et al., 2023). Since milk is a perishable product, it is of great importance both in terms of health and economy to determine the quality quickly.

Since milk is the raw material of many products, it is of great importance to determine its quality. Milk quality is determined by employees in many companies. This can lead to time-consuming and very erroneous determinations. Therefore, it will be very useful to determine the quality of milk by an automated system (Çelik, 2022). In the literature, studies have been conducted in which milk quality classification is estimated by machine learning algorithms (Frizzarin et al., 2021).

Neware, (2023) used KNN, LR, ANN, and SVM machine learning algorithms to predict milk quality. Among these algorithms, when $k=3$ is used in the KNN algorithm, it has achieved successful results. Ahmad et al. (2010) proposed a model to detect milk quality prediction. In study used the milk temperature, time of the milk travel and fat attributes to divide the milk quality of 4 classes. The dataset obtained from a local dairy of Thailand. In the study, for classified of the milk dataset by using Artificial Neural Network (ANN) and K-Nearest neighbor (KNN) and Multiple Linear Regression (MLR) algorithms were used. Frizzarin et al. (2021) proposed to predict milk quality characteristics from existing milk spectra using machine learning methods. Using mid-infrared spectra, they created a dataset of 622 milk samples with protein composition and other data. They suggested that this dataset could be used by different regression and classification algorithms. Çelik, (2022) proposed a model which are Neural Network (NN) and Adaptive Boosting (AdaBoost: AB)

algorithms. In the study with Classification Accuracy (CA) metric was obtained 99.9% success rate by using AdaBoost algorithm and obtained 95.4% success rate by NN algorithm. Kumari et. al. (2023) divided the milk samples into three grades - low, medium, and high class by using a machine learning algorithm called Artificial Neural Network (ANN). In the study, by using the ANN model classified milk samples with high accuracy 99.88%.

In this proposed model, seven attributes are used to determine quality of milk which pH value, Temperature, Taste, Odor, Color, Fat, and Turbidity. In this study, Orange interface is used, which is open source code and written in python software. Orange is a widely used because of the user interface is easy.

Materials and Methods

In this study, C4.5 tree algorithm, which is one of the decision tree algorithms, was used. In the study, the milk quality dataset shared from Kaggle (2023) open source storage was used. The flowchart of the designed model is shown in Figure1. In the designed model, 70% of the data from the data set was randomly selected for training and 30% was used for testing. Learning was carried out on the C4.5 algorithm with the training data, and Low, Medium and High classification of the test data was realized.

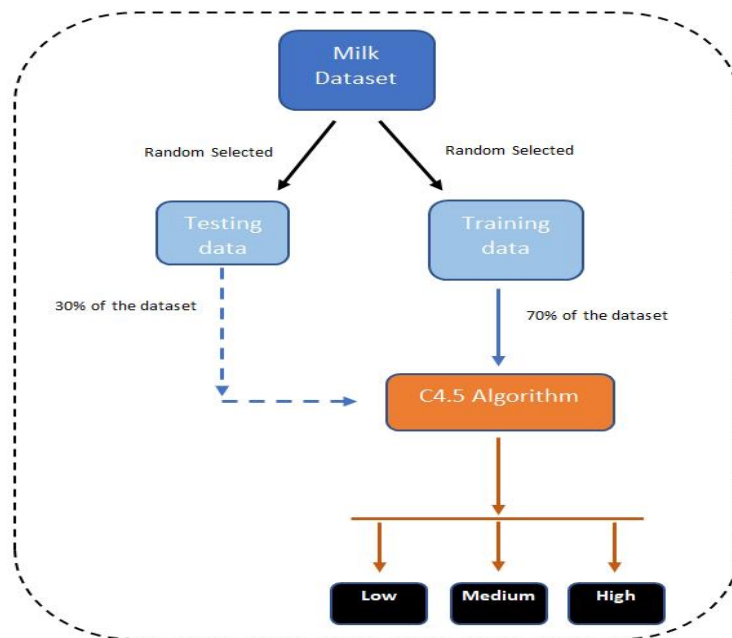


Figure1. Flow chart of the designed model

Figure 2 shows the classification successes and errors of some specimens on the designed model. It is seen that the error rate is 0.000 in 17 of the 21 examples shown in the figure. In addition, it is seen that there is a small error value of 0.016 on the figure, although the correct determination is made in 4 examples.

	Tree	error	Grade	id
1	0.00 : 1.00 : 0.00 → low	0.000	low	672
2	0.00 : 1.00 : 0.00 → low	0.000	low	684
3	0.00 : 0.00 : 1.00 → medium	0.000	medium	248
4	0.00 : 1.00 : 0.00 → low	0.000	low	666
5	0.00 : 0.00 : 1.00 → medium	0.000	medium	232
6	0.00 : 0.00 : 1.00 → medium	0.000	medium	196
7	0.00 : 1.00 : 0.00 → low	0.000	low	498
8	0.98 : 0.02 : 0.00 → high	0.016	high	11
9	0.00 : 0.00 : 1.00 → medium	0.000	medium	388
10	0.00 : 1.00 : 0.00 → low	0.000	low	755
11	0.00 : 0.00 : 1.00 → medium	0.000	medium	255
12	0.00 : 0.00 : 1.00 → medium	0.000	medium	221
13	0.00 : 0.00 : 1.00 → medium	0.000	medium	413
14	0.98 : 0.02 : 0.00 → high	0.016	high	146
15	0.00 : 1.00 : 0.00 → low	0.000	low	525
16	0.98 : 0.02 : 0.00 → high	0.016	high	45
17	0.00 : 1.00 : 0.00 → low	0.000	low	506
18	0.00 : 1.00 : 0.00 → low	0.000	low	539
19	0.00 : 0.00 : 1.00 → medium	0.000	medium	428
20	0.00 : 0.00 : 1.00 → medium	0.000	medium	209
21	0.98 : 0.02 : 0.00 → high	0.016	high	115

Figure 2.Classification Estimates and Error Rates of Some Samples

Milk Quality Dataset

The dataset used in the study was downloaded from Kaggle, which is shared as open source (Kaggle, 2023). Information about the data set is given on Table 1. There are 1059 records on the dataset. Each of these records have 7 attribute information which are pH value, Temperature, Taste, Odor, Color, Fat, and Turbidity. Using these data, milk quality is divided into "low", "medium" and "high" classes.

Table 1.Details of attributes in the dataset (Kumari et. al., 2023)

Number	Attributes	Information about attributes
1	pH	Potential of hydrogen value in the milk Milk samples of the data set.
2	Temperature	Value of the milk samples
3	Taste	Binary format value where 1 is for good taste and 0 for bad taste.
4	Odour	Binary format value where 1 is for good odour and 0 for bad odour.
5	Fat	Binary format value where 1 is for high-fat content and 0 for low-fat content.
6	Turbidity	Binary format value where 1 is for high turbidity and 0 for low turbidity.
7	Colour	Numerical values for the colour of the milk samples. White, yellowish white and slight bluish-white indicates good milk samples.

C4.5 Decision Tree Algorithm

The C4.5 decision tree algorithm was developed by J. Ross Quinlan in 1993. The C4.5 algorithm is one of the widely used classification algorithms within machine learning algorithms (Andrienko & Andrienko, 1999; Çelik, 2023).

F1 Score Metric

Using the F1 Score metric, consistent results are obtained in terms of precision and sensitivity in multi-label classification (Lipton & Elkan, 2014). The results obtained from precision and sensitivity calculations are

used to calculate the F1 score metric. The precision calculation is shown on equation 1. The sensitivity calculation is shown on equation 2.

$$\text{Precision} = \frac{(TP)}{(TP+FP)} \quad (1)$$

$$\text{Recall} = \frac{(TP)}{(TP+FN)} \quad (2)$$

The F1 score metric is obtained as a result of precision and recall calculations. The F1 score metric calculation is shown on equation 3.

$$\text{F1 score} = 2 * \frac{\text{Precision} * \text{Recall}}{\text{Precision} + \text{Recall}} \quad (3)$$

TP is True Positive, FP is False Positive, TN is True Negative and FN is False Negative.

TP

Matthews Correlation Coefficient (MCC)

The MCC metric was first used by B.W. Matthews in 1975 to evaluate the performance of a structure prediction. The MCC metric is used as a measurement metric that shows the correlation between the predicted and actual labels (Matthews, 1975).

In unbalanced data sets, classes with a large number of data may have high classification success. As a solution to this situation, the MCC metric is a performance measurement metric designed to solve class imbalance in data sets containing unbalanced class data (Boughorbel et al., 2017). MCC calculation is shown on equation 4 (Chicco et al., 2021).

$$\text{MCC} = \frac{(TP * TN) - (FP * FN)}{\sqrt{(TP + FP) * (TP + FN) * (TN + FP) * (TN + FN)}} \quad (4)$$

Findings and Discussion

In addition to F1 score and MCC success metrics, complexity matrix data and ROC curve graphs were also used for success comparisons. Figure 3 shows the complexity matrix of the classification process made with the designed model. On the figure, it is seen that 82 of the 83 samples with a "high" class were correctly determined, and 1 of them was estimated as a "medium" class. In addition, it is seen that 108 data belonging to the "medium" class were determined correctly with the model. However, 124 of the 126 samples that actually belong to the "low" class were correctly determined, while 1 was the "high" class and 1 was the "medium" class.

		Predicted			Σ
		high	low	medium	
Actual	high	82	0	1	83
	low	1	124	1	126
	medium	0	0	108	108
Σ		83	124	110	317

Figure 3. Confusion Matrix of the model.

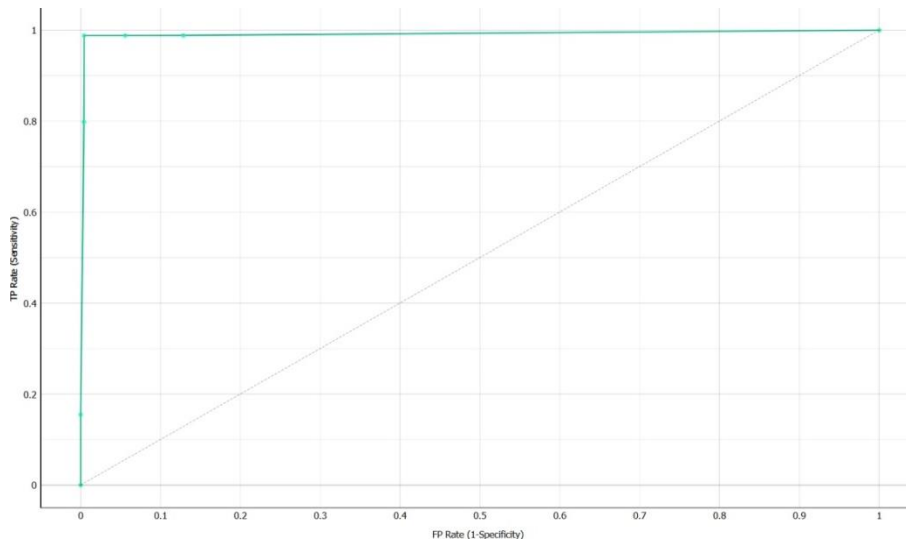
Table 2 shows the success rates according to the training, test data dimensions and performance metrics used in the designed model. In the model using the C4.5 decision tree, 70% of the data set, that is, 742 data, were selected for training. In addition, 30% of the data set, that is, 317 data, selected for the test. In the results

obtained, 99.1% classification success was achieved according to the F1 score metric and 98.6% according to the MCC metric.

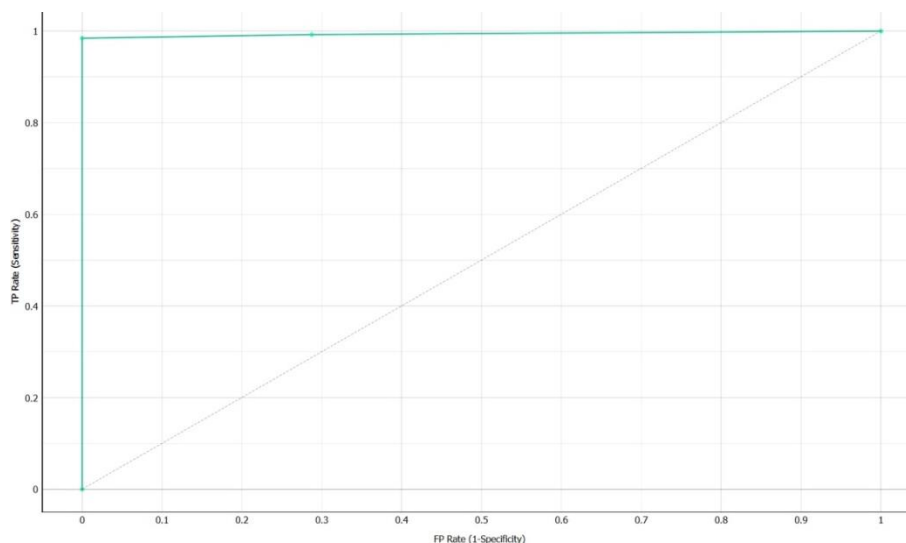
Table 2.Details of the model and performance rates

Algorithm	Training Size	Test Size	F1 Score	MCC
C4.5 Decision Tree	70% (742 pieces of data)	30% (317 pieces of data)	99.1%	98.6%

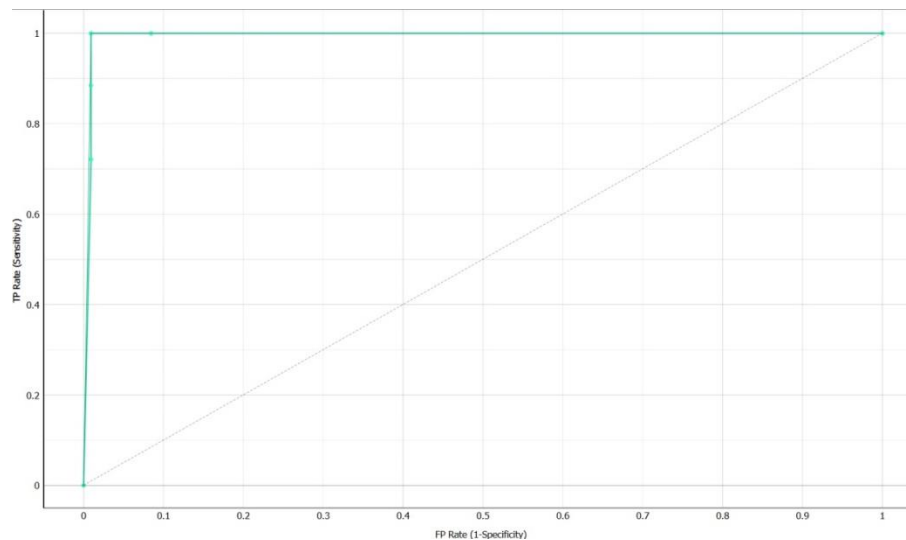
Figure 4 shows the ROC curves of the classification achievements of each class. Classification success ROC curve graphs of the class "high" on figure 4.a, "low" on figure 4.b and "medium" on figure 4.c are shown. ROC (Receiver Operating Characteristic Curve) means the area under the curve. In these graphs, success comparisons are made with the size of the areas under the curve. When the graphs are examined, it is seen that the success rates are high, but there is a very small difference. The highest successful classification is shown on figure 4.c, where the "medium" classification is. The lowest successful classification is shown in figure 4.b, where the "low" classification is located.



a) ROC curve of the "high" class



b) ROC curve of the "low" class



c) ROC curve of the "medium" class

Figure 4. ROC curve plots of the model's Classification achievements

Conclusion and Recommendations

In this study, classification was performed with the C4.5 decision tree algorithm on the Milk Quality dataset downloaded from the Kaggle data store. There are 1059 records in the data set. These records are divided into 3 classes using 7 attributes. In the designed model, 70% of the data were randomly selected from the data set and used for training. 30% of random data were selected from the data set and used for testing.

The results were compared using F1 score and MCC metric. In the designed model, 99.1% classification success was achieved according to the F1 score metric and 98.6% according to the MCC metric. These results show that classification can be performed with the C4.5 decision tree algorithm with a high rate of success. In future studies, classification is considered according to different educational dimensions.

References

- Ahmad, I., Komolavanij, S., and Chanvarasuth, P. 2010. Prediction of raw milk microbial quality using data mining techniques. *Agricultural Information Research*, 19(3), p.64–70.
- Andrienko, G., Andrienko, N. (1999). GIS Visualization Support To The C4. 5 Classification Algorithm of KDD. *In Proceedings of the 19th International Cartographic Conference*, Ottawa, Canada, p. 1-7.
- Boughorbel, S., Jarray, F., & El-Anbari, M. (2017) Optimal classifier for imbalanced data using Matthews Correlation Coefficient metric. *PLoS ONE*, 12(6), e0177678.
- Chicco, D., Warrens M. J. & Jurman, G. (2021). The Matthews Correlation Coefficient (MCC) is More Informative Than Cohen's Kappa and Brier Score in Binary Classification Assessment. *IEEE Access*, 9, p. 78368-78381. <https://doi.org/10.1109/ACCESS.2021.3084050>.
- Çelik, A. (2022). Using Machine Learning Algorithms to Detect Milk Quality. *Eurasian Journal of Food Science and Technology*, 6(2), p.76-87.
- Çelik, A. (2023). Buğday Tohumu Sınıflandırmasının Karar Ağacı Algoritmasıyla Gerçekleştirilmesi ve Değişken Eğitim Verisine Göre Başarı Kıyaslaması. *International Journal of Advanced Natural Sciences and Engineering Researches*, 7(11), p.44-48.
- Frizzarin, M., Gormley, I. C., Berry, D. P., Murphy, T. B., Casa, A., & Lynch, A. & Mcparland, S. (2021). Predicting cow milk quality traits from routinely available milk spectra using statistical machine learning methods. *Journal of Dairy Science*. 104.

- Kaggle, 2023, Milk Quality Prediction, Retrieved: November 3, 2023, from <https://www.kaggle.com/datasets/cpluzshrijayan/milkquality/code>.
- Kumari, S., Gourisaria, M. K., Das H. & Banik, D. (2023). Deep Learning Based Approach for Milk Quality Prediction. In: *11th International Conference on Emerging Trends in Engineering & Technology - Signal and Information Processing (ICETET - SIP)*, Nagpur, India, p. 1-6. <https://doi.org/10.1109/ICETET-SIP58143.2023.10151626>.
- Lipton, Z., Elkan, C. & Narayanaswamy, B. (2014). F1-Optimal Thresholding in the MultiLabel Setting. 2014. arxiv: <https://arxiv.org/abs/1402.1892>
- Matthews, B. (1975). Comparison of the predicted and observed secondary structure of T4 phage lysozyme. *Biochimica et biophysica acta*, 405(2), p.442–451. [https://doi.org/10.1016/0005-2795\(75\)90109-9](https://doi.org/10.1016/0005-2795(75)90109-9) PMID: 1180967
- Neware, S. (2023). Cow Milk Quality Grading using Machine Learning Methods. *International Journal of Next-Generation Computing - Special Issue*, 14(1), p. 1-8.

DDOS ATTACKS DETECTION WITH A RULE-BASED APPROACH USING ROUGH SET

Rasım ÇEKİK

*Şırnak University, Faculty of Engineering, Department of Computer Engineering, Şırnak-Türkiye
(Responsible Author) ORCID: 0000-0002-7820-413X*

ABSTRACT

DDoS attacks are among the most dangerous and common network attacks. The goal of these attacks is to disrupt service providers. Various methods for stopping and neutralizing these attacks have been developed. This study presents a rule-based approach for detecting DDoS attacks using rough sets. The method took advantage of rough sets' ability to make effective inferences from data. The rules obtained by the LEM2 algorithm in rough sets were used to create a decision-making model. The model was trained on 6450 pieces of data and tested on 3250 pieces of data. According to experimental results, it has been observed that the proposed model can detect a high rate of 80.2450%. Additionally, the dataset used is an unbalanced dataset. Despite this, the proposed model made a close determination for each log and achieved a balanced classification process.

Keywords: DDoS Attacks, Network Security, Rough Set, Data Mining.

Introduction

With the advancement of network technology, the great bulk of work done in daily life is now done on digital networks. Therefore, networks are now the foundation of many key domains, including communication, data transport, financial transactions, and information sharing. However, security flaws in these networks can expose users to a variety of dangers and threats, including DDoS attacks, data leaks and theft, phishing, firewall flaws, malware exploitation, and encryption flaws. These network security breaches can cost you time, money, and your reputation. Furthermore, network assaults can harm systems by destroying, modifying, disrupting, or leaking data (Kothari et al., 2011, August). Malware, viruses, worms, trojans, spyware, phishing, and other similar threats can cause these harms. Network protocol architecture can potentially cause vulnerabilities that can lead to network attacks. Incorrect or incomplete use of applications that use network protocols can cause losses in attacked systems (Cao et al., 2019). For example, TCP side-channel vulnerabilities are hard-to-predict, hard-to-find and often manually detected by experts. Moreover, over the last 20 years, DDoS attacks have evolved significantly, with several attack variants developed (Li et al., 2023). Equipped with a range of attack options to choose from, attackers can precisely target victims' vulnerabilities by identifying their targets and combining attack methods according to their demands (Shan et al., 2017, October). There are more than a hundred types of DDoS attacks recorded worldwide. Before discussing the research trends in DDoS attacks and the challenges faced in dealing with these attacks, we need to briefly understand DDoS attacks. DDoS attacks are the most common attacks on the network. DDoS stands for "Distributed Denial of Service". DDoS attacks are malicious online attacks that aim to make a target's services unavailable. Such attacks occur when many computers or devices, usually as part of a large network called a botnet (zombie army), send massive amounts of traffic to the target in a coordinated manner. This excess traffic drains the target's resources and interferes with its ability to serve legitimate users. DDoS attacks can affect many organizations such as internet service providers, large enterprises, financial institutions and government sites. To counter such attacks, methods such as security measures, traffic filtering, high availability configurations and frequently updated security policies are used.

Many studies have been conducted to develop early warning and detection systems for DDoS attacks. The classification results of DDoS attacks are thought to be useful for developing attack detection and early prevention systems for attacks caused by protocol or application vulnerabilities (Kührer et al., 2014). For example, Lonea et al. (2013) proposed using Dempster-Shafer Theory (DST) processes and Fault Tree Analysis (FTA) for virtual machine (VM) detection system (IDS)-based attacks to detect and analyze DDoS

attacks in cloud computing services. Similarly, the communication rules for IoT-based sensor networks are evolving with new standards over time. DDoS attacks, on the other hand, endanger resource availability by threatening sensor nodes with high-volume network attacks. Baig et al. (2020) presented an ADE (Averaged Dependence Estimator)-based DDoS detection scheme for IoT sensors to prevent this. Also, the authors in (Huang et al., 2016) address the challenges associated with large-scale Software Defined Networking (SDN) in terms of implementation, technologies used, and test beds utilized. They discuss the management of the Open Flow protocol as well as different implementation alternatives of the SDN architecture, according to (Nunes et al., 2014). The deployment in SDNs is analyzed in (Zhang et al., 2015). The study is examined challenges, design principles, deployment, performance and architectures. SDN layers are discussed in terms of implementation challenges, possible architectures and performance improvements in (Xia et al., 2018). Examples can be multiplied in this manner.

Rough Set Theory

The rough set theory, initially introduced by Pawlak in 1985 (Pawlak, Z. 1991), has gained popularity in various disciplines. This theory presents a novel mathematical approach to handling imperfect knowledge, specifically addressing vagueness or imprecision. In this framework, vagueness is represented by a boundary region of a set, and rough set concepts are defined through topological operations, namely lower and upper, referred to as approximations. Assume you have a collection of objects, each of which has several attributes. Some attributes may be more important than others when it comes to classifying these objects. Rough sets assist you in identifying key attributes and developing decision rules based on them.

Basic Concepts of Rough Sets:

- Information/Decision Systems (Tables)
- Indiscernible Relation
- Set Approximation
- Reducts and Core
- Rough Membership
- Dependency of Attributes

Information/Decision Systems (Tables): Real-world information is presented in the form of an information table (also known as a decision table). An information system (IS) is defined as:

$$IS = (U, A \cup \{d\}) \quad (1)$$

where, U is a non-empty finite set of objects. A is a non-empty finite set of features such that for every $a \in A$. $a: U \rightarrow V_a$. V_a is called the value set of a . $d \notin A$ is the decision feature and the elements of A are called the condition features.

Indiscernible Relation: Given an attribute set $B \subseteq A$ subset, an indiscernible relation $ind(B)$ on the universe U can be defined as follows:

$$ind(B) = \{(x, y) \mid (x, y) \in U^2, \forall b \in B (b(x) = b(y))\} \quad (2)$$

The equivalence relation is indistinguishable. If there is no confusion, the equivalence class of an object x is denoted by $[x]_{ind(B)}$, or $[x]_B$ and $[x]$. An approximation space is defined as the pair $(U, [x]_{ind(B)})$.

Reducts and Core: If the set of attributes is dependent, one might want to find all possible minimal subsets of attributes that lead to the same number of elementary sets as the entire set of attributes (reducts), as well

as the set of all indispensable features (core). Rough set theory is founded on two fundamental ideas: core and reduct. The reduct is a critical component of an IS that can discern all objects discernible by the original IS. The core is the same in all reducts. The discernibility matrix is used to calculate reducts and core. The dimension of the discernibility matrix is $n \times n$, where n denotes the number of elementary sets, and its elements are defined as the set of all attributes that discern elementary sets $[x]_i$ and $[x]_j$.

Set Approximation: Set approximations in rough sets consist of two concepts: *lower* and *upper*. The lower refers to objects that definitely belong to a set, while the upper refers to objects that are likely to belong to a set.

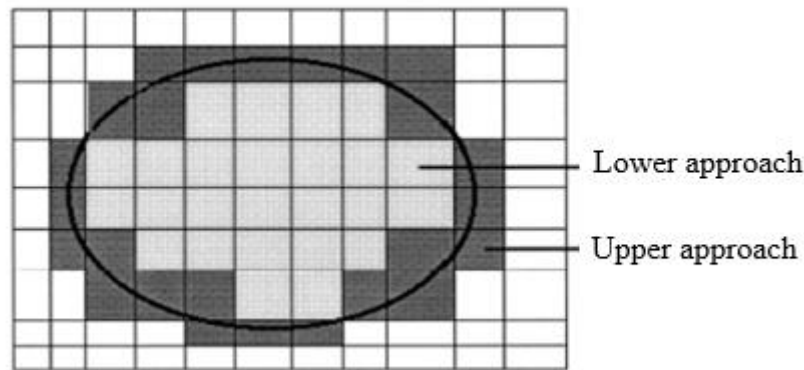


Figure 1. Lower and upper approaches for rough sets

Let $X (X \subset U)$ be a subset of the universal set and $B (B \subseteq A)$ be a subset of the attribute set.

The lower approach notation:

$$\underline{BX} = \{X_i \in U \mid [x]_i \text{IND}(B) \subset X\} \quad (3)$$

The upper approach notation:

$$\overline{BX} = \{X_i \in U \mid [x]_i \text{IND}(B) \cap X \neq \emptyset\} \quad (4)$$

Reducts and Core: The reduced set of attributes, also known as *Reducts*, determines the bare minimum of attributes required to represent the data structure in an information system. Also, the *Core* attributes set is made up of the common elements of the reduced attributes sets.

Rough Membership: Rough sets can also be defined using a rough membership function rather than an approximation. In rough set theory, a rough membership function is associated with a set, and it describes the degree of membership of an element in that set. The rough membership function reflects the uncertainty or imprecision in the classification of elements into sets. Notation:

$$\mu_X^R: U \rightarrow \langle 0,1 \rangle$$

where,

$$\mu_X^R(x) = \frac{|X \cap R(x)|}{|R(x)|} \quad (5)$$

Proposed Method

Rough sets are a mathematical approach to vagueness and uncertainty. To put it another way, the rough set approach can be thought of as a formal framework for discovering facts from imperfect data. The rough set approach's results are presented as classification or decision rules derived from a set of examples. The rule-removing skill of rough sets approach was used in this study. The LEM2 algorithm was used in this process. The LEM2 algorithm is a rule induction algorithm that handles inconsistent data sets using rough set theory (Grzymala & Werbrouck, 1998). There are several methods in the LEM2 algorithm, including basic minimal covering, extent minimal covering, and satisfactory description. The basic minimal covering method was used in this study. This method is used to generate a set of decision rules based on a minimal covering algorithm (the fewest possible rules that cover all of the examples). It only has one parameter, which is the name of the decision feature.

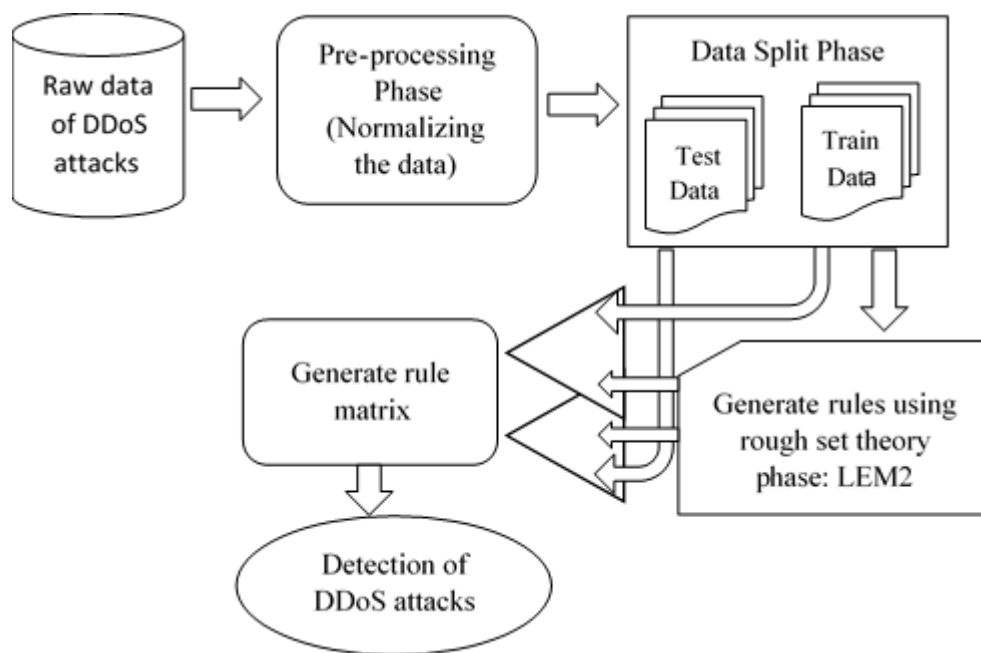


Figure 2. Architecture of proposed method

The processes discussed in this study are given below in order. First, preprocessing of the used dataset was performed by transforming the non-numeric data. Then the processes applied are as follows:

1. **Selecting a subset data within the entire dataset:** Since the used datasets are very large, they are divided into smaller subset. the division operation has been made based on features using any feature selection method.
2. **Divide subset data as train and test data:** Subset data is divided as at randomly 66% train and 33 % test data.
3. **Generation rules on train data:** ROSE2 (Rough Set Data Explorer) was used to generate generation rules on train data. ROSE2 is a piece of software that implements the fundamentals of rough set theory and rule discovery techniques. All computations are based on Z. Pawlak's rough set fundamentals. W. Ziarko's variable precision rough set model is used in one of the implemented extensions. It is especially useful when analyzing data sets with large boundary regions. Another extension implements R. Slowinski's rough set approach based on a similarity relation. Inductive learning is used to assess the similarity relationship from data (Kryszkiewicz, M.,1998).

The system contains several tools for rough set based knowledge discovery, e.g.:

- data preprocessing, including discretization of numerical features,
- performing a standard and an extended rough set based analysis of data,
- search of a core and reducts of features permitting data reduction,
- inducing sets of decision rules from rough approximations of decision classes,
- evaluating sets of rules in classification experiments,
- using sets of decision rules as classifiers.

4. Calculate similarity and decision making: In the phase, a new matrix called the Rule Matrix is generated. This matrix is also the new information system for the rough set. The Rule Matrix consists of rules created by LEM2. So, each cell of the Rule Matrix, which is formed with rules in a row and each attribute in a column, contains the attribute value mentioned in the relevant rule. Moreover, the last column is the class column and contains the relevant class label. According to this matrix, the similarity for the test data is calculated as in Equation 6 below:

$$\text{similarity}(tt_i) = \sum_{k=1}^{N_i} \{1 \mid (x, y) \in R^2, \forall b \in B (b(x) = b(y))\} \quad (6)$$

and $i = 1, 2, 3 \dots M$

In this case, N_i is the number of rules that produce class i . Likewise, R is a non-empty finite set of rules and B be a subset of the attribute set. M denotes the number of classes. Once the similarity has been calculated for each class, Equation -2 below is used to decide the label of a test data.

$$\text{Decision}(tt_i) = \max(\text{similarity}(tt_i)) \text{ and } i = 1, 2, 3 \dots M \quad (7)$$

Accordingly, the test data with the highest similarity value is given the label of that class.

Experimental Work

In this section, information about the dataset is shared, followed by an analysis of the experimental studies.

Dataset

In the study, the reduced subset of the "DDoS Attack Network Logs" set, which can be downloaded for free on the Kaggle platform, consisting of more than 1 million data, was used. The data set is in .csv format and contains 27 different attributes. The last column contains the class information of the data. There are 1048575 records belonging to 'NORMAL', 'HTTP-FLOOD', 'SIDDOS', 'SMURF', 'UDP-FLOOD' classes in the dataset. Within the scope of this study, a certain number of data from each class in this dataset has been taken. Information about the data received is presented in Table-1 below.

Table 1. Information about the data set used

	NORMAL	HTTP-FLOOD	SIDDOS	SMURF	UDP-FLOOD
TRAIN	2000	1400	800	1200	1050
TEST	1000	600	300	800	550

In the study, Class tags were changed to NORMAL→1, HTTP-FLOOD→2, SIDDOS→3, SMURF→4, UDP-FLOOD→5. The features in the data set are numeric or categorical. In the study, categorical data were converted into numerical data. In addition, with the help of rough sets, 4 attributes that were found to be super flush were discarded. From the train and test data prepared in this way, train data was presented for the rough sets to work on.

Success Analysis

At this stage, the success of the model proposed in this study was tested. Previously, the rough set-based model on training data was run on test data and its success was observed.

A total of 4007 rules were obtained by running the rough set-based LEM2 method. According to these rules, it is determined to which label the incoming data belongs. A part of the rules obtained with LEM2 is shown below on Table 2.

Table 2. A Part/Samples from rules created by LEM2

#	LEM2
#	C:\Users\rasimcekik\Desktop\Bildiri\DDoS_Train2.isf
#	objects = 11012
#	attributes = 24
#	decision = D
#	classes = {1, 2, 3, 4, 5}
#	Thu Dec 07 22:53:03 2023
#	559 s
RULES	
rule 1.	(A12 = 16) & (A20 = 22) => (D = 1); [4, 4, 0.13%, 100.00%][4, 0, 0, 0] [{239, 970, 2344, 2781}, {}]
rule 2.	(A8 = 1599) => (D = 1); [1, 1, 0.03%, 100.00%][1, 0, 0, 0] [{131}, {}]
rule 3.	(A12 = 16) & (A13 = 19) => (D = 1); [3, 3, 0.10%, 100.00%][3, 0, 0, 0] [{295, 2063, 2288}, {}]
rule 4.	(A8 = 6059) => (D = 1); [1, 1, 0.03%, 100.00%][1, 0, 0, 0] [{539}, {}]
rule 5.	(A2 = 1) & (A13 = 2) => (D = 1); [3, 3, 0.10%, 100.00%][3, 0, 0, 0] [{1908, 2111, 2650}, {}]
rule 6.	(A18 = 18057) & (A20 = 17) => (D = 1); [5, 5, 0.17%, 100.00%][5, 0, 0, 0] [{92, 1231, 1636, 1743, 2280}]
rule 7.	(A7 = 3) & (A21 = 13) => (D = 1); [6, 6, 0.20%, 100.00%][6, 0, 0, 0] [{766, 1145, 1216, 1374, 1867, 2396}, {}]
rule 8.	(A12 = 5) & (A15 = 8) => (D = 1); [3, 3, 0.10%, 100.00%][3, 0, 0, 0] [{74, 1329, 2618}, {}]
rule 9.	(A3 = 23) & (A7 = 2) & (A13 = 19) => (D = 1); [5, 5, 0.17%, 100.00%][5, 0, 0, 0] [{212, 334, 352, 2290, 2327}]
rule 10.	(A7 = 4) & (A15 = 46) => (D = 1); [10, 10, 0.33%, 100.00%][10, 0, 0, 0] [{974, 1536, 1549, 1649, 1951, 2044, 2053, 2186, 2547, 2909}, {}]
rule 11.	(A8 = 13413) => (D = 1); [1, 1, 0.03%, 100.00%][1, 0, 0, 0]
.	.
.	.
.	.
rule 2371.	(A4 = 21) & (A8 = 4192) => (D = 2); [1, 1, 0.04%, 100.00%][0, 1, 0, 0] [{5907}, {}]
rule 2372.	(A3 = 22) & (A8 = 9934) => (D = 2); [1, 1, 0.04%, 100.00%][0, 1, 0, 0] [{6261}, {}]

rule 2373. (A5 = 3) & (A8 = 4978) => (D = 2); [1, 1, 0.04%, 100.00%][0, 1, 0, 0][{7174}, {}]

rule 2374. (A4 = 23) & (A8 = 7017) => (D = 2); [1, 1, 0.04%, 100.00%][0, 1, 0, 0][{6497}, {}]

rule 2375. (A8 = 112) => (D = 2); [1, 1, 0.04%, 100.00%][0, 1, 0, 0][{5759}, {}]

rule 2376. (A8 = 293) => (D = 2); [4, 4, 0.17%, 100.00%][0, 4, 0, 0][{5971, 6794, 7018, 7185}, {}]

rule 2377. (A5 = 3) & (A8 = 1523) => (D = 2); [2, 2, 0.08%, 100.00%][0, 2, 0, 0][{6376, 7394}, {}]

rule 2378. (A8 = 9902) & (A18 = 505455) => (D = 2); [1, 1, 0.04%, 100.00%][0, 1, 0, 0][{6799}, {}]

rule 2379. (A8 = 1357) & (A11 = 16) => (D = 2); [1, 1, 0.04%, 100.00%][0, 1, 0, 0][{6187}, {}]

rule 2380. (A2 = 12) & (A8 = 524) => (D = 2); [1, 1, 0.04%, 100.00%][0, 1, 0, 0][{5119}, {}]

.

.

.

rule 2387. (A8 = 11487) => (D = 3); [1, 1, 0.05%, 100.00%][0, 0, 1, 0, 0][{3425}, {}]

rule 2388. (A8 = 10936) => (D = 3); [1, 1, 0.05%, 100.00%][0, 0, 1, 0, 0][{3507}, {}]

rule 2389. (A8 = 1782) => (D = 3); [3, 3, 0.15%, 100.00%][0, 0, 3, 0, 0][{3370, 4008, 4290}, {}]

rule 2390. (A8 = 14806) => (D = 3); [1, 1, 0.05%, 100.00%][0, 0, 1, 0, 0][{3664}, {}]

rule 2391. (A8 = 2268) => (D = 3); [1, 1, 0.05%, 100.00%][0, 0, 1, 0, 0][{3671}, {}]

rule 2392. (A8 = 5006) => (D = 3); [1, 1, 0.05%, 100.00%][0, 0, 1, 0, 0][{3092}, {}]

rule 2393. (A2 = 3) & (A13 = 25) => (D = 3); [2, 2, 0.10%, 100.00%][0, 0, 2, 0, 0][{4613, 4721}, {}]

rule 2394. (A1 = 2) & (A7 = 3) & (A15 = 46) => (D = 3); [3, 3, 0.15%, 100.00%][0, 0, 3, 0, 0][{3981, 4259, 4697}]

rule 2395. (A4 = 1) & (A15 = 40) => (D = 3); [2, 2, 0.10%, 100.00%][0, 0, 2, 0, 0][{3253, 3898}, {}]

rule 2396. (A3 = 3) & (A7 = 4) & (A15 = 5) => (D = 3); [2, 2, 0.10%, 100.00%][0, 0, 2, 0, 0][{4085, 4919}]

rule 2397. (A8 = 3351) => (D = 3); [1, 1, 0.05%, 100.00%][0, 0, 1, 0, 0][{3062}]

rule 2398. (A4 = 23) & (A7 = 3) & (A20 = 4) => (D = 3); [2, 2, 0.10%, 100.00%][0, 0, 2, 0, 0][{3326, 3618}]

.

.

.

rule 3592. (A8 = 13896) => (D = 4); [1, 1, 0.05%, 100.00%][0, 0, 0, 1, 0][{7433}, {}]

rule 3593. (A8 = 1258) => (D = 4); [1, 1, 0.05%, 100.00%][0, 0, 0, 1, 0][{8525}, {}]

rule 3594. (A8 = 15919) => (D = 4); [1, 1, 0.05%, 100.00%][0, 0, 0, 1, 0][{8319}, {}]

rule 3595. (A8 = 9540) => (D = 4); [1, 1, 0.05%, 100.00%][0, 0, 0, 1, 0][{7783}, {}]

rule 3596. (A8 = 8233) => (D = 4); [1, 1, 0.05%, 100.00%][0, 0, 0, 1, 0][{8846}, {}]

rule 3597. (A8 = 7387) => (D = 4); [1, 1, 0.05%, 100.00%][0, 0, 0, 1, 0][{8024}, {}]

rule 3598. (A8 = 14410) => (D = 4); [1, 1, 0.05%, 100.00%][0, 0, 0, 1, 0][{9032}, {}]

rule 3599. (A8 = 15487) => (D = 4); [1, 1, 0.05%, 100.00%][0, 0, 0, 1, 0][{8331}, {}]

rule 3600. (A8 = 5536) => (D = 4); [1, 1, 0.05%, 100.00%][0, 0, 0, 1, 0][{7790}, {}]

rule 3601. (A8 = 10431) => (D = 4); [1, 1, 0.05%, 100.00%][0, 0, 0, 1, 0][{8028}, {}]

.

.

.

rule 3933. (A6 = 20980) => (D = 5); [1, 1, 0.06%, 100.00%][0, 0, 0, 0, 1][{10942}]

rule 3934. (A6 = 8791) => (D = 5); [1, 1, 0.06%, 100.00%][0, 0, 0, 0, 1][{10913}]

rule 3935. (A13 = 64) & (A14 = 65) & (A19 = 55) => (D = 5); [1, 1, 0.06%, 100.00%][0, 0, 0, 0, 1][{10598}]

rule 3936. (A6 = 12189) => (D = 5); [2, 2, 0.12%, 100.00%][0, 0, 0, 0, 2][{9671, 10738}]

rule 3937. (A11 = 17) & (A14 = 68) & (A15 = 69) => (D = 5); [1, 1, 0.06%, 100.00%][0, 0, 0, 0, 1][{10369}]

rule 3938. (A18 = 782884) => (D = 5); [1, 1, 0.06%, 100.00%][0, 0, 0, 0, 1][{9953}]

rule 3939. (A18 = 543178) => (D = 5); [1, 1, 0.06%, 100.00%][0, 0, 0, 0, 1][{10849}]

rule 3940. (A4 = 25) & (A14 = 55) & (A21 = 56) => (D = 5); [1, 1, 0.06%, 100.00%][0, 0, 0, 0, 1][{9909}]

A Rule Matrix was created based on the specified rules. According to the Rule Matrix, the similarity of each data in the test data was calculated. In this way, the labels of 2250 data in total were tried to be identified. The result is also shown on Figure 3.

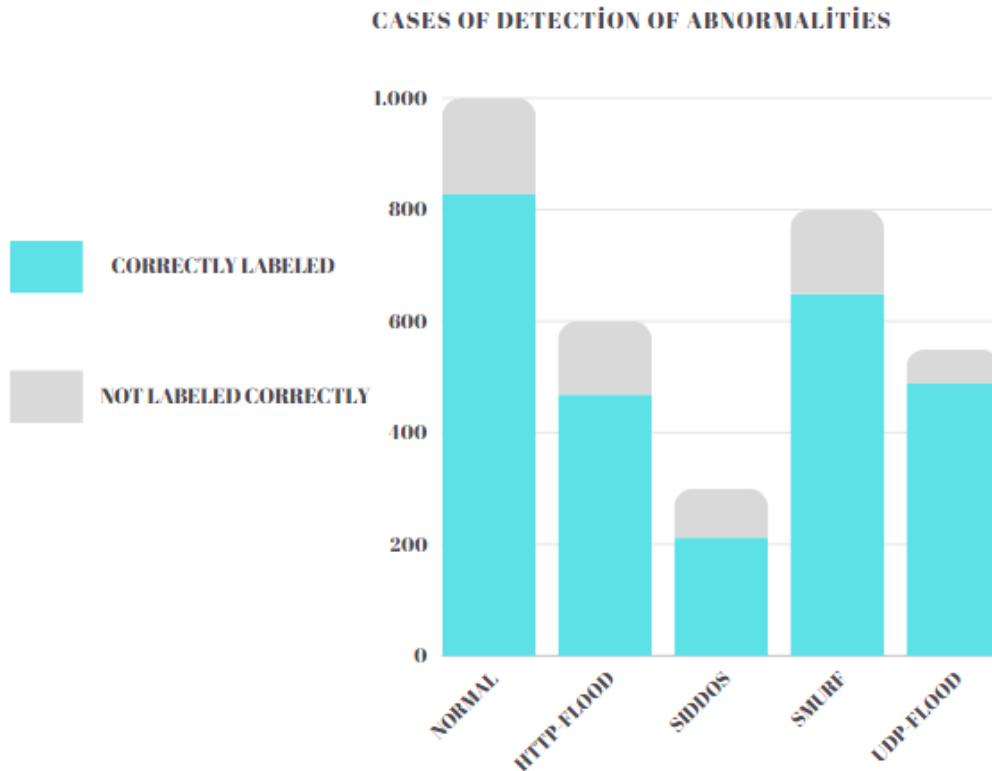


Figure 3. Tag detection results for each log generated on the network using the proposed model

The proposed model correctly labeled 827 out of 1000 normal data and 468 out of 600 for HTTP-FLOOD. Similarly, 212 out of 300 for SIDDOS, 649 out of 800 for SMURF and 488 out of 550 for UDP-FLOOD. When the figure is analyzed, it is seen that the method performs a highly class-efficient categorization on this unbalanced dataset, which does not have a balanced distribution by class. It is observed that a close classification rate is achieved for all classes. In order to see this situation more clearly, it is useful to perform further analysis, for this, it is first necessary to see that the data is not balanced and to show the classification made on this basis. Therefore, the percent accuracy for each case is also given in Figure 4. So, for each Log, the percentage of correctly labeled data among all correctly labeled Logs is given.

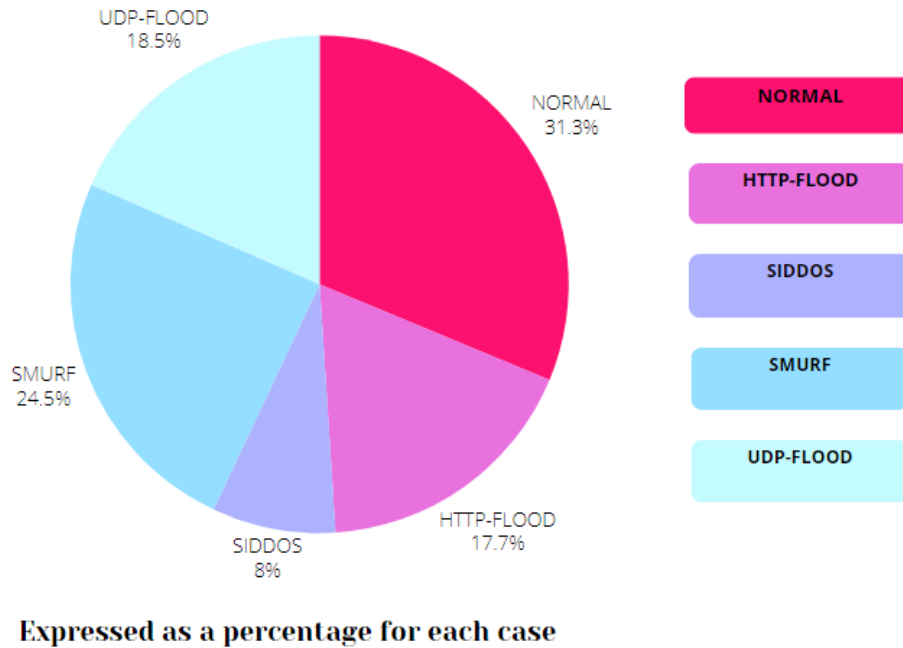


Figure 4. Percentage of correctly labeled data for each Log over all correctly labeled Logs

When Figure 4 is analyzed, it is seen that there is a balanced classification on log basis. This is because it is seen that each Log is parsed with a decomposition close to the number ratio. This implies that the model can offer stability in the direction of quantification. Moreover, in order to understand that the model is statistically significant, it is necessary to look at the accuracy percentages on Log/label basis. Figure 5 is obtained for this purpose. The figure shows the classification rates for each Log.

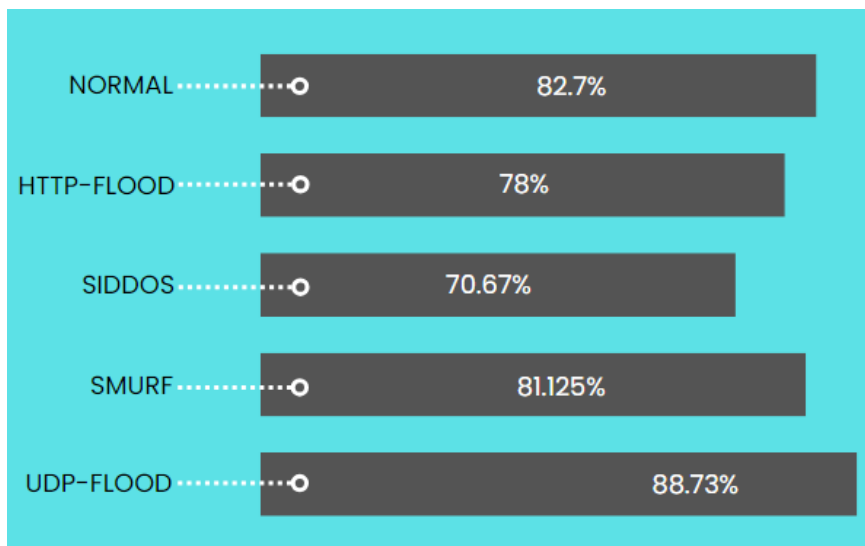


Figure 5. Log-based classification results

The Figure 5 shows that the highest results are obtained for the UDP-FLOOD logs, while for many other logs the ratio is not much lower. Finally, it is seen that the proposed model works with an average accuracy of 80.2450% on the basis of all logs. This is a significant achievement for unbalanced data.

Conclusion and Recommendations

Rapid technological advancement has increased risks while also bringing innovations in web technologies and other fields. Cyber attacks, such as DDoS, are one of these risks. The prevalence of DDoS attacks in digital environments has heightened the importance of research in this area. Detecting these attacks has become both popular and necessary. This study analyzes studies in the field of DDoS and presents a model that can work efficiently in this field. Because the model is built using the effective information extraction technique of rough sets, it is expected that the model will be used in experimental studies. This study may also be said to shed light on future studies in this field. Finally, this study examines the significance of DDoS attacks in the digital environment and presents a viable solution for detecting such attacks.

AL-JAZARI: ANCIENT WISDOM'S INFLUENCE ON MODERN TECHNOLOGY

Mahmut Dirik

Department of Computer Engineering, Sirnak University, Turkey

ABSTRACT

This study examines the influence of the 12th-century inventor and engineer Al-Jazari on contemporary technology and engineering disciplines. It examines how Al-Jazari's innovations in areas such as automation, robotics, fluid mechanics, time measurement, and mechanical design have inspired modern technological and engineering applications. His pioneering work in the field of robotic design and automation is evidenced by his descriptions of pistons, cylinders, crankshafts, valves, and their integrated operation in pumping systems, which are detailed in his book. This treatise illuminates the depth and significance of Al-Jazari's contributions to science and explores the technological legacy that stretches from the 12th century to the present day.

Keywords: Al-Jazari, Historical Innovation, History of Technology, Contemporary Engineering Practices

1. Introduction

Al-Jazari is considered one of the most important figures in the history of technology and the Islamic world in the 12th and 13th centuries [1]. His historical legacy, in particular his contributions to the development of automated machines and robotic systems, is outstanding. Al-Jazari's innovative designs and mechanical knowledge make him both an inventor and a scientist. His works represent a significant turning point in the fields of engineering and mechanics and serve as a source of inspiration for future generations [2].

Al-Jazari's legacy is mainly summarized in his work "The Book of Knowledge of Ingenious Mechanical Devices", which contains designs for water clocks, automatic pitchers, jugs, and many other innovative mechanical devices [3]–[6]. These designs not only testify to the depth of technical knowledge and engineering skill of Al-Jazari's era but also lay the foundation for modern technology and robotics [3]–[5].

The era in which Al-Jazari lived is also considered one of the most brilliant periods of scientific and technological advancement in the Islamic world. Significant progress was made in various fields, from mathematics to astronomy and from medicine to engineering. As part of this progress, Al-Jazari made revolutionary contributions to technology and automation. His works continue to inspire contemporary studies in engineering and technology.

Al-Jazari contributed his first thoughts to the fields of robotics and artificial intelligence and produced groundbreaking design drawings. His book, "The Book of Knowledge of Ingenious Mechanical Devices," offers insights into his life and work. It is an important source to understand the scientific content of his inventions and their place in the history of technology, as well as to determine his position in the history of technology [3], [4].

In order to accurately evaluate Al-Jazari's works, an in-depth study of the position of his automata in the history of technology and his place in the history of technology is necessary. His main work, the book, includes 50 different devices in six categories and serves as a basic reference to determine his place in the history of technology [7].

When examining the works of Al-Jazari, it is noticeable that most of his constructed devices are described in detail with measurements and geometric shapes. Among the geometric terms that frequently appear in his explanations are circles, right angles, rectangles, circumferences, radii, and cylinders [5], [7], [8].

Al-Jazari's work represents the pinnacle of theoretical and practical knowledge in this field in the Islamic world [6], [9]. Al-Jazari does not deal with theoretical topics such as air and vacuum, but his expertise in the

manufacture of devices demonstrates his mastery of the subject. His works contain detailed and innovative designs that emphasize his importance in the history of engineering and technology.

2. Al-Jazari's innovative mechanisms in technology and their effects

Al-Jazari, a Muslim scientist known for his exceptional technical intellect and contributions in the fields of engineering and design, lived in Mesopotamia in the 12th century during the Artuqid dynasty. He lived in Mesopotamia in the 12th century. He lived in Mesopotamia in the 12th century. He lived in Mesopotamia in the 12th century. His works include significant innovations in automation and robotics and served as an early inspiration for the development of modern robotics and automation. Al-Jazari focused on automatic systems, programmable robots, and mechanical animals and developed designs that illustrated the integration of complex mechanical systems and moving parts [6], [9]. These inventions laid the foundation for modern robotic and automation systems and pushed the boundaries of mechanical design.

Al-Jazari also made remarkable advances in fluid mechanics. His inventions, which ingeniously utilized water and hydraulics, have influenced the foundations of modern fluid mechanics in fields such as hydraulic engineering, aeronautics, and automotive engineering [10]. His work on complex water clocks made an important contribution to modern mechanical engineering and timekeeping technology. These clocks incorporate important concepts such as gear systems, flow control, and feedback mechanisms and demonstrate an advanced understanding.

Al-Jazari's designs include various machines such as pumps, cranks, suction devices, and valves. These designs laid the foundation for modern machinery and have found their way into today's technology and design in various forms [11]. His approach to finding creative mechanical solutions to practical problems laid the foundation for today's engineering methods. The emphasis on functionality, efficiency, and aesthetics in his designs is in line with modern engineering principles [12], [13].

Al-Jazari's work epitomizes an interdisciplinary approach where art, science, and technology intersect and is becoming increasingly important in today's research and development. The detailed documentation of mechanical devices is an important educational resource for understanding the history and development of technology. The influence of ancient technologies on contemporary designs and applications can be explored through these documents. In particular, Al-Jazari's work, which inspires modern designers and artists in the fields of kinetic art and automata, often references the creative use of mechanical systems and aesthetic design elements in contemporary art and design. Al-Jazari's work is characterized by its importance in the history of engineering and design and its contribution to technological advancement, and it continues to inspire creativity, interdisciplinary thinking, and technological advancement in contemporary engineering and design [14].

3. Impact on Modern Technology

Al-Jazari's innovative designs laid an important foundation for modern automation and robotics technologies. His devices showed how mechanical systems could be programmed and operated automatically, and they served as a source of inspiration for the development of modern industrial robots and automated control systems. Al-Jazari's work emphasizes the crucial importance of integrating complex mechanical systems and moving parts in modern engineering and robotics [9], [15], [16]. Some of the most notable examples of programmable robots and automatic systems by Al-Jazari are:

Automatic water clocks: Al-Jazari designed sophisticated water clocks that measured time based on the flow and pressure of water. These clocks were programmed to activate mechanical figures or produce sounds at certain intervals. They not only showed the time but also gave visual and acoustic signals at certain hours.

Automated water clocks: Al-Jazari designed sophisticated water clocks that measured time based on the flow and pressure of water. These clocks were programmed to activate mechanical figures or produce sounds at certain intervals. They not only showed the time but also gave visual and acoustic signals at certain hours.



Figure 1. The Elephant Water Clock [6]



Figure 2. Al-Jazari's Boat Water Clock [6]

Automated musical instruments: One of Al-Jazari's most famous inventions are robotic musicians that can play music automatically. These robots were equipped with a water-powered system that allowed them to play various musical instruments in a specific order. This is considered one of the earliest examples of robotics and programmable machines.



Figure 3. Al-Jazari's Automated Musical Instruments [6]

Automatic washing machines and washbasins: Al-Jazari also designed automatic washbasins for ablutions or hand washing. These washbasins were equipped with mechanisms that could automatically supply the user with water.

These inventions illustrate Al-Jazari's understanding of how mechanical systems could be programmed and operated automatically. With these technologies, he laid the foundation for the principles used today in the fields of robotics and automation. Al-Jazari's work is therefore of great importance to the history of modern engineering and technology.



Figure 4. Al-Jazari's Peacock Ablution Machine [6]



Figure 5. Al-Jazari's Peacock Ewer [6]

4. The influence of ancient automation on modern robotics

The automatic systems developed by Al-Jazari are based on mechanical parts that work in a specific order and according to a specific schedule, and they are one of the earliest examples of the programming concepts of modern robots. Today's robots are similarly programmed to perform complex tasks in a specific order.

Al-Jazari's designs utilized mechanisms that detect physical changes such as water flow and pressure. This function can be considered a precursor to the sensor and actuator technology found in modern robotics. In addition, Al-Jazari's designs, such as automatic beverage dispensers and water clocks, incorporate complex mechanical systems and automatic control mechanisms. This complexity is widely used in modern industrial automation and robotics [17].

Al-Jazari's designs include automatic control mechanisms based on the principle that one action triggers another. This principle forms the basis for automatic control systems in today's robotics [6]. In addition, his work is characterized by its functionality and aesthetics, emphasizing that today's robot designs should be both functionally efficient and visually impressive. These historical examples show how ancient automation has contributed to the fundamental concepts and principles of modern robotic technology. In this respect, Al-Jazari's work is not only of historical significance but also a source of inspiration for modern technology and engineering.

5. The importance of fluid mechanics and hydraulic systems in engineering and technology

Fluid mechanics and hydraulic systems are recognized as fundamental disciplines in the fields of engineering and technology. These disciplines study the behaviour of fluids, including liquids and gases, and explore how these fluids can be used in various engineering applications.

Fluid Mechanics:

Fundamental Concepts: Fluid mechanics covers fundamental concepts such as pressure, flow velocity, viscosity, and density and analyses both the motion and static state of fluids.

Areas of application: This scientific field has a wide range of applications, from aviation to shipbuilding, from chemical engineering to environmental engineering. Examples such as the aerodynamic design of aeroplane wings or flow management in sewage treatment plants are practical applications of fluid mechanics.

Computational Fluid Dynamics (CFD): Modern computer simulations enable the modelling and analysis of complex problems in fluid mechanics. This makes it possible to optimize designs before they are tested under real conditions.

Hydraulic systems:

Basic principles: Hydraulic systems work by transmitting force and motion using the pressure and flow of fluids, based on physical laws such as Pascal's principle.

Areas of application: Hydraulic systems are used in various fields, including construction machinery, aviation, automotive, and industrial machinery. Applications such as the arm mechanisms of excavators or the braking systems of cars are examples of the effectiveness of hydraulic systems.

Energy efficiency and control: Hydraulic systems offer high energy efficiency and precise control options, which is particularly beneficial in situations that require the lifting of heavy loads or precise movements.

The extensive application areas of fluid mechanics and hydraulic systems emphasise their role as fundamental engineering disciplines that influence and shape many aspects of modern technology. Innovations in these fields play a crucial role in solving modern engineering challenges ranging from energy efficiency to environmentally friendly solutions [18]–[23].

6. Al-Jazari's Contributions to Hydraulic Engineering and their Contemporary Applications

Al-Jazari's innovations had a profound influence on the field of modern hydraulic engineering. His groundbreaking designs laid the foundation for numerous fundamental principles that are used in many technical applications today. Al-Jazari's achievements in the field of hydraulic pumps, valves, and water clocks and their contribution to today's applications are described in detail below [24], [25].

Today's applications of hydraulic pumps:

Application in construction machinery: Hydraulic pumps are often used in construction machinery, particularly in excavators and other heavy machinery. These pumps help to lift and transport heavy materials.

Use in automotive systems: In automotive systems, hydraulic pumps are an integral part of steering and braking systems that improve vehicle control and provide a safer driving experience.

Industrial applications: In factories and production plants, hydraulic pumps are used in a variety of machines to increase the efficiency and effectiveness of production processes.

Contemporary applications of valves:

Use in water treatment systems: In water treatment systems, valves are crucial for controlling and regulating the flow of water.

Use in heating and cooling systems: Valves in heating, ventilation, and air conditioning systems play a central role in regulating the flow of water and other fluids to control temperature.

Use in the oil and gas industry: In the oil and gas sector, valves are essential for regulating the pressure and flow rate in pipelines to ensure the safe and efficient transport of liquids.

Modern applications for water clocks:

Historical and educational applications: Water clocks have been used to measure time since ancient times and are precursors to modern clock technology. They are still used today for educational purposes.

Use in garden irrigation systems: Today, water clocks are used in automatic garden irrigation systems to promote efficient water use.

Use in scientific research: Water clocks are used in scientific experiments and studies to explore the principles of fluid dynamics and time measurement.

These examples illustrate the fundamental role that hydraulic pumps, valves and water clocks play in various applications. Al-Jazari's inventions are considered innovative and groundbreaking and have contributed significantly to progress in the fields of hydraulic engineering, mechanical automation and robotics.

6.1. Al-Jazari's Dual-Action Pump

Al-Jazari's dual-action pump with its two-piston system is designed so that each piston alternately draws in and discharges water. This innovative design allows one piston to draw in water while the other simultaneously discharges water, resulting in a seamless and efficient water flow. This mechanism is an example of an ingenious and continuous flow system, a significant advance in hydraulic technology [25], [26].

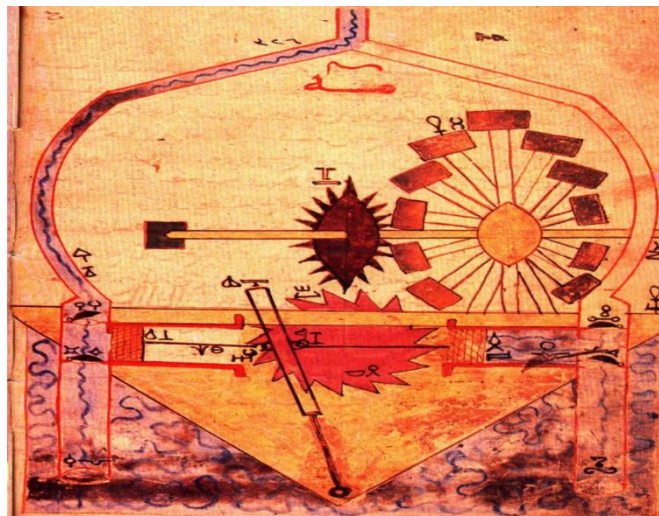


Figure 6. Al-Jazari's Dual-Action Pump [6]

Innovative features of the work of Al-Jazari

Al-Jazari's innovation of the crankshaft: Al-Jazari was a pioneer in the use of the crankshaft to regulate and synchronise piston movements. This innovation can be clearly seen in the automatic crank mechanisms of the water-catching machines. His contributions were decisive for the automatic movement and further development of crankshaft technology. The crankshaft, which functions as an eccentric shaft, is praised for its ability to convert circular motion into linear or other types of motion. Al-Jazari's efforts in this field are considered a significant milestone in the history of crankshaft technology, and some sources refer to him as the inventor of the crankshaft. This innovation is of great importance when considering the historical development of the crankshaft across different eras and cultures.

Continuous flow: The dual-action pump developed by Al-Jazari enables a constant and uninterrupted flow of water, which proves particularly beneficial for scenarios that require a continuous supply, such as agricultural irrigation or mining.

Efficiency and performance: The dual-action configuration of the pump increases its efficiency and allows larger volumes of water to be transported at higher pressure.

Al-Jazari's pioneering designs have had a lasting impact on the development of modern hydraulic pumps and water management systems. His dual-action pump is still a fundamental principle in hydraulic systems and continues to influence various modern engineering applications [3], [27].

To understand the integrated motion mechanism of Al-Jazari, you can follow the steps below that explain how this complicated device works.

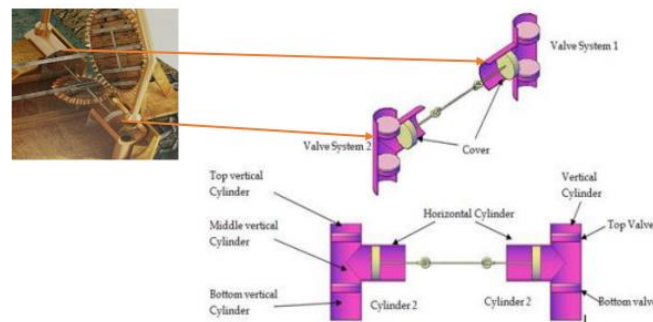


Figure 7. An illustration of hydraulic and gear system [27], [28]

Rotating panels around a shaft: The first component of the system consists of a central shaft around which the panels rotate. These panels, which are driven by the force of water or wind, generate energy through their rotation, which in turn influences the subsequent elements of the mechanism.

Gear wheels: The rotation of these plates sets a horizontal shaft in the centre in motion. This horizontal shaft engages with a gear wheel that is aligned perpendicular to the plane of the side and sets it in rotation.

Piston mechanism: The system has a piston mechanism in which a crankshaft, connected at both ends by joints, carries a piston at one end. This arrangement facilitates the generation and operation of the piston.

Cylinders: To enable the movement of these pistons, the cylinders are strategically placed on either side. Each cylinder is equipped with two valves at its base: one to draw in water and the other to expel water.

This intricate arrangement represents an integrated movement system designed by Al-Jazari. The design is highly compatible with the principles of contemporary engineering, and its pioneering approach has profoundly influenced the development of various modern movement mechanisms and machine designs.

7. Al-Jazari's Technical Designs Rooted in Air, Vacuum, and Equilibrium Principles

Al-Jazari's technical designs, based on the principles of air, vacuum, and equilibrium, contain significant examples that demonstrate the sophisticated technical skills and creativity of his era.

Al-Jazari's pneumatic water fountain: Al-Jazari used the principles of air pressure to design an original water fountain. This design cleverly utilised the ability of air pressure to lift water in various forms. Air pressure was used strategically to control both the force and direction of the water jet, resulting in a visually captivating water feature. This system was praised not only for its aesthetics but also for its technical ingenuity.

Al-Jazari's designs, imbued with the principles of air, vacuum, and equilibrium, are full of examples that show the advanced technical ingenuity and creativity of his time.

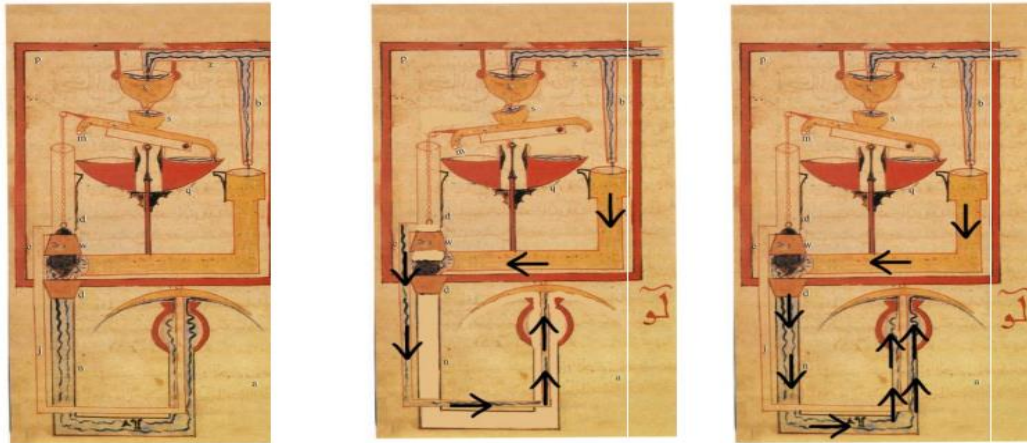


Figure 8. Al-Jazari's Pneumatic Water Fountain [6], [9]

8. The Influence of Al-Jazari on Mechanical Engineering

Innovations in automation and robotics: Al-Jazari is considered a pioneer in the development of mechanical automation and robotics. His designs laid the foundation for the automated operation of complicated mechanical devices and thus created the infrastructure for modern automation and robotics.

Revolutionary developments in timekeeping: Al-Jazari's contributions to the design of water clocks and timekeeping mechanisms were crucial to precise timekeeping and laid the foundation for today's timekeeping technologies.

Advances in hydraulic systems: In the field of hydraulics, Al-Jazari played a crucial role in the development of hydraulic pumps, valves, and water clocks. His work in these areas shaped the fundamental principles of fluid control and transmission and enabled the development of modern hydraulic systems.

The principle of mechanical equilibrium: Al-Jazari's development of the principle of mechanical equilibrium is a fundamental concept that ensures the stability and balanced operation of mechanical devices and is crucial for accurate weight distribution.

Pioneering fluid mechanics: Al-Jazari's contributions to fluid mechanics, particularly his designs of water fountains and fluid control systems, represent significant advances in the field.

Influence on microcontrollers and electronic control systems: The principles of mechanical equilibrium and fluid control established by Al-Jazari have influenced the fundamental concepts for the development of modern microcontrollers and electronic control systems.

The Future Impact of Al-Jazari's Legacy

Promoting technological innovation: Al-Jazari's pioneering work in automation, robotics, and mechanical devices continues to have the potential to inspire future technological breakthroughs and contribute to the advancement of modern robotics and automation.

A resource for education and learning: Al-Jazari's works are invaluable to students and researchers in the fields of engineering and mechanics and play an important role in imparting fundamental engineering knowledge to future generations.

Historical significance and research: An in-depth analysis of Al-Jazari's contributions is crucial for understanding the development of engineering progress in history and provides a rich source for future historical studies.

Contributions to green technologies: Al-Jazari's designs, particularly in the field of hydraulic systems and water clocks, have the potential to make a significant contribution to the development of sustainable technologies that address today's environmental challenges.

Preservation and dissemination of cultural heritage: Al-Jazari's legacy is a testament to the rich scientific and technological heritage of the Middle East and the Islamic world. Its preservation and dissemination are key to passing on this cultural wealth to future generations.

Al-Jazari's contributions and legacy retain their importance, both in their historical context and in their continuing influence on the development of technical and scientific progress.

9. CONCLUSION

Al-Jazari, a 12th-century scientist, is best known for his early contributions to modern disciplines such as automation, robotics, and artificial intelligence. His innovative work in these fields sheds light on the history of science and technology in Islamic civilization and is considered an important source of inspiration for future generations.

Al-Jazari's works are of crucial importance for the education of younger generations and for people interested in the history of science and technology. It is important to use his works to promote interest in these fields and to provide a broader perspective on the history of science. In particular, Al-Jazari's mechanical constructions and technological innovations should be the focus of efforts to better understand and recognize the contributions of Islamic civilization in science and technology.

Al-Jazari's mechanical knowledge and its applications should be recognized as important indicators of the scientific and technological progress of his time. His contributions need to be emphasized more in terms of their role in the advancement of science. This enables a deeper understanding of the origins of civilization and cultural values and creates a strong motivation for the preservation and promotion of this historical heritage.

To summarize, Al-Jazari's work has an important place in understanding and interpreting the history of science and technology. More attention needs to be paid to these topics in academic research, not only to preserve scientific heritage but also to inspire future innovation.

References

- [1] Y. Korkutata and Z. F. Toprak, "El- Cezerî ile ilgili yapılan çalışmaların değerlendirilmesi," no. 484, pp. 37–49, 2013.
- [2] G. Sarton, *Introduction to the History of Science*. Robert E. Krieger Publishing Company, Huntington, New York, 1975.
- [3] S. Al-Hassani, "Al-Jazari: The Mechanical Genius," *MuslimHeritage.com*, 2001.
- [4] H. Invented, "AL-JAZARI," pp. 1–14, 2020.
- [5] M. Dirik, "Al-Jazari: The Ingenious Inventor of Cybernetics and Robotics 1", Accessed: Feb. 18, 2023. [Online]. Available: www.dergipark.org.tr/en/pub/jscai
- [6] "The Book of Knowledge of Ingenious Mechanical Devices: (Kitāb fī ma 'rifat ... - P. Hill - Google Books." Accessed: May 31, 2020. [Online]. Available: https://books.google.com.tr/books/about/The_Book_of_Knowledge_of_Ingenious_Mecha.html?id=EUtqCAAQBAJ&printsec=frontcover&source=kp_read_button&redir_esc=y#v=onepage&q&f=false
- [7] "Al-Jazari: The Mechanical Genius - Muslim HeritageMuslim Heritage." Accessed: Feb. 19, 2023. [Online]. Available: <https://muslimheritage.com/al-jazari-the-mechanical-genius/>
- [8] A. Uzun and F. Vatansever, "Ismail al Jazari machines and new technologies," *Acta Mechanica et Automatica*, vol. 2, no. 3, pp. 91–94, 2008.
- [9] D. Hill, *A History of Engineering in Classical and Medieval Times*. Routledge, 1996.
- [10] Z. Şen, "Ancient water robotics and Abou-I Iz Al-Jazari," *Water Sci Technol Water Supply*, vol. 13, no. 3, pp. 699–709, 2013, doi: 10.2166/ws.2013.031.

- [11] S. Al-Hassani, "The Machines of Al-Jazari and Taqi Al-Din | Muslim Heritage," Muslim Heritage.
- [12] I. al-R. al-Jazari, *The Book of Knowledge of Ingenious Mechanical Devices*. 1973. doi: 10.1007/978-94-010-2573-7.
- [13] R. V Jones, "The Book of Knowledge of Ingenious Mechanical Devices," *Physics Bulletin*, vol. 25, no. 10, pp. 474–474, Oct. 1974, doi: 10.1088/0031-9112/25/10/040.
- [14] G. Nadarajan, "Islamic Automation : A Reading of al-Jazari ' s The Book of Knowledge of Ingenious Mechanical Devices (1206)," 2007.
- [15] E. Wiedeman, *Über die Uhren im Bereich der islamischen Kultur (German Edition)*: saxoniabuch, 2017. Accessed: May 31, 2020. [Online]. Available: <https://www.amazon.com/Uhren-Bereich-islamischen-Kultur-German/dp/3957705053>
- [16] Z. Şen, "How to Improve the Science and Engineering Education in Islamic Countries ?," vol. 1, no. 3, pp. 121–131, 2018, doi: 10.26701/uad.484662.
- [17] T. Akman, "Sekiz Yüzyıl Önce Otomatik Makine Yapan Türk Bilgini Ebül -İz," *Bilim ve Teknik*, vol. 7, no. 77, pp. 1–6, 1974.
- [18] "Fluid Mechanics Measurements - R. Goldstein - Google Kitaplar." Accessed: Dec. 11, 2023. [Online]. Available: https://books.google.com.tr/books?hl=tr&lr=&id=jGQ-DwAAQBAJ&oi=fnd&pg=PP15&dq=Fluid+mechanics&ots=I-kNC9Fv_v&sig=vpbNOD0UVP-gF_aPovnhFuOYpZ8&redir_esc=y#v=onepage&q=Fluid%20mechanics&f=false
- [19] S. L. Brunton, B. R. Noack, and P. Koumoutsakos, "Machine Learning for Fluid Mechanics," <https://doi.org/10.1146/annurev-fluid-010719-060214>, vol. 52, pp. 477–508, Jan. 2020, doi: 10.1146/ANNUREV-FLUID-010719-060214.
- [20] H. Marzbani, R. N. Jazar, and M. Fard, "Hydraulic engine mounts: a survey," <https://doi.org/10.1177/1077546312456724>, vol. 20, no. 10, pp. 1439–1463, Apr. 2013, doi: 10.1177/1077546312456724.
- [21] S. Shakerin, "Engineering Art," *Mechanical Engineering*, vol. 123, no. 07, pp. 66–69, Jul. 2001, doi: 10.1115/1.2001-JUL-5.
- [22] L. Romdhane and S. Zeghloul, "AL-JAZARI (1136–1206)," pp. 1–21, 2009, doi: 10.1007/978-90-481-2346-9_1.
- [23] M. Ceccarelli, Ed., "Distinguished Figures in Mechanism and Machine Science," vol. 7, 2010, doi: 10.1007/978-90-481-2346-9.
- [24] K. V Raju, S. Manasi, A. Roots, and S. Development, *Water and Scriptures*. 2017. doi: 10.1007/978-3-319-50562-6.
- [25] G. A. H. Emeritus, "Innovation of Mechanical Machinery in Medieval Centuries, Part IV: Mechanisms, Gear Trains and Cranes," 2014. Accessed: Jun. 04, 2020. [Online]. Available: www.ijarcsst.com
- [26] G. A. Hassaan, "Computer Science and Management Studies Innovation of Mechanical Machinery in Medieval Centuries, Part III: Hydraulic Control Components and Feedback Control Systems," *International Journal of Advance Research in*, vol. 2, no. 11, 2014, Accessed: Dec. 11, 2023. [Online]. Available: www.ijarcsms.com
- [27] M. Dirik, "Al-Jazari: The Ingenious Inventor of Cybernetics and Robotics 1", Accessed: Dec. 11, 2023. [Online]. Available: www.dergipark.org.tr/en/pub/jscai
- [28] A. A. Bin, M. Yazid, M. Fahmi, and A. Ruskam, "The Mechanical Engineer: Abu'l-'Izz Badi'u'z-Zaman Ismail ibnu'r-Razzaz al Jazari."

DRILLING STICK SLIP PREDICTION USING MACHINE LEARNING

Dastan Begaliyev

Department of Petroleum Engineering, Nazarbayev University, Astana, Kazakhstan

Masoud Riazi

Department of Petroleum Engineering, Nazarbayev University, Astana, Kazakhstan

ABSTRACT

Drill string vibration modelling poses inherent challenges due to complex variables, necessitating simplifying assumptions that may lack universal transferability across Bottom Hole Assemblies (BHAs), reservoirs, and formations. This study advocates a data-driven approach using open-source machine learning to mitigate drill string vibrations. Stick-slip severity, quantified by the Stick-Slip Index (SSI), is classified (Model 1) and predicted (Model 2) using publicly available drilling data, specifically Weight on Bit (WOB) and torque values from 12 limestone and sandstone formations.

Utilizing Decision Tree Classifier-based predictions, the models demonstrate feasibility and utility, particularly in two distinct formations with varied WOB and torque values. Minor parameter changes leading to shifts in stick-slip severity are accurately predicted, suggesting potential generalization to formations with similar geological characteristics. The study contributes to the understanding of mitigating drill string vibrations through practical data-driven models, paving the way for future refinements and broader applications in drilling operations.

Keywords: Stick-slip, Drill String Vibrations, Machine Learning, Decision Tree Classifier.

ROLE OF BIG DATA IN INDIAN BANKING OPERATIONS

Yashvanth M

Management student, CMS B School, Jain Deemed to be University

Shivani singh

Management Student, CMS B School, Jain Deemed to be University

Dr. Shalini R

Associate Professor, CMS B School, Jain Deemed to be University

ABSTRACT

Big data plays a very important role in the development of the banking and financial sector. The banks are not just keeping the money safe, they are also securing the customers information by the help of Big Data. Big data is all about how the data is collected, processed, analyzed and utilized. The objectives of this study is to understand Big data's key characteristics and its benefits in banking operations. Another objective is to analyze the impact of big data analytics in Indian banking sector. The present study collects data from secondary sources like books, magazine articles, academic journals and official websites of RBI and other banks. The studies on Indian banks like HDFC, ICICI, Axis, State Bank of India, and ING Vysya, shows how big data analytics have been instrumental in improving customer-specific solutions, customer segmentation, and effective customer feedback analysis. Furthermore, it has played a vital role in fraud prevention and detection, ensuring the security and integrity of the banking industry. In conclusion, big data is a critical force on driving innovation in banking operations, shaping customer experiences and strengthening security in constantly changing financial sectors.

Key words: Big data, Banking Operations, Fraud prevention, Customer segmentation, Financial sector.

INTRODUCTION

Big data is regarded as a significant revolution. It's evolving essential in all commercial areas and will facilitate establishing a firm's long-term competitive advantage. All kinds of organizations need to give big data sources strategic importance because the technology platform is constantly evolving and changing. This is necessary so that they can learn more about customer behavior and customize their products and services to the needs of customers.

In-depth analysis of the effects of big data on the enormous amounts of data produced and stored at higher rates of size, speed, and variety of banking activities is provided in this paper. Incredible growth in data and the rapid advancement of new technologies have resulted in substantial changes to corporate strategies and management across the board, including blockchain, Artificial Intelligence (AI), Big Data analytics and cloud. The improvement of the banking or financial services sector depends more and more on big data. (Gonsalves & Jadav,2012)

Big data's influence on the development of the banking and financial services sectors has diminished. A smart system may offer bankers priceless tools to enhance their decision-making process when managing complicated portfolios based on the vast amount of controlled data. In any case, due to the relentless and rapid growth of data analytics, the banking sector now has access to a greater selection of services and the extraordinary ability to specialize and personalize its products and services. (Nafis Alam,2022)

LITERATURE REVIEW:

Author	Title	Source	Findings
Kumar et. al.	"Imperative Role of Artificial Intelligence and Big Data in Finance and Banking Sector"	International Conference on Sustainable Computing and Data Communication Systems (ICSCDS), Erode, India, 2023,	AI and Big Data are indispensable tools in the banking and finance sector. They enhance decision-making, reduce risks, improve customer experiences, and drive operational efficiency. Embracing these technologies is essential for staying competitive and meeting the evolving demands of the industry while ensuring security and compliance.
Morshadul Hasan, Thi Le, Ariful Hoque	The Impact of Big Data on Banking Operations	Nanjing Audit University and Murdoch University journal	The development of big data Generates favorable requirements for expanding the commercial reach of financial companies and offering services to banking customers.
Moody Amakobe	The Impact of Big Data Analytics on the Banking Industry	Moody Amakobe CS872-1503C-01- Introduction to Big Data Analytics Colorado Technical University	The study claims that banks with big data analytics maintain a 4% point market share better than banks without big data analytics. The main subjects of the article will be the following. (Marketing, credit risk management, and fraud detection)
Rimvydas Skyrius, Igor Katin, et. al.	The Potential of Big Data in Banking	S. Srinivasan Editor (27 May 2017) Guide to Big Data Applications	To fully harness this potential, banks must invest in data infrastructure, analytics capabilities, and data privacy measures while ensuring compliance with regulatory requirements. Those that effectively leverage Big Data will have a competitive advantage in the rapidly evolving financial landscape.
Rahul More, et. al.	Big Data Analysis in Banking Sector	International Journal of Engineering Research and Applications	Applications for big data analytics frequently involve data from both internal and third-party sources, such as forecasting, describing, recommending or treating consumer data gathered by outside information service providers.

OBJECTIVES:

- To understand Big Data's key characteristics and apply examples from Indian banks.
- To learn about and understand big data analytics
- How Big Data Analytics Impact on Indian Banking Sector

RESEARCH METHODOLOGY

Review of secondary data was used to perform the study for this paper. The information is taken from Books, magazine articles, academic journals and websites were only a few of the many sources of information that were used.

Characteristics of Big Data are 3 Vs (Nagham Saeed, Laden Husamaldin 2021)

- Volume
- Variety
- Velocity

Volume

Big Data refers to a scale that is enormous in itself. Assessing the value of the results depends heavily on sample size. Whether or not a particular set of data can be categorized as Big Data also depends on its volume. When working with Big Data, another attribute that must be taken into consideration is "size."

Velocity

Collecting data from multiple sources (Accessibility) at a faster speed can help in getting a better picture and making better decisions. Is about how fast the data can be analyzed and interpreted in an understandable way

Variety

The data can be structured and unstructured by Variety the data can be organized. Variety provides the flexibility to store and analyze different types of data by obtaining real time information. (Nagham Saeed, Laden Husamaldin 2021)

Sectors Ranking according to their engagement with the growth of the V's.

Rank	Sector/s	No. of V's	The V's
First	Retail & Oil and Gas	7 V's	(1) Volume, (2) Velocity, (3) Variety, (4) Veracity, (5) Value, (6) Variability, and (7) Visualisation.
Second	Agriculture, Manufacturing, Health Care, Law enforcement & Education	5 V's	(1) Volume, (2) Velocity, (3) Variety, (4) Veracity, and (5) Value.
Third	Waste Management	4 V's	(1) Volume, (2) Velocity, (3) Variety and (4) Veracity
Fourth	Telecommunication	3 V's	(1) Volume, (2) Variety, and (3) Veracity.

DATA ANALYTICS USE CASE FROM INDIAN BANKING

In India, the banking sector is expanding rapidly. The banking sector in India has the potential to grow to be the third largest banking sector in the world by 2025, according to a KPMG-CII report. Indian banks are using data analytics to entice new clients, keep them, discover opportunities for upselling , cross-selling and they cut their own losses to be ahead in the sector. (Mr. RAMPRAVESH, Dr. RASHI GUPTA 2017)

HDFC Bank Using Analytics to Get a Complete Picture of the Customer

The LiveMint study says, HDFC Bank Ltd, set up a Data center and started allocation of funds in technology in the 2000s to support it to make sense of the vast quantity of unorganized data that its information technology (IT) systems had gathered. This is one of the earliest instances of analytics being used. According to its analytics engines, HDFC Bank can keep track of every detail of a typical **customer's financial behavior**.

The bank can use the insights into the personal behaviors of its customers provided by the analytics technologies to customize the promotions . Analytics is also used to lessen the possibility of money laundering by spotting suspicious behavior, such as the sudden activity in inactive accounts or the movement of funds to various accounts or huge cash transactions in a day . The bank can monitor consumer credit histories using analytics and make loan decisions based on those histories. (Utkarsh Srivastavaa 2015)

ICICI Bank Decreasing Credit Losses using BI and Analytics

India was also affected by the US subprime mortgage crisis of 2007. Banks had to manage the difficulties of declining money supply and the upswing interest rates while making sure that their clients were satisfied. ICICI Bank has recognized debt collection as a critical stage where a considerate approach may increase client satisfaction. One of the most important steps in the debt collection process was **choosing the optimum customer-approach channel for each situation.**

The bank decided to use technology to achieve the objective of converting debt collection into a software for customer loyalty. The Business Intelligence system used by ICICI Bank was developed internally and uses different types of software, they are Posidex, SAS, TRIAD, Data Clean, and Blaze Advisor. Solution takes into consideration a number of aspects, including the efficacy of the data like customer profile, risk tolerance, and vulnerability. (Santosh Gopalkrishnanb 2015)

Axis Bank Analytics Of Risk Management and Customer behavior

Axis Bank has experienced a five times increase in the productivity of its sales team due to big data analysis. For instance, when their sales representatives visit a client to discuss a loan, they make an effort to learn more about the client's history and the possibility that he/she will accept a certain loan. Analytics are also used by Axis Bank to lower loan prepayments brought on by refinancing with other institutions and boost customer loyalty. SAS is used by Axis Bank to give client intelligence throughout the company. **By providing early warning signals,** The bank is also able to improve risk management across the board due to the SAS tool.

State Bank of India implementation of data analytics

Public sector banks are not far behind private sector banks. SBI's financial data center presently has more than 120 TB of data. In an effort to reduce the percentage of defaulted student borrowing, auto loans, housing loans, and SME loans, they are employing data analytics to develop their data models. For instance, income tax departments and credit ratings agencies in the case to find appropriate individuals and then to send them letters of reminder. To determine where and **how much money should be put at each ATM branch,** they use Big data analytics.

ING Vysya Bank as implemented business intelligence (BI)

Business intelligence (BI) became necessary for ING Vysya (now owned by Kotak Mahindra Bank) when the bank noticed that various end users frequently showed up to meetings with incomplete reports. They needed a solution that would enable users to produce reliable reports rapidly. They developed a common data repository with SAP BO, **which enabled users to receive accurate reports** and thereby increase productivity. (Managing Director 2012)

Benefits of Big Data in the Banking Industry (Aishwarya Banik, 2022)

1. Customer-specific banking solutions are provided

When used in addition to Efficient instruments and technology, big data may provide banks a deeper knowledge of Specific users depending on the inputs collected.

This covers their spending habits, reasons for investing, and past financial or personal transactions. For instance, they are able to forecast spending patterns. Big data is used by the banking industry for better comprehension of its customers. As a result, they create products, services, and other offers that fit the requirements of their current clients.

2. Segmentation of Customers

According to customer segmentation, banks are better able to target their clients with the most effective advertising campaigns. With the help of big data they can modify advertisements that are able to understand the customer.

Banks will get valuable insight into consumer behavior by merging big data, artificial intelligence, and machine learning. They may also use it to customize the consumer experience.

Moreover, financial institutions will be able to organize their clients based on multiple factors such as preferred credit card spending or even net worth, by being able to track each customer transaction.

3. Effective Customer Feedback Analysis

Financial institutions can utilize big data solutions to acquire insights into customer inquiries, feedback and issues. This data empowers them to respond promptly, fostering customer loyalty through perceived appreciation and rapid responsiveness.

Fraud Prevention and Detection Strategies Identifying fraudulent activities stands out as a primary challenge in today's banking sector. Leveraging big data within banking operations is instrumental in ensuring the prevention of unauthorized transactions, offering a robust defense against illegal activities.

Moreover, this approach serves as a fundamental pillar for enhancing the security and integrity of the banking industry. Through vigilant monitoring of customer spending patterns and the timely detection of any unusual activities, banks use the power of big data to not only battle fraud but also boost customer safety.

Impact of Big Data on Banking Institutions and major areas of work

In the financial industry, experts often describe big data as the tool that empowers an organization to generate, handle, and manipulate extensive datasets within a specified timeframe. It also encompasses the necessary storage capacity to manage these data volumes, which are known for their diversity, magnitude, and velocity.

In order to increase company openness, accountability and executive control of risk, financial institutions are utilizing big data in a number of key areas as they strengthen their enterprise risk management frameworks. (Utkarsh Srivastava, Santosh Gopalkrishnan, 2015)

● Customer Centric

In order to be more customer-focused, banks must reassess what they already know about their clients and develop a deeper understanding of who they are, what excites them, what they value, and what motivates them.

Client experience closed feedback loop	Customer life event analysis
Next best offer	Real time allocation based offerings
Sentiment analysis-enabled strategy management	Sentiment analysis-enabled lead/referral management
Quality of lead analytics	Micro-segmentation
Customer Gamification	Sentiment analysis-enabled sales forecasting

● Risk Management

The methods for using data analysis to discover and assess financial crime management (FCM) solution guidelines are as follows: early identification of the connection between financial Violation.

MIS/ Regulatory reporting	Disclosure reporting
Real time keyboard conversation tracking	Anti-money laundering

- **Transactions**

When transactions are monitored from time to time, a vast amount of Information about the nature of Transactions, log analytics, trading views, and other factors usually becomes clear. The following are some ways that banks and other financial organizations use big data under this heading:

IVR analysis	B2B merchant insights
Real time capital calculations	Log analytics

India's Advantage in the Big Data Opportunity

India's domestic demand for big data analytics is still in its early stages because the majority of Indian businesses still view big data as a fading trend. The opportunity for Indian service providers comes from providing outsourcing services for big data technology implementation and analytics, which is experiencing strong growth.

Customer needs may be better understood by banking organizations with the use of a lot of client data, which will eventually enhance service levels, boost revenue, and Fulfill customer requirements. The development of the banking or financial services sector depends increasingly on big data. (David Floyer, 2013)

The Future of Big Data

The main big data technologies for practical applications are suggested based on the fundamental big data idea and the history of their development. The information-spectrum-based framework is suggested for the interaction between large data collecting and applications. The shortcomings of the existing technology and the main barriers to innovation are examined in terms of the big data model technique. Big data model groups are suggested in both horizontal and vertical dimensions. Two aspects may be used to describe the major technologies: (Xuewei Li , Xueyan Li , 2018)

1. **Scope of service aims:** Enforcing Data Collection Consistency and Service Standards
2. **Transformation in Data presentation :** To increase the application of the data analysis model, break the hard division of qualitative notions using quantitative methods.

CONCLUSION OF STUDY

Big Data is transforming how businesses are run and managed. The 3Vs, or volume, variety and velocity are frequently used to describe big data. There are many types of data sets that make up big data and are combined to create meaningful data. Other datasets, such corporate, public, and social information will be combined to give even more insights. Big data development makes it easier for financial organizations to expand their company operations and offer services to banking customers. The banking industry must carefully consider how to address the problems carried on by big data. large data has a large influence on a number of banking operations. The market for information mining technology in decision guidance is significant. It will be used for duties related to business management including Anti-fraud Measures, market research, borrower credit scoring, client information verification , financial database marketing strategies and retail banking customer segmentation. Since a majority of Indian businesses still see big data as a passing trend, the domestic demand for big data analytics is still in its initial stage in India.

References:

1. R. Kumar, N. Grover, R. Singh, S. Kathuria, A. Kumar and A. Bansal, 2019, "Imperative Role of Artificial Intelligence and Big Data in Finance and Banking Sector," International Conference on Sustainable Computing and Data Communication Systems (ICSCDS), pp. 523-527, doi: 10.1109/ICSCDS56580.2023.10105062. <https://www.semanticscholar.org/paper/Digital-Banking-Transformation%3A-Application-of-and-Indriasari-Gaol/74b1b9d71a97f87c8c6400a6cfb42f4fbccec07f>
2. Nafis Alam, The Impact of Big Data Analytics on Banking Sector, 2022, International journal of accounting research, Department of Accounting, Western Sydney University, Sydney, Australia. https://www.researchgate.net/publication/280446380_The_Impact_of_Big_Data_Analytics_on_the_Banking_Industry
3. Mrs. Flavia Gonsalves and Samiksha Jadhav, (2012) Big Data Application in Banking Sector, International Research Journal of Engineering and Technology (IRJET). <https://www.irjet.net/archives/V7/i6/IRJET-V7I61197.pdf>
4. Iraqi Journal of Industrial Research, June 2021, Big Data Characteristics (V's) in Industry, Nagham Saeed, Laden Husamaldin., Vol. 8, No. 1. <https://ijoir.gov.iq/ijoir/index.php/jou/article/view/52>
5. Mr. Rampravesh Gond, Research Scholar, JTT University, Rajasthan, 2017, AN Empirical Study Of Big Data Analytics In Indian Banking Sector Volume 2, Issue 4 (2017, April) (Issn-2455-6602) Online Anveshana's International Journal Of Research In Regional Studies, Law, Social Sciences, Journalism And Management Practices, Page 5. <http://publications.anveshanaindia.com/wp-content/uploads/2017/04/An-Empirical-Study-of-Big-Data-Analytics-in-Indian-Banking-Sector.pdf>
6. Utkarsh Srivastava, Santosh Gopalkrishnan, (2015) 2nd International Symposium on Big Data and Cloud Computing (ISBCC'15) Impact of Big Data Analytics on Banking Sector: Learning for Indian Banks, MBA-I (Finance), Symbiosis Institute of Business Management, Symbiosis International University, Lavale, Pune 412115, Indian Research Scholar, Dr. D.Y. Patil University Pune & Assistant Professor, SIBM, Symbiosis International University, Lavale, Pune 412115, India. <https://www.sciencedirect.com/science/article/pii/S1877050915005992>
7. Aishwarya Banik, 2022 Benefits of Big Data in the Banking Industry <https://www.analyticsinsight.net/10-reasons-why-big-data-is-the-future-of-india/>
8. Utkarsh Srivastava, Santosh Gopalkrishnan, Impact of Big Data Analytics on Banking Sector: Learning for Indian Banks, 2nd International Symposium on Big Data and Cloud Computing (ISBCC'15) <https://www.sciencedirect.com/science/article/pii/S1877050915005992>
9. David Floyer. Financial Comparison of Big Data MPP Solution and Data Warehouse Appliance; 2013. http://wikibon.org/wiki/v/Financial_Comparison_of_Big_Data_MPP_Solution_and_Data_Warehouse_Appliance#Big_Data_Approach
10. Akter, S., Michael, K., Uddin, M. R., McCarthy, G., & Rahman, M. (2020). Transforming business using digital innovations: the application of AI, blockchain, cloud and data analytics. Annals of Operations Research. <https://doi.org/10.1007/s10479-020-03620-w>

ENHANCING NETWORK SECURITY: AN INTRUSION DETECTION AND PREVENTION APPROACH

Oyewale Mustapha Akinola

Dept. of Computer Engineering, the Federal Polytechnic Ilaro, Ogun State, Nigeria.

Adaramola Ojo Jayeola

Dept. of Computer Engineering, the Federal Polytechnic Ilaro, Ogun State, Nigeria.

ABSTRACT

The field of cyber security is constantly evolving, and protecting networks from cyber-attacks is more crucial than ever. There is a need to demonstrate the effectiveness of IDPS in detecting and preventing intrusions on a network system. Therefore, this research focuses on the implementation of an Intrusion Detection and Prevention System (IDPS) that uses Snort and pfSense as a mechanism for network intrusion detection and prevention to create a cost-effective, efficient, and reliable IDPS. The pfSense was deployed on a virtual machine (VM) alongside a Windows 10 operating system. The configuration facilitated the configuration of firewall settings and Snort rule sets via the pfSense web GUI, offering a user-friendly interface. The IDPS's efficacy was tested by utilizing malicious websites to generate network traffic. However, the combined capabilities of snort and pfSense provide real-time intrusion detection, comprehensive threat prevention, and adaptable security policies, making them invaluable tools for enterprises of all scales. By leveraging the strengths of these two software, organizations can safeguard their networks and sensitive data from a wide spectrum of cyber threats.

Keywords: Cyber-attacks, IDPS, PfSense, Security, Snort.

A PROPOSED AES-CBC ALGORITHM TO IMPROVE IOT SYSTEMS SECURITY

Belgacem Bouallegue

*College of Computer Science, King Khalid University, Abha 61421, Saudi Arabia
Electronics and Micro-Electronics Laboratory (E. μ . E. L), Faculty of Sciences of Monastir, University of Monastir, Monastir
5000, Tunisia*

Mouna Bedoui

*Electronics and Micro-Electronics Laboratory (E. μ . E. L), Faculty of Sciences of Monastir, University of Monastir, Monastir
5000, Tunisia*

Hosam El-Sofany

*College of Computer Science, King Khalid University, Abha 61421, Saudi Arabia
Cairo Higher Institute for Engineering, Computer Science and Management, Cairo 4735320, Egypt*

Mohsen Macchout

*Electronics and Micro-Electronics Laboratory (E. μ . E. L), Faculty of Sciences of Monastir, University of Monastir, Monastir
5000, Tunisia
Cairo Higher Institute for Engineering, Computer Science and Management, Cairo 4735320, Egypt*

ABSTRACT

The security of Internet of Things (IoT) systems has become a paramount concern as their usage continues to proliferate. To address this issue, this paper presents a proposed solution to enhance IoT systems' security through the implementation of the AES-CBC (Advanced Encryption Standard in Cipher Block Chaining) algorithm. By adopting this algorithm, the proposed solution aims to improve the confidentiality and integrity of data transmitted and stored within IoT systems. The core concept of the proposed solution involves utilizing the AES-CBC algorithm to encrypt IoT data. The Cipher Block Chaining mode enhances security by introducing interdependence between blocks of data, making it more resistant to various types of attacks.

To evaluate the effectiveness of the proposed solution, comprehensive tests and simulations were conducted. The results demonstrate the enhanced security provided by the AES-CBC algorithm, particularly in terms of data privacy and protection against tampering. Furthermore, the proposed solution takes into account the scalability and compatibility requirements of IoT systems. The AES-CBC algorithm can be implemented across various IoT devices and communication protocols, making it a versatile solution for improving security in diverse IoT environments.

A SYSTEMATIC REVIEW ON VEHICULAR AD HOC NETWORK (VANET) SECURITY CHALLENGES AND SOLUTIONS

Idris Lawal Bagiwa

Department of Computer Studies, Hassan Usman Katsina Polytechnic P.M.B. 2052, Katsina State, Nigeria

ABSTRACT

The security of vehicular communication systems is critical to their implementation. In reality, security is critical in a vehicular ad hoc network (VANET). The purpose of this study is to give complete and unbiased information regarding many current model security conceptions, ideas, challenges, and solutions in VANET for safe transportation. A total of 184 publications relating to the security model in VANET published between 2018 and 2023 were collected from the most relevant scholarly sources for this purpose (using Google Scholar Academic Search Premier (via EBSCOHost, EdITLib Education & Information Technology Digital Library, ScienceDirect, Scientific.Net, ACM Digital Library, IEEE Xplore, Springer, World Scientific Journal, Wiley Online Library, JSTOR, Microsoft Academic, Cornell University Library, SAGE Publishing, Taylor, Francis Online Academic Journals and IEEE Computer Society). However, 54 papers were eventually evaluated for a variety of reasons, including relevance and the breadth of the topic given in the pieces. Using a systematic review technique, this study is able to highlight the key security risks, security difficulties, security requirements in VANET, and future research within this area.

Keywords: Challenges, Solutions, Security, Systematic Review, VANET

SYNTHESIS OF BINDER-FREE AND HIGHLY CONDUCTING MoS₂ NANOFLOWERS LIKE ELECTRODE MATERIAL FOR SUPERCAPACITOR APPLICATIONS

A. Raza

Plasma Processing of Electrode Materials Lab, Department of Physics, Government College University Faisalabad 38000, Faisalabad

I. A. Khan

Plasma Processing of Electrode Materials Lab, Department of Physics, Government College University Faisalabad 38000, Faisalabad

ABSTRACT

Binder-free Molybdenum disulfide (MoS₂) nanoflowers have been synthesized on nickel-foam (NiF) by simple chemical vapor deposition technique. The structural analysis confirmed low intense hexagonal nanostructure formation of MoS₂/NiF electrode materials (E-Ms). The synthesized MoS₂/NiF nanoflowers exhibited the maximum specific capacitance of 4200 F/g at a current density of 1 A/g. The energy density and power density for synthesized E-Ms are in the range of 53-145 Wh/kg and 250-3000 W/kg which enable them to be used as E-Ms for excellent electrochemical performance of supercapacitors. The excellent electrical conductivity, absence of charge transfer resistance, high porosity and binder-free synthesis persuaded the synthesized MoS₂/NiF nanoflowers to exhibit excellent cyclic stability of 98.76 % over 4000 continuous charging-discharging cycles. The simulations of Power's law and Dunn's model also confirmed that the overall excellent electrochemical performance of synthesized E-Ms is contributed by capacitive and diffusion-controlled processes.

Keywords: Binder free, Nanostructure, Nanoflowers, Cyclic stability, Specific capacitance, Conductivity

EVALUATION OF THE EFFECTIVENESS OF FAULT-TOLERANT OPERATION OF BROKEN BARS USING DIRECT TORQUE CONTROL IN AN INDUCTION MACHINE

Ibrahim Chouidira

Research Laboratory on the Electrical Engineering, Faculty of Technology, University of M'Sila, PO Box 166 Ichebilia, 28000 M'sila, Algeria.

Djala Eddine Khodja

Research Laboratory on the Electrical Engineering, Faculty of Technology, University of M'Sila, PO Box 166 Ichebilia, 28000 M'sila, Algeria.

ABSTRACT

The objective of this study is the fault-tolerant control to compensate for the effect of faults that affect the system and capable of maintaining a certain level of performance on stability in the presence of the faults. To achieve this, we use models: a multi-winding model to appear the broken bars to monitor the behavior of the device when it is exposed to faults. By direct torque control "DTC", this method consists of indirectly controlling the closing or opening of the switches of the two-level inverter from the pre-calculated values of the stator flux. The results appear the importance of this technique and ensure performance continuous the machine by providing fault tolerance.

Keywords: Passive fault-tolerant, broken bars, direct torque control 'DTC'.

HYSTERESIS CONTROL FOR COMPENSATION OF CURRENT HARMONICS BY USING ACTIVE PARALLEL FILTER

Ibrahim Choudira

*Research Laboratory on the Electrical Engineering, Faculty of Technology, University of M'Sila, PO Box 166 Ichebilia, 28000
M'sila, Algeria.*

Djala Eddine Khodja

*Research Laboratory on the Electrical Engineering, Faculty of Technology, University of M'Sila, PO Box 166 Ichebilia, 28000
M'sila, Algeria.*

ABSTRACT

The main goal of the proposed study of the active parallel filter to improve the quality of electrical energy. Based on network currents and voltages measurements respectively. Through the method of identifying harmonic currents such as the instantaneous power method for extracting the disturbing current, on the other hand, the filter consists of the study of a two-level voltage inverter controlled by a regulator at hysteresis a detailed comparison is made with criteria the before and after filtering to determine stability the systems. The simulation results obtained showed good performance for the proposed control.

Keywords: *Active parallel filter, current, harmonic, hysteresis.*

ELECTRONIC DISASTERS: THE HIDDEN DANGERS AND TOXICITY OF EMF'S POLLUTION PRODUCED IN THE 21 ST CENTURY AND THEIR NEGATIVE EFFECTS ON THE ENVIRONMENT AND HUMAN HEALTH

Mamoun Lyes HENNACHE

Department of Electronics and Communication Engineering, College of Engineering, Ankara Yildirim Beyazıt University (AYBU), Turkey. (Responsible Author)

Ali HENNACHE

Imam Mohammad Ibn Saud Islamic University (IMSIU), College of Engineering, Department of Electrical Engineering, Riyadh, Kingdom of Saudi Arabia

ABSTRACT

Electromagnetic fields are ubiquitous in modern society. They occur in connection with use of electric power, electronic equipment like, computers, TVs, radios, microwaves, light dimmers, digital clocks and cell phone chargers, electronic surveillance systems and various types of wireless communications. While these fields differ with respect to strengths and physical characteristics, they all give rise to concern among those exposed about the possibility of health risks. It is well established that strong fields can give rise to acute health effects, such as burns. Current concerns are instead directed towards the possibility that long-term exposure to weak fields might have detrimental health effects.

Nowadays there is a lot of concern for our environment in terms of clean air and water, growing organic foods, heavy metals and industrial organic chemicals out of our systems. But now there is a new pollutant to worry about – it is not something you can see, smell, taste, or touch. It is not something you can sense, making it difficult for one to be aware of the presence of electromagnetic radiation. It is found in our homes, schools, even our hospitals. The culprit is dirty electricity (electrical pollution) and that what is more, a less-well known kind of EMF, known as "dirty" or transient electricity, may play an even more damaging role. Transients are largely by-products of modern energy-efficient electronics and appliances—from computers, refrigerators, and plasma TVs to compact fluorescent light bulbs and dimmer switches—which tamp down the electricity they use. This manipulation of current creates a wildly fluctuating and potentially dangerous electromagnetic field that essentially charges up the electrons in every cell of the body. The dirt follows the electrical lines around houses and out of houses following the wires that supply electricity to houses. The neighbor's dirt and the office's dirt, and the factory's dirt follow the same paths and ends up in every house, office and factory. With this in mind, it is important in this paper to understand what causes electrical pollution and what to look for in your everyday environment and home, how it is controlled and measured, the health effects, and protection against electrical pollution from harmful radiations.

Keywords: Dirty electricity, Power quality, Pollution, Electromagnetic radiations and Human health.

Introduction

A disaster and a crisis are two different and related events. The two terms are sometimes used interchangeably. Crisis can happen to any organization. It has been noted that there were no universally accepted definitions yet developed for disaster and crisis. There is also no universally available criteria, to define the disaster in terms of the consequences, such as the casualties and the cost of damage. Traditionally disasters are divided into "natural" phenomena such as meltdowns, hurricanes, floods, tsunamis, tornadoes, oil spills or earthquakes such disasters can contribute to the transmission of some diseases, especially since water supplies and sewage systems may be disrupted, and hygiene may be compromised by population displacement and overcrowding, and normal public health services may be interrupted and "man-made" disaster that occurs at an industrial organization may develop into an industrial crisis. Pollution in all its various types (soil pollution, water pollution, thermal pollution, air pollution, radioactive pollution, light pollution and noise pollution) is categorized based on the part of the environment which they affect or result

which the particular pollution causes. Each of these types has its own distinctive causes and consequences but all of them cause immense damage and thus a categorized study of pollution helps to understand the basics in more detail and produce protocols for the specific types.

Materials and Methods

Environment represents the totality of physical, chemical, biological, behavioral and socio-economic factors. The electromagnetic radiation pervading the environment is now increasingly realized and this has added to the list of another pollutant in the environment i.e. electro-pollution.

This paper reviews the man-made disasters caused by this marvelous but dangerous technology known as the electronic disasters which are the most pervasive environmental exposure in industrialized countries today called the Electro Magnetic Radiation (EMR) or Electro Magnetic Fields (EMFs) exposures created by the vast array of electronic equipments and wireless technologies and offer a thorough presentation of the current information on EMF health effects, safety standards, and protection solutions.

Electricity plays a vital role in modern society, as it is used to light homes, operate household devices such as air conditioners, radios and TVs., washers, dryers, computers, it is also found in industry and the workplace and administrations using photocopiers, fax machines, scanner etc... The increasing demand of electric power for industrial, workplace and home use has led to the extensive developments of the generation, transmission and distribution of electricity. As a result, high-voltage transmission lines (1 Bonneville Power Administration, 1993, 2002) and prominent distribution lines have become common outdoor features and due to the intensive use of electronic device and the advanced use of Information and communication technologies, the current age is somehow called the electronic age because of the inventions of transistors and diode electronic industry boomed to gigantic proportions. Everyday newer and newer items are sent to market. If we purchase one new gadget today, it will be outdated within six months. The end result is electronic waste generation. There is contamination of earth, air, water due to the waste generation. Plastic was considered harmful. This is known as the electronic waste, and is supposed to be one of the most dangerous pollution and contamination of the environment, although the electronic waste is one of the most important type of the electronic disasters, it is unfortunately beyond the scope of this paper and this latter is just concentrating on what is called "dirty electricity" electrical pollution or power quality (2 Graham, M. 2002) where its major causes and effects are radiations and health.

Safety Standards

In Saudi Arabia, alternating current (AC) electricity operates at a power frequency of 60 hertz (Hz), which is in the extremely low frequency (ELF) range. The term "extremely low" is used to describe any frequency below 300 Hz. The use of AC electricity results in the production of electric and magnetic fields (EMFs), which oscillate at 60 Hz. These fields are emitted by transmission and distribution lines (Health effects from exposure, 2009), power transformers, service wires, electrical panels, indoor wires and household electrical and electronic appliances.

EMF means electromagnetic field. It is a physical energetic field that radiates from all things in nature and from man- made electronic systems. Electromagnetic radiation is made up of electric and magnetic fields that move at right angles to each other at the speed of light.

- 1- An electric field which is dependent on the voltage and is always present when the power is switched on .This means that an electric field is always present in power lines, home wiring, and any appliance which is plugged in (but not in use) , it is therefore produced whenever two objects are at a different potential (voltage). Physical objects such as vegetation, buildings, fences and towers can reduce electric field to a lower level. The strength of the electric field is described in terms of volts per meter (V/m) or kilovolts per meter (kV/m). [For 1 kV/m means that there is a difference of 1 kV (1000 V) between two points, 1 meter (m) apart]. Electric fields are blocked by most building materials.
- 2- A magnetic field which is generated by electric current flowing in the line when appliances, machinery and the like are in use. This means that, a magnetic field only occurs when electric power is in use in

power lines, home wiring, appliances, and machines and therefore can vary considerably depending on demand (load current) and is usually measured in amperes per meter (A/m) or in Tesla (T) or Gauss (G). [1 A/m corresponds to 1.257 T or 12.57 milligauss (mG)]. Magnetic fields can pass through most objects and are reduced mainly by increasing distance from the source. As such, EMF shielding works well for power-frequency electric fields but not usually for power-frequency magnetic fields.

Both electric and magnetic fields are strongest when close to their source. As we move away from the source, the strength of the fields falls rapidly. Exposure limits for electrical power frequencies should thus include both electric and magnetic fields.

Radiation Pollution

Radiation pollution is any form of ionizing or non-ionizing radiation that results from human activities. The most well-known radiation results from the detonation of nuclear devices and the controlled release of energy by nuclear-power generating plants. Other sources of radiation include increased exposure to medical X rays and to radiation emissions from microwave ovens and other household appliances, although of considerably less magnitude, all constitute sources of environmental radiation.

Electromagnetic Radiation

Electromagnetic radiation (radio waves, light, etc.) is a form of energy and consists of interacting, self-sustaining electric and magnetic fields that propagate in straight lines through empty space at 299,792 km per second (the speed of light, c), it slows as it passes through a medium such as air, water, glass, and other media. Electromagnetic energy decreases as if it were dispersed over the area on an expanding sphere, expressed as $4\pi R^2$ where radius R is the distance the energy has travelled. The amount of energy received at a point on that sphere diminishes as $1/R^2$. This relationship is known as the inverse-square law of (electromagnetic) propagation. It accounts for loss of signal strength over space, called space loss.

From an electrical point of view, the electromagnetic spectrum (Figure 1) can be divided into three main bands or fields:

- Extremely Low Frequency (**ELF**) fields usually concern all frequencies up to 300 Hz.
- Intermediate Frequency (**IF**) fields concern all frequencies from 300 Hz to 10 MHz and
- Radiofrequency (**RF**) fields concern frequencies between 10 MHz and 300 GHz.

The effects of electromagnetic fields on the human body depend not only on the concerned field intensity but on its frequency and energy as well.

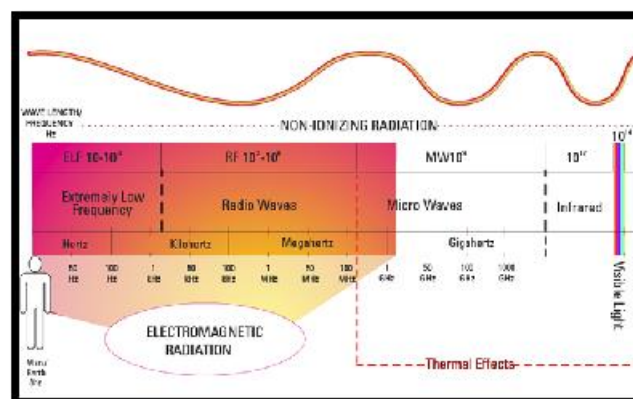


Figure 1. Electromagnetic Spectrum

Source: <http://www.safespaceprotection.com/harmful-effects-electromagnetic-fields.aspx>

Electrical Pollution “ Dirty Electricity ”

Electricity has been a lifesaver for modern civilization and we would be lost without it; but, research has brought to light the existence of different kinds of electricity, namely clean and dirty (Havas, M., 2004).

Clean electricity is safe electricity. Clean electricity has a smooth sine wave that goes up and down 50 or 60 times a second depending on the frequency of the country's electrical supply.

1- Dirty electricity (electrical pollution) is a term used to describe a type of electrical phenomenon occurring worldwide and is electromagnetic pollution called transients and harmonics - operating in the 4 to 100 kilohertz frequency range - which contaminate the electrical supply.

Dirty electricity, also known as Poor power quality is a ubiquitous pollutant. It has been a concern for the electric utility for decades. Dirty electricity is ubiquitous. It is generated by electronic equipment such as computers, plasma televisions, energy efficient appliances, dimmer switches, etc... Dirty electricity refers to electromagnetic energy that flows along a conductor and radiates from them and involves both extremely low frequency electromagnetic fields and radio frequency radiation and deviates from a pure 60-Hz sine wave (Figure 2). It has both harmonic and non harmonic (transient) components and emerged as a problem in the late 1970s with the increasing use of electronic devices that produce nonlinear loads. Until recently, dirty electricity has been largely ignored by the scientific community. Recent inventions of metering and filter equipment provide scientists with the tools to measure and reduce dirty electricity on electrical wires.

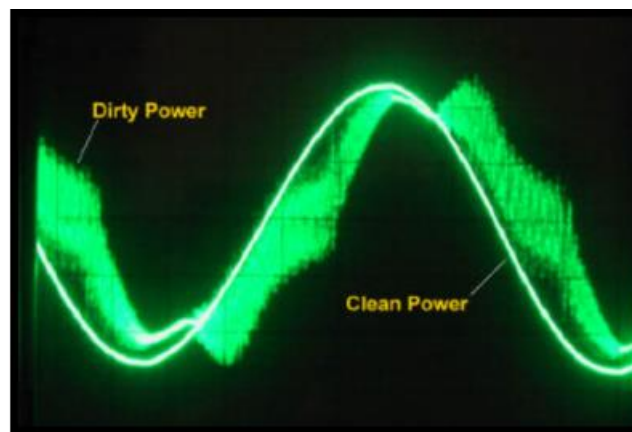


Figure 2. Dirty and Clean Power

The Adverse Health Effects Of Emfs From Modern Technology

Today we face a threat to our health that did not exist just over 100 years ago. Our modern technology has created a new form of pollution which we can't see, taste, or smell and its invisible nature has most unaware of its ever-increasing presence in both our personal and public environments. With the now conclusive evidence of negative health effects from unnatural EMFs, it has become paramount that we learn not only what type and how much of this harmful radiation we are being exposed to, but also the best and most effective measures to protect ourselves.

7. SOURCES OF DIRTY ELECTRICITY

Electricity is the most common source of power throughout the world because it is easily generated and transmitted to where it is needed. As electricity moves through wires and machines, it produces EMF (Kazakhstan Health Department, 2003). The power grids of nations consist of electrical generation, transmission and distribution facilities. As electricity is sent along the wires of the power grid, EMF is created (Henshaw D.L. 2002).

Once electricity is delivered to the user, it continues to produce EMF throughout the wiring systems of offices, homes, schools, factories and other structures. The appliances and electrical equipment connected to these wiring systems produce their own EMF as well.

- **Electrical Equipment and Wiring**

Electrical and electronic appliances, external electrical power lines (Draper G., 2005), IT equipment such as computers, printers, fax machines, copiers, etc..., home wiring.

- **Metallic Objects** These objects do not emit EMFs on their own, but rather act as antennae which will collect and then radiate unnatural energies. Electrical Circuits, Watches, Jewelry Telephone Lines Keys,

- **Microwave / Radiofrequency Technology**

This includes all Wireless and Digital Technology such as digital TV broadcasts, cell phones, digital cordless phone, Radar, home alarm systems, Wi-Fi, electric water, refrigerators, heaters, electric shaver, vacuum cleaners, coffee makers, and microwave ovens.

- **Transportation methods** such as automobiles, trucks, airplanes, electrical and magnetic trains and subway systems are significant sources of EMF.

This invisible radiation, as shown by the above list, is everywhere – home, office, school, coffee-shop, hospital, highways – even the countryside is littered with cell towers. It is easy to understand how we are being exposed to such Huge amount of radiation. This source of contamination can also be brought into buildings and homes through their electrical wiring, ground and plumbing currents. Two experts in this field of study found correlations between communities using little or no electricity and those using dirty electricity. The communities exposed to dirty electricity had a much higher incidence of many chronic diseases and other

health affections.

Health Effects Of Man-Made Electromagnetic Frequencies

Today we face a threat to our health that did not exist just over 100 years ago. Our modern technology has created a new form of pollution which we can't see, taste, or smell and its invisible nature has most unaware of its ever-increasing presence in both our personal and public environments. With the now conclusive evidence of negative health effects from unnatural EMFs, it has become paramount that we learn not only what type and how much of this harmful radiation we are being exposed to, but also the best and most effective measures to protect ourselves.

Electromagnetic radiation is always and everywhere around us. The potential effects of electromagnetic fields on human health vary widely depending on the frequency and intensity of the fields (Ahlbom A., 2001). Some EMFs are very strong and toxic like X-rays and UV light, and others are weak and trivial at usual exposures. Communities might be facing a public health disaster from mobile phones electrical power lines if no prevention and protection techniques are taken.

Research in western countries have found a positive correlation between exposure to ELF magnetic fields and childhood leukemia (Greenland S., 2000). It has been shown that exposure to magnetic fields greater than 3 – 4 mG double childhood leukemia rates.

Protection Solutions From Emfs

Grounding / Earthing

This is one of the most profoundly simple and effective measures to help the body deal with unnatural EMFs. All life on Earth (Chevalier G. 2007), including human beings, have developed and evolved with the natural direct current and electromagnetic field of the planet. This current produces an abundant supply of free electrons on the surface of the Earth. The land masses and oceans of our planet are therefore providing an abundant supply of electrons to the human body when it is directly connected to the Earth. It is this direct connection with the Earth which is the key to the utter simplicity of the benefits of Grounding / Earthing in

protecting us from the harmful effects of EMFs. Also of great importance is the fact that the electromagnetic field of the Earth provides the reference point for the biological cycles of the human body. This means that the Earth's EMF directly regulates the healthy functioning of our biological rhythms. These functions include sleep cycles (Wilbur V. 2006), hormone production, digestive processes, and nervous system function, immune response, and stress responses. Research has shown that being connected directly to the Earth (i.e. grounded) reduces the stress and inflammation hormone (Ghaly M. , 2004), improves sleep and increases the anti-cancer hormone melatonin (Ober A.C. (n.d., 2009) and improved autonomic balance of musculature and the left hemisphere of the brain (Chevalier G., 2009).

When the body is insulated from the Earth. The body then absorbs this radiation, but cannot get rid of it. This radiation gets converted to electric currents which cause vibration at the cellular level (Goldsworthy, A., 2009). This then causes damage to the cell by displacing ions and destabilizing the membrane. Ultimately, this leads to membrane leakage and can produce the negative biological effects discussed earlier (Goldsworthy, A., 2009). However, if the body is in direct contact with the Earth, then the Earth becomes the 'sink' for the electromagnetic radiation. This means that the body functions as a conductor and allows the radiation to pass through it before any current can be generated on a cellular level and cause damage (Goldsworthy, A., 2009).

Radiation Protection Basics

Although some radiation exposure is natural in our environment, it is desirable to keep radiation exposure as low as reasonably (National Council on Radiation Protection, 1995) achievable in an occupational setting. This is accomplished by the techniques of time, distance, and shielding.

Time: The amount of radiation exposure increases and decreases with the time people spend near the source of radiation.

Distance: The farther a person is from a source of radiation, the lower the radiation dose. Levels decrease by a factor of the square of the distance. Distance is a prime concern when dealing with gamma rays, because they can travel long distances. Alpha and beta particles don't have enough energy to travel very far. As a rule, if the distance is doubled, the exposure is reduced by a factor of four. Halving the distance, increases the exposure by a factor of four.

Shielding: Placing a radioactive source behind a massive object provides a barrier that can reduce radiation exposure.

Administrative and Engineering Controls: The use of administrative and engineering controls is essential for keeping radiation exposure **As Low As Reasonably Achievable (ALARA)**.

Shielding: The greater the shielding around a radiation source, the smaller the exposure. Shielding simply means having something that will absorb radiation between you and the source of the radiation (but using another person to absorb the radiation doesn't count as shielding). The amount of shielding required to protect against different kinds of radiation depends on how much energy they have.

Simulation And Results

Electromagnetic Fields in Human Body

Exposures to a dirty power raise the question of the effects of electromagnetic field on human health. Although there are some restrictions and some limitations to the authorized radiated fields by the power systems. Electromagnetic fields play a positive role as well. On one hand, electromagnetic fields can be considered as harmful to health and on the other hand, the latter are used for medical diagnosis (medical Scanning MRI) or for medical treatment.

The electrical properties of any material, including biological tissue (Blank, M., 2004), can be broadly separated into two categories: conducting and insulating. In a conductor, the electric charges move freely in response to the application of an electric field, whereas in an insulator (dielectric), the charges are fixed and not free to move. A more detailed discussion of the fundamental processes underlying the electrical properties

of tissue can be found in Foster and (Foster K. R. 1989). Since biological tissues mainly consist of water, they behave neither as a conductor nor a dielectric, but as a dielectric with losses. Some simulation results from the calculation of the dielectric properties of human body tissues in the frequency range from 10 Hz to 100 GHz using the parametric model and the parameter values developed by

C.Gabriel et al (<http://niremf.ifac.cnr.it/tissprop/>) are presented for different tissues (Blood, Hear, Stomach, Kidney, fat etc...) and are presented in Figure 3 shows conductivity versus frequency for 4 type of tissues (skin dry, skin wet, tooth and fat) in the frequency range 10 Hz - 100 GHz and it is clear and obvious that skin wet has the highest conductivity.

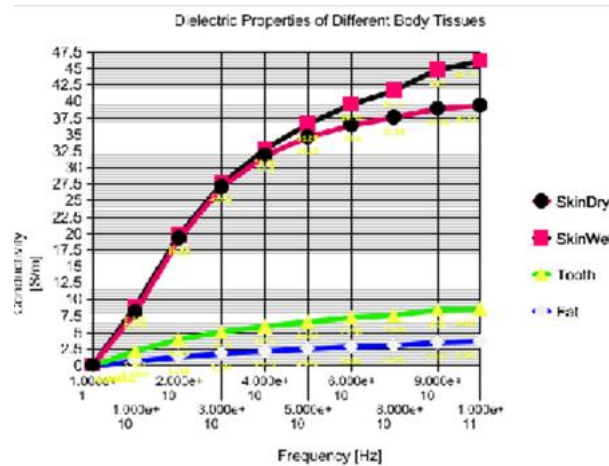


Figure 3. Conductivity versus frequency for different tissues

Conductivity results for tissues of the main part of the body are shown in figure 4 the conductivity is higher in blood and heart while the lowest in the brain white matter.

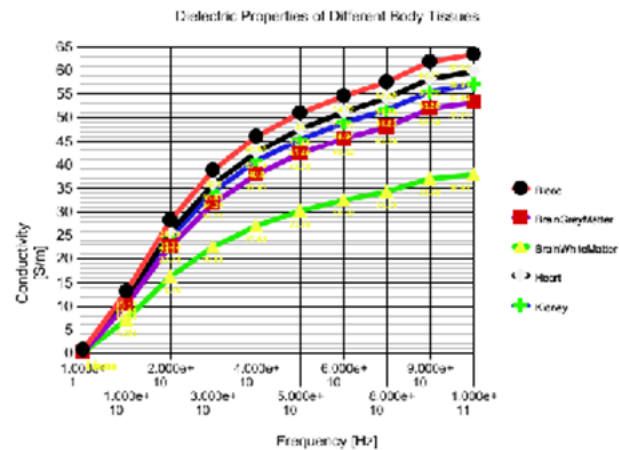


Figure 4. Conductivity versus Frequency for the most important organs in the bod

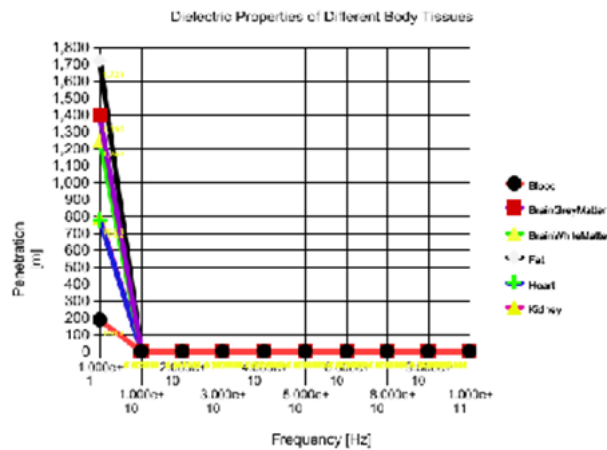


Figure 5. Penetration versus Frequency for different tissues

Electromagnetic radiation produces by mobile

As the number of mobile phone usage increased exponentially nowadays, issues related to the Electromagnetic radiation produce by mobile phone is becoming a big concern in the society. Radio frequency used to communicate by mobile phone is known as Mobile communication and this latter has the ability to penetrate through semi-solid substances like meat, and living tissue to a distance proportional to its power density and is where signal is transferred via electromagnetic wave through radio frequency and microwave signals. This signal produces electromagnetic radiation in the form of thermal radiation that consists of harmful ionizing radiation and harmless non-ionizing radiation. People using cell phones are prone to high blood pressure and other symptoms such as hot ears, burning skin, headaches and fatigue. There have been various studies into the connection between mobile phones and memory loss. Because of their smaller heads, thinner skulls and higher tissue conductivity, children may absorb more energy from a given phone than adults.

When using mobile phone, electromagnetic wave is transferred to the body which causes health problems especially at the place near ear skull region where they are known to affect the neurones. It also can cause dielectric heating effect or thermal effect. Thermal effects are the temperature rise in the body cause of energy absorption from oscillating electric fields or electromagnetic radiation. Thermal radiation is generated when heat from the movement of charged particles within atoms of the mobile phone's (Goldsworthy, A., 2009). Electromagnetic Radiation towards Adult Human, 2010) case is converted to electromagnetic radiation (Hardell L, 1999, Hardell L, 2002). Due to the danger caused by the absorption of energy from a mobile phone and its effect on human brain, many research have been done and still going on by tens of experts around the world and most of them lead to the conclusion that non-thermal radiation affects the human brain and Figure 6 given by (Electromagnetic Radiation towards Adult Human, 2010) shows the result collected Head before and after the used of Mobile Phone and it is clear that the results are confirming what was already explained.

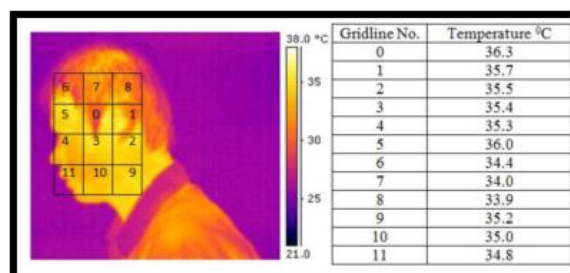


Figure 6. Heat Distribution on Head before the used of Mobile Phone

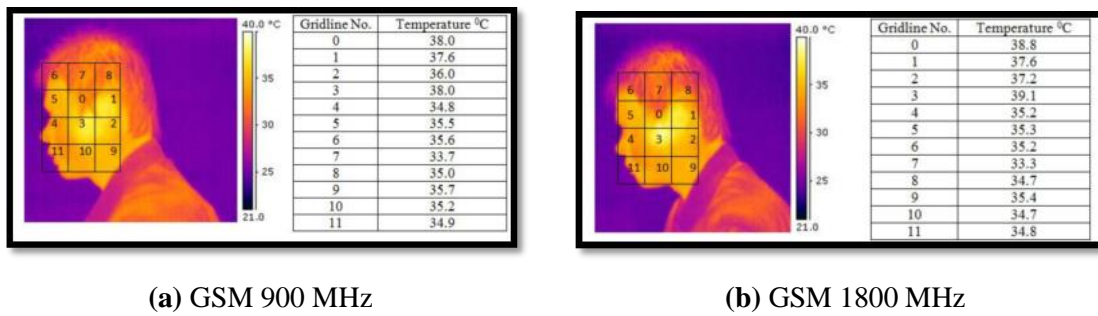


Figure 7. Heat Distribution using Mobile Phone (External Antenna) after 45 minutes talking time

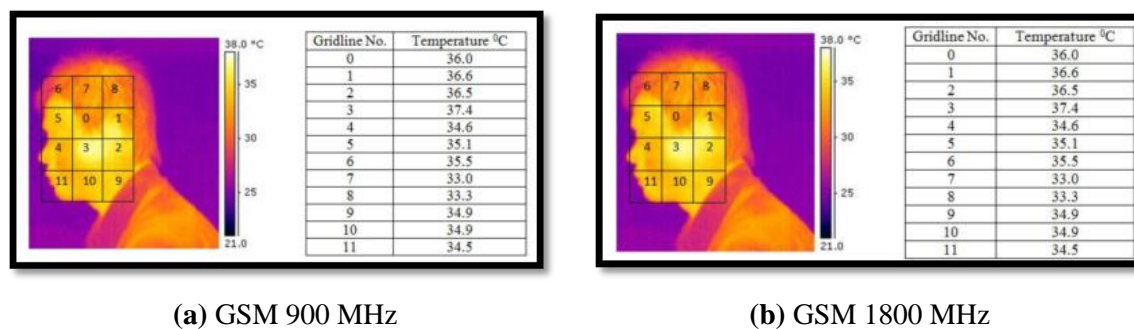


Figure 8. Heat Distribution using Mobile Phone (Built-in Antenna) after 45 minutes talking time

It can be seen from the above figures as the time becomes longer, due to blood circulation of our body, the level of temperature decreased slowly. From the result, this shows that, our body has the limitation of absorbing heat transfer due to electromagnetic radiation which will take several times to low down the heat level.

Conclusions

In our push to develop and then exploit our technological advances, very little attention is given to how these new and ever-increasing devices interact and influence our human biology and the biology of all living things. As a society we have become dependent upon, even addicted to our technology. But as the mounting evidence shows we are paying a very steep price for all the advantages and conveniences of our modern lifestyle. While it is obviously unrealistic and far too simplistic to suggest going backwards, we can however find a more healthful way forward. In order to do this we need to see our technology with new eyes and its ability to serve mankind not only for its commercial benefits, but for the protection of all life on the planet.

Dirty electricity is biologically active. Once dirty electricity is reduced, people's health improves. Providing scientists with the tools needed for research and according to dramatic results outcome of the research done in western countries, further investigation to determine the mechanisms involved and the percentage of the population affected in Saudi Arabia is indeed needed and the connection between electromagnetic pollution and these disorders needs to be investigated and the percentage of people sensitive to this form of energy (Dirty Electricity) needs to be determined.

References

- Ahlbom A., cardis E., Green A., Linet M., Savitz D., & Swerdlow A. (2001). Review of the epidemiologic literature on emf and health. *Environmental Health Perspectives (EHP)*. *Environ Health Perspect.* 109(Suppl 6): 911-933.
- Blank, M., Goodman, R. (2004). Comment: a biological guide for electromagnetic safety: the stress response. *Bioelectromagnetics* 25(8):642–646.
- Bonneville Power Administration. *Electrical and Biological Effects of Transmission Lines: A Review*. The U.S. Department of Energy, Portland, Oregon, USA, 1993. National Institute of Environmental Health Sciences (NIEHS). *Questions and Answers about EMF*. NIEHS, Research Triangle Park, North Carolina, USA, 2002 (available at the NIEHS website: www.niehs.nih.gov/emfrapid/home.htm).
- Chevalier G. (2007). *The earth's electrical surface potential: A summary of present understanding*. California Institute for Human Science, Encinitas, CA. January 2007.
- Chevalier G., Mori K., and Oschman J.L. (n.d.). *The effect of earthing on human physiology*. California Institute for Human Science, Retrieved December 7, 2009 from http://www.sleepingearthed.com/pdf/EFX_science_Physiology.pdf.
- Draper G., Vincent T., Kroll M.E., & Swanson J. (2005). Childhood cancer in relation to distance from high voltage power lines in England and Wales: A case-control study. *BMJ.* 330(7503): 1290.
- Electromagnetic Radiation towards Adult Human Head from Handheld Mobile Phones D.A.A. Mat1, W.T. Kho2, A. Joseph3, K. Kipli4, K. Lias5, A.S.W. Marzuki6 and S. Sahrani7 ISSN 1832-6758 Electronic Version., Vol. 1 / Issue 2 / November 2010 ,2010 INTI University College.
- K. R. Foster and H. P. Schwan, Dielectric properties of tissues and biological materials: a critical review. *Crit. Rev. Biomed. Eng.* 1989; 17:25–104
- Ghaly M. and Teplitz D. (2004). The biologic effects of grounding the human body during sleep as measured by cortisol levels and subjective reporting of sleep, pain, and stress. *The Journal of Alternative and Complementary Medicine.* 10(5): 767-776.
- Graham, M. (2002). Mitigation of electrical pollution in the home. *Memorandum No. UCB/ERL M02/18*. 19 April 2002, Electronics Research Laboratory, College of Engineering, University of California, Berkeley.
- Greenland S., Sheppard A.R., Kaune W.T., Poole C., & Kelsh M.A. (2000). A pooled analysis of magnetic fields, wire codes, and childhood leukemia. *Childhood leukemia-EMF study group. Epidemiology.* 11(6): 624-634.
- Goldsworthy, A. (July 2009). Some facts about cell phone radiation. Retrieved August 4, 2009 from <http://www.mastsanity.org>.
- Hardell L, Nasman A, Pahlson A, Hallquist A, Hansson Mild K. (1999). Use of cellular telephones and the risk for brain tumours: A case-control study. *Int J Oncol* 1999, 15, 113-116.
- Hardell L, Hallquist A, Mild KH, Carlberg M, Pahlson A, Lilja A. (2002). Cellular and cordless telephones and the risk for brain tumours. *Eur J Cancer Prev* 2002, 11, 377-386.
- Havas, M., Stetzer, D. (2004). *Dirty electricity and electrical hypersensitivity: five case studies*. World Health Organization Workshop on Electrical Hypersensitivity 25–26 October 2004, Prague, Czech Republic.
- Henshaw D.L. (2002). Does our electricity distribution system pose a serious risk to public health? *Med Hypotheses.* 59(1): 39-51.
- <http://niremf.ifac.cnr.it/tissprop/>
- Kazakhstan Health Department. (2003). Permissible levels of high-frequency electromagnetic pollutions voltage in wires of industrial frequency alternating current. Confirmed: The Order of the Head State Sanitary Physician of the Republic of Kazakhstan. November 28, 2003, No. 69.

National Council on Radiation Protection and Measurements. (June 13, 1995). NCRP draft recommendations on emf exposure guidelines (section 8). Retrieved December 5, 2009 from www.microwavenews.com/ncrp1.html

National Institute of Environmental Health Services, National Institute of Health. (May 1999). Health effects from exposure to power-line frequency electric and magnetic fields. Retrieved December 5, 2009 from www.niehs.nih.gov/health/docs/niehs-report.pdf.

Ober A.C. (n.d.). Grounding the human body to neutralize bio-electrical stress from static electricity and emfs. ESD Journal. Retrieved December 7, 2009 from <http://www.esdjournal.com/articles/cober/ground.htm>.

Wilbur V. (2006). Insomnia and sleep disorders. In V.P. Arcangelo and A.M. Peterson (Eds.), *Pharmacotherapeutics for advanced practice* (pp. 639-654). Philadelphia: Lippincott Williams and Wilkins.

SUPERCONDUCTING MATERIALS AND THEIR IMPACT ON THE DEVELOPMENT OF ELECTRONIC DEVICES

Mamoun Lyes HENNACHE

Department of Electronics and Communication Engineering, College of Engineering, Ankara Yildirim Beyazit University (AYBU), Turkey.

Ali HENNACHE

Imam Mohammad Ibn Saud Islamic University (IMSIU), College of Engineering, Department of Electrical Engineering, Riyadh, Kingdom of Saudi Arabia,

ABSTRACT

Superconducting is a fascinating phenomenon of exactly zero electrical resistance and expulsion of magnetic fields occurring in certain materials when cooled below a characteristic critical temperature that allows us to observe quantum mechanical effects at the macroscopic scale. The importance of superconductivity for fundamental science can be seen from the fact that there are at least 12 Nobel Laureates in physics, who obtained the price of research related to superconductivity. Besides being of great interest in themselves, superconductors have been vehicles for the development key concepts and methods in modern theoretical physics and find more and more practical applications in our society. Those range from high-power applications, strong superconducting magnets used in medicine, diagnostics, and particle accelerators; to the most sensitive quantum devices capable of measuring 10^{-11} of the earth's magnetic field and a millionth part of the electron charge.

The aims and objectives of this paper are to help new researchers learn to understand and demonstrate the basic features of the most important, fascinating, and challenging field of physics "Superconductivity", and to introduce them to the unusual properties that are exhibited by superconducting materials that can have an impact on the development of electronic devices and their applications to many diverse areas such as medicine, transport, computers, production and transport of electric energy, information, and communication technologies, as well as many other areas. Some envisioned applications are discussed in this paper.

Keywords: Superconductors, zero electrical resistance, Meissner effect, resistivity, levitating action, critical temperature.

Introduction

As most people know (or don't know, whichever is the case) the component of an electrical circuit that causes energy loss is called "resistance," which can be defined as a materials opposition to current being passed through it. Usually, this resistance results in the production of heat, sound, or another form of energy. In many cases, this transformation of energy is useful in such applications as toasters, heaters, and light bulbs. Even though it is a useful property, resistance often gets in the way of performance in such cases as high voltage transmission wires, electric motor output, and other cases where internal system energy losses are unwanted. This is where the phenomenon of superconducting (Introduction: Superconductivity Basics) materials comes into play and may present the solution to this energy loss problem.

Definition of Superconductivity

Superconductivity is an absolutely remarkable phenomenon (The Physics of Superconductivity) discovered in 1911 by a student working with the famous Dutch scientist, Kamerlingh-Onnes. Kamerlingh-Onnes pioneered work at very low temperatures — temperatures just a few degrees above the absolute zero of temperature. He succeeded in reaching temperatures much colder than anyone before him and thus opened a new frontier for science — a field of science previously unexplored, the field of low temperature physics.

Kamerlingh-Onnes and his students set to work to study what happened to various properties of materials when they were that cold. One of his students was studying the electrical resistance of wires. He found that as he cooled mercury wire the electrical resistance of the wire took a precipitous drop when he got to about 3.6 degrees above absolute zero. The drop was enormous - the resistance became at least twenty thousand times smaller. The drop took place over a temperature interval too small for them to measure. As far as they could tell, the electrical resistance completely vanished.

To test for the complete vanishing of the electrical resistance, Kamerlingh-Onnes devised an ingenious experiment. He took a closed circle of mercury wire and caused a current to flow around the circle. With his experimental arrangement one would expect ordinarily that resistance would cause the current to die out quickly, much as friction and air resistance cause a bicycle coasting on a level road to come to a stop. He found that for a loop of mercury wire the current, once started, would persist for as long as the wire was kept cold (Fig.1) . The persistence of the electrical current in the circuit is a kind of perpetual motion — it's a totally startling phenomenon for physicists.



Figure 1. A loop of mercury wire

Superconductors are thus, materials that display zero resistance under certain conditions (The Physics of Superconductivity). These conditions are called the "critical temperature" and "critical field," denoted T_c and H_c respectively. The T_c is the highest temperature state the material can attain and remain superconductive. The H_c is the highest magnetic field the material can be exposed to before reverting to its normal magnetic state. Within the substances currently known to superconduct, there is a divide between what has come to be called type I and type II superconductors. Type I are composed of pure substances, usually metals, and type II are composite compounds, usually some sort of ceramic.

For some materials, the resistivity vanishes at some low temperature: they become superconducting. Superconductivity is the ability of certain materials to conduct electrical current with no resistance. Thus, superconductors can carry large amounts of current with little or no loss of energy.

History Of Superconductors

In the early 1900's a dutch physicist by the name of Heike Kammerlingh Onnes (pictured above), discovered superconductivity. Before his discovery, Onnes had spent most of his scientific career studying extreme cold. The first step he took toward superconductivity was on July 10, 1908 when he liquified helium and cooled it to an astonishing 4 K, which is roughly the temperature of the background radiation in open space. Using this liquid helium, Onnes began experimenting with other materials and their properties when subjected to intense cold. In 1911, he began his research on the electrical properties of these same materials. It was known to Onnes that as materials, particularly metals, cooled, they exhibited less and less resistance. Bringing a mercury wire to as close to absolute zero as possible, Onnes observed that as the temperature dropped, so to

did the resistance, until 4.2 K was reached. There resistance vanished and current flowed through the wire unhindered. Below (Fig.2) is an approximate graph displaying resistance as a function of temperature for the experiment Onnes conducted with mercury:

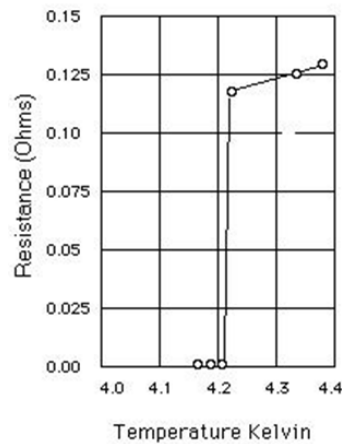


Figure 2. Resistance as a Function of Temperature for the experiment Onnes conducted with mercury
 .Source:<http://www.physnet.uni-hamburg.de/home/vms/reimer/htc/pt2.html>

Continuing with his experiments, Onnes discovered what he came to call "persistent currents," which were electrical currents that flowed continuously in a superconductor without a voltage to drive them. Additionally, the currents in superconductors flowed without dissipating energy, a fact that Onnes proved when he instigated a current in a conductor and found that a year later the current was still flowing and had not degraded! In 1913, Onnes was awarded the Nobel Prize for his discovery and the field of superconductors was officially created (Past, Present and Future , High-Temperature Superconductivity). However, in 1933 Meissner and Ochsenfeld discovered another property of superconductors, which is in fact believed by many to be an even more basic characterization. This phenomenon, which is popularly called the Meissner effect, has to do with the magnetism of a superconductor. You're no doubt familiar with the fact that iron has remarkable magnetic properties. Iron tends to draw to it the lines of magnetic force of a magnet. That's why iron is often used to make electromagnets. It helps to guide the magnetic lines of force around in space where you wish to have them. The superconductor is just the opposite. It's what is called a perfect diamagnet. A superconductor excludes the lines of magnetic force. If you bring a small bar magnet up to a superconductor, the superconductor bends the lines of force away from it and doesn't allow them to penetrate.

Then in 1986, researchers at an IBM laboratory in Switzerland discovered that ceramics from a class of materials called perovskites were superconductors at a temperature of about 35 Kelvin. This event sparked great excitement in the world of physics, and earned the Swiss scientists a Nobel Prize in 1987. As a result of this breakthrough, scientists began to examine the various perovskite materials very carefully. In February of 1987, a perovskite ceramic material was found that was a superconductor at 90 Kelvin. This was very significant because now it became possible to use liquid nitrogen as the refrigerant. Since these materials superconduct at a significantly higher temperature, they are called High Temperature Superconductors .

There are several advantages in using liquid nitrogen instead of liquid helium. Firstly, the 77 Kelvin temperature of liquid nitrogen is far easier to attain and maintain than the chilly 4.2 Kelvin of liquid helium. Liquid nitrogen also has a much greater capacity to keep things cold than does liquid helium. Most importantly, nitrogen constitutes 78% of the air we breathe, and thus unlike liquid helium, for which there are only a few limited sources, it is relatively much cheaper.

The interest in the new superconductors continues to mount (Fig.3) Past, Present and Future , High-Temperature Superconductivity. Many Governments, Corporations and Universities are investing large sums of money in this to investigate this major breakthrough that many have hailed as important as the invention of the transistor.

Nowadays the discovery of novel superconductors continues. In 2001, magnesium diboride (MgB_2) was found to be a superconductor with $T_c = 39^\circ K$. The technology of magnesium diboride wire production is

being actively developed at the moment. Although the magnesium diboride wire performance is not high for the time being, in future MgB₂ wires might replace more expensive Nb₃Sn and Nb-Ti wires. In spring 2008 Japanese researchers discovered a new family of superconductors based on the elements from the 5th group of the Mendeleev Table (pnictides, LaO_{1-x}F_xFeAs with T_c=26°K).

1986: Bednorz and Muller discover superconductivity at high temperatures in layered materials comprising copper oxide planes.

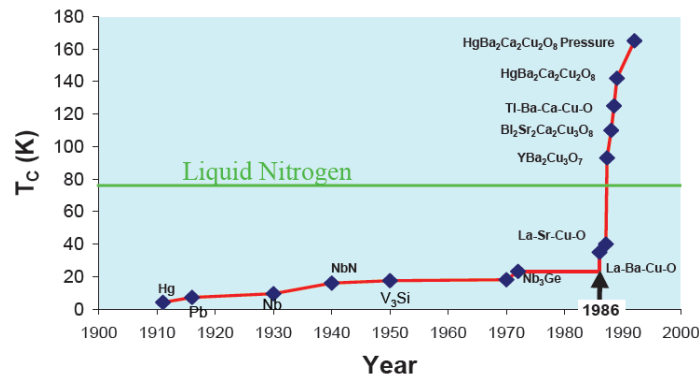


Figure 3. The chronology of discoveries of superconductors with higher critical temperatures.

Source: http://mrs.engr.uconn.edu/PDFs/BWells_Talk_March21-2012.pdf

Nobel Prizes

1. Heike Kamerlingh-Onnes

1913 Nobel Laureate in Physics :for his investigations on the properties of matter at low temperatures which led, inter alia to the production of liquid helium.

2. Lev Davidovich Landu

1962 Nobel Laureate in Physics : for his pioneering theories for condensed matter, especially liquid helium.

The prize was awarded jointly to:

3. John Bardeen, Leon N. Cooper and J. Robert Schrieffer

1972 Nobel Laureate in Physics : for developing theory of superconductivity, usually called the BCS-theory.

The prize was divided, one half being equally shared between:

4. Leo Esaki and Ivar Giaever

1973 Nobel Laureate in Physics : for their experimental discoveries regarding tunneling phenomena in semiconductors and superconductors, respectively, and the other half to

Brian D. Josephson

1973 Nobel Laureate in Physics : for his theoretical predictions of the properties of a supercurrent through a tunnel barrier, in particular those phenomena which are generally known as the Josephson effects.

The prize was awarded jointly to:

5- J. Georg Bednorz and K. Alexander Müller

1987 Nobel Laureate in Physics : for their important breakthrough in the discovery of superconductivity in ceramic materials.

1987 Nobel Laureate in Physics

The prize is being awarded jointly to:

- Alexei A. Abrikosov, Vitaly L. Ginzburg and Anthony J. Leggett

2003 Nobel Laureate in Physics : for pioneering contributions to the theory of superconductors and superfluids

Physics Of Superconductors

As it was already explained that superconductivity is the ability of certain metals, alloys and ceramic materials to let electrical current flow with no electrical resistance and energy dissipation (Fig. 4). Superconductivity appears at below a certain (critical) temperature, which is between 30K and 120K (-243°C and -153°C) for high-temperature superconductors (HTS) and below 20K (-253°C) for the low-temperature superconductors (LTS). Superconducting properties disappear if the temperature rises above the critical value, but also in the presence of high current density or strong external magnetic fields (Physics Today, June 1991) . The critical values of temperature, magnetic field and current density are specific characteristics of each superconductor material. Almost all of today's superconductors are based on Nb (niobium) and Nb-alloys LTS wires, which have already reached a high level of industrialization.

An important parameter such as Absolute zero is needed to be defined this latter is thus the lowest possible temperature, at which point the atoms of a substance transmit no thermal energy - they are completely at rest. It is 0 degrees on the Kelvin scale, which translates to -273.15 degrees Celsius (or -459.67 degrees Fahrenheit).

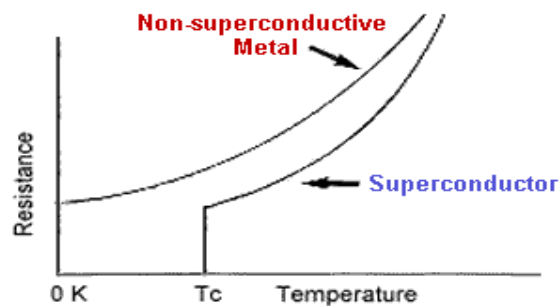


Figure 4. Resistance versus Temperature for Superconductor and Non-Superconductor

Superconductors have two outstanding features:

- i. **Zero electrical resistivity.** This means that an electrical current in a superconducting ring continues indefinitely until a force is applied to oppose the current.
- ii. **The magnetic field inside a bulk sample is zero (the Meissner effect).** When a magnetic field is applied current flows in the outer skin of the material leading to an induced magnetic field that exactly opposes the applied field. The material is strongly diamagnetic as a result. In this experiment, a magnet floats above the surface of the superconductor .

Technical Characteristics

The main technical characteristics of superconductors important for commercial use:

T – temperature at which a superconducting element operates;

I_c – the critical current of a superconducting element (a film or a wire) without an external field ;

J_c(B) – the critical current of a superconducting element in an external magnetic field

L – the length of a superconducting element. I_c is the exact point at which a superconducting element loses its ability to carry current without electrical resistance

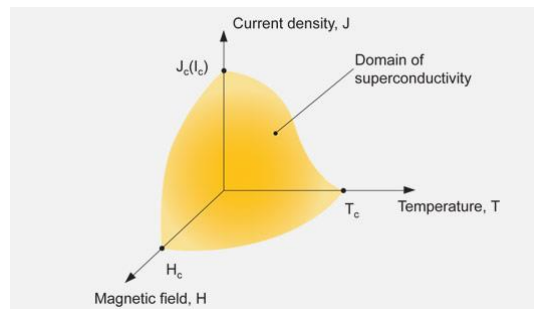


Figure 5. Critical area limiting existence domain of superconductivity

In addition to the requirement that the temperature and magnetic field must be below some value, there is also a limit on the current density in a superconducting material. Hence the three critical values T_c , H_c and J_c , which are all interdependent are shown in figure 5, and a material will only remain in the superconducting state within the volume shaded.

Critical temperature (T_c)

As long as the superconductor is cooled to very low temperatures, the Cooper pairs stay intact, due to the reduced molecular motion. As the superconductor gains heat energy the vibrations in the lattice become more violent and break the pairs. As they break, superconductivity diminishes. Superconducting metals and alloys have characteristic transition temperatures from normal conductors to superconductors called Critical Temperature (T_c). Below the superconducting transition temperature, the resistivity of a material is exactly zero. Superconductors made from different materials have different T_c values.

Critical current density (J_c)

If too much current is passed through a superconductor, it will revert to the normal state even though it may be below its transition temperature. The value of Critical Current Density (J_c) is a function of temperature; i.e., the colder you keep the superconductor the more current it can carry.

Critical magnetic field (H_c)

The maximum value for the magnetic field at which the material remains in the Super-conducting state even below its T_c is known as the critical magnetic field (H_c). When a superconductor is cooled below its transition temperature (T_c) and applied magnetic field is increased gradually above certain magnetic field (H_c) the superconductivity is lost. It was found that in addition to a critical temperature, both current density and applied magnetic field have to be kept below their respective critical values (J_c and H_c) to maintain the superconducting state. Figure 1 illustrates the superconducting state as a region beneath a shaded 'critical surface' defined by the three critical parameters, J_c , H_c , and T_c .

Categories of Superconductors.

Superconductors are divided into two types depending on their characteristic behavior in the presence of a magnetic field. Type I superconductors are comprised of pure metals, whereas Type II superconductors are comprised primarily of alloys or intermetallic compounds. Both, however, have one common feature: below a critical temperature, T_c , their resistance vanishes.

Type 1 superconductors:

The first group encompasses superconducting metals and metalloids which have some resistance at normal temperatures, but when cooled past a certain point their resistance becomes 0. The theory currently used to explain this phenomenon is the BCS theory. It states that when sufficiently cooled, electrons form "Cooper Pairs" which enable them to flow unimpeded by molecular obstacles such as vibrating nuclei. It is sort of like two bicyclists drafting behind one another to go faster. The phenomenon is called phonon-mediated coupling because sound is produced in the flexing of the crystal lattice as the electrons pass through it. Type 1 superconductors are perfect diamagnets, meaning they completely repel any magnetic field they are placed in. Another cool property of both types of superconductors is that once set up, a current loop will last indefinitely because there is no resistance. This has the potential to store a lot of energy, and American Superconductors Co. already has energy storage backup units for sale for major power companies.

Type 2 superconductors:

The second group is made up of metallic compounds and alloys. These compounds (usually a metal-oxide ceramic) can usually attain higher T_c values, but the mechanism for why they do this is unknown. It is most likely due to planar layering in the crystal lattice (see image in upper left corner of web page - taken from superconductors.org). Some theories predict an upper limit on the T_c of type 2 superconductors, while other theories claim there is no limit. Right now, research in type 2 superconducting is mainly trial and error with different combinations of chemicals. As of the time of this writing, 138K was the highest T_c . Type 2 superconductors are not perfect diamagnets; they allow some penetration of a magnetic field. And they also do not change suddenly from having resistance to having none. There is generally a range of temperatures where there is a mixed state.

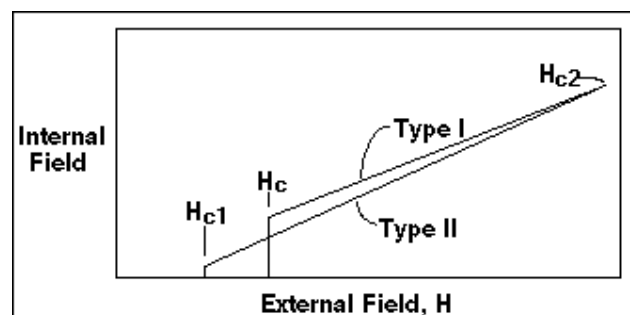


Figure 6. Internal Field Versus External Field for Type I and Type II Superconductor. Source: <http://www.americanmagnetics.com/tutorial/supercon.html>

The critical temperature at which the resistance vanishes in a superconductor is reduced when a magnetic field is applied. The maximum field that can be applied to a superconductor at a particular temperature and still maintain superconductivity is called the critical field, or H_c . This field varies enormously between Type I and Type II superconductors (Fig. 6) (Superconductivity Basics and Superconductivity Concepts). The maximum critical field (H_c) in any Type I superconductor is about 2000 Gauss (0.2 Tesla), but in Type II materials superconductivity can persist to several hundred thousand Gauss (H_{c2}). At fields greater than H_c in a Type I superconductor and greater than H_{c2} in a Type II superconductor, the conductor reverts to the normal state and regains its normal state resistance.

Superconductors and Magnetism

A Type 1 superconductor in a magnetic field will completely repel all field lines. This is called the Meissner effect, and it is an example of perfect diamagnetism. The perfect exclusion of a magnetic field can be explained by using Faraday's law.

Additional differences between type I and type II exist, mainly that type II display superconducting qualities at much higher temperatures and can remain superconductive in the presence of much higher magnetic fields

(Superconducting Magnets, 1983). While type I have T_c 's that hover just a few degrees from absolute zero, type II can have T_c 's of over 130 K. The graph below (Fig.7) shows how type I and type II superconductors compare as related to T_c and H_c :

The difference in magnetic fields is also quite large. Type I superconductors can stand fields up to approximately 2000 Gauss, which translates to about .2 Tesla, while type II can with stand fields of up to several hundred thousand Gauss, which translates to more than 10 Tesla.

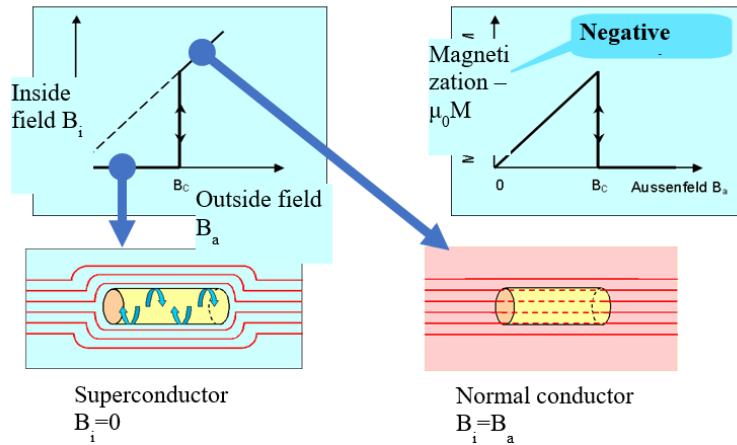


Figure 7. Inside field versus outside field for Normal and Superconductor

Meissner Effect

When a superconductor is placed in a magnetic field (Fig.8) the field is expelled below T_c .

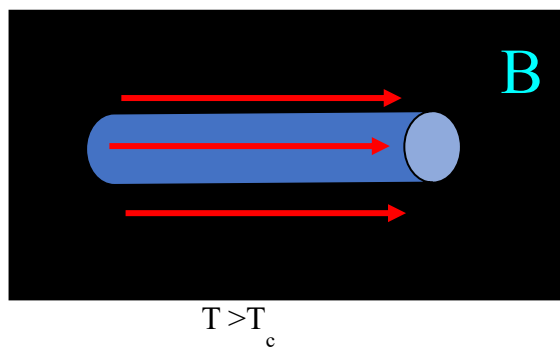


Figure 8. superconductor is placed in a magnetic field

- a- $T > T_c$ Not Superconductivity
- b- $T < T_c$ Superconductivity



Figure 9. Meissner Effect , Source:<http://www.americanmagnetics.com/tutorial/supercon.htm>

The physics that govern the superconducting qualities themselves are very involved and complex, and are beyond the scope of this chapter, however, a basic explanation of their function will be given. A very interesting property of superconductors is their ability to "push" magnetic flux out of itself. This is done when eddy currents are induced in the superconductor that produces a magnetic field that is equal and opposite to the initial magnetic field. As shown in the above diagram, when a magnet comes close to a superconducting material, the magnetic flux is "pushed" out and the magnet hovers. This is an amazing phenomena called the Meissner Effect, shown in Figures 8 and 9.

Research And Potential Uses

The prospects for technological applications of superconductivity (Applications of Superconductivity, 2000) have been long evident. However, the first superconductors were operable at low temperatures and only could produce low currents; and superconductivity was destroyed when critical current density was exceeded. Real superconductivity applications only became possible following a considerable advancement made in research and development in the 1970s. For the sake of convenience, the areas in which superconductors are used are grouped into two categories: relatively low-capacity electronics (such as high-performance computers, magnetic field and radiation detectors, microwave filters) and large scale (cables, current limiters, magnets, motors, generators, power accumulators). These two areas of applications differ greatly from each other and have practically nothing in common. Superconducting materials used in electronics production are based on epitaxial thin films not larger than 100 cm², while power applications require flexible wires more than one kilometer long and capable to transmit large amounts of power.

Applications of Superconductors

Applications of superconductors can be classified as follow (Fig.10) (Applications of Superconductivity, 2000).

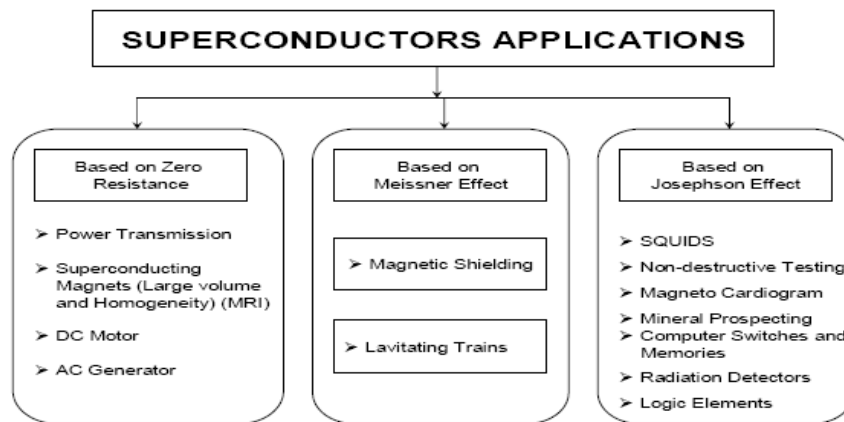


Figure 10. Classification of applications of superconductors.

The third Group “Based on Josephson Effect” is beyond the scope of this project.

5.3 Maglev Trains

Superconductors have many modern day uses and have many potential uses that could better many different areas of science. As pictured below (Fig.5.1), superconductors could be used to magnetically levitate trains (maglev trains), creating a system that does not lose energy in the form of friction with a track, instead the train floats a above the track and is propelled by the magnetic forces caused by the induced currents.

Maglev trains are trains that levitate about 10 mm off the tracks using repulsive electromagnets on both the tracks and the train itself. This levitation greatly reduces friction, potentially allowing the train to move faster

and consume less power than it would otherwise. This enables them to operate without friction, and therefore achieve unheard of speeds. Maglevs, with sufficient track, can reach speeds over 300 mph. A new Maglev train in Shanghai recently broke the 500 Km/h barrier (310 mph). These trains are also more efficient because there less energy loss to friction between the train and the track.

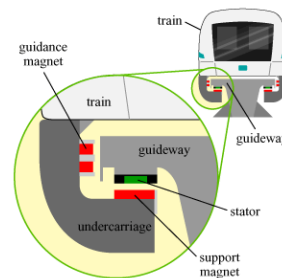


Figure 11. Maglev trains use superconductors to levitate the train above magnetic rails, **Source:** <http://superconductors.org/Uses.htm>

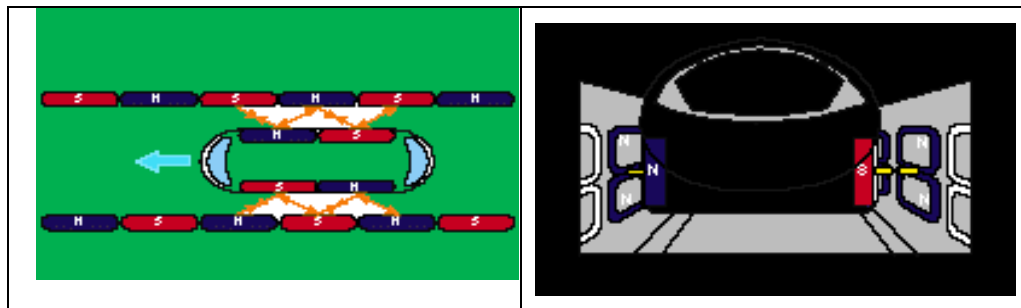


Figure 12. Maglev Train and how they magnetically work, **Source :** <http://www.spacecable.org.uk/Images/Inductrack.j>

Running alongside the track are walls (Fig.11 and 12) with a continuous series of vertical coils of wire mounted inside. The wire in these coils is not a superconductor. As the train passes each coil, the motion of the superconducting magnet on the train induces a current in these coils, making them electromagnets. The electromagnets on the train and outside produce forces that levitate the train and keep it centered above the track. In addition, a wave of electric current sweeps down these outside coils and propels the train forward (see drawings).

Drawings of Maglev train showing magnets both on-board and built into sidewalls; drawings courtesy of Railway Technical Research Institute Maglev Systems Development Department

Magnetism in elementary science states that like poles repel and opposites attract. When two magnets of the same poles are brought towards each other, a repulsion force can be felt and likewise a pair of the same poles will attract (Case studies in superconducting magnets :1994). Maglev trains use these basic principles to force the train upwards above the track surface. The simple way of visualizing this is to imagine the train repelling away from the track surface. By arranging magnets in a certain way, a train can be made to float on repelling magnetic fields. This enables it to move with every little friction (there is still air resistance).

Maglev trains work in one of two ways; both methods are based on the same concept but involve different approaches. German engineers have developed Electromagnetic (Case studies in superconducting magnets 1994). Suspension (EMS) while the Japanese engineers have developed Electrodynamic Suspension (EDS), the newest EDS technology being the inductrack (Fig.13).

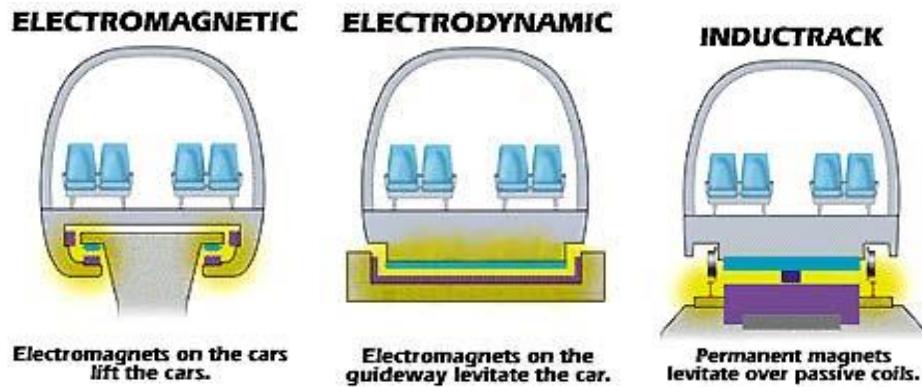


Figure 13. Type of Suspension

Maglev trains need strong magnetic fields, faster changing fields, thicker material with lower resistivity such as copper, silver, aluminum etc... in order to go fast

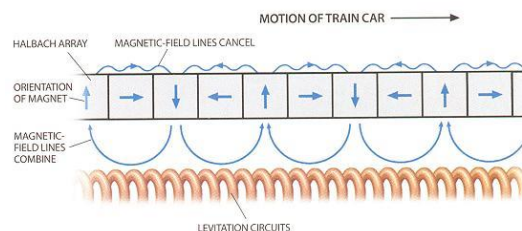


Figure 14 . Maglev Train and its Levitation Circuits, Source:
<http://www.spacecable.org.uk/Images/Inductrack.j>

A power supply is used to accelerate the train until it levitates and if the power fails it can safely slow down on its auxiliary wheels. The magnets are made from a neodymium-iron-boron alloy (creates a bigger magnetic field) and are arranged in a Halbach array, concentrating the magnetic field above it. The track is an array of short-circuited wires (Fig. 14) which create a magnetic field and repels the magnets allowing the train to levitate. These types of trains levitate higher, (about 2.54 cm) and are much more stable. There are two designs, Inductrack I which is designed for high speeds and Inductrack II which is designed for slower speeds.

Magnetic Resonance Imaging (MRI)

Another use of superconductors is in Magnetic Resonance Imaging, or MRI, in which the superconductor helps in creating a non-invasive method of looking at a person's brain and internal organs activities. Magnetic resonance imaging (MRI) machines (Fig.15) allow doctors to see a three-dimensional scan of a patient's internal organs. MRI machines use very powerful magnets to charge the protons of hydrogen atoms in the body's cells. A radio frequency is then aimed at the charged protons. The charged protons absorb the frequency and then reflect it back at the machine. The machine ultimately uses the reflected data to form a three-dimensional image of the area being scanned.

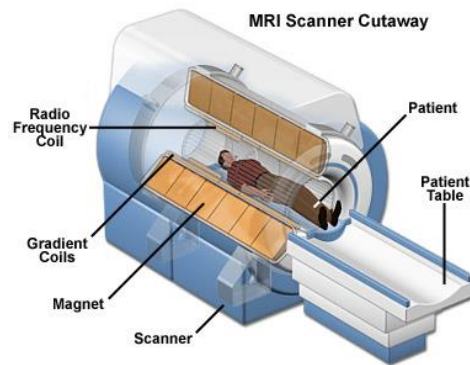


Figure 15. MRI Machine

MRI machines use superconductors to deliver a strong enough magnetic field so that hydrogen atoms in the body's fat and water molecules will pick up energy from the field which can then be detected by special instruments. SQUIDS (Superconducting QUantum Interference Device) can be used like an MRI, but without the need for a strong magnetic field. They can detect magnetic fields of infinitely small magnitudes. They can also be used for extremely precise motion detection (Fig.16).



Figure 16. Output Picture from a MRI test, Source: <http://superconductors.org/Uses.htm>

Electronics and Computer Technology

In the area of electronics superconductivity will be widely used in computer technology. Superconducting elements will ensure short switching time, low capacity losses when using thin-film elements and large circuit assembly density. The most efficient industrial application of superconductivity is related to generating, transmitting and efficient use of electrical power (Fig. 17). The ability of superconductors to conduct electricity with zero resistance can be exploited in the use of electrical transmission lines.



Figure 17: Production and Transmission of Electrical Power, Source: <http://superconductors.org/Uses.htm>

The field of electronics holds great promise for practical applications of superconductors. The miniaturization and increased speed of computer chips (Fig.18) are limited by the generation of heat and the charging time of capacitors due to the resistance of the interconnecting metal films. The use of new superconductive films may result in more densely packed chips which could transmit information more rapidly by several orders of

magnitude. The electronics industry thus would benefit from faster switching times, smaller components, and greater circuit efficiency.

Superconducting electronics have achieved impressive accomplishments in the field of digital electronics. Logic delays of 13 picoseconds and switching times of 9 picoseconds have been experimentally demonstrated. Through the use of basic Josephson junctions (Josephson Computer Technology, 1980) scientists are able to make very sensitive microwave detectors, magnetometers, SQUIDs and very stable voltage sources.

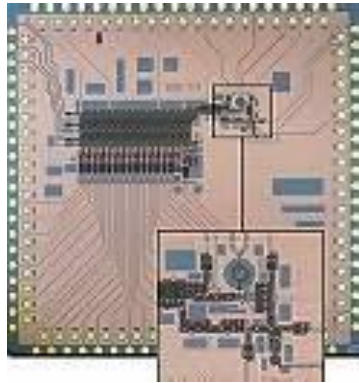


Figure 18. More densely packed chips (Superconducting Electronics), Source: <http://superconductors.org/Uses.htm>

Conclusions

Superconductivity is becoming one of the key constituents of the technical progress. Many aspects of superconductivity in complex compounds remain unexplained. On the one hand, it hampers discovery of new superconductors, on the other, it gives no answer to the question if there is a maximum temperature at which superconductivity occurs. The latter fact gives hope that in future materials with abnormally high transition temperature can be discovered.

Superconductors are already used in many fields: electricity, medical applications, electronics and even trains. They are used in laboratories, especially in particle accelerators, in astrophysics with the use of bolometers, in ultrasensitive magnetic detectors called SQUIDs,,,, and in superconducting coils to produce very strong magnetic fields. However, they need to be cooled to very low temperatures, which restricts their use in our everyday life. But new applications are already operational in laboratories and will be able to spread to our cities and our homes if the cooling process becomes less expensive or, better, if we discover superconducting materials that do not require any cooling. If this happens, we can expect an actual revolution in energies and environment on the one side, and transportation and computer science on the other.

The possible discovery of room temperature superconductors has the potential to bring superconducting devices into our every-day lives.

References

A Guide to Superconductivity: <http://www.physnet.uni-hamburg.de/home/vms/reimer/htc/contents.html> A Guide to Superconductivity:

<http://www.physnet.uni-hamburg.de/home/vms/reimer/htc/contents.html>

Applications of Superconductivity, H. Weinstock, Kluwer (2000).

Case studies in superconducting magnets: design and operational issues, Y. Iwasa, New York: Plenum Press (1994).

Handbook of Applied Superconductivity, B. Seeber, IOP (1998).

<http://almaz.com/nobel/physics/>

http://www.superox.ru/en/application_superconductivity.htm

Introduction: Superconductivity Basics:

<http://supercon.lbl.gov/MCoccoli/Files/Supercon/Thesis/ThesisBook/Chapters/Introduction.pdf>

Josephson Computer Technology, special issue of IBM Journal of Research and Development 24, Number 2, pp. 105-264, 1980.

Past, Present and Future , High-Temperature Superconductivity: History and Outlook

<http://www.jsap.or.jp/jsapi/Pdf/Number04/PastPresentFuture.pdf>

Physics Today, June 1991, (volume 44), Special Issue on High-Temperature Superconductors.

Proceedings of the IEEE 77, Number 8, 1989, Special Issue on Superconductivity.

SerwayCh12-Superconductivity.pdf:

http://academic.cengage.com/resource_uploads/static_resources/0534493394/4891/SerwayCh12-Superconductivity.pdf

Superconducting Magnets, M.N. Wilson, Oxford (1983).

Superconductivity Basics: <http://www.americanmagnetics.com/tutorial/basics.html>

Superconductivity Concepts:<http://hyperphysics.phy-astr.gsu.edu/hbase/solids/supcon.html>

Superconductors: The Long Road Ahead, by S. Foner and T.P. Orlando, Technology Review 91, pp. 36-47, 1988.

Superconductivity in Doped Fullerenes, A.F. Hebard, Physics Today, November 1992, p. 26.

Superconductivity by A. Leggett and D.M. Ginzburg in Encyclopedia Britannica at

<http://search.eb.com/bol/topic?idxref=507241>)

The Physics of Superconductivity: <http://www.physics.uoguelph.ca/nicol/supercond/resources.html>

<http://www.physics.usyd.edu.au/~khachan/PTF/Superconductivity.pdf>

The Rise of Superconductors - What Causes Superconductivity?

http://www.qudev.ethz.ch/phys4/studentspresentations/supercond/Ford_The_rise_of_SC_6_7.pdf

CONVERTING THE ENERGY OF SEA WAVES INTO ELECTRICAL ENERGY

Kassayeva Assyl Zhvlamanovna,

Candidate Of Pedagogical Sciences, Associated Professor of Natural Sciences Department, Caspian University of Technology and Engineering, Kazakhstan, ORCID NO: 0009-0006-9479-9096

Sagindvkova Elvira Umirovna

Candidate Of Pedagogical Sciences, Associated Professor of Natural Sciences Department, Caspian University of Technology and Engineering, Kazakhstan, ORCID NO: 0009-0006-9479-9096

ABSTRACT

The amount of ocean wave energy available worldwide is large enough to generate serious interest in its extraction and use, and to make a significant contribution to meeting the energy aspirations of various consumers. The amount of marine energy is fundamentally greater than the amount of energy on land, yet the introduction of wave energy conversion systems in offshore power plants remains a costly initiative. The relevance of the published study is justified by the fact that ocean waves provide an inexpensive and environmentally friendly energy resource suitable for simple wave energy generation through offshore power plants. The purpose of this study is to analyse the technological characteristics, depending on the localisation resource potential of wave energy generating offshore power plants, focusing on the hydrodynamic characteristics of offshore power plants during the analysis. The subject of the study is modern technologies for harnessing ocean wave energy in an offshore power plant format, with realistic prospects for reaching the commercial stage of power generation, along with wind and solar power. PFERRET software was used to analyse the data. The Ferret software was upgraded to the PFERRET version based on the Python application. The PyFERRET software is a carrier of complex and multiple data for analysis. It is designed and produced specifically for meteorologists and oceanographers, and runs on UNIX and Mac operating systems. The PFERRET software applies data on wind and atmospheric pressure obtained from the ECMWF database, in formats such as Netcdf, ASCII and binary code. The originality of the published study is related to the technological trend to improve the efficiency and competitiveness of the wave energy generating offshore power plants, to reduce the cost and congestion of deployed offshore power plant systems, especially in remote areas.

Keywords: Energy storage system; technological advances; wave energy conversion; optim solution; efficient operation; achieving resonance.

DESIGN AND ANALYSIS OF REDUCED SWITCH MULTILEVEL INVERTERS FOR ELECTRIC VEHICLE APPLICATIONS

Reshmi Soyinka V

Department of Electrical & Electronics Engineering, Sri Sivasubramaniya Nadar College of Engineering, Kalavakkam – 603 110, Chennai, Tamil Nadu, INDIA

Vaduhammal V

Department of Electrical & Electronics Engineering, Sri Sivasubramaniya Nadar College of Engineering, Kalavakkam – 603 110, Chennai, Tamil Nadu, INDIA

Sneka C

Department of Electrical & Electronics Engineering, Sri Sivasubramaniya Nadar College of Engineering, Kalavakkam – 603 110, Chennai, Tamil Nadu, INDIA

Dr V Thiagarajan

Department of Electrical & Electronics Engineering, Sri Sivasubramaniya Nadar College of Engineering, Kalavakkam – 603 110, Chennai, Tamil Nadu, INDIA

ABSTRACT

The efficient and compact design of multilevel inverters (MLI) serves as a driving force across various applications, notably in solar photovoltaic (PV) systems and electric vehicles (EVs). Multilevel inverters have garnered increasing attention as they strive to meet specific requirements and offer an attractive alternative for delivering high-quality power. They present a range of advantages, including a reduced device count, operation at lower switching frequencies, decreased dv/dt stress, and lower harmonic distortions. Recent advancements in multilevel inverter topologies have led to designs with fewer components compared to conventional inverters like the flying capacitor type (FC), cascaded H-bridge type (CHB), and neutral point clamped type (NPC). The number of components in the circuit is directly linked to the number of levels in the multilevel inverter, which can increase both cost and structural complexity. In the case of FC MLI and NPC MLI, maintaining capacitor voltage balance presents a formidable challenge, limiting them to five levels and preventing further cascading. This limitation results in an output voltage that is only half of the input voltage, leading to higher switching frequencies and increased losses. To address these issues, a wide range of research efforts has been dedicated to reducing the component count in multilevel inverters, resulting in the proposal of various topologies tailored to different levels, each with its unique set of challenges. In this study, a novel multilevel inverter architecture utilizing a switched capacitor approach is presented. The proposed configuration is distinguished by its simplicity and ease of implementation, especially for higher-level applications. A key advantage is the reduced number of active switches, resulting in a corresponding reduction in driver circuitry. In the context of solar energy systems, the integration of solar panels, alongside a perturb and observe (P&O) algorithm, ensures a stable DC voltage. Furthermore, a single input and multi-output converter is employed to boost the DC link voltage. A comprehensive comparative analysis is conducted, encompassing parameters such as switch count, gate driver boards, source count, diode and capacitor quantities, and overall component count. For the proposed MLI configurations, simulation results are meticulously aligned with experimental data. The total harmonic distortion (THD) consistently remains below 5%, conforming to IEEE standards. To corroborate our findings, we have implemented a hardware prototype in our laboratory, subjecting it to dynamic load variations, while the simulations have been executed using MATLAB/Simulink.

Keywords: Multilevel Inverter, Reduced switch count, Symmetrical, Asymmetrical, Photovoltaic, P&O algorithm, THD

**STRATEGIC ENERGY OPTIMIZATION IN A HYBRID POWER SYSTEM WITH
PHOTOVOLTAIC, WIND, AND BATTERY INTEGRATION USING A THREE-LEVEL
CONVERTER**

Abdelkader BOUAZZA

L2GEGI Laboratory, University of Tiaret, 14000 Tiaret, Algeria

ABSTRACT

On a global scale, this work presents an extensive examination of a hybrid energy system encompassing three distinct energy sources: wind energy, photovoltaic power (PV), and battery storage. Each energy source is governed by precise control strategies to ensure the efficient delivery of energy. The integration of a sophisticated multi-level inverter enhances the quality of energy injected into the AC load. Fuzzy logic control techniques are employed for the optimization of power transfer to the DC bus voltage. Furthermore, a meticulously devised management system facilitates the coordination of power flow among the system components to meet specific load requirements. This system was globally implemented using MATLAB / Simulink, and the results unequivocally demonstrate the efficacy of the proposed approach, which has been validated through extensive global experimentation.

KEYWORDS: wind power, photovoltaic energy, energy storage, hybrid energy system, Maximum Power Point Tracking (MPPT), three-level inverter, Fuzzy Logic Control (FLC)

DYNAMIC FUZZY CONTROL STRATEGY FOR INTEGRATING PHOTOVOLTAIC, FUEL CELL, AND BATTERY SYSTEM VIA THREE-LEVEL T TYPE INVERTER

KOULALI Mostefa

L2GEGI Laboratory, University of Tiaret, 14000 Tiaret, Algeria

ABSTRACT

This research focuses on examining an electrical energy generation setup comprising three distinct energy sources: photovoltaic energy, a fuel cell, and a battery. To optimize this hybrid production system, precise control mechanisms are employed for each component. Integration of a three-level T-type inverter within the hybrid system chain enhances the quality of energy supplied to the alternating load, subsequently reducing harmonic distortion. The Renewable Energy Management System offers a comprehensive overview of the hybrid system's performance. It enables swift analysis for identifying underlying issues, enhances efficiency through power curve comparisons, and facilitates visualizing production trends. Implementing the proposed system in Matlab/Simulink showcases its effectiveness. Additionally, an energy management algorithm is developed to optimize power flow across various segments of the production line, aimed at mitigating load fluctuations. To evaluate this approach, a prototype is designed, simulated using Matlab/Simulink, and can be implemented in an experimental test bench to further analyze its efficacy.

Keywords: Fuel Cell, Photovoltaic PV, Battery, Hybrid System, Three Level T type Inverter, Adaptive Fuzzy Logic Control (AFLC).

THE CURRENT STATUS AND FUTURE PROJECTION OF PEM FUEL CELLS

Selman İLBEYOĞLU

*Şırnak University, Postgraduate Education Institute, Department of Energy Science and Technology, Şırnak- Türkiye
(Responsible Author) ORCID: 0009-0006-5374-7548*

Hüseyin GÜRBÜZ

*Şırnak University, Faculty of Engineering, Mechanical Engineering, Department of Automotive Şırnak-Türkiye
ORCID: 0000-0002-3561-7786*

ABSTRACT

Due to the existing energy crisis, many industries have embarked on the quest for renewable and sustainable energy sources and systems. Hydrogen, as an alternative energy source, holds great promise as an environmentally friendly energy carrier. In this context, fuel cells have become a significant energy system that is actively researched both scientifically and commercially, alongside renewable energy sources like solar and wind energy. Fuel cells are components that directly convert chemical energy into electrical energy. These systems operate with significantly higher efficiency compared to traditional power generation systems based on combustion processes. Among fuel cells, proton exchange membrane (PEM) fuel cells are particularly noteworthy due to their operational conditions, compact structure, operation at low temperatures (60-90°C), high power density, and use of clean fuel. In this study, a general assessment of PEM fuel cells is conducted, examining their current state and potential position in the future. The prominent features of this technology have been emphasized in terms of environmental sustainability and high energy efficiency. Additionally, enhancing the efficiency, reducing the cost, and commercializing the electrocatalyst used in the electrode structure of PEM fuel cells are crucial aspects. The outcomes of this study indicate that when investigations are conducted on existing issues in PEM fuel cells, such as catalyst material costs (typically platinum), durability, hydrogen production, and storage, and efforts are made towards finding solutions, PEM fuel cells have the potential to play a highly effective role in the future energy market.

Keywords: Hydrogen, PEM Fuel Cell, Energy Conversion Technologies

Introduction

With the impact of rapid societal growth globally, particularly in developing economic powers, world energy consumption has shown a steady increase in recent years (Wang et al., 2021). For decades, internal combustion engines have been the primary propulsion equipment in the automotive industry. Most engines in the transportation sector utilize fossil fuels such as gasoline and diesel (Van Vliet et al., 2011). As of 2015, the industrial sector holds the position of being the largest energy consumer compared to all other sectors. More than half of the energy distribution is consumed in sectors such as food, paper, and metal manufacturing, which particularly require high heat and energy. Considering sector demand, as seen in Figure 1, approximately 50% of global energy is consumed by the industrial sector, 29% by residential and commercial building usage, and 20% by the transportation sector. No doubt, as the world population increases, the energy demand in residential buildings also rises accordingly, particularly for electrical appliances, lighting, and heating systems. However, due to the current advancements in electric vehicle technology, the increase in energy demand in the transportation sector is somewhat slower (Ndayishimiye et al., 2019).

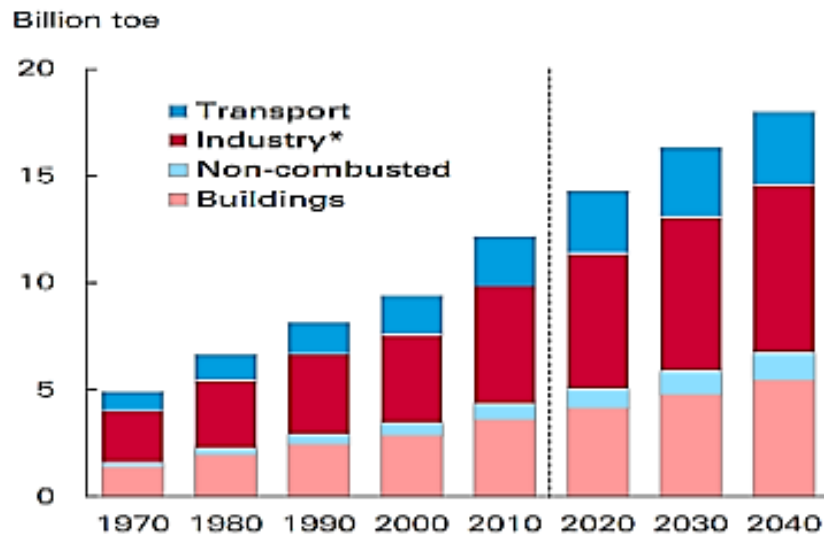


Figure 1. Primary energy consumption by end use sector

It is widely accepted that renewable energy sources are increasingly being used in place of depleting energy resources. Hydrogen emerges as a crucial sustainable alternative fuel and energy source, surpassing fossil fuels (İlbeyoğlu et al., 2020). Hydrogen-based fuel cells are sustainable energy conversion systems that transform the chemical energy of fuel into electrical energy without generating any harmful emissions. These fuel cells are not limited by the Carnot cycle and exhibit high energy efficiency. Among various types, Proton Exchange Membrane (PEM) fuel cells are the most commonly used, operating at low temperatures (60-90°C) with good dynamic characteristics and high power density (Madheswaran et al., 2022). Proton Exchange Membrane Fuel Cells (PEMFCs) are energy conversion technologies with the potential to reduce energy consumption, pollutant emissions, and dependence on fossil fuels. These technologies have gained widespread attention globally in recent years due to their high efficiency and low emissions. Moreover, they are produced using proton exchange membrane (especially Nafion) as a proton conductor for electrochemical reactions at low temperatures, along with electrochemical catalysts (Wang et al., 2020). Compared to other types of fuel cells, PEM fuel cell technology has predominated in the automotive industry so far, primarily due to its rapid reaction initiation times and numerous advantages (Olabi et al., 2021). The primary factor contributing to this is their ability to have zero exhaust emissions and their utility as an electric power source while in motion. Additionally, PEMFCs, like internal combustion engine vehicles, have the capability for rapid refueling and can cover more than 500 km with a full hydrogen tank (Alaswad et al., 2020). These types of fuel cells offer versatile energy solutions that can be effectively utilized not only for power generation but also in distributed generation, residential applications, and the portable electronics sector (Wilberforce et al., 2023). The operational principle of a PEM fuel cell, as depicted in Figure 2, involves the transfer of gas fuels at the anode and oxidizing gases like air at the cathode. During this process, oxidation reactions occur at the anode, while reduction reactions take place at the cathode. An ion transfer occurs in the electrolyte between the electrodes, moving from the anode to the cathode. These electrochemical reactions, utilizing chemical transformations between hydrogen and oxygen, lead to the generation of electrical energy. The electrochemical interactions between the anode and cathode establish the fundamental operating principles of the fuel cell, ensuring efficient energy conversion (Karanfil, 2020).

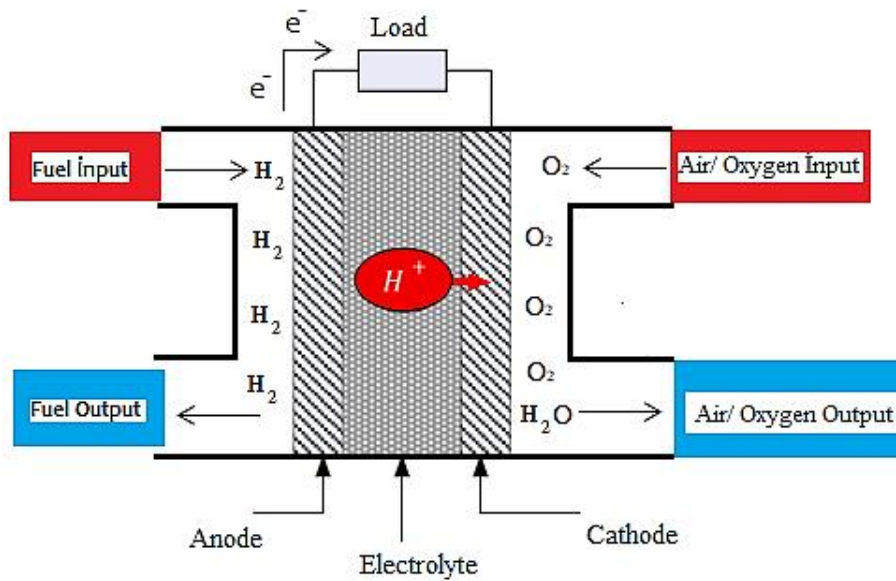
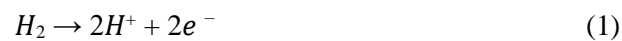
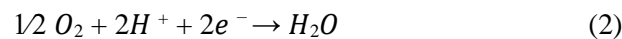


Figure 2. Schematic diagram of proton exchange membrane fuel cell (Wilberforce et al. 2023).

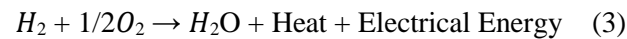
At the anode side: (Hydrogen oxidation reaction)



At the cathode side: (Oxygen reduction reaction)



All reactions:



The reactions occurring at the anode and cathode sides in the fuel cell are represented by equations 1, 2, and 3 (Li et al., 2023). The Proton Exchange Membrane (PEM) fuel cell has a complex structure. As depicted in Figure 3, this fuel cell typically consists of a proton membrane, anode and cathode electrodes, gas diffusion layers, bipolar plates, and, finally, outer plates.

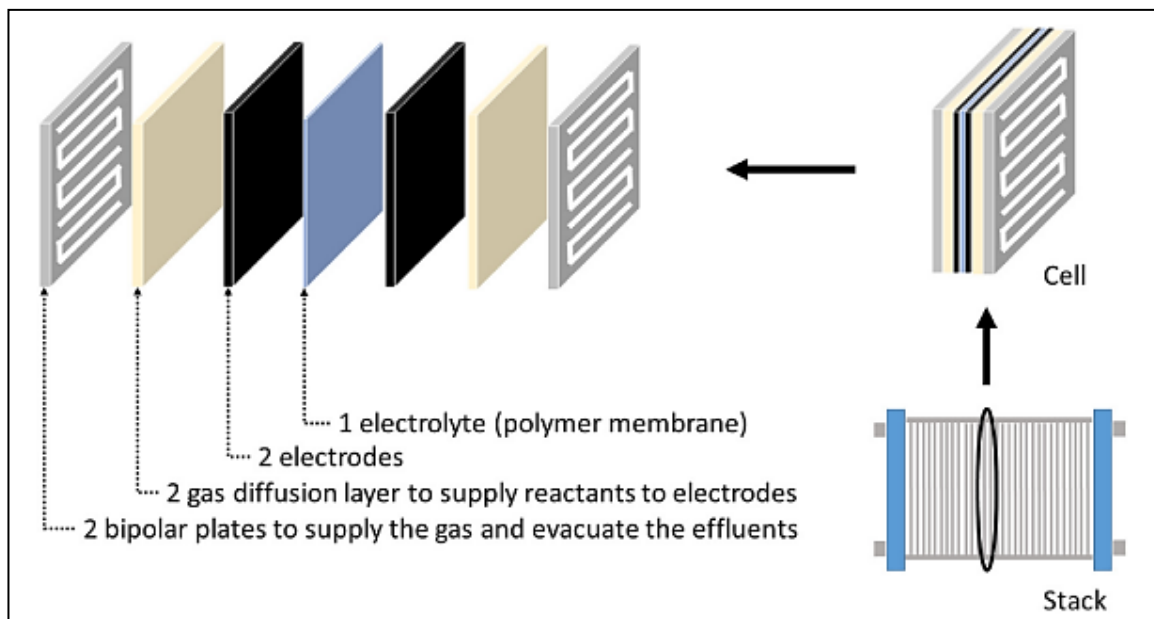


Figure 3. Structure of a single cell in a PEMFC stack (Yue et al., 2021).

The Current State of PEM Fuel Cells

In the last decade, significant progress has been made in understanding and addressing the fundamental mechanisms responsible for voltage losses and performance degradation in proton exchange membrane fuel cells (PEMFCs). However, cost and durability continue to persist as the two primary obstacles hindering the widespread use of PEMFC-based power systems. There is a close relationship between these obstacles, as the expensive Pt (platinum) catalyst is also the main source of performance degradation in PEMFCs (Borup et al., 2020). In current fuel cells, degradation is mitigated by using a cathode catalyst with lower Beginning of Life (BOL) activity, requiring higher catalyst loadings and alleviated by using system controls that prevent known conditions. However, degradation processes, such as limiting the voltage range of the fuel cell stack, intensify (Borup et al., 2020). PEM fuel cells use hydrogen as fuel and produce water as the sole byproduct with practical efficiency of up to 65%; this efficiency is significantly better than Otto and diesel engines. Standard hydrogen refueling takes less than 5 minutes, providing an advantage over the current charging time of electric battery vehicles (Wang et al., 2021). The incorporation of fuel cells into the automotive industry is increasing due to the advantages involved, but notwithstanding the forward movement made, fuel cells still have a long way to go for widespread commercialization. Fundamental research gaps that need consideration in future studies include the development of efficient membranes and the reduction or replacement of platinum catalysts with more cost-effective but equally efficient materials. Membrane thickness, bipolar plate geometry design, current collector material, and material weight significantly impact the overall cost of the operating cell (Alaswad et al., 2020). In Figure 4, a hydrogen fuel cell electric bus (FCEB) is compared to a diesel-fueled bus over a one-year operational period at UC Irvine. This comparison demonstrates that hydrogen-based FCEB operation significantly reduces greenhouse gas emissions and other pollutants.

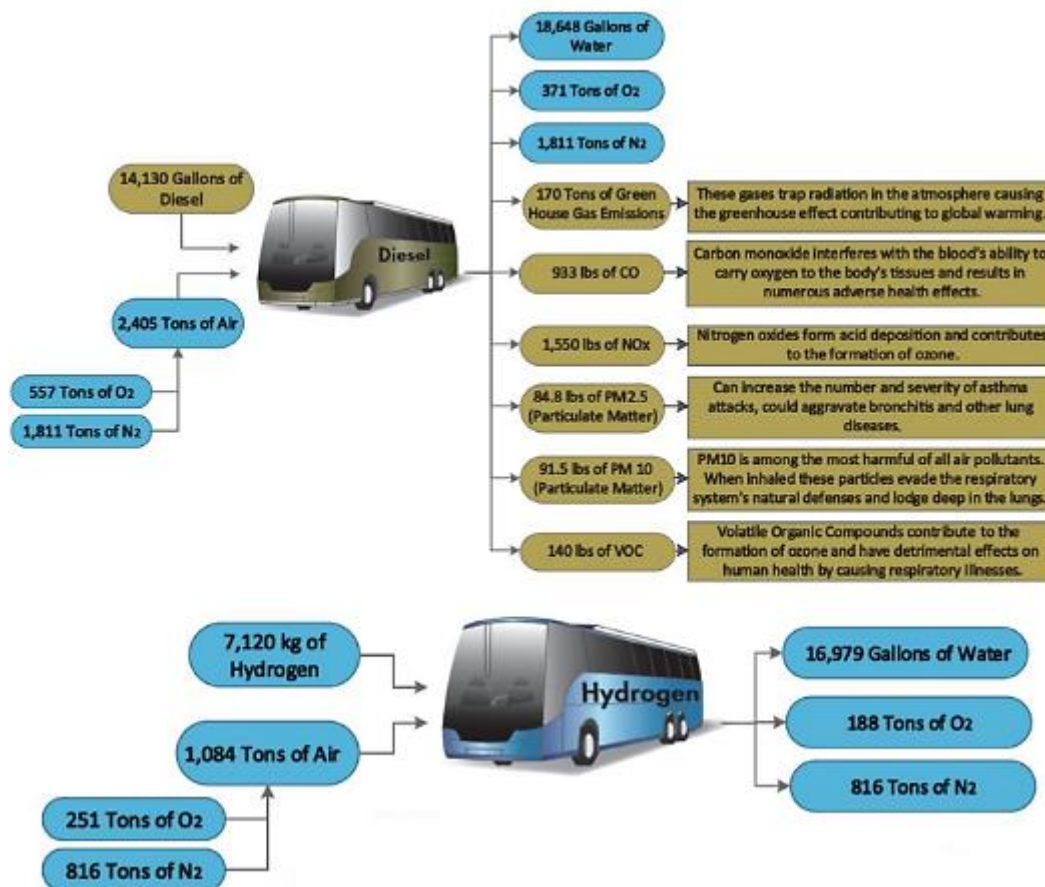


Figure 4. Comparison of a bus with a diesel engine and a PEM fuel cell (Wang et al., 2020).

Currently, hydrogen fuel cells are actively used in several brands and models of vehicles, including Toyota Mirai, Honda Clarity, and Hyundai Nexo. This highlights the focus of these brands on hydrogen fuel cells in

their research and development efforts. Among the key studies related to fuel cells, there is a significant emphasis on the development of polymeric membranes. Proton exchange membrane fuel cells, due to their ability to achieve high efficiency at low operating temperatures, operate silently, produce only pure water, and no other waste except heat, have become the most prominent type of fuel cell in hydrogen fuel cell vehicles. The membrane is considered the most crucial component of PEM fuel cells (Hydroborpem, 2023). The hydrogen tanks of Mirai are made of carbon fiber, and the components of the car resemble those of a high-end vehicle. The main elements of the Toyota Mirai are illustrated in Figure 5 below.

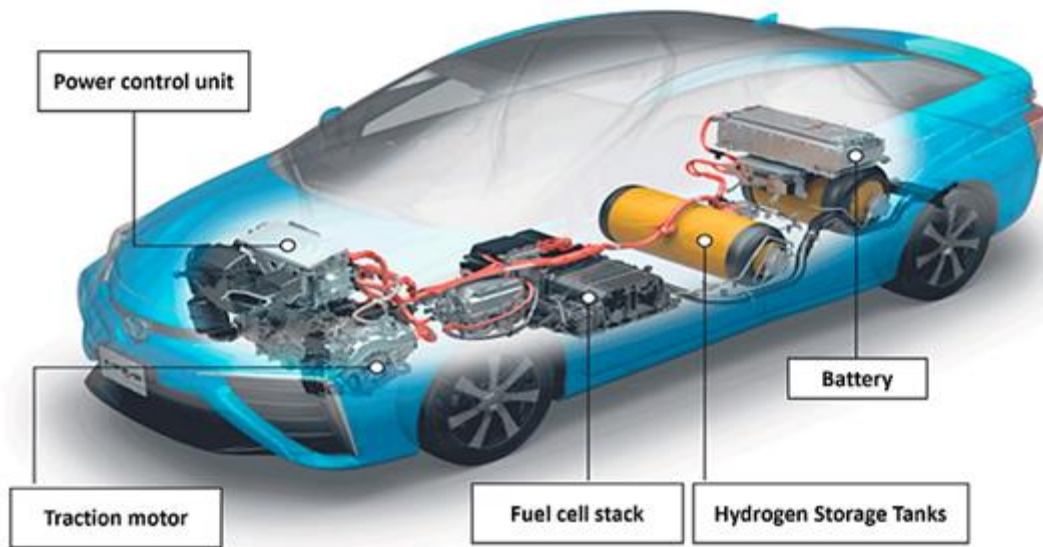


Figure 5. Components in Toyota Mirai (Olabi et al., 2021).

Fueling the hydrogen tank from a pump takes less than five minutes. Hydrogen fuel cell electric vehicles (FCEVs) play a unique role in decarbonizing transportation and the broader economy. They are crucial in achieving zero emissions across various road transport types, from passenger cars like Mirai to vans, trucks, and buses. A real image of the Toyota Mirai's fuel cell is provided in Figure 6.



Figure 6. Actual image of the fuel cell in the Toyota Mirai vehicle

Future Projection

Although much success in recent years, fuel cell technologies for automotive applications face remarkable technical challenges. Overcoming these challenges requires intensive efforts from both automotive manufacturers and researchers in areas such as pure hydrogen production, on-board hydrogen storage, fuel cell durability and reliability, consumer access to and safety with hydrogen. Alongside all these challenges, the high costs currently reduce the preferability of fuel cell electric vehicles (FCEVs) (İnci et al., 2021). Further cost reductions in fuel cell technology are necessary to be competitive with internal combustion engines without relying on government incentives. As of June 2018, there are approximately 5000 Fuel Cell Vehicles (FCVs) operating in the United States since 2015. In the United States, there are more than 20,000 forklifts and over 20 buses powered by PEM fuel cells across four states. California alone hosts operational hydrogen fueling stations numbering over 30, with plans to install over 200 by 2025 (Satyapal, 2019). The advancement of technologies utilized in hydrogen production, including components like FC and battery, is anticipated to reduce the production costs of hydrogen FCEVs, consequently boosting production to meet growing demand. The market size of hydrogen FC-based vehicles, valued at \$651.9 million in 2018, is projected to reach \$42,038.9 million by 2026, exhibiting an annual compound growth rate of 66.9% from 2019 to 2026 (Jadhav, 2020). Fig. 7 illustrates fluctuations in the number of FCEVs between 2013 and 2030 across three regions: North America, Europe, and Asia-Pacific. The count of FCEVs, a mere 20 in 2013, surged to 11,900 in 2018 and was expected to reach around 31,000 by the close of 2020, marking an approximate 160% increase from 2018 projections (Han et al., 2014). The anticipated figures for future vehicles in these regions reveal a consistent year-over-year rise in FC-based electric vehicles' production. The total number forecasted for FCEVs in 2030 is 582,400, with an assumed 1784% increase in the next decade (Secondary Research, 2020).

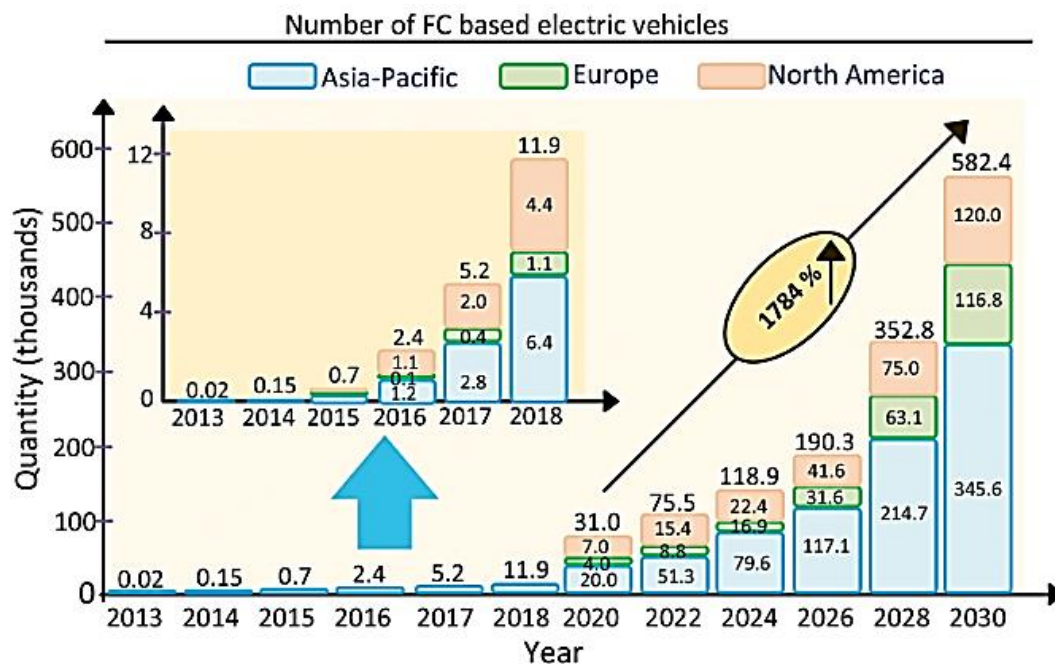


Figure 7. The number of FCEVS according to regions (İnci et al., 2021).

Conclusion and Recommendations

PEM fuel cells have the capability to decrease our energy consumption, emissions of pollutants, and reliance on fossil fuels. By utilizing hydrogen as fuel, PEM fuel cells achieve practical efficiencies of up to 65%, producing water as a byproduct—significantly outperforming Otto and diesel engines. Standard hydrogen refueling takes less than 5 minutes, providing a distinct advantage over the current charge status of electric vehicles. While substantial progress has been made in recent years towards commercialization, challenges persist, particularly in terms of durability and cost. Further scientific research is needed to overcome these

barriers and advance fuel cell technology in the commercialization process. With the advantages PEM fuel cells offer to the automotive industry, an increased interest can be anticipated. The results of this study focus on examining existing issues in PEM fuel cells, such as the cost of catalyst materials like platinum, durability, and hydrogen production and storage. These analyses suggest that PEM fuel cells have the potential to play an effective role in the energy market and that solution strategies for current issues could enhance this potential.

References

- Alaswad, A., Omran, A., Sodre, J. R., Wilberforce, T., Pignatelli, G., Dassisti, M., ... & Olabi, A. G. (2020). Technical and commercial challenges of proton-exchange membrane (PEM) fuel cells. *Energies*, *14*(1), 144.
- Borup, R. L., Kusoglu, A., Neyerlin, K. C., Mukundan, R., Ahluwalia, R. K., Cullen, D. A., ... & Myers, D. J. (2020). Recent developments in catalyst-related PEM fuel cell durability. *Current Opinion in Electrochemistry*, *21*, 192-200.
- Empowering Automotive with Hydrogen. <https://hydroborpem.com/index.html>, 04.12.2023.
- Han, W., Zhang, G., Xiao, J., Bénard, P., & Chahine, R. (2014). Demonstrations and marketing strategies of hydrogen fuel cell vehicles in China. *international journal of hydrogen energy*, *39*(25), 13859-13872.
- İlbeyoğlu, S., Gürbüz, H., & Bayat, M. (2023, June). Hidrojen PEM Yakıt Hücresinin Performansını Etkileyen Faktörler ve Genel Bir Değerlendirme. In *International Conference on Pioneer and Innovative Studies* (Vol. 1, pp. 47-52).
- İnci, M., Büyük, M., Demir, M. H., & İlbey, G. (2021). A review and research on fuel cell electric vehicles: Topologies, power electronic converters, energy management methods, technical challenges, marketing and future aspects. *Renewable and Sustainable Energy Reviews*, *137*, 110648.
- Jadhav, A. J. A. (2020). Hydrogen fuel cell vehicle market by vehicle type (passenger vehicle and commercial vehicle) and technology (proton exchange membrane fuel cell, phosphoric acid fuel cells, and others). *Global Opportunity Analysis and Industry Forecast*.
- Karanfil, G. (2020). Proton değişim membran yakıt hücreleri: Termodinamiği, bileşenleri ve uygulama Alanları. *Mühendis ve Makina*, *61*(698), 57-76.
- Li, N., Cui, X., Zhu, J., Zhou, M., Liso, V., Cinti, G., ... & Araya, S. S. (2023). A review of reformed methanol-high temperature proton exchange membrane fuel cell systems. *Renewable and Sustainable Energy Reviews*, *182*, 113395.
- Madheswaran, D. K., Jayakumar, A., & Varuvel, E. G. (2022). Recent advancement on thermal management strategies in PEM fuel cell stack: a technical assessment from the context of fuel cell electric vehicle application. *Energy Sources, Part A: Recovery, Utilization, and Environmental Effects*, *44*(2), 3100-3125.
- Ndayishimiye, V., Zhang, X., Nibagwire, D., Simiyu, P., Dushimimana, G., & Bikorimana, S. (2019). Environmental benefits of modern power system and clean energy. In *E3S Web of Conferences* (Vol. 107, p. 02006). EDP Sciences.
- Olabi, A. G., Wilberforce, T., & Abdelkareem, M. A. (2021). Fuel cell application in the automotive industry and future perspective. *Energy*, *214*, 118955.
- Satyapal, S. (2019). Hydrogen and fuel cell program overview. *2019 Annual Merit Review*, Crystal City, VA. Secondary Research. Expert Interviews, Analysis Markets and Markets Analysis. Automotive fuel cell market global forecast 2028; 2020.
- Van Vliet, O., Brouwer, A. S., Kuramochi, T., van Den Broek, M., & Faaij, A. (2011). Energy use, cost and CO₂ emissions of electric cars. *Journal of power sources*, *196*(4), 2298-2310
- Wang, Y., Diaz, D. F. R., Chen, K. S., Wang, Z., & Adroher, X. C. (2020). Materials, technological status, and fundamentals of PEM fuel cells—a review. *Materials today*, *32*, 178-203.

- Wang, Y., Yuan, H., Martinez, A., Hong, P., Xu, H., & Bockmiller, F. R. (2021). Polymer electrolyte membrane fuel cell and hydrogen station networks for automobiles: Status, technology, and perspectives. *Advances in Applied Energy*, 2, 100011
- Wilberforce, T., Rezk, H., Olabi, A. G., Epelle, E. I., & Abdelkareem, M. A. (2023). Comparative analysis on parametric estimation of a PEM fuel cell using metaheuristics algorithms. *Energy*, 262, 125530.
- Yue, M., Jemei, S., Zerhouni, N., & Gouriveau, R. (2021). Proton exchange membrane fuel cell system prognostics and decision-making: Current status and perspectives. *Renewable Energy*, 179, 2277-2294.

BLADE PITCH ANGLE CONTROL OF A WIND TURBINE WITH PI-PD DESIGNED WITH THE WEIGHTED GEOMETRIC CENTER METHOD

Abdullah TURAN

*Sirnak University, Sirnak Vocational School, Department of Mechanical and Metal Technologies, Sirnak-Turkey
(Responsible author) ORCID: 0000-0002-0174-2490*

Hebat GUNEL

*Sirnak University, Postgraduate Training Institute, Department of Energy Science and Technologies, Sirnak-Turkey
ORCID: 0009-0004-9446-2464*

ABSTRACT

The impact of renewable energy sources on the energy market is increasing. The most important of these resources is wind energy. At high speeds, the turbine and other critical components must be kept under control to avoid damage. In this study, a time-delayed PI-PD controller was designed using the weighted geometric center method (WGC) to control the blade pitch angle of a wind turbine. The design procedure is based on obtaining the stable region drawn using the stability limit curve on the controller parameters plane and calculating the WGC of this region. However, choosing the parameters that can provide the best system performance within this region is an important problem. The WGC method offers a very practical and useful solution to this problem. The advantage of the proposed PI-PD control design approach is that the resulting parameters are calculated numerically without using graphical methods or iterative optimization processes, thus ensuring closed-loop stability. Simulations were carried out in the MATLAB/Simulink environment. Here, the performance analysis of the method used was made by examining the unit step responses. According to the simulation results, it was observed that the PI-PD controller designed with the proposed adjustment technique was applied more successfully compared to the PI-PD controller designed with the Ziegler Nichols method on the blade pitch angle model of the wind turbine.

Keywords: PI-PD controller, weighted geometric center, wind turbine, blade pitch angle, time delay.

Introduction

Renewable energy sources are becoming more important day by day due to the depletion of conventional energy resources and their negative effects on the environment. One of the prominent energy sources among these sources is wind energy. Wind energy is a very environmentally friendly energy source, considering the reductions it causes in CO₂ emissions released into the atmosphere. Despite their high initial investment costs in the past, wind turbines are at the forefront in electrical energy production because these costs have decreased with developing technology and they do not require raw materials after production (Senel et al., 2015). There are some advantages to using wind energy. This energy has a recyclable feature, there is no transportation problem and it does not require very high technology for energy production. In addition, this energy source is found freely and abundantly in the atmosphere and does not cause environmental pollution. As long as the sun and the earth exist, wind energy must be converted into another form of energy in order to benefit from it. Wind turbines are used for this purpose (Ilkılıc et al., 2015). Wind turbines are examined in two groups, depending on their speed: fixed speed and variable speed. Variable speed wind turbines have advantages such as being able to be directly connected to the grid and having higher energy efficiency compared to fixed speed models (Koc, et al., 2011). The output power of the turbine in a fixed-speed wind power plant is constant, while the output power of a variable-speed wind turbine varies according to the air speed (Isık & Unal, 2020). It has been confirmed that the output power depends on variable wind speeds (Ciftci & Dursun, 2017). Wind power plants (RES) have been installed in many places around the world, but problems have occurred because they depend on the output power and variable wind speed. If the power produced by the wind turbine is not constant, there will be fluctuations in the grid. Controller is used to solve these problems and there are different controllers. In recent years, classical PID, fuzzy logic, etc. Many

studies have been investigated in which the pitch angle of the wind turbine is controlled using controllers (Civelek, 2013). PI-PD controllers are modifications of PID controllers and are often used to address special cases that better suit specific application needs. PI-PD controllers represent a different type of PID controllers, which are especially preferred in astable and holistic systems (Onat, 2019).

Many studies have been carried out in the literature to control the blade pitch angle. Classic PI (Hwas & Sougueh, 2022), PID controller (Karthik & Habibi, 2018; Ziegler & Nichols, 1942), fuzzy logic-based PI-PID type hybrid controllers (Civelek & Naik, 2020), which are modeling in uncertain and complex systems, are some of them.

It is important to ensure that the pitch angle remains at a certain value in certain wind conditions. The choice of PI-PD controller depends on the specified performance goals and the dynamic characteristics of the system. The PI part can help correct fixed errors in pitch angle, while the PD part can provide stability against rapid changes in pitch angle.

In this study, a PI-PD design procedure based on the WGC method is proposed for the blade pitch angle of the wind turbine. At the beginning of the procedure, the controller parameters region (proportional gain: k_f and derivative gain: k_d) that stabilize the inner loop with the PD controller and WGC were calculated. The inner loop was then reduced to a single block using PD control parameters. Finally, the procedure over the reduced model was repeated with the PI controller for the outer loop. Using the coordinates of the boundary points, the WGC points of the resulting stable region can be easily calculated. The advantage of the WGC method over other methods is that there is no need for any optimization process to numerically calculate the control parameters (Hamamci et al., 2006; Onat et al., 2021; Onat et al., 2017; Turan et al., 2019).

Materials and Methods

Wind turbine

Based on aerodynamic theories, the mechanical power produced by a wind turbine is expressed by Eq. (1) (Ghasemi et al., 2014).

$$P_w = \frac{1}{2} \rho A C_p(\lambda, \beta) v^3 \quad (1)$$

In this context, ρ represents the air density (kg/m^3), A represents the area covered by the wind turbine blades (m^2), and v represents the wind speed (m/s). $C_p(\lambda, \beta)$ is generally a non-linear wind turbine power coefficient and has been determined experimentally. One of the limits determined for the power coefficient (C_p) obtained according to Equation 2, which expresses the relationship between the wing tip-speed ratio (λ) and the wing pitch angle (β), is the Betz limit. This limit cannot exceed 59% of the maximum value of C_p (Garcia et al., 2012).

$$C_p(\lambda, \beta) = 0.5176 \left(\frac{116}{\lambda_i} - 4\beta - 5 \right) e^{-\frac{21}{\lambda_i}} + 0.0068\lambda \quad (2)$$

$$\frac{1}{\lambda_i} = \frac{1}{\lambda + 0.08\beta} + \frac{0.035}{B_3 + 1} \quad (3)$$

The wing tip-speed ratio (λ) represents the ratio of the wing angular speed to the wind speed, specified as in Eq. (4).

$$\lambda = \frac{W_t R}{v} \quad (4)$$

Here W_t is the angular velocity (rad/s) and R is the wing radius.

Actuator model

An electric or hydraulic drive system is needed to move the turbine blades along the target axis. In this study, wing dynamic behavior and wing angle of attack are assumed to be linear. A DC servo motor was used as the actuator and the position transfer function was given by Eq. (5). Here, the time delay is taken as 0.1 s.

$$G_p(s) = \frac{1}{s(s+1)} e^{-0.1s} \quad (5)$$

PI-PD controller design with weighted geometric center method

They differ at certain points, while PI-PD controllers are similar to PID controller structures. PID controllers have some structural limitations in providing the desired performance in the control of astatic, integrative and resonant systems. On the other hand, PI-PD controllers tend to provide very successful results in such systems (Tan, 2009). While PID controllers contain three parameters, the PI-PD controller structure has four parameters. The inner loop with PD feedback provides better positioning of the poles, improving the transfer function and response of the system in (Figure 1). Then, in the second cycle with the PI controller, the system performance is tried to be reduced to the target level. Thanks to the inner loop with PD feedback, the open loop instability is corrected, thus the stable open loop poles are brought to the appropriate position (Tan, 2009). Therefore, the PI-PD controller structure is advantageous over classical PID controllers.

PI-PD controllers represent a control structure that provides effective results in the control of stable, unstable, integrative and resonant processes. Therefore, it is important to obtain stable coefficients that make the system stable with these controllers (Kaya, 2003). However, the selection of appropriate parameters for the system within the stable region is still a critical issue that requires research. This study offers a practical solution based on the (k_f, k_d) and (k_p, k_i) planes on the stability limit curve. The stability limit curve, which varies depending on controller parameters and frequency, is the focus of this study. For example, the notation $l(k_f, k_d, \omega)$ expresses the stability limit curve in the (k_p, k_i) plane. Since the stability boundary curve depends on ω , ω can vary from 0 to ∞ . However, it has been shown in the study in which frequency range stable controller parameters can be found and the frequency range required for drawing can be assumed. Therefore, with the outlined method, all PI-PD parameters with which a control system can be stabilized can be quickly calculated. The effects of selected controllers on the performance of the system can be easily examined by using the WGC method in the calculated stable region. With this method, a simple PI-PD controller setting was made using the WGC method for time-delayed systems.

Obtaining stability regions for PI-PD controller

In the control system shown in (Figure 1), let $G_p(s)$ be defined as follows.

$$G_p(s) = \frac{N_p(s)}{D_p(s)} e^{-Ts} \quad (6)$$

$C_{PD}(s)$ and $C_{PI}(s)$;

$$C_{PD}(s) = k_f + k_d(s) \quad (7)$$

$$C_{PI}(s) = k_p + \frac{k_i}{s} = \frac{k_p(s) + k_i}{s} \quad (8)$$

It is in the form and refers to PD and PI controllers, respectively. Obtaining the PI and PD controller parameters that stabilize the given system constitutes the main problem.

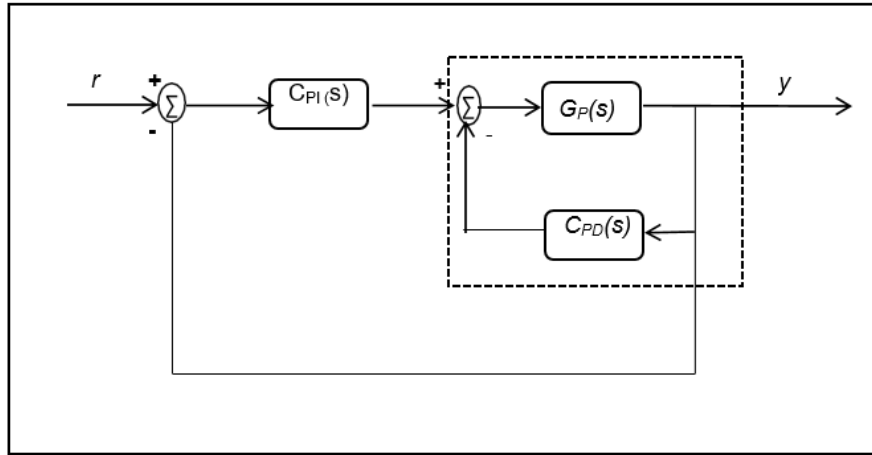


Figure 1. PI-PD control system

Stability region for PD controller

When we consider the first loop with PD controller in (Figure 1), the characteristic equation of this loop is obtained as follows.

$$\Delta_{PD}(s) = 1 + C_{PD}(s)G_P(s) \quad (9)$$

This expression can be written as follows using Eq. (6) and Eq. (7).

$$\Delta_{PD}(s) = D_P(s) + (k_f + k_d(s)N_P(s))e^{-Ts} \quad (10)$$

In the parameter space approach, there are three possible cases for the roots of a stable polynomial: Real root limit, infinite root limit and complex root limit.

By writing $s = j\omega$ in Eq. (6), the numerator and denominator of $G_P(s)$ can be written as follows (Tan, 2009).

$$G_P = \frac{N_{PE}(-\omega^2) + j\omega N_{PO}(-\omega^2)}{D_{PE}(-\omega^2) + j\omega D_{PO}(-\omega^2)} \quad (11)$$

In this case, the characteristic equation expression given in Eq.(10) can be written by dividing it into real and imaginary parts as follows.

$$\Delta_{PD}(j\omega) = [D_{PE} + (k_f N_{PE} - \omega^2 k_d N_{PO}) \cos(\omega T) + (\omega k_f N_{PO} + \omega k_d N_{PE}) \sin(\omega T)] + j[\omega D_{PO} + \omega k_f N_{PO} + \omega k_d N_{PE}] \cos(\omega T) + (-k_f N_{PE} + \omega^2 k_d N_{PO}) \sin(\omega T) \quad (12)$$

$$\Delta_{PD}(j\omega) = R_e + jI_m = 0 \quad (13)$$

When the real and imaginary parts are set equal to zero separately, as in Eq. (13), the following equations are obtained, respectively.

$$k_f(N_{PE} \cos(\omega T) + \omega N_{PO} \sin(\omega T)) + k_d(-\omega^2 N_{PO} \cos(\omega T) + \omega N_{PE} \sin(\omega T)) = -D_{PE} \quad (14)$$

$$k_f(N_{PO} \cos(\omega T) - \omega N_{PE} \sin(\omega T)) + k_d(-\omega^2 N_{PO} \sin(\omega T) + \omega N_{PE} \cos(\omega T)) = -\omega D_{PO} \quad (15)$$

Eq. (14) and Eq. (15) can be restated as follows.

$$k_f Q + k_d B = C$$

$$k_f M + k_d N = L \quad (16)$$

$$k_f = \frac{CN - LB}{QN - MB} \quad (17)$$

$$k_d = \frac{QL - MC}{QN - MB} \quad (18)$$

Here;

$$Q = N_{PE} \cos(\omega T) + \omega N_{PO} \sin(\omega T) \quad (19)$$

$$B = -\omega^2 N_{PO} \cos(\omega T) + \omega N_{PE} \sin(\omega T) \quad (20)$$

$$C = -D_{PE} \quad (21)$$

$$M = \omega N_{PO} \cos(\omega T) - N_{PE} \sin(\omega T) \quad (22)$$

$$N = \omega^2 N_{PO} \sin(\omega T) + \omega N_{PE} \cos(\omega T) \quad (23)$$

$$L = -\omega D_{PO} \quad (24)$$

It is in the form. If the above equations are substituted into Eq. (17) and Eq. (18), k_f and k_d are obtained as follows.

$$k_f = \frac{-(N_{PE} D_{PE} + \omega^2 N_{PO} D_{PO}) \cos(\omega T) + \omega (N_{PE} D_{PO} - N_{PO} D_{PE}) \sin(\omega T)}{(N_{PE}^2 N + \omega^2 N_{PO}^2)} \quad (25)$$

$$k_d = \frac{(\omega N_{PO} D_{PE} - \omega N_{PE} D_{PO}) \cos(\omega T) - (N_{PE} D_{PE} - \omega^2 N_{PO} D_{PO}) \sin(\omega T)}{\omega (N_{PE}^2 + \omega^2 N_{PO}^2)} \quad (26)$$

Using Eq. (25) and Eq. (26), the stability limit curve $I(k_d, k_f, \omega)$ can be drawn on the (k_d, k_f) plane. However, it should not be forgotten that the frequency value that makes the denominator of Eq. (25) and Eq. (26) zero will cause a discontinuity in obtaining the stability limit curve. However, this does not constitute an obstacle for the calculation of stable controllers (Tan, 2009). If present, the real root boundary and the infinite root boundary (k_d, k_f) can divide the parameter plane into stable and unstable regions. Therefore, after the stability limit curve $I(k_d, k_f, \omega)$ is obtained, it should be tested whether there are stable controller parameters (Tan, 2009). The real root limit $k_f = k_f(0)$ is obtained by writing $s = 0$ in Eq. (12) as in Eq. (27), and at $s = 0$ there is a real virtual root of $\Delta_{PD}(s)$ given by Eq. (10). Since it may exceed the axis, it is set equal to zero.

$$k_f = k_f(0) = -\frac{D_{PE}(0)}{N_{PE}(0)} \quad (27)$$

$$k_f = \frac{\omega (N_{PE} D_{PO} - N_{PO} D_{PE}) \sin(\omega T)}{(N_{PE}^2 + \omega^2 N_{PO}^2)} \quad (28)$$

In Eq. (26), the imaginary part is zero for $\omega=0$. The line is the limiter of the stability boundary curve so that the real part becomes equal to zero at $\omega=0$ (Tan, 2009).

In the transfer function of the system, as long as the degree of the denominator $D_P(s)$ is greater than the degree of the numerator $N_P(s)$ (which is usually the case), there will be no infinite root limit. The stability limit curve is obtained depending on $I(k_d, k_f, \omega)$. ω can vary from zero to infinity. As mentioned above, since the $k_f = k_f(0)$ line is the limiter of the stability boundary curve, the frequency below the positive real value of ω can be considered to satisfy Eq. (28) and If this positive real value of the frequency is called ω_a , drawing the stability boundary curve in the range $\in [0, \omega_a]$ will be sufficient to obtain the parameters (k_d, k_f) that provide stability.

Stability region for PI controller

If the closed-loop transfer function of the inner loop with PD feedback is expressed as $G_p(s)$ for the given system in (Figure 1), the equivalent block diagram of the system will be as shown in (Figure 2).

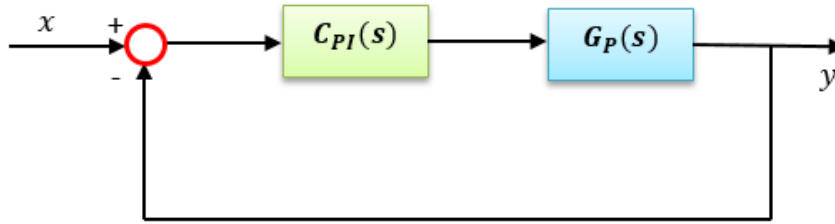


Figure 2. Reduced block diagram

$G_p(s)$ is obtained as in Eq. (29).

$$G_p(s) = \frac{N_p(s)}{D_p(s)} = \frac{N_p(s)e^{-Ts}}{D_p(s) + (k_f + k_d s)N_p(s)e^{-Ts}} \quad (29)$$

Here, when $s = j\omega$ is taken, $G_p(s)$ can be expressed as follows.

$$G_p(j\omega) = \frac{(N_{PE} + j\omega N_{PO})(\cos(\omega T) - j\sin(\omega T))}{\Delta_{PD}(j\omega)} \quad (30)$$

Here;

$$N_E = N_{PE}(\cos(\omega T) + \omega N_{PO} \sin(\omega T)) \quad (31)$$

$$N_O = N_{PE}(\cos(\omega T)) - \frac{N_{PE}(\sin(\omega T))}{\omega} \quad (32)$$

$$D_E = D_{PE} + (k_f N_{PE} - \omega^2 k_d N_{PO})\cos(\omega T) + (\omega k_f N_{PE})\sin(\omega T) \quad (33)$$

$$D_O = D_{PO} + (k_f N_{PO} + k_d N_{PE})\cos(\omega T) + \left(-\frac{k_f N_{PE}}{\omega}\right)\sin(\omega T) \quad (34)$$

are in the form.

Calculation of WGC Point

The proposed WGC method is based on two basic processes: calculating the control parameter region that makes the system stable using the stability boundary curve method and determining the WGC point of the stability area through the points that form the boundary curve of this region.

Step 1: For the PI-PD controller design consisting of two loops, the PD controller design is detailed in the first (inner) loop. Therefore, first of all, when the two equations with two unknowns (k_f , k_d) in Eq. (31) are solved depending on the frequency (ω) (rad/s), the stability limit curve of the PD controller system is obtained as in (Figure 3). Here, the real root boundary line formed by changing the system parameters is the line showing the location of the closed loop roots in the s plane. The selected frequency range (0, 20 rad/s) was sufficient to see the stable region.

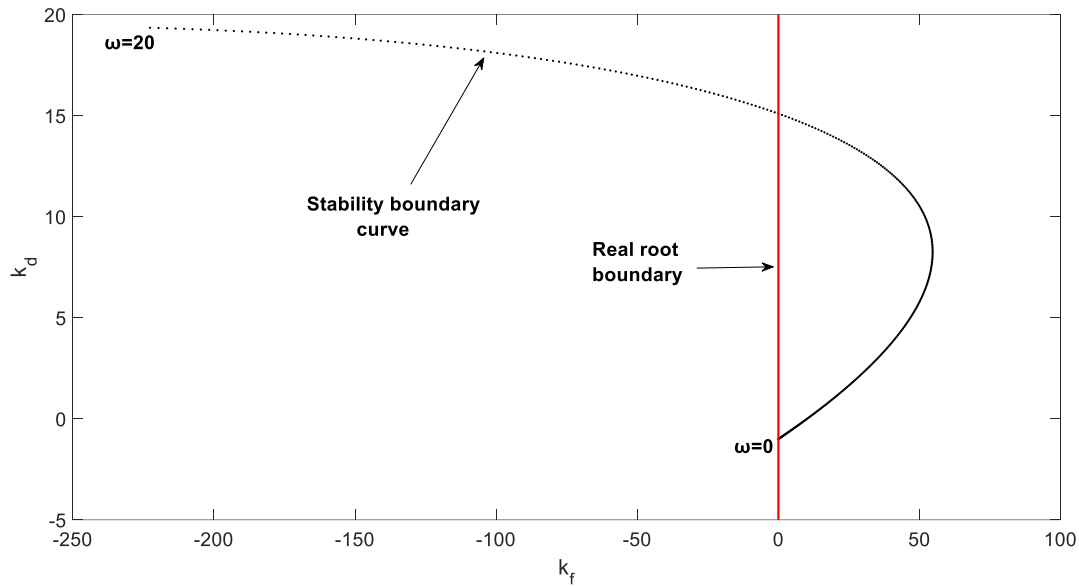


Figure 3. Real root boundary and stability boundary curve for ω (rad / s) [0 20]

In Figure (3), the stability region is obtained by randomly selecting points from different areas seen in the graph. The stability region with PD controller is given in (Figure 4).

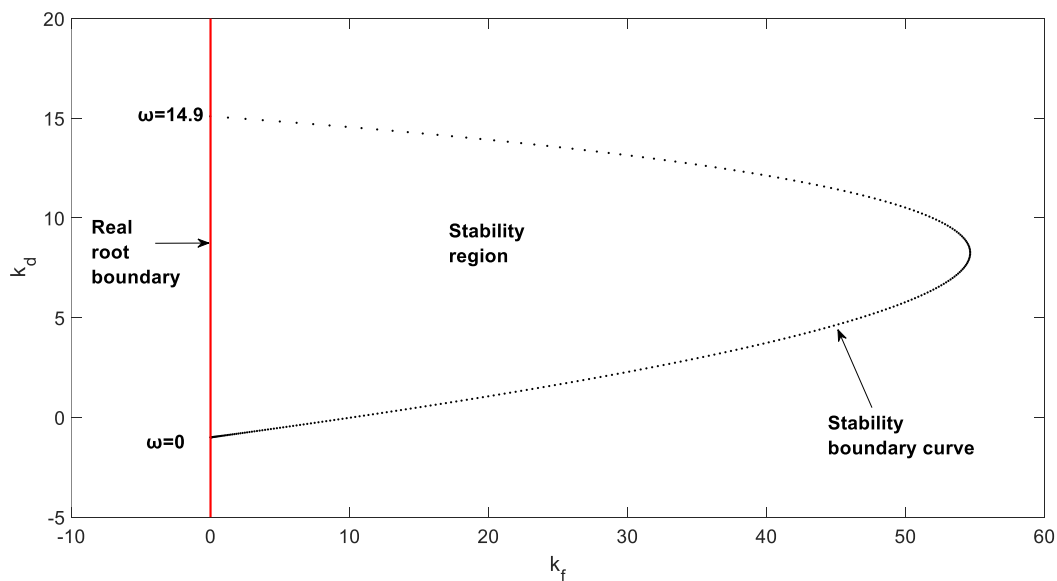


Figure 4. Stability region of the PD controller

In this process, k_f and k_d are calculated for each ω value and each w value is obtained in a different range. In Figure (4), the red line with $k_f = 0$ shows the boundary of the stable boundary curve. The closed stability region consists of m boundary position points expressed as $(k_{f1}, k_{d1}), (k_{f2}, k_{d2}), \dots, (k_{fm}, k_{dm})$ coordinates. Their reflection points to the real root line can be expressed as $(0, k_{d1}), (0, k_{d2}), \dots, (0, k_{dm})$ coordinates. In other words, the stability region is surrounded by $2 \cdot m$ points. $k_{f1} = 0$ can be considered independent of ω because the stability boundary curve is limited to the real root line $k_{f1} = 0$ (Onat, 2013).

As a result, using the coordinate values of the stability boundary curve points and their reflection points, the WGC points of the stable region are calculated using Eq. (35) and Eq. (36), is determined by (Figure 5).

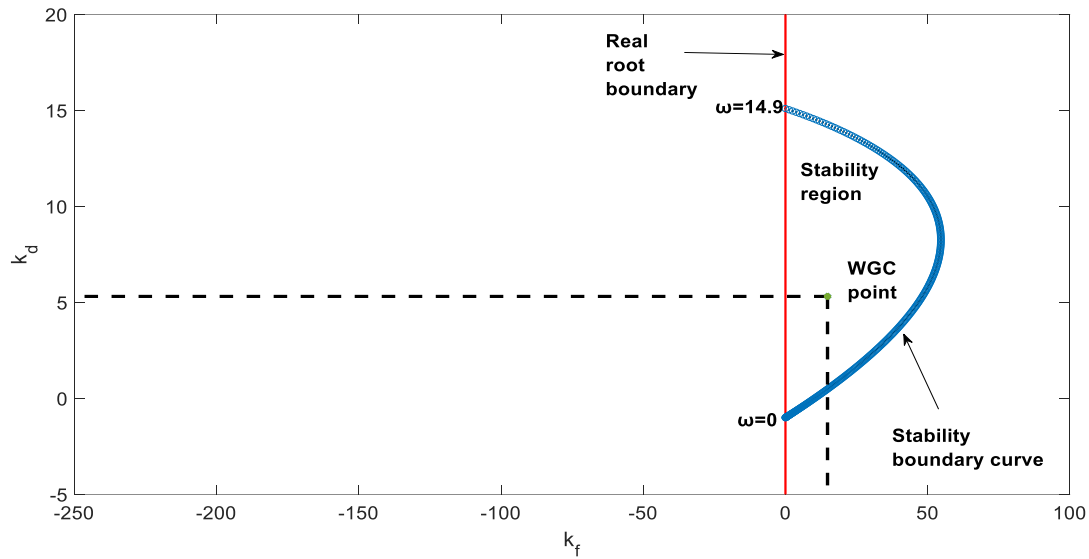


Figure 5. WGC point of PD controller

$$k_{dwgc} = \frac{1}{m} \sum_{i=1}^m k_{dj} \quad (35)$$

$$k_{pwgc} = \frac{1}{2m} \left[\sum_{i=1}^m k_{fj} + (0. m) \right] \quad (36)$$

Here ω is chosen in steps of 0.05. Step values may affect the result values. However, it does not have a significant effect on stability (Ozyetkin, et al., 2020). As a result, the WGC point of the PD controller is obtained as $(k_f, k_d) = (14.79, 5.312)$.

Step 2: The inner loop is reduced using the selected PD control parameters ($k_f = 14.79$, $k_d = 5.312$). Reduced inner loop transfer function is given in Eq. (36).

$$G(s) = \frac{N(s)}{D(s)} = \frac{G_P(s)}{1 + G_{PD}(s)G_P(s)} = \frac{N_P(s)D_{PD}(s)e^{-\tau s}}{D_P(s)D_{PD}(s) + N_{PD}(s)N_P(s)e^{-\tau s}} \quad (37)$$

The stability region is obtained for the PI controller by means of the reduced transfer function in the k_p - k_i plane. PI controller parameters can also be obtained using the given procedure for calculating the C_{PD} parameters. The application of $s = j\omega$ change to the characteristic equation of the outer loop is given in Eq. (38).

$$\Delta_{PI}(j\omega) = D(j\omega)D_{PI}(j\omega) + N(j\omega)N_{PI}(j\omega)e^{-j\tau\omega} = 0 \quad (38)$$

If Δ_{PI} is decomposed into its virtual and real parts;

$$\Delta_{PI} = R_{\Delta,PI} + I_{\Delta,PI} = 0 \quad (39)$$

If the procedure described above to obtain the PD controller parameters is also used to obtain the PI parameters, the following equations are obtained. Figure (6) shows the area created by the stability boundary curve and a zoomed view of this area.

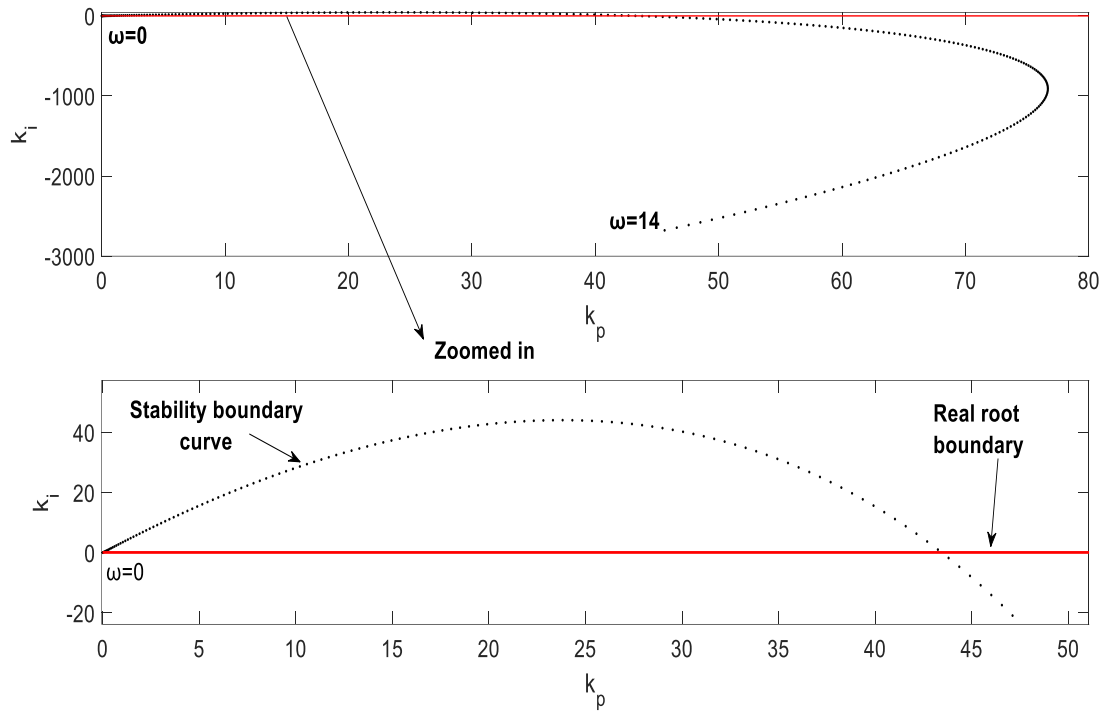


Figure 6. Real root boundary and stability boundary curve for ω (rad / s) [0 14]

By solving the set of (linear) equations depending on the frequency (ω), the stability region as in (Figure 7) and WGC are determined by plotting the obtained k_p and k_i parameters in the $k_p - k_i$ plane in (Figure 8). It is a fact that choosing ω with a smaller step size (eg 0.05 also results in larger m values) will allow us to get more accurate results than with a larger step size. Thus, the WGC point of the PI controller is obtained as $(k_p, k_i) = (7.96, 23.7)$.

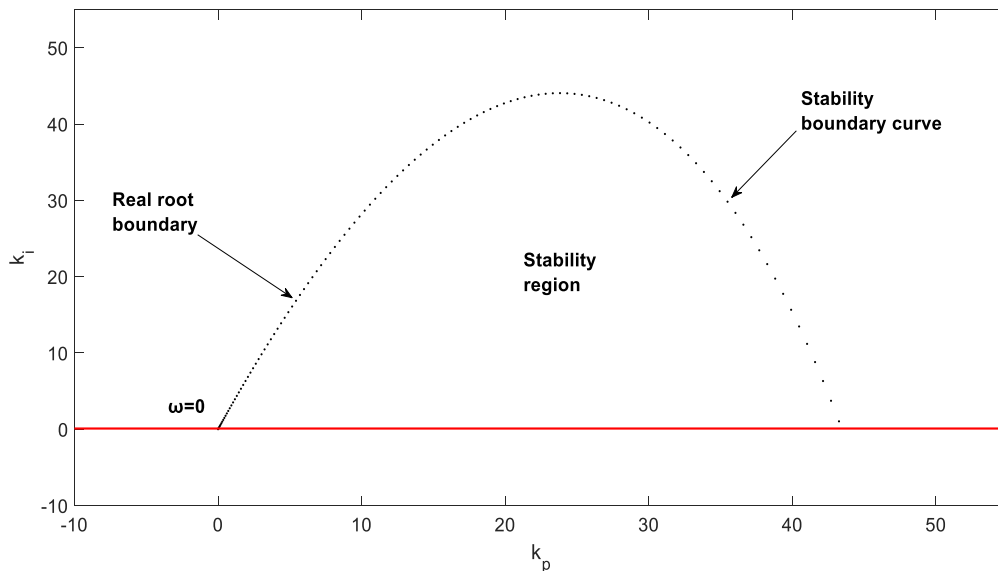


Figure 7. Stability region of the PI controller

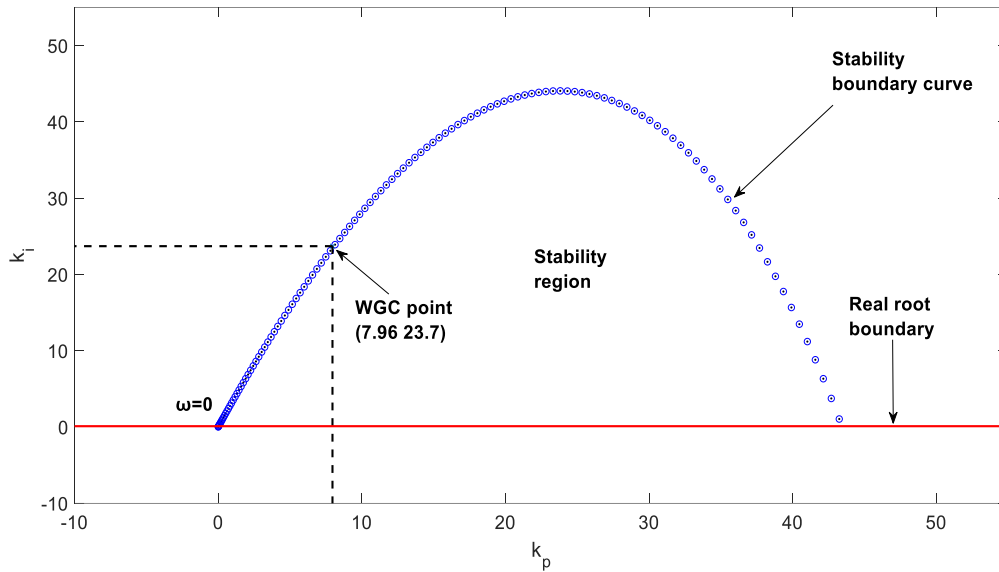


Figure 8. WGC point of PI controller

Simulation Results

In the simulations carried out in the Matlab/Simulink environment, the unit step responses of the PI-PD controller designed with the proposed method were analyzed. Figure (9) shows the answers of the PI-PD controller designed with the WGC method and the PI-PD controller designed with the Ziegler-Nichols method. It is clearly seen that the settling time is less and there is no maximum overshoot in the PI-PD controlled response designed with the proposed method. Therefore, it is understood that the proposed method gives very good results for the blade pitch angle model of the time-delayed wind turbine.

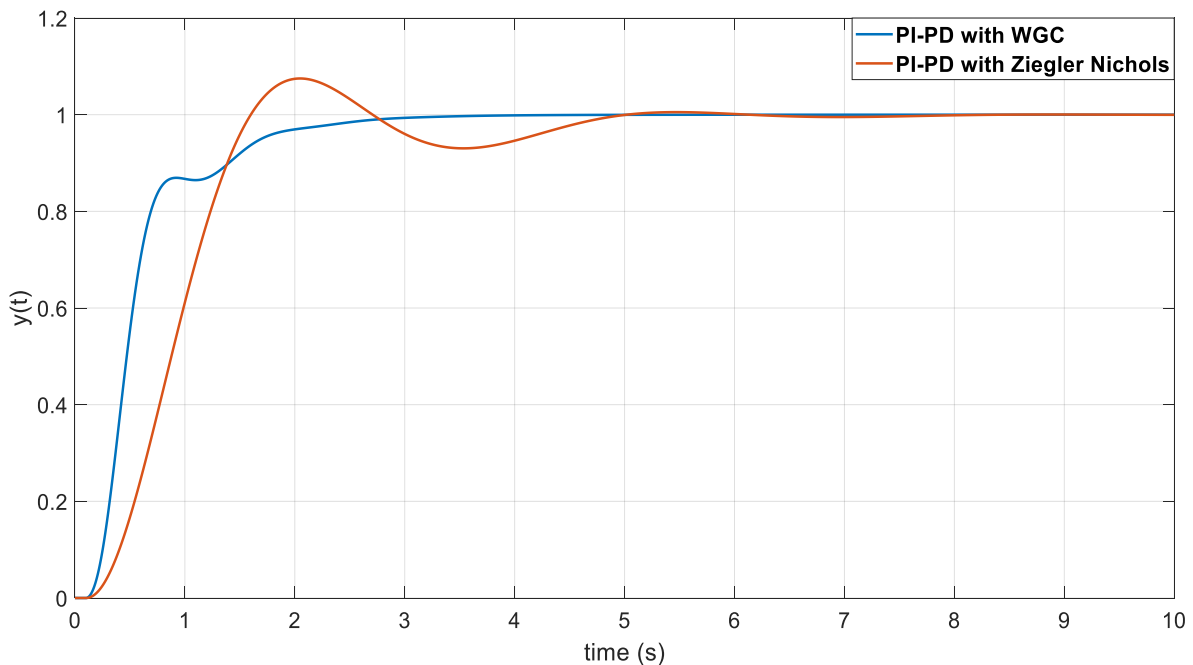


Figure 9. Unit step response of the system

Conclusion

In this study, a time-delayed PI-PD controller was designed using the WGC method to control the blade pitch angle of a wind turbine in order to keep the turbine and other critical components under control at high speeds to prevent damage. The advantage of the proposed PI-PD control design approach is that the resulting parameters are calculated numerically without using graphical methods or iterative optimization processes, thus ensuring closed-loop stability. The proposed method does not use any cyclic optimization algorithm. The fact that the method allows the controller parameters to be calculated numerically through the model offers a nice numerical solution to control engineers, especially for practical applications. According to the simulation results, it is seen that more successful results are obtained with the PI-PD controller designed with the proposed method for the blade pitch angle model of the wind turbine with the targeted delay time, compared to the PI-PD controller designed with the Ziegler-Nichols method.

References

- Ali, H. I. & Saeed, A. H. (2016). Robust PI-PD controller design for systems with parametric uncertainties. *Engineering & Technology Journal*, 34, p.2167-2173.
- Civelek, Z. (2013). Bulanık PID kontrolör ile rüzgâr türbininin hatve açısının kontrolü (M.S. thesis). Kırıkkale University.
- Civelek, Z., Lüy, M., Çam, E. & Barışçı, N. (2016). Control of pitch angle of wind turbine by fuzzy PID controller. *Intelligent Automation & Soft Computing*, 22(3), 463-471.
- Çiftçi, A. & Dursun, M. (2017). Değişken hızlı rüzgâr türbinlerinde kullanılan sürekli mıknatıslı senkron generatörün maksimum güç izleme algoritması ile vektör kontrolü. *Düzce Üniversitesi Bilim ve Teknoloji Dergisi*, 5(2), p.356-369.
- Garcia-Sanz, M. & Houpis, C. H. (2012). *Wind Energy Systems: Control Engineering Design*. Taylor & Francis Group CRC press. Boca Raton, Florida, USA, 613s.
- Ghasemi, S., Tabesh, A. & Askari-Marnani, J. (2014). Application of fractional calculus theory to robust controller design for wind turbine generators. *IEEE Transactions on Energy Conversion*, 29(3), 780-787.
- Habibi, H., Nohooji, H. R. & Howard, I. (2018). Adaptive PID control of wind turbines for power regulation with unknown control direction and actuator faults. *IEEE Access*, 6, 37464-37479.
- Hamamci, S. E. & Tan, N. (2006). Design of PI controllers for achieving time and frequency domain specifications simultaneously. *ISA transactions*, 45(4), p. 529-543.
- Hwas, A. & Katebi, R. (2012). Wind turbine control using PI pitch angle controller. *IFAC Proceedings Volumes*, 45(3), 241-246.
- İlkılıç, C. & Aydın, H. (2015). Wind Power Potential and Usage in the Coastal Regions of Turkey. *Renewable and Sustainable Energy Reviews*, 44, p. 78-86.
- İşik, E. & Ünal, O. (2020). Rüzgâr Türbini Kanat Tasarımı ve Analizi. Makina mekanik tasarım projesi. Kocaeli Üniversitesi, Kocaeli, Türkiye.
- İlkılıç, C. (2009). Türkiye’de Rüzgâr Enerjisi Potansiyeli ve Kullanımı. *Mühendis ve Makine Dergisi*, 50(593), p.26-32.
- Karthik, R., Hari, A. S., Kumar, Y. P. & Pradeep, D. J. (2020). Modelling and control design for variable speed wind turbine energy system. *International Conference on Artificial Intelligence and Signal Processing (AISP)*, IEEE, 1-6.
- Kaya, İ. (2003). A PI-PD controller design for control of unstable and integrating processes. *ISA transactions*, 42, p.111-121
- Koç, E. & Güven, A. N. (2011). Değişken Hızlı Rüzgâr Türbinlerinin Modellenmesi ve Arıza Sonrası Sisteme Katkı Yeteneklerinin İncelenmesi/Modeling and Investigation of Fault Ride Through Capability of Variable Speed Wind Turbines. *EMO Bilimsel Dergi*, 1(1), p.51-55.

- Naik, K. A., Gupta, C. P. & Fernandez, E. (2020). Design and implementation of interval type-2 fuzzy logic-PI based adaptive controller for DFIG based wind energy system. *International Journal of Electrical Power & Energy Systems*, 115, 105468.
- Onat, C. (2019). "A new design method for PI–PD control of unstable processes with dead time," *ISA transactions*, 84, p. 69-81.
- Onat, C., Daşkın, M., Turan, A. & Özgüven, Ö. (2021). Manyetik Levitasyon Sistemleri İçin Ağırlıklı Geometrik Merkez Yöntemi ile PI-PD Kontrolcü Tasarımı. *Mühendis ve Makina*, 62(704), p.556-579. <https://doi.org/10.46399/muhendismakina.877649>.
- Onat, C., Daşkın, M. & Turan, A. (2017). WGC Based PID Tuning Method for Integrating Processes with Dead-time and Inverse Response. *International Conference On Mathematics And Engineering* 10-12 May, 2017 Istanbul, Turkey.
- Onat, C., Sahin, M. & Yaman, Y. (2013). Optimal Control of a Smart Beam by Using a Luenberger Observer. In *ICEAF III, 3rd International Conference of Engineering Against Failure*, June, 26, 2013 28.
- Ozyetkin, M.M., Onat, C. & Tan, N. (2020). PI-PD controller design for time delay systems via the weighted geometrical center method. *Asian Journal of Control*, Vol:22, No:5 p. 1811-1826.
- Sougueh, I. M. & Görel, G.(2022). PI, PID ve GA-PID Kontrolör ile Rüzgâr Türbinin Kanat Hatve Açısı Kontrolü. *International Journal of Engineering Research and Development*, 14(2), p.502-513.
- Şenel, M. C. & Koç, E. (2015). Dünyada ve Türkiye’de rüzgâr enerjisi durumu-genel değerlendirme. *Mühendis ve Makina*, 56(663), p.46-56.
- Turan, A., Onat, C. & Sahin, M. (2019). Active Vibration Suppression Of A Smart Beam Via PID Controller Designed Through Weighted Geometric Center Method. *10th Ankara International Aerospace Conference*. 18-20 September, 2019 METU, Ankara, Turkey.
- Ziegler, J. G. & Nichols, N. B. (1942). Optimum settings for automatic controllers. *Transactions of the American Society of Mechanical Engineers*, 69(8), 759–765.

THE ROLE AND IMPORTANCE OF COAL IN ENERGY PRODUCTION**Edip TASKESEN**

*Dr., Sirnak University, Faculty of Engineering, Department of Energy systems Engineering, Sirnak-Türkiye
ORCID: 0000-0002-3052-9883*

Ruzgar ÜREN

*Mr., Sirnak University, Postgraduate Education Institute, Department of Energy Science and Technologies, Sirnak-Türkiye
(Responsible Author) ORCID: 0000-0002-0313-9337*

Selman İLBEYOĞLU

*Mr., Sirnak University, Postgraduate Education Institute, Department of Energy Science and Technologies, Sirnak-Türkiye
ORCID: 0009-0006-5374-7548*

Ceylan ÜREN

*Mrs., Sirnak University, Postgraduate Education Institute, Department of Energy Science and Technologies, Sirnak-Türkiye
ORCID: 0009-0004-0899-5089*

ABSTRACT

The relationship between the world economy and energy is well-known. The unquestionable importance and place of coal, a primary energy source preferred for centuries, are undeniable. However, the increasing shift towards renewable energy is causing a change in the points from which energy needs will be supplied. In this context, studies have been conducted on the changes in both Turkey and other countries. Emphasis has been placed on the cleaning, refining, and improvement of coal, especially. A general overview of the tar formed by organic substances through pyrolysis has been given by focusing on the fundamental components of the integration system. Along with coal reserves and production, global energy production and consumption have also been addressed. In addition to a general overview of coal and energy, its structure has been discussed. A literature review has been conducted along with coal processing and usage technologies. The gasification of coal and its significance, along with its place and importance in world energy, has been highlighted. Coal reserves, production, consumption, and responses to demands have been examined.

In conclusion, it has been observed that the place, importance, and structure of coal are significant factors for energy needs. The development of clean coal power plants such as Integrated Gasification Combined Cycle (IGCC) and ultra-supercritical (USC) power plants has increased the efficiency of coal-fired power plants while reducing emissions.

Keywords: Coal, Energy, Coal Gasification, Refined

Introduction

As known, there is a natural connection between the world economy and the energy used. The general trend of the world's energy and economy is tracked (Q. Wang et al., 2022). Coal has been one of the primary sources of energy for centuries and continues to be an important fuel for electricity generation and industrial processes. Despite the increasing interest in renewable energy sources, coal still plays a significant role in global energy consumption. However, its use has been scrutinized, particularly in terms of greenhouse gas emissions and air pollution, due to its environmental impact. In order to address these concerns, recent research has focused on developing new technologies to process and use coal more efficiently and exploring cleaner and more sustainable alternative energy sources.

Environmental concerns, whether related to the pollution of nature or political initiatives, have led to an increase in coal use in the Philippines. However, due to oppositional political steps, regional decisions have been made to completely ban its use in some areas like 'Bohol' (Delina, 2022).

In recent years, the ecological and environmental problems arising from the use of coal, oil, and other high-

carbon energy sources have become increasingly apparent. The intensive use of coal and other high-carbon energy sources is the main cause of the smog in London at the beginning of the 20th century and the serious smog and haze in China today. With the increasing demand for a green ecological environment, natural gas and new methods of obtaining energy as clean energy sources will take a higher share at the top of the list to be used as a primary energy source (Zou et al., 2016).

In addition to the increasing demand for a green ecological environment, the separation and utilization of waste plastics, specifically known as high-density polyethylenes, from medical waste as a fuel source are of great importance. Polyethylene plastics constitute nearly a quarter of the total waste plastics. The heightened health needs, especially during the Covid-19 pandemic, have led to an increasing amount of medical waste every day, becoming a significant environmental issue. Considering this information, the conversion of high-density polyethylenes into synthesis gas is not only important for energy production but also a crucial step in reducing waste.

Gasification, particularly the preference for Indian coals with ash content ranging from 20% to 40%, is common. Elevating the heating value of synthesis gas through gasification with suitable fuels is crucial (Aktan, 2020). In this context, Indian coals with low calorific values are ideal to produce low-value gas. Due to the natural structure of polyethylenes, they are volatile, resulting in higher carbon and hydrogen emissions in tar and gaseous forms (P. Sahu and P. Vairakannu, 2022) (Sahu & Vairakannu, 2022).

This study emphasizes the relationship and importance between the global coal economy and energy (TAŞKESEN et al., 2022). However, the increasing interest in renewable energy has altered the demand for energy sources. Studies on these changes have been conducted in Turkey and other countries. Information has been provided about the structure, cleaning, refining, and improvement of coal. Additionally, information has been given about coal reserves and global energy production and consumption. The study also includes a literature review on coal processing and usage technologies.

Overview of Coal and Energy

Coal reserves and production provide a general overview of the global distribution of coal reserves, as well as current production levels and trends. Different types of coal, such as anthracite, bituminous, and lignite, along with their respective characteristics and uses, can be discussed.

Global energy consumption and demand examine the overall energy demand worldwide, including the energy sources currently used to meet this demand. It may highlight different sectors with the highest energy consumption, such as industry, transportation, and buildings, and discuss factors influencing energy demand, such as population growth and economic development.

As known, new systems integrated into power plants are rapidly advancing. Thermal power plants frequently undergo operational adjustments, and updates continue to occur in both their systems and operating algorithms. One potential solution is to integrate energy storage. Specifically, molten salt systems with thermal storage are integrated into heat sources. Simulations have shown significant increases in thermal efficiency as a result of this integration (Figure 1). The effects of key system parameters, such as turbines, regenerative and molten salt heaters, and condensers, on system performance have been (Zhang et al., 2022).

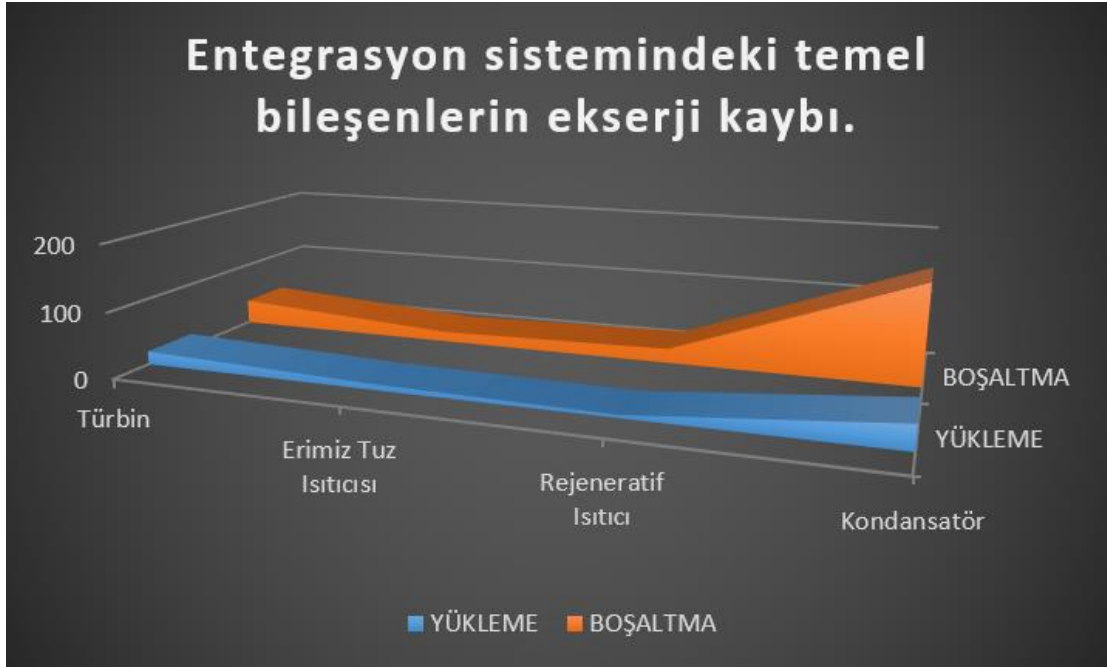


Figure 1. Exergy loss of the fundamental components in the integration system.

Tar is a black and sticky organic substance formed through the pyrolysis of organic materials (*Piroliz Nedir?*, 2023). These organic materials typically include plant-based materials such as bark, wood, or coal. The ultimate analysis of tar involves determining the chemical and physical properties of the organic and inorganic substances in its composition.

The ultimate analysis of tar (Figure 2) is carried out using analytical techniques such as gas chromatography, mass spectrometry, nuclear magnetic resonance spectroscopy, elemental analysis, and X-ray fluorescence spectroscopy. These techniques assist in the identification and determination of organic and inorganic components. The ultimate analysis of tar is crucial for determining its quality and intended uses. Additionally, it aids in assessing the impacts of tar on human health and the environment.

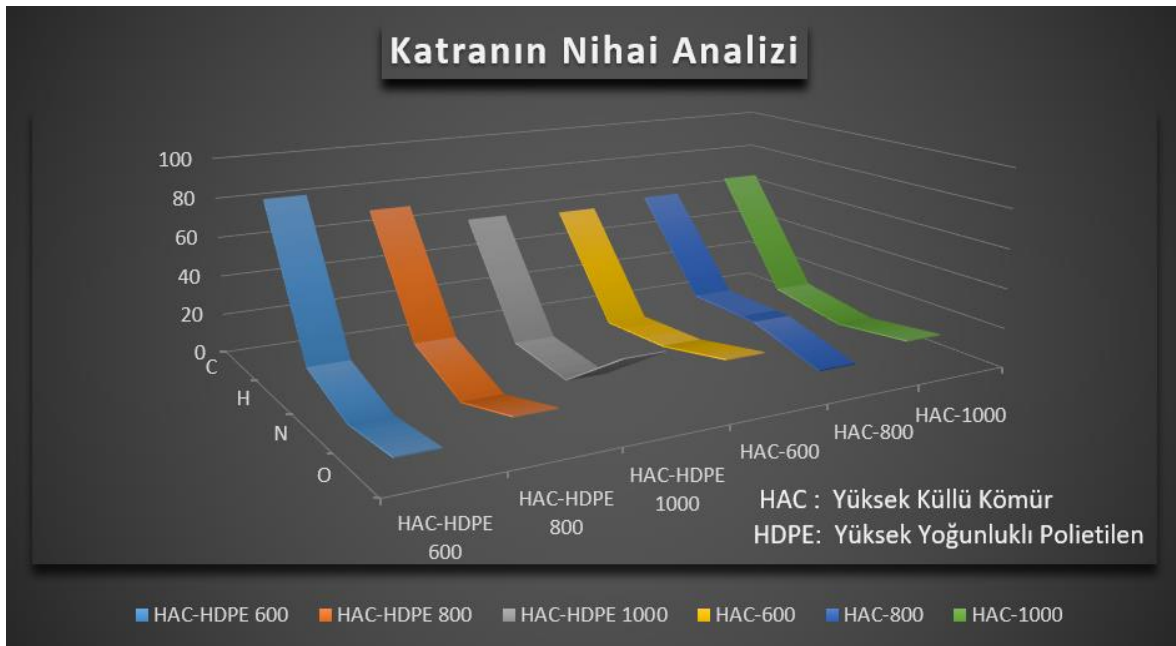


Figure 2. The ultimate analysis of tar.

Coal Reserves and Production

Coal reserves and production represent the quantity of coal located underground and the annual amount extracted and produced. This information is crucial for understanding the role of coal as an energy source and its potential future use.

Coal reserves denote the estimated quantity of coal known to exist underground and economically recoverable with current technology. Typically measured in tons or metric tons, these reserves can be categorized into different types such as anthracite, bituminous, and lignite based on geological and physical characteristics.

Coal production (*Coal*, 2021) signifies the amount of coal extracted from underground and processed for use. It encompasses mining, transportation, and processing activities, typically reported annually in tons or metric tons. Coal production can vary depending on factors such as market demand, technological advancements, and government policies. Coal reserves and production are important due to factors like meeting energy needs, industrial processes, and economic growth (Ali et al., 2018; *Coal*, 2021; TAŞKESEN et al., 2022). For instance, providing insights into how much coal is available and can be produced aids in energy planning and policy decisions. Additionally, it offers information for energy companies and other stakeholders to make investment decisions and provides an idea of market supply and demand for coal. Lastly, it can assist researchers and scientists in developing more efficient and sustainable new technologies and strategies for coal processing and usage (Ali et al., 2018; *Yenilenebilir Enerji Kaynakları Nelerdir*, 2018; Zou et al., 2016).

Global Energy Consumption and Demand

Global energy consumption and demand refer to the total amount of energy consumed worldwide, and the energy sources used to meet this demand. Understanding patterns and trends in global energy usage is also important (Ali et al., 2018).

Energy consumption (Ali et al., 2018) represents the total amount of energy used by various sectors such as industry, transportation, buildings, and residences to provide power for different activities and services. This energy can take the form of electricity, fossil fuels, renewable energy sources, or other types of energy. Global energy consumption has been rapidly increasing in recent years due to factors such as population growth, urbanization, economic development, and technological advancements (Ali et al., 2018; *Yenilenebilir Enerji Kaynakları Nelerdir*, 2018).

Energy demand refers to the amount of energy needed to meet this consumption and is influenced by various factors such as the type of economic activities, the level of energy efficiency, and the availability and cost of different energy sources. The energy sources used to meet this demand can vary by country and region but generally include fossil fuels such as coal, oil, and natural gas, along with renewable energy sources like hydroelectric, wind, solar, and bioenergy (*Yenilenebilir Enerji Kaynakları Nelerdir*, 2018). Visual representations of renewable energy sources such as hydroelectric, wind, solar, and bioenergy are provided in Figure 3.



Figure 3. Renewable energy sources such as hydroelectric, wind, solar, and bioenergy (Ali et al., 2018).

Information about global energy consumption and demand is important for several reasons. Firstly, it can assist governments and international organizations in making energy policy decisions, as well as inform private sector investment decisions for energy companies and other corporate stakeholders. Additionally, it can aid researchers and scientists in developing new technologies, initiatives, and strategies for more efficient, sustainable, and environmentally friendly energy production and consumption. Finally, awareness and understanding of the challenges and opportunities related to global energy usage can help educate the public about the need for transitioning to a more sustainable energy system (Coal, 2021).

The Role of Coal in Energy Production, Gasification Techniques, and Reasons for Preferring Gasification

Coal serves as an example of sedimentary rocks consisting of inorganic and organic components (Aktan, 2020; ÖNAL, n.d.; TAŞKESEN et al., 2022). Its basic structure includes oxygen, hydrogen, and carbon, with trace amounts of nitrogen and sulfur. Throughout various periods in history, coal has been a dominant energy raw material, finding applications in our daily lives. It is considered in the chemical industry for products ranging from dyes to pharmaceuticals, fertilizers, and plastic raw materials. Gasification, the process of reacting the carbon in coal with gasification agents to obtain gas products, is employed for various purposes (Yan et al., 2022).

One of the most effective strategies is gasifying coal under specific conditions, which proves to be an efficient way to increase the conversion rate of coal. The fundamental principle is to gasify coal with the least processing to achieve the highest heat efficiency possible, serving its purpose. There are various gasification processes for coal, such as fixed-bed gasification, fluidized-bed gasification, Lurgi gasifier, Winkler fluidized-bed gasifier, and Westinghouse fluidized-bed gasifier (Aktan, 2020).

Particularly, underground gasification methods offer a key advantage by minimizing the need for human labor in producing low-calorific-value gas. This allows the utilization of coal beds that are not economically feasible to extract for this purpose. One of the reasons for the preference of underground gasification methods for these fossil fuels (Figure 4) is the ability to burn coal in its own bed and convert it into industrially usable gas (Ali et al., 2018; Canel, 1986).



Figure 4. The role and place of fossil fuels in energy production (Yan et al., 2022).

The separation of non-recyclable chemical waste materials (Ertaş & Güden, 2019) and their incineration, without causing harm to the environment, result in the production of synthetic gas called Specific Gravity Number (SGN). This synthetic gas can be utilized as an alternative fuel for the chemical industry, contributing to heat and electricity generation.

The fundamental composition, emphasizing the presence of oxygen, carbon, and hydrogen, along with small amounts of sulfur and nitrogen, has been highlighted. Regarding the diffusion of hydrogen from the structural elements, hypotheses and results related to geo (Yan et al., 2022) graphical storage have been explored (Keshavarz et al., 2022; C. Wang et al., 2022; Yan et al., 2022). The existence of numerous underground formations aside, having micro-porous structures capable of absorbing significant amounts of gas and releasing them when needed provides a substantial advantage. Due to this structure, coal is indicated as the most suitable among underground formations (Keshavarz et al., 2022; Yan et al., 2022).

Materials and Methods

Various polymerization methods are employed to produce polyethylene using different forms of ethylene. Polyethylenes are thermoplastics used in various products, with over 100 million tons of thermoplastic resins produced annually. These resins, constituting 34% of the plastic market, are preferred in packaging areas, including geomembranes, plastic bags, plastic bottles, and plastic films (*Polyethylene*, n.d.).

The study simulated the spontaneous combustion of coal, subjecting it to heating and cooling processes under different oxygen concentrations. Additionally, analyzed parameters included oxygen concentration, air supply, coal temperature, gas production rate, oxidation kinetics, and index gases. Based on the data obtained from these analyses, it was observed that the heating and cooling processes did not overlap in terms of hot spot mobility. One of the results obtained from the analyses is that oxygen consumption is much higher in cooling than in heating, indicating that coal actively captures oxygen very strongly (C. Wang et al., 2022).

There are fundamental studies in the literature regarding the diffusion of hydrogen in the structure of coal. Hydrogen adsorption measurements at 13 bars equilibrium pressure and at temperatures of 20, 30, 45, and 60 degrees Celsius (Figure 5) and coefficients at different temperatures have been observed (Keshavarz et al., 2022).

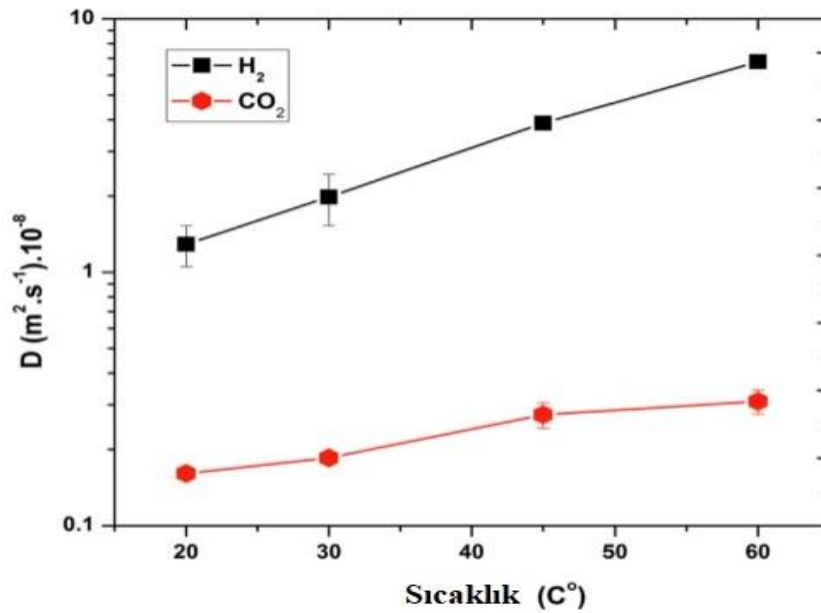


Figure 5. Hydrogen (H₂) and carbon dioxide (CO₂) diffusion coefficients at different temperatures (Keshavarz et al., 2022).

The diffusion rates of hydrogen and carbon dioxide were measured in processes at different temperatures on the same sample under common conditions, and an increase in temperature with constant pressure was observed (Keshavarz et al., 2022).

Global Position of Coal

In recent years, coal continues to hold a significant position in the energy sector, but it is gradually giving way to renewable energy sources. One notable development regarding the global position of coal is that, in 2021, the United Kingdom experienced a coal-free day in electricity generation for the first time. This marks the end of the coal era that began when the UK opened its first coal-fired power plant in 1882. Similarly, in 2020, China witnessed a decline in coal consumption for the first time, interpreted as a step towards the country's energy transition. Coal is the most abundant fossil energy worldwide, with a total amount exceeding 100 trillion tons. It is primarily distributed across three regions: Europe and Eurasia, Asia-Pacific, and North America (Figure 6). As of the end of 2014, proven coal reserves worldwide were 8915×10^8 tons (or 4457.5×10^8 feet). The coal reserves in Europe and Eurasia, Asia-Pacific, and North America account for 34.8%, 32.3%, and 27.5%, respectively. The United States has the most abundant coal reserves with 2373×10^8 tons, followed by Russia (1570×10^8 tons) and China (1145×10^8 tons) (*BP Weighs Ending Its 70-Year-Old Statistical Review of World Energy*, 2022).

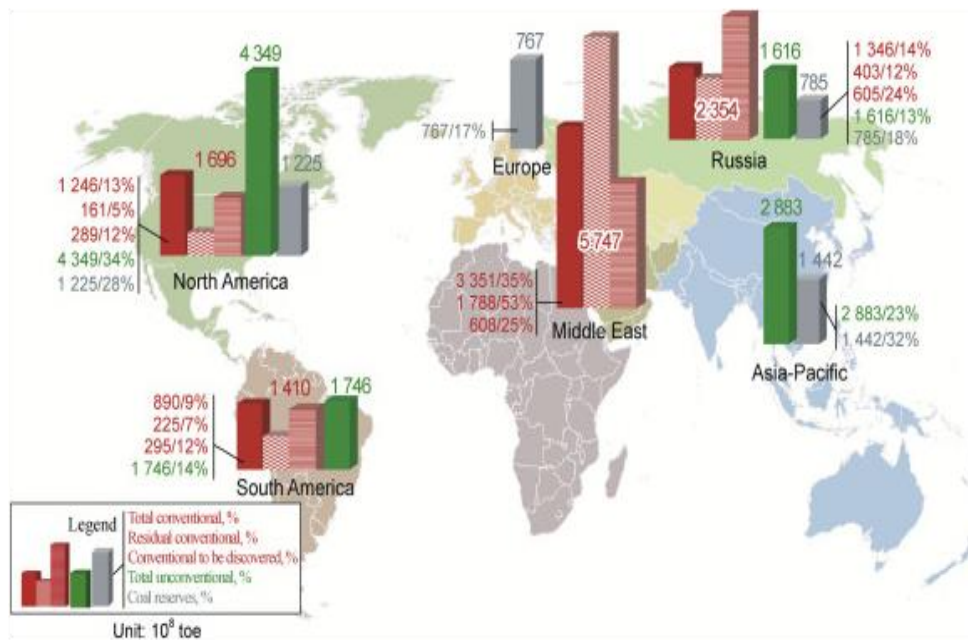


Figure 6. Distribution of global fossil energy (Zou et al., 2016).

The share of coal in the global primary energy mix will continue to decline, and the trend towards cleaner use of coal will become more pronounced (Zou et al., 2016). In 2014, global coal production was 8,165 million tons, a 0.7% decrease compared to the previous year, and global coal consumption increased by 0.4%, remaining at a level lower than the average of the past 10 years, at 2.9%. The share of coal in global energy consumption has decreased to 30.0%. Coal production and consumption in North America, Europe, and Eurasia are decreasing (Yang et al., 2011). For example, coal use in Europe has halved since 1990. Coal consumption in the United States has declined in recent years and accounted for approximately 23% in 2019. On the other hand, coal use in developing countries remains high and is rapidly increasing. Particularly in Asia, especially in China and India, coal use is still widespread and constitutes a significant portion of global coal demand. In conclusion, the position and use of coal worldwide vary by country and region. However, factors such as efforts to combat climate change and transition to renewable energy sources are expected to continue reducing the future importance of coal use.

Coal Processing and Utilization Technologies

Coal processing and utilization technologies (Aydin & Karakurt, 2009) have made significant progress in recent years with the development of new technologies aiming to improve the efficiency, sustainability, and environmental impact of coal mining, processing, and utilization. Coal processing refers to the methods used to clean, refine, and enhance coal, while coal utilization technologies refer to the ways in which coal is burned or otherwise used to generate energy.

One of the most important developments in coal processing is the advancement of enhanced coal cleaning technologies. Coal cleaning involves removing impurities from coal to improve its quality and reduce emissions when burned. Advanced coal cleaning technologies, such as dense medium cyclones, froth flotation, and magnetic separation, have been developed to clean coal more efficiently and effectively. These technologies employ advanced techniques to separate impurities from coal, resulting in a cleaner, higher-quality product.

Another significant development in coal processing is the improvement of coal upgrading technologies (*Temiz Kömür Teknolojileri*, n.d.). Coal upgrading includes processes that increase the energy content of coal or make it more suitable for specific applications. One example of coal upgrading is coal liquefaction, which involves converting coal into liquid fuels such as diesel and gasoline. Other coal upgrading technologies include coal gasification (Canel, 1986; ÖNAL, n.d.), which converts coal into synthesis gas that can be used

to produce various liquid fuels and chemicals, and coal-to-liquid (CTL) technologies (*Temiz Kömür Teknolojileri*, n.d.).

In addition to advancements in coal processing, there have been significant developments in coal utilization technologies (Aydın & Karakurt, 2009). For example, advanced coal-fired power plants designed to produce electricity more efficiently and with lower emissions have been developed. These power plants utilize advanced technologies such as ultra-supercritical steam cycles, operating at higher temperatures and pressures than traditional coal-fired power plants, leading to higher efficiency and lower emissions (Ali et al., 2018).

Results and Recommendations

In recent years, advancements in the coal and energy sectors have led to significant developments in energy production, storage, and utilization. The growing interest in renewable energy sources supports sustainability efforts and has prompted various technological innovations aimed at reducing carbon emissions. The global need to decrease greenhouse gas emissions, coupled with the increasing demand for energy worldwide, has driven the development of cleaner and more efficient coal technologies. Some of the notable advancements in the coal and energy field include high-efficiency, low-emission (HELE) coal technologies, carbon capture, utilization, and storage (CCUS) technologies, and the development of clean coal power plants. These technologies contribute to making coal a more sustainable and reliable energy source while reducing its environmental impact.

High-efficiency, low-emission (HELE) coal technologies have increased the efficiency of coal-fired power plants while reducing greenhouse gas emissions.

Carbon capture, utilization, and storage (CCUS) technologies have the potential to capture and store carbon dioxide emissions from coal-fired power plants.

The development of clean coal plants such as Integrated Gasification Combined Cycle (IGCC) and ultra-supercritical (USC) power plants has improved the efficiency of coal-fired power plants while reducing emissions. Coal can be converted into cleaner-burning fuels such as synthetic natural gas (SNG) and coal-to-liquid (CTL) through advanced coal conversion technologies.

The use of coal in electricity generation and industrial processes is expected to continue for many more years, making the development of cleaner and more efficient coal technologies crucial. Overall, recent developments in coal and energy have the potential to make coal a more sustainable and reliable energy source while reducing its environmental impact. These technologies will play a significant role in meeting the world's growing energy demands while addressing the issue of climate change.

References

Polyethylene. (n.d.). Wikipedia. <https://en.wikipedia.org/wiki/Polyethylene>

Aktan, M. (2020). Kömür gazlaştırma ürünlerinin gerçek opsiyonlar yöntemi ile değerlendirilmesi.

Ali, K. O. Ç., YAĞLI, H., Yıldız, K. O. Ç., & Uğurlu, İ. (2018). Dünyada ve Türkiye’de enerji görünümünün genel değerlendirilmesi. *Mühendis ve Makina*, 59(692), 86–114.

Aydın, G., & Karakurt, İ. (2009). YERALTI KÖMÜR DAMARLARINDAN ÜRETİLEN METANIN KULLANIM TEKNOLOJİLERİ. *Pamukkale Üniversitesi Mühendislik Bilimleri Dergisi*, 15(1), 129–136.

BP Weighs Ending Its 70-Year-Old Statistical Review of World Energy. (2022, December 6). *JPT Journal of Petroleum Technology*. https://jpt.spe.org/bp-weighs-ending-its-70-year-old-statistical-review-of-world-energy?gclid=Cj0KCCQjw2cWgBhDYARIsALggUhp98ySR_sGL3oKAgR290Mn6HISh2d6pZSuTNzr_15zui0JXjT1I-PgaAiaiEALw_wcB

Canel, M. (1986). Coal Gasification. *Scientific Mining Journal*, 25(2), 35–42. <https://www.acarindex.com/pdfs/1292779>

- Coal. (2021). Republic of Türkiye Ministry of Energy and Natural Resources . <https://enerji.gov.tr/bilgimerkezi-tabiiikaynaklar-komur>
- Delina, L. L. (2022). Coal development and its discontents: Modes, strategies, and tactics of a localized, yet networked, anti-coal mobilisation in central Philippines. *The Extractive Industries and Society*, 9, 101043.
- Ertaş, H., & Güden, M. A. (2019). Hastanelerde Tibbi Atık Yönetimi. *Sosyal Araştırmalar ve Yönetim Dergisi*, 1, 53–67.
- Keshavarz, A., Abid, H., Ali, M., & Iglauer, S. (2022). Hydrogen diffusion in coal: Implications for hydrogen geo-storage. *Journal of Colloid and Interface Science*, 608, 1457–1462.
- ÖNAL, G. (n.d.). Enerjide kömür'ün önemi.
- Piroliz Nedir? (2023). Enovon. <http://www.enovon.com.tr/teknolojilerimiz/piroliz-nedir/>
- Sahu, P., & Vairakannu, P. (2022). CO₂ based synergistic reaction effects with energy and exergy (2E) analysis of high density polyethylene with high ash bituminous coal for syngas production. *Fuel*, 311, 122500.
- TAŞKESEN, E., Şükürü, A., ERTUĞRUL, G., Fatih, A., DUMRUL, H., & BULBUL, S. (2022). Şırnak-Uludere bölgesinde yaygın olarak bulunan asfaltitlerden doğal hüyük asit elde edilebilirliğinin incelenmesi. *Politeknik Dergisi*, 25(2), 691–697.
- Temiz Kömür Teknolojileri. (n.d.). Türkiye Kömür İşletmeleri Kurumu (TKİ). Retrieved December 4, 2023, from <https://www.tki.gov.tr/temiz-komur-teknolojileri>
- Wang, C., Deng, Y., Zhang, Y., Xiao, Y., Deng, J., & Shu, C.-M. (2022). Coal oxidation characteristics and index gases of spontaneous combustion during the heating and cooling processes. *Fuel*, 307, 121806.
- Wang, Q., Yang, X., & Li, R. (2022). The impact of the COVID-19 pandemic on the energy market—A comparative relationship between oil and coal. *Energy Strategy Reviews*, 39, 100761.
- Yan, S., Qu, X., Xia, Z., Chen, C., & Bi, J. (2022). Effect of experimental variables on coal catalytic hydrogasification in a pressurized fluidized bed. *Fuel*, 307, 121761.
- Yang, Z., Zhang, J., Kintner-Meyer, M. C. W., Lu, X., Choi, D., Lemmon, J. P., & Liu, J. (2011). Electrochemical energy storage for green grid. *Chemical Reviews*, 111(5), 3577–3613.
- Yenilenebilir Enerji Kaynakları Nelerdir? (2018, February 2). *Ekolojist*. <https://ekolojist.net/yenilenebilir-enerji-kaynaklari-nelerdir>
- Zhang, K., Liu, M., Zhao, Y., Yan, H., & Yan, J. (2022). Design and performance evaluation of a new thermal energy storage system integrated within a coal-fired power plant. *Journal of Energy Storage*, 50, 104335.
- Zou, C., Zhao, Q., Zhang, G., & Xiong, B. (2016). Energy revolution: From a fossil energy era to a new energy era. *Natural Gas Industry B*, 3(1), 1–11.

ELECTROCHEMICAL ENERGY CONVERSION AND STORAGE SYSTEMS

Edip TAŞKESEN

*Dr., Sirnak University, Faculty of Engineering, Department of Energy systems Engineering, Sirnak-Türkiye
ORCID: 0000-0002-3052-9883*

Fatih ARLI

*Dr., Sirnak University, Faculty of Engineering, Department of Energy systems Engineering, Sirnak-Türkiye
ORCID: 0000-0002-0899-3460*

Hamza ALAHMAD

*Mr., Sirnak University, Postgraduate Education Institute, Department of Energy Science and Technologies, Sirnak-Türkiye
(Responsible Author) ORCID: 0000-0002-6261-3449*

Elif Nur BİLEN

*Mr., Sirnak University, Postgraduate Education Institute, Department of Energy Science and Technologies, Sirnak-Türkiye
(Responsible Author) ORCID: 0000-0002-7385-3704*

ABSTRACT

This study underscores the imperative of adopting clean energy technologies, particularly electrochemical systems, to meet escalating global energy demands and mitigate greenhouse gas emissions. Emphasizing the role of sustainable resources like wind and solar power, the paper explores the challenges posed by their intermittent nature and advocates for modifications in power generation and consumer behavior. It highlights the critical role of tailored materials in electrochemical systems and discusses ongoing research on basic-level candidate materials. The study delves into various applications of electrochemical energy technologies, including fuel cells, batteries, and capacitors, elucidating their classifications and working principles. In conclusion, the study posits that ongoing innovations in materials and technologies are integral to achieving a sustainable and efficient energy future.

Keywords: Electrochemical Energy, Fuel Cells, Energy Storage Systems, Batteries

1. Introduction

Given the surge in global energy requirements and increasing levels of greenhouse gases, the importance of adopting clean and eco-friendly energy technologies cannot be overstated. Sustainable resources such as wind and solar power will contribute to the resilience of domestic power networks. The incorporation of renewable energy will be pivotal in shaping the future energy landscape. As escalating amounts of sustainable energy become part of national electricity grids, a better comprehension of the intermittent nature's effects ensues. Modifications in power generation and intelligent meters enhance the efficiency of energy utilization. Tailored generators and grid providers are urging consumers to alter their energy consumption patterns. This transition underscores expenses and intensifies the need for energy storage. In the forthcoming years, electrochemical energy systems will assume a critical role in promoting sustainability, offering both heightened efficiency and reduced overall pollution.

In real-life applications, the limitations of energy solutions are now being noticed. Solutions based on single power generation or storage technologies often exceed current performance limits, and hybrid energy solutions are driving global demand. In this context, the importance of electrochemical energy technologies is increasing.

In electrochemical energy technologies, the electrode and electrolyte materials must have the necessary properties. Research at a basic level on candidate materials, composites and assemblies is ongoing, and practical materials must be carefully adapted to factors such as chemical stability, compatibility and affordability. At high temperatures, particularly above 500°C, issues such as gas tightness, interface

compatibility and stability become critical. These challenges should be solved by experimental studies and theoretical modelling, but when overcome, electrochemical energy technologies will have a variety of practical applications (Badwal et al., 2014).

Some electrochemical energy technologies developed in the past have been used in areas such as chemical sensors, energy efficiency, quality control, clean energy devices, energy storage, electrochemical reactors, smart windows, air separation membranes and supercapacitors (Guth et al., 2009; Stiegel et al., 2006; Yang et al., 2011). While technologies are optimised for cost, life and performance, they are in increasing demand for advanced electrochemical energy systems in areas ranging from transport vehicles to energy storage. New generation technologies such as high-efficiency fuel cells, membrane reactors, gas separation devices and hybrid energy systems have significant potential.

In this study, an overview of the technologies being addressed is presented and the challenges ahead of development are discussed.

2. Electrochemical Energy Conversion and Energy Storage Systems

Electrochemical energy conversion and storage systems are devices designed to transform chemical energy into electrical energy. Electrochemical capacitors and rechargeable (secondary) batteries are examples of the mechanisms responsible for this conversion, and the reversal of this process is possible. Fundamental electrochemical energy storage and conversion systems encompass electrochemical batteries, capacitors, and fuel cells. Commercial applications employ these systems based on performance metrics like energy density, power density, and cycle life.

Electrochemical energy conversion is a subject in the field of energy technology, and involves fuel cells and photoelectrochemical methods (Badwal et al., 2014). In addition, batteries and supercapacitors are also included in this technology area among electric storage devices. This is becoming increasingly important, especially in the context of automotive drive systems (Electrochemical Energy Conversion, 2011). Efforts have increased to develop stronger and longer-lasting batteries that allow longer operating times in electric vehicles (Electrochemical Energy Conversion, 2011; Juda, 2011). These systems will cover a wide range of Energy-conversion fuel cells and photoelectrochemicals.

Electrochemical energy storage encompasses diverse secondary batteries. The chemical energy within their active components is transformed into electrical energy via an electrochemical redox reverse process. Presently, batteries are manufactured for a broad spectrum of uses in various dimensions, generating energy from W to several hundred kW (as an illustration, one can juxtapose batteries for rapid chargers and batteries for large motorized vehicles or energy plants) (Krivik & Bac, 2013).

Based on the electrochemical systems employed, commonly available secondary batteries encompass traditional batteries (e.g., lead-acid, Ni-Cd), contemporary batteries (e.g., Ni-MH, Li-ion, Li-pol), unique batteries (e.g., lead-acid, Ni-Cd), Ag-Zn can be categorized into fundamental clusters like Ni-H₂), flow batteries (e.g., Br₂-Zn, vanadium redox), and elevated temperature batteries (e.g., Na-S, Na-metal-chloride) (Krivik & Bac, 2013).

2.1. Fuel Cells

The fuel cell is a power generation element that converts the chemical energy of an oxidant required for the realization of fuel supplied from outside the system and for the electrochemical reaction into usable energy such as electricity and heat (Bilen et al., 2022).

A fuel cell system consists of four units. These basic units are the fuel processing unit consisting of the power generation unit (fuel cell assembly module), the power conversion unit and the control unit assembly (Figure 1) (Bilen et al., 2022).

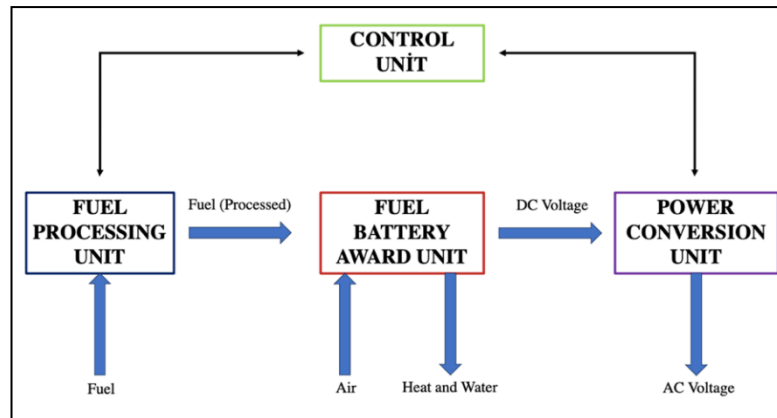


Figure 1. General structure and elements of the fuel cell system (Bilen et al., 2022).

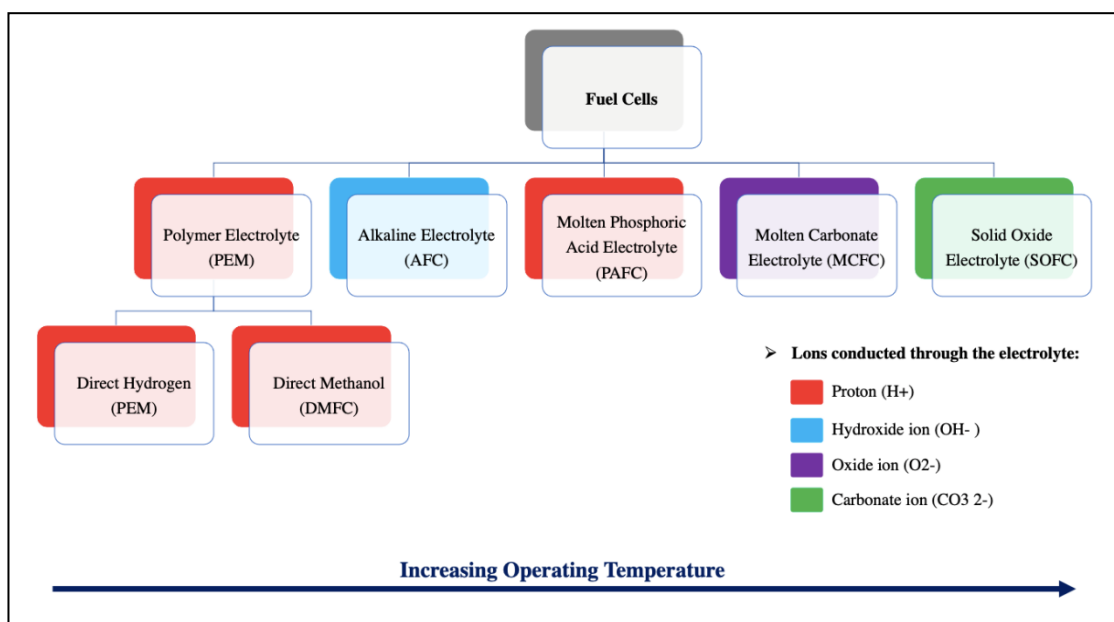
- **Fuel Processing Unit** The fuel processing unit is a unit in which hydrogen is purified and used directly from the used fuel if it is not used directly and is prepared before the fuel is sent to the fuel cell. It is the indirect feeding unit that is performed in three operations in the fuel-fed unit [11,14].
- **Power Generation System** can consist of more than one fuel cell module. It is the unit that produces electricity in the system [14,15].
- **Power Converter System** A unit that converts the direct current generated by a cell into a commercial alternating current. It is conditioned by a transducer or converted into alternating current [12,16,17].
- **Control System** The operation of the whole system is monitored and controlled by the control system. The most important controls at this point are; humidification, fuel/air flow control, fuel cell temperature control, voltage/current output control, waste heat-waste water control, refrigerant control, etc item. These include equipment such as fans, compressors, humidifiers and heat exchangers [13,14,15].

Many types of fuel cells are in development. They can be divided into two classes according to the working temperature range of fuel cells. These are; Low-temperature fuel cells and High-temperature fuel batteries. However, today, instead of this classification, fuel cells are classified according to the material from which the electrolyte part is made. This variety does not affect the basic principle of operation, but it makes a difference in performance, working conditions and application. These include the type of fuel and oxidant used, the preparation of fuel outside or inside the fuel cell (external reforming), the type of electrolyte, the working temperature, the type of fuel supply, etc. Includes [9,16,17]. The most common classification of fuel cells is based on the type of electrolyte used in the cell. According to this classification, there are seven types of fuel cells (Table 1) [18].

Table 1. Depending on fuel type, operating temperature and electrolyte (Badwal et al., 2014; Bilen et al., 2022).

Type Of Fuel Cell	Fuel	Electrolyte	Operating Temperature (°C)
Alkaline Fuel Cell (AFC)	H ₂ (Hydrogen)	KOH	50-90
Proton Replacement Membrane Fuel Cell (PEMFC)	NG (Natural Gas)	Polymer	0-125
Proton Replacement Membrane Fuel Cell (PEMFC)	H ₂ (Hydrogen)	Polymer	100–200
Fuel Cell Used Direct Methanol (DMFC)	CH ₃ OH (Methanol)	Sulfuric Acid or Polymer	50–120
Phosphoric Acid Fuel Cell (PAFC)	NG (Natural Gas)	Ortho Phosphoric Acid	190–120
Molten Carbonate Fuel Cell (MCFC)	NG (Natural Gas)	Li/K Carbonate Mixture	630–650
Solid Oxide Fuel Cell (SOFC)	NG (Natural Gas)	Stabilized Zirconium	900–1000
Direkt Carbon Fuel Cell (DCFC)	C (Carbon)	Stabilised Zirconia	500-1000

Various commercially accessible fuel cell systems, spanning a range of scales from a few watts (W) to megawatts (MW), are currently accessible, and their operational patterns, along with widely diverse performance attributes, have been examined in scholarly works (Badwal et al., 2014; Kulkarni & Giddey, 2012). Traditionally, these devices have been classified primarily based on the electrolyte type and subsequently on the fuel type employed. Further categorization of fuel cells can be undertaken considering the operational temperature, with polymer electrolyte membrane fuel cells (PEMFC) typically exhibiting the lowest operational temperatures, falling below 100 °C, while solid oxide fuel cells (SOFCs) manifest the highest operational temperatures, reaching around 800 °C or beyond (Refer to Figure 2).

**Figure 2.** Commercial or nearly commercial fuel cell systems are classified accordingly (Badwal et al., 2014).

Emerging fuel cell technologies defy conventional classifications due to diverse fuel handling systems and a departure from traditional electrolytes. Categorization based on fuel types, such as direct methanol, ethanol, or carbon fuel cells, proves more relevant for system design and application. However, ambiguity arises in classifying fuel cells based on operating conditions, where the fuel may be either gas or liquid. Figure 3 provides a color-coded fuel-based classification, indicating potential end-user applications.

Solid fuels appeal for their cost-effectiveness and abundance, while gaseous fuels offer transport advantages through pipe networks. Liquid fuels, less abundant but highly energy-dense, suit transport and mobile applications.

Within solid fuels, Microbial Fuel Cells (MFC) and Direct Carbon Fuel Cells (DCFC) hold the potential for a transformative impact on power generation and applications.

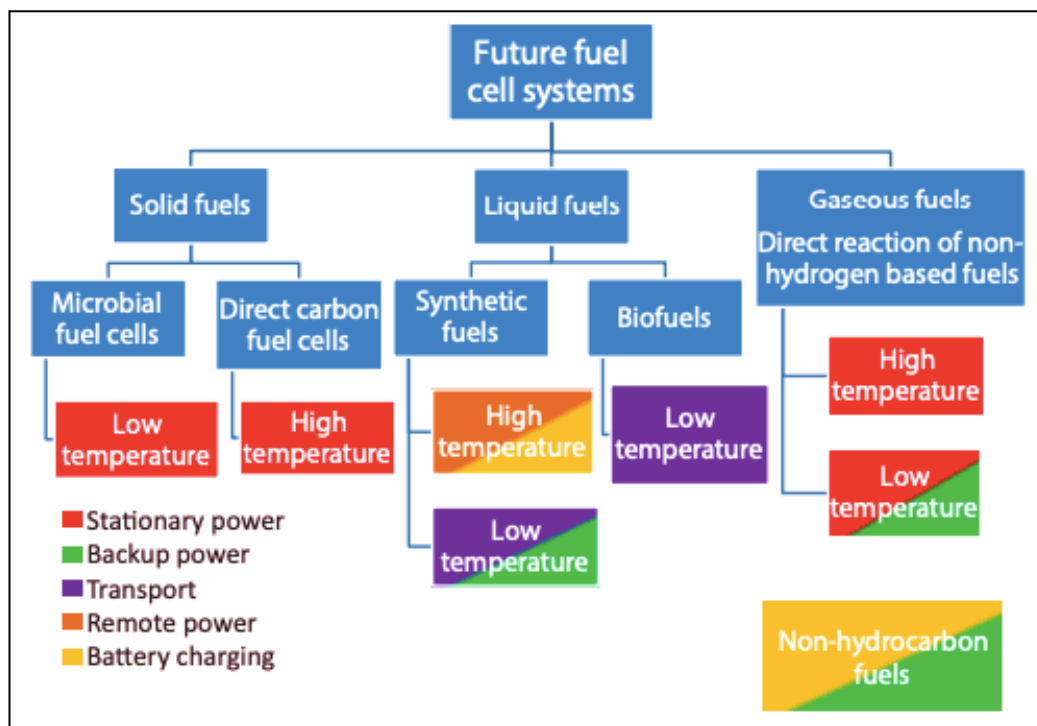


Figure 3. Future fuel cell systems can be categorized based on their classification (Badwal et al., 2014).

2.2. Electrochemical Energy Storage Technologies

Electrochemical energy devices are employed for transforming chemical energy into electricity. Throughout the conversion procedure, it experiences at least two typical chemical reaction sequences.

There are two main branches of electrochemical storage technologies. Electrochemical batteries and electrochemical capacitors (Carnegie et al., 2013). Depending on the design, structural characteristics, nature of the chemical reaction and electrochemical storage systems vary (Daniel & Besenhard, 2012). According to operating principles, electrochemical batteries and cells can be classified into 4 categories: primary cell or battery, secondary cell or battery, backup cell and fuel cell (Emeksiz & Burak, 2022). They are also classified depending on the types of chemicals used to make batteries (Şükran & Güngör, 2021).

Key application areas of electrochemical energy storage systems include transportation and micropower (fixed/portable) production, including the use of wind and solar power (Zhang et al., 2011).

Another helpful categorization relates to the extent of discharge; shallow or profound cycle batteries. Profound cycle batteries possess a thinner plate as composition, appropriate for renewable applications. The third categorization pertains to the nature of the electrolyte in the battery (water-imprinted or damp and leak-

resistant). Flooded or moist batteries are extensively employed in renewable applications. Sealed batteries come in two varieties: Gel and Absorbable Glass Mat for renewable applications (Emeksiz & Burak, 2022).

2.2.1. Batteries According to Working Principle

2.2.1.1. Primary Cell or Battery

Typically, recharging the primary battery is not feasible. The majority of initial cells utilize electrolytes found in absorptive materials or dividers (Emeksiz & Burak, 2022). Primary batteries with electrolytes can be categorized as aqueous and non-aqueous. Batteries with aqueous electrolytes contain water-based solutions. Zinc-Carbon and Zinc-Chloride, Alkaline Zinc-Manganese Dioxide, Zinc-Air, Zinc-Silver Oxide, and Zinc-Curve Oxide are examples of aqueous electrolyte batteries. The anhydrous electrolyte type includes Lithium-Tionyl Chloride, Lithium-Sulfuryl Chloride, Lithium-Sulfur Dioxide, Lithium-Mangan Dioxide, Lithium-Carbon Monofluoride, Lithium-Iron Disulfide, Lithium-Iodine, and Lithium-Silver Vanadium Oxide species.

2.2.1.2. Secondary Cell or Battery

A secondary cell or battery can be charged by passing through the circuit by moving in the opposite direction of the current during discharge (Emeksiz & Burak, 2022). Rechargeable battery systems are divided into two according to the type of electrolyte. They have both aqueous and anhydrous electrolytes, which are based on water and solvents, respectively. Aqueous electrolyte batteries are Lead Acid, Nickel-Metal Hydride, Nickel-Cadmium, and Alkaline Zinc-Mangan Dioxide. Waterless electrolyte batteries are Lithium Ion, Lithium Metal, Sodium Sulfur, Metal Air and Sodium Nickel Chloride (Kiehne, 2003; Root, 2011).

2.2.1.3. Backup Cell or Battery

The substitute cell or battery belongs to the primary battery category. They are commonly favoured for extended-term storage. The active components of the cell are segregated and quarantined until required (Emeksiz & Burak, 2022). Substituted batteries are fitted without electrolytes. By negatively impacting the efficiency of activated cells, they can be securely upheld under circumstances that may present a risk. The absent section of the batteries can be incorporated before utilization (Root, 2011).

2.2.1.4. Fuel Cell

They are devices that primarily produce electricity by using the chemical energy of hydrogen or another fuel to reveal the hidden chemical energy of a fuel and generate electrical energy (Emeksiz & Burak, 2022). The principle of operation of fuel cells is like batteries. However, they do not run out or need to be recharged. They generate electricity and heat when there is a fuel continuity.

2.2.2. Batteries According to the Type of Chemical Used

2.2.2.1. Lead Acid Batteries

It is the preferred type of battery in photovoltaic systems. They are the most important factor to prefer to be long-lasting and low cost. High maintenance costs and low energy densities are among the disadvantages. In addition, although the sulfuric acid in the structure creates a danger, there is a risk of explosion in case of overcharging of these batteries (Emeksiz & Burak, 2022).

2.2.2.2. Lithium-ion Batteries

Lead acid is the most preferred battery structure after batteries. Lithium-ion batteries can produce more voltage than older battery technologies. It is easy to destroy because it does not contain toxic substances. The possibility of damage to overheating and high voltages is among the disadvantages (Abraham, 2020).

2.2.2.3. Sodium-ion Batteries

They are the next generation of energy storage systems that are expected to replace lithium-ion batteries. However, sodium causes a disadvantage due to its heavy structure. Sodium ion batteries are not yet able to demonstrate sufficient properties in terms of commercial use (Emeksiz & Burak, 2022).

2.2.2.4. Nickel Cadmium Batteries

It is a battery technology that has been used for many years. It can produce a voltage up to 1.3 volts. Because the presence of cadmium in it poses a risk to environmental influences, there are problems with its destruction and recycling (Emeksiz & Burak, 2022).

2.2.2.5. NanoBolt Lithium Tungsten Batteries

As a result of the studies carried out in the new anode material, it has been observed that nano tubes formed with tungsten and carbon-coated multi-stratification technology for the binding of copper can reveal the possibility of a new battery. With its large surface technology, which allows for more connection of ions, it allows batteries to store more energy and charge faster (Emeksiz & Burak, 2022).

2.2.2.6. Redox Current Batteries

Hydrochloric and sulfuric acid were added to it and %70 higher density than Li-ion derivatives were observed. This type of battery has been used to store energy from wind turbines and solar panels. If applied to electric vehicles, it allows 1600 km of driving on a charge. These batteries offer lighter weight and higher energy storage (Emeksiz & Burak, 2022).

2.2.2.7. Aluminum Graphite Batteries

These batteries offer the possibility of charging at fairly high speeds. It has been seen that batteries developed at Stanford University can charge the phone in 60 seconds if used on smartphones. Only 1.5 V energy output can be provided in the prototype produced. This is insufficient for existing electronic devices. In case of a more useful form of use, it will be lighter, the energy capacity will be high and safe (Emeksiz & Burak, 2022).

2.2.2.8. Bioelectrochemical Batteries

These batteries use the oxidation method by producing acetic acid with the help of anaerobic bacteria. The work veri on it is still ongoing. The biggest advantage of this battery technology is that the bacteria in it constantly renew themselves and have an infinite life (Emeksiz & Burak, 2022). With bioelectrochemical battery technology, Microbial Fuel Cells are capable of handling the future inexhaustible battery capability (Emeksiz & Burak, 2022).

2.2.2.9. Organosilicon Electrolyte Batteries

Li-ion revealed that despite the risks of fire and explosion in electrodes in batteries, organosilicon-based solvents were used in batteries to eliminate the risks. This technology is still in the research phase and studies have gained momentum (Emeksiz & Burak, 2022).

2.2.2.10. Solid State Batteries

Solid-state drives (Solid State Drive-SSD) have revolutionized data storage technology with fast and secure data storage. Accordingly, this technology, which is considered in energy storage, promises serious changes in battery technology. Using the SSD battery, the heating problem is eliminated, eliminating the risk of fire and providing a lifetime possibility of use without loss of performance. Composed of ceramic, sulfate, glass and solid polymer components, these batteries have the potential to provide 2-10 times more energy intensity than Li-ion batteries in the future (Emeksiz & Burak, 2022).

2.2.2.11. Gold Nanocable Gel Electrolyte Batteries

The researchers, who coated the gold nanocables with manganese dioxide and put them in electrolytic gel, observed that they charged 200,000 times without any wear. Compared to the charging status of traditional batteries 6000 times, it is a very successful design (Emeksiz & Burak, 2022).

Conclusion and Recommendations

Electrochemical Energy Conversion and Storage Systems is an energy technology that is increasingly important today. Fuel cells are power generation elements that convert the chemical energy of fuel and oxidant provided by the external system into usable energy. This system mainly consists of four units: a fuel processing unit, a power generation unit (fuel cell assembly module), a power conversion unit and a control unit assembly.

- The fuel processing unit is a unit where hydrogen is purified from the fuel used before being sent to the fuel cell. The power generation system is the unit that produces electricity in the system. A power conversion system is a unit that converts the direct current produced by a cell into a commercial alternating current. The control system is a unit that monitors and controls the operation of the entire system. These controls include elements such as humidification, fuel/air flow control, fuel cell temperature control, voltage/current output control, waste heat-wastewater control and a coolant control.
- Various fuel cells are being developed and can be divided into two classes based on operating temperature range: low-temperature fuel cells and high-temperature fuel cells. However, nowadays, classification according to the material from which the electrolyte part is made is common. This diversity does not affect the basic operating principle, but differs in terms of performance, operating conditions and application.
- Electrochemical energy storage technologies are used to convert chemical energy into electrical energy. These storage systems can be examined in two main branches: electrochemical batteries and electrochemical capacitors. According to their operating principles, electrochemical batteries and cells can be divided into four categories: primary battery or battery, secondary battery or battery, backup battery and fuel cell. These systems can also be classified according to the substances used in battery chemistry.
- The main application areas of electrochemical energy storage systems include transportation and micropower generation (stationary/portable), wind and solar energy use. Storage systems can be classified as shallow or deep cycle batteries based on depth of discharge. Batteries containing water or wet and sealed, depending on the characteristics of the electrolyte, are widely used in renewable energy applications. There are two types of sealed batteries commonly used in renewable energy applications: gel and absorbable glass mat type.

As a result, electrochemical energy conversion and storage systems have a wide range of applications through the combination of different technologies. Fuel cells and batteries have made significant advances in energy production and storage. Innovative technologies are constantly being researched to increase energy storage capacity and provide more efficient energy conversion.

References

- Abraham, K. M. (2020). How comparable are sodium-ion batteries to lithium-ion counterparts? *ACS Energy Letters*, 5(11), 3544–3547.
- Badwal, S. P. S., Giddey, S. S., Munnings, C., Bhatt, A. I., & Hollenkamp, A. F. (2014). Emerging electrochemical energy conversion and storage technologies. *Frontiers in Chemistry*, 2, 79.
- Bilen, E. N., TAŞKESEN, E., & ALAHMAD, H. (2022). Yakıt Pillerinin Tarihsel Gelişimi, Çalışma Prensipleri ve Çeşitleri İncelenmesi.
- Carnegie, R., Gotham, D., Nderitu, D., & Preckel, P. V. (2013). Utility scale energy storage systems. State Utility Forecasting Group. Purdue University, 1.
- Daniel, C., & Besenhard, J. O. (2012). *Handbook of battery materials*. John Wiley & Sons.
- Electrochemical Energy Conversion. (2011). Wikipedia. https://en.wikipedia.org/wiki/Electrochemical_energy_conversion#External_links
- Emeksiz, C., & Burak, K. (2022). Enerji Depolama Teknolojilerinin İncelenmesi ve Karşılaştırmalı Analizi. *International Journal of Multidisciplinary Studies and Innovative Technologies*, 6(2), 134–142.
- Guth, U., Vonau, W., & Zosel, J. (2009). Recent developments in electrochemical sensor application and technology—a review. *Measurement Science and Technology*, 20(4), 042002.
- Juda, Z. (2011). Advanced Batteries And Supercapacitors For Electric Vehicle Propulsion Systems With Kinetic Energy Recovery. *Journal of KONES Powertrain and Transport*, 18(4), 165–171.
- Kiehne, H. A. (2003). *Battery technology handbook* (Vol. 118). CRC Press.
- Krivic, P., & Bac, P. (2013). Electrochemical Energy Storage. In *Energy Storage- Technologies and Applications*. InTech. <https://doi.org/10.5772/52222>
- Kulkarni, A., & Giddey, S. (2012). Materials issues and recent developments in molten carbonate fuel cells. *Journal of Solid State Electrochemistry*, 16, 3123–3146.
- Root, M. (2011). *The Tab Battery Book: An in-depth guide to construction, design, and use*. (No Title).
- Stiegel, G. J., Bose, A., & Armstrong, P. (2006). Development of ion transport membrane (ITM) oxygen technology for integration in IGCC and other advanced power generation systems. US Dept. of Energy.
- Şükran, E. F. E., & Güngör, Z. A. (2021). Geçmişten Günümüze Batarya Teknolojisi. *Avrupa Bilim ve Teknoloji Dergisi*, 32, 947–955.
- Yang, Z., Zhang, J., Kintner-Meyer, M. C. W., Lu, X., Choi, D., Lemmon, J. P., & Liu, J. (2011). Electrochemical energy storage for green grid. *Chemical Reviews*, 111(5), 3577–3613.
- Zhang, J., Zhang, L., Liu, H., Sun, A., & Liu, R.-S. (2011). *Electrochemical technologies for energy storage and conversion*, 2 volume set (Vol. 1). John Wiley & Sons.

ELECTROCATALYTIC TECHNIQUE INVESTIGATION IN BIODIESEL PRODUCTION

Edip TAŞKESEN

Dr., Sirnak University, Faculty of Engineering, Department of Energy systems Engineering, Sirnak-Türkiye
ORCID: 0000-0002-3052-9883

Hakan DUMRUL

Dr., Sirnak University, Faculty of Engineering, Department of Energy systems Engineering, Sirnak-Türkiye
ORCID: 0000-0003-1122-3886

Hamza ALAHMAD

Mr., Sirnak University, Postgraduate Education Institute, Department of Energy Science and Technologies, Sirnak-Türkiye
(Responsible Author) ORCID: 0000-0002-6261-3449

ABSTRACT

Biodiesel is an important alternative fuel with environmental advantages and suitable physico-chemical properties, and this fuel is produced from vegetable oils. However, the cost factor is one of the main barriers to the commercialization process. Traditional transesterification methods include processes that require high ambient temperatures and special catalysts for production. However, due to the large number of restrictions of existing catalysts, electrocatalytic processes that do not require high temperatures are evaluated. In this context, the electrocatalytic transesterification process can be performed depending on the presence or absence of a catalyst or co-solvent. In this study, the basic principles of the electrocatalytic transesterification process examine the reaction mechanism.

Keywords: Biodiesel, Energy conversion, Electrocatalytic, Electrocatalytic reactor

Introduction

Biodiesel emerges as a substitute energy source derived from plant-based oil, possessing renewability, biodegradability, and environmentally friendly characteristics (Atabani et al., 2012a; Özdemir & Mutlubas, 2016; Thangaraj et al., 2016). In the contemporary era, biodiesel has garnered escalating interest owing to the swift exhaustion of fossil fuels and their detrimental effects on the ecosystem (Hayyan et al., 2010). Substantial portions of the expenses associated with biodiesel manufacturing are frequently allocated to raw material expenditures, such as plant-based oil or animal adipose tissue. To mitigate these costs, non-edible oils sourced from arboreal flora are employed as foundational materials (Demirbas, 2009; Sunde et al., 2011).

The elevated consistency, mass, and free fatty acids (FFA) levels in ligneous plant-based oils and used cooking oil (UCO) diminish their appeal as raw materials. Consequently, diverse methodologies (dilution, amalgamation, microemulsion, pyrolysis, and esterification) have been explored, and esterification is considered the most efficacious among these approaches (Thangaraj & Solomon, 2020). In the esterification procedure, a brief alcohol chain (methanol or ethanol) is employed alongside a catalyst, resulting in the production of glycerol and fatty acid methyl or ethyl esters (FAME) from triglycerides (Atabani et al., 2012b; Thanh et al., 2012).

Throughout this procedure, the temperature of the chemical reaction typically falls within the 50-65°C spectrum, and commonly, NaOH or KOH is employed as a catalytic agent (Singh et al., 2006). Nevertheless, oils containing elevated levels of free fatty acids (FFA) may exhibit a heightened susceptibility to saponification. To mitigate this potentiality, acid-based catalysts are generally favored; nonetheless, such a preference might necessitate an increased quantity of alcohol (Thangaraj et al., 2019; Thangaraj & Piraman, 2016; Thangaraj & Solomon, 2021).

Contemporary catalysts encompass metal oxides, molecular sieves, activated alumina, and sodium bicarbonate. Furthermore, lipase enzymes find application, albeit at a substantial expense. These enzymes

are frequently immobilized to enhance stability and facilitate separation. Diverse catalytic systems leverage metal oxides due to elevated specific surface area and robust alkaline potency. Nevertheless, the susceptibility of heterogeneous catalysts to elevated free fatty acid concentrations or subpar raw materials may impose constraints (Thangaraj & Solomon, 2021).

Recently, the focus has shifted towards nanostructured substances owing to their exceptional physical and chemical characteristics. The utilization of nanocatalysts facilitates proximity between reactants and the catalyst site, attributable to their elevated surface-to-volume ratio. This feature enables heterogeneous nanocatalytic systems to exhibit reaction rates akin to those observed in homogeneous systems (Refaat, 2011; Veljković et al., 2015).

An electrocatalytic approach has been introduced to address issues specific to the transesterification process. The electrocatalytic process, characterized by its environmental sustainability, facilitates electron transfer between the electrode and reactants. This method ensures heightened efficiency at a reduced cost, rendering it applicable to numerous sustainable energy technologies. Notably, the electrocatalytic process has proven effective in averting saponification in oils with elevated free fatty acid (FFA) and water content, and it can be executed at a comparatively modest expense (Thangaraj & Solomon, 2021).

Electrocatalytic Mechanism in The Transesterification Process

During electrolytic processes, a continuous electric current, specifically direct current (DC), is applied across liquefied salts or solvated ionic compounds, leading to the disintegration of the compounds into elemental constituents (Kim et al., 2014; Lauka et al., 2015). The electrocatalytic reactor encompasses an electrochemical cell with electrodes fabricated from graphite (Fereidooni & Mehrpooya, 2017; Helmi & Tahvildari, 2016; Putra et al., 2015, 2017; Thangaraj & Solomon, 2021) or activated charcoal (Sivachidambaram et al., 2017) or carbon nanotubes (Zhu et al., 2020) or graphene (Ke & Wang, 2016), maintaining a separation distance typically ranging between 10 and 20 millimeters (Fereidooni & Mehrpooya, 2017; Guan & Kusakabe, 2009; Helmi & Tahvildari, 2016; Putra et al., 2014, 2015; Thangaraj & Solomon, 2021) (refer to Fig. 1).

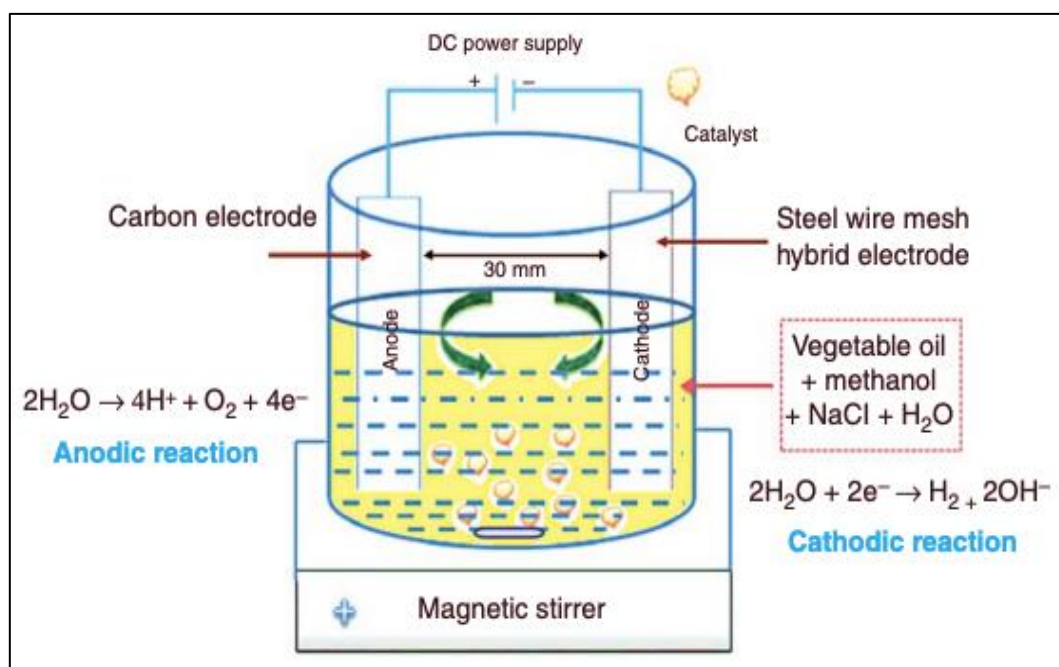


Figure 1. Electrocatalytic reactor arrangement and processes take place at the electrode interface (Thangaraj & Solomon, 2021).

The process of electrolytic transesterification is elucidated through Equations (1)–(5). The electrocatalytic reactor is charged with a blend comprising plant-derived oil, ethanol, catalyst, auxiliary solvents, and an electrolytic solution (sodium chloride + water). The reaction is delineated by Equations (1)–(3). The anode facilitates the oxidation of chloride and hydroxyl ions into chlorine (Cl₂) and oxygen (O₂); concurrently, hydroxyl ions and hydrogen are generated at the cathode (Equations (4)). The methoxide ion is produced by the interaction of ethanol with hydroxyl (OH⁻), exhibiting nucleophilic solid characteristics. Subsequently, it engages the carbonyl moiety in glyceride molecules, yielding methyl ester and glycerin. Glycerin emerges as a by-product in the transesterification process (Fereidooni & Mehrpooya, 2017; Helmi & Tahvildari, 2016; Putra et al., 2015; Thangaraj & Solomon, 2021).



anodic reaction



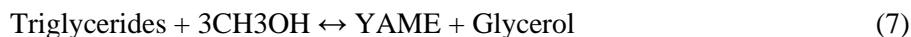
cathodic reaction



proton-transfer reaction



and transesterification reaction



Electrode Types

Electrochemical applications employ two types of electrodes: metallic electrodes prepared through conventional microfabrication and electrodes with a thin layer of metal or metal oxide deposited onto the substrate surface through electroplating. The performance of electrodes, particularly platinum, depends on factors such as conductivity and chemical stability. Quadruple metal oxide anodes (Ti, Ru, Sn, Sb) demonstrate stability and electrochemical activity without a soluble supporting electrolyte. Carbon materials find widespread use in electrochemical applications due to their high conductivity, diverse morphologies, and cost-effectiveness. Additionally, nano-sized carbon-based materials, such as carbon quantum dots (CQDs) and graphene quantum dots (GQDs), are considered promising electrode materials, offering advantages like redox properties and biocompatibility. Finally, carbon-based electrocatalysts derived from biomass have been explored for their potential in various electrochemical conversion processes, showcasing high performance, especially in methanol oxidation, and representing a low-cost and sustainable alternative (Thangaraj & Solomon, 2021).

Biodiesel Yield in Electrocatalytic Processes

Key factors influencing biodiesel yield include voltage, stirring rate, electrode type, water content, co-solvent type, reaction temperature, reaction duration, oil-to-methanol molar ratio, and NaCl concentration. Ion-exchange resins, particularly hybrid ion-exchange resin-grafted electrodes, prove effective in electrocatalytic systems. Notably, a PtIrRu electrode demonstrates superior performance in transesterification, attributed to its high surface area, conductivity, and catalytic activity. Electrolysis voltage significantly impacts biodiesel conversion, with higher voltages enhancing transesterification but posing challenges in large-scale operations. Electrolysis time influences yield, showcasing the importance of optimizing reaction duration. Co-solvents, like acetone, enhance reactant contact but may reduce electrical conductivity. The oil-to-alcohol molar ratio and reaction temperature are intertwined, with the former affecting electrical conductivity and

the latter influencing miscibility. pH shifts during electrolysis, and electrical conductivity rises with NaCl concentration, impacting biodiesel production. The PtIrRu electrode emerges as a promising catalyst, offering high efficiency and conversion rates in electrocatalytic biodiesel production (Thangaraj & Solomon, 2021).

Advantages and Disadvantages of Electrocatalytic Technique in Biodiesel Production

The electrocatalyst method is an alternative approach in the field of biodiesel production. This technique treats the biodiesel production process as an alternative to traditional chemical transesterification and accelerates electrochemical reactions with catalysts.

- **Advantages:**
 - **Low Energy Consumption:** The electrocatalytic method is characterized by low energy consumption. Since the amount of energy consumed to speed up chemical reactions is low, energy efficiency increases,
 - **Low Temperature and Pressure:** In conventional chemical methods, biodiesel production can be carried out by electrocatalytic technique without the need for high temperature and pressure conditions. This saves energy and maintains product quality,
 - **Reduced Catalyst Use:** Electrocatalytic reactions enable more efficient use of catalysts. This increases the reaction speed and reduces catalyst costs,
 - **Product Quality and Purity:** The electrocatalytic technique allows for acquiring more pure and homogeneous products. This can improve product quality and minimize the formation of decomposition products (Osman et al., 2023; Taft & Canchaya, 2022).
- **Disadvantages:**
 - **High Initial Costs:** Special equipment and electrodes may be required to apply the electrocatalytic method. This can lead to high costs initially,
 - **Process Control Challenges:** Electrocatalytic reactions may be more complex than traditional chemical methods. Therefore, the control and optimization of the reaction parameters can be challenging,
 - **High Technical Expertise Requirement:** Applying the electrocatalytic method may require expertise in electrochemical knowledge and experience. This can lead to operating and maintenance challenges,
 - **Longer Reaction Times:** Electrocatalytic reactions may take longer than traditional methods. This can affect production efficiency (Osman et al., 2023; Taft & Canchaya, 2022).

Conclusion and Recommendations

This study aimed to examine electrocatalytic techniques in biodiesel production and to understand the factors that influence the efficiency of these techniques. Considering the information in the literature, the types of electrodes used in electrocatalytic reactions and the physical and chemical properties of these electrodes play an essential role. Metallic electrodes are preferred because of their high electrical conductivity and durability, while electrodes modified with coating layers can provide higher surface area and catalytic activity.

When the factors affecting the efficiency of electrocatalytic reactions in biodiesel production are examined, the electrolysis voltage, mixing speed, electrode type, water content, auxiliary solvent type, reaction temperature, reaction time, oil/parameters such as methanol molar ratio and NaCl concentration are essential. Careful optimization of these factors can improve efficiency in producing electrocatalyst biodiesel.

When evaluating the advantages and disadvantages of electrocatalytic techniques in biodiesel production, it was seen that this method has advantages such as performing under low-temperature conditions, decreasing by-products and high product purity.

As a result, the potential of electrocatalytic techniques in biodiesel production is of great interest. Further research and development of these techniques could be essential for environmentally friendly and sustainable biodiesel production. Future studies are proposed to focus on a more detailed understanding of the

electrocatalytic reaction mechanisms, the optimization of electrode materials and the exploration of applicability on an industrial scale. Advanced studies in this field are expected to contribute to the wide acceptance and industrial application of electrocatalytic techniques in biodiesel production.

References

- Atabani, A. E., Silitonga, A. S., Badruddin, I. A., Mahlia, T. M. I., Masjuki, Hh., & Mekhilef, S. (2012a). A comprehensive review of biodiesel as an alternative energy resource and its characteristics. *Renewable and Sustainable Energy Reviews*, 16(4), 2070–2093.
- Atabani, A. E., Silitonga, A. S., Badruddin, I. A., Mahlia, T. M. I., Masjuki, Hh., & Mekhilef, S. (2012b). A comprehensive review on biodiesel as an alternative energy resource and its characteristics. *Renewable and Sustainable Energy Reviews*, 16(4), 2070–2093.
- Demirbas, A. (2009). Progress and recent trends in biodiesel fuels. *Energy Conversion and Management*, 50(1), 14–34.
- Fereidooni, L., & Mehrpooya, M. (2017). Experimental assessment of electrolysis method in production of biodiesel from waste cooking oil using zeolite/chitosan catalyst with a focus on waste biorefinery. *Energy Conversion and Management*, 147, 145–154.
- Guan, G., & Kusakabe, K. (2009). Synthesis of biodiesel fuel using an electrolysis method. *Chemical Engineering Journal*, 153(1–3), 159–163.
- Hayyan, A., Alam, M. Z., Mirghani, M. E. S., Kabbashi, N. A., Hakimi, N. I. N. M., Siran, Y. M., & Tahiruddin, S. (2010). Sludge palm oil as a renewable raw material for biodiesel production by two-step processes. *Bioresource Technology*, 101(20), 7804–7811.
- Helmi, M., & Tahvildari, K. (2016). The effect of changing the concentration of loaded KOH to a zeolite heterogeneous catalyst activity in biodiesel production by electrolysis. *International Journal of Advanced Biotechnology and Research*, 7, 79–85.
- Ke, Q., & Wang, J. (2016). Graphene-based materials for supercapacitor electrodes—A review. *Journal of Materiomics*, 2(1), 37–54.
- Kim, J., Ryu, B.-G., Lee, Y.-J., Han, J.-I., Kim, W., & Yang, J.-W. (2014). Continuous harvest of marine microalgae using electrolysis: effect of pulse waveform of polarity exchange. *Bioprocess and Biosystems Engineering*, 37, 1249–1259.
- Lauka, D., Gusca, J., Kalnins, S., Vigants, E., & Blumberga, D. (2015). Analysis of use of bioenergy production by-products to enhance electrolysis process. 28th ECOS Conference, Pau, France, 28, 1.
- Osman, A. I., Elgarahy, A. M., Eltaweil, A. S., Abd El-Monaem, E. M., El-Aqapa, H. G., Park, Y., Hwang, Y., Ayati, A., Farghali, M., & Ihara, I. (2023). Biofuel production, hydrogen production and water remediation by photocatalysis, biocatalysis and electrocatalysis. *Environmental Chemistry Letters*, 21(3), 1315–1379.
- Özdemir, Z. Ö., & Mutlubaş, H. (2016). Biyodizel üretim yöntemleri ve çevresel etkileri. *Kırklareli Üniversitesi Mühendislik ve Fen Bilimleri Dergisi*, 2(2), 129–143.
- Putra, R. S., Hartono, P., & Julianto, T. S. (2014). Effect of co-solvent on transesterification of used frying oil: the enhancement of electrolytic process by organocatalyst chitosan. *Proceedings of the 3rd Applied Science for Technology Application, ASTECHNOVA 2014 International Energy Conference*, Yogyakarta, Indonesia.
- Putra, R. S., Hartono, P., & Julianto, T. S. (2015). Conversion of methyl ester from used cooking oil: the combined use of electrolysis process and chitosan. *Energy Procedia*, 65, 309–316.
- Putra, R. S., Liyanita, A., Arifah, N., Puspitasari, E., & Hizam, M. N. (2017). Enhanced electro-catalytic process on the synthesis of FAME using CaO from eggshell. *Energy Procedia*, 105, 289–296.

- Refaat, A. A. (2011). Biodiesel production using solid metal oxide catalysts. *International Journal of Environmental Science & Technology*, 8, 203–221.
- Singh, A., He, B., Thompson, J., & Van Gerpen, J. (2006). Process optimization of biodiesel production using alkaline catalysts. *Applied Engineering in Agriculture*, 22(4), 597–600.
- Sivachidambaram, M., Vijaya, J. J., Kennedy, L. J., Jothiramalingam, R., Al-Lohedan, H. A., Munusamy, M. A., Elanthamilan, E., & Merlin, J. P. (2017). Preparation and characterization of activated carbon derived from the *Borassus flabellifer* flower as an electrode material for supercapacitor applications. *New Journal of Chemistry*, 41(10), 3939–3949.
- Sunde, K., Brekke, A., & Solberg, B. (2011). Environmental impacts and costs of hydrotreated vegetable oils, transesterified lipids and woody BTL—a review. *Energies*, 4(6), 845–877.
- Taft, C. A., & Canchaya, J. G. S. (2022). Overview: Catalysts, feedstocks in biodiesel production. *Research Topics in Bioactivity, Environment and Energy: Experimental and Theoretical Tools*, 337–357.
- Thangaraj, B., Jia, Z., Dai, L., Liu, D., & Du, W. (2016). Lipase NS81006 immobilized on FeO magnetic nanoparticles for biodiesel production. *Ovidius University Annals of Chemistry*, 27(1), 13–21.
- Thangaraj, B., Jia, Z., Dai, L., Liu, D., & Du, W. (2019). Effect of silica coating on Fe₃O₄ magnetic nanoparticles for lipase immobilization and their application for biodiesel production. *Arabian Journal of Chemistry*, 12(8), 4694–4706.
- Thangaraj, B., & Piraman, S. (2016). Heteropoly acid coated ZnO nanocatalyst for *Madhuca indica* biodiesel synthesis. *Biofuels*, 7(1), 13–20.
- Thangaraj, B., & Solomon, P. R. (2020). Scope of biodiesel from oils of woody plants: a review. *Clean Energy*, 4(2), 89–106.
- Thangaraj, B., & Solomon, P. R. (2021). Biodiesel production by the electrocatalytic process: a review. *Clean Energy*, 5(1), 19–31.
- Thanh, L. T., Okitsu, K., Boi, L. Van, & Maeda, Y. (2012). Catalytic technologies for biodiesel fuel production and utilization of glycerol: a review. *Catalysts*, 2(1), 191–222.
- Veljković, V. B., Banković-Ilić, I. B., & Stamenković, O. S. (2015). Purification of crude biodiesel obtained by heterogeneously-catalyzed transesterification. *Renewable and Sustainable Energy Reviews*, 49, 500–516.
- Zhu, S., Ni, J., & Li, Y. (2020). Carbon nanotube-based electrodes for flexible supercapacitors. *Nano Research*, 13, 1825–1841.

EXPLORING BUILDING-INTEGRATED PHOTOVOLTAIC/THERMAL SYSTEMS

Lecturer Mazlum CENGİZ

*Sirnak University, Machinery and Metal Technologies, Sirnak-Türkiye
(Responsible Author) ORCID: 0002-3724- 6894*

Lecturer Yahya CELEBI

*Sirnak University, Motor Vehicles and Transportations, Sirnak-Türkiye
ORCID: 0002-4686-9794*

Prof. Dr. Huseyin AYDIN

*Batman University, Faculty of Engineering, Department of Mechanical Engineering, Batman-Türkiye
ORCID: 0002-5415-0405*

ABSTRACT

Energy consumption in the building sector accounts for 30-40% of worldwide energy consumption and is responsible for almost 40% of the total carbon dioxide emissions. The present energy usage in buildings constitutes over 40% of the overall primary energy consumption in both the United States and the European Union, and more than 35% of the total energy consumption in Turkey. Thus, improving the energy efficiency of buildings can propose a key solution to energy shortages, and environmental issues. The ultimate solution involves transforming the buildings into self-sustainable structures as a medium for generating energy by harvesting different renewable energy sources with appropriate design, construction, and operation. Solar energy is preferable renewable energy for use in buildings because it is extensively accessible, pollution-free, and viable. The integration of photovoltaics and thermal technologies into photovoltaic/thermal system can eliminate the need of external electrical energy for solar thermal systems. Employing this integrated system in buildings leads to the innovation of building-integrated photovoltaic/thermal systems, delivering a self-sufficient energy supply for the buildings. This study investigates the working principle of main building-integrated photovoltaic/thermal systems. Moreover, it presents advantages, disadvantage, and applications of these systems.

Keywords: Building-integrated photovoltaic/thermal (BIPV/T); Solar energy; Working principles; Applications; Advantages/Disadvantages

Introduction

Nowadays, most individuals spend 90% of their daily routines indoor, utilizing energy on artificial heating and air conditioning systems (Cao et al., 2016). In addition, growing population and the desire for a more modern way to live causes a significant increase in energy consumption in the building sector that accounts for 30-40% of worldwide energy consumption and is responsible for almost 40% the total carbon dioxide emissions (Cao et al., 2016; Maghrabie et al., 2021; Yu et al., 2021). The present energy usage in buildings constitutes over 40% of the overall primary energy consumption in both the United States and the European Union, and more than 35% of the total energy consumption in Turkey (Cao et al., 2016; 8th NC of Turkey, 2023). Furthermore, buildings utilize over 55% of the global electricity, with an annual growth rate of 2.5% (Maghrabie et al., 2021). Figure 1 illustrates that both residential and non-residential buildings are responsible for 30% of the world's energy consumption and 28% of the worlds' emissions in 2019. Thus, improving the energy efficiency of buildings can offer a crucial solution to energy shortages, and environmental issues such as the melting of snow caps, global warming, stratospheric ozone depletion, drought, and desertification (Maghrabie et al., 2021; Pandey et al., 2018; Rabaia et al., 2021).

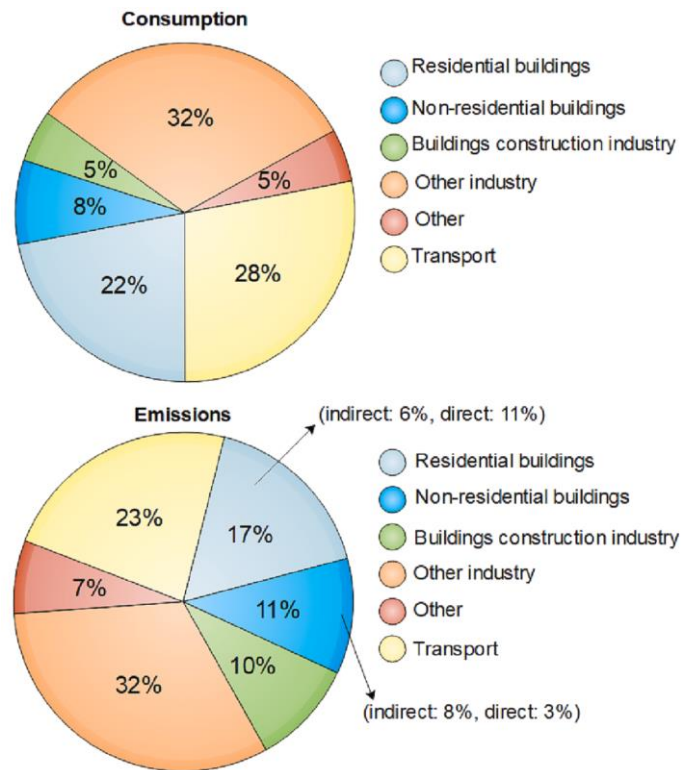


Figure 1. Global energy usage and emissions by sector in 2019 (Sirin et al., 2023).

The ideal solution for reducing energy consumption and emissions from buildings involves transforming the buildings into self-sustainable structures as a medium for generating energy by harvesting different renewable energy sources with appropriate design, construction, and operation. In comparison to other renewable energy resources, solar energy is preferable for use in buildings because it is extensively accessible, pollution-free, and viable (Maghrabie et al., 2021; George et al., 2019). Photovoltaics (PVs), which directly transform solar irradiance into electrical energy, and thermal systems, which convert solar energy into thermal energy such as heat, are solar energy technologies. The integration of both technologies into photovoltaic/thermal system can eliminate the need of external electrical energy for solar thermal systems. Employing this integrated system in buildings leads to the innovation of building-integrated photovoltaic/thermal (BIPV/T) systems, delivering a self-sufficient energy supply for the buildings. The BIPV/T systems can be implemented either as a roofing structure or as a part of a building's façade. These systems have a great potential to serve as the primary energy source in urban areas (Maghrabie et al., 2021; Shukla et al., 2016). There are several advantages and disadvantages of the BIPV/T systems, which are listed below.

Advantages of the BIPV/T systems:

1. Eco-friendly
2. Offers sun and weather shielding
3. Generates both electrical and thermal energies
4. Mitigate cooling and heating demands in buildings
5. Diminishes electrical expenses of a building
6. Decreases operational energy costs
7. Lowers the carbon footprint of the building
8. Acts as thermal insulation

9. Improves the value of the building

Disadvantages of the BIPV/T systems:

1. High capital cost, and maintaining expenses
2. System and building overheating
3. Achieving maximum performance requires optimal design parameters and graphical analysis of the building
4. Its viability relies on the national and local supporting policy

There are substantial global market opportunities for the BIPV/T systems because they are innovative, practical, and offers a promising solution for attaining net-zero emission buildings (Shukla et al., 2017). It is an energy-generating technology that incorporates solar photovoltaic (PV) panels in the design of windows, roof, façades, and shading structures (Yang, 2015).

A review study presented by Yu et al. (2021) focused on development and designs of solar systems integrated with building façades and classified façade-based BIPV/T systems into 7 categories: air cooling for PVs, space heating, ventilation, water heating, PV-phase change material, BIPV/T with heat pump, and PV thermoelectric wall. The review stated that BIPV/T systems are really promising to diminish the heating/cooling load of heating, ventilation, and air conditioning. Hence, they demonstrate great potential in reducing energy consumption, and contributing to the advancement of energy-efficient buildings.

Additionally, Abdelrazik et al. (2022) introduced a review study that investigated the multi numerical and experimental studies carried out to examine the design and performance of the different BIPV/T systems. It was revealed that with selecting ideally designed features, including tilt angles, configuration arrangements, and fluid flow rates, optimal performance in BIPV/T air systems can be achieved. BIPV/T water cooled systems exhibited superior thermal performance over BIPV/T air systems, but with increased manufacturing expenses. Moreover, relative to air, and water cooled BIPV/T, BIPV/T with phase change material and BIPV/T with concentrators displayed better outcomes under the same testing settings.

Furthermore, a comprehensive review written by Sirin et al. (2023) explained the operation of BIPV/T systems, outlined their categorization, advantages, performance improvement methods, and possible contributions to energy-efficient buildings. It was indicated that it is essential to determine the energy loads in the design and operational stages. Choosing materials such as concentrators, phase change materials, and deciding on the optimal system location in a building are crucial steps to improve the efficiency of BIPV/T systems. In addition to achieving the optimal engineering design and performance, the future of these systems is also affected by energy policies and incentives.

Working principle of BIPV/T Systems

Majority of solar irradiance reaching PV cells is not transformed into electricity, but rather into heat energy, leading to increase in the temperature of the cells and reduction in the conversion efficiency and lifetime of the cells (Elnozahy et al., 2015; Spertino et al., 2016). Therefore, BIPV/T systems basically extract the unwanted heat from PV panels producing electrical energy by working fluids like water, air, refrigerant. Furthermore, these systems recover the electrical efficiency of the PV cells and prolong their lifetime and use the extracted heat for various applications.

The illustrated diagram of a façade BIPV/T system with air circulation is presented in Figure 2, displaying the directional movement of active air through the system to contribute to the warming interior spaces (Quesada et al., 2012). Fresh air goes into the lower part of the air gap, undergoes heating, rises, and then circulates into the room via the upper wall opening in the wintertime (Yu et al., 2021).

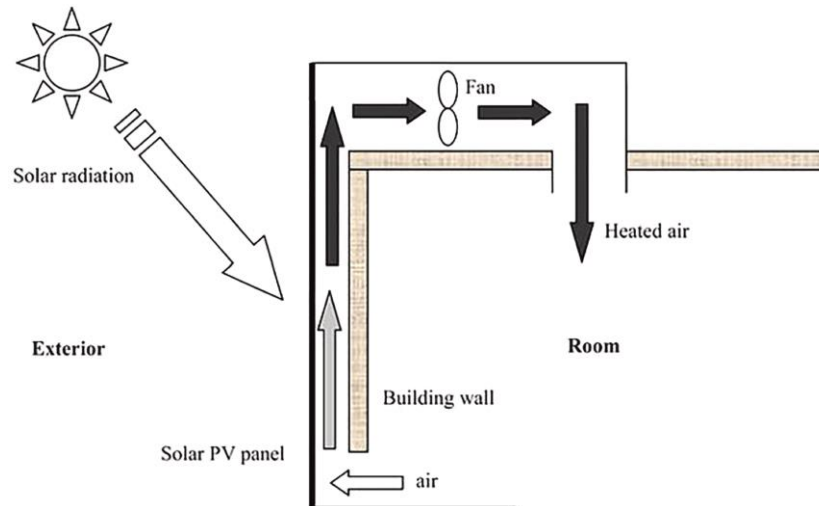


Figure 2. An illustrated diagram of a façade BIPV/T system with air circulation (Quesada et al., 2012; Maghrabie et al., 2021).

Additionally, a BIPV/T system can be operated for ventilation in summer besides fresh air preheating, as shown in Figure 3.

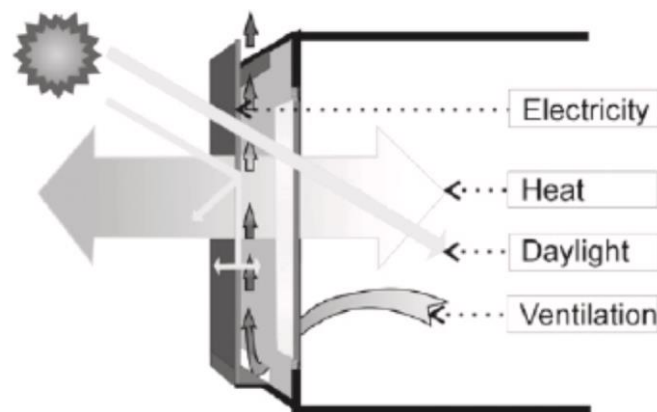


Figure 3. The ventilation mode of a façade BIPV/T system with air circulation (Yu et al., 2021)

In the summertime, the air in the room flows through the air inlet into the lower section of the air gap, undergoes warming, and is subsequently expelled outdoors (Yu et al., 2021). A typical view of a rooftop BIPV/T system with air circulation is exhibited in Figure 4. Its working principle is similar to the façade BIPV/T system with air circulation.

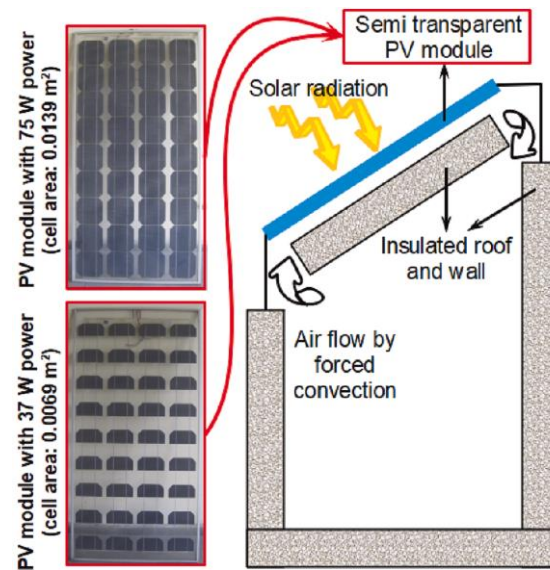


Figure 4. A rooftop BIPV/T system with air circulation (Sirin et al., 2023)

Moreover, installing BIPV/T systems with air circulation on Trombe walls has gained increasing interest because this combined system has the capability to harness more solar irradiance for space heating in addition to generating electrical power, and contributes to improve the architectural aesthetics of conventional Trombe walls (Lin et al., 2019).

BIPV/T systems with heat pipe or heat pump evaporator use a phase change material as a working medium. The phase change material in BIPV/T undergoes a phase change from a solid to a liquid state during daytime, cooling down the PV panel. It then releases the stored heat during the night time. It is important to choose the right type and amount of phase change material based on temperature requirements and thermal load to guarantee effective cooling of the PV panel (Yang, 2015). Roof BIPV/T system with phase change material, and Façade BIPV/T system with air circulation and phase change material are presented in Figure 5 and 6, respectively. Although BIPV/T systems with air circulation are convenient, their performance is lower when they compare to cooling with phase change materials. Climate conditions determine the mass of required phase change material. In hot climates, a phase change material with broader phase change temperature is preferred to address issues related to overheating. (Asefi et al., 2021).

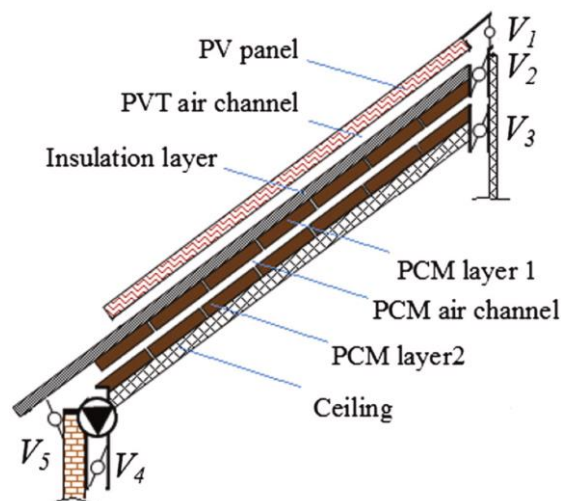


Figure 5. Roof BIPV/T system with phase change material (Asefi et al., 2021)

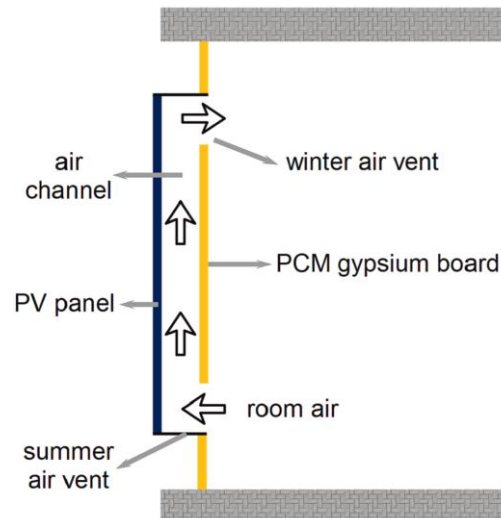
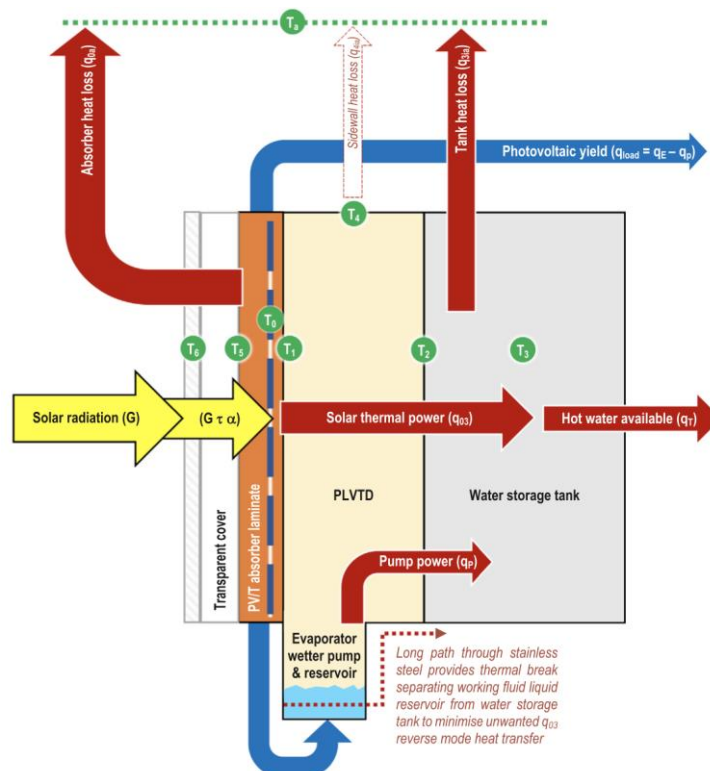


Figure 6. Façade BIPV/T system with phase change material (Sirin et al., 2023)

The working principle of a novel BIPV/T façade system utilizing a PV panel combined with an integrated collector-storage system for solar water heating is demonstrated in Figure 7. The system control absorbs temperature and minimizes thermal losses with utilizing a planar liquid-vapor thermal diode (PLVTD) and store hot water in an integrated tank. Thus, it provides a solution for overheating heat losses and BIPV/T overheating (Pugsley et al., 2020).



G	Incident solar radiation flux	$G_{\tau\alpha}$	Absorbed solar radiation
T_a	Ambient environmental temperature	Q_{03}	Thermal power transferred from the absorber to the water storage tank through the thermal diode
T_0	Photovoltaic cell temperature	Q_T	Net rate of heat gained by the stored water bulk
T_1	Temperature of absorber laminate substrate and PLVTD evaporator plate	Q_{0a}	Heat loss from PV cells
T_2	Temperature of condenser plate and tank mantle	Q_{3ia}	Heat loss from the back and sides of the water storage tank not covered by the thermal diode
T_3	Temperature of water bulk stored in the tank	Q_{4ia}	Heat loss from PLVTD sidewalls
T_4	Thermal diode sidewall temperature	Q_E	Electrical power yielded from PV
T_5	Absorber laminate surface temperature	Q_P	Electrical power consumed by the evaporator wetter pump which is then all converted to heat
T_6	Transparent cover temperature	Q_{load}	Electrical power delivered to load

Figure 7. BIPV/T system with PLVTD and collector-storage solar water heater (Pugsley et al., 2020).

Even though BIPV/T systems utilizing water as a coolant have extra manufacturing expenses, they display better thermal performance relative to the ones using air as a coolant (Abdelrazik et al., 2022).

Applications of BIPV/T Systems

The BIPV/T systems utilize the extracted thermal energy for various applications such as residential and non-residential space heating, water heating, drying procedures, agricultural process, industrial food processing and water desalination. In addition, they provide daylighting, shading, architectural aesthetics. Applications of BIPV/T systems on the roof and façade are introduced in Figure 8 (Maghrabie et al., 2021).



Figure 8. Applications of BIPV/T systems on the roof and façade (Maghrabie et al., 2021).



Figure 8. Applications of BIPV/T systems on the roof and façade (Maghrabie et al., 2021). (continued)

Photovoltaic/Thermal (PV/T) systems can behave as a thermal insulation material, and windows for buildings with utilization of right materials (Sirin et al., 2023). The BIPV/T systems can be assembled in different arrangements to ensure that it is elegant and invisible with the architectural design of a building, providing a convenient and modest appearance (Buker and Riffat, 2015).

Conclusion and Recommendations

The BIPV/T systems significantly improves building performance and reduces harmful emissions and provides an opportunity to develop low energy buildings and achieve the net zero building target. Therefore, implementation of these systems guarantees high performance of next generation eco-friendly buildings with producing the electrical and thermal energy.

The BIPV/T systems can utilize different fluids as a heat extraction medium and have various application areas. The systems are summarized in Figure 9.

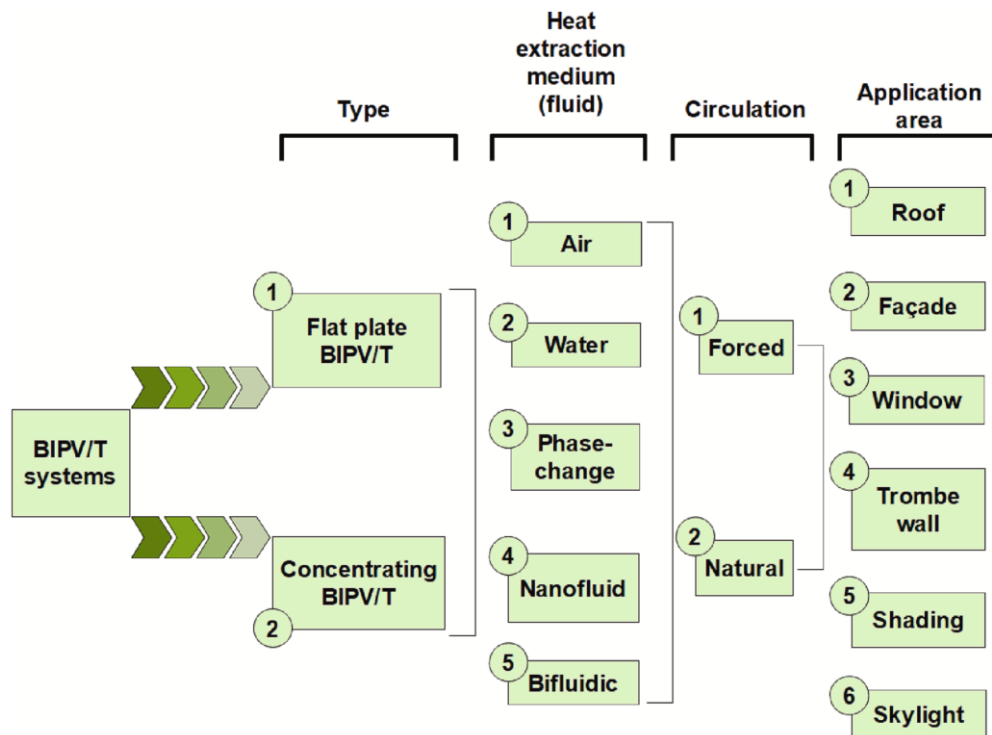


Figure 9. Classification of BIPV/T systems (Sirin et al., 2023)

Façades BIPV/T systems are vulnerable to shading from surrounding buildings in urban areas relatively roof BIPV/T system. This can significantly diminish the electrical and thermal efficient of façade-based BIPV/T systems. Also, the roof of a building provides a broader area of installation.

The type of PV panel and working fluid can play an essential role in the performance of the BIPV/T systems. Refrigerants can be used as a working fluid to absorb heat from PV panels rather than air or water.

To encourage the adoption of building-integrated photovoltaic/thermal (BIPV/T) systems, some incentives such as government subsidies, tax credits, and awareness campaigns can be implemented. Additionally, some successful case studies, promoting the long-term cost savings, and emphasizing the positive environmental impact of BIPV/T systems can further motivate many individuals and organizations to support this sustainable technology. For instance, Apple Inc. has already had a target of using 100% renewable electricity and making all its products carbon neutral by 2030, covering the entire supply chain and the energy consumption of devices of its customer. Apple Inc. indicated that there are notable opportunities to conserve energy by retrocommissioning buildings currently used or managed by Apple, including energy-intensive facilities such as data centres (Apple Environmental Progress Report, 2023). Therefore, Apple Inc. can consider the BIPV/T systems in their buildings to achieve its goal. Additionally, Tesla Inc. produces traditional PVs and has installed 3000 solar roof systems in the United States (CNBC, 2023) but has not consider manufacturing PV/T roof systems or using them in their buildings.

In conclusion, BIPV/T systems are vital technology for buildings, contributes to the realization of sustainable buildings that offer safe, heathy, and comfortable environment for their residents.

References

- Abdelrazik, A. S., Shboul, B., Elwardany, M., Zohny, R. N., & Osama, A. (2022). The recent advancements in the building integrated photovoltaic/thermal (BIPV/T) systems: An updated review. *Renewable and Sustainable Energy Reviews*, 170, 112988. <https://doi.org/10.1016/j.rser.2022.112988>
- Apple Environmental Progress Report. (2023). Access address (04.12.2023): https://www.apple.com/environment/pdf/Apple_Environmental_Progress_Report_2023.pdf
- Asefi, G., Habibollahzade, A., Ma, T., Houshfar, E., & Wang, R. (2021). Thermal management of building-integrated photovoltaic/thermal systems: A comprehensive review. *Solar Energy*, 216, 188-210. <https://doi.org/10.1016/j.solener.2021.01.005>
- Buker, M. S., & Riffat, S. B. (2015). Building integrated solar thermal collectors—A review. *Renewable and Sustainable Energy Reviews*, 51, 327-346. <https://doi.org/10.1016/j.rser.2015.06.009>
- Cao, X., Dai, X., & Liu, J. (2016). Building energy-consumption status worldwide and the state-of-the-art technologies for zero-energy buildings during the past decade. *Energy and buildings*, 128, 198-213. <https://doi.org/10.1016/j.enbuild.2016.06.089>
- Eight National Communication and Fifth Biennial Report of Türkiye Under the UNFCCC (8th NC of Türkiye). (2023). Access Address (02.12.2023): <https://unfccc.int/sites/default/files/resource/8NC-5BR%20Türkiye.pdf>
- Elnozahy, A., Rahman, A. K. A., Ali, A. H. H., Abdel-Salam, M., & Ookawara, S. (2015). Performance of a PV module integrated with standalone building in hot arid areas as enhanced by surface cooling and cleaning. *Energy and Buildings*, 88, 100-109. <https://doi.org/10.1016/j.enbuild.2014.12.012>
- George, M., Pandey, A. K., Abd Rahim, N., Tyagi, V. V., Shahabuddin, S., & Saidur, R. (2019). Concentrated photovoltaic thermal systems: A component-by-component view on the developments in the design, heat transfer medium and applications. *Energy Conversion and Management*, 186, 15-41. <https://doi.org/10.1016/j.enconman.2019.02.052>
- Lin, Y., Ji, J., Zhou, F., Ma, Y., Luo, K., & Lu, X. (2019). Experimental and numerical study on the performance of a built-middle PV Trombe wall system. *Energy and Buildings*, 200, 47-57. <https://doi.org/10.1016/j.enbuild.2019.07.042>
- Maghrabie, H. M., Elsaid, K., Sayed, E. T., Abdelkareem, M. A., Wilberforce, T., & Olabi, A. G. (2021). Building-integrated photovoltaic/thermal (BIPVT) systems: Applications and challenges. *Sustainable energy technologies and assessments*, 45, 101151. <https://doi.org/10.1016/j.seta.2021.101151>
- Pandey, A. K., Hossain, M. S., Tyagi, V. V., Abd Rahim, N., Jeyraj, A., Selvaraj, L., & Sari, A. (2018). Novel approaches and recent developments on potential applications of phase change materials in solar energy. *Renewable and Sustainable Energy Reviews*, 82, 281-323. <https://doi.org/10.1016/j.rser.2017.09.04>
- Pugsley, A., Zacharopoulos, A., Mondol, J. D., & Smyth, M. (2020). BIPV/T facades—A new opportunity for integrated collector-storage solar water heaters? Part 2: Physical realisation and laboratory testing. *Solar Energy*, 206, 751-769. <https://doi.org/10.1016/j.solener.2020.05.098>
- Quesada, G., Rouse, D., Dutil, Y., Badache, M., & Hallé, S. (2012). A comprehensive review of solar facades. Opaque solar facades. *Renewable and Sustainable Energy Reviews*, 16(5), 2820-2832. <https://doi.org/10.1016/j.rser.2012.01.078>
- Rabaia, M. K. H., Abdelkareem, M. A., Sayed, E. T., Elsaid, K., Chae, K. J., Wilberforce, T., & Olabi, A. G. (2021). Environmental impacts of solar energy systems: A review. *Science of The Total Environment*, 754, 141989. <https://doi.org/10.1016/j.scitotenv.2020.141989>
- Shukla, A. K., Sudhakar, K., & Baredar, P. (2016). A comprehensive review on design of building integrated photovoltaic system. *Energy and Buildings*, 128, 99-110. <https://doi.org/10.1016/j.enbuild.2016.06.077>
- Shukla, A. K., Sudhakar, K., & Baredar, P. (2017). Recent advancement in BIPV product technologies: A review. *Energy and Buildings*, 140, 188-195. <https://doi.org/10.1016/j.enbuild.2017.02.015>

Spertino, F., D'angola, A., Enescu, D., Di Leo, P., Fracastoro, G. V., & Zaffina, R. (2016). Thermal–electrical model for energy estimation of a water cooled photovoltaic module. *Solar Energy*, 133, 119-140. <https://doi.org/10.1016/j.solener.2016.03.055>

Şirin, C., Goggins, J., & Hajdukiewicz, M. (2023). A review on building-integrated photovoltaic/thermal systems for green buildings. *Applied Thermal Engineering*, 120607. <https://doi.org/10.1016/j.applthermaleng.2023.120607>

CNBC, Tesla has only installed 3,000 Solar Roof systems in the U.S., far below forecast, study finds. Access address (04.12.2023): <https://www.cnbc.com/2023/03/30/tesla-has-installed-3000-solar-roof-systems-in-the-us-study-finds.html>

Yang, R. J. (2015). Overcoming technical barriers and risks in the application of building integrated photovoltaics (BIPV): hardware and software strategies. *Automation in Construction*, 51, 92-102. <https://doi.org/10.1016/j.autcon.2014.12.005>

Yu, G., Yang, H., Yan, Z., & Ansah, M. K. (2021). A review of designs and performance of façade-based building integrated photovoltaic-thermal (BIPVT) systems. *Applied thermal engineering*, 182, 116081. <https://doi.org/10.1016/j.applthermaleng.2020.116081>

THEORETICAL ANALYSIS OF AN ORGANIC RANKINE CYCLE WITH PARABOLIC TROUGH COLLECTOR IN ŞIRNAK CLIMATE CONDITIONS

Erhan KIRTEPE

*Assist. Prof. Dr., Şırnak University, Şırnak Vocational School, Şırnak- Türkiye
(Responsible Author) ORCID: 0000-0002-1824-2599*

Mert Sinan TURGUT

*Dr., Ege University, Faculty of Engineering, Department of Mechanical Engineering, İzmir-Türkiye
ORCID: 0000-0002-5739-2119*

ABSTRACT

With technology, industrial development, and increasing population, energy demand is increasing day by day. Interest in renewable energy sources has increased because fossil fuels used to obtain energy are depleting and harming the environment. In this context, using renewable energy sources is essential in every area where energy is needed. Using both environmentally friendly and inexhaustible renewable energy resources will enable us to leave a liveable world to future generations. For this purpose, many researchers are carrying out studies on systems that will enable us to benefit from renewable energies and increase the efficiency of these systems. In this study, the theoretical analysis of the Organic Rankine Cycle (ORC) with a Parabolic Trough Collector (PTC), which is used to generate electricity from solar energy, one of the most important renewable energy sources in Şırnak climate conditions, has been carried out. Analyses for days representing the summer months have been carried out hourly during daylight hours. PTC, which has been used to produce useful energy from solar energy, tracks the sun throughout the day. The radiation on the PTC has been calculated using a method for the estimation of clear-sky radiation. Energy analyses of the PTC, ORC, and the entire system have been made hourly for the average days of summer months. As a result of the theoretical studies, the results showed that the highest electrical energy generation at the generator is achieved on June 11 with 169.811 kW, and the maximum overall system efficiency is reached on August 16 with 0.16303.

Keywords: Solar Energy, Parabolic Trough Collector, Organic Rankine Cycle, Efficiency.

Introduction

The ever-growing need for energy worldwide and the environmental hazards of fossil-based fuels gave rise to the utilization of renewable energy sources. The development of energy systems that use renewable energy sources will allow engineers and scientists to benefit from the advantages of these kinds of sources. Numerous studies can be found in the literature about the thermal performance analysis of solar energy-assisted thermodynamic systems that employ different kinds of refrigerants.

Bellos and Tzivanidis (2017) investigated the utilization of nanofluids in a solar field in an effort to achieve higher system performance. The system consists of a Parabolic Trough Collector, a storage tank, and an organic Rankine cycle. The authors investigated four different nanoparticles: Al_2O_3 , CuO, TiO_2 , and Cu. Syltherm 800 is utilized as the base fluid, and pure thermal oil is employed as the working fluid. Moreover, four different refrigerants are employed in the organic Rankine cycle, namely toluene, MDM, cyclohexane, and n-pentane, and their performances are compared with each other. The authors considered the concentration of the nanoparticles and the ratio of the turbine inlet pressure to critical pressure as the optimization parameters. The results showed that toluene is the most desirable organic fluid and CuO is the best nanoparticle. The combination of these two fluids results in 167.05 kW of electricity production and 20.11% system efficiency. Singh et al. (2023) proposed a solar-powered hybrid power system that includes a Kalina Cycle (KC) and an organic Rankine cycle (ORC). The parabolic trough collector is modeled with two different working fluids: Syltherm-800 and Mxene/Syltherm-800 nanofluid. The usage of Mxene-based nanofluid resulted in an 11.10% increase in generated useful heat. Moreover, the Mxene-based nanofluid

gave rise to superior performance in converting solar energy into usable power with higher efficiency. Shahverdi et al. (2021) analyzed a solar-driven ORC system that provides the required power to an irrigation system. The parabolic trough collectors are used to provide the heat required in the evaporator. The authors have analyzed the performances of eight different organic fluids in the ORC. The results revealed that the most optimal ORC performance is acquired by employing the MDM working fluid with a system efficiency of 12.19%. And the minimum collecting area is obtained to be about 22.6 m². Pina et al. (2021) introduced and analyzed a novel hybrid solar-biomass ORC-based poly-generation thermal system from economic, energy, and environmental viewpoints. The poly-generation system is designed to be used in Zaragoza, Spain. The thermal and economic analyses revealed that the system is not economically viable because the electricity production (279.07 €/MWh) is much costlier than the current electricity purchase price in Spain. Li et al. (2023) investigated a 300 kW ORC-based hybrid solar-geothermal power generation system at four different places in China. The optimal design configuration of the thermal system is calculated by minimizing the levelized cost of energy (LCOE) with regard to a certain annual electricity generation (E). The results showed that the hybrid system minimized the LCOE and maximized the E by 25.34% and 16.28%, respectively, compared to the individual solar system. Karthikeyan and Kumar (2023) proposed a novel trigeneration system as an alternative approach to cooling systems in dairy plants. The system absorbs and utilizes solar power during the day, and uses abundant cotton waste biomass during the night. The authors studied the system for different conditions in cities around India. The results revealed that, for the cold region city of Sundernagar, the highest electricity and hydrogen production rates are achieved, which are 220 kW and 1.9 kg/h, respectively. Furthermore, the selected cities displayed impressive CO₂ emission decreases ranging between 364 kg/h to 43 kg/h.

This study investigates the energy production performance of a parabolic trough collector (PTC)-assisted ORC that operates in Şırnak climatic conditions. It is very well known that the solar energy potential of Şırnak is remarkably high in summer. The heat energy absorbed from the sun in the PTC is transferred to the secondary fluid of the ORC to achieve the evaporation process in the evaporator. The mathematical modeling of the thermal system is accomplished. A daily energy production analysis of the thermal system is conducted for the summer days. To the best of the authors' knowledge, the daily energy production analysis of an ORC that operates with a PTC in Şırnak climatic conditions has never been studied in the literature before. This aspect of the study marks its novelty.

Mathematical Modeling of the System

The thermal system analyzed in this study is depicted in Figure 1. Syltherm 800 is employed as the refrigerant in the PTC and heat storage tank, and toluene is utilized as the main refrigerant in the ORC. The heat absorbed from the PTC is transferred to the fluid in the storage tank by a heat exchanger without mixing with the fluid in the tank. The main refrigerant of the ORC absorbs heat from the Syltherm 800 and vaporizes in the evaporator. Afterward, it enters the turbine, where it expands and produces useful work. Then, the refrigerant leaves the turbine and moves into the condenser, where it is cooled down to the desired temperature. Finally, the refrigerant exits the condenser and goes into the expansion valve, where its pressure is regulated to the evaporator level. These processes repeat during the operation of the cycle.

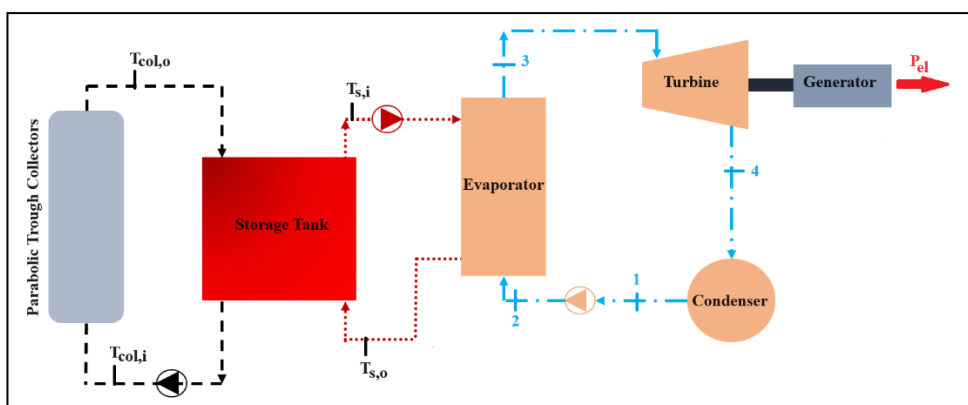


Figure 1. Schematic depiction of the system

Modeling of the PTC

The sun radiation angle received by the collector, which is rotated in the east-west direction to follow the sun during the day, is calculated as follows (Duffie et al., 2020; Kırtepe & Güngör, 2023),

$$\cos \theta = \left(\cos^2 \theta_z + \cos^2 \delta \sin^2 \omega \right)^{1/2} \quad (1)$$

where δ is the declination angle, and ω is the hour angle. The declination angle is determined with the Cooper equation (Duffie et al., 2020),

$$\delta = 23.45 \sin(360(284 + n) / 365) \quad (2)$$

where n is the number of days passed since the first day of the year. The solar zenith angle is obtained with the following equation (Duffie et al., 2020),

$$\cos \theta_z = \sin \delta \sin \phi + \cos \delta \cos \phi \cos \omega \quad (3)$$

where ϕ is the altitude angle. The angle of the sun tracking surface is computed as,

$$\tan \beta = \tan \theta_z \left| \cos(\gamma - \gamma_s) \right| \quad (4)$$

where γ represents the relative surface azimuth angle to the sun azimuth angle. The sun azimuth angle is calculated as follows,

$$\gamma_s = \text{sign}(\omega) \cdot \cos^{-1} \left(\frac{\cos \theta_z \sin \phi - \sin \delta}{\sin \theta_z \cos \phi} \right) \quad (5) \text{ The instant}$$

solar radiation received by the PTC in clear weather conditions is determined with the following equations (Kırtepe & Güngör, 2019; Duffie et al., 2020),

$$\tau_b = a_0 + a_1 \exp \left(\frac{-k}{\cos \theta_z} \right) \quad (6)$$

where τ is the transparency ratio, and a and k are the correction factor parameters. The direct solar radiation in clear weather conditions is,

$$G_{cnb} = G_{on} \tau_b \quad (7)$$

where G_{on} is the extraterrestrial radiation incident on the plane normal to the radiation on the n th day of the year. The clear-sky horizontal solar beam radiation is calculated as follows,

$$G_{cb} = G_{cnb} \cos \theta_z \quad (8)$$

The solar radiation received by the tilted collector surface is determined with the following equation,

$$G_{ctb} = G_{cb} R_b \quad (9)$$

where R_b is the ratio of beam radiation on the tilted surface to that on a horizontal surface at any time (Duffie et al., 2020). The effects of solar beams reflected from the ground and non-uniform radiations arriving at the collector surface are neglected in the calculations.

The mathematical model of the PTC is accomplished with the below-given equations (Forristall, 2003; Kırtepe et al., 2019). The absorbed radiation from the cylindrical receiver is determined as,

$$S = G_{ctb} \left(\prod_{i=1}^6 \gamma_i \right) \tau_c \alpha_r K(\theta) \quad (10)$$

where $K(\theta)$ is a parameter that incident angle modifier, and τ_c and α_r are the transmittance of the glass envelope and absorptance of absorber, respectively. The numerical values of the PTC parameters, γ , are given in Table 1 (Forristall, 2003).

Table 1. PTC optical parameter values.

Optical Property	Value
Collector shadowing effect (γ_1)	0,974
Tracking error (γ_2)	0,994
Mirror alignment geometry error (γ_3)	0,980
Dirt on mirrors (γ_4)	0,995
Dirt on collector (γ_5)	0,997
Unaccounted factors (γ_6)	0,960
Clean mirror reflectance (λ)	0,935

The amount of heat transferred to the fluid that flows through the collector and the thermal efficiency of PTC is calculated with the following equations (Duffie et al., 2020),

$$\dot{Q}_u = A_a F_R \left(S - \frac{A_r}{A} U_L (T_{col,i} - T_{amb}) \right) \quad (11)$$

$$\eta_{col} = \frac{\dot{Q}_u}{G_{ctb} A_a} \quad (12)$$

where U_L and F_R are the overall heat loss coefficient and collector heat recovery factors, respectively, and A is the surface area. The mass flow rate of the refrigerant passing the collector is determined with respect to the surface area of the collector (Bellos & Tzivanidis, 2018),

$$\dot{m}_{col} = 0.02 A_a \quad (13)$$

The heat loss occurring in the glass cover is computed as,

$$\dot{Q}_c = \varepsilon_c \pi D_{c,o} L \sigma (T_{c,o}^4 - T_{amb}^4) + h_{c,amb} \pi D_{c,o} L (T_{c,o} - T_{amb}) \quad (14)$$

where D and L are the diameter and length of the glass cover, respectively. The McAdams equation is utilized to obtain the heat convection coefficient between the glass and the ambient (Duffie et al., 2020). The heat transfer occurring on the glass surface is calculated with the following equation,

$$\dot{Q} = \frac{2\pi k L (T_{c,i} - T_{c,o})}{\ln \left(\frac{D_{c,o}}{D_{c,i}} \right)} \quad (15)$$

The emissivity factor of the cylindrical receiver is computed with respect to the outer surface temperature,

$$\varepsilon_r = 0.000327 T_{r,o} - 0.06597 \quad (16)$$

And the heat transfer to the fluid flowing through the collector is determined with the following equation,

$$\dot{Q} = \dot{m}_{col} c_p (T_{col,o} - T_{col,i}) \quad (17)$$

Modeling of the ORC and Thermal Storage Tank

The following assumptions have been taken into account to simplify the calculations and computational burden during the modeling of the ORC and thermal storage tank (Li et al., 2014);

- The ORC operates under steady-state conditions.
- Heat losses and leakages from the pipes are neglected.
- The evaporator and condenser are shell-and-tube type heat exchangers.
- The ORC working fluid leaves the condenser at the saturated liquid phase
- The potential and kinetic energy changes are neglected.

- The working fluid performs a fully developed flow during the operation of the cycle.
- The PTC-side fluid enters the collector at 300°C.
- The ORC working fluid leaves the evaporator at the saturated vapor phase.

The heat and mass balance equations form the backbone of the thermodynamic model of the system. The mass balance equation is as follows,

$$\sum \dot{m} = 0 \quad (18)$$

The energy balance in each system component is determined with the following equation,

$$\sum \dot{Q} + \sum P + \sum (\dot{m}.h) = 0 \quad (19)$$

where Q is the rate of heat transfer and P is the work. The operating parameter values of the overall system are listed in Table 2 (Bellos & Tzivanidis, 2018; Kırtepe & Güngör, 2019; Kırtepe & Turgut, 2021).

Table 2. Overall system operating parameter values.

Parameter	Value
Cylindrical receiver outer diameter ($D_{r,o}$)	0,07 m
Cylindrical receiver inner diameter ($D_{r,i}$)	0,066 m
Cylindrical receiver heat conduction coefficient (k_r)	54 W/mK
Cylindrical receiver absorption rate (α_r)	0,96
Glass cover outer diameter ($D_{c,o}$)	0,115 m
Glass cover inner diameter ($D_{c,i}$)	0,109 m
Glass cover heat conduction coefficient (k_c)	1,2 W/mK
Glass cover emissivity (ϵ_c)	0,88
Glass cover transparency (τ_c)	0,95
PTC clearance area	5x7,8 m ²
Heat storage tank volume (V_t)	10 m ³
Turbine isentropic efficiency ($\eta_{turbine}$)	0,85
Pump isentropic efficiency (η_{pump})	0,70
Generator electromechanic efficiency ($\eta_{generator}$)	0,98
Condenser temperature (T_{cond})	45 °C

Validation of the PTC Model

A model validation study is accomplished to assess the accuracy of the developed PTC mathematical model. The outcomes of the developed PTC model are compared with that of the experimental study done at Sandia National Laboratory (Dudley et al., 1994). The variations of the reduced temperature parameter with respect to the PTC efficiency for both models are depicted in Figure 2. It is realized that the outcomes of both models agree well, and the behavior differences between the models are negligible. The maximum deviation between the two models is observed as 7.65%.

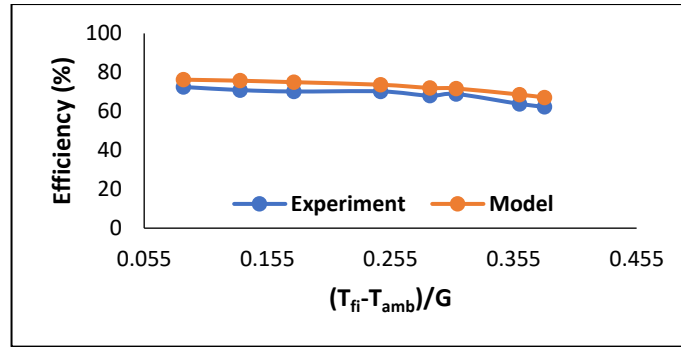


Figure 2. The prediction capability assessment of the developed PTC model.

Findings and Discussion

The theoretical analysis of the solar energy-assisted ORC system is carried out on three different summer days, namely June 11, July 17, and August 16, between 7 a.m. and 6 p.m. The PTCs used in the examined system tracked the sun in the east-west direction. The hourly solar radiation received by PTC was calculated using the clear-sky model. The average daily wind speed and hourly ambient temperature are determined by averaging the 2017-2023 data obtained from the Şırnak Meteorology Station Directorate. Figure 3 shows the solar radiation and ambient temperature variations throughout the analyzed hours and days.

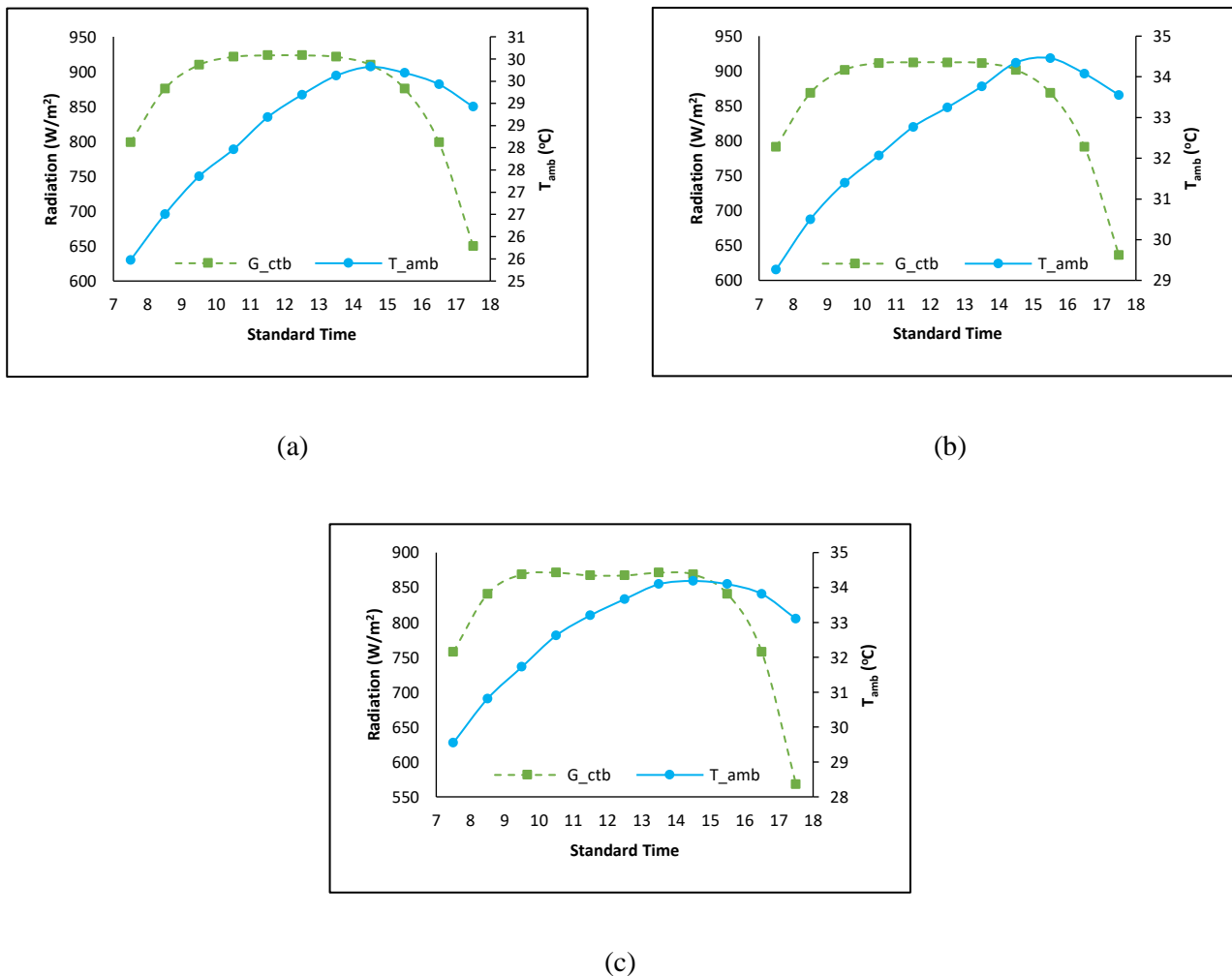
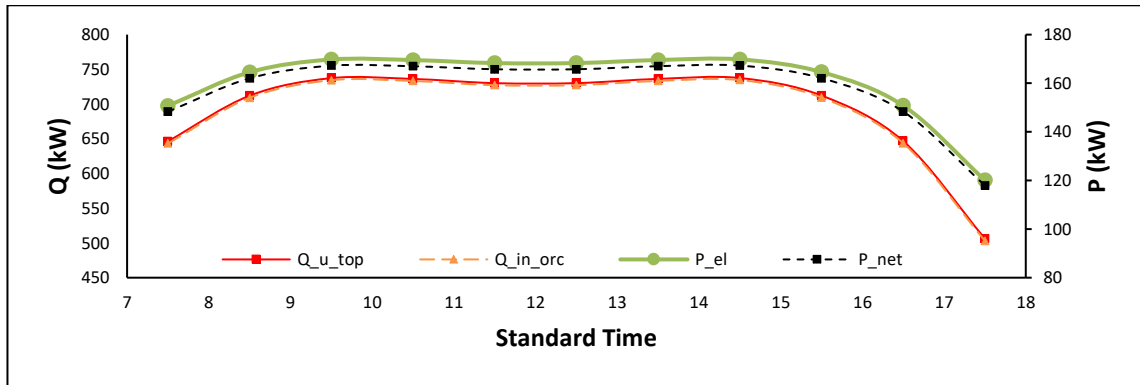
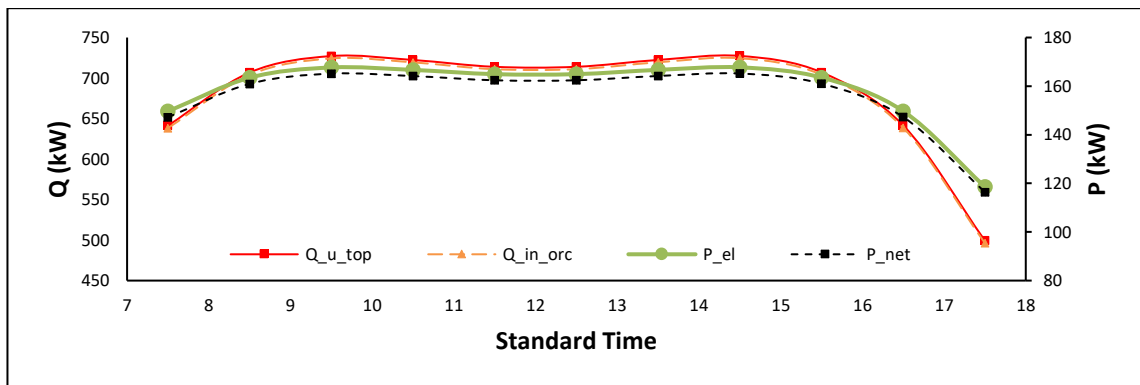


Figure 3. The solar radiation and ambient temperature variations on a) June 11 b) July 17 c) August 16.

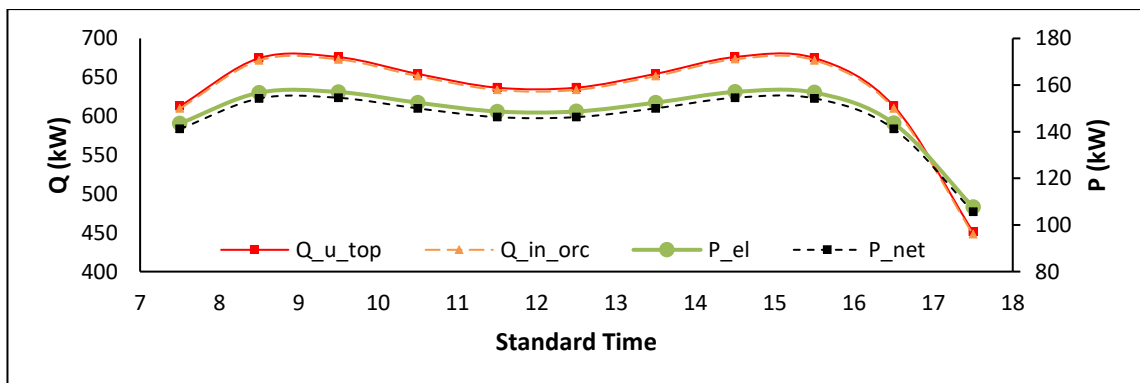
Figure 4 depicts the hourly changes in the heat transfer rates in collectors and ORC evaporator and the electrical energy generated at the generator and net ORC system for the three analyzed summer days. The maximum generated electrical energies at the generator for June 11, July 17, and August 16 are 169.811 kW, 167.729 kW, and 157.052 kW, respectively. The highest electrical energy is generated on June 11. Moreover, the maximum heat rates absorbed from collectors for June 11, July 17, and August 16 are 737.493 kW, 727.322 kW, and 676.133 kW, respectively.



(a)

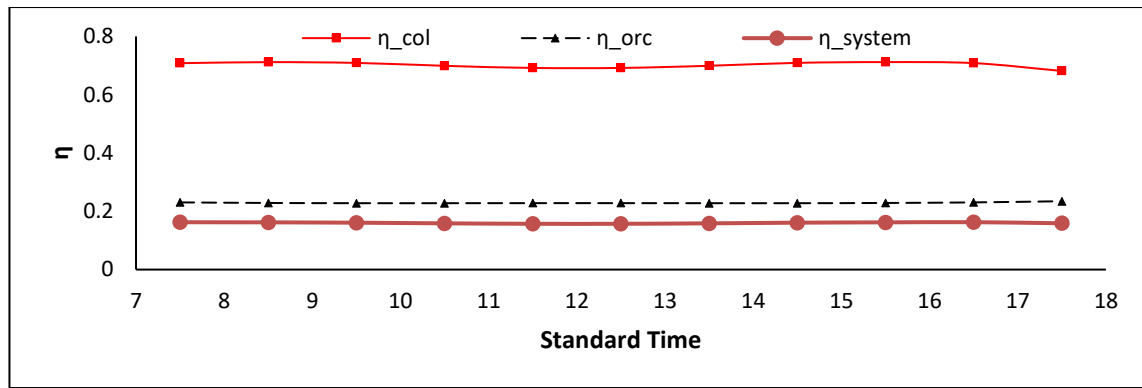


(b)

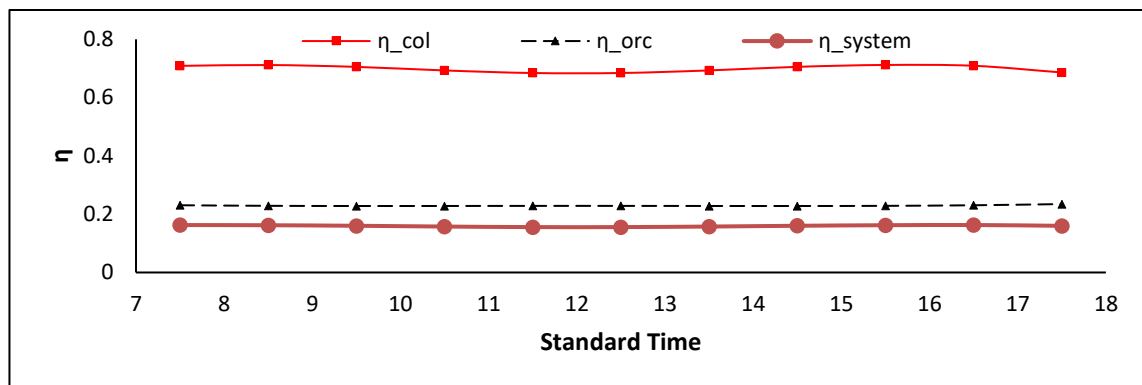


(c)

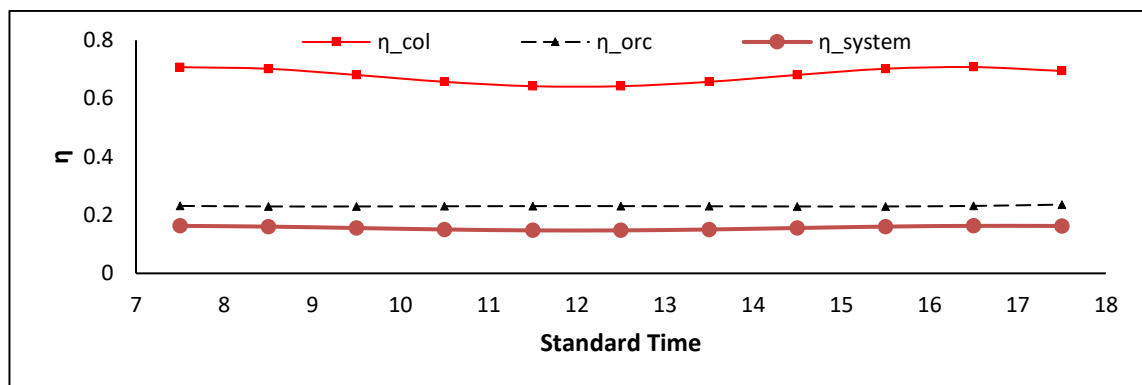
Figure 4. The hourly variations of the heat transfer rate obtained from collectors and supplied to the ORC, and electrical energy generated at the generator and overall net ORC energy for the days a) June 11 b) July 17 c) August 16.



(a)



(b)



(c)

Figure 5. The hourly changes of the ORC, PTC, and overall system efficiencies for the days a) June 11 b) July 17 c) August 16.

Figure 5 shows the hourly changes in the ORC, PTC, and overall system efficiencies for the analyzed summer days. It is observed that the maximum ORC efficiencies for June 11, July 17, and August 16 are 0.23446, 0.23465, and 0.23591, respectively. Moreover, the highest overall system efficiencies for the same days are 0.16252, 0.16282, and 0.16303.

Conclusion and Recommendations

This study analyzes the operation and power production performance of a solar energy-assisted ORC. The wind speed and temperature data are collected from Şırnak Meteorology Station Directorate. The hourly solar radiation received by the sun-tracking PTC is calculated by using the clear-sky method. The mathematical

model of the thermodynamic system is developed. The prediction accuracy of the PTC model is validated by comparing its outcomes with that of a system with similar configurations. The theoretical investigations are carried out for three different average days of summer months between 7 a.m. and 6 p.m. The results showed that the highest electrical energy generation at the generator is achieved on June 11 with 169.811 kW, and the maximum overall system efficiency is reached on August 16 with 0.16303.

References

- Bellos, E. & Tzivanidis, C. (2017). Parametric analysis and optimization of an Organic Rankine Cycle with nanofluid based solar parabolic trough collectors. *Renewable Energy*. 114, 1376-1393.
- Bellos, E. & Tzivanidis, C. (2018). Parametric Analysis and Optimization of a Cooling System with Ejector-Absorption Chiller Powered by Solar Parabolic Trough Collectors. *Energy Conversion and Management*, 168, 329-342. <https://doi.org/10.1016/j.enconman.2018.05.024>.
- Dudley, V.E., Kolb, G.J., Mahoney, A.R., Mancini, T.R., Matthews, C.W., Sloan, M. & Kearney, D. (1994). Test Results: SEGS LS-2 Solar Collector. *Report of Sandia National Laboratories (SANDIA-94-1884)*.
- Duffie, J.A., Beckman, W.A. & Blair, N. (2020). *Solar Engineering of Thermal Processes, Photovoltaics and Wind*. 5th ed., John Wiley and Sons.
- Forristall, R. (2003). Heat Transfer Analysis and Modelling of a Parabolic Trough Solar Receiver Implemented in engineering Equation Solver. NREL/TP-550-34169.
- Karthikeyan, B. & Kumar, G.P. (2023). Thermo-economic and optimization approaches for integrating cooling, power, and green hydrogen production in dairy plants with a novel solar-biomass cascade ORC system. *Energy Conversion and Management*. 295, 117645. <https://doi.org/10.1016/j.enconman.2023.117645>.
- Kırtepe, E., Yılmaz, R. & Özbalta, N. (2019). Parabolik Yoğunlaştırıcı Toplayıcıların Teorik Modellenmesi ve Farklı Sistem Parametrelerinin Verime Etkisinin İncelenmesi. 22. Ulusal Isı Bilimi ve Tekniği Kongresi, 11-14 September 2019, Kocaeli, Turkey.
- Kırtepe, E. & Güngör, A. (2019). İzmir Koşullarında Açık Gökyüzü Işınımı için Fotovoltaik Termal (PV/T) Kolektörün Teorik Modellenmesi. 14. Ulusal Tesisat Mühendisliği Kongresi. 17-20 April 2019. İzmir, Turkey.
- Kırtepe, E. & Turgut, O.E. (2021). Theoretical Modeling and Investigation of System Parameters of Organic Rankine Cycle With Nanofluid Used Solar Parabolic Trough Collector. 5th International Anatolian Energy Symposium. 24-26 March 2021, Karadeniz Technical University, Trabzon/Turkey.
- Kırtepe, E. & Güngör, A. (2023). Güneş Enerjili Absorpsiyonlu Soğutma Sisteminin Şirnak İli İklim Koşullarındaki Davranışının Teorik İncelemesi. *Tesisat Mühendisliği*. Sayı: 198, sf. 23-33, Eylül-Ekim 2023.
- Li, D., Rao, Z., Zhuo, Q., Chen, R., Dong, X., Liu, G. & Liao, S. (2023). Resource endowments effects on thermal-economic efficiency of ORC-based hybrid solar-geothermal system. *Case Studies in Thermal Engineering*. 52, 103739. <https://doi.org/10.1016/j.csite.2023.103739>.
- Li, Y-R., Du, M-T., Wu, C-M., Wu, S-Y. & Liu, C. (2014). Potential of organic Rankine cycle using zeotropic mixtures as working fluids for waste heat recovery. *Energy*, 171, p. 95-108. <https://doi.org/10.1016/j.energy.2014.09.035>.
- Pina, E.A., Lozano, M.A., Serra, L.M., Hernandez, A. & Lazaro, A. (2021). Design and thermo-economic analysis of a solar parabolic trough - ORC – Biomass cooling plant for a commercial center. *Solar Energy*. 215, p. 92-107. <https://doi.org/10.1016/j.solener.2020.11.080>.
- Shahverdi, K., Bellos, E., Loni, R., Najafi, G. & Said, Z. (2021). Solar-driven water pump with organic Rankine cycle for pressurized irrigation systems: A case study. *Thermal Science and Engineering Process*. 25, 100960. <https://doi.org/10.1016/j.tsep.2021.100960>.

Singh, S.S., Tiwari, A.K. & Paliwal, H.K. (2023). Thermo-economic assesment of hybrid Kalina cycle and organic Rankine cycle system using a parabolic trough collector solar field. *Thermal Science and Engineering Progress*, 46, 102132. <https://doi.org/10.1016/j.tsep.2023.102132>.



HYDROGEN - FUEL OF THE FUTURE

Kassayeva Assylkanym Zhulamanovna, associate professor.

Yessenov University, Aktau, Kazakhstan

Savelkin Nikita Kirillovich, assistant.

Yessenov University, Aktau, Kazakhstan

ABSTRACT

Hydrogen is the most common element on earth, but it is chemically bound in water, hydrocarbons, carbohydrates and other substances. To separate hydrogen, you need to invest energy. There are several methods for producing hydrogen, such as steam conversion of natural gas, production from biomass, high-temperature decomposition of water and electrolysis.

The production of green hydrogen by low-temperature electrolysis makes it possible to obtain hydrogen up to 80% of energy consumption. During its decomposition, the resulting products, in addition to hydrogen, are oxygen and water vapor. The received energy will be generated at the expense of a power plant, the principle of operation of which is based on the use of alternative energy sources (water, wind, sun). It is recommended to install a hydrogen production plant on the shore of the Caspian Sea to reduce transportation costs and to increase production efficiency.

Electrolyzer installations are commercially available. The limit of the net efficiency of low-temperature electrolysis systems producing hydrogen at pipeline pressures is ~ 99%. With this method of hydrogen production, the cost will be three times lower than when using conventional methods of hydrogen production.

Keywords: Alternative energy, green hydrogen, electrolyzer, technological complex, sea, station, efficiency, economy, consumption.

EVALUATION THE PERFORMANCE OF SHELL/TUBE HEAT EXCHANGERS USING HYBRID NANO FLUID

Maissa Bouselsal

Departement of Physics, Faculty of Sciences University of 20 Aout 1955-Skikda- Algeria

Fateh Mebarek - Oudina

Departement of Physics, Faculty of Sciences University of 20 Aout 1955-Skikda- Algeria

ABSTRACT

Our work consists in studying by numerical simulation the phenomenon of natural convection in a square saturated by a nanofluid (nanofluids and hybrid nanofluids) and mixtures of this basic fluid and nanoparticles (Al_2O_3 , Cu) and hybrid nanoparticles (Al_2O_3 - CuO), with a cylindrical heat source.

The resolution of the system of equations describing the thermal transfer and hydrodynamic flow of the two models is solved numerically using Comsol Multiphysics software based on the Galerkin finite element method.

The effects of Rayleigh Ra, nanoparticle density fraction (ϕ) and nanoparticle type on temperature contours and Nusselt number were studied.

The results of this study show that increasing the density fraction of nanoparticles (ϕ) promotes heat transfer as well as increasing the number of Rayleigh Ra improves heat transfer. Heat transfer is preferred for Al_2O_3 -CuO/water nanofluids.

Keywords: heat transfer, natural convection, nanofluid, nanoparticles, square

PRODUCTION, IMPROVEMENT AND CHARACTERIZATION OF ACTIVATED CARBON FIBERS FROM DATE PALMS

Huda Assi ALBAYATI

*MSc Student, Bolu Abant İzzet Baysal University, Faculty of Engineering, Department of Chemical Engineering, Bolu-Türkiye
(Responsible Author) ORCID: 0009-0005-4225-9912*

Waleed M. SH. ALABDRABA

*Prof. Dr., Tikrit University, Faculty of Engineering, Department of Environment Engineering, Tikrit-Iraq
ORCID: 0000-0002-2357-0597*

Cem GÖL

*Assist. Prof. Dr., Bolu Abant İzzet Baysal University, Faculty of Engineering, Department of Chemical Engineering, Bolu-Türkiye
(Responsible Author) ORCID: 0000-0001-9258-1866*

ABSTRACT

This research focuses on the production of activated carbon fibers using different activation methods, with emphasis on chemical treatment to improve resistance and process efficiency, in order to obtain an effective adsorbent from agricultural waste that would be used for the removal of organic pollutants and heavy metals in wastewater. The raw material chosen for this endeavour is palm fiber, due to Iraq's global leadership in date production and the significant amount of agricultural waste generated. The chemical treatment process involves two basic steps: coating the carbon with a layer of N-doped carbon and then applying a layer of double hydroxide (LDH) to increase the efficiency of the process. In this study, three samples were obtained and examined by XRD, SEM and BET. The results showed that the produced carbon fibers had good surface area and pore size. As a result of this study, the obtained activated carbon fibers can be used in the process of removing pollutants from water.

Keywords: Activated Carbon Fibers, ACFs, Date Palm Fibers.

Introduction

Water and land resources will suffer if petroleum products leak into the environment (Al-Majed et al., 2012; Sajida & Hemlata, 2021). Several authors (Boehm et al., 2011; Burton et al., 2010) have reported on the detrimental effects on birds, marine life, and other species. Oil spills have been cleaned up using a variety of techniques, including in-situ burning, the use of sorbents, chemical techniques like the use of dispersants, mechanical techniques like skimming and solidification, and biological techniques like the use of bacteria or enzymes (Cumio et al., 2007; Etkin & Nedwed, 2021; Iriakuma et al., 2016; Perkovic, 2016; Saleem et al., 2018; Sundaravadivelu, 2015). Many of these techniques, according to some researchers, are expensive and don't eliminate the components from the spills (Guia et al., 2018). Planning for environmental cleanup should take into account a solution that won't cause further environmental issues. Natural sorbents are numerous, affordable, and extremely effective in cleaning up oil spills, making them a highly promising option for environmental rehabilitation. Numerous writers have discussed the efficiency and environmental friendliness of using natural sorbents to clean up oil spills (Kandanelli et al., 2018). Peat moss, rice straws, raw cotton, kapok, milkweed, sugarcane bagasse, maize cobs, rice hulls, and various sorbents have all been examined (Abdullah et al., 2010; Alaa El-Din et al., 2018; AlAmeri et al., 2019; Ben Jmaa & Kallel, 2022; Praba Karana et al., 2011).

Activated carbon fiber (ACF) was made using acrylic textile fibers by Carrott et al. With the active fibers at 900 °C. It was discovered that, with one fiber in particular, the number of micropores tripled, the average pore width abruptly rose, the average stack height, L, abruptly fell, and the reactivity decreased by more than half throughout a relatively constrained burn range between 40 and 50%. The observed variations point to a shift in the c-activation process from one that largely involves single crystal attack and rearrangement at

greater combustion to one that primarily involves gasification of amorphous or more reactive carbon at lower combustion (Carrott et al., 2001).

An N-doped AC was created by Li et al. using urea as the nitrogen supply and corncob as the carbon precursor. This AC demonstrated good electrochemical performance. To increase the ammonia removal capacity, Soo-Jin et al. (Park & Kim, 2010) fluoro-oxidized activated carbon fibers (ACFs). By using XPS analysis, it was established that polar groups, such as C-F, C-O, and COOH, had been introduced into the ACFs. BET and t-plot techniques were used to examine the $N_2/77K$ adsorption isotherms' specific surface area, aggregate volumes, and tiny holes. The use of the gas detection tube approach demonstrated the effectiveness of ammonia removal. As a result, when the surface treatment duration rose, the ACFs' unique surface area and micropore size were partially damaged. However, the oxygen-fluorinated ACF enhanced the polar functional groups on the surfaces of the ACF that contained fluorine and oxygen, which boosted the effectiveness of the ACFs generated by removing ammonia (Li et al., 2023).

Activated carbon fiber (ACF) was created by Ka-Lok Chiu et al. by annealing and activating cotton with $ZnCl_2$ in argon. It was discovered that the cotton preserved its original fiber structure and transformed it into microporous ACF. Its 2060 m^2/g BET surface area. The adsorption of methylene blue (MB) in water at various pH levels was used to assess the adsorption capability of this ACF product. It is discovered that the Langmuir isothermal model and the pseudo 2nd-order kinetic model both did an excellent job of explaining the adsorption procedure. The ACF sample could successfully adsorb the methyl bromide in both neutral and alkaline conditions (Chiu & Ng, 2012).

The ACF generated from Oil Palm Empty Fruit Bunch fibers by the one-step direct activation technique (ACF-D) was compared to the ACF produced by the traditional two-step carbonization and activation (ACF-ND) by Chee-Heong Ooi et al. The various characteristics of the created ACFs were looked at. EDS, SEM, FTIR, and XRD were used to characterize raw EFB and ACFs. According to the findings, EFB has an oxygen content of 36.67 wt% and a carbon content of 63.33 wt%. ACF-D was discovered to have a lot of carbon (93.63 weight percent), but little oxygen (5.19 weight percent). ACF-ND produced a sample with a lower oxygen content (3.85 wt%) and a greater carbon content (95.68 wt%). For both ACF samples, there is no obvious distinctive peak in the XRD findings (Ooi et al., 2013).

The adsorption of pollutants by activated carbon with their removal efficiencies as parameters of total suspended solids (TSS), total dissolved solids (TDS), chemical oxygen demand (COD) and biochemical oxygen demand (BOD) in the literature are summarized in Table 1.

Table 1. Literature on adsorption of pollutants by activated carbon with their respective removal efficiencies.

Ref.	Type	Year	Pollutants	Raw materials	Removal efficiency %
(Raji et al., 2021)	AC	2021	COD	-	76.2
			Colors		88.4
(Khalaf Erabee & M. Ethaib, 2018)	AC	2018	COD	Date pits	41.8
			BOD		39.8
			TDS		67.7
			TSS		81.8
(Nayl et al., 2017)	AC	2017	COD	Date palm	95.4
			BOD		92.8
(Ferraz & Yuan, 2020)	AC	2020	COD	Oat hulls	90.0
(Nabavi et al., 2022)	AC	2022	COD	Commercial	44.8
			BOD		44.1
			TDS		46.0
(Pophali et al., 2021)	ACF	2021	COD	Commercial	94.0
			Cr(VI)		97.0
(Samuchiwal et al., 2021)	ACF	2021	COD	Commercial	72.0
			Colors		91.0
(Sharma & Lee, 2017)	ACF	2017	COD	Commercial	82.3
			TOC		79.5
(Berhe et al., 2023)	ACF	2023	COD	Commercial	71.2
			TOC		67.4
			NH ₄ ⁺ -N		69.3
(Dehghani et al., 2021)	ACF	2021	COD	Commercial	96.0
			BOD		95.6
			TDS		91.0
			TSS		76.6

Materials and Methods

Experiments and calculations were conducted in the Water Treatment Laboratory of the College of Engineering at Tikrit University in Iraq. The raw material for producing activated carbon fiber is date palm fiber, which is obtained locally from palm plantations.

The working system consists of laboratory devices used to carry out burning, activation, treatment, measurement and calibration operations. First, the raw material is prepared, then it is cleaned well from dirt and dust. A muffle furnace was used to complete the carbonization process. After the activation process, the sample is washed, and a pH meter is used to ensure that the pH has reached equilibrium. Samples are then prepared for carbonization, activation and curing processes, each of which will be explained in detail (Figure 1).

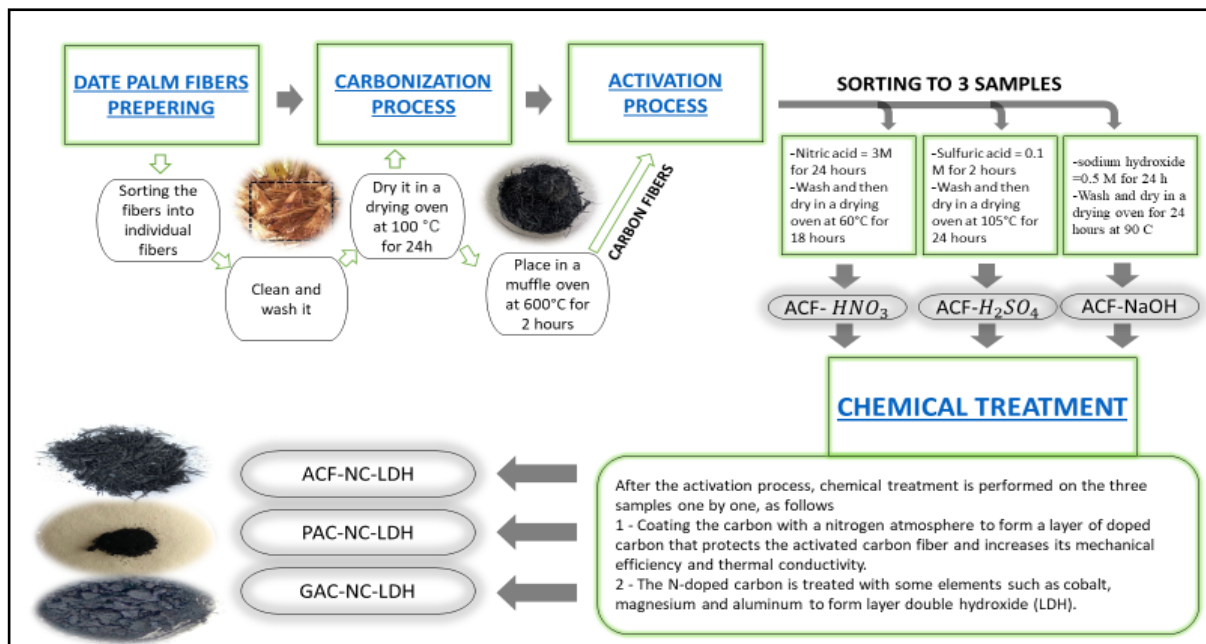


Figure 1. Experimental Setup of Production processes.

The primary cell-wall and additional secondary walls of date palm fibers are made up of a number of helically wrapped cellular micro-fibrils made of long chain cellulose molecules, which might affect the fiber's mechanical characteristics. The three primary components of every cell wall are cellulose, hemicelluloses, and lignin. The most important structural elements in most natural fibers are cellulose and lignin. Chemical composition of date palm fibers are listed in Table 2 (Saba, 2020). Despite being resistant to hydrolysis, strong alkalis, and oxidizing agents, cellulose is also somewhat degradable when subjected to chemical treatments.

Table 2. Chemical Composition (%) of Date Palm Fibers (Saba, 2020).

Constituents	Cellulose	Hemicelluloses	Lignin	Ash	Extractive
Leaflet	40.21	12.80	32.2	10.54	4.25
Leaf	54.75	20.00	15.30	1.75	8.20
Rachis	38.26	28.17	22.53	5.96	5.08

Date palm tree (Figure 2) fibers were identified as a raw material for the production of activated carbon fibers and powder activated carbon. The fallen date palm fibers were collected from the trees located locally, considering the selection of the good ones.

The fibers are broken up in the form of separate strands, then cleaned and washed well with distilled water to get rid of pollutants that may harm the production process. In addition, it was washed again with non-ionic (DI) water to remove any impurities or ions that could cause undesirable reactions. After the washing process, the fibers are dried in a drying oven at 100 degrees for 24 hours to get rid of any moisture, and then the material is ready for the carbonization process.

The dried palm fibers were previously placed in special packages, taking into account that they are closed tightly to ensure that no air enters them, then they are inserted into the muffling oven at a temperature of 600 degrees Celsius for a period of two hours. The packages are removed from the muffle furnace, and thus we have obtained (inactive) carbon fibers (Czerwińska et al., 2022; L. Wang et al., 2019).

After completing the carbonization process, inactivated carbon fibers were obtained. The chemical activation process was carried out on carbon fibers using nitric acid HNO_3 at a concentration of 3 M, where the sample is soaked in the acid for 24 hours. Then the sample is washed in deionized water repeatedly for the purpose

of obtaining a neutral pH value. Then the sample is dried at 60 °C for 18 hours. To activate the second sample, Dilute sulfuric acid H_2SO_4 at a concentration of 0.1 M was used. The second sample was soaked in the acid for 2 hours (Lee et al., 2014). Then the sample is washed in de-ionized water repeatedly, then the sample is dried in a drying oven at 105 °C for 24 hours. In addition, a third sample of carbon fibers was prepared and activated using sodium hydroxide at a concentration of 0.5 M for 24 hours, then washed with non-ionic water several times, then dried in a drying oven for 24 hours at 90 °C (Moon et al., 2006).



Figure 2. Date Palm Tree

Chemical treatment by carbon coating with a nitrogen atmosphere leads to the creation of a layer of doped carbon that protects the activated carbon fibers and increases their mechanical efficiency and thermal conductivity. In addition, some elements such as cobalt, magnesium and aluminum are treated to form double-layer hydroxide (LDH). The activated carbon fibers are laminated with a hydroxide network after creating the doped carbon layer (Ulla Gro Nielsen, 2021). This network stimulates the activated carbon to absorb the largest possible number of pollutants, which greatly increases the removal efficiency. For the sample that activated by nitric acid HNO_3 , the encapsulation process is carried out by preparing two solutions of hydrochloric acid HCl (1M, 50ml), then 2.3 ml of aniline is added to one of the solutions, and 5.8 g of ammonium persulfate is added to the second solution. The first solution containing aniline is added to the activated carbon fibers. Then the second solution containing ammonium persulfate is gradually added to the mixture for 25 minutes using a burette. Finally, the resulting mixture is placed in an ice atmosphere (a container covered with ice) and placed in a magnetic mixer for 6 hours moving speed 800 rpm. Then the sample is placed in a muffle furnace at a temperature starting from 5 °C and up to 400 °C gradually for a period of 3 hours. Thus, we have obtained ACFs coated with an N-doped carbon layer (ACF-NC). Then 1 g of urea, $CoSO_4 \cdot 7H_2O$, $MgSO_4 \cdot 7H_2O$, and $Al_2(SO_4)_3 \cdot 18H_2O$ are added to 100 ml of deionized water (DI), then the mixture is placed in a stainless-steel container and placed in a drying oven at 100 °C for 12 hours. Then it is rinsed with non-ionic water and placed in a drying oven at 60 °C for 6 hours.

The nanosheets have grown on the surface of ACF-NC in the form of a lattice structure, whereby we have obtained (ACF-NC-LDH). The same treatment steps were carried out on the second sample activated by dilute sulfuric acid, after completing the treatment steps, an activated carbon coated with a layer of N-doped carbon with a lattice structure (PAC-NC-LDH) was produced. That is, the product may change from fiber form to powder form. More specifically, the turning point was immediately after using the ice bath. As for the third sample activated with sodium hydroxide, after performing the same chemical treatment stages, the sample appeared in the form of granular agglomerates coated with a layer of N-doped carbon with a network structure (GAC-NC-LDH) (Figure 3).

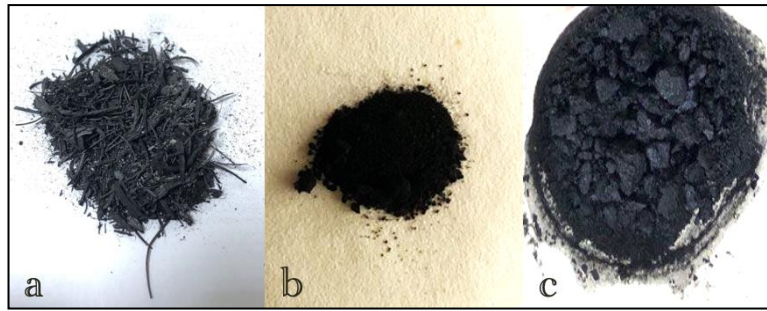


Figure 3. Three samples produced, (a) ACF-NC-LDH, (b) PAC-NC-LDH, (c) GAC-NC-LDH.

Findings and Discussion

The Brunauer Emmett-Teller (BET) analyses were carried out to assess the porosity and ultrastructural characteristics of the as-prepared ACF-NC-LDH, PAC-NC-LDH, and GAC-NC-LDH. BET technique determines the surface area of any adsorbent. The outcome revealed that the ACF-NC-LDH that had been produced had a surface area of $275.62 \text{ m}^2/\text{g}$. The pore size distribution is decreased using the Berrett-Joyner-Halenda (BJH) method. The average pore width was 2.7812 (nm) , and the pore size was $0.1957 \text{ (cm}^3/\text{g)}$. The produced PAC-NC-LDH has a surface area of $147.75 \text{ m}^2/\text{g}$, pore volume of $0.0942 \text{ (cm}^3/\text{g)}$, and an average pore diameter of 2.466 (nm) . The values indicate that the surface area and pore size of ACF-NC-LDH are much larger than that of PAC-NC-LDH and this explains the resulting difference in adsorption efficiency between them. Pore diameters are classified by IUPAC (Zdravkov et al., 2007) as belonging to one of three categories: micropores (diameters less than 2 nm), mesopores (diameters between 2 and 50 nm), or macropores (diameters more than 50 nm). As for GAC-NC-LDH, the surface area was very small, about $10 \text{ m}^2/\text{g}$, the pore volume was $0.016 \text{ (cm}^3/\text{g)}$, and the average pore diameter was 0.62 (nm) , so it was neglected and not included in the experiments because the acceptable limits The surface area of activated carbon must be greater than $10 \text{ m}^2/\text{g}$ (Hu & Srinivasan, 2001). BET analysis results of the samples are summarized in Figure 4.

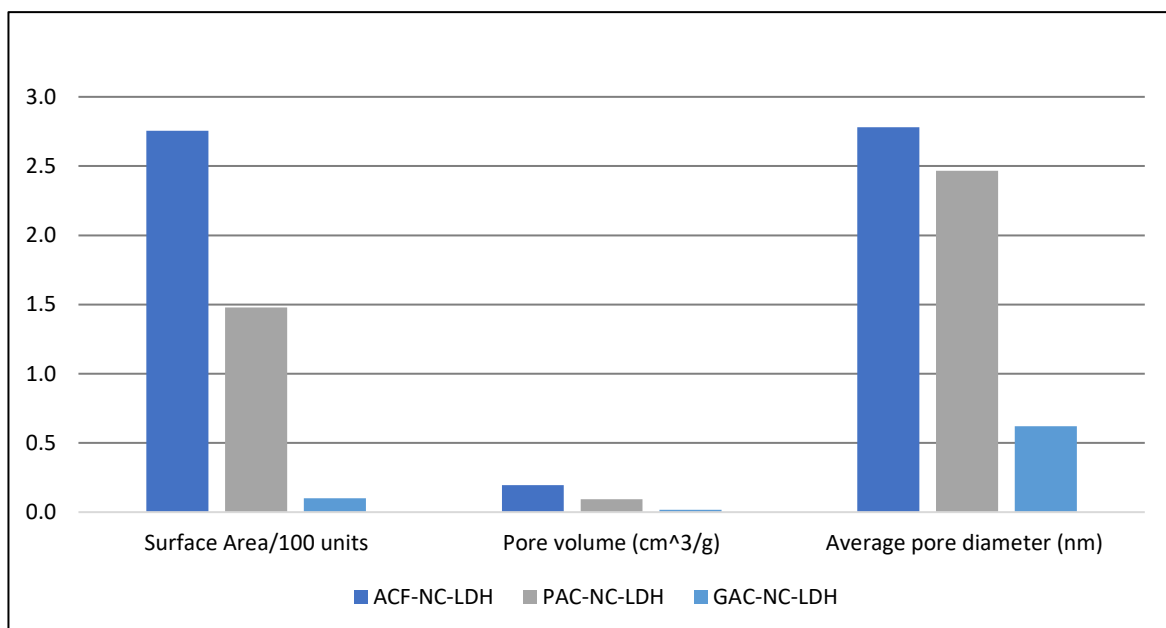


Figure 4. BET analysis for ACF-NC-LDH, PAC-NC-LDH and GAC-NC-LDH.

Figure 5 (a) shows the transformation of the ACFs fibers from twisted and interlaced to rougher after being coated with an N-doped carbon layer, which may provide sufficient active sites for the in-situ creation of MgCoAl-LDH. Some used a network topology in order to give a bimodal pore size distribution (pore size was mostly distributed between 40 and 50 m). The virgin fibers' surface was quite smooth and had a diameter of about 41 m (Figure 5(c)), (J. Wang et al., 2022). After a normal hydrothermal reaction, a substantial number of evenly distributed, vertically oriented LDH sheets with a width of about 2 μm were adhered to the carbon fiber surface.

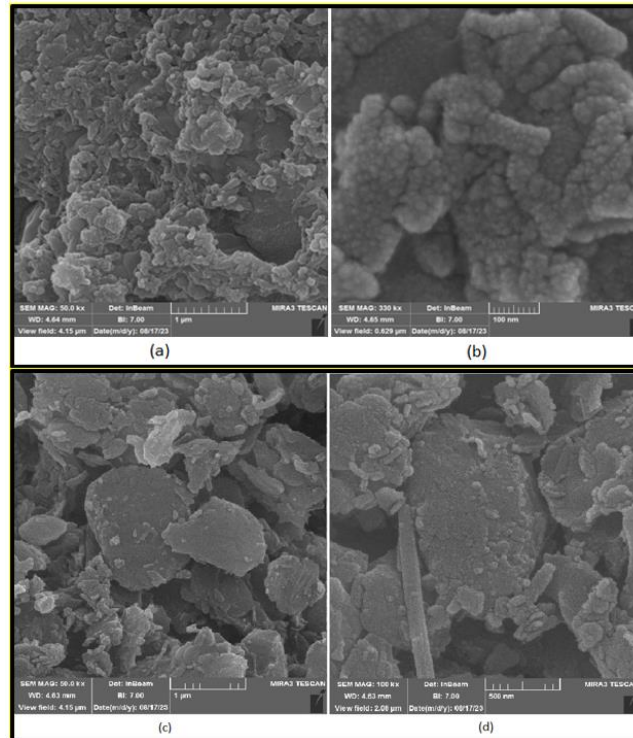


Figure 5. SEM images of ACFs (a,b) Activated carbon fiber ACF after treatment process (ACF-NC-LDH) (b,c) carbon fiber (CFs)

However, due to the inclusion of the N-doped carbon layer and the constrained growth of LDH on the fiber surface, which covered several naturally existing microscopic holes (2 nm) on the surface of the fiber. Figure 5(b) On the surface of pristine ACFs, a buildup of irregular and microscopic LDH sheets known as ACF-NC-LDH develops randomly and is spread, in contrast to pure fibers with smooth surfaces (Figure 5(d)).

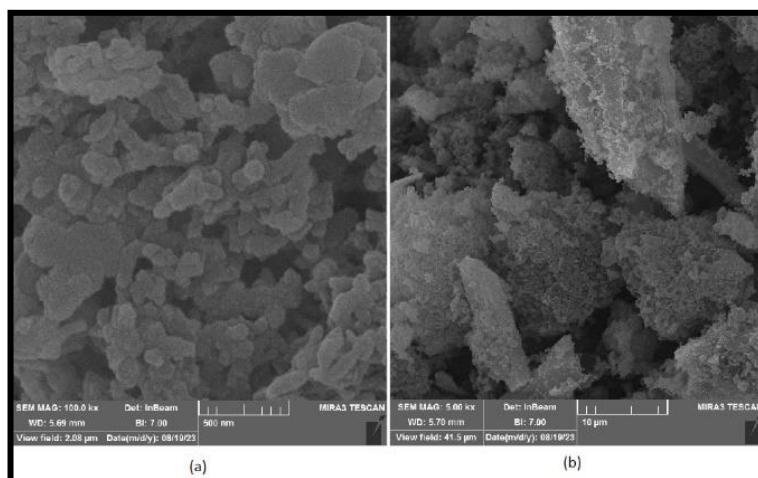


Figure 6. SEM images of Powdered activated carbon PAC after treatment process (PAC-NC-LDH)

Figure 6 (b) clearly shows the granular layer randomly spread on the surface of the activated carbon powder. This is called PAC-LDH. Activation of the N-doped layer led to the bonding of some carbon molecules to each other, making them appear in the form of individual PAC-NC-LDH blocks, as in Figure 6 (a). The diameter of the grains ranged between 30-50nm.

The prepared ACF-NC-LDH's XRD data is displayed in (Figure 7). Sample peaks may be found in ($2\theta = 24.62341, 43.9242$). The crystallization sizes, according to these statistics, are 0.993 and 1.569, respectively. The crystal size L was calculated using Scherrer's equation as follows:

$$B(2\theta) = \frac{K\lambda}{L\cos\theta}$$

where:

B: is the Full Width at Half Maximum (FWHM) of the peak at 2θ .

K: is the Scherrer's constant, which, depending on the crystal shape, can range from 0.6 to 2.08; in this case, we focus on it.

The average crystal size obtained by applying Scherrer's equation to X-ray diffraction data is 1.2815 nm. It has been observed that the closest value was achieved by Ali Hashem et al. (Hashem et al., 2021) and that it has the same peak at 2θ equal to 24.62 by comparing the sharp peak acquired at that value. This indicates that a good level of crystallinity was attained. On the other hand, for PAC-NC-LDH, a peak appeared at 2θ equal to 23.42 (Figure 9), and its crystallization volume was equal to 0.7434 nm. The same result was found by Li-an Xing et al. (Xinga et al., 2023) when 2θ equals 21 demonstrating that the contaminants produced by KOH during the activation process were entirely eliminated by washing with a solution of hydrochloric acid and deionized water. The resultant activated carbon is an amorphous substance. The large peak at about 23 indicates that the material had just a little amount of graphitization throughout the activation phase.

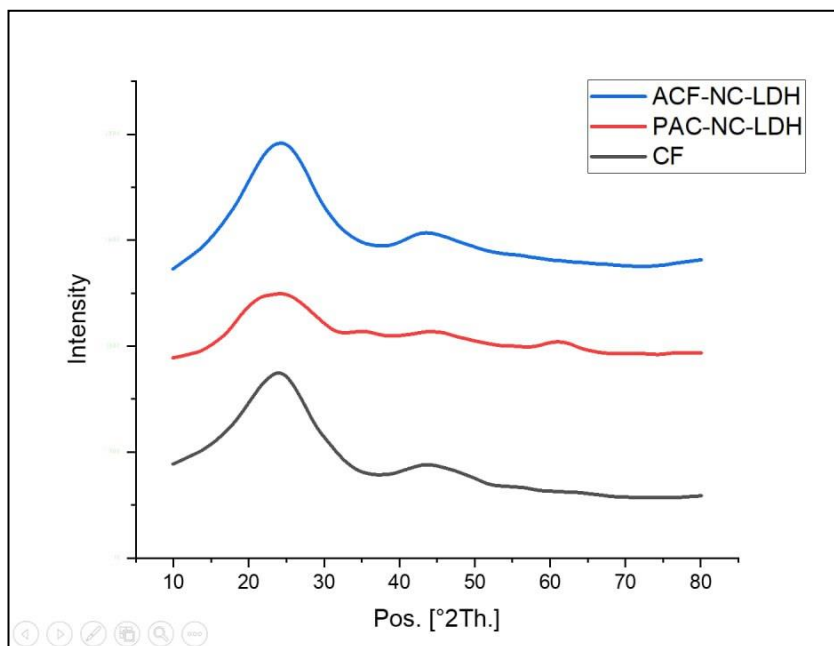


Figure 7. X-Ray analysis for the samples.

For CF before the chemical treatment process, two peaks appeared at 2θ equal to 24.26 and 43.9 (Figure 7), and the average size of the crystals was equal to 1.496 nm, which means that the size of the crystallization decreased slightly during the chemical treatment process, and the reason for this is due to the repeated washing operations during the treatment.

Conclusion and Recommendations

The findings of this study affirm the successful completion of the activated carbon fiber production process, highlighting the substantial influence of activation and treatment procedures on the resulting product's structure and shape. Three distinct samples were obtained: ACF-NC-LDH, PAC-NC-LDH, and GAC-NC-LDH. The potential application of these products in adsorption processes for the removal of organic pollutants from contaminated industrial water appears promising. BET analyses were instrumental in assessing the porosity and structural attributes of ACF-NC-LDH and PAC-NC-LDH. These results underscore the considerable differences in surface area and pore volume between ACF-NC-LDH and PAC-NC-LDH. The morphological transformations of ACFs, captured in Figure 5, reveal the impact of the N-doped carbon layer coating. The hydrothermal reaction resulted in well-distributed LDH sheets on the carbon fiber surface. Conversely, PAC-NC-LDH displayed granular layers (Figure 6), indicating the effect of N-doped layer activation. The calculated average crystal size of 1.2815 nm aligns with existing literature, affirming a satisfactory level of crystallinity.

Further exploration of the structural nuances of ACF-NC-LDH and PAC-NC-LDH is recommended to optimize the synthesis process. Fine-tuning parameters may enhance adsorption performance. Continued research on the practical applications and scalability of ACF-NC-LDH in real-world scenarios is warranted. This includes pilot studies to assess its effectiveness in large-scale environmental remediation efforts. Comprehensive characterization studies, including additional techniques such as TEM and FTIR, can provide deeper insights into the microstructure and chemical composition of the produced materials. Conducting an environmental impact assessment of the activated carbon fibers, considering factors such as reusability, disposal, and long-term effects, will contribute to a holistic understanding of their suitability for environmental remediation.

References

- Abdullah, M. A., Rahmah, A. U., & Man, Z. (2010). Physicochemical and sorption characteristics of Malaysian *Ceiba pentandra* (L.) Gaertn. as a natural oil sorbent. *Journal of Hazardous Materials*, 177(1–3), 683–691. <https://doi.org/10.1016/j.jhazmat.2009.12.085>
- Al-Majed, A. A., Adebayo, A. R., & Hossain, M. E. (2012). A sustainable approach to controlling oil spills. *Journal of Environmental Management*, 113, 213–227. <https://doi.org/10.1016/j.jenvman.2012.07.034>
- Alaa El-Din, G., Amer, A. A., Malsh, G., & Hussein, M. (2018). Study on the use of banana peels for oil spill removal. *Alexandria Engineering Journal*, 57(3), 2061–2068. <https://doi.org/10.1016/j.aej.2017.05.020>
- AlAmeri, K., Giwa, A., Yousef, L., Alraeesi, A., & Taher, H. (2019). Sorption and removal of crude oil spills from seawater using peat-derived biochar: An optimization study. *Journal of Environmental Management*, 250(August), 109465. <https://doi.org/10.1016/j.jenvman.2019.109465>
- Ben Jmaa, S., & Kallel, A. (2022). Chemically Treated Seagrass Fibers as Biosorbent for Crude Oil Removal. In *New Prospects in Environmental Geosciences and Hydrogeosciences: Proceedings of the 2nd Springer Conference of the Arabian Journal of Geosciences (CAJG-2), Tunisia 2019*. Cham: Springer International Publishing. 328–325 .
- Berhe, R. N., Kassahun, S. K., Kang, J. W., Lee, I., Verma, M., & Kim, H. (2023). Performance evaluation of Fe₃O₄@ACF-supported bio-electro Fenton system for simultaneous sewage treatment and methyl orange degradation. *Materials Today Communications*, 35(April), 106331. <https://doi.org/10.1016/j.mtcomm.2023.106331>
- Boehm, P. D., Gundlach, E. R., & Page, D. S. (2011). The phases of an oil spill and scientific studies of spill effects. *Oil in the Environment: Legacies and Lessons of the Exxon Valdez Oil Spill*, January, 37–53. <https://doi.org/10.1017/CBO9781139225335.006>
- Burton, N. H. K., Musgrove, A. J., Rehfisch, M. M., & Clark, N. A. (2010). Birds of the Severn Estuary and Bristol Channel: Their current status and key environmental issues. *Marine Pollution Bulletin*, 61(1–3), 115–123. <https://doi.org/10.1016/j.marpolbul.2009.12.018>
- Carrott, P. J. M., Nabais, J. M. V., Ribeiro Carrott, M. M. L., & Pajares, J. A. (2001). Preparation of activated

- carbon fibres from acrylic textile fibres. *Carbon*, 39(10), 1543–1555. [https://doi.org/10.1016/S0008-6223\(00\)00271-2](https://doi.org/10.1016/S0008-6223(00)00271-2)
- Chiu, K., & Ng, D. H. L. (2012). Synthesis and characterization of cotton-made activated carbon fiber and its adsorption of methylene blue in water treatment. *Biomass and Bioenergy*, 46, 102–110. <https://doi.org/10.1016/j.biombioe.2012.09.023>
- Cumo, F., Gugliermetti, F., & Guidi, G. (2007). Best available techniques for oil spill containment and clean-up in the Mediterranean Sea. *WIT Transactions on Ecology and the Environment*, 103, 527–535. <https://doi.org/10.2495/WRM070491>
- Czerwińska, K., Śliz, M., & Wilk, M. (2022). Hydrothermal carbonization process: Fundamentals, main parameter characteristics and possible applications including an effective method of SARS-CoV-2 mitigation in sewage sludge. A review. *Renewable and Sustainable Energy Reviews*, 154(October 2021). <https://doi.org/10.1016/j.rser.2021.111873>
- Dehghani, Y., Honarvar, B., Azdarpour, A., & Nabipour, M. (2021). Treatment of wastewater by a combined technique of adsorption, electrocoagulation followed by membrane separation. *Advances in Environmental Technology*, 7(3), 171–183. <https://doi.org/10.22104/AET.2021.5133.1394>
- Etkin, D. S., & Nedwed, T. J. (2021). Effectiveness of mechanical recovery for large offshore oil spills. *Marine Pollution Bulletin*, 163(November 2020), 111848. <https://doi.org/10.1016/j.marpolbul.2020.111848>
- Ferraz, F. M., & Yuan, Q. (2020). Performance of oat hulls activated carbon for COD and color removal from landfill leachate. *Journal of Water Process Engineering*, 33(November 2019), 101040. <https://doi.org/10.1016/j.jwpe.2019.101040>
- Guia, J., Teixeira, A. P., & Guedes Soares, C. (2018). Probabilistic modelling of the hull girder target safety level of tankers. *Marine Structures*, 61(January), 119–141. <https://doi.org/10.1016/j.marstruc.2018.04.007>
- Hashem, A., Aniagor, C. O., Nasr, M. F., & Abou-Okeil, A. (2021). Efficacy of treated sodium alginate and activated carbon fibre for Pb(II) adsorption. *International Journal of Biological Macromolecules*, 176(February), 201–216. <https://doi.org/10.1016/j.ijbiomac.2021.02.067>
- Hu, Z., & Srinivasan, M. P. (2001). Mesoporous high-surface-area activated carbon. *Microporous and Mesoporous Materials*, 43(3), 267–275. [https://doi.org/10.1016/S1387-1811\(00\)00355-3](https://doi.org/10.1016/S1387-1811(00)00355-3)
- Iriakuma, C. T., Obomanu, T., Idogun, A. K., Rowland Ukotije-Ikwut, P., & Idogun, A. K. (2016). *A Novel Method for Adsorption using Human Hair as a Natural Oil Spill Sorbent Want more papers like this? A Novel Method for Adsorption using Human Hair as a Natural Oil Spill Sorbent*. 7(8), 1754–1764. <http://www.ijser.org>
- Kandanelli, R., Meesala, L., Kumar, J., Raju, C. S. K., Peddy, V. C. R., Gandham, S., & Kumar, P. (2018). Cost effective and practically viable oil spillage mitigation: Comprehensive study with biochar. *Marine Pollution Bulletin*, 128(January), 32–40. <https://doi.org/10.1016/j.marpolbul.2018.01.010>
- Khalaf Erabee, I., & M. Ethaib, S. (2018). Performane of Activated Carbon Adsorption in Removing of Organic Pollutants from River Water. *International Journal of Engineering & Technology*, 7(4.20), 356. <https://doi.org/10.14419/ijet.v7i4.20.26134>
- Lee, T., Zubir, Z. A., Jamil, F. M., Matsumoto, A., & Yeoh, F. Y. (2014). Combustion and pyrolysis of activated carbon fibre from oil palm empty fruit bunch fibre assisted through chemical activation with acid treatment. *Journal of Analytical and Applied Pyrolysis*, 110(1), 408–418. <https://doi.org/10.1016/j.jaap.2014.10.010>
- Li, B., Dai, F., Xiao, Q., Yang, L., Shen, J., Zhang, C., & Caib, M. (2023). Nitrogen-doped Activated Carbon for High Energy Hybrid Supercapacitor. *Energy & Environmental Science*. <https://doi.org/10.1039/x0xx00000x>
- Moon, S. Y., Kim, M. S., Hahm, H. S., & Lim, Y. S. (2006). Preparation of Activated Carbon Fibers by Chemical Activation Method with Hydroxides. *Materials Science Forum*, 510–511, 750–753. <https://doi.org/10.4028/www.scientific.net/msf.510-511.750>

- Nabavi, E., Sabour, M., & Dezvareh, G. A. (2022). Ozone treatment and adsorption with granular activated carbon for the removal of organic compounds from agricultural soil leachates. *Journal of Cleaner Production*, 335(December 2021), 130312. <https://doi.org/10.1016/j.jclepro.2021.130312>
- Nayl, A. E. A., Elkhatab, R. A., El Malah, T., Yakout, S. M., El-Khateeb, M. A., Ali, M. M. S., & Ali, H. M. (2017). Adsorption studies on the removal of COD and BOD from treated sewage using activated carbon prepared from date palm waste. *Environmental Science and Pollution Research*, 24(28), 22284–22293. <https://doi.org/10.1007/s11356-017-9878-4>
- Ooi, C.-H., Ang, C.-L., & Yeoh, F.-Y. (2013). *The Properties of Activated Carbon Fiber Derived from Direct Activation from The Properties of Activated Carbon Fiber derived from Direct Activation from Oil Palm Empty Fruit Bunch Fiber*. April. <https://doi.org/10.4028/www.scientific.net/AMR.686.109>
- Park, S., & Kim, B. (2010). *Ammonia removal of activated carbon fibers produced by oxyfluorination*. 291(2005), 597–599. <https://doi.org/10.1016/j.jcis.2005.05.012>
- Perkovic, M. (2016). *Oil Spill Modeling and Combat*. February.
- Pophali, A., Singh, S., & Verma, N. (2021). A dual photoelectrode-based double-chambered microbial fuel cell applied for simultaneous COD and Cr (VI) reduction in wastewater. *International Journal of Hydrogen Energy*, 46(4), 3160–3170. <https://doi.org/10.1016/j.ijhydene.2020.06.162>
- Praba Karana, C., Rengasamy, R. S., & Das, D. (2011). Oil spill cleanup by structured fibre assembly. *Indian Journal of Fibre and Textile Research*, 36(2), 190–200.
- Raji, M., Mirbagheri, S. A., Ye, F., & Dutta, J. (2021). Nano zero-valent iron on activated carbon cloth support as Fenton-like catalyst for efficient color and COD removal from melanoidin wastewater. *Chemosphere*, 263, 127945. <https://doi.org/10.1016/j.chemosphere.2020.127945>
- Saba, N. (2020). Date Palm Fiber Composites. In *Date Palm Fiber Composites*. <https://doi.org/10.1007/978-981-15-9339-0>
- Sajida, S., & Hemlata, B. (2021). Sorption studies of radionuclides from simulated low level waste using green biosorbent. *Research Journal of Chemistry and Environment*, 25(1), 68–73.
- Saleem, J., Adil Riaz, M., & Gordon, M. (2018). Oil sorbents from plastic wastes and polymers: A review. *Journal of Hazardous Materials*, 341, 424–437. <https://doi.org/10.1016/j.jhazmat.2017.07.072>
- Samuchiwal, S., Bhattacharya, A., & Malik, A. (2021). Treatment of textile effluent using an anaerobic reactor integrated with activated carbon and ultrafiltration unit (AN-ACF-UF process) targeting salt recovery and its reusability potential in the pad-batch process. *Journal of Water Process Engineering*, 40(October). <https://doi.org/10.1016/j.jwpe.2020.101770>
- Sharma, A., & Lee, B. K. (2017). Growth of TiO₂ nano-wall on activated carbon fibers for enhancing the photocatalytic oxidation of benzene in aqueous phase. *Catalysis Today*, 287, 113–121. <https://doi.org/10.1016/j.cattod.2016.11.019>
- Sundaravadivelu, D. (2015). Parametric Study to Determine the Effect of Operational Variables on Oil Solidifier Performance for Oil Spill Remediation .. *Doctoral Dissertation, University of Cincinnati*.
- Ulla Gro Nielsen. (2021). Chapter Two - Solid state NMR studies of layered double hydroxides,. *Annual Reports on NMR Spectroscopy*, 104, 75–140.
- Wang, J., Duan, H., Wang, M., Shentu, Q., Xu, C., Yang, Y., Lv, W., & Yao, Y. (2022). Construction of durable superhydrophilic activated carbon fibers based material for highly-efficient oil/water separation and aqueous contaminants degradation. *Environmental Research*, 207(July 2021), 112212. <https://doi.org/10.1016/j.envres.2021.112212>
- Wang, L., Chang, Y., & Li, A. (2019). Hydrothermal carbonization for energy-efficient processing of sewage sludge: A review. *Renewable and Sustainable Energy Reviews*, 108(June 2018), 423–440. <https://doi.org/10.1016/j.rser.2019.04.011>
- Xinga, L., Yanga, F., Zhonga, X., Liua, Y., Lua, H., Guoc, Z., Lva, G., & Jinbei Yange, Aihua Yuana,* , J. P. (2023). Ultra-microporous cotton fiber-derived activated carbon by a facile one-step chemical activation

strategy for efficient CO₂ adsorption. *Separation and Purification Technology*, 324.

Zdravkov, B. D., Čermák, J. J., Šefara, M., & Janků, J. (2007). Pore classification in the characterization of porous materials: A perspective. *Central European Journal of Chemistry*, 5(2), 385–395. <https://doi.org/10.2478/s11532-007-0017-9>

DETERMINATION OF THE OPTIMUM PLACEMENT OF THE SEMI-ACTIVE CONTROL ELEMENT USED IN STRUCTURAL VIBRATION CONTROL

Huseyin AGGUMUS

*Sirnak University, Sirnak Vocational School, Department of Mechanical and Metal Technologies, Sirnak-Turkey
ORCID: 0000-0002-7158-677X*

Abdullah TURAN

*Sirnak University, Sirnak Vocational School, Department of Mechanical and Metal Technologies, Sirnak-Turkey
(Responsible author) ORCID: 0000-0002- 0174-2490*

ABSTRACT

Many different control devices are used to control structural systems. These control devices are placed in the systems as active, semi-active, and passive control applications to control vibration. In active and semi-active control applications, the type of the control device applied to the system and the algorithms required to operate this device are important, as well as the points where it is applied to the building. This study investigates the optimum location of a semi-active controller added to a building model. MR damper, a semi-active control device, is used for this purpose. The optimum placement of the MR damper is investigated by examining the response of the building model to earthquake excitations with simulations created by placing it separately on all floors of the building model, both inside and outside. MR dampers are semi-active control devices that change the damping force according to the applied voltage. Therefore, the required voltage is transmitted by the Groundhook control algorithm. Numerical simulations evaluate the optimum placement of the MR damper on the structure through the Matlab-Simulink program.

Keywords: Structural control, MR damper, Optimum placement, Groundhook control.

Introduction

Many systems have been developed and implemented in buildings to suppress vibrations caused by natural disasters such as earthquakes (Aggumus & Guclu, 2020; Aggumus & Cetin, 2018; Cetin et al., 2011a; Guclu & Yazici, 2007). Active, passive and semi-active control devices are used to suppress structural system responses. Performance is high in active control applications. However, concerns such as high power consumption, costs and security restrict active control applications. Passive control applications have lower performance than active control but are more convenient in terms of applicability. Semi-active control applications perform better than passive control applications. Security is more advantageous than active control in terms of cost and applicability.

In semi-active control applications, MR dampers provide important advantages such as high power production and ease of applicability. MR dampers are semi-active control devices that can produce variable forces with transmitted voltages (Terasawa et al., 2004a; Dyke et al., 1996). The performance of MR dampers on the system depends on both the control algorithm by which the transmitted voltage is determined and where they are placed on the structure. There are many studies in the literature regarding the placement of the MR damper. MR dampers were placed on the first floor of a three-story building (Kim et al., 2009; Dyke et al., 1996), on the first two floors of a six-story building model (Aggumus & Cetin, 2018; Cho et al., 2005; Jansen & Dyke, 2000), only on the first floor (Aggumus & Cetin, 2018; Cetin et al., 2011b), and only on the second floor (Aggumus & Cetin, 2018), performance analysis was made. Studies have shown that MR dampers placed in different parts of the structure affect the performance of the system (Aggumus & Cetin, 2018).

In this study, MR dampers were placed on all floors of a six-storey building model separately from outside and inside, and performance tests were carried out through simulation studies. The MR damper was first added to the floors of the building from the outside in six different ways, and then it was added from the

inside in five different ways to determine the optimum placement for both situations. The groundhook control algorithm was used to determine the voltage transmitted to the MR damper.

Materials and Methods

Equations of motion of the building model

The control situations where the MR damper is applied in the six-storey building examined in this study are shown in (Figure 1). For all control cases, only lateral vibrations of the structure were considered.

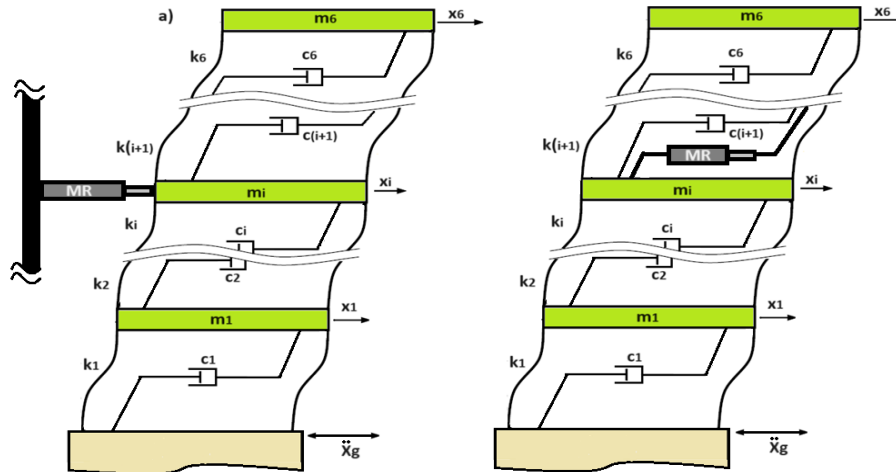


Figure 1. MR damper placements in the building model, **a)** Application of MR damper from outside **b)** Application of MR damper from inside

The generalized equation of the system is as follows.

$$M_s \ddot{x}(t) + C_s \dot{x}(t) + K_s x(t) = -H_s f(t) - M_s L \ddot{x}_g(t) \quad (1)$$

Here M_s , C_s ve $K_s \in R^{6 \times 6}$ are the mass, damping and stiffness matrices, respectively. $\ddot{x}(t)$, $\dot{x}(t)$ ve $x(t) \in R^{6 \times 1}$ are the acceleration, velocity and displacement vectors, respectively. The seismic input vector L is shown as follows.

$$L = [1 \ 1 \ 1 \ 1 \ 1 \ 1]^T \quad (2)$$

The vector H_s showing the location of the controller is shown in six different ways as follows, if the MR damper is connected to the floors separately as in (Figure 1a).

$$\begin{aligned} H_{sd1} &= [1 \ 0 \ 0 \ 0 \ 0 \ 0]^T \\ H_{sd2} &= [0 \ 1 \ 0 \ 0 \ 0 \ 0]^T \\ H_{sd3} &= [0 \ 0 \ 1 \ 0 \ 0 \ 0]^T \\ H_{sd4} &= [0 \ 0 \ 0 \ 1 \ 0 \ 0]^T \\ H_{sd5} &= [0 \ 0 \ 0 \ 0 \ 1 \ 0]^T \\ H_{sd6} &= [0 \ 0 \ 0 \ 0 \ 0 \ 1]^T \end{aligned} \quad (3)$$

H_s vector is shown in five different ways as follows if the MR damper is connected to the floors separately, as shown in (Figure 1b).

$$\begin{aligned} H_{s112} &= [1 \quad -1 \quad 0 \quad 0 \quad 0 \quad 0]^T \\ H_{s123} &= [0 \quad 1 \quad -1 \quad 0 \quad 0 \quad 0]^T \\ H_{s134} &= [0 \quad 0 \quad 1 \quad -1 \quad 0 \quad 0]^T \\ H_{s145} &= [0 \quad 0 \quad 0 \quad 1 \quad -1 \quad 0]^T \\ H_{s156} &= [0 \quad 0 \quad 0 \quad 0 \quad 1 \quad -1]^T \end{aligned} \quad (4)$$

Mass values for system parameters $m_{1...5} = 862.85 \text{ kg}$, $m_6 = 803.98 \text{ kg}$, stiffness values $k_1 = 1.26 * 10^6 \text{ N/m}$, $k_{2..6} = 1.23 * 10^6 \text{ N/m}$ and damping values are $c_{1...6} = 36.7052 * 10^6 \text{ N/m}^2 \text{ dir}$ (Loh et al., 2008).

MR damper model and groundhook control

This study used the MR damper as a semi-active control element. According to the LuGre friction model, the force produced by the MR damper is obtained by the following expression. (Terasawa et al., 2004b).

$$f = \sigma_a z + \sigma_0 z v + \sigma_1 \dot{x}_1 - \sigma_1 a_0 |\dot{x}_1| z + \sigma_2 \dot{x}_1 + \sigma_b \dot{x}_1 v \quad (5)$$

The variable z is the internal dynamic variable of the MR fluid, v is the stress, σ_0 is the stiffness of $z(t)$, σ_1 is the damping coefficient of $z(t)$, σ_2 is the viscous damping coefficient, σ_a is the stiffness of $z(t)$, σ_b is the viscous is the damping coefficient and a_0 is the constant coefficient (Sakai et al., 2003).

MR dampers are control devices that produce force with transmitted voltage. Therefore, the displacement Groundhook control algorithm was used to determine the voltage delivered to the MR damper. Groundhook control is a control algorithm achieved by imitating the ideal structural configuration of a passive damper between the structure and the soil (Kim & Kang, 2012; Koo et al., 2004). If the MR damper is added to the building model from outside, the algorithm applied is as in Eq. (6), and if it is applied from inside the floors, it is applied as in Eq. (7).

$$V = \begin{cases} V_{\max} & \text{eğer } x_i(\dot{x}_i) \leq 0 \\ V_{\min} & \text{eğer } x_i(\dot{x}_i) > 0 \end{cases} \quad (i = 1 \dots 6) \quad (6)$$

$$V = \begin{cases} V_{\max} & \text{eğer } x_j(\dot{x}_j - \dot{x}_{(j+1)}) \leq 0 \\ V_{\min} & \text{eğer } x_j(\dot{x}_j - \dot{x}_{(j+1)}) > 0 \end{cases} \quad (j = 1 \dots 5) \quad (7)$$

V_{\min} is the minimum voltage, V_{\max} is the maximum voltage. The maximum and minimum voltages to be transmitted to the MR damper are determined as $V_{\max} = 10\text{v}$ and $V_{\min} = 0$.

Findings and Discussion

In this study, the suppression performances of different placements of the MR damper on a six-storey building model were examined. There are two ways to apply the MR damper to the building. The first was added to the floors from the outside in six different ways to each floor, and the second was added to the interior of the floors in five different ways. System responses were analyzed under the influence of the El-Centro earthquake. Simulations were carried out in the Matlab-Simulink program.

The maximum displacement and displacement RMS responses of the system were examined. Figure (2) shows the displacement and displacement RMS responses of the application of the MR damper to the interior floors of the building. It is seen that the control performance of the MR damper decreases towards upper floor locations. It showed the best performance in placements within floors between the 1st and 2nd floors.

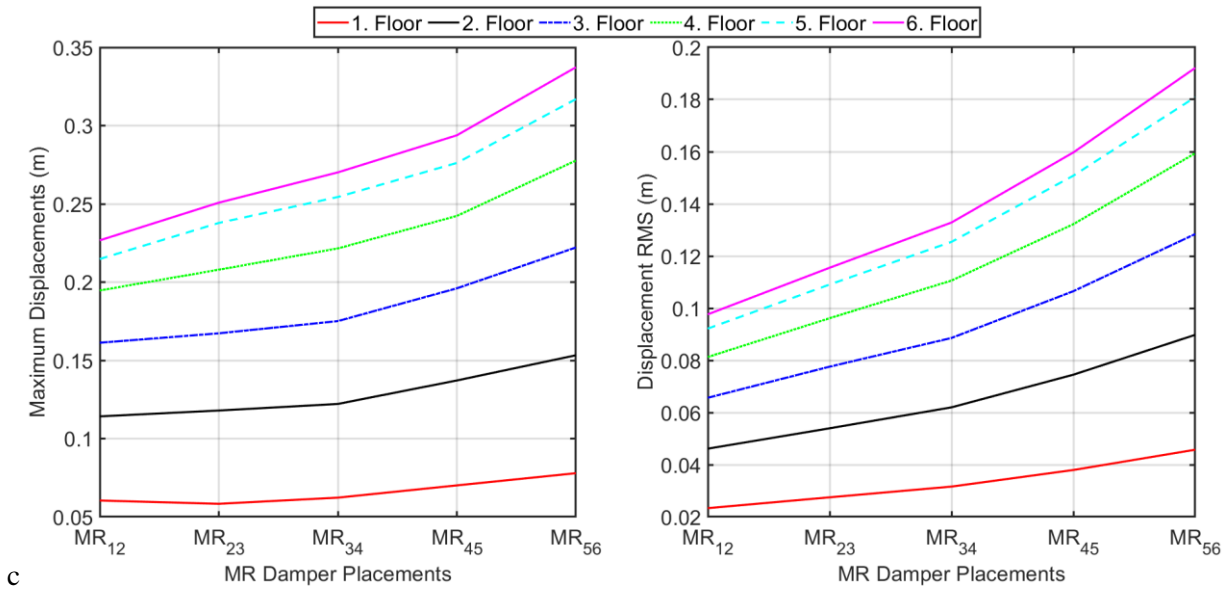


Figure 2. The situation where MR damper is placed inside the floors of the building

Figure (3) shows the displacement and displacement RMS responses of the MR damper applied from the outside of the building. It has been observed that the vibration suppression performance of the system increases when MR dampers are placed towards the upper floors. However, the rate of increase again decreased towards multiples. The best performance in the placement of the MR damper outside the floor was seen on the 6th floor.

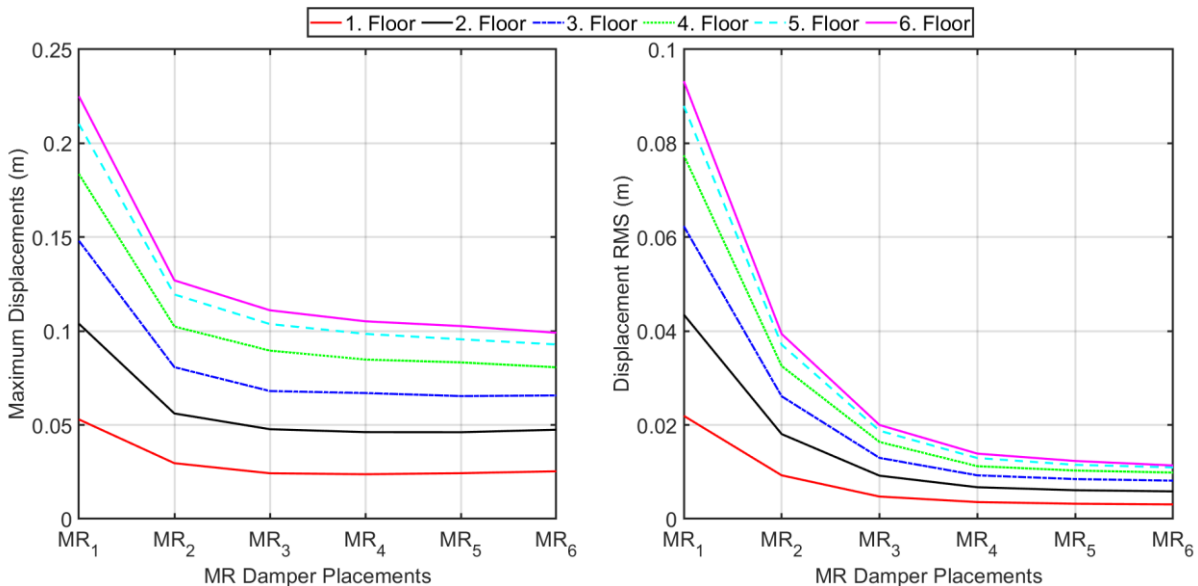


Figure 3. The situation where the MR damper is placed on the floors of the building from outside

There are performance differences between placing the MR damper on the inside of the floors and on the outside. While the performance decreases inside the floors towards the upper floors, the performance increases towards the upper floors outside the floors. In Figure (4), the situation where there is no control in the building model is compared with MR₁₂, which is the best performance of the MR damper when placed inside floors, and MR₆, which is the best performance when placed outside floors. The best control performance was obtained in the MR₆ case on all floors.

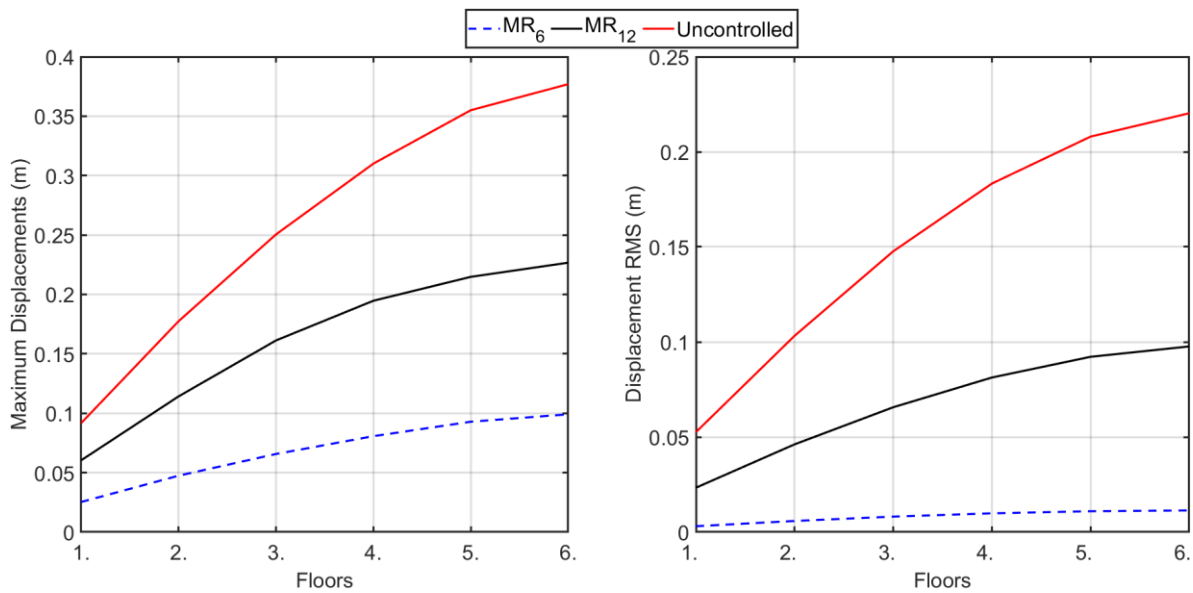


Figure 4. Comparisons of optimum placements of MR damper

Conclusion and Recommendations

In this study, the optimum placement of the MR damper, a semi-active control element, on a six-storey building model was investigated. The MR damper was placed in the building in 11 different ways, six from outside the floors and five from inside the floors, and its effect on the system responses was examined. The voltage transmitted to the MR damper was transmitted with the Groundhook control algorithm. The system was excited by the El Centro earthquake, and its control performances were examined. Simulations were carried out in the Matlab-Simulink program. Structural system responses are different in all MR damper placements. When the MR damper was added to the building model from the outside, the best performance was obtained in the 6th-floor placement, and when added inside the floors, the best performance was obtained in the layout between the 1st and 2nd floors. When comparing both MR damper layouts, it was concluded that MR6 exhibited better control performance.

References

- Aggumus, H. & Cetin, S. (2018). Experimental investigation of semiactive robust control for structures with magnetorheological dampers. *Journal of Low Frequency Noise, Vibration and Active Control*, 37(2), p.216–234. <https://doi.org/10.1177/0263092317711985>
- Aggumus, H. & Guclu, R. (2020). Robust H_{∞} Control of STMDs used in structural systems by hardware in the loop simulation method. *Actuators*, 9(3), 55. <https://doi.org/10.3390/act9030055>
- Cetin, S., Zergeroglu, E., Sivrioglu, S. & Yuksek, I. (2011a). A new semiactive nonlinear adaptive controller for structures using MR damper. *Design and experimental validation. Nonlinear Dynamics*, 66(4), p.731–743. <https://doi.org/10.1007/s11071-011-9946-0>
- Cetin, S., Zergeroglu, E., Sivrioglu, S., & Yuksek, I. (2011a). A new semiactive nonlinear adaptive controller for structures using MR damper: Design and experimental validation. *Nonlinear Dynamics*, 66(4), 731–743. <https://doi.org/10.1007/s11071-011-9946-0>
- Cetin, S., Zergeroglu, E., Sivrioglu, S. & Yuksek, I. (2011b). A new semiactive nonlinear adaptive controller for structures using MR damper: *Design and experimental validation. Nonlinear Dynamics*, 66(4), p.731–743.
- Cho, S.-W., Kim, B.-W., Jung, H.-J. & Lee, I.-W. (2005). Implementation of Modal Control for Seismically Excited Structures using Magnetorheological Dampers. *Journal of Engineering Mechanics*, 131(2), p.177–184. [https://doi.org/10.1061/\(ASCE\)0733-9399\(2005\)131:2\(177\)](https://doi.org/10.1061/(ASCE)0733-9399(2005)131:2(177))

- Dyke, S. J., Spencer, B. F., Sain, M. K. & Carlson, J. D. (1996). Modeling and control of magnetorheological dampers for seismic response reduction. *Smart Materials and Structures*, 5(5), p.565–575. <https://doi.org/10.1088/0964-1726/5/5/006>
- Guclu, R. & Yazici, H. (2007). Fuzzy Logic Control of a Non-linear Structural System against Earthquake Induced Vibration. *Journal of Vibration and Control*, 13(11), p.1535–1551. <https://doi.org/10.1177/1077546307077663>
- Jansen, L. M. & Dyke, S. J. (2000). Semiactive control strategies for MR dampers: Comparative study. *Journal of Engineering Mechanics*, 126(8), 795–803.
- Kim, H.-S. & Kang, J.-W. (2012). Semi-active fuzzy control of a wind-excited tall building using multi-objective genetic algorithm. *Engineering Structures*, 41, p.242–257. <https://doi.org/10.1016/j.engstruct.2012.03.038>
- Koo, J.-H., Ahmadian, M., Setareh, M. & Murray, T. (2004). In Search of Suitable Control Methods for Semi-Active Tuned Vibration Absorbers: *Journal of Vibration and Control*. <https://doi.org/10.1177/1077546304032020>
- Loh, C.-H., Agrawal, A. K., Lynch, J. P. & Yang, J. N. (2008). Development of experimental benchmark problems for international collaboration in structural response control. *Saf Manag Heal Monit Inf, Bridg Maint*, p.3298–3305.
- Sakai, C., Ohmori, H. & Sano, A. (2003). Modeling of MR damper with hysteresis for adaptive vibration control. *42nd IEEE International Conference on Decision and Control (IEEE Cat. No.03CH37475)*, 4, p.3840–3845 vol.4. <https://doi.org/10.1109/CDC.2003.1271748>
- Terasawa, T., Sakai, C., Ohmori, H. & Sano, A. (2004a). Adaptive identification of MR damper for vibration control. *Undefined*. <https://www.semanticscholar.org/paper/Adaptive-identification-of-MR-damper-for-vibration-Terasawa-Sakai/d3c8367e399761b180eb13c9e63d2335fbc64acd>
- Terasawa, T., Sakai, C., Ohmori, H. & Sano, A. (2004b). Adaptive identification of MR damper for vibration control. *2004 43rd IEEE Conference on Decision and Control (CDC) (IEEE Cat. No.04CH37601)*, 3, p.2297-2303. <https://doi.org/10.1109/CDC.2004.1428732>

CHANGE OF KEY MECHANICAL PERFORMANCE PARAMETERS OF Bi-2223 CERAMIC PHASE WITH CdO ADDITION IN MAIN MATRIX

Asaf Tolga Ulgen

Sirnak University, Department of Electric-Electronic Engineering, Sirnak-Turkey, 73000

Ümit Erdem

Scientific and Technological Research Application Center, Kirikkale University, Kirikkale-Turkey

G. Yildirim

Abant İzzet Baysal University, Department of Mechanical Engineering, Bolu-Turkey, 14280

ABSTRACT

The impact of cadmium oxide addition on the fundamental mechanical properties of $\text{Bi}_{2.1}\text{Sr}_{2.0}\text{Ca}_{2.1}\text{Cu}_{3.0}\text{O}_y(\text{CdO})_x$ (Bi-2223) superconductors has been scrutinized through Vickers hardness (H_v) experiments. The materials studied are prepared with the molar ratios interval $0 \leq x \leq 0.1$ by means of the standard ceramic method and Vickers experiments are made in the test loads between 0.245 N-2.940 N. The hardness results deduced from experiments indicate a notable degradation in characteristic features depending on the increase in the CdO impurity amount in Bi-2223 matrix as a consequence of not only the decrease in the crystallinity quality and slip systems but also the rise in the stress amplified sites, stress raiser regions, and crystallinity problems. Consequently, the cadmium oxide addition decreases the mechanical durability and fracture strength against applied loads due to the encouragement of propagation of non-recoverable defects, cracks and dislocations throughout transgranular sites rather than transcrySTALLINE regions. That is exactly why the new Bi-2223 matrices including CdO particles (especially the maximum CdO added sample) are found to be much more response to the applied forces. In fact, the material may fracture more easily due to rapid access to terminal velocity for the critical crack size. At the same time, it is observed that all prepared samples exhibit an indentation size effect (ISE) behavior (but within the decrement trend with increasing CdO amount) due to the dominant nature of the elastic recovery mechanism. Moreover, we determine the differentiation of elastic hardness coefficient (C_{11}), fracture toughness (K_{IC}), yield strength (Y), and brittle index (B) parameters form the H_v versus loads graphs.

Keywords: Bi-2212 ceramics; CdO particles; Micro hardness; ISE.

1. Introduction

The discovery of the first superconductor in mercury metal at the critical transition temperature below 4.2 K dates back to 1911 [1]. With the discovery, the researchers have focused to find new materials exhibiting the superconductivity. Hence, in the history, several materials including rare earth borocarbides, pure elements, nitrides, organic compounds, sulfides, oxides, A-15 inorganics, magnesium diboride, metal-based compounds, chalcogens, chevrel phase, pyrochlorine oxides, heavy fermions, metals, semi-metal-containing materials, alloys, carbon/silicon-based compounds, fullerites, ruteno-cuprates, and cuprate-layered perovskite types [2, 3]. Of the compounds studied, the last parents composed of the high-temperature superconducting cuprate-layered perovskite compounds (Bi-, Tl-, and Hg-containing), particularly the Bi-based superconducting ceramics (Bi-2212 with 85 K critical transition temperature, Bi-2223 with critical transition temperature of 100 K, and Bi-2201 phase with 20 K critical transition temperature) have garnered immense attention due to their exceptional characteristics [4]. Especially, the Bi-2223 superconducting phase with superior thermodynamic stability, high superconductive temperatures, magnetic field and current carrying capacity, optical and electronic characteristics, resistivity toward humidity, simple chemical contents, easily deforming/shaping/rolling for long cables, easy access to cooling system, stabilization performance to oxygen contents and low energy losses has widely been used in applied sciences, non-toxic chemicals, innovative energy infrastructure, energy-related industries, generators, electro-optics, sensitive

process control, refrigeration systems, power transmission, networks, and various large-scale applications [5–17]. Moreover, the presence of BiO layers (incorporating Vander Waal bonds) in Bi-based compounds facilitates easy shaping, deformation, and rolling for long tape-casting and cable construction. Consequently, these Bi-containing superconducting components (particularly Bi-2223 phase) have gained significant prominence in the literature. However, practical utilization of the components faces challenges due to their inherent brittleness within the micaceous structure [18]. Additionally, issues like randomly oriented microcrystals, intergranular boundaries, characteristics of mobile carriers in space, layered anisotropic micaceous structure, high sensitivity to applied magnetic fields, multiple phase compositions, large penetration depth, coupling problems between layers, granular structure, stabilization of main phases, short coherence length, and mechanical stabilization require resolution through appropriate preparation methods. These methods include doping mechanisms, metallic interfaces, cation or anion substitutions in crystal structures, transition metal evaporation/diffusion, multilayered structures, and chemical additions in crystal lattices [19–22]. One of the preferred methods to enhance crystallinity quality and grain connectivity while mitigating crystal structure problems, crack-initiating defects, and non-recoverable stress concentration regions involves the doping mechanisms [23, 24].

In the present study, significant alterations in key mechanical properties such as critical crack size, crystallinity quality, slip systems, stress amplified sites, mechanical durability, fracture strength, stress raiser regions, crystallinity problems, microhardness, elastic hardness coefficient, fracture toughness, yield strength, and brittle index parameters of CdO added Bi-2223 materials have been investigated in detail. At the same time, the preformed microhardness results have enabled us to discuss the effect of different CdO addition amount on the movement of dislocations, defects, and cracks thorough the transgranular sites and transcrystalline regions. Likewise, the behavior of main mechanical characteristic property of pure and CdO added Bi-2223 samples to addition mechanism and external forces has been determined [25, 26].

2. Experimental procedures for $\text{Bi}_{2.1}\text{Sr}_{2.0}\text{Ca}_{2.1}\text{Cu}_{3.0}\text{O}_y$ samples prepared with different CdO impurity addition level

The preparation of $\text{Bi}_{2.1}\text{Sr}_{2.0}\text{Ca}_{2.1}\text{Cu}_{3.0}\text{O}_y$ ceramic materials within various cadmium oxide impurity intervals ranging from 0.00 to 0.10 in mole-to-mole ratios has been conducted using the classic ceramic preparation method under the atmospheric air conditions. High-purity chemical components (CdO, CuO, Bi_2O_3 , SrCO_3 , and CaCO_3 chemicals) with a purity level exceeding 99.99% have been used to synthesize the compounds.

The procedure has begun by weighing 2 grams of the chemical powders according to stoichiometric ratios using an electronic balance in ambient air. The powders have been then mixed in a porcelain crucible in the air medium for 9 hours in a grinding machine to reduce particle size and ensure a homogeneous mixture. Following the procedure, the powders has been undergone a 40-minute grinding process in an agate mortar without solvents so as to not only reduce particle size further but also promote new atomic bonding within the compounds.

Then, the chemical powders in 2 gr are weighed in line with the stoichiometric ratios with the aid of an electronic balance in the medium of air. The powders are exposed to the mixture process in a porcelain crucible. The mixture of powders is mixed for 9 hours in a grinding machine in the air medium condition both to diminish the powder particle size growth and to enhance the homogenous structure of chemical mixture. The mixture of powders is exposed to the grinding process by hands in an agate mortar without any solvents 40 min not only to bring closer the particles together by minimizing the particles but also to form new bonding between the atoms in the compounds. The calcination process is performed in the porcelain crucibles placed into a programmable muffle furnace at the environment temperature of 800 °C at the duration of 36 hours under atmospheric air conditions. During the calcination process of homogenous mixed chemicals, cooling/heating rates are set at 5°C per minute. Main reason is to remove impurity phases from the bulk $\text{Bi}_{2.1}\text{Sr}_{2.0}\text{Ca}_{2.1}\text{Cu}_{3.0}\text{O}_y(\text{CdO})_x$ ceramic structures. After that, the homogenous mixture calcined is subjected to the pressing process to be formed in a rectangular shape with the size of $2.0 \times 0.5 \times 0.2 \text{ cm}^3$ in the medium of atmospheric air so that new forms possess much more grain boundary coupling strength between the stacked planes in the Bi-2223 crystal lattice. Correspondingly, we automatically overcome the microscopic structural problems to be formed in the main system. After this process, a series of polycrystalline bulks of $\text{Bi}_{2.1}\text{Sr}_{2.0}\text{Ca}_{2.1}\text{Cu}_{3.0}\text{O}_y(\text{CdO})_x$ were sintered at the temperature of 850°C for 36 h under

medium of air in the furnace. Hereafter, the bulk $\text{Bi}_{2.1}\text{Sr}_{2.0}\text{Ca}_{2.1}\text{Cu}_{3.0}\text{O}_y(\text{CdO})_x$ compounds produced at different cadmium oxide concentration including $x=0.000, 0.005, 0.010, 0.050, 0.070,$ and 0.100 will be shown as pure or unadded, CdO/1, CdO/2, CdO/3, CdO/4, and CdO/5, respectively.

The influence of cadmium oxide addition on $\text{Bi}_{2.1}\text{Sr}_{2.0}\text{Ca}_{2.1}\text{Cu}_{3.0}\text{O}_y(\text{CdO})_x$ ceramic superconductors on the fundamental mechanical properties has extensively been via the standard Vickers microhardness experiments that have been conducted with a SHIMADZU HVM-2 model digital tester. The measurements have been taken between the external test forces between 0.245 N and 2.940 N . Throughout the experiments, pyramidal geometry diamond indenter has been used to leave indentation diagonal traces on the specimen surfaces. The forces have been applied to the various selected regions of sample surfaces for 10 seconds with the calibrated microscope. The experimental measurements have been repeated 5 times to find the average impression lengths on the surface. By using the conventional formula given below, the microhardness parameters have been determined. The effect of cadmium oxide addition on the elastic recovery mechanism has also been discussed in detail. Similarly, the variation of critical crack size, crystallinity quality, slip systems, stress amplified sites, mechanical durability, fracture strength, stress raiser regions, and crystallinity problems with the cadmium oxide addition and applied test loads.

With the aid of the experiment results including the change of indentation diagonal lengths with the test loads applied, we have found some critical mechanical strength parameters such as the elastic hardness coefficient (C_{II}), fracture toughness (K_{IC}), yield strength (Y), and brittle index (B) parameters of the pure and $\text{Bi}_{2.1}\text{Sr}_{2.0}\text{Ca}_{2.1}\text{Cu}_{3.0}\text{O}_y(\text{CdO})_x$ ceramic superconductors [15]. At the same time, the role of addition mechanism on the movement of dislocations, defects, and cracks through the transgranular sites and transcrySTALLINE regions has also been discussed extensively. Lastly, the differentiation in the mechanical characteristic property (indentation size effect, ISE, and reverse indentation size effect, RISE) with respect to the cadmium oxide addition has been found in detail.

3. Results and discussion

The impact of cadmium oxide addition amount ranging from 0.000 to 0.100 on various crucial mechanical properties has extensively been investigated in $\text{Bi}_{2.1}\text{Sr}_{2.0}\text{Ca}_{2.1}\text{Cu}_{3.0}\text{O}_y(\text{CdO})_x$ ceramics using a SHIMADZU HVM-2 model tool. The Vickers hardness measurements have been conducted under different applied loads (0.245 N - 2.940 N). The study has encompassed an exploration of microhardness, critical crack size, crystallinity quality, slip systems, stress amplified sites, mechanical durability, fracture strength, resistance to fatigue failure, stress raiser regions, crystallinity problems, residual compressive stress regions, elastic hardness coefficient, fracture toughness, yield strength, and brittle index parameters. Besides, the Vickers hardness results have enabled us to determine the preference of dislocations, defects, and cracks movements through the transgranular sites or transcrySTALLINE regions. As widely acknowledged, fundamental mechanical properties have closely been linked to the crystal structure quality, microscopic structural problems, lattice strain fields, impurity scattering, defects, stress concentration and amplified regions, deformations, coupling problems, and dislocation propagation throughout the ceramic matrix. These factors have established the relationship between material deformation and forces applied on the surfaces. Coefficients of H_v (Vickers hardness) have been determined using standard equations given below:

$$H_v = 1854.4 \left(\frac{F}{d^2} \right) \quad (1)$$

The graphical representation in Fig. 1 showcases the variation of H_v parameters concerning cadmium oxide levels ($0.000 \leq x \leq 0.100$) and forces within the range of 0.245 N to 2.940 N for pure and CdO added Bi-2223 superconducting ceramics. As seen from the curves in Fig. 1 that all the samples prepared have exhibited various mechanical performances with rising the CdO added particles. This means that concentration of CdO particles in the bulk Bi-2223 structures has successfully been performed. Similarly, with the enhancement in the external test forces on the specimen surface, the pure and CdO added Bi-2223 superconducting ceramics have exhibited different behaviors due to the varied sensitive to the loads. In more detail, the microhardness parameters determined from Eq. 1 have been displayed to truncate with the augment in the CdO amounts in the main structure due to the harsh augmentation in the crystal structure problems, microscopic structural problems, lattice strain fields, impurity scattering, defects, stress concentration and amplified regions, deformations, coupling problems, and dislocation propagation throughout the Bi-2223 ceramic matrix. The

rapid increment in the crystallinity problems have damaged to the durable tetragonal phase and led to the revival of the stress-induced phase. Shortly, the presence of CdO impurity ions in the crystal lattice of Bi-2223 system has triggered the deformation degree and interaction between the grains of system and thus the force barrier regions have been blocked immediately as a result of the combination of the degradation of the slip systems and enhancement in the stored internal strain regions. Accordingly, propagations belonging to the defects, dislocations and cracks have been found to reach speedily the critical velocity under even lower test loads. Furthermore, the maximum CdO added sample (CdO/5) exhibits the highest response to the external test forces. In fact, the defects, dislocations and cracks propagations have been noted to proceed much more along with the intergranular sites rather than the transcrystalline regions. On this basis, the CdO/5 compound may be broken more easily in the case of the applied test loads. All in all, the cadmium oxide addition has damaged seriously the main mechanical performance behaviors.

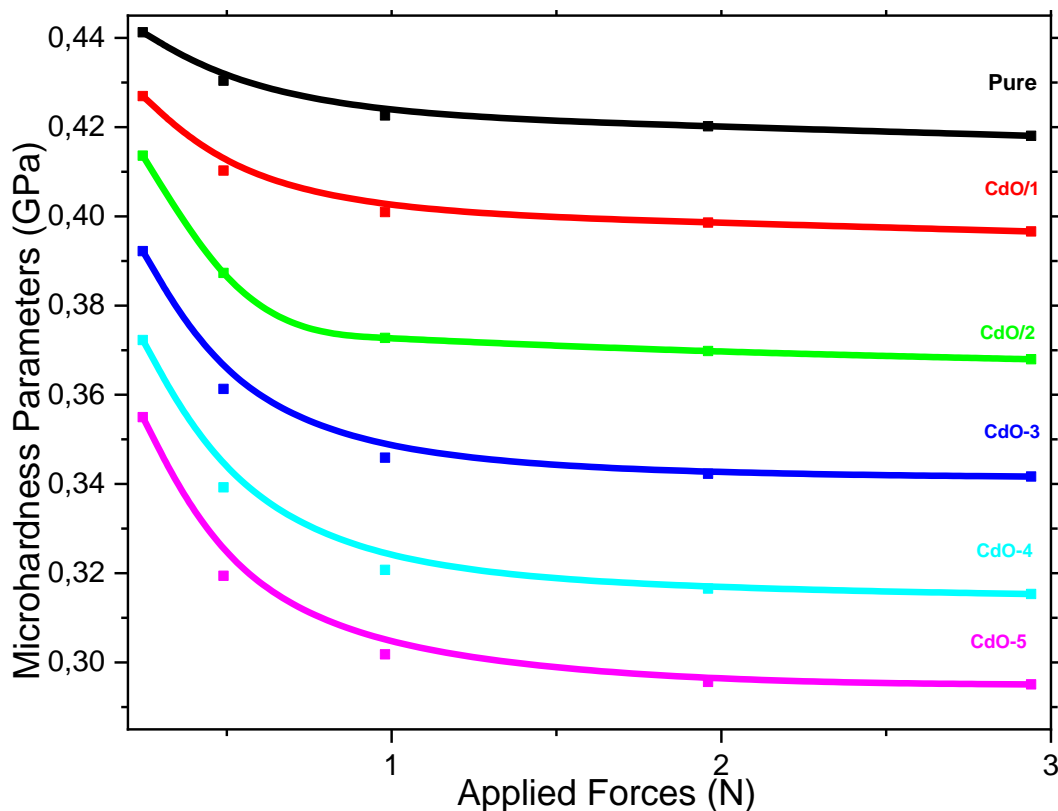


Fig. 1 Change of Microindentation hardness parameters of $\text{Bi}_{2.1}\text{Sr}_{2.0}\text{Ca}_{2.1}\text{Cu}_{3.0}\text{O}_y(\text{CdO})_x$ with applied test forces

At the same time, the hardness graphics given in Fig. 1 have shown that all the materials have exhibited the standard indentation size effect (ISE) behavior due to the predominant character of recovery mechanism related to the appearance of elastic and plastic deformations simultaneously in the crystal systems [27]. As well known that the non-linear truncate of Vickers hardness constants in terms of the applied test forces are typical behavior of ISE characteristic [28–30].

It is another interesting result deduced from Fig. 1 that the behavior of ISE has been noted to decrease regularly depending on the enhancement of the cadmium oxide addition level. This is line with the dramatic increase in the crystal structure problems, microscopic structural problems, lattice strain fields, impurity scattering, defects, stress concentration and amplified regions, deformations, and coupling problems between the ordered layers in the bulk Bi-2223 system. Hence, it has been observed that the unadded has exhibited the highest ISE nature whereas the CdO/5 compound has noticed to show the lowest ISE feature among the compounds. To increase visibility and understanding of mechanical behavior of the pure and coefficients in Table 1. As appeared that the pure sample have had the greatest H_v values between 0.4412 GPa and 0.4181

GPa whereas the minimum values of 0.3550 GPa-0.2951 GPa have been found for the CdO/5 compound. In this respect, among the H_v parameters, the maximum value of 0.4412 GPa has been noted to belong to the unadded one under an applied force of 0.245 N, after the applied test load, the values have been found to be about 0.4304 GPa at 0.490 N, 0.4226 GPa at 0.980 N, 0.4202 GPa at 1.960 N, and the minimum value of 0.4181 GPa at 2.940 N test load. As for the minimum values, the value of 0.3550 GPa has been observed for the CdO/5 compound under an applied force of 0.245 N. Conversely, the value has been noted to decrease towards to the minimum value of 0.2951 GPa under 2.940 N. the other samples produced have been found to present the moderate H_v values. Accordingly, the numerical H_v findings have indicated that the un-added Bi-223 ceramic has exhibited the least response to the test forces applied. Conversely, the maximum CdO added CdO/5 material has been noted to reveal the most response to the microindentation force applied.

Table 1 Variation of H_v , C_{II} , Y , K_{IC} , and B constants with applied test forces

<i>Samples</i>	<i>F (N)</i>	<i>H_v (GPa)</i>	<i>C_{II} (GPa)^{7/4}</i>	<i>Y (GPa)</i>	<i>K_{IC} (MPam^{1/2})</i>	<i>B (m^{-1/2})</i>
<i>Pure</i>	0.245	0.4412	0.2389	0.1471	0.1369	3.2236
	0.490	0.4304	0.2287	0.1435	0.1352	3.1839
	0.980	0.4226	0.2215	0.1409	0.1339	3.1549
	1.960	0.4202	0.2193	0.1401	0.1336	3.1460
	2.940	0.4181	0.2173	0.1394	0.1332	3.1381
<i>CdO-1</i>	0.245	0.4270	0.2255	0.1423	0.1513	2.8224
	0.490	0.4103	0.2103	0.1368	0.1483	2.7666
	0.980	0.4010	0.2020	0.1337	0.1466	2.7351
	1.960	0.3986	0.2000	0.1329	0.1462	2.7269
	2.940	0.3966	0.1982	0.1322	0.1458	2.7201
<i>CdO-2</i>	0.245	0.4136	0.2133	0.1379	0.1815	2.2785
	0.490	0.3873	0.1901	0.1291	0.1757	2.2049
	0.980	0.3727	0.1778	0.1242	0.1723	2.1629
	1.960	0.3698	0.1754	0.1233	0.1716	2.1545
	2.940	0.3680	0.1738	0.1227	0.1712	2.1492
<i>CdO-3</i>	0.245	0.3922	0.1944	0.1307	0.1855	2.1147
	0.490	0.3613	0.1684	0.1204	0.1780	2.0297
	0.980	0.3459	0.1560	0.1153	0.1742	1.9860
	1.960	0.3423	0.1532	0.1141	0.1733	1.9756
	2.940	0.3417	0.1527	0.1139	0.1731	1.9739
<i>CdO-4</i>	0.245	0.3723	0.1774	0.1241	0.1969	1.8912
	0.490	0.3392	0.1508	0.1131	0.1879	1.8052
	0.980	0.3207	0.1367	0.1069	0.1827	1.7552
	1.960	0.3166	0.1336	0.1055	0.1813	1.7463
	2.940	0.3153	0.1327	0.1051	0.1814	1.7381
<i>CdO-5</i>	0.245	0.3550	0.1632	0.1183	0.1997	1.7780
	0.490	0.3194	0.1357	0.1065	0.1894	1.6865
	0.980	0.3018	0.1229	0.1006	0.1841	1.6394
	1.960	0.2956	0.1185	0.0985	0.1822	1.6225
	2.940	0.2951	0.1181	0.0984	0.1820	1.6211

Similarly, the elastic hardness coefficient, fracture toughness, yield strength, and brittle index (B) parameters have been calculated by using the following relations:

$$K_{IC} = \sqrt{2E\alpha} \quad (\alpha \text{ means the surface energy value}) \quad (2)$$

$$B = \frac{H_v}{K_{IC}} \quad (3)$$

$$C_{11} = H_v^{7/4} \quad (4)$$

$$Y \approx \frac{H_V}{3} \quad (5)$$

All the computation data have been given in Table 1. The variation in the values of K_{IC} , Y , C_{11} and B parameters over both the CdO addition amount and external forces has extensively been investigated by using the standard Vickers microhardness measurement results performed on the different regions for 10 seconds under test loads ranging from 0.245 N to 2.940 N test loads. Based on the computations, the mechanical performance properties have been obtained to truncate methodically with rising the cadmium oxide concentration in the crystal system. This behavior has stemmed from the typical ISE nature of pure and CdO added Bi-2223 ceramic compounds.

We have also determined the change of yield strength parameters with the applied test forces and CdO impurity addition amounts in detail by using the equations. The computations performed have been depicted in Table 1. It has been visible from the table that the un-added Bi-2223 ceramic compound has been noted to have the highest values of Y parameters at any applied test loads while the smallest values of Y parameters have been found for the CdO/5 material. In this context, the highest value of about 0.1471 GPa has ascribed to the pure sample under an applied force of 0.245 N. With the increase of test loads, the yield strength value has been observed to decrease regularly and obtained to be about 0.1394 GPa at an applied force of 2.940 N. The decrement with the applied test loads has been due to the typical ISE nature of material studied. On the other hand, the bulk CdO/5 sample has exhibited the value of 0.1183 GPa at 0.245 N test force and value of 0.0984 GPa at 2.940 N applied test force. The other materials have exhibited the moderate yield strength parameters.

Additionally, according to the numerical values for the fracture toughness parameters (related to the granular structure) given in Table 1, with augmentation of cadmium oxide level the K_{IC} constants were obtained to increase systematically. Hence, the unadded Bi-2223 sample have possessed the lowest K_{IC} constants under any applied test forces whereas the maximum values have been detected for the bulk CdO/5 material. Among the K_{IC} values given in Table 1, the minimum value has been noted to be about of 0.1369 MPam^{1/2} at 0.245 N for unadded product. With enhancing the test forces, the value has been observed to decrease towards to the K_{IC} value of 0.1332 MPam^{1/2} at the external force of 2.940 N. Conversely, the maximum values changing from 0.1820 MPam^{1/2} to 0.1997 MPam^{1/2} have been obtained for the CdO/5 ceramic material. Similarly, at the applied external force of 2.940 N, the value has fallen in the minimum value of 0.1820 MPam^{1/2}. Similar to the values of yield strengths, the decrement trend with the applied test load has been because of ISE nature of pure and CdO added Bi-2223 samples. The other materials exhibit moderate fracture toughness values. Correspondingly, it can be summarized that of the materials studied the unadded ceramic has been observed to have the best crystallinity quality and thus presented the least response to the applied forces. To contrast that the CdO/5 ceramic material has been observed to exhibit the largest response to the applied external test forces due to its worst crystal quality.

Moreover, the change of Vickers microhardness parameters as a function of applied force for the

Bi_{2.1}Sr_{2.0}Ca_{2.1}Cu_{3.0}O₇(CdO)_x superconductors has enabled us to define the role of cadmium oxide addition on the elastic stiffness coefficient parameters. Table 1 has shown that the presence and rise of cadmium oxide in the Bi-2223 main matrix led to the diminish in the elastic stiffness coefficient values. The decrement trend in the elastic stiffness coefficient parameters have stemmed from the regression of the crystallinity quality and slip systems based on the increase in the stress amplified sites, stress raiser regions, and crystallinity problems in the Bi-2223 ceramic system. Similarly, as the test forces applied to the specimen surface of materials have increased, the values of C_{11} parameters were noticed to truncate regularly due to the typical ISE nature of pure and CdO added Bi-2223 ceramic compounds. On this basis, the unadded sample has been found to possess the highest values of C_{11} coefficients at any applied test forces. In numerical detail, the maximum value has been obtained

to be about $0.2389 \text{ (GPa)}^{7/4}$ at the applied test load of 0.245 N for the C_{11} parameter of the pure sample. In the case of 2.940 N test load applied, the value of C_{11} coefficients has been found to be about $0.2173 \text{ (GPa)}^{7/4}$. On the other hand, the smallest values of C_{11} parameters have been determined to be about $0.1632 \text{ (GPa)}^{7/4}$ and $0.1181 \text{ (GPa)}^{7/4}$ under the external forces of 0.245 N and 2.940 N, respectively. The other samples have had the moderate elastic stiffness coefficient parameters.

Another mechanical performance finding inferred from the change of indentation diagonal lengths with the test loads applied is brittleness index parameters that have been found for the equations. We have tabulated the numerical values of B parameters in Table 1 where the brittleness index parameters have been found to decrease with increase in both the cadmium oxide impurity amount in the Bi-2223 system and test forces applied to the surface of materials studied. Hence, the maximum values of B parameter have been found for the pure sample at any applied test forces. Numerically, the highest B value of $3.2236 \text{ m}^{-1/2}$ has been found for the pure sample when the force of 0.245 N has been applied. In the case of maximum test force of 2.940 N, the value of brittleness index parameter has been recorded to be about $3.1381 \text{ m}^{-1/2}$ for the unadded sample. As for the CdO/5 ceramic material, under the test force of 0.245 N, the material has been found to exhibit the B value of about $1.7780 \text{ m}^{-1/2}$. As the external forces applied has increased, the B parameter has been noted to be about $1.6211 \text{ m}^{-1/2}$. The other samples prepared has presented the moderate values. Hence, it is normal to confirm that the increment trend for the brittleness index parameters has resulted from the enhancement of the granular structure in the Bi-2223 structures.

To sum up, all the mechanical performance parameters including microhardness, elastic hardness coefficient, fracture toughness, yield strength, and brittle index parameters have been observed to diminish the durable tetragonal phase, slip systems, and crystal structure quality of the Bi-2223 ceramic system. Further, the regression of the mechanical performance parameters with the external forces applied has stemmed from the ISE feature of $\text{Bi}_{2.1}\text{Sr}_{2.0}\text{Ca}_{2.1}\text{Cu}_{3.0}\text{O}_y(\text{CdO})_x$ systems.

4. Conclusion

In the current work, the role of cadmium oxide addition on the fundamental mechanical properties including the microhardness, elastic hardness coefficient, fracture toughness, yield strength, and brittle index parameters of $\text{Bi}_{2.1}\text{Sr}_{2.0}\text{Ca}_{2.1}\text{Cu}_{3.0}\text{O}_y(\text{CdO})_x$ ceramics the aid of Vickers microhardness experimental measurements performed at 0.245 N-2.940 N applied external forces. It has been obtained that Bi-2223 crystal structure has seriously been affected by both the CdO impurity addition amount and test force magnitudes. In more detail, with the increase in the cadmium oxide impurity addition in the main system all the mechanical performance parameters have been affected negatively due to the decrease in the mechanical durability, fracture strength, crystallinity quality, and slip systems based on the increase in the

stress amplified sites, stress raiser regions, and crystallinity problems in the Bi-2223 ceramic materials. Hence, the movement of defects, cracks, and dislocations have preferred to proceed thorough the transgranular sites rather than transcrystalline regions in the crystal structure. Similarly, the presence of CdO impurity has led to the access to terminal velocity of the critical crack size for the bulk Bi-2223 system. Further, the CdO/5 compound has been noted to be broken more easily under even lower test loads as a result of the increased response to the applied test forces. Furthermore, all the $\text{Bi}_{2.1}\text{Sr}_{2.0}\text{Ca}_{2.1}\text{Cu}_{3.0}\text{O}_y(\text{CdO})_x$ ceramics have been recorded to present ISE feature, however, the CdO impurity has affected negatively.

References

- [1] Kamerlingh Onnes, H. (1911). Further experiments with Liquid Helium. D. On the change of Electrical Resistance of Pure Metals at very low Temperatures, etc. V. The Disappearance of the resistance of mercury. Koninklijke Nederlandse Akademie van Wetenschappen Proceedings Series B Physical Sciences, 14, 113-115.
- [2] Erdem, U. (2021). Homovalent Ho/Bi substitution effect on characteristic properties of Bi-2212 superconducting ceramics. Journal of Materials Science: Materials in Electronics, 32(24), 28587-28604.

- [3] Turgay, T., & Yildirim, G. (2019). Effect of aliovalent Si/Bi partial substitution on propagation mechanisms of cracking and dislocation in Bi-2212 crystal system. *Journal of Materials Science: Materials in Electronics*, 30, 7314-7323.
- [4] Ghahfarokhi, S.M., Shoushtari, M.Z. (2010). Structural and physical properties of Cd-doped Bi_{1.64}Pb_{0.36}Sr₂Ca_{2-x}Cd_xCu₃O_y superconductor, *Physica B: Condensed Matter*, 405(22), 4643-4649.
- [5] Zalaoglu, Y., Terzioğlu, C., Turgay, T., & Yildirim, G. (2018). Detailed survey on minimum activation energy for penetration of Ni nanoparticles into Bi-2223 crystal structure and temperature-dependent Ni diffusivity. *Journal of Materials Science: Materials in Electronics*, 29(4), 3239-3249.
- [6] Slimani, Y., Almessiere, M. A., Hannachi, E., Baykal, A., Manikandan, A., Mumtaz, M., & Azzouz, F. B. (2019). Influence of WO₃ nanowires on structural, morphological and flux pinning ability of YBa₂Cu₃O_y superconductor. *Ceramics International*, 45(2), 2621-2628.
- [7] Slimani, Y., Almessiere, M. A., Hannachi, E., Mumtaz, M., Manikandan, A., Baykal, A., & Azzouz, F. B. (2019). Improvement of flux pinning ability by tungsten oxide nanoparticles added in YBa₂Cu₃O_y superconductor. *Ceramics International*, 45(6), 6828-6835.
- [8] Hannachi, E., Slimani, Y., Ekicibil, A. H. M. E. T., Manikandan, A., & Azzouz, F. B. (2019). Magneto-resistivity and magnetization investigations of YBCO superconductor added by nano-wires and nanoparticles of titanium oxide. *Journal of Materials Science: Materials in Electronics*, 30, 8805-8813.
- [9] Hannachi, E., Slimani, Y., Ekicibil, A. H. M. E. T., Manikandan, A., & Azzouz, F. B. (2019). Excess conductivity and AC susceptibility studies of Y-123 superconductor added with TiO₂ nanowires. *Materials Chemistry and Physics*, 235, 121721.
- [10] Jankovský, O., Antončík, F., Hlášek, T., Plecháček, V., Sedmidubský, D., Huber, Š., ... & Bartůněk, V. (2018). Synthesis and properties of YBa₂Cu₃O_{7-δ}-Y₂Ba₄CuWO₁₀. 8 superconducting composites. *Journal of the European Ceramic Society*, 38(6), 2541-2546.
- [11] Deng, Z., Zhang, W., Zheng, J., Wang, B., Ren, Y., Zheng, X., & Zhang, J. (2017). A high-temperature superconducting maglev-evacuated tube transport (HTS Maglev-ETT) test system. *IEEE Transactions on Applied Superconductivity*, 27(6), 1-8.
- [12] Dondapati, R. S., Kumar, A., Kumar, G. R., Usurumarti, P. R., & Dondapati, S. (2017). Superconducting magnetic energy storage (SMES) devices integrated with resistive type superconducting fault current limiter (SFCL) for fast recovery time. *Journal of Energy Storage*, 13, 287-295.
- [13] Jeong, S. H., Song, J. B., Choi, Y. H., Kim, S. G., Go, B. S., Park, M., & Lee, H. (2016). Effect of micro-ceramic fillers in epoxy composites on thermal and electrical stabilities of GdBCO coils. *Composites Part B: Engineering*, 94, 190-196.
- [14] Fallah-Arani, H., Sedghi, A., Baghshahi, S., Moakhar, R. S., Riahi-Noori, N., & Nodoushan, N. J. (2022). Bi-2223 superconductor ceramics added with cubic-shaped TiO₂ nanoparticles: Structural, microstructural, magnetic, and vortex pinning studies. *Journal of Alloys and Compounds*, 900, 163201.
- [15] Wang, Y., & Zheng, Y. (2014). Review of research and measurement for application properties of HTS tapes. *Science China Technological Sciences*, 57(8), 1568-1577.
- [16] A.K. Saxena, *High-Temperature Superconductors*, 2nd Ed., Springer Heidelberg New York Dordrecht London, 2012.
- [17] T.P. Sheahan, *Introduction to High-temperature Superconductivity*, 1st ed., Kluwer Academic Publishers, New York, Boston, 2002.
- [18] Plakida, N. (2010). High Temperature Cuprate Superconductors. Springer Series in Solid-State Sciences. Springer. p. 480. ISBN 9783642126321.
- [19] M.B. Turkoz, M. Oz, T. Turgay, G. Yildirim, Gece Kitapligi, Evaluation of Magneto-Resistivity performances and Flux Pinning Centers with Vanadium Addition in Bi-2223 Main Matrix, pp. 139 -158, Ankara, Turkey.

- [20] Hilgenkamp, H., & Mannhart, J. (2002). Grain boundaries in high-T_c superconductors. *Reviews of Modern Physics*, 74(2), 485.
- [21] Autret-Lambert, C., Pignon, B., Gervais, M., Monot-Laffez, I., Ruyter, A., Ammor, L., ... & Decourt, R. (2006). Microstructural and transport properties in substituted Bi₂Sr₂CaCu₂O_{8+δ} modulated compounds. *Journal of Solid State Chemistry*, 179(6), 1698-1706.
- [22] Salama, 9., Selvamanickam, V., Gao, L., & Sun, K. (1989). High current density in bulk YBa₂Cu₃O_x superconductor. *Applied Physics Letters*, 54(23), 2352-2354.
- [23] Tsuei, C. C., Kirtley, J. R., Hammerl, G., Mannhart, J., Raffy, H., & Li, Z. Z. (2006). Doping effect on pairing symmetry in cuprate superconductors. *Journal of Physics and Chemistry of Solids*, 67(1-3), 64-67.
- [24] Fujita, K., Noda, T., Kojima, K. M., Eisaki, H., & Uchida, S. (2005). Effect of disorder outside the CuO₂ planes on T_c of copper oxide superconductors. *Physical review letters*, 95(9), 097006.
- [25] M.E. Takayama, High-pressure synthesis of homologous series of high critical temperature (T_c) superconductors, *Chem. Mater.* 10 (1998) 2686–2698.
- [26] Saunders, P.J.; Ford, G.A. (2005). *The Rise of the Superconductors*. Boca Raton, FL: CRC Press.
- [27] Y. Zalaoglu, B. Akkurt, M. Oz, G. Yildirim, Transgranular region preference of crack propagation along Bi-2212 crystal structure due to Au nanoparticle diffusion and modeling of new systems, *J. Mater. Sci. Mater. Electron.* 28 (2017) 12839–12850.
- [28] A.A. Elmustafa, D.S. Stone, Nanoindentation and the indentation size effect: Kinetics of deformation and strain gradient plasticity, *J. Mech. Phys. Solid.* 5 (2003) 357–381.
- [29] K. Sangwal, On the reverse indentation size effect and microhardness measurement of solids, *Mat. Chem. Phys.* 63 (2000) 145–152.
- [30] R. Awad, A.I. Abou-Aly, M. Kamal, M. Anas, Mechanical properties of (Cu_{0.5}Tl_{0.5})-1223 substituted by Pr, *J. Supercond. Nov. Magn.* 24 (2011) 1947–1956.

INFLUENCE OF APPLIED LOADS AND CdO IMPURITY ON MECHANICAL STABILIZATION AND GRANULARITY DEGREE OF Bi-2223

Asaf Tolga Ulgen

Sirnak University, Department of Electric-Electronic Engineering, Sirnak-Turkey, 73000

Ümit Erdem

Scientific and Technological Research Application Center, Kirikkale University, Kirikkale-Turkey

G. Yildirim

Abant İzzet Baysal University, Department of Mechanical Engineering, Bolu-Turkey, 14280

ABSTRACT

This study seeks meaningful solutions to two main problems related to the change of Vickers hardness (H_v), Young's moduli of elasticity (E), ductility (D), resilience (U_r), and shear modulus of rigidity (G) with (i-) cadmium oxide (CdO) impurity addition and (ii-) test applied forces between 0.245 N and 2.940 N of $\text{Bi}_{2.1}\text{Sr}_{2.0}\text{Ca}_{2.1}\text{Cu}_{3.0}\text{O}_y(\text{CdO})_x$ (Bi-2223) ceramics. It is observed from the curves associated with the variation of average indentation diagonal lengths as a function of applied test loads that the microhardness parameters are noted to decrease with the rise of CdO impurity amount and applied test loads. The former decrement results from the increase in crack-initiating cracks/defects/dislocations, non-recoverable stress concentration and amplification sites based on the crystal structure problems (microvoids and lattice strains) whereas the latter behavior stems from the typical indentation size effect (ISE) behavior of $\text{Bi}_{2.1}\text{Sr}_{2.0}\text{Ca}_{2.1}\text{Cu}_{3.0}\text{O}_y(\text{CdO})_x$ ceramics. On this basis, the un-added Bi-2223 ceramic shows the best crystallinity quality, durable tetragonal phase, and mechanical stabilization. In other words, cadmium oxide impurity damages the fundamental mechanical strength of Bi-2223 ceramic system. All the differentiations are correlated by strong links established by fitting equations from the third-order formulas. Similarly, the role of CdO impurity on the crystal structure quality of Bi-2223 samples is confirmed by the change in the granularity degree with Young's moduli of elasticity.

Keywords: Bi-2223 ceramics; CdO impurity; Third-order formulas; Young's modulus of elasticity; Granularity degree.

1. Introduction

Following the 1911 discovery of superconductivity in mercury heavy-metal elements [1], a significant breakthrough occurred in 1986 with the identification of a novel high-temperature perovskite oxide material, $\text{La}_{2-x}\text{Ba}_x\text{CuO}_4$. This material displayed distortions and oxygen deficiency, resulting in critical transition temperatures reaching around 35K [2], marking a pivotal moment in exploring superconductivity in ceramic materials [3]. Subsequently, lanthanum replaced yttrium in cuprate perovskite system, achieving a superconductive transitions larger than 77 K that is boiling point for liquid nitrogen temperature for the first time [4]. Following these developments, various other ceramic parents, including Tl-, Ga-, Hg-, and Bi-based perovskite systems, were subsequently discovered.

Of cuprate ceramic materials, the Bi-based ceramic superconductors within the distorted and perovskite systems stood out for their notably higher critical transition temperatures, robust magnetic field capabilities (≥ 100 T), exceptional current carrying ($\approx 10^7 \text{A/cm}^2$) abilities, minimal energy losses, and dissipation [5, 6]. The properties are highly promising for applications in advanced engineering, industrial technology, and small to large-scale applications. Moreover, they exhibit superior thermodynamic stability, ease of rolling/deforming/shaping for lengthy cable constructions exceeding one kilometer and tape-casting, facilitated by the presence of Vander Waal bonded BiO layers within the micaceous structure. Additionally, their simple preparation process using cost-effective and non-toxic chemicals, resistance to water/humidity, and accessibility for nitrogen cooling systems contribute to their appeal [7–10].

However, these Bi-containing systems, akin to other ceramic cuprates, have inherent issues such as brittleness in wire fabrication, different phases, challenges in mechanical stabilization, granular structure, inter-granular boundaries, sensitivity to magnetic fields/currents, randomly oriented microcrystals, structural characteristic problems, weak interlayer connections, low carrier transporters, short coherence length, limited operating temperature ranges, spatial characteristics of mobile hole carriers, and significant penetration depth. These inherent characteristics limit their potential applications [11, 12]. Over the years, researchers have strived to address these issues using diverse techniques involving sample preparation conditions, purity of powders, content quality, dopant types, and various fabrication techniques [13, 14].

Here role of cadmium oxide impurity intervals 0.00 to 0.10 on several mechanical features including Young's moduli of elasticity (E), ductility (D), resilience (U_r), and shear modulus of rigidity (G) using the Vickers hardness experiments measured at varied forces applied ranging from 0.245N to the value of 2.940 N. Further, the dependence of mechanical performance behavior on the CdO impurity addition level and forces applied has been discussed in detail. The experimental results and calculations have displayed that the enhancement in the factors such as applied test loads and impurity level has been noted to affect negatively the main mechanical performances mentioned above because of the enhancement in the crystal structure problems attributed to the interaction between the adjacent layers, microvoids, lattice strains, crack-initiating cracks/defects/dislocations, non-recoverable stress concentration, and amplification sites in the Bi-2223 crystal system. We have also been interested in the change of mechanical characteristic behavior of Bi-2223 systems with the addition mechanism.

2. Experimental procedures for $\text{Bi}_{2.1}\text{Sr}_{2.0}\text{Ca}_{2.1}\text{Cu}_{3.0}\text{O}_y$ samples prepared with different CdO impurity addition level

The preparation of $\text{Bi}_{2.1}\text{Sr}_{2.0}\text{Ca}_{2.1}\text{Cu}_{3.0}\text{O}_y$ ceramic materials within various cadmium oxide impurity intervals ranging from 0.00 to 0.10 in mole-to-mole ratios has been conducted using the classic ceramic preparation method. High-purity chemical components (CdO, CuO, Bi_2O_3 , SrCO_3 , and CaCO_3 chemicals) with a purity level exceeding 99.99% have been used to synthesize the compounds.

The procedure has begun by weighing 2 grams of the chemical powders according to stoichiometric ratios using an electronic balance in ambient air. The powders have been then mixed in a porcelain crucible in the air medium for 9 hours in a grinding machine to reduce particle size and ensure a homogeneous mixture. Following the procedure, the powders has been undergone a 40-minute grinding process in an agate mortar without solvents so as to not only reduce particle size further but also promote new atomic bonding within the compounds.

Subsequently, the calcination process has occurred in porcelain crucibles placed in a programmable furnace at an environmental of 800 °C under atmospheric conditions for 36 hours. Purpose of calcination has been to eliminate impurity phases from the solid $\text{Bi}_{2.1}\text{Sr}_{2.0}\text{Ca}_{2.1}\text{Cu}_{3.0}\text{O}_y(\text{CdO})_x$ ceramic structures. The heating and cooling rates during the calcination process has been maintained at 5°C per minute.

The homogeneous mixture obtained after calcination has been undergone a pressing process to form rectangular shapes with the volume of $2.0 \times 0.5 \times 0.2 \text{ cm}^3$, aiming to enhance the connections within the Bi-2223 and mitigate the systematic issues in the main system. Subsequently, a series of polycrystalline bulk $\text{Bi}_{2.1}\text{Sr}_{2.0}\text{Ca}_{2.1}\text{Cu}_{3.0}\text{O}_y(\text{CdO})_x$ compounds have been sintered at 850°C for 36 h, each compound representing different cadmium oxide concentrations including $x=0.000, 0.005, 0.010, 0.050, 0.070$, and 0.100, denoted as pure or unadded, CdO/1, CdO/2, CdO/3, CdO/4, and CdO/5, respectively.

Role of CdO particles on main mechanical properties of $\text{Bi}_{2.1}\text{Sr}_{2.0}\text{Ca}_{2.1}\text{Cu}_{3.0}\text{O}_y(\text{CdO})_x$ ceramic superconductors has extensively been analyzed through standard Vickers microhardness experiments conducted using a SHIMADZU HVM-2 model digital tester. Measurements have been taken with external test forces ranging between 0.245 N and 2.940 N under atmospheric conditions. A pyramidal geometry diamond indenter has been employed to create indentation diagonal traces on specimen surfaces. Varied external forces have been applied to various selected regions of the sample surfaces for 10 seconds using a calibrated microscope. Experimental measurements have been repeated five times to determine mean impression traces on the surface. Microhardness parameters have been calculated using a conventional formula. Furthermore, the study has delved into the effect of cadmium oxide addition on the crystal structure problems attributed to the

interaction between the adjacent layers, lattice strains, microvoids, crack-initiating cracks/defects/dislocations, non-recoverable stress concentration, and amplification sites in the Bi-2223 crystal system.

At the same time, the role of cadmium oxide impurity addition on the Vickers hardness (H_V), Young's moduli of elasticity (E), ductility (D), resilience (U_r), and shear modulus of rigidity (G) parameters extracted from microhardness experiments has thoroughly been examined via equations depicted below (1–4):



(1)

$$E = 81.9635H_V \quad (2)$$

$$U_r = Y^2 / 2E \quad (3)$$

$$E = 2G(1 + \nu) \quad (4)$$

3. Results and discussion

3.1. Inspection of Young's moduli of elasticity, ductility, resilience, and shear modulus of rigidity of bulk CdO added Bi-2223 ceramics

The variation in some critical mechanical performance quantities including the Young's moduli of elasticity (E), ductility (D), resilience (U_r), and shear modulus of rigidity (G) parameters using the Vickers test findings deduced from 0.245 N-2.940 N applied test loads has been analyzed using the related equations that have been gathered in Table 1.

Table 1 Values of U_r , D , G and E mechanical parameters belonging to the $\text{Bi}_{2.1}\text{Sr}_{2.0}\text{Ca}_{2.1}\text{Cu}_{3.0}\text{O}_y(\text{CdO})_x$ superconductors

Samples	F (N)	U_r (MPa)	G (GPa)	D ($m^{1/2}$)	E (GPa)
Pure	0.245	0.2992	14.4649	0.3102	36.1623
	0.490	0.2919	14.1108	0.3141	35.2771
	0.980	0.2866	13.8551	0.3170	34.6378
	1.960	0.2850	13.7764	0.3179	34.4411
	2.940	0.2835	13.7076	0.3187	34.2689
CdO/1	0.245	0.2893	13.9994	0.3543	34.9984
	0.490	0.2782	13.4519	0.3615	33.6296
	0.980	0.2719	13.1470	0.3656	32.8674
	1.960	0.2703	13.0683	0.3667	32.6707
	2.940	0.2688	13.0027	0.3676	32.5067
CdO/2	0.245	0.2805	13.5600	0.4389	33.9000
	0.490	0.2625	12.6978	0.4535	31.7445
	0.980	0.2525	12.2191	0.4623	30.5481
	1.960	0.2508	12.1240	0.4642	30.3102
	2.940	0.2496	12.0650	0.4653	30.1626
CdO/3	0.245	0.2657	12.8584	0.4729	32.1461
	0.490	0.2448	11.8454	0.4927	29.6134
	0.980	0.2345	11.3405	0.5035	28.3512
	1.960	0.2320	11.2224	0.5062	28.0561
	2.940	0.2316	11.2028	0.5066	28.0069
CdO/4	0.245	0.2523	12.2060	0.5288	30.5150
	0.490	0.2300	11.1208	0.5540	27.8020
	0.980	0.2174	10.5143	0.5697	26.2857
	1.960	0.2145	10.3799	0.5727	25.9496
	2.940	0.2137	10.3372	0.5753	25.8431

	0.245	0.2405	11.6388	0.5624	29.0970
	0.490	0.2166	10.4717	0.5929	26.1791
<i>CdO/5</i>	0.980	0.2046	9.8946	0.6100	24.7366
	1.960	0.2002	9.6914	0.6163	24.2284
	2.940	0.2002	9.6750	0.6169	24.1874

According to the calculations performed from the equations, firstly we have extensively investigated the effect of cadmium oxide impurity addition amount on the moduli of elasticity of pure and CdO added Bi-2223 ceramics. One can see the numerical values belonging to the moduli of elasticity in Table 1. It has been seen from the table that with the increase in the applied test forces on the specimen surface and CdO impurity addition level in the system, value of E parameters has been noted to mitigate methodically due to the standard indentation size effect (ISE) mechanical characteristic behavior. Moreover, the negative effects on the crystallinity quality related to the degradation in microscopic structural problems, defects, lattice strain fields, and impurity scattering faults have caused to the decrease in the moduli of elasticity of the bulk Bi-2223 systems. On this basis, the values of E parameters have been found to be in a range of 36.1623 GPa-24.1874 GPa under the applied test loads. The pure sample has had the largest E coefficients at any external forces. Numerically, the sample exhibited the highest value of 36.1623 GPa under an applied force of 0.245 N. As the test forces have increased, the parameters have been calculated to be about 35.2771 GPa at 0.490 N applied load, 34.6378 GPa under 0.980 N, 34.4411 GPa under 1.960 N, and 34.2689 GPa under a test load of 2.940 N, respectively. As for the minimum moduli of elasticity parameters, the CdO/5 ceramic compound has been noted to present the E value of 29.0970 GPa under a test load of 0.245 N. Under 2.940 N test load, the unadded has had the global minimum value of 29.0970 GPa. The other materials exhibit moderate values of E parameters. Accordingly, the numerical E results observed have shown that the pure material has had the least sensitive to the applied external forces. On other hand, the CdO/5 sample with the maximum CdO impurity addition level has been obtained to possess the most sensitive to the applied test loads.

Another mechanical performance finding inferred from the change of indentation diagonal lengths with the test loads applied is ductility (failure parameter) that have been calculated for the pure and CdO added Bi-2223 ceramic structures. One can see the D parameters in Table 1. It has been observed from the table that the ductility parameter has been recorded to depend on both the external force magnitudes and also CdO impurity amounts in the Bi-2223 system. According to the data given in Table 1, the values of D parameters have been observed to increase (inversely proportional to brittleness) with enhancing the CdO level because of the enhancement of the crystallinity problem in the system. Similarly, the increase in the applied test force has also led to the enhancement in the ductility parameter. Hence, the smallest value of ductility parameter has been noted to be about $0.441 m^{1/2}$ for the unadded ceramic at an applied test load of 0.245 N. With the increase in the text force up to the value of 2.940 N, the D parameter has been observed to increase to the value of $0.453 m^{1/2}$. Conversely, the CdO/5 ceramic material has been found to have the highest D values at any forces applied to the specimen surfaces. Numerically, this sample has shown the D parameter of $0.817 m^{1/2}$ at a force of 0.245 N. Under the largest force of 2.940 N, the D parameter has been found to reach to the maximum value of $0.897 m^{1/2}$. That is to say, the minimum D parameters have been observed for the better crystal structure materials. The decrement trend has resulted from the enhancement of the granular structure in the Bi-2223 structures.

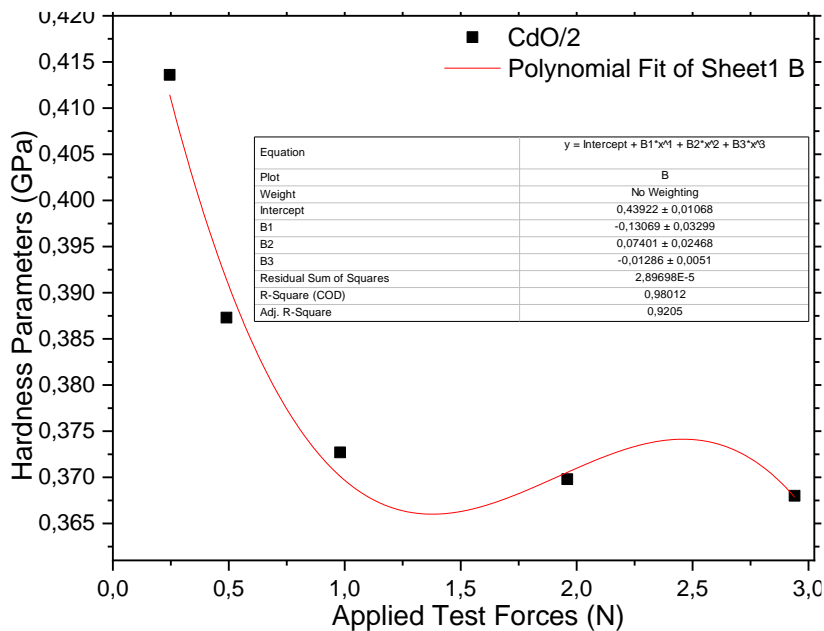
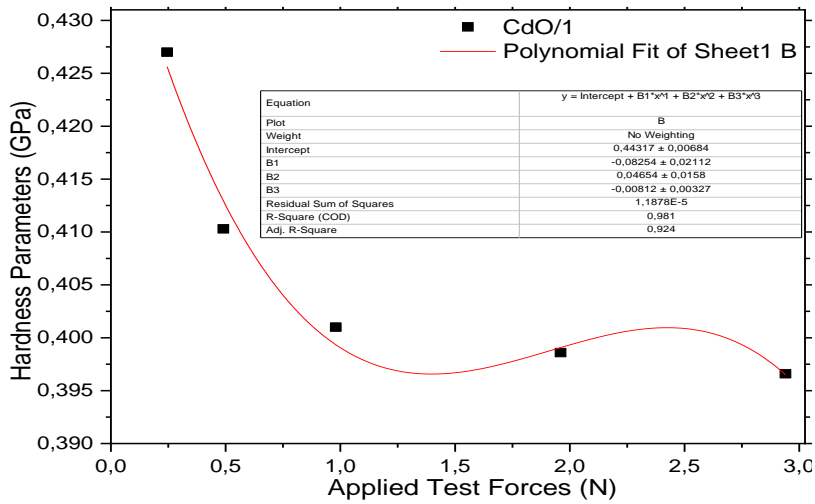
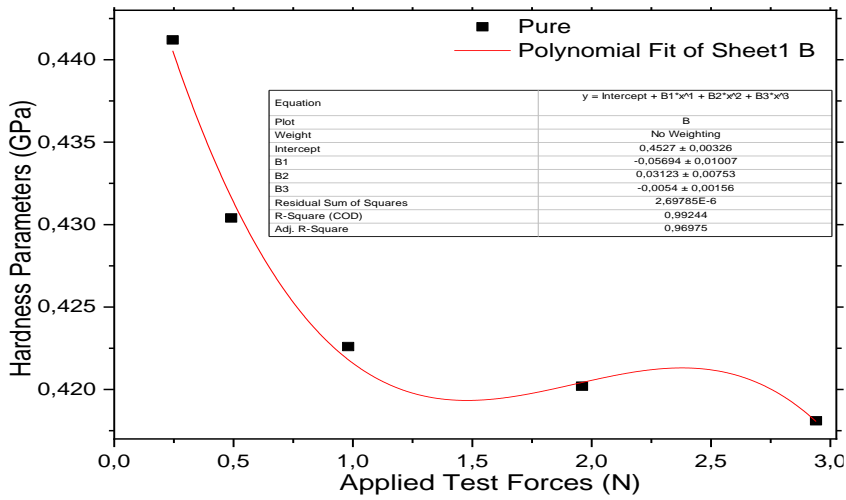
Thirdly, the variation of indentation diagonal lengths with the applied external forces has enabled us to find the role of cadmium oxide impurity addition on the other mechanical performance property such as shear (G) moduli of pure and CdO added Bi-2223 systems. As well known that the shear moduli can be determined from Poisson's ratio inserted in the strong equation including the moduli of elasticity and shear moduli. In the equation related to the value of G moduli, it is obvious that the shear modulus is directly related to the Young's moduli, and the Poisson ratio shown as the letter of ν is used to be 0.25 in the formula [15]. The value of Poisson ratio is defined by the random alignment of adjacent stacked layers within the bulk Bi-2223 ceramic system, characterized by its isotropic structure. Table 1 illustrates the numerically calculated shear moduli for both the pure and CdO added bulk Bi-2223 crystal systems. It has been observed that the values of G parameters were found to depend strongly on both CdO level and applied test forces. In this respect, with the increase in the CdO impurity amount in the Bi-2223 crystal system, the values of G parameters have

been noted to mitigate scientifically. Similarly, the increase in the applied test forces has led to the degradation in the values of G parameters. Correspondingly, the unadded Bi-2223 materials have exhibited the maximum G values. Namely, the value of 14.4649 GPa has been found for the pure sample at the applied test load of 0.245 N whereas in the case of the maximum test force of 2.940 N, the value has been found to decrease toward to the value of 13.7076 GPa. As for the G parameter of maximum CdO added Bi-2223 sample, the value has been noticed to be about 11.6388 GPa. However, the force value of 2.940 N has been applied to the specimen surface, the value of G parameter has been obtained to be about 9.6750 GPa. The other samples exhibit moderate G moduli parameters at any applied microindentation test load. It can be noted that the reduction of the G moduli parameters has stemmed the enhancement of the granularity degree and crystallinity problems in the Bi-2223 system.

The last mechanical performance property deduced from the variation of typical microhardness parameters with the applied test forces is the resilience that is an ability of a sample to absorb energy when elastically deformed, and release of energy after unloading. In the current work, we have studied the variation in the values of U_r parameters of the bulk Bi-2223 ceramic compounds with the cadmium oxide impurity level and applied test loads in detail. One can see the computations for the U_r coefficients in Table 1. As seen from the table that system the values of U_r parameters have been observed to reduce regularly at any applied test loads with the enhancement in the cadmium oxide impurity level. For example, the pure Bi-2223 sample has been obtained to exhibit 0.2992 MPa (global maximum value) under 0.245 N force. In the same test force, the value of U_r parameter has been recorded to decrease to the value of 0.2405 MPa. Likewise, with the enhancement of the applied test force on the specimen surface, the parameter has been found to diminish the values of 0.2835 MPa for the pure sample and 0.2002 MPa for the CdO/5 sample (global minimum value). The other samples have shown the moderate U_r parameters at any applied test loads. The degradation of the values of resilience coefficients based on the augmentation of the cadmium oxide impurity addition amount in the Bi-2223 materials and test forces applied to the specimen surface has resulted from the diminish in the recovering elastic energy capability after unloading. Accordingly, the maximum CdO added Bi-2223 ceramic sample has presented the most sensitive to the test forces applied. To sum up, the Vickers hardness tests have indicated that the decrease in the fundamental mechanical performance parameters (U_r , D , G , and E parameters) with the cadmium oxide impurity addition amount has been because of the increase in the crack-initiating cracks/defects/dislocations, non-recoverable stress concentration and amplification sites based on the crystal structure problems (microvoids and lattice strains) in the Bi-2223 crystal system. Further, the reduction of the mechanical performance parameters with the test forces applied has been stemmed from the typical ISE property of the pure and CdO added Bi-2223 samples.

3.2. High correlation between Vickers hardness findings and applied test loads

It has been found that there has been a strong relationship between the values of Vickers microhardness parameters and applied test forces for CdO added Bi-2223 ceramics due to the variation in the interaction between the adjacent layers, cracks/defects/dislocations, non-recoverable stress concentration regions based on the main lattice problems, microvoids, and lattice strains. On this basis, we have endeavored to find a strong correlation utilizing from the graphs between the Vickers hardness tests and applied test loads as given in Fig. 2.



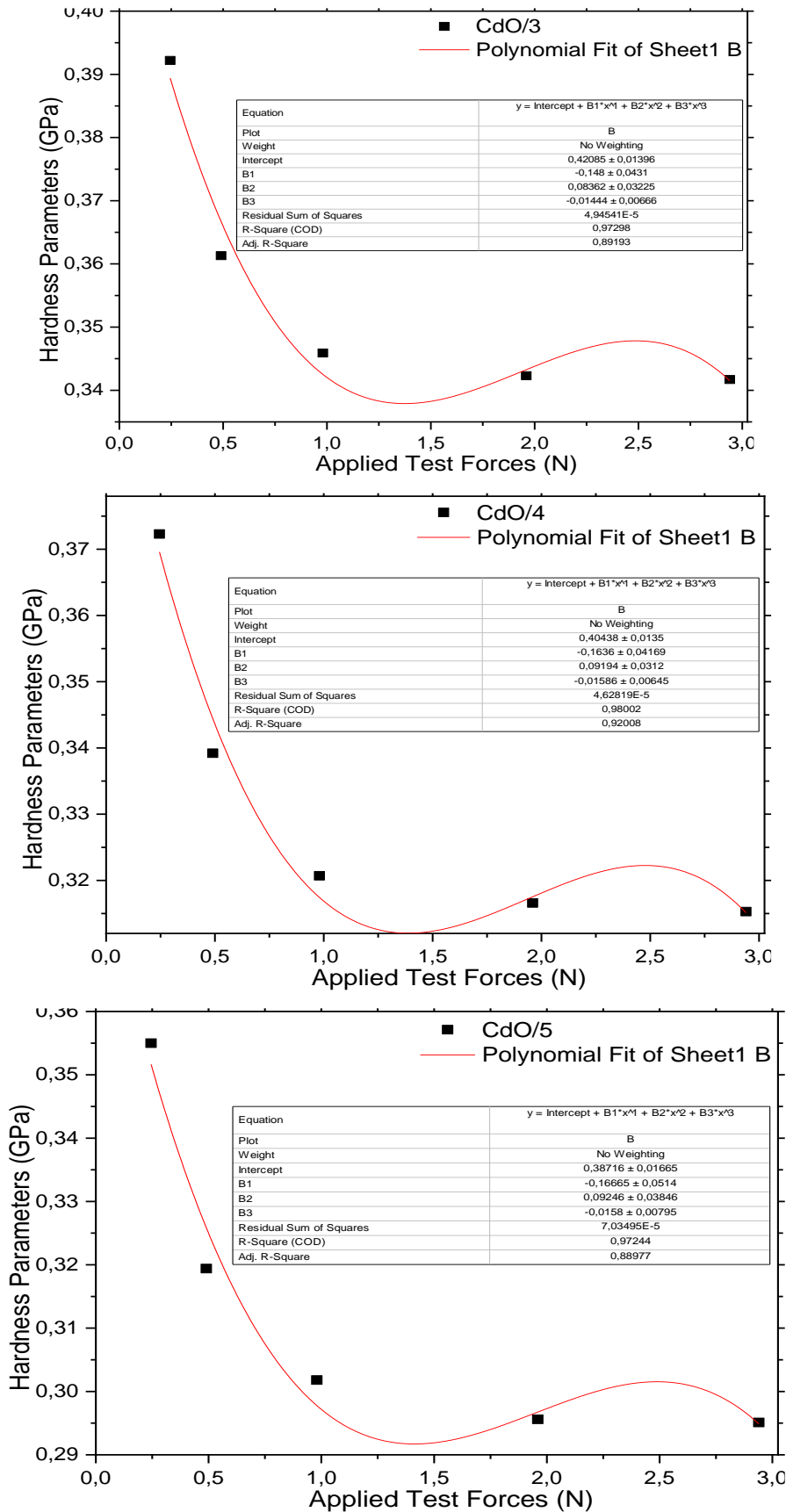


Figure 2. Fitting equations based on microindentation hardness and force applied for pure and CdO added Bi-2223 compounds

In this aim, we have determined the equations (for fitting) from the third-order equations. The correlation values have been obtained to be high enough to establish a link between Vickers hardness parameters and applied test forces. The fitting relations have been listed in Table 2.

Table 2. Link between microindentation hardness and force applied for CdO added Bi-2223 ceramics

<i>Samples</i>	*Fitting equations for pure and CdO added Bi-2223 compounds
Pure	$y = -0.00540x^3 + 0.03123x^2 - 0.05694x + 0.45270$
CdO/1	$y = -0.00812x^3 + 0.04654x^2 - 0.08254x + 0.44317$
CdO/2	$y = -0.01286x^3 + 0.07401x^2 - 0.13069x + 0.43922$
CdO/3	$y = -0.01444x^3 + 0.08362x^2 - 0.14800x + 0.42085$
CdO/4	$y = -0.01586x^3 + 0.09194x^2 - 0.16360x + 0.40438$
CdO/5	$y = -0.01588x^3 + 0.09246x^2 - 0.16665x + 0.38716$

It has been seen from the table that every x^3 , x^2 , and x term has been obtained to depend considerably on the cadmium oxide impurity addition amount. Especially for the CdO/5, the excess dependence has been found. The negative value of x^3 term has stemmed from the characteristic ISE nature of samples. In more detail, the numerical values of x^3 term have been calculated between -0.00540 and -0.01588. With the increase in the CdO impurity addition in the system, the dependence of x^3 term has increased to the impurity addition. In this context, the smallest absolute value of 0.0540 has belonged to the pure sample with the least response to the applied external test forces while the maximum parameter of 0.01588 has been computed for the CdO/5 material with the most response to the applied test loads. The change of the x^3 term depending on the CdO impurity addition level has resulted from the enhancement in the crystal structure problems mentioned above. Correspondingly, the mechanical durability and strength have been obtained to decrease dramatically with the enhancement in the impurity addition.

3.3. Differentiation in granularity degree of Bi-22223 ceramics with CdO impurity addition

In this part of paper, the variation in the values of granularity degree (porosity) parameters deduced from the change in the moduli of elasticity of the bulk Bi-2223 ceramics has been determined with respect to the cadmium oxide impurity addition amount. The more detail can be observed from Ref. [16]. On this basis, the equation used to determine the degrees of granularity degree parameters has been provided below [15]:

$$E = E_0(1 - 1.9P + 0.9P^2) \quad (4)$$

According to formulization, the value of E_0 parameter has been determined to be about 36.1623 GPa belonging to the pure sample due to the exhibition of densest character and largest elastic modulus parameter in the $\text{Bi}_{2.1}\text{Sr}_{2.0}\text{Ca}_{2.1}\text{Cu}_{3.0}\text{O}_y(\text{CdO})_x$ ceramics. The other moduli of elasticity belonging to the CdO/1, CdO/2, CdO/3, CdO/4, and CdO/5 ceramic samples at any applied test forces have been gathered from table 1. The relative porosity degree values found by using the moduli of elasticity have numerically been depicted in Table 3.

Table 3. Dependence of porosity degree parameters on CdO impurity addition level and applied test forces.

<i>Materials</i>	<i>Microhardness Test Forces (N)</i>				
	<i>0.245</i>	<i>0.490</i>	<i>0.980</i>	<i>1.960</i>	<i>2.940</i>
	Relative volume fraction porosity (%)				
Pure	----	1.296	2.243	2.536	2.793
CdO/1	1.708	3.753	4.910	5.210	5.462
CdO/2	3.346	6.639	8.514	8.892	9.127
CdO/3	6.017	10.006	12.057	12.543	12.625
CdO/4	8.567	12.964	15.515	16.090	16.273
CdO/5	10.840	15.697	18.198	19.096	19.169

As obtained that both CdO impurity concentration in Bi-2223 ceramic system and external forces applied to the specimen surface have affected seriously the relative granularity degree parameters. In this context, with augmentation in both the loads and CdO impurity level, it has been found to enhance significantly the granularity degree. Numerically, the minimum granularity degree has been noted to be about 1.296 % for the pure sample when the test force of 0.490 N has been applied to the sample. With the increase in the applied test force up to the value of 2.940 N, the porosity was determined to rise towards to the value of 2.793%. Similarly, as the CdO impurity addition amount has increased in the Bi-2223 crystal system, the parameter has increased and reached to the maximum value of 19.169% for the CdO/5 sample under an applied test force of 2.940 N. The calculations have presented that both the CdO impurity addition in the Bi-2223 ceramic system and external forces applied to the specimen surface have revived the crystal structure problems attributed to the interaction between the adjacent layers, microvoids, lattice strains, crack-initiating cracks/defects/dislocations, non-recoverable stress concentration, and amplification sites in the Bi-2223 crystal system. Thus, the impurity addition mechanism has been noted to damage fundamental mechanical strength, durable tetragonal phase, crystallinity quality, and mechanical stabilization of Bi-2223 ceramic system.

4. Conclusion

In this work, we have investigated the variation of the fundamental mechanical performance parameters, strength, durable tetragonal phase, crystallinity quality, and mechanical stabilization of Bi-2223 ceramic system with the cadmium oxide impurity addition in the crystal lattice. The materials have been prepared by means of the standard ceramic preparation method and mechanical measurements have been performed by the Vickers hardness tests between 0.245 N and 2.940 N. The experimental curves have enabled us to determine the Vickers microhardness, Young's moduli of elasticity, ductility, resilience, and shear modulus parameters to discuss the role of impurity. The results observed have indicated that all the mechanical findings have been found to depend on harshly both the external force magnitudes and cadmium oxide impurity addition level. This finding has shown that the CdO impurity has been entered into the crystal system. At the same time, the experimental results have been observed to decrease with the rise of CdO impurity amount and applied test loads due to the enhancement in the crystal structure problems attributed to the interaction between the adjacent layers, microvoids, lattice strains, crack-initiating cracks/defects/dislocations, non-recoverable stress concentration, and amplification sites in the Bi-2223 crystal system. Hence, the pure sample have been observed to exhibit the least response to forces; on the other hand, the maximum CdO impurity added Bi-2223 have presented the most response to the applied test load. Besides, all the materials studied have exhibited the standard ISE character.

References

- [1] H.K. Onnes, Further experiments with Liquid Helium. D. On the change of Electrical Resistance of Pure Metals at very low Temperatures, etc. V. The Disappearance of the resistance of mercury, Koninklijke Nederlandsche Akademie van Wetenschappen Proceedings, 14 (1911) 113–115.
- [2] Saunders, P.J.; Ford, G.A. (2005). The Rise of the Superconductors. Boca Raton, FL: CRC Press.
- [3] A.K. Saxena, High-temperature superconductors, Springer, Berlin, 2010.
- [4] P. Marsh, R.M. Fleming, M.L. Mandich, A.M. Desantolo, J. Kwo, M. Hong, L.J. Martinez-Miranda, Crystal-Structure of the 80K Superconductor $\text{YBa}_2\text{Cu}_4\text{O}_8$, Nature 334 (1988) 141–143.
- [5] U. Erdem, Y. Zalaoglu, A.T. Ulgen, T. Turgay, G. Yildirim, Role of trivalent Bi /Tm partial substitution on active operable slip systems in Bi 2212 crystal structure, Cryogenics, 113 (2021) 103212.
- [6] M. Chen, W. Paul, M. Lakner, L. Donzel, M. Hoidis, P. Unternaehrer, R. Weder, M. Mendik, 6.4 MVA resistive fault current limiter based on Bi-2212 superconductor, Physica C 372 (2002) 1657–1663.
- [7] H. Yamauchi, M. Karppinen, Application of High-Pressure Techniques: Stabilization and Oxidation-State Control of Novel Superconductive and Related Multi-Layered Copper Oxides, Supercond. Sci. Technol. 13 (2000) R33–R52.

- [8] S.Y. Oh, H.R. Kim, Y.H. Jeong, O.B. Hyun, C.J. Kim, Joining of Bi-2212 high- T_c superconductors and metals using indium solders, *Physica C* 463–465 (2007) 464–467.
- [9] U. Erdem, Y. Zalaoglu, A.T. Ulgen, T. Turgay, G. Yildirim, Role of trivalent Bi /Tm partial substitution on active operable slip systems in Bi 2212 crystal structure, *Cryogenics*, 113 (2021) 103212.
- [10] A.K. Saxena, *High-Temperature Superconductors*, 2nd Ed., Springer Heidelberg New York Dordrecht London, 2012.
- [11] K. Salama, V. Selymanickam, L. Gao, K. Sun, High-current Density in Bulk $\text{YBa}_2\text{Cu}_3\text{O}_x$ superconductor, *Appl. Phys. Lett.* 54 (1989) 2352–2354.
- [12] C. Autret-Lambert, B. Pignon, M. Gervais, I. Monot-Laffez, A. Ruyter, L. Ammor, F. Gervais, J.M. Bassat, R. Decourt, Microstructural and transport properties in substituted $\text{Bi}_2\text{Sr}_2\text{CaCu}_2\text{O}_{8+\delta}$ modulated compounds, *J. Solid State Chem.* 179 (2006) 1698–1706.
- [13] J.J. Roa, E. Jiménez-Piqué, X.G. Capdevila, M. Segarra, Nanoindentation with spherical tips of single crystals of YBCO textured by the Bridgman technique: Determination of indentation stress-strain curves, *J. Eur. Ceram. Soc.* 30 (2010) 1477–1482. doi:10.1016/j.jeurceramsoc.2009.10.021.
- [14] S. Dadras, S. Dehghani, M. Davoudiniya, S. Falahati, Improving superconducting properties of YBCO high temperature superconductor by Graphene Oxide doping, *Mater. Chem. Phys.* 193 (2017) 496–500. doi:https://doi.org/10.1016/j.matchemphys.2017.03.003.
- [15] Jr. W.D. Callister, D.G. Rethwisch, *Materials Science and Engineering: An Introduction*, 9th ed., Wiley Binder Version, USA, 2013.
- [16] W. Abdeen, S. Marahba, R. Awad, A.I. Abou Aly, I.H. Ibrahim, M. Matar, Electrical and mechanical properties of (Bi, Pb)-2223 substituted by holmium, *J. Advanced Ceramics* 5 (2016) 54–69.

**RECENT METHODOLOGIES IN SYNTHESIZING THIENOTHIOPHENES: A PROMISING
FRAMEWORK FOR THE DEVELOPMENT OF BIOLOGICALLY ACTIVE COMPOUNDS****Ayesha Rafiq***Department of Chemistry, Government College University Faisalabad, Pakistan***Prof. Dr. Matloob Ahmad***Department of Chemistry, Government College University Faisalabad, Pakistan**ORCID: 0000-0003-1302-8056***ABSTRACT:**

Heterocyclic chemistry has emerged as a dynamic and important subfield within the larger field of organic chemistry as a result of the growing interest in the field of pharmacology. The numerous applications of heterocyclic compounds in the scientific and physical sciences make them desirable candidates. Dithioenthiophene (TT) is a stable, electron-rich annulated ring made up of two thiophene rings. Thienothiophenes (TTs) are a complete representation of the planar system that can significantly change or enhance the basic characteristics of organic, π -conjugated components that are incorporated into a molecular structure. The optoelectronic and pharmacological capabilities of these compounds were just two of their many uses. Thienothiophene's many isomeric forms have demonstrated a range of uses, including those in semiconductors, solar cells, organic field effect transistors, antiviral, anticancer, antiglaucoma, and electroluminescents. To create thienothiophene derivatives, several techniques were used. We have discussed several synthesis approaches of different isomeric forms of thienothiophene that have been discovered during the previous six years.

Keyword: Thieno[3,2-*b*]Thiophene • Thieno[2,3-*b*]Thiophene • Thieno[3,4-*b*]Thiophene • Synthesis

DEVELOPMENT OF COMPOSITES BASED ON BIODEGRADABLE POLYMERS AND LOCAL MINERAL MATERIALS AND THEIR APPLICATIONS IN WASTEWATER TREATMENT

TAFRAOUT Fatiha

University Abdelmalek Essaâdi, Al-Hoceima, Morocco

ABSTRACT

Chemical pollution of water largely results from effluents containing organic pollutants and heavy metals. Various conventional processes exist to treat these effluents on a large scale in wastewater treatment plants, but these processes are not very selective and often lead to the formation of sludge which is itself difficult to treat. In the global dynamic concerning the environment and its protection, the valorization of natural resources is making major progress in the development of bio-based products and new eco-technologies. In this sense, agro-resources could constitute a sustainable raw material for use in wastewater treatment. This thesis aims to design composites from various biodegradable biopolymers and mineral materials, and evaluate their ability to remove emerging pollutants.

Keywords: composites, biopolymers, mineral materials, wastewater, emerging pollutants.

INVESTIGATION ON MECHANICAL AND WEAR BEHAVIOUR OF FLYASH REINFORCED AA6068 ALUMINIUM ALLOY FABRICATED THROUGH POWDER METALLURGY TECHNIQUE

U. Elaiyaran

Department of Automobile Engineering, Easwari Engineering College, Chennai-600089

J. Paulmar Pushparaj

Department of Mechanical Engineering, Easwari Engineering College, Chennai-600089

C. Asokan

Department of Mechanical Engineering, SNS College of Technology, Coimbatore- 641035

S. Prathiban

Department of Mechanical Engineering, SRM Institute of science and Technology, Chennai-600089

ABSTRACT

Powder metallurgy (PM) aluminum composites involve the fabrication of composite materials by blending aluminum powder with other materials to improve specific properties. The process typically includes steps such as powder production, mixing, compaction, and sintering. The incorporation of fly ash particles into aluminum matrix composites is a common strategy to enhance the mechanical properties and wear resistance of the resulting material. Fly ash is a byproduct of coal combustion and is rich in silica, alumina, and other oxides. When dispersed in an aluminum matrix, it can impart several desirable properties to the composite material. In the research, AA6068 aluminum metal matrix composites were developed through the powder metallurgy method, incorporating fly ash particles at weight percentages of 5, 10, 15%. Microscopic examinations using scanning electron microscope indicate a uniform distribution of fly ash particles throughout the matrix. It was observed that the aluminum alloy prepared with 10% of flyash showed increased hardness than the base alloy. Additionally, the wear behavior of base metal and its composite has been investigated using a pin-on-disc tribometer under dry sliding conditions. Three different loads of 10N, 20N, and 30N constant sliding velocity of 1.3ms⁻¹ have been used for wear experiments. According to wear debris and microstructural investigations of worn surfaces, the wear mechanism in base metal is regulated by adhesion, while the wear mechanism in composites is abrasive. The AA6068-10% Fly Ash composite has the lowest wear rate. It is found that the AA6068-10% Fly Ash has the best wear rate and mechanical properties.

Keywords: AA6068, Flyash, Powder metallurgy, hardness, wear properties.



SMART NANOCOMPOSITE IN THE TiC-BN-SiC-B₄C-SiAlON-Al₂O₃ SYSTEM

Z. Kovziridze

Georgia Technical University, Institute of Bionanoceramics and Nanocomposite Technology, Georgia, 0175, Tbilisi

N. Nijaradze

Georgia Technical University, Institute of Bionanoceramics and Nanocomposite Technology, Georgia, 0175, Tbilisi
Georgia Technical University, Institute of Bionanoceramics and Nanocomposite Technology, Georgia, 0175, Tbilisi,

T. Cheishvili

Georgia Technical University, Institute of Bionanoceramics and Nanocomposite Technology, Georgia, 0175, Tbilisi

Ts. Danelia

Georgia Technical University, Institute of Bionanoceramics and Nanocomposite Technology, Georgia, 0175, Tbilisi

N. Darakhvelidze

Georgia Technical University, Institute of Bionanoceramics and Nanocomposite Technology, Georgia, 0175, Tbilisi

ABSTRACT

Goal - to obtain on first stage β - SIALON containing nanocomposites by reactive sintering method at 1400°C, with nitrogen process from origin composition in TiC-BN-SiC-B₄C-Si-Al-Al₂O₃ system. By using this method of synthesis, it became possible to receive nanocomposites with different percentages of β - SIALON. Our task was also to study the phase composition of received consolidated materials in the TiC-BN-SiC-B₄C- β -SiAlON-Al₂O₃ (nanopowder-400nm.) system.

Method. The obtained mass was grounded in an attritor and the consolidated composite was obtained by hot pressing at 1620°C during 40 minutes, with glass perlite (Armenia) dope 2 mass%, delaying at final temperature for 8 min, under 30 MPa pressure and vacuum – 10⁻³ Pa. Perlite from Aragatc contained 96 mas. % glass.

To study the phase composition of the composites, we conducted an X-ray structural analysis on the DRON-3 device. And to study the microstructure, we conducted research on an optical microscope -AC100 and a raster electron microscope “Nanolab 7” of the company “OPTON”. The values of the electrical parameters of the studied composites were calculated on the basis of the obtained “lgp- t” dependence. We have studied mechanical properties.

Result. In TiC-BN-SiC-B₄C- β -SiAlON-Al₂O₃ system we obtained nanocomposites with high mechanical properties and a matrix composed of: β -SIALON, silicon carbide, corundum nanoparticles, titanium carbide, boron carbide and of boron nitride.

Conclusion. The phase composition of the obtained composite provides high physical-technical and performance properties of these nanocomposites. Compression strength-2187 MPa, Bending strength-285 MPa, Thermal expansion coefficient a_{20-700} -3.8 10⁻⁶ °C.

Key words: nanocomposite; hot press; electron microscope; phase composition; B₄C-BN-TiC-SiC- β -SIALON-Al₂O₃ nano-powder system.

MODELLING TOPOGRAPHICAL PROPERTIES OF 3D PRINTING METAL MATERIAL

Matej Babič

Faculty of information studies, Novo mesto, Slovenia

ABSTRACT

3D printing or additive manufacturing is a process of making three dimensional solid objects from a digital file. 3D printing is an additive technology used to manufacture parts. It is 'additive' in that it doesn't require a block of material or a mold to manufacture physical objects, it simply stacks and fuses layers of material. It's typically fast, with low fixed setup costs, and can create more complex geometries than 'traditional' technologies, with an ever-expanding list of materials. It is used extensively in the engineering industry, particularly for prototyping and creating lightweight geometries. The creation of a 3D printed object is achieved using additive processes. In an additive process an object is created by laying down successive layers of material until the object is created. Each of these layers can be seen as a thinly sliced cross-section of the object. 3D printing is the opposite of subtractive manufacturing which is cutting out / hollowing out a piece of metal or plastic with for instance a milling machine. 3D printing enables you to produce complex shapes using less material than traditional manufacturing methods. 3D printing encompasses many forms of technologies and materials as 3D printing is being used in almost all industries you could think of. It's important to see it as a cluster of diverse industries with a myriad of different applications. In this article, we use multiple regression for modelling topographical properties of 3D printing metal material.